Terms and Conditions of Use of Digitised Theses from Trinity College Library Dublin

Copyright statement

All material supplied by Trinity College Library is protected by copyright (under the Copyright and Related Rights Act, 2000 as amended) and other relevant Intellectual Property Rights. By accessing and using a Digitised Thesis from Trinity College Library you acknowledge that all Intellectual Property Rights in any Works supplied are the sole and exclusive property of the copyright and/or other IPR holder. Specific copyright holders may not be explicitly identified. Use of materials from other sources within a thesis should not be construed as a claim over them.

A non-exclusive, non-transferable licence is hereby granted to those using or reproducing, in whole or in part, the material for valid purposes, providing the copyright owners are acknowledged using the normal conventions. Where specific permission to use material is required, this is identified and such permission must be sought from the copyright holder or agency cited.

Liability statement

By using a Digitised Thesis, I accept that Trinity College Dublin bears no legal responsibility for the accuracy, legality or comprehensiveness of materials contained within the thesis, and that Trinity College Dublin accepts no liability for indirect, consequential, or incidental, damages or losses arising from use of the thesis for whatever reason. Information located in a thesis may be subject to specific use constraints, details of which may not be explicitly described. It is the responsibility of potential and actual users to be aware of such constraints and to abide by them. By making use of material from a digitised thesis, you accept these copyright and disclaimer provisions. Where it is brought to the attention of Trinity College Library that there may be a breach of copyright or other restraint, it is the policy to withdraw or take down access to a thesis while the issue is being resolved.

Access Agreement

By using a Digitised Thesis from Trinity College Library you are bound by the following Terms & Conditions. Please read them carefully.

I have read and I understand the following statement: All material supplied via a Digitised Thesis from Trinity College Library is protected by copyright and other intellectual property rights, and duplication or sale of all or part of any of a thesis is not permitted, except that material may be duplicated by you for your research use or for educational purposes in electronic or print form providing the copyright owners are acknowledged using the normal conventions. You must obtain permission for any other use. Electronic or print copies may not be offered, whether for sale or otherwise to anyone. This copy has been supplied on the understanding that it is copyright material and that no quotation from the thesis may be published without proper acknowledgement.

Characterization of Sfh, a novel H-NS-like protein

By

Marie Doyle

A dissertation presented for the degree of Doctor of Philosophy, in the Faculty of Science, University of Dublin, Trinity College

Department of Microbiology
Moyne Institute of Preventive Medicine
Trinity College Dublin

August 2006

Declarations

I, Marie Doyle, am the sole author of this thesis. The work presented herein represents my own work except where duly acknowledged in the text, and has not been previously presented for a higher degree at this or any other University. Some parts of this work have been published in the following paper:

Beloin, C., Deighan, P., Doyle, M., and Dorman, C.J. (2003) *Shigella flexneri* 2a strain 2457T expresses three members of the H-NS-like protein family: characterization of the Sfh protein. *Mol Genet Genomics* **270**: 66-77.

I agree that the Library of Trinity College Dublin may lend or copy this thesis upon request.

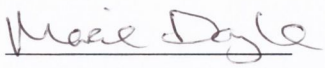

Marie Doyle

Summary

Members of the H-NS protein family are widespread among Gram-negative bacteria and are known to influence gene expression at a global level. *Shigella flexneri* serotype 2a strain 2457T expresses three members of the H-NS protein family, namely, H-NS, StpA, and the recently identified Sfh protein. Unlike the *hns* and *stpA* genes, the *sfh* gene is not located on the chromosome, but on the large self-transmissible plasmid pSf-R27. In this study, the regulation of growth phase-dependent Sfh expression was examined and several novel roles for Sfh *in vivo* were elucidated.

Growth-phase-dependent expression of Sfh was shown to be controlled at the level of transcription and also post-transcriptionally at the translational level. The *sfh* transcript was predicted to fold into a *cis*-inhibitory structure that hinders efficient translation of the message. At the onset of stationary phase, *sfh* mRNA is translated due to the presence of a translation stimulatory factor, leading to high levels of Sfh protein in the cell. The factor that stimulates translation of the *sfh* transcript has yet to be identified, but is thought to be a stationary phase-specific riboregulator or RNA chaperone. Importantly, H-NS and StpA were shown not to influence the translation of the *sfh* transcript, but were observed to directly repress transcription of the *sfh* gene. Furthermore, Sfh was found to be subject to regulated proteolysis in the absence of H-NS, but to be stable irrespective of the presence or absence of StpA. These data show the potential importance of heteromerization among H-NS family members. It is proposed that different homomeric and heteromeric H-NS-like protein complexes could modulate distinct subsets of genes.

A novel role for Sfh, H-NS, and StpA in modulating conjugative transfer of plasmid pSf-R27 was identified, although the proteins were shown not to regulate the thermosensitive transfer of plasmid pSf-R27. Consistent with members of the H-NS protein family being transcriptional repressors, all three proteins were shown to negatively influence *tra* gene

expression. Mating assays revealed that conjugative transfer of plasmid pSf-R27 from donor strains lacking one or more H-NS-like protein was dramatically reduced. This paradoxical observation suggests that plasmid pSf-R27 conjugative transfer is subject to complex regulation at both the transcriptional and post-transcriptional level.

Significantly, a distinct role for Sfh in pSf-R27 plasmid biology was elucidated. Sfh was shown to have a 'stealth-like' role that allows plasmid pSf-R27 to disseminate into a new host virtually without detection at the level of the host transcriptome. DNA microarray analysis revealed that horizontal transfer of plasmid pSf-R27 lacking a functional *sfh* gene, but not of the wild-type plasmid has a profound effect on the host transcriptome. It is proposed that H-NS is less active in strains that acquire plasmid pSf-R27 lacking the *sfh* gene, due to a titration effect exerted by the introduced plasmid. Consequently, acquisition of plasmid pSf-R27 lacking the *sfh* gene dramatically reduces the fitness of the recipient bacterium. Importantly, expression of Sfh *in trans* was shown to minimize the fitness cost of plasmid pSf-R27 and several other unrelated plasmids on host cells.

Finally, Sfh was shown to influence *Shigella* and *Salmonella* virulence gene expression. Sfh can repress *Shigella* virulence gene expression under non-permissive conditions by binding to the promoter regions of the *virF* and *virB* genes. In addition, horizontal acquisition of Sfh on plasmid pSf-R27 was shown to contribute to *Salmonella* virulence signaling pathways. Notably, acquisition of plasmid pSf-R27 by *Salmonella* Typhimurium correlated with an increase in bacterial survival within the macrophage. These findings suggest that plasmid pSf-R27 might encode novel virulence factors, which protect *Salmonella* in the macrophage's intracellular environment and thus could enhance the systemic spread of *Salmonella* in the host.

Acknowledgements

Firstly I would like to thank Charlie for giving me the wonderful opportunity to work in his lab and for all his encouragement and advice throughout this project. I would also to thank my thesis committee, Cyril, Tim and Stephen for their constant guidance and helpful comments over the past four years.

A special thanks to all the prep room staff Henry, Dave, Margaret, Miriam, Fionnuala, Paddy Joe and Ronan, thanks to your hard work I was never short of media, flasks, pipettes or anything else.

I would like to thank all the members of the CJD lab past and present Padraig, Ronan, Colin, Antonia, Paul, Matt, Arlene, Libby, Tadhg, Gar, Mick, Jenny and Kirsty. Thanks for all the help and the craíc both in and out of the lab, especially the mad nights out! Connie thanks for everything, without you the lab would fall to pieces. A huge thanks to Padraig, who from day one in the lab always came to my rescue and even when you left you still managed to give me great advice and encouragement all the way from Boston. A special word of thanks to Arlene and Libby for the daily girlie chats, I'll miss our coffee and scones.

Fiona, my 'twin' as Tim likes to call you, we've managed to choose the same career path ever since school. I've been so lucky to have you as a friend all these years, thanks for always being there and listening to me moan when things didn't work out. Thanks also to Matthew for all the jokes and laughs.

Also thanks to my non-Moyne friends Niamh, Paula, Sarah, Helen and Caitrin for your friendship and support, you were my escape from the 'science world'.

A huge thank you must go to my family, my parents, my brothers and sister, for all their love and support. Mum and Dad I think I owe you a fortune by now!

Last but not least I'd like to thank Darragh, you always know what to say to brighten my day. Thanks for all the support and encouragement.

For my parents

with thanks

Table of Contents

List of Figures

(Number shown is that of the page previous to the figure)

List of Tables

(Number shown is that of the page previous to the figure)

Chapter 1

General Introduction

1.1 Introduction

Enterobacteriaceae are capable of adapting to diverse environmental conditions due to their sophisticated genetic regulatory systems that can sense and swiftly respond to environmental stress. As a result, *Enterobacteriaceae* can successfully tranverse fundamentally different habitats, such as the soil and water in the environment, to the intestinal gut of the host (Rhen and Dorman, 2005). The complex genetic regulatory networks that are key to sensing these environmental changes often overlap (Rhen and Dorman, 2005), and are controlled by global gene regulators, such as the nucleoid-associated proteins (Dorman and Deighan, 2003; Rhen and Dorman, 2005). These proteins can co-ordinate the transcription of a large number of genes scattered around the genome, including bacterial virulence genes located within horizontally acquired pathogenicity islands and plasmids (Dorman and Porter, 1998; Dorman and Deighan, 2003; Rhen and Dorman, 2005).

The aim of this chapter is to provide some background to the genetics of virulence in the bacterial species, *Shigella flexneri* and *Salmonella enterica* serovar Typhimurium. It also aims to introduce the major nucleoid-associated proteins, in particular H-NS and its role in global gene expression. In addition, the general characteristics of H-NS-like proteins are discussed, with an emphasis on StpA and Sfh. Finally, it provides a detailed review of IncHI1 plasmids and bacterial conjugation systems.

1.2 *Shigella*

Shigella is an enteroinvasive Gram-negative bacterium that causes bacillary dysentery or shigellosis in humans. *Shigella* is considered to be a clonal lineage of *Escherichia coli* that arose approximately 80 million years ago (Pupo *et al.*, 2000; Rolland *et al.*, 1998). The two bacteria share a high degree of genomic sequence similarity. However, the *Shigella* species have evolved to occupy a specialized pathogenic niche. There are four *Shigella* species, namely, *Shigella flexneri, Shigella sonnei, Shigella dysenteriae* and *Shigella boydii*, which are subdivided into serotypes based on the O-specific polysaccharide antigen of the

lipopolysaccharide (LPS) (Niyogi, 2005). All four *Shigella* species are pathogenic, but the epidemiology of each is slightly different. *S. dysenteriae* is most commonly responsible for rapidly spreading and deadly epidemics of the disease, *S. flexneri* and *S. sonnei* account for the endemic forms of the disease, while *S. boydii* is pathogenic, but rarely encountered, except in the Indian sub-continent (Niyogi, 2005; Sansonetti, 2001). *S. flexneri* is responsible for around 50% of all shigellosis cases, which occur mainly in developing countries. Transmission is via the faecal-oral route, and the disease is particularly prevalent in areas with poor hygiene standards. *Shigella* is highly infectious, with as few as 10–100 viable organisms being required to establish an infection (DuPont *et al.*, 1989). *Shigella* causes disease by invading the epithelium of the colon, resulting in an intense acute inflammatory response. The infection process involves uptake through the colonic epithelium via M-cells, engulfment by macrophages, induction of apoptosis of the macrophage, and then basolateral invasion of colonic epithelial cells, where the bacteria replicate and spread directly into adjacent cells (Blocker *et al.*, 1999; Dorman and Porter, 1998; Wassef *et al.*, 1989; Zychlinsky *et al.*, 1992). The resulting inflammation and mucosal destruction lead to the symptoms of dysentery.

The clinical manifestations of shigellosis vary from short-lasting watery diarrhoea to acute inflammatory bowel disease characterized by fever, intestinal cramp and bloody diarrhoea with mucopurulent faeces (Sansonetti, 2001). Most episodes of shigellosis are self-limiting in healthy individuals, but *Shigella* can cause acute, life-threatening complications such as sepsis, intestinal perforation, and severe malnutrition and dehydration in the very young and immunocompromised (Niyogi, 2005). According to the World Health Organisation, there are approximately 150 million cases of dysentery per year, with 600,000 fatalities, almost all of which occur in the developing world. Efforts to control disease transmission include improved sanitation practices and antibiotic treatment. However, the variety of antimicrobials effective for the treatment of shigellosis is becoming limited due to globally emerging drug resistance (Sack *et al.*, 1997).

1.2.1 *Shigella* infection process

Shigella infections are acquired by the ingestion of contaminated food or water. Infection occurs specifically in the rectal and colonic mucosae, where *Shigella* first invades and then spreads between the cells of the epithelium (Sansonetti, 2001). Unlike enteroinvasive *E. coli* and *Salmonella*, *Shigella* is unable to enter colonic epithelial cells by their apical surfaces. Instead, *Shigella* exploits the antigen-sampling M-cells in the gut to gain access to the basolateral surfaces of epithelial cells (Fig. 1.1; Wassef *et al.*, 1989). Bacteria are passively translocated through the M-cells in a phagosome, and engulfed by macrophage located in the basolateral layer below. In contrast to *Salmonella*, which remains and multiplies within the macrophage phagosome, *Shigella* escapes the macrophage phagosomal vacuole, and once free in the cytoplasm, induces apoptosis of the macrophage (Fig. 1.1; Sansonetti, 2001; Zychlinsky *et al.*, 1992). The subsequent activation of caspase 1 in the dying macrophage causes the release of two potent pro-inflammatory cytokines, IL-1βand IL-18 (Dockrell, 2001; Zychlinsky *et al.*, 1992). Cytokine release results in the recruitment of polymorphonuclear (PMN) cells to the site of infection. These cells migrate through the epithelium into the lumen of the colon, resulting in destabilization of the integrity of the epithelial barrier. This allows more bacteria to gain access to the basolateral membrane and leads to the characteristic symptoms of the disease (Perdomo *et al.*, 1994a; Perdomo *et al.*, 1994b; Philpott *et al.*, 2000).

Upon contact with the basolateral surface of host colonic epithelial cells, *Shigella* secretes effector proteins into the host cell cytosol via a bacterial type III secretion system (TTSS). These effector proteins induce major cytoskeletal rearrangements at the site of bacterial interaction with the cell membrane (Adam *et al.*, 1995), which leads to the formation of large membrane ruffles that surround and engulf the bacterium in a macropinocytosis-like process (Fig. 1.1). Once internalized, *Shigella* release factors that cause lysis of the phagocytic vacuole, thereby releasing bacteria in the cell cytoplasm, where conditions are optimal for growth and multiplication (High *et al.*, 1992; Sansonetti *et al.*, 1996). Within two hours of entry into the epithelial cell, *Shigella* nucleates and assembles actin tails (Fig. 1.1). These

Fig. 1.1. Schematic model of the principal steps of *Shigella* infection. *Shigella* infections are acquired through consumption of contaminated food or water and the infection process can be divided into six steps. (1) Following ingestion, *Shigella* pass the stomach specifically to infect the rectal and colonic mucosae. The bacteria cross the epithelium barrier by entering M-cells. (2) They are delivered to resident macrophage located in the basolateral layer below. (3) *Shigella* escapes the macrophage phagosomal vacuole, and once free in the cytoplasm, induces apoptosis of the macrophage. (4) Upon contact with the basolateral surface of host colonic epithelial cells, *Shigella* secretes effector proteins into the host cell cytosol via the Mxi-Spa type III secretion system, which subsequently induce bacterial uptake. (5) Once internalized, *Shigella* lyses the phagocytic vacuole and (6) forms actin tails, which propel the bacteria through the cell cytoplasm and into adjacent cells, spreading infection across the tissue layer. Figure adapted from Porter (1998).

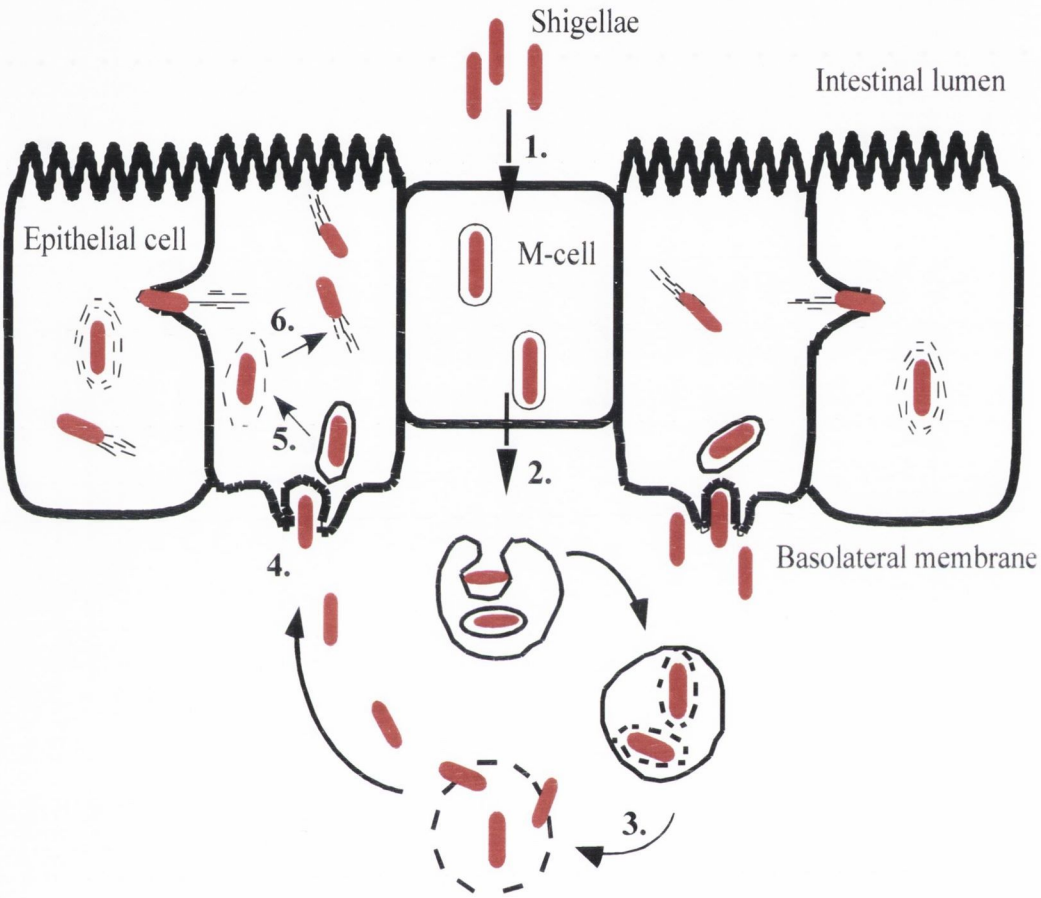
Shigellae
Intestinal lumen
1.
Epithelial cell
M-cell
6.
5.
2.
4.
Basolateral membrane
3.

polarize at one end of the cell and their polymerization generates momentum, propelling the bacteria through the cell cytoplasm and into adjacent cells, spreading infection across the tissue layer (Fig. 1.1; Bernardini *et al.*, 1989). In response to bacterial invasion, colonic epithelial cells express an array of proinflammatory factors such as NF-κB and IL-8. In addition, LPS released by intracellular bacteria accounts for a strong sustained release of IL-8, which consequently attracts more PMNs to the site of infection and further aggravates inflammation (Philpott *et al.*, 2000). The additive effect of the invasion process and the host inflammatory response probably explains the severity of the tissue destruction typically associated with shigellosis (Sansonetti, 2001).

1.2.2 *Shigella* large virulence plasmid

The entire complement of genes critical for *Shigella* invasion of epithelial cells is located on a large 220-kb plasmid, termed the *Shigella* large virulence plasmid (LVP). Consistent with this, the LVP is sufficient to confer an invasive phenotype onto avirulent strains of *Shigella* and *E. coli* (Blattner *et al.*, 2001; Sansonetti, 1991b). The core genes required for *Shigella* virulence are located within a 31-kb region of the LVP, known as the entry region (Fig. 1.2; Maurelli *et al.*, 1985; Sasakawa *et al.*, 1988). There are 37 open reading frames in this region, which encodes the Mxi-Spa TTSS and its associated effector proteins. The overall G+C content of the entry region is 35% compared with an estimated 50% G+C content for the *Shigella* chromosome, and the entry region is flanked by truncated insertion sequences. These data indicate that the virulence genes were acquired by horizontal transfer. The Mxi-Spa TTSS is homologous to the *Salmonella* Inv/Spa TTSS, which is also required for epithelial invasion. The Mxi-Spa apparatus has been visualized by electron microscopic analysis and consists of a multi-ring base composed of the MxiG, MxiJ, MxiD and MxiM proteins and a slender needle-like structure, which protrudes outwards from the bacterial envelope and consists of the proteins MxiH and MxiM (Fig. 1.3; Parsot, 2005). Assembly of the TTS apparatus (TTSA) proceeds in sequential steps that require reprogramming of the secretion machine (Marlovits *et al.*, 2006). A recent *Salmonella* study demonstrated that

completion of the inner rod results in the firm anchoring of the needle to the base, which triggers a conformational change on the cytoplasmic side of the TTSA. Consequently, the TTSA stops secretion of the inner rod and needle proteins and starts secretion of effector proteins. Hence this mechanism determines the length of the needle substructure (Marlovits *et al.,* 2006). The *Shigella* TTSA is activated upon bacterial contact with epithelial cells and is responsible for the secretion of the invasion plasmid antigen (Ipa) proteins, which mediate invasion of the epithelial mucosa (Menard *et al.*, 1993; Schuch and Maurelli, 2001).

Four Ipa proteins –IpaA, IpaB, IpaC and IpaD– together with IpgD are required for host cell invasion. The Ipa proteins exhibit a high degree of amino acid sequence similarity to the Sip proteins of *Salmonella* (Galan, 1996). They are produced and stored in the cytoplasm of bacteria, before being released through the Mxi-Spa secretion system upon contact with host cells (Menard *et al.*, 1994). The IpaB and IpaC proteins form a 'translocon' or pore-like structure in the eukaryotic cell membrane, through which other Ipa proteins are thought to enter the cytoplasm (Fig. 1.3; Blocker *et al.*, 1999; Page *et al.*, 2001). In addition, the translocon complex is thought to regulate the rate of secretion (Menard *et al.*, 1996).

The two Ipa proteins, IpaA and IpaC are known to be involved in actin cytoskeleton rearrangements of the host cell, which mediate *Shigella* uptake by phagocytosis (Osiecki *et al.*, 2001; Schuch *et al.*, 1999). IpaC triggers activation of members of the Rho family of GTPases, namely, Rac and CDC42, via its C-terminal domain, once it is inserted into the host cell membrane. The mechanism of GTPase activation mediated through IpaC is currently unknown (Sansonetti *et al.*, 1999; Tran Van Nhieu *et al.*, 1999). The IpaA protein is secreted into the host cell cytosol, where it binds directly to the focal adhesion protein vinculin, promoting depolymerization of actin filaments (Tran Van Nhieu *et al.*, 2000). Furthermore, another secreted protein, IpgB1, was shown recently to stimulate the activation of Rac and CDC42, thus contributing to membrane ruffle formation during *Shigella* invasion (Ohya *et al.*, 2005). Once internalized the bacterium escapes from the phagocytic vacuole via IpaB-

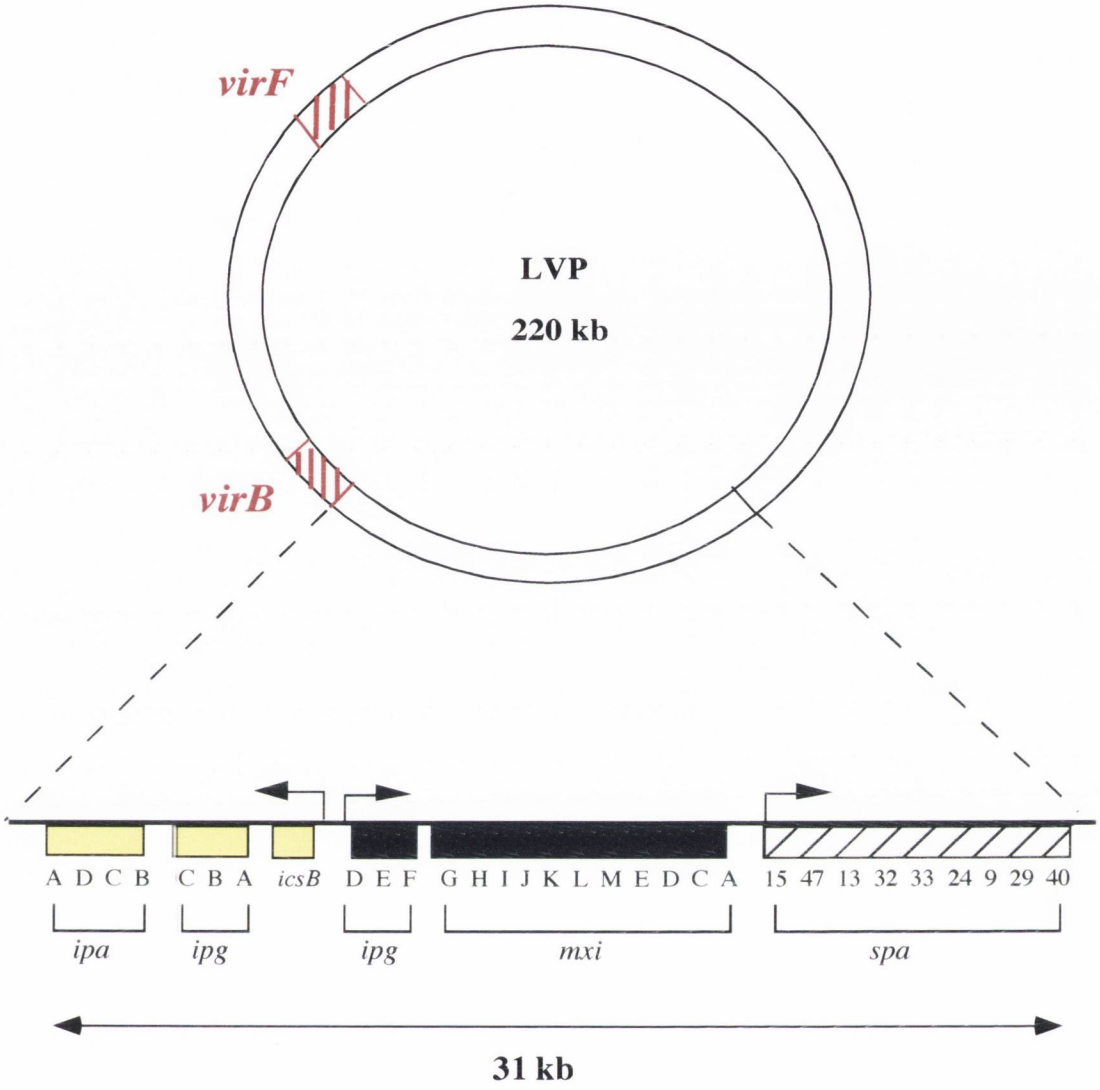

Fig. 1.2. Schematic map of the *Shigella* large virulence plasmid (LVP). The core genes required for *Shigella* virulence are located within a 31-kb region of the LVP, known as the entry region. The genes in this region encode the Mxi-Spa type III secretion system and its associated effector proteins. Arrows indicate the locations of the promoters of the three operons. The genes encoding the two essential regulatory proteins, VirF and VirB, are located outside the entry region and are indicated in red. Figure adapted from Mc Kenna (2002).

Fig. 1.3. Schematic model of the *Shigella* Mxi-Spa type III secretion apparatus. The Mxi-Spa apparatus consists of a multi-ring base composed of the MxiG, MxiJ, MxiD and MxiM proteins and a slender needle-like structure, which protrudes outwards from the bacterial envelope, consisting of the proteins MxiH and MxiM. The IpaB and IpaC proteins form the translocon, a pore-like structure in the eukaryotic cell membrane, through which the other secreted effectors enter the host cell cytoplasm.

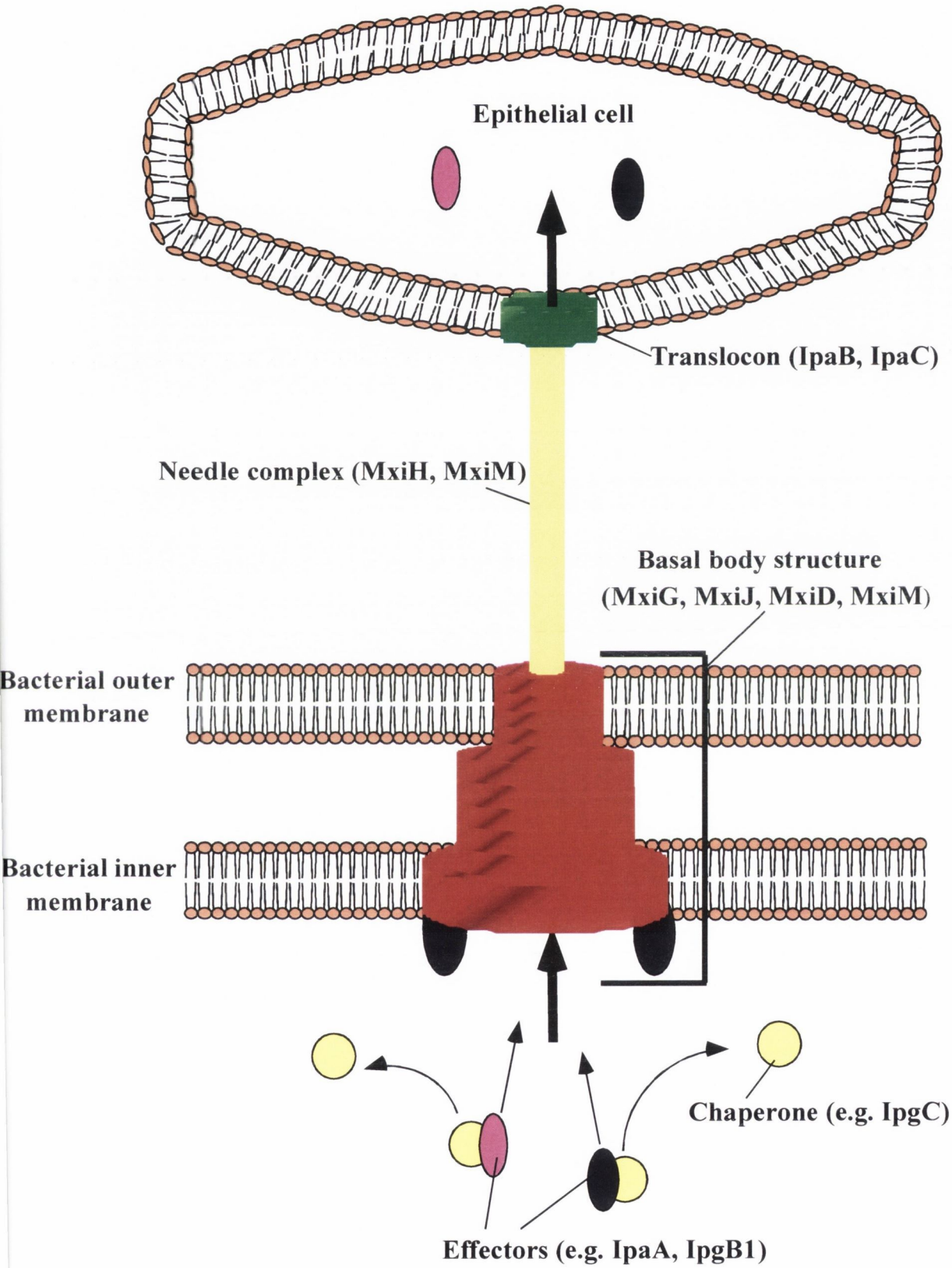
Epithelial cell
Translocon (IpaB, IpaC)
Needle complex (MxiH, MxiM)
Basal body structure
(MxiG, MxiJ, MxiD, MxiM)
Bacterial outer membrane
Bacterial inner membrane
Chaperone (e.g. IpgC)
Effectors (e.g. IpaA, IpgB1)

mediated lysis (High *et al.*, 1992). In addition to vacuolar escape, IpaB is also responsible for the induction of apoptosis in macrophage via interaction with caspase 1.

Several of the Ipa proteins interact with chaperones, encoded by the *ipg* genes, inside the bacterial cell. These include the IpaC and IpaB proteins, both of which interact with IpgC (Menard *et al.*, 1994; Page *et al.*, 2001). Consequently, IpgC is only free to interact with the regulatory protein MxiE (to facilitate virulence gene activation) following secretion of IpaB and IpaC.

In addition to the Ipa proteins, a repertoire of effectors encoded outside of the entry region of the LVP, are secreted by the Mxi-Spa TTSS. These include the IpaH proteins, which are characterized by a N-terminal leucine rich motif, and also the Osp proteins. These proteins appear to be produced and secreted at a later stage than the Ipa invasins and their roles in *Shigella* virulence are not clear, although it is thought they might play a role in the survival of bacteria in the intracellular environment (Buchrieser *et al.*, 2000).

The ability of *S. flexneri* to spread from cell to cell via actin polymerization is an essential part of the infection process. This mobility is mediated by a single outer membrane protein, IcsA, encoded by the LVP (Bernardini *et al.*, 1989). IcsA localises at the old pole of the cell, which is critical for unidirectional movement, and its activity is modulated by the outer membrane protease, IcsP (Egile *et al.*, 1997; Shere *et al.*, 1997). IcsA forms a ternary complex with the host proteins, N-WASP and Arp2/3, which leads to actin nucleation and polymerization, resulting in forward momentum and the formation of actin tails (Suzuki and Sasakawa, 2001).

Expression of the Mxi-Spa TTSS and its effectors is thought to represent a large metabolic burden for the bacteria. Therefore, unsurprisingly *Shigella* has evolved a complex regulatory system that integrates several environmental signals to prevent inappropriate expression. Optimal expression of the genes occurs under conditions which approximate those in the

lower intestine, i.e., at pH 7.4, moderate osmolarity and 37°C (Maurelli *et al.*, 1984; Nakayama and Watanabe, 1998; Porter and Dorman, 1994). Two LVP-encoded proteins, VirF and VirB, are essential for virulence gene activation and their expression is tightly regulated by several chromosomal loci, which include the genes coding for the major nucleoid-associated proteins, FIS, IHF and H-NS (Beloin and Dorman, 2003; Dorman and Porter, 1998; Dorman *et al.*, 2001; Falconi *et al.*, 2001; Porter and Dorman, 1997a).

1.3 *Salmonella*

Salmonella is a Gram-negative facultative intracellular pathogen. The genus *Salmonella* is divided into two species, *Salmonella enterica* and *Salmonella bongori*, which are subdivided into subspecies or serovars. The species *S. bongori* is thought to be phylogenetically older than *S. enterica* (Hensel, 2000) and is usually only isolated from cold-blooded animals. In contrast, *S. enterica* is associated with infection of a wide variety of animal hosts including poultry, cattle, pigs, mice and humans (Ohl and Miller, 2001). Certain serovars of *S. enterica* have adapted to cause infection only in specific hosts, while others display a broader host range and can cause diseases of different severity, depending on the host organism (Darwin and Miller, 1999b). *Salmonella* infections are usually acquired from contaminated food or water and are commonly associated with ingestion of improperly cooked poultry products, particularly eggs. Salmonellosis (the disease caused by *Salmonella*) has several clinical manifestations ranging from gastroenteritis to typhoid fever and bacteraemia. Serotypes associated with gastroenteritis orchestrate an intestinal inflammatory and secretory response, whereas serovars concerned with causing typhoid fever establish a systemic infection through their ability to survive and proliferate in mononuclear phagocytes (Ohl and Miller, 2001). The nature and severity of the disease caused depend largely on the infecting *Salmonella* serovar and the recipient host (Darwin and Miller, 1999b).

In humans, *Salmonella* infection causes two types of disease. Infection with the exclusively human pathogens *S. enterica* serovar Typhi (*S.* Typhi) and *S. enterica* serovar Paratyphi (*S.*

Paratyphi) results in a systemic infection called typhoid fever. Typhoid fever is still a major health problem in developing countries. According to World Health Organisation estimates, 16 million cases of typhoid fever occur annually worldwide with approximately 600,000 deaths (Jones, 2005). Transmission of this disease within the human population is generally a result of poor sanitation in developing nations. Clinical manifestations include fever, abdominal pain and transient diarrhoea or constipation. The pathological hallmark of enteric fever is mononuclear cell infiltration and hypertrophy of the reticuloendothelial system, including the intestinal Peyer's patches, mesenteric lymph nodes, spleen, and bone marrow. Without treatment mortality is 10–15% (Ohl and Miller, 2001). Efforts to control disease transmission include improved sanitation practices and antibiotic treatment. However, infections with antibiotic-resistant *Salmonella* species have surfaced, posing a greater risk to human populations in endemic areas (Jones, 2005). In contrast, infection with non-typhoidal *Salmonella* strains, such as *S. enterica* serovar Enteriditis (*S.* Enteriditis) and *S. enterica* serovar Typhimurium (*S.* Typhimurium), usually cause a self-limiting gastroenteritis characterized by diarrhoea in healthy humans, and bacteraemia is a rare complication of the very young and immunocompromised (Jones and Falkow, 1996; Wallis and Galyov, 2000). These broad host-range *Salmonella* are the most common cause of food-borne illness worldwide, and it is estimated that up to 1.3 billion cases of acute gastroenteritis are caused by non-typhoidal *Salmonella*, leading to 3 million deaths annually (Jones, 2005; Pang *et al.*, 1995).

1.3.1 *Salmonella* infection process

As mentioned previously, all *Salmonella* infections are acquired by the ingestion of contaminated food or water. Following oral ingestion, the bacteria must survive the acidic pH of the stomach before entering the small intestine. Once inside the small intestine the bacteria traverse the intestinal mucus layer and adhere to intestinal epithelial cells, which is mediated by several types of surface-expressed appendages called fimbriae (Fig. 1.4; Baumler *et al.*, 1996). These include type I fimbriae, long polar fimbriae, plasmid-encoded fimbriae and thin

aggregative fimbriae (Clegg *et al.*, 1996; Darwin and Miller, 1999b; Finlay and Brumell, 2000; Lucas and Lee, 2000). Upon contact with intestinal epithelial cells, *Salmonella* promotes its own uptake into these non-phagocytic cells by a process known as bacteria-mediated endocytosis (Francis *et al.*, 1992). This involves *Salmonella* translocating a set of deleterious effector proteins into the host cell cytosol via a bacterial TTSS (Galan, 1996). The effector proteins induce major cytoskeletal rearrangement of the host cell in the vicinity of the adhering bacteria, resulting in denuding of the microvilli and ruffling of the cell membrane (Fig. 1.4). Subsequently, the membrane ruffles surround and engulf the invading bacteria into vacuoles (Fig. 1.4). In mice, *Salmonella* appear to adhere preferentially to and enter the M-cells (Jones *et al.*, 1994). However, in bovine ligated ileal loops *Salmonella* invade both M-cells and enterocytes (Frost *et al.*, 1997). It has also been reported that *Salmonella* may passively cross the intestinal epithelial barrier following phagocytosis by migrating CD18-positive phagocytes (Vazquez-Torres *et al.*, 1999). Following bacterial internalization, a fraction of the *Salmonella*-containing vacuoles transcytose to the basolateral surface of the intestinal epithelia where the *Salmonella* exit and reach the Peyer's patches (Fig. 1.4). Here *Salmonella* encounter submucosal macrophages. *Salmonella* serotypes that cause systemic infection enter macrophages by bacteria-mediated endocytosis and are able to survive and grow inside the phagosomal vacuole (Fig. 1.4; Alpuche-Aranda *et al.*, 1994). The ability of *Salmonella* to survive in macrophages is dependent upon several virulence mechanisms that interfere with the normal antimicrobial functions of the macrophage (Cirillo *et al.*, 1998; Hensel, 2000; Vazquez-Torres and Fang, 2001). Subsequent migration of infected phagocytes to other organs of the reticuloendothelial system allows dissemination of *Salmonella* in the host (Fig. 1.4).

Clearly, *Salmonella* pathogenesis is very complex and requires the coordinate regulation of many bacterial virulence factors utilized at different anatomical sites within the animal host. In *S.* Typhimurium many of the genes encoding these virulence factors are found clustered together in groups. Small groups consisting of a few genes are called pathogenicity islets, while large groups containing many genes organized into operons are called pathogenicity

Fig. 1.4. Schematic model of the principal steps of *Salmonella* infection. *Salmonella* infections are typically acquired through consumption of contaminated food or water and the infection process can be divided into four steps. (1) Following ingestion, the bacteria pass the stomach to infect the small intestine. Upon contact with intestinal epithelial cells, *Salmonella* promotes its own uptake by translocating a set of deleterious effector proteins into the host cell cytosol via the SPI-1-encoded TTSS. (2) Following bacterial internalization, a fraction of the *Salmonella*-containing vacuoles transcytose to the basolateral surface of the intestinal epithelia where the *Salmonella* exit and encounter resident macrophage. (3) *Salmonella* serotypes that cause systemic infection enter macrophages by bacteria-mediated endocytosis, and reside in a *Salmonella*-containing vacuole (SCV) where they have the ability to survive and replicate. SPI-2 is essential for survival and proliferation in macrophages. (4) Subsequent migration of infected phagocytes to other organs of the reticuloendothelial system allows dissemination of *Salmonella* in the host. Figure adapted from Kelly (2005).

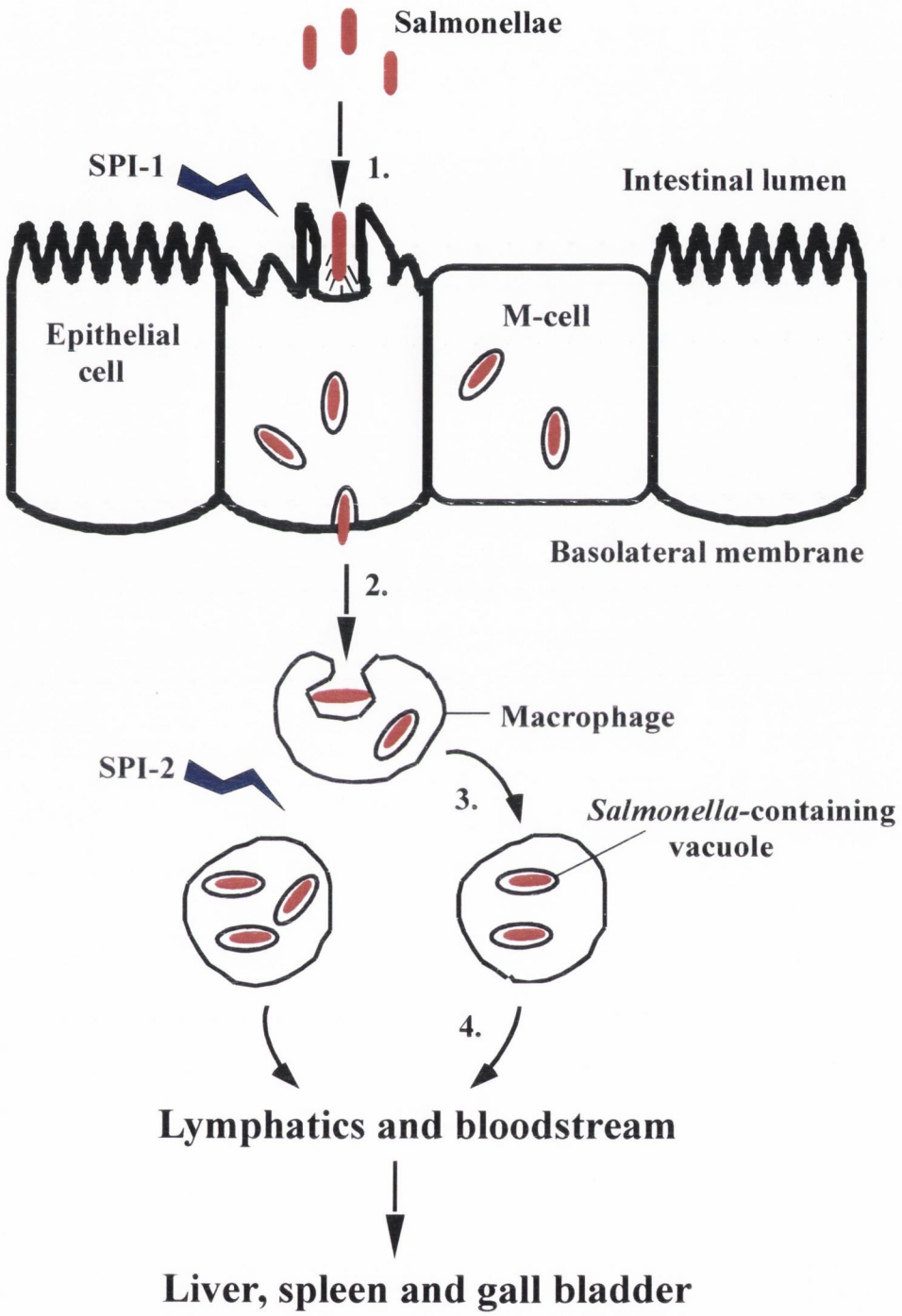
Salmonellae
SPI-1
1.
Intestinal lumen
Epithelial cell
M-cell
Basolateral membrane
2.
Macrophage
SPI-2
3.
Salmonella-containing vacuole
4.
Lymphatics and bloodstream
Liver, spleen and gall bladder

islands (Groisman and Ochman, 1996; Hansen-Wester and Hensel, 2001; Hensel, 2004; Kingsley and Baumler, 2002). Pathogenicity islands are genetic elements, which have a different percentage G+C content and codon usage to the rest of the genome as a whole, and are not found in closely related non-pathogenic species. Pathogenicity islands are often found integrated at tRNA loci or contain the remnants of bacteriophage or transposons at their borders, indicating that they were acquired by horizontal transfer (Blanc-Potard *et al.*, 1999; Groisman and Ochman, 1996; Hensel, 2004; Marcus *et al.*, 2000).

1.3.2 *Salmonella* pathogenicity island-1 (SPI-1)

Salmonella pathogenicity island-1 (SPI-1) is required by *S.* Typhimurium for invasion of intestinal epithelial cells and induction of intestinal secretory and inflammatory responses (Galyov *et al.*, 1997; Watson *et al.*, 1995). SPI-1 is located at 63 centisomes on the *S.* Typhimurium chromosome, is approximately 40 kb in size, and includes no less than 35 genes (Fig. 1.5; Collazo and Galan, 1997). The SPI-1 genes code for regulatory proteins, structural components of the Inv/Spa TTSS, and several secreted proteins and their chaperones (Wallis and Galyov, 2000). The ability of *S.* Typhimurium to induce its own uptake by non-phagocytic cells is dependent on the activity of the SPI-1 Inv/Spa TTSS (Watson *et al.*, 1995) and correlates with the observation that mutants lacking a functional SPI-1 are attenuated in mice when infected by the oral but not by the intraperitoneal route (Galan and Curtiss, 1989). Electron microscopic analysis of the SPI-1 type III secretion needle complex revealed that its size and morphology are virtually identical to that of the *Shigella* TTSA (Kimbrough and Miller, 2002). It consists of a multi-ring base composed of the SPI-1-encoded proteins Prgk, PrgH and InvG and a slender hollow needle-like structure, which protrudes outwards from the bacterial envelope, consisting of the SPI-1 proteins PrgI and PrgJ (Kimbrough and Miller, 2000). The translocation of SPI-1 effectors into the host cell also requires three SPI-1-encoded effectors –SipB, SipC and SipD– which are thought to insert into the eukaryotic cell membrane to form a 'translocon' of unknown structure (Darwin and Miller, 1999b). Recently, it was shown that SipB binds to cholesterol with high affinity

and that host-cell plasma membrane cholesterol is essential for TTSS-dependent effector translocation (Hayward *et al.*, 2005).

At least 13 effector proteins encoded both within and outside of SPI-1 are delivered into the host epithelial cell via the translocon (Knodler *et al.*, 2002). The precise function of many of these effectors remains to be elucidated, but generally they are thought to be involved in actin cytoskeleton rearrangements of the host cell, which mediate bacterial invasion. Previous studies have deciphered the roles of six translocated effectors, namely, SopE, SopE2, SopB, SptP, SipA and SipC, in orchestrating host-cell cytoskeletal rearrangements. SopE, SopE2 and SopB cooperatively activate Cdc42 and Rac-1, two members of the Rho family of GTP binding proteins (Bakshi *et al.*, 2000; Hardt *et al.*, 1998a; Stender *et al.*, 2000). Activation of Cdc42 and Rac triggers actin cytoskeleton rearrangements, resulting in massive ruffling and extrusion of the plasma membrane to engulf *Salmonella*. SipA and SipC then further modulate actin activity by binding and stabilizing actin during entry (Hayward and Koronakis, 1999; Zhou *et al.*, 1999). Remarkably another secreted effector protein, SptP, functions as a GTPase-activating protein to antagonize Cdc42 and Rac activation to help stabilize the eukaryotic cell membrane after bacterial endocytosis (Fu and Galan, 1999). In addition, SopB also promotes intestinal inflammation and fluid secretion by subverting inositol phosphate signaling pathways (Norris *et al.*, 1998).

The regulation of SPI-1 gene expression is complex and involves many factors (Eichelberg and Galan, 1999). Multiple environmental and physiological conditions are known to influence expression of SPI-1 genes including oxygen tension, osmolarity, growth phase of bacteria and pH (Bajaj *et al.*, 1996; Lucas and Lee, 2000). The experimental environmental cues that induce SPI-1 gene expression approximate to those found in the lumen of the small intestine, the location where SPI-1 activity is required (Eichelberg and Galan, 1999). On a molecular level several SPI-1-encoded transcriptional activators are essential for SPI-1 induction. Expression of these activators is regulated by a number of global regulatory proteins including the nucleoid-associated proteins FIS, H-NS, IHF, Hha, and HU (Fahlen *et*

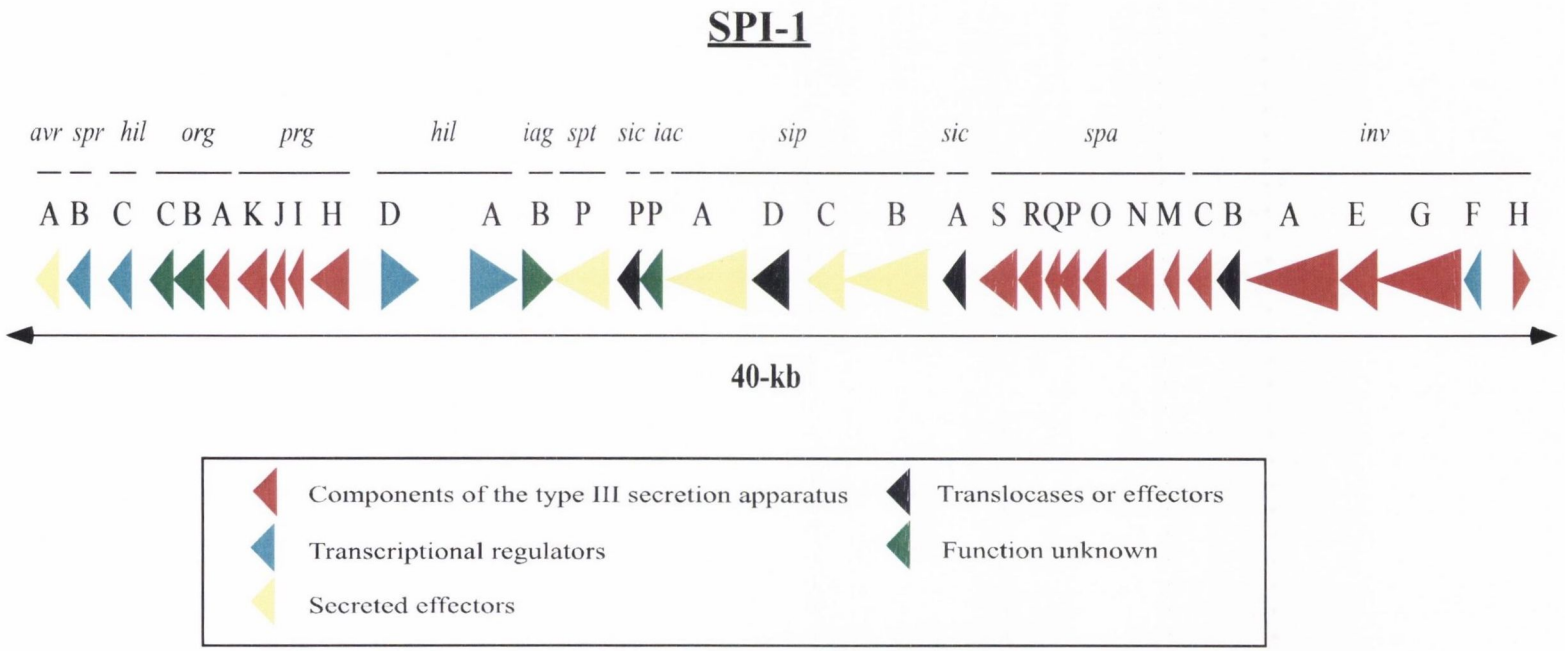

Fig. 1.5. Genetic organisation of *Salmonella* pathogenicity island-1 (SPI-1). SPI-1 genes encoding the Inv/Spa type III secretion structural components, transcriptional regulators, secreted effectors, and translocase/effectors are indicated. The length of each gene is approximately to scale. Figure adapted from Carroll (2003).

al., 2001; Kelly *et al.*, 2004; Lucas and Lee, 2000; Mangan *et al.*, 2006; Schechter *et al.*, 2003; Wilson *et al.*, 2001).

1.3.3 *Salmonella* pathogenicity island-2 (SPI-2)

Salmonella pathogenicity island-2 (SPI-2) is required by *S.* Typhimurium for intracellular survival and replication in host cells such as the macrophage (Cirillo *et al.*, 1998; Hensel *et al.*, 1998; Hensel, 2000; Ochman *et al.*, 1996) and for systemic infection (Hensel *et al.*, 1995; Shea *et al.*, 1996). Consistent with this, SPI-2 mutants are severely attenuated in virulence in the mouse model of systemic infections (Shea *et al.*, 1996) and fail to proliferate in infected organs like the liver and spleen (Shea *et al.*, 1999). SPI-2 is located at 31 centisomes on the *S.* Typhimurium chromosome, is approximately 40-kb in size, and encodes 42 open reading frames (Fig. 1.6). SPI-2 is inserted adjacent to the $tRNA^{ValV}$ gene and is only present in *S. enterica* and not the phylogenetically older species *S. bongori* (Beuzon *et al.*, 1999). Therefore, it is postulated that SPI-2 has been acquired more recently than SPI-1, since the latter is found in both *S. enterica* and *S. bongori.* Further molecular analyses of SPI-2 revealed that this locus is not the result of a single horizontal acquisition event (Deiwick *et al.*, 1999). A portion of about 15-kb appears to be phylogenetically older, and has no function in the systemic pathogenesis of *Salmonella* infections. The second portion of SPI-2 of about 25-kb is required for systemic infection and harbours the genes coding for the structural components of the TTSS (*ssa* genes), and putative secreted effectors (*sse*) as well as their specific chaperones (*ssc*) (Fig. 1.6; Freeman *et al.*, 2002). In total there are 31 genes in the 25-kb section of SPI-2, which are organized into four operons termed regulatory, structural I, structural II, and effector/chaperone (Fig. 1.6; Cirillo *et al.*, 1998; Hensel *et al.*, 1998; Shea *et al.*, 1996).

The SPI-2 TTSS mediates replication of intracellular bacteria within membrane-bound *Salmonella*-containing vacuoles (SCVs) (Cirillo *et al.*, 1998; Hensel *et al.*, 1998) and is essential for systemic infection (Hensel *et al.*, 1995; Shea *et al.*, 1996). Molecular analyses of

the SPI-2 TTSS *in vitro* and *in vivo* revealed that its structure is unique compared to other TTSS structures (Chakravortty *et al.*, 2005). The SPI-2-dependent secretory apparatus is composed of a filamentous needle-like structure that is *in vitro,* sheathed with secreted protein. In contrast to other TTSS, the secretory apparatus encoded by SPI-2 is only present singly or in few copies at one pole of the bacterial cell. Acidic pH is essential to trigger the formation of the SPI-2 TTSS surface structure and for its translocation function for the delivery of effector proteins (Chakravortty *et al.*, 2005). In addition, the translocation of SP1-2 effectors into the host cell requires the three SPI-2 secreted proteins SseB, SseC, and SseD, which are thought to form the SPI-2 translocon pore in the host cell membrane (Klein and Jones, 2001; Nikolaus *et al.*, 2001). Furthermore it was revealed that SseA (initially described as a putative effector protein) is a chaperone for SseB and SseD (Ruiz-Albert *et al.*, 2003).

The SPI-2 TTSS secretes a diverse set of effectors encoded both within and outside of SPI-2 (Beuzon *et al.*, 2000; Miao and Miller, 2000; Worley *et al.*, 2000) that have a variety of functions including inhibition of fusion between lysosomes and SCVs (Uchiya *et al.*, 1999), avoidiance of NADPH oxidase-dependent killing (Vazquez-Torres and Fang, 2001), delay of apoptosis-like host-cell death (van der Velden *et al.*, 2000), control of SCV membrane dynamics (Beuzon *et al.*, 2000; Ruiz-Albert *et al.*, 2002), assembly of a meshwork of F-actin around the SCV (Meresse *et al.*, 2001), accumulation of cholesterol around the SCV (Catron *et al.*, 2002) and interference with the localization of inducible nitric oxide synthase to the SCV (Chakravortty *et al.*, 2002).

Through mutational studies, the specific functions of a few SPI-2 effectors have been elucidated. The SPI-2-encoded effectors SseF and SseG [which are translocated to the SCV membrane *Salmonella*-induced filaments (Sifs) and other endosomal compartments] are involved in Sif production (Guy *et al.*, 2000; Kuhle and Hensel, 2002). Another effector protein encoded within SPI-2 is SsaB (also called SpiC). This prevents fusion of the SCV with endosomes and lysosomes (Uchiya *et al.*, 1999). However, additional studies revealed

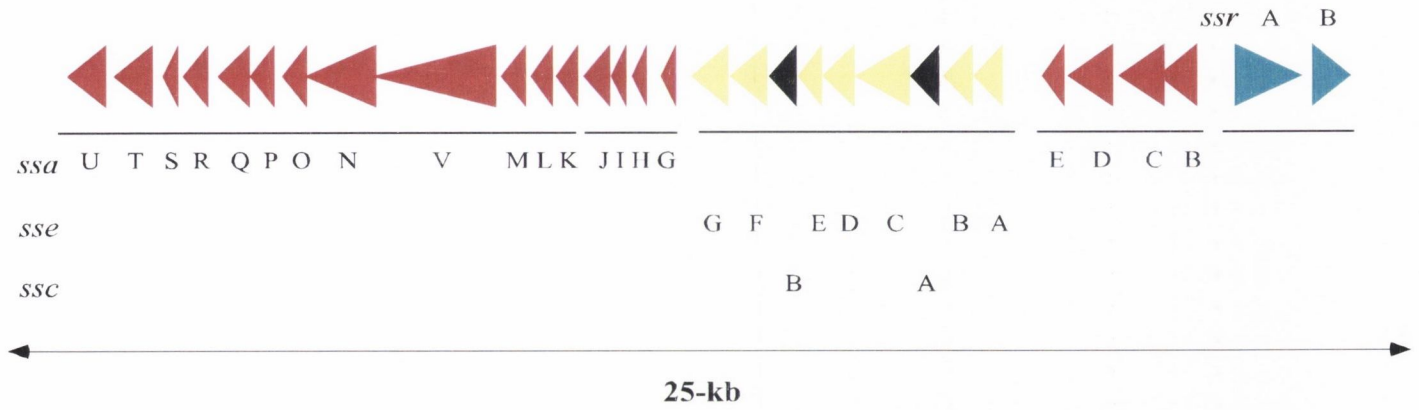

Fig. 1.6. Genetic structure and organisation of *Salmonella* pathogenicity island-2 (SPI-2). The 25-kb virulence region of SPI-2 includes genes encoding the type III secretion apparatus (*ssa*, red boxes), regulatory proteins (*ssr*, blue boxes), effector proteins (*sse*, yellow boxes), and chaperones (*ssc*, black boxes). Figure adapted from Carroll (2003).

that SsaB is necessary for the translocation of SPI-2 effectors into macrophages and is necessary for the *in vitro* secretion of the SPI-2 translocon proteins SseB, SseC and SseD (Freeman *et al.*, 2002; Yu *et al.*, 2002). These data imply that the SsaB phenotype observed by Uchiya *et al.* (1999) might be a consequence of the lack of effector translocation in the mutant, and that the SsaB protein *per se* does not prevent fusion of lysosomes with the SCV. Several non-SPI-2 encoded effectors are also translocated to the host-cell cytosol via the SPI-2 TTSS (Waterman and Holden, 2003). These include SifA, SifB, SspH1, SspH2, SlrP, SseI, and SseJ (Miao *et al.*, 1999; Miao and Miller, 2000), all of which contain a conserved amino terminal motif that targets them for translocation across the phagosome membrane by the SPI-2 TTSS (Miao and Miller, 2000). SspH1 and SlrP are also translocated by the SPI-1 TTSS during *S.* Typhimurium invasion (Miao and Miller, 2000).

Unlike SPI-1, very little is known about the environmental conditions that influence SPI-2 gene expression. Some studies report that low pH, Mg^{2+} deprivation and phosphate starvation activate SPI-2, while other studies refute this (Beuzon *et al.*, 1999; Cirillo *et al.*, 1998; Deiwick *et al.*, 1999; Lee *et al.*, 2000; Miao *et al.*, 2002; Rathman *et al.*, 1996). In the case of pH, it now appears that low pH is required for the assembly and function of the SPI-2 TTSS, but does not trigger SPI-2 gene expression (Chakravortty *et al.*, 2005). Thus, the environmental conditions that induce SPI-2 is a contentious topic of investigation, but it is known that SPI-2 genes are preferentially expressed in the intracellular environment of the macrophage (Cirillo *et al.*, 1998; Valdivia and Falkow, 1997). The regulation of SPI-2 has not been characterized in detail but is known to involve both SPI-2- and chromosome-encoded regulators. The SPI-2-encoded two-component regulatory system SsrA/SsrB is pivotal for activation of SPI-2 gene expression (Ochman *et al.*, 1996; Worley *et al.*, 2000) and is itself under the positive control of two other sensor-regulator systems, namely, EnvZ/OmpR and PhoP/PhoQ (Bijlsma and Groisman, 2005; Lee *et al.*, 2000). Other positive regulators of SPI-2 include SlyA, and the nucleoid-associated proteins FIS (Kelly *et al.*, 2004; Linehan *et al.*, 2005) and IHF (Mangan *et al.*, 2006).

1.3.4 *Salmonella* plasmid virulence genes

All pathogenic non-typhoidal *Salmonella* serovars that cause systemic infection (including *S.* Typhimurium) possess high molecular weight virulence plasmids (Gulig, 1990). These virulence plasmids are essential for the bacteria to cause an efficient systemic infection (Gulig *et al.*, 1992; Gulig *et al.*, 1993) and can vary in size from 50 to 100-kb depending on the serovar (Chu *et al.*, 1999; McClelland *et al.*, 2001). The *S.* Typhimurium virulence plasmid is approximately 90-kb in size and contributes to systemic infection in the mouse by increasing the replication rate of the bacteria inside host cells (Gulig *et al.*, 1993). It has been shown that an 8-kb region of this virulence plasmid, which is highly conserved among pathogenic *Salmonella* serovars, is sufficient to replace the entire plasmid for mediating systemic infection and increased growth rate in mice (Gulig *et al.*, 1992). Encoded on this 8-kb region is a cluster of genes termed the *Salmonella* plasmid virulence (*spv)* genes. The *spv* system consists of five genes designated *spvRABCD* (Fig. 1.7).

The *spv* system is expressed from two main promoters, one situated in front of the *spvR* gene (P_{spvR}) and the other upstream of the structural genes *spvABCD* (P_{spvA}) (Grob and Guiney, 1996; Marshall *et al.*, 1999; Rhen *et al.*, 1993). The four structural genes form an operon and are all transcribed from the *spvA* promoter (Fig. 1.7), although some post-transcriptional modifications do occur (El-Gedaily *et al.*, 1997). The *spvR* gene is located immediately upstream of *spvABCD* and encodes a LysR-like positive regulator (Fig. 1.7), which activates both its own expression and that of the structural genes by binding to the two promoters, P_{spvA} and P_{spvR}. SpvR has been shown to bind to the *spvA* promoter in a hierarchical fashion at two sites, with binding to a proximal site being dependent on binding to a more distal site (Sheehan and Dorman, 1998). SpvB is an ADP-ribosyltransferase that specifically ADP-ribosylates actin and depolymerizes actin filaments in infected host cells, leading to cytotoxic effects such as rounding (Lesnick *et al.*, 2001; Otto *et al.*, 2000; Tezcan-Merdol *et al.*, 2001). Recently, it was shown that SpvB ADP-ribosylates actin G molecules at arginine-177, which is the same target residue used by binary clostridial ADP-ribosylating toxins such as the C2 toxin of *Clostridium botulinum*, and the iota toxin of *Clostridium perfringens* (Hochmann *et*

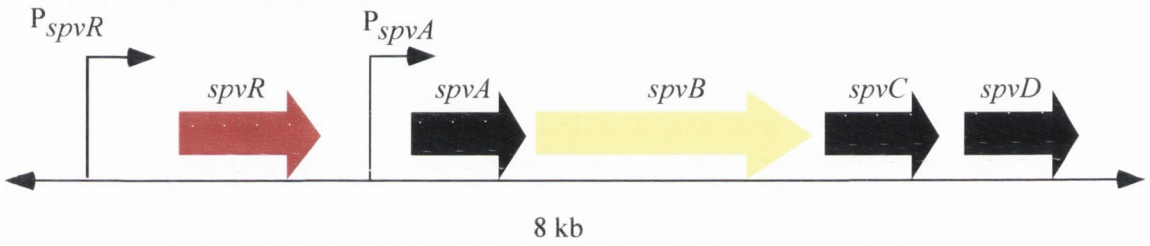

Fig. 1.7. Genetic organisation of the *Salmonella* plasmid virulence (*spv*) genes. The *spv* system consists of five genes designated *spvRABCD,* which are encoded within a highly conserved 8-kb region of *Salmonella* virulence plasmids. The *spvR* gene encodes a member of the LysR family of transcriptional regulators and is transcribed from the P_{spvR} promoter. The *spvA*, *spvB*, *spvC* and *spvD* genes are transcribed as an operon from the P_{spvA} promoter. The SpvB protein is a ADP-ribosyltransferase. Figure adapted from Carroll (2003).

al., 2006). Unlike binary ADP-ribosylating toxins that have a separate binding/translocation component to deliver the enzyme component into the cytosoplasm of cells (Hochmann *et al.*, 2006), it is not clear how SpvB is translocated to the host-cell cytosol. However, it is known that secretion of SpvB is independent of the *Salmonella* TTSS *in vitro* and *in vivo* under conditions that approximate intracellular ion concentrations (Gotoh *et al.*, 2003). The functions of the other structural proteins SpvA, SpvC and SpvD have yet to be elucidated, but it was shown that the *spvC* gene along with the *spvB* gene were sufficient to restore partial virulence to plasmid-cured strains of *S.* Typhimurium (Matsui *et al.*, 2001). In addition, signature tagged mutagenesis (STM) has shown them to be required for virulence (Hensel *et al.*, 1995).

1.3.5 *Salmonella* flagellar gene expression and assembly

Bacterial flagella facilitate the motility of an organism towards favourable conditions or away from detrimental environments. In addition, bacterial flagella play a crucial role in bacterial adhesion, biofilm formation and colonization (Soutourina and Bertin, 2003). Indeed, motility in pathogenic bacteria such as *S.* Typhimurium is usually considered a virulence factor essential for colonization of a host organism or target organ (Soutourina and Bertin, 2003). *S.* Typhimurium possesses ~6–10 flagella that are peritrichiously arranged around the cell (Bonifield and Hughes, 2003). The individual flagella are composed of three distinct substructures – the basal body consisting of a central rod and several rings, the short curved structure called the hook, and the long helical filament that acts as a propeller (Aldridge and Hughes, 2002; Macnab, 1996). The filament is ~10 μm in length and is composed of ~20, 000 subunits of flagellin protein, FliC or FljB (Bonifield and Hughes, 2003).

Assembly and function of the *S.* Typhimurium flagellar system requires the expression of more than 50 genes, which are divided among at least 17 operons scattered around the *Salmonella* chromosome (Fig. 1.8; Aldridge and Hughes, 2002; Chilcott and Hughes, 2000; Soutourina and Bertin, 2003). Flagellar gene expression is strictly controlled by an elaborate

regulatory cascade, which couples flagellar gene transcription to flagellar assembly. The various operons of the flagellar regulon are divided into three temporally regulated, hierarchical transcriptional classes designated early, middle and late, and their respective promoters are referred to as class 1, class 2, and class 3 (Fig. 1.8; Aldridge and Hughes, 2002; Chilcott and Hughes, 2000; Soutourina and Bertin, 2003).

Flagellar biosynthesis is initiated by activation of the single class 1 promoter that transcribes the *flhDC* operon. FlhD and FlhC are the master regulators of the flagellar regulon, and their expression is required for activation of the class 2 promoters, which transcribe the middle gene operons (Fig.1.8; Aldridge and Hughes, 2002; Chilcott and Hughes, 2000; Soutourina and Bertin, 2003). Middle genes encode proteins required for the structure and assembly of the hook–basal body complex, in addition to the flagellum-specific sigma factor σ^{28}, FliA, and its cognate anti-sigma factor, FlgM (Fig. 1.8; Aldridge and Hughes, 2002; Chilcott and Hughes, 2000; Soutourina and Bertin, 2003). FlgM binds to σ^{28} and prevents transcription of the class 3 σ^{28}-dependent promoters until completion of the flagellum basal body and hook. At that time, FlgM is secreted from the cell leading to σ^{28}-dependent transcription of the class 3 promoters. The late genes encode proteins that are required for maturation of the flagellum and chemosensory system (Aldridge and Hughes, 2002; Chilcott and Hughes, 2000; Soutourina and Bertin, 2003).

The crucial regulatory point of the flagellar regulon is the *flhDC* class 1 promoter and therefore, unsurprisingly its expression is regulated by a number of global regulatory signals. These include cAMP-CRP, temperature, several heat shock proteins (DnaK, DnaJ, and GrpE), high concentrations of either organic salts, carbohydrates, or alcohols, growth phase, phosphatidylethanolamine and phosphatidylglycerol synthesis, and surface-liquid transition (Adler and Templeton, 1967; Chilcott and Hughes, 2000; Li *et al.*, 1993; Shi *et al.*, 1992). The *flhDC* promoter is also sensitive to DNA supercoiling, and several nucleoid-associated proteins regulate flagellar gene expression, including FIS, IHF and H-NS (Kelly *et al.*, 2004; Ko and Park, 2000; Mangan *et al.*, 2006; Yona-Nadler *et al.*, 2003). Interestingly, H-NS

Fig. 1.8. The flagellar regulatory network. (A) Chromosomal locations of the various operons that constitute the flagellar regulon of *S.* Typhimurium. (B) The flagellar operons are divided into three temporally regulated, hierarchical transcriptional classes designated early, middle and late, and their respective promoters are referred to as class 1 (red arrow), class 2 (green arrow), and class 3 (blue arrow). Flagellar biosynthesis is initiated by activation of the single class 1 promoter that transcribes the *flhDC* operon. FlhD and FlhC are the master regulators of the flagellar regulon, and their expression is required for activation of the class 2 promoters, which transcribe the middle genes. Middle gene operons encode proteins required for the structure and assembly of the hook–basal body complex. Middle genes also encode the sigma factor σ^{28}, FliA, and its cognate anti-sigma factor, FlgM. FlgM binds to σ^{28} and prevents transcription of the class 3 σ^{28}-dependent promoters until completion of the flagellum basal body and hook. At that time, FlgM is secreted out of the cell, which subsequently leads to σ^{28}-dependent transcription of the class 3 promoters. The late genes encode proteins required for maturation of the flagellum and chemosensory system. Figure adapted from Chilcott and Hughes (2000).

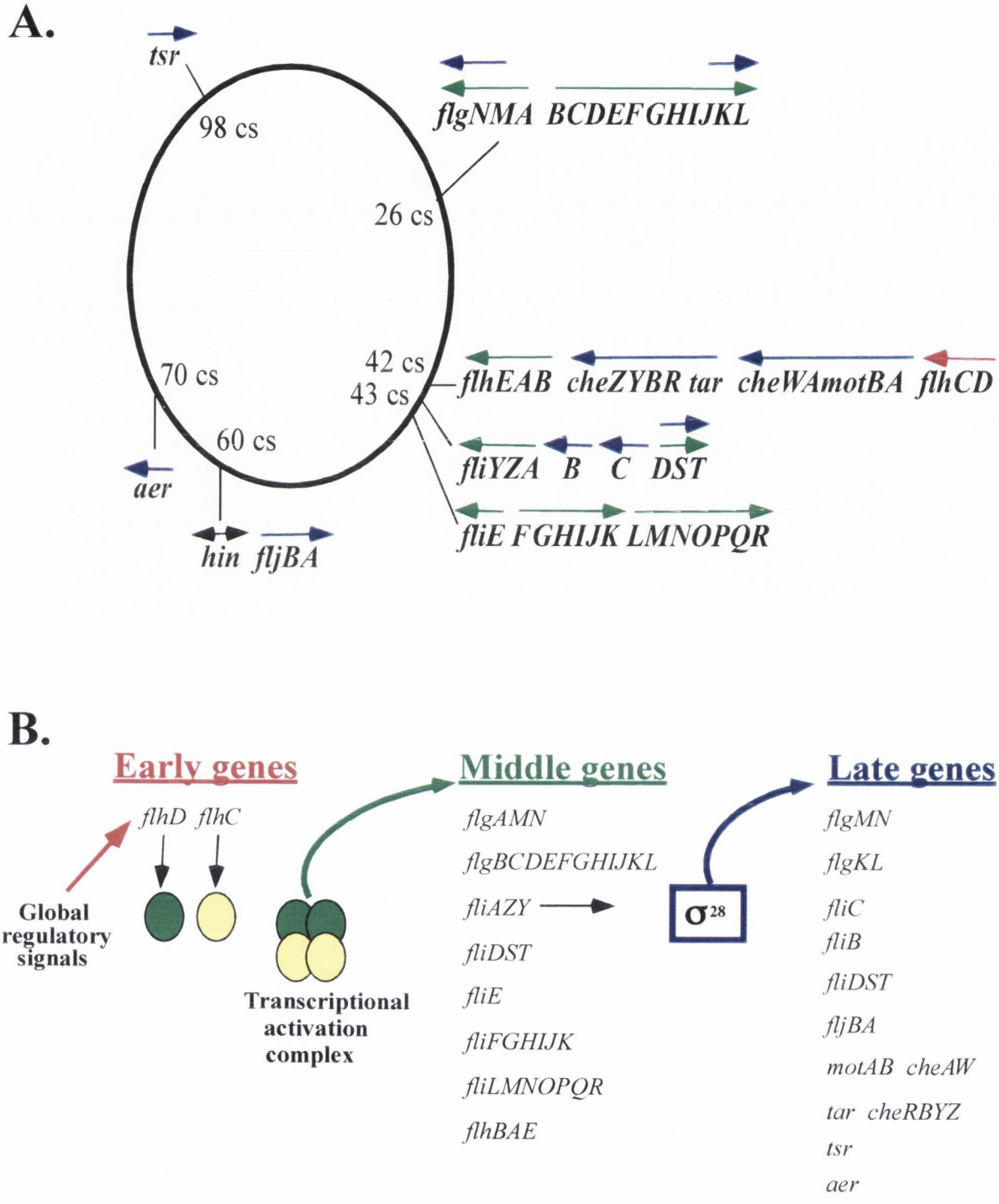
A.
tsr
98 cs
flgNMA BCDEFGHIJKL
26 cs
42 cs
43 cs
flhEAB cheZYBR tar cheWAmotBA flhCD
70 cs
60 cs
aer
fliYZA B C DST
fliE FGHIJK LMNOPQR
hin fljBA
B.
Early genes
flhD flhC
Global regulatory signals
Transcriptional activation complex
Middle genes
flgAMN
flgBCDEFGHIJKL
fliAZY
σ28
fliDST
fliE
fliFGHIJK
fliLMNOPQR
flhBAE
Late genes
flgMN
flgKL
fliC
fliB
fliDST
fljBA
motAB cheAW
tar cheRBYZ
tsr
aer

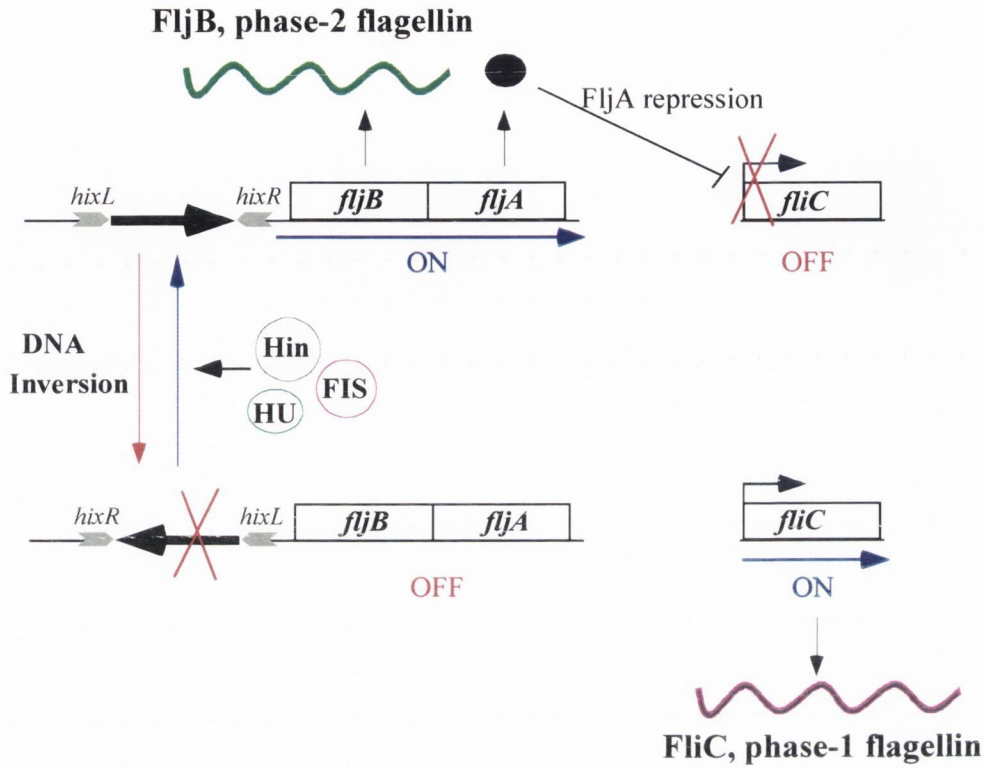

Fig. 1.9. Mechanism for flagellar phase variation in *S.* Typhimurium. The two genes *fliC* and *fljB* are located at distinct regions of the chromosome and encode the flagellins, FliC and FljB, respectively. The promoter for the *fljBA* operon is flanked by an inverted repeat, which can be inverted by site-specific recombination mediated by the Hin recombinase, in conjunction with the nucleoid-associated proteins, FIS and HU. In one direction the promoter drives *fljBA* operon expression, which results in the production of FljB or phase-2 flagellin, and also FljA, which represses the unlinked *fliC* gene. In the opposite orientation, the promoter is unable to transcribe the *fljBA* operon. Therefore, no FljB flagellin is produced and *fliC* repression is alleviated, which results in the production of FliC or phase-1 flagellin. Figure adapted from Macnab (1996).

positively influences flagellar gene expression in *S.* Typhimurium and *E. coli* (Bertin *et al.*, 1994; Hinton *et al.*, 1992; Ko and Park, 2000). In addition, expression of the *flhDC* operon is also controlled at the post-transcriptional level by several factors including CsrA (Lawhon *et al.*, 2003; Wei *et al.*, 2001) and the ClpXP protease (Tomoyasu *et al.*, 2002; Tomoyasu *et al.*, 2003).

Recently, flagellin was determined as the major molecular trigger by which *S.* Typhimurium activates gut epithelial proinflammatory gene expression (Zeng *et al.*, 2003). In fact, *Salmonella* flagellin is a target of both the innate and adaptive immune responses of the host during infection (Salazar-Gonzalez and McSorley, 2005). Therefore, it seems likely that *S.* Typhimurium alternately expresses two different flagellins, FljB and FliC, as a strategy to evade immune detection. The two flagellin proteins are highly similar, but the surface-exposed amino acids in the central part of the proteins are divergent, resulting in distinct antigenicities (Bonifield and Hughes, 2003). *Salmonella* alternates expression of FljB and FliC at a rate of 10^{-3} to 10^{-5} switches per cell generation. The molecular mechanism mediating this flagellar phase variation involves a site-specific DNA inversion event in the chromosome encompassing the *fljBA* operon (Fig. 1.9; Bonifield and Hughes, 2003; Macnab, 1996). The promoter of the *fljBA* operon is flanked by two *hix* sites (*hixL* and *hixR*) and also located between these two inverted repeats is the *hin* gene, which codes for the Hin recombinase (Fig. 1.9). Thus, Hin is expressed in either orientation of the switch (Bonifield and Hughes, 2003; Haykinson *et al.*, 1996; Macnab, 1996). The Hin recombinase, in conjunction with the nucleoid-associated proteins, FIS and HU, mediates a reversible recombination reaction between the *hix* sites (Bonifield and Hughes, 2003; Haykinson *et al.*, 1996; Macnab, 1996). In one orientation, the *fljBA* promoter is in the correct position for transcription of the *fljBA* operon (Fig. 1.9; Bonifield and Hughes, 2003; Macnab, 1996). This results in the production of FljB flagellin and also FljA, which represses the unlinked *fliC* gene at both the transcriptional and translational levels. In the alternative orientation, the *fljBA* operon cannot be transcribed and hence, *fliC* repression is alleviated, which results in the production of FliC flagellin (Fig. 1.9; Bonifield and Hughes, 2003; Macnab, 1996).

1.4 The bacterial nucleoid and nucleoid-associated proteins

Bacterial chromosomal DNA and its associated proteins form a highly organized compact structure called the bacterial nucleoid. Formation of the nucleoid allows bacteria to fit their large genomes into the small volume of a bacterial cell. For example, the *E. coli* 4.6-Mb chromosome, which has a contour length of 1.6 mm, is condensed to fit into a cell that measures only 2 μm by 1 μm (Dame, 2005; Taludker *et al.*, 1999; Travers and Muskhelishvili, 2005). The shape and size of the bacterial nucleoid is determined by a number of factors, including DNA supercoiling, macromolecular crowding and nucleoid-associated proteins (Dame, 2005). Within the nucleoid, the bacterial chromosomal DNA is organized into large supercoiled loops that emanate from a central core. These superhelical domains are about 10-kb in size (Cunha *et al.*, 2001; Postow *et al.*, 2004; Travers and Muskhelishvili, 2005) and are topologically closed, due to the binding of proteins that create cross-links between DNA tracts (Case *et al.*, 2004; Dame, 2005). The overall superhelicity of the different domains is determined primarily by the antagonistic effects of DNA gyrase, which introduces negative supercoils and removes positive supercoils, and DNA topoisomerase I, which relaxes supercoiled DNA (Dorman, 1995).

The bacterial proteins that associate with the nucleoid and help organize and compact it, are known as histone-like nucleoid-associated proteins, due to their functional similarity to eukaryotic histone proteins (Azam and Ishihama, 1999; Travers and Muskhelishvili, 2005). Gram-negative bacteria, such as *E. coli*, have at least 12 distinct types of nucleoid-associated proteins. The four most abundant and best characterized are H-NS (histone-like nucleoid structuring), HU (heat unstable), FIS (factor for inversion and stimulation) and IHF (integration host factor) (Azam and Ishihama, 1999; Dorman and Deighan, 2003; Dorman, 2004). Nucleoid-associated proteins are known to act antagonistically or in concert, and the ratio between them is dynamically linked to the growth phase of the bacterium (Azam *et al.*, 1999; Taludker *et al.*, 1999). In exponential phase the most abundant nucleoid-associated proteins are FIS, HU, IHF, StpA (suppressor of *td* mutant phenotype A) and H-NS, whereas in stationary phase, the protein composition of the nucleoid changes primarily to Dps (DNA-

binding protein from starved cells), IHF and HU (Azam *et al.*, 1999; Taludker *et al.*, 1999). This fluctuation in the intracellular levels of the nucleoid-associated proteins not only influences the conformation of the nucleoid, but also DNA functions such as replication, recombination, repair and transcription (Atlung and Ingmer, 1997; Finkel and Johnson, 1992; Ishihama, 1997; Travers and Muskhelishvili, 2005; Williams and Rimsky, 1997).

1.4.1 HU

HU is a major protein component of the bacterial nucleoid and is well conserved among bacterial species (Azam *et al.*, 1999; Oberto and Rouviere-Yaniv, 1996; Taludker *et al.*, 1999). In most bacteria HU exists as a 18-kDa homodimer, but in *E. coli, S.* Typhimurium and *Serratia marcescens* HU is predominantly found as a heterodimer composed of two subunits, HUα and HUβ, encoded by the *hupA* and *hupB* genes, respectively. The *hupA* and *hupB* genes are unlinked on the chromosome, and their expression in *E. coli* is regulated at the transcriptional level by the proteins CRP and FIS (Claret and Rouviere-Yaniv, 1996). CRP activates expression of both genes, whereas FIS positively regulates the *hupA* gene but negatively regulates the *hupB* gene (Claret and Rouviere-Yaniv, 1996). Consequently, the two HU subunits have distinct growth phase-dependent expression profiles, which results in the formation of three different HU protein complexes *in vivo* (Claret and Rouviere-Yaniv, 1996, 1997). Throughout the growth curve, the composition of HU varies from homomeric $HU\alpha_2$ complexes (early exponential phase), to heteromeric HUαHUβ complexes (mid to late exponential phase), to homomeric $HU\beta_2$ complexes (stationary phase) (Claret and Rouviere-Yaniv, 1997). The different HU complexes have distinct effects on cellular physiology (Claret and Rouviere-Yaniv, 1997). For example, $HU\beta_2$ does not induce negative supercoiling like HUαHUβ and $HU\alpha_2$ (Boubrik and Rouviere-Yaniv, 1995). HU binds DNA with low affinity in a sequence independent manner, but displays a high affinity for DNA recombination and repair intermediates such as gapped, nicked or kinked DNA. HU can also bind RNA (Balandina *et al.*, 2001; Taludker *et al.*, 1999; Talukder and Ishihama, 1999). HU is known to restrain negative supercoils (Broyles and Pettijohn, 1986; Rouviere-Yaniv *et al.*,

1979), but overexpression of the HU protein does not lead to increased compaction of the bacterial nucleoid (McGovern *et al.*, 1994). Recently, it was shown that HU at low concentrations can compact DNA, but at high HU concentrations DNA becomes extended (Skoko *et al.*, 2004; van Noort *et al.*, 2004).

1.4.2 IHF

The IHF protein was first identified in *E. coli* by its role in the integration and excision of the phage λ (Miller and Friedman, 1980). In *S. enterica* and *E. coli,* the IHF protein is a heterodimer, whose subunits (IHFα and IHFβ) are encoded by the *ihfA* and *ihfB* genes. The *ihfA* and *ihfB* genes are found at distinct locations on the chromosome, and are subject to independent regulatory influences (Aviv *et al.*, 1994). Although IHF is predominantly a heterodimer, its subunits are capable of forming homodimers, and these have DNA-binding activity (Werner *et al.*, 1994; Zablewska and Kur, 1995; Zulianello *et al.*, 1994). Recently, the three IHF complexes ($IHF\alpha_2$, $IHF\beta_2$, IHFαIHFβ) were shown not to be equivalent, as their regulons contain both overlapping and distinct genes (Mangan *et al.*, 2006). IHF is closely related to HU and shares approximately 30% amino acid identity with the HU protein (Drlica and Rouviere-Yaniv, 1987). The intracellular concentration of IHF is growth phase-dependent, and increases at the onset of stationary phase (Azam *et al.*, 1999; Talukder and Ishihama, 1999). This suggests that IHF could have a potential role in the structural and functional conversion of the nucleoid during the phase transition of growth. Unlike HU, IHF binds to a conserved DNA sequence, 5′-WATCAANNNNTTR-3′ (where W=A/T, R=purine and N=any base) (Craig and Nash, 1984). When bound to DNA, IHF is able to bend the DNA by angles of up to 180°. Consequently, IHF can bring distant sites on the genome together. This DNA-bending activity is critical to its transcriptional role in several systems (Rice *et al.*, 1996; Rice, 1997). In addition, IHF is known be involved in other DNA transactions such as transposition, site-specific recombination and replication initiation (Bushman *et al.*, 1985; Crellin *et al.*, 2004; Dorman and Higgins, 1987; Esposito *et al.*, 2001; Makris *et al.*, 1990; Ryan *et al.*, 2002).

1.4.3 FIS

The FIS protein was originally identified by its ability to stimulate Hin-, Gin-, and Cin-mediated DNA inversion (Haffter and Bickle, 1987; Johnson and Simon, 1985; Kahmann *et al.*, 1985). Subsequently, FIS was shown to stimulate both excisive and integrative recombination of bacteriophage λ DNA (Ball and Johnson, 1991a, b; Thompson *et al.*, 1987), and to regulate transcription of a wide variety of genes, including those encoding stable RNA (Auner *et al.*, 2003; Gonzalez-Gil *et al.*, 1996; Ross *et al.*, 1990). FIS is also known to influence the topological state of DNA in the cell by repressing DNA gyrase and activating topoisomerase I gene expression (Keane and Dorman, 2003; Schneider *et al.*, 1999; Weinstein-Fischer *et al.*, 2000) and is required for *oriC*-directed DNA replication (Filutowicz *et al.*, 1992; Gille *et al.*, 1991). Expression of the 11.2-kDa FIS protein is rapidly and transiently induced when stationary phase cells are subcultured into a rich medium (Ball *et al.*, 1992). Consequently, FIS is very abundant in early exponential phase but virtually undetectable in the late exponential and stationary phases of growth (Ball *et al.*, 1992). Although FIS binds DNA in a sequence-specific manner, the proposed consensus sequence for FIS-binding sites, 5′-GNNYRNNTNNYRNNC-3′ (Y=pyrimidine R=purine), is highly degenerate (Finkel and Johnson, 1992; Hubner and Arber, 1989). The *E. coli* FIS protein has been shown to preferentially bind to intrinsically curved DNA, and is known to bind DNA as a dimer (Wagner, 2000). Upon binding DNA, FIS introduces a bend of between 40° and 90° (Hengen *et al.*, 1997). Crystal structural studies revealed that the FIS protein consists of four α-helices (A-D) and two N-terminal β-sheets (Kostrewa *et al.*, 1991; Safo *et al.*, 1997; Yuan *et al.*, 1991). The two N-terminal β-sheets are involved in activation of DNA inversion reactions catalyzed by the Hin and Gin recombinases, while the C-terminal α-helices C and D form the helix-turn-helix DNA-binding domain of the protein (Koch *et al.*, 1991; Kostrewa *et al.*, 1991; Osuna *et al.*, 1995; Safo *et al.*, 1997).

1.5 H-NS

The H-NS protein was originally identified as a heat-stable transcription factor (Jacquet *et al.*, 1971), and subsequently was shown to play an important role in the structure and functioning of the nucleoid (Varshavsky *et al.*, 1977). Upon further analysis H-NS was shown to condense DNA *in vivo* and *in vitro,* in a similar way to eukaryotic histones (Spassky *et al.*, 1984; Spurio *et al.*, 1992) and hence it was named histone-like nucleoid structuring protein. The *hns* gene is located at 27.8 centisomes on the *E. coli* chromosome and encodes a polypeptide of ~15-kDa (Falconi *et al.*, 1988). H-NS is a very abundant protein in the cell, and it is estimated that there are about 20,000 molecules per genome equivalent (Dorman, 2004; Schroder and Wagner, 2002; Tendeng and Bertin, 2003). Mutations in the *hns* gene are highly pleiotropic, due to the fact that H-NS regulates the expression of many unrelated genes, which are scattered around the genome. Proteomic and transcriptomic studies have demonstrated that ~5% of all the annotated genes in *E. coli* display altered expression in an *hns*$^-$ background (Deighan *et al.*, 2000; Hommais *et al.*, 2001). Many of the genes affected by H-NS are linked to the stress response or to changes in environmental conditions, such as osmolarity, temperature, anaerobosis, pH or growth phase (Atlung and Ingmer, 1997; Hommais *et al.*, 2001; Schroder and Wagner, 2002). The ability of H-NS to exert such widespread effects on gene expression probably reflects the fact that it does not bind DNA in a sequence-specific manner, but instead preferentially binds to intrinsically curved DNA, which is commonly found at promoters (Bracco *et al.*, 1989; Jauregui *et al.*, 2003; Tolstorukov *et al.*, 2005; Yamada *et al.*, 1990; Zuber *et al.*, 1994). H-NS can also bind RNA, albeit with a lower affinity than for DNA (Brescia *et al.*, 2004; Cusick and Belfort, 1998). H-NS acts predominantly as a transcriptional repressor, although some rare exceptions are known where it functions as an activator (Dorman, 2004; Schroder and Wagner, 2002).

1.5.1 Structure of H-NS

Genetic and biochemical data have shown that the 137 amino acid-long H-NS protein is composed of two distinct functional domains separated by a flexible linker (Fig. 1.10; Bertin

Fig. 1.10. Structure and dimerization of the H-NS protein. (A) Schematic diagram of the 137 amino acid-long H-NS protein, which is composed of two distinct functional domains separated by a flexible linker. The N-terminal domain (residues 1–65) of H-NS contains the oligomerization activity of the protein and consists of 2 short α-helices followed by a longer α-helix. It is connected to the C-terminal nucleic acid-binding domain of H-NS (residues 90–137) by a protease-sensitive linker. The C-terminal DNA-binding domain has a mixed αβ-structure. (B) 3D structure (Esposito *et al.*, 2002) and schematic diagram of the H-NS dimeric N-domain of *S.* Typhimurium. (C) 3D structure (Bloch *et al.*, 2003) and schematic diagram of the H-NS dimeric N-domain of *E. coli*. (D) Schematic diagram of an alternative dimer structure in which both the linker and the C-terminal domain, in addition to the N-terminal domain, play an important role in dimerization. Figure adapted from Stella *et al.* (2005).

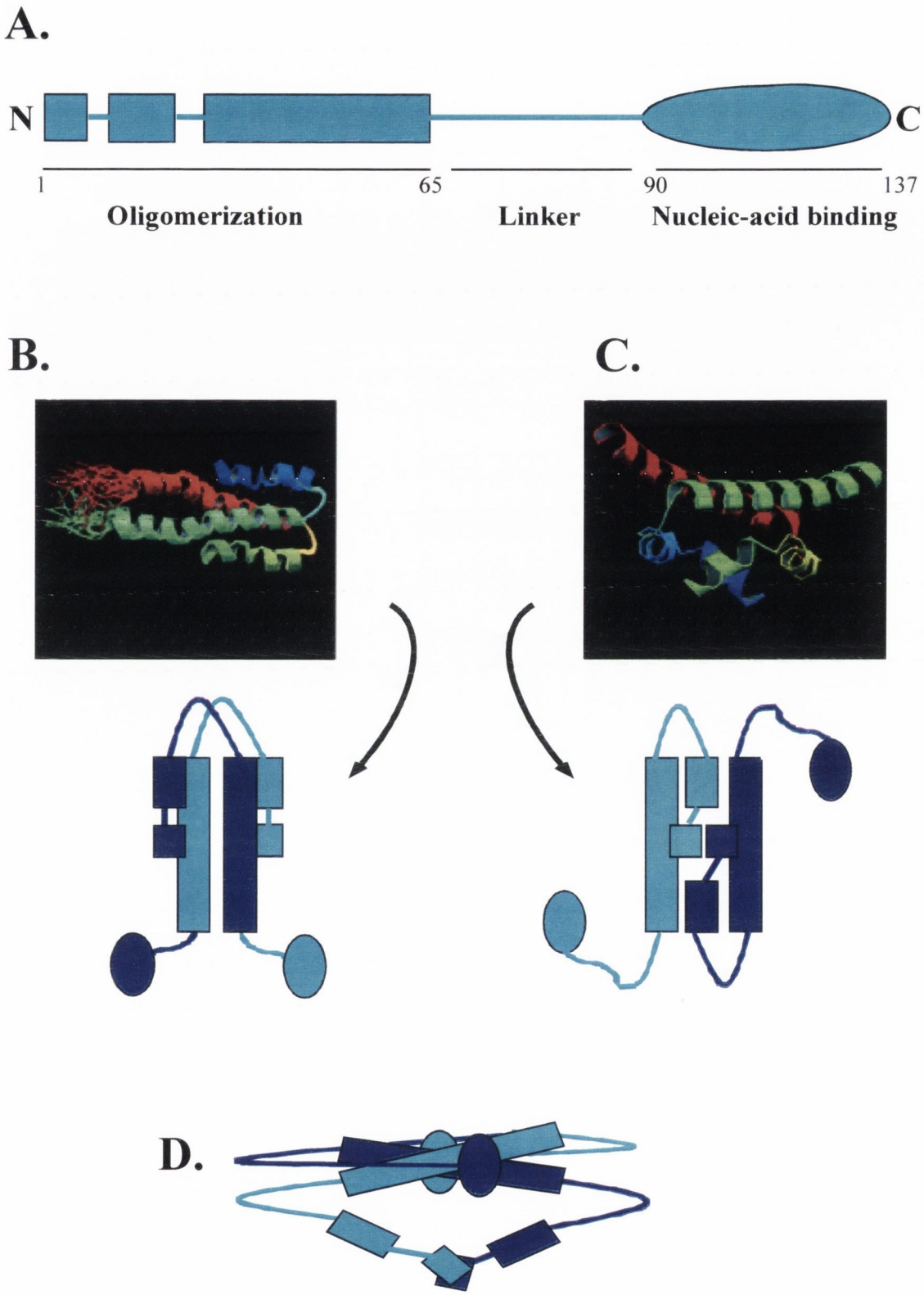
A.
N
C
1
65
90
137
Oligomerization
Linker
Nucleic-acid binding
B.
C.
D.

et al., 1999; Dorman *et al.*, 1999). The N-terminal domain (residues 1–65) of H-NS contains the oligomerization activity of the protein and is connected by a protease-sensitive linker to the C-terminal nucleic acid-binding domain (residues 90–137) (Fig. 1.10; Dorman *et al.*, 1999; Dorman, 2004). Oligomerization and nucleic-acid binding are both crucial to the biological activity of H-NS. The oligomerization domain of H-NS consists mainly of α-helices and is predicted to adopt a coiled-coil formation, which is essential for dimerization of H-NS (Esposito *et al.*, 2002). H-NS dimers are able to self-associate in a concentration-dependent manner to give rise to higher-order oligomers (Ceschini *et al.*, 2000; Smyth *et al.*, 2000; Spurio *et al.*, 1997; Ueguchi *et al.*, 1996). The ability of H-NS to form higher-order oligomers is essential for transcriptional regulation (Nye and Taylor, 2003; Ueguchi *et al.*, 1997), as well as for chromosome condensation (Badaut *et al.*, 2002). Consistent with this, substitution of proline for leucine at position 30 of H-NS produces a protein that has lost the ability to both dimerize and bind DNA (Ueguchi *et al.*, 1997). Furthermore, substituting the arginines at positions 12 and 15 also has a deleterious effect on DNA binding (Bloch *et al.*, 2003).

The C-terminal DNA-binding domain of H-NS has a mixed αβ-structure and contains the core DNA-binding motif, TWTGXGRXP (where X is any amino acid), which lies betweens residues 108 and 116 of the protein (Fig. 1.10; Bertin *et al.*, 1999; Dorman *et al.*, 1999). This motif is highly conserved among H-NS proteins and its importance in DNA-binding has been shown by biochemical and mutational analysis. Fluorescence analysis of the H-NS protein revealed that the fluorescence of the tryptophan at position 109 is enhanced when the protein interacts with curved DNA, but decreases on interaction with non-specific competitor DNA (Tippner and Wagner, 1995). Moreover, substituting the proline at position 116 for alanine or serine abolishes the ability of H-NS to bind preferentially to curved DNA (Badaut *et al.*, 2002; Spurio *et al.*, 1997). In addition, deletion or substitution of the proline at position 116 impairs the ability of H-NS to oligomerize *in vitro* (Spurio *et al.*, 1997).

1.5.2 H-NS oligomerization and activity

Recently, two NMR spectroscopy studies elucidated the secondary structure of the H-NS N-terminal oligomerization domain (Bloch *et al.*, 2003; Esposito *et al.*, 2002). It consists of 2 short α-helices (H1 residues 2–7; H2, residues 10–16 respectively) followed by a longer α-helix (H3, residues 22–49), but the relative orientation of the helices is a contentious topic. The *S.* Typhimurium study determined that H3 forms a parallel coiled-coil, onto which the two shorter α-helices, H1 and H2, fold back (Fig 1.10; Esposito *et al.*, 2002). In contrast, data from the *E. coli* study showed that H3 and H2 form a U-shaped structure, against which H1 lies perpendicularly (Fig. 1.10; Bloch *et al.*, 2003). A similar structure to the *E. coli* one was also obtained from crystals of the H-NS homologue, VicH, from *Vibrio cholerae* (Cerdan *et al.*, 2003). Subsequently, Stella *et al.* (2005) proposed another alternative model, in which both the linker and the C-terminal domain, in addition to the N-terminal domain, play an important role in oligomerization (Fig. 1.10; Stella *et al.*, 2005). This model is consistent with previous data showing that deletion or substitution of the proline at position 116 impairs the ability of H-NS to oligomerize *in vitro* (Spurio *et al.*, 1997).

In addition, Stella *et al.* (2005) demonstrated that *in vivo* H-NS forms both dimers and tetramers, with the latter being the active form (Stella *et al.*, 2005). Furthermore, another study by the same group showed the tetramerization efficiency of H-NS is strongly reduced by an increase in osmolarity and a decrease in temperature (<26°C), but is unaffected by changes in pH or an increase in temperature above 28°C (Stella *et al.*, 2006). These data suggest a mechanism by which osmotic-shock genes, transcriptionally regulated by H-NS, become derepressed in response to an increase in osmolarity. Moreover, these findings indicate that the oligomerization properties of H-NS do not play a role in temperature-dependent control of virulence gene expression and conflict with a previous report on *Salmonella* H-NS (Ono *et al.*, 2005). However, the *Salmonella* study involved *in vitro* experiments with a H-NS fragment lacking the C-terminal domain, which is known to play a fundamental role in H-NS tetramerization and H-NS-DNA interactions (Badaut *et al.*, 2002; Spurio *et al.*, 1997; Stella *et al.*, 2005).

The mechanisms by which H-NS affects transcription remain unclear and several models have been proposed that are not mutually exclusively. Significantly, all the models are dependent on H-NS oligomerization. It is now apparent that H-NS-mediated DNA bridging plays an important role in both compaction of the nucleoid and global gene expression. Scanning force microscopy has shown that H-NS can form bridges between adjacent tracts of double-stranded DNA (Dame *et al.*, 2000), and recent structural data suggests this might be achieved via interactions between the flexible linker regions of H-NS dimers that are bound to the different strands (Bloch *et al.*, 2003; Dorman, 2004). Often H-NS represses gene expression by binding to two distinct regions within a gene's promoter region, e.g., the *virF, hdeAB* and *rrnB* P1 promoters. In the case of the *virF* promoter, the two H-NS binding sites are separated by an intrinsically curved piece of DNA (Prosseda *et al.*, 2004). At temperatures below 32°C, H-NS represses *virF* transcription via DNA bridging of the two H-NS-binding sites, which excludes RNA polymerase from the promoter. With an increase in temperature, the concomitant melting of the intrinsic bend between the two H-NS-binding sites disrupts the H-NS nucleoprotein repression complex, and thus *virF* is expressed (Prosseda *et al.*, 2004). More complex mechanisms have been proposed for repression of the *rrnB* P1 and *hdeAB* promoters. At the *rrnB* P1 promoter RNA polymerase is physically trapped in a competent open complex by the DNA bridging of upstream and downstream regions by H-NS, thus preventing transcript elongation (Dame *et al.*, 2002). A similar mechanism has been proposed for the *hdeAB* promoter, except that formation of the H-NS repressive nucleoprotein complex that traps RNA polymerase is dependent on whether the RNA polymerase holoenzyme contains σ^{38} or σ^{70} (Shin *et al.*, 2005). As mentioned above, changes in the local topology of a promoter can disrupt H-NS repressive nucleoprotein complexes, but often sequence-specific regulatory factors bind to the promoter and antagonize the repressive activity of H-NS, thereby acting as H-NS anti-repressors (Beloin and Dorman, 2003; Haack *et al.*, 2003; Jordi *et al.*, 1992; Prosseda *et al.*, 2004; Yu and DiRita, 2002).

Finally, another model for H-NS repression does not involve DNA bridging but H-NS binding to DNA at a region of curvature (nucleation site) followed by polymerizing along the

DNA (Amit *et al.*, 2003; Rimsky *et al.*, 2001). In this model, H-NS acts as a transcriptional silencer of a specific DNA region that contains a target promoter. It should also be noted that H-NS could indirectly, through its effect on supercoiling, regulate a subset of promoters that are sensitive to changes in supercoiling (Higgins *et al.*, 1988).

1.5.3 Regulation of *hns* gene expression

Expression of the *hns* gene is controlled at both the transcriptional and post-transcriptional levels. H-NS negatively autoregulates its own expression (Atlung and Ingmer, 1997; Free and Dorman, 1995) and is also subject to negative cross-regulation by its paralogues, StpA and Sfh (Deighan *et al.*, 2003). In contrast, the nucleoid-associated protein, FIS, positively influences *hns* gene expression. FIS activates transcription of the *hns* gene by binding directly to its regulatory region, and also indirectly by antagonizing H-NS-mediated repression (Falconi *et al.*, 1996). Furthermore, *hns* gene expression is dynamically linked to the growth cycle through a positive correlation between *hns* transcription and DNA synthesis (Free and Dorman, 1995). Consequently, production of *hns* mRNA is mainly confined to exponential growth and at the onset of stationary phase, when DNA synthesis ceases, the cellular level of *hns* mRNA concomitantly declines (Free and Dorman, 1995). This unique regulatory mechanism seems to ensure that H-NS protein levels remain relatively constant throughout the growth cycle, at least during growth in batch culture in LB medium at 37°C (Deighan *et al.*, 2003; Free and Dorman, 1995).

Although H-NS regulates genes linked to the stress response and to changes in environmental conditions, expression of the *hns* gene itself does not alter significantly in response to heat shock, osmotic shock, carbon starvation, and growth in minimal medium (Dorman *et al.*, 1999; Hinton *et al.*, 1992). However, *hns* mRNA and protein levels are induced ~4-fold during cold shock due to the direct binding of the cold-shock transcriptional enhancer protein, CspA, to the 5′-end of the *hns* gene (Giangrossi *et al.*, 2001; La Teana *et al.*, 1991). H-NS protein levels are also reported to increase ~3-fold upon phosphate deprivation (Van Bogelen

et al., 1996) and during growth at elevated hydrostatic pressure (Welch *et al.*, 1993). At the post-transcriptional level, the small non-coding RNA, DsrA, negatively influences *hns* gene expression. When overexpressed, DsrA enhances the rate of *hns* mRNA turnover by specifically base-pairing to two distinct regions of the *hns* transcript (Lease and Belfort, 2000).

1.6 H-NS-like proteins

H-NS-like proteins constitute a large family of proteins that are widespread in Gram-negative bacteria (Bertin *et al.*, 1999). Originally, H-NS-like proteins were thought to be restricted to members of the *Enterobacteriaceae* and related bacteria (Atlung and Ingmer, 1997), until the subsequent isolation of BpH3, a H-NS-like protein from *Bordetella pertussis,* which is a non-enteric bacterium belonging to the β-proteobacteria (Goyard and Bertin, 1997). More recently, the family of known H-NS-like proteins has expanded rapidly, largely resulting from the pace of complete bacterial genome sequencing (Tendeng and Bertin, 2003). The role of many H-NS-like proteins in bacterial physiology remains to be elucidated, but a few such as BpH3 of *B. pertussis*, HvrA of *Rhodobacter capsulatus,* and MvaT of *Pseudomonas spp.* have been shown to complement several *hns* mutant phenotypes (Bertin *et al.*, 1999; Tendeng *et al.*, 2003). The relationships of 54 proteins belonging to the H-NS family with ≥40% amino acid sequence identity to the H-NS protein of *E. coli* K-12 are summarized in the cladogram in Fig. 1.11. The cladogram shows that members of the H-NS protein family form three distinct groups, which correspond to H-NS proteins, H-NS paralogues (sequences in the same species that share a direct common ancestor with H-NS proteins) and H-NS orthologues (sequences in other species that share a direct common ancestor with H-NS proteins). Furthermore, it highlights that some bacterial species contain multiple *hns*-like genes, as exemplified by *S. flexneri* (Fig. 1.11). It has also become apparent from sequencing studies that the genes coding for these additional copies of H-NS-like proteins are frequently encoded on self-transmissible elements (Tendeng and Bertin, 2003), as is the case for KorB and Sfh, which are encoded on the conjugative plasmids R46 and pSf-R27, respectively. On this basis

it has been proposed that the H-NS protein family has evolved from a global regulatory ancestral protein (H-NS). This family has come to include more specialized proteins either by duplication (paralogues like StpA), divergence (orthologues like VicH), or horizontal transfer (Sfh and KorB) (Tendeng and Bertin, 2003).

Members of the H-NS protein family display an evolutionarily conserved structural and functional organization into two modules, i.e., an N-terminal oligomerization domain and a C-terminal nucleic acid-binding domain, which are separated by a flexible linker (Bertin *et al.*, 1999; Dorman *et al.*, 1999). The N-terminal oligomerization domain displays strong amino acid divergence, but is predicted to adopt an α-helical structure and a coiled-coil conformation in all H-NS-like proteins identified so far (Bertin *et al.*, 2001; Tendeng and Bertin, 2003). In contrast, the C-terminal nucleic acid-binding domain of H-NS-like proteins is a mixed αβ-structure, whose amino acid sequence is largely conserved and contains the consensus motif (TWTG-GR-P), which can be used as a signature to identify the protein (Bertin *et al.*, 2001; Dorman *et al.*, 1999). Since H-NS-like proteins have an overall conserved structure, members of this protein family can potentially form both homomeric and heteromeric protein-protein interactions. This raises the possibility that the various homomeric and heteromeric protein complexes could have different physiological properties depending on their subunit composition (Bertin *et al.*, 1999; Deighan *et al.*, 2003; Dorman *et al.*, 1999).

1.6.1 StpA

The StpA protein was first identified as a multicopy repressor of a splicing defective *td* operon in bacteriophage T4 (Zhang and Belfort, 1992; Zhang *et al.*, 1995). Subsequently, the *stpA* gene was isolated by its ability to restore repression of arginine decarboxylase gene expression in a *hns* mutant (Shi and Bennett, 1994). The *stpA* gene is located at 60.26 centisomes on the *E. coli* chromosome and encodes an ~15-kDa protein that has 57% amino acid sequence identity to H-NS. Given this similarity it is not surprising that StpA and H-NS

Fig. 1.11. Cladogram of H-NS proteins. The cladogram shows the relationships of 54 proteins belonging to the H-NS family. H-NS, StpA and H-NS-like proteins were retrieved from the genomic databases based on their amino acid sequence similarity to the *E. coli* K-12 H-NS protein sequence. Proteins that had ≥40% amino acid sequence identity to the *E. coli* K-12 H-NS protein were then used to construct the cladogram with the Blast Tree View program. *S. flexneri* serotype 2a strain 2457T has three members of the H-NS protein family, namely, H-NS, StpA and Sfh, which are indicated in red.

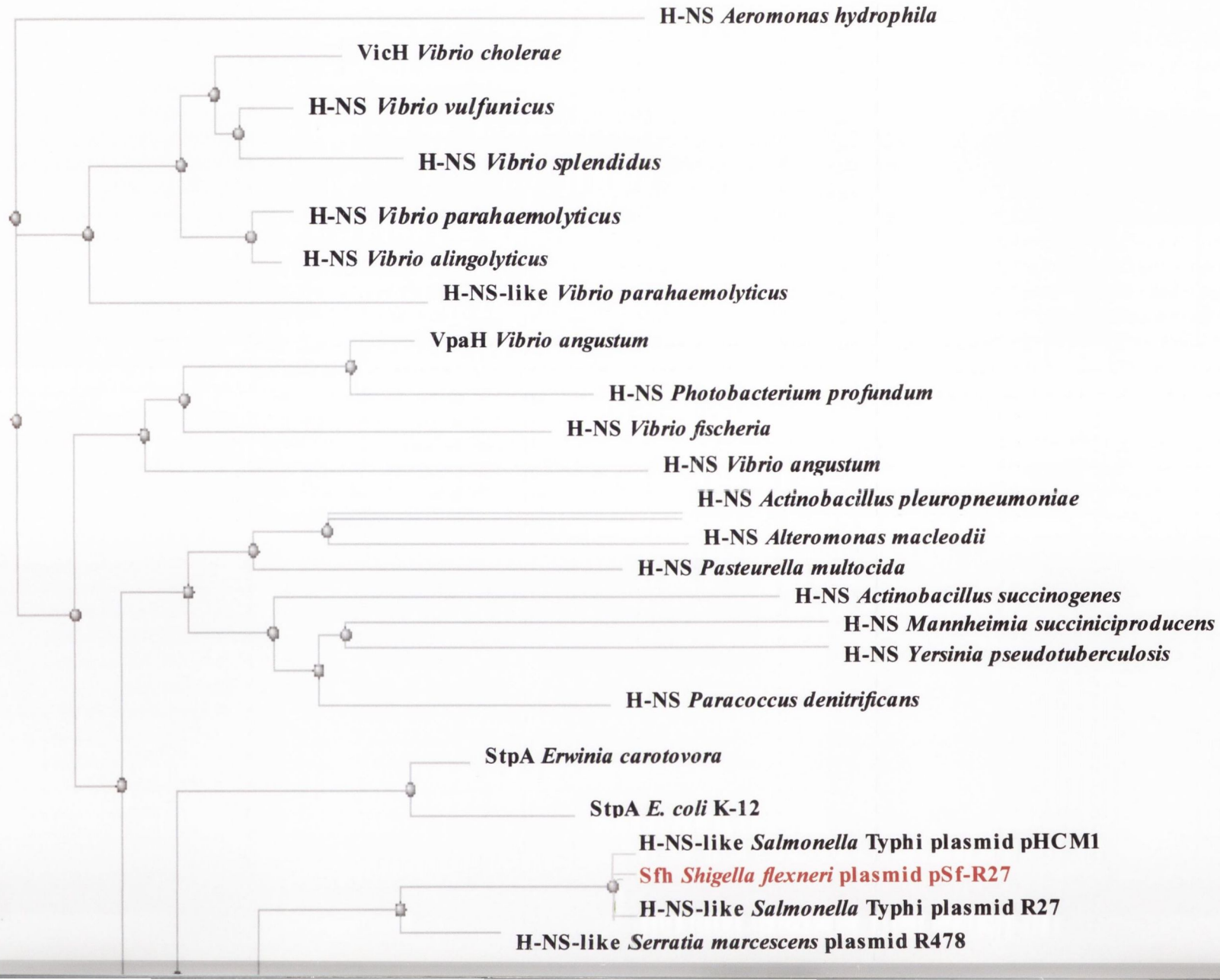
H-NS *Aeromonas hydrophila*
VicH *Vibrio cholerae*
H-NS *Vibrio vulfunicus*
H-NS *Vibrio splendidus*
H-NS *Vibrio parahaemolyticus*
H-NS *Vibrio alingolyticus*
H-NS-like *Vibrio parahaemolyticus*
VpaH *Vibrio angustum*
H-NS *Photobacterium profundum*
H-NS *Vibrio fischeria*
H-NS *Vibrio angustum*
H-NS *Actinobacillus pleuropneumoniae*
H-NS *Alteromonas macleodii*
H-NS *Pasteurella multocida*
H-NS *Actinobacillus succinogenes*
H-NS *Mannheimia succiniciproducens*
H-NS *Yersinia pseudotuberculosis*
H-NS *Paracoccus denitrificans*
StpA *Erwinia carotovora*
StpA *E. coli* K-12
H-NS-like *Salmonella* Typhi plasmid pHCM1
Sfh *Shigella flexneri* plasmid pSf-R27
H-NS-like *Salmonella* Typhi plasmid R27
H-NS-like *Serratia marcescens* plasmid R478

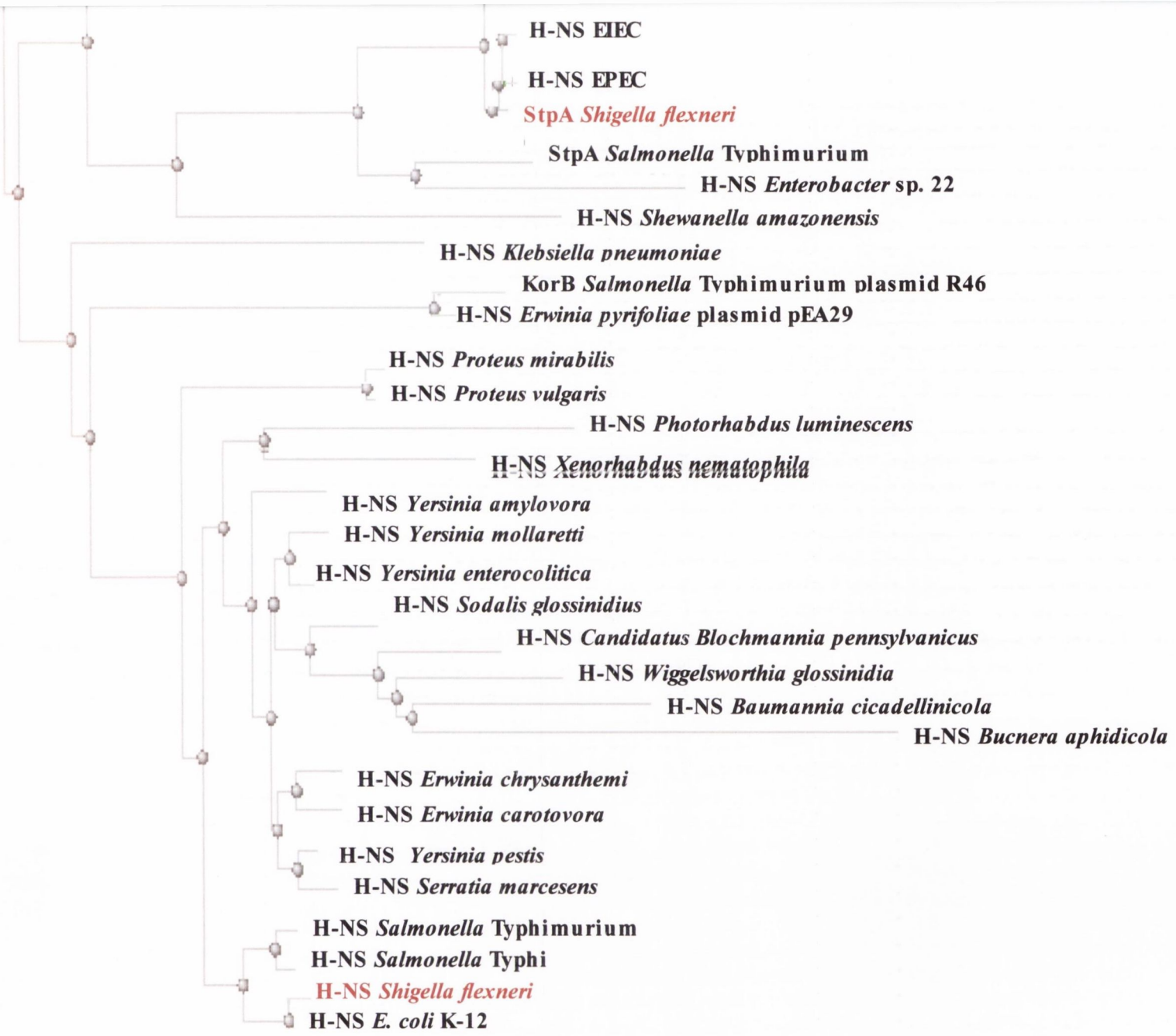
H-NS EIEC
H-NS EPEC
StpA Shigella flexneri
StpA Salmonella Typhimurium
H-NS Enterobacter sp. 22
H-NS Shewanella amazonensis
H-NS Klebsiella pneumoniae
KorB Salmonella Typhimurium plasmid R46
H-NS Erwinia pyrifoliae plasmid pEA29
H-NS Proteus mirabilis
H-NS Proteus vulgaris
H-NS Photorhabdus luminescens
H-NS Xenorhabdus nematophila
H-NS Yersinia amylovora
H-NS Yersinia mollaretti
H-NS Yersinia enterocolitica
H-NS Sodalis glossinidius
H-NS Candidatus Blochmannia pennsylvanicus
H-NS Wiggelsworthia glossinidia
H-NS Baumannia cicadellinicola
H-NS Bucnera aphidicola
H-NS Erwinia chrysanthemi
H-NS Erwinia carotovora
H-NS Yersinia pestis
H-NS Serratia marcesens
H-NS Salmonella Typhimurium
H-NS Salmonella Typhi
H-NS Shigella flexneri
H-NS E. coli K-12

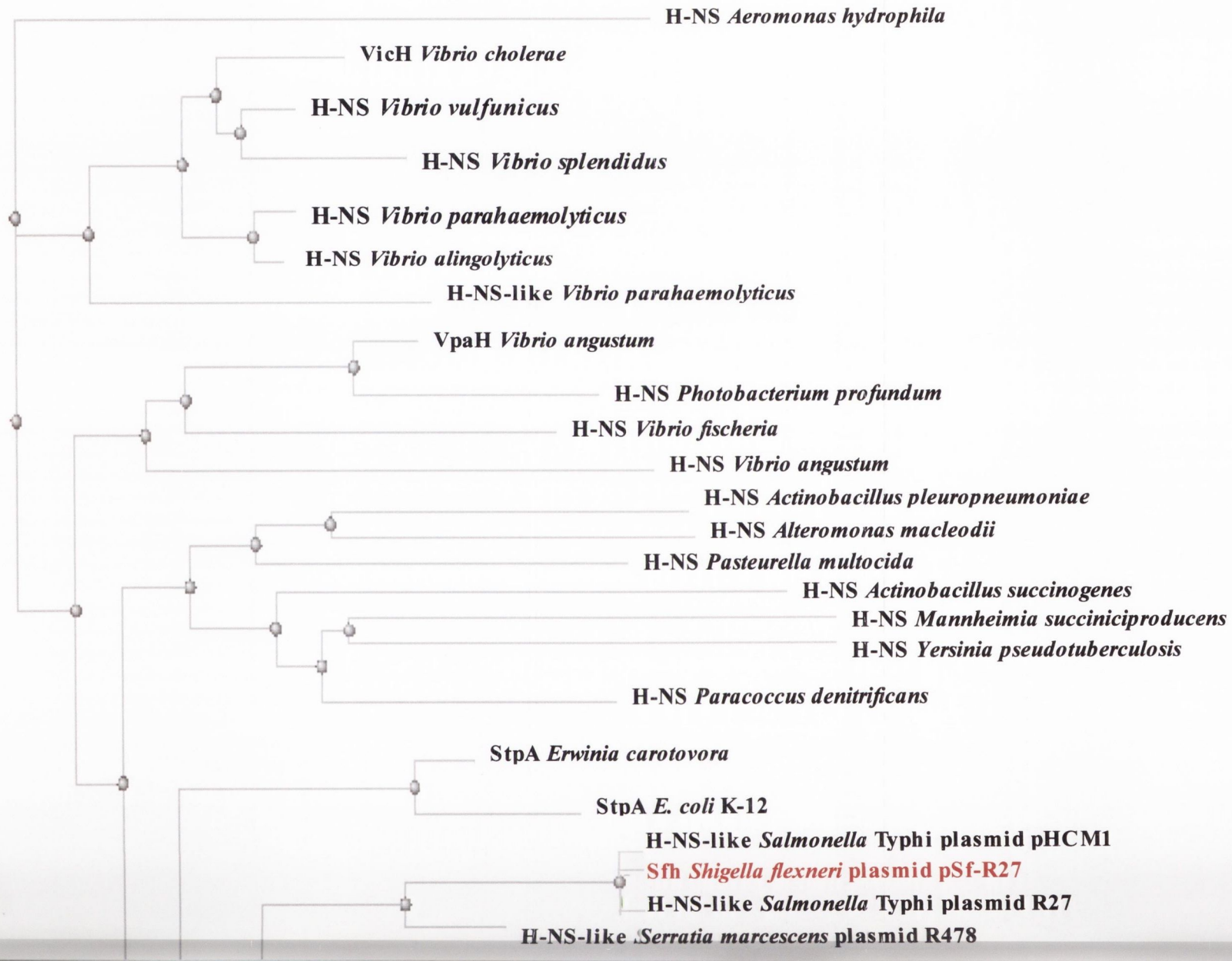
H-NS *Aeromonas hydrophila*
VicH *Vibrio cholerae*
H-NS *Vibrio vulfunicus*
H-NS *Vibrio splendidus*
H-NS *Vibrio parahaemolyticus*
H-NS *Vibrio alingolyticus*
H-NS-like *Vibrio parahaemolyticus*
VpaH *Vibrio angustum*
H-NS *Photobacterium profundum*
H-NS *Vibrio fischeria*
H-NS *Vibrio angustum*
H-NS *Actinobacillus pleuropneumoniae*
H-NS *Alteromonas macleodii*
H-NS *Pasteurella multocida*
H-NS *Actinobacillus succinogenes*
H-NS *Mannheimia succiniciproducens*
H-NS *Yersinia pseudotuberculosis*
H-NS *Paracoccus denitrificans*
StpA *Erwinia carotovora*
StpA *E. coli* K-12
H-NS-like *Salmonella* Typhi plasmid pHCM1
Sfh *Shigella flexneri* plasmid pSf-R27
H-NS-like *Salmonella* Typhi plasmid R27
H-NS-like *Serratia marcescens* plasmid R478

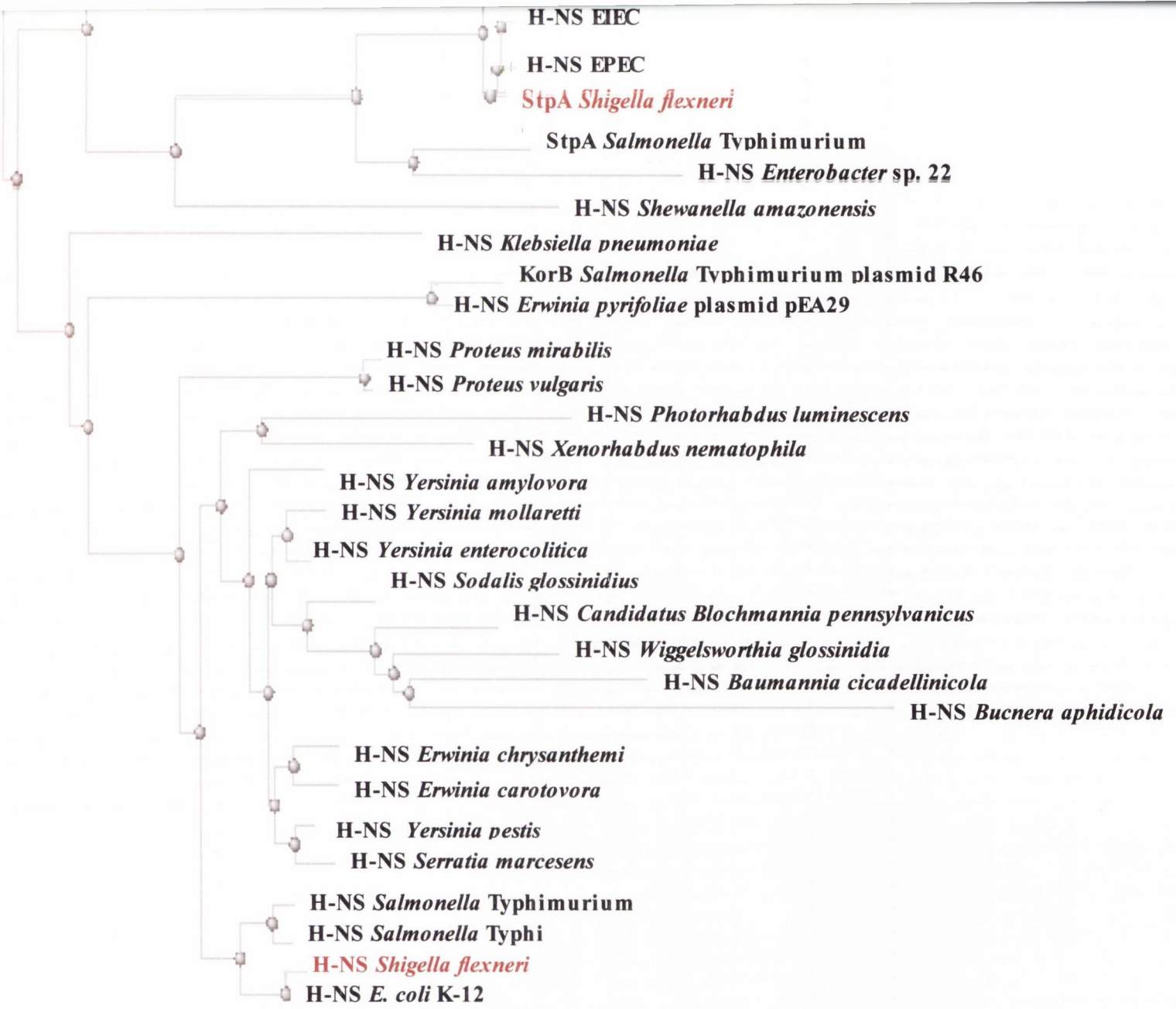
H-NS EIEC
H-NS EPEC
StpA Shigella flexneri
StpA Salmonella Typhimurium
H-NS Enterobacter sp. 22
H-NS Shewanella amazonensis
H-NS Klebsiella pneumoniae
KorB Salmonella Typhimurium plasmid R46
H-NS Erwinia pyrifoliae plasmid pEA29
H-NS Proteus mirabilis
H-NS Proteus vulgaris
H-NS Photorhabdus luminescens
H-NS Xenorhabdus nematophila
H-NS Yersinia amylovora
H-NS Yersinia mollaretti
H-NS Yersinia enterocolitica
H-NS Sodalis glossinidius
H-NS Candidatus Blochmannia pennsylvanicus
H-NS Wiggelsworthia glossinidia
H-NS Baumannia cicadellinicola
H-NS Bucnera aphidicola
H-NS Erwinia chrysanthemi
H-NS Erwinia carotovora
H-NS Yersinia pestis
H-NS Serratia marcesens
H-NS Salmonella Typhimurium
H-NS Salmonella Typhi
H-NS Shigella flexneri
H-NS E. coli K-12

have many overlapping biochemical activities, but importantly they also have distinct functions. For example, both proteins can constrain DNA supercoils *in vitro* and preferentially bind to intrinsically curved DNA. Moreover, overexpression of StpA can functionally repress a subset of H-NS-regulated genes (Sonden and Uhlin, 1996; Zhang *et al.*, 1996). However, StpA has a high affinity for RNA and is a far superior RNA chaperone than H-NS (Zhang *et al.*, 1995; Zhang *et al.*, 1996). H-NS and StpA have also been shown to differentially regulate OmpF porin expression in *E. coli*. H-NS influences transcription of the *micF* antisense RNA gene, whereas StpA modulates the interaction of the *ompF* mRNA with the MicF antisense RNA, and thus influences *ompF* expression at the translational level (Deighan *et al.*, 2000).

Another difference between the paralogues is the degree to which they are expressed, and their growth phase-dependent expression profiles. During growth in rich medium, the *stpA* gene is only transiently expressed during log phase but transcription of the *stpA* gene is significantly enhanced in minimal medium in an Lrp (leucine responsive protein)-dependent manner (Free and Dorman, 1997). In addition, several environmental conditions can modulate *stpA* gene expression. Increases in medium osmolarity and in growth temperature stimulate *stpA* gene expression, while carbon starvation causes a rapid repression of the gene (Free and Dorman, 1997; Sonden and Uhlin, 1996). Additionally, StpA negatively autoregulates its own expression, and H-NS negatively cross-regulates the *stpA* gene (Sonden and Uhlin, 1996; Zhang *et al.*, 1996). Thus, both paralogues negatively cross-regulate each other's gene expression. However, the dominant effect is repression of the *stpA* gene by H-NS, which subsequently results in the low cellular content of StpA (200 molecules per cell), compared to that of H-NS (20,000 molecules per cell) (Free and Dorman, 1997; Sonden and Uhlin, 1996; Spassky *et al.*, 1984; Williams and Rimsky, 1997).

Like H-NS, the StpA protein has bipartite organization and consequently is able to form both homomeric and also heteromeric protein complexes with H-NS. This has led to speculation that the properties of these homomeric and heteromeric complexes could vary depending on

their protein subunit composition (Dorman *et al.*, 1999; Johansson and Uhlin, 1999). Consistent with this, a mutation in the *stpA* gene seems to affect the expression of only a few proteins. However, the number of proteins affected in an *hns stpA* double mutant is far greater than those affected in an *hns* mutant alone (Zhang *et al.*, 1996). The importance of StpA:H-NS heteromerization has been shown in the differential turnover of H-NS and StpA by the Lon protease. StpA is degraded by the Lon protease *in vivo,* whereas H-NS is not. Oligomerization of StpA to H-NS protects the StpA protein from Lon-mediated degradation. Thus, it is believed that StpA exists mainly in StpA:H-NS heteromeric complexes *in vivo* (Johansson and Uhlin, 1999; Johansson *et al.*, 2001).

1.6.2 Sfh

The H-NS homologue Sfh (*Shigella flexneri* H-NS-like protein) was discovered three years ago in the *S. flexneri* serotype 2a strain 2457T using bioinformatics analyss (Beloin *et al.*, 2003). Sfh has 59% and 61% amino acid identity to H-NS and StpA, respectvely (Fig. 1.12). Unlike the *hns* and *stpA* genes, the *sfh* gene is not located on the chromosone but on a large ~165-kb plasmid that is 99.7% identical to the prototype IncHI1 plasmid, R27 (Beloin *et al.*, 2003; Wei *et al.*, 2003). Consequently, its closest homologues (98% amino acid sequence identity) are the H-NS-like proteins encoded by the IncHI1 plasmids, R27and pHCM1, of *Salmonella* (Fig. 1.11). Like *stpA* mutants, no obvious phenotypes can be associated with mutations in the *sfh* gene. However, Sfh can complement an *hns* mutation in*E. coli*, restoring wild-type expression of the *fliC* and *proU* genes, and restoring wild-type Fgl, porin protein and mucoidy phenotypes (Beloin *et al.*, 2003). The overall domain structure of Sfh closely matches that of its homologues, H-NS and StpA (Fig. 1.12). Consistent with this, chemical crosslinking and yeast two-hybrid assays showed the Sfh protein, like H-NS and StpA, is capable of forming homomeric complexes and that Sfh can form heteromeric complexes with both of its homologues (Deighan *et al.*, 2003). This raises the possibility that Sfh may modulate the activities of H-NS and StpA, and *vice versa.* Expression of Sfh is regulated in a growth phase-dependent manner. During growth in rich media, Sfh expression is only

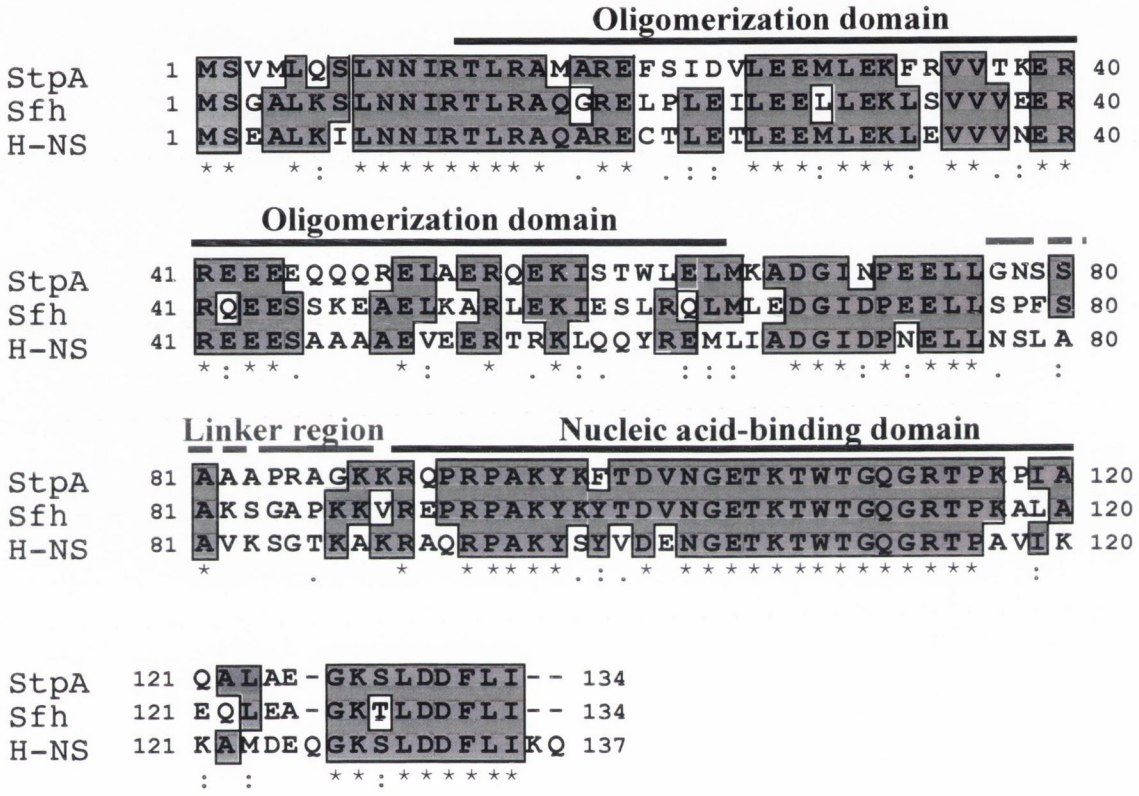

Fig. 1.12. Protein sequence alignment of the three *Shigella* H-NS-like proteins. Conserved amino acids are shaded in grey and are indicated by an asterisk. The oligomerization domains, linker region and nucleic acid-binding domains of the three proteins are also indicated. Reproduced from Deighan *et al.* (2003).

induced in early stationary phase, while correspondingly *sfh* mRNA levels rapidly decrease (Deighan *et al.*, 2003). Thus, the three H-NS-like proteins, H-NS, StpA, and Sfh, all have distinct growth phase expression profiles, at least in rich media. The inconsistency between *sfh* mRNA and Sfh protein profiles suggests there is a post-transcriptional aspect to *sfh* growth-phase regulation, distinguishing it from both H-NS and StpA (Deighan *et al.*, 2003). Like H-NS and StpA, Sfh can negatively autoregulate transcription of its own gene and when overexpressed all three proteins can negatively cross-regulate transcription of each other's genes (Deighan *et al.*, 2003).

1.7 IncHI plasmids

Plasmids are semi-autonomous genetic elements that synchronize their replication with the host cell chromosome, thus ensuring that each daughter cell contains at least one plasmid copy (Bingle and Thomas, 2001). Plasmids of the *Enterobacteriaceae* are classified into incompatibility groups based upon their ability (or inability) to co-exist within the same cell alongside another plasmid. Consequently, plasmids of the same incompatibility group share common replication and/or partitioning systems (Gilmour *et al.*, 2004). Plasmids of the H incompatibility group (IncH) were first isolated in Mexico in 1972 during an epidemic of chloramphenicol-resistant typhoid fever (Anderson and Smith, 1972). IncH plasmids are divided into two subgroups, HI and HII (Bradley *et al.*, 1982). IncHI plasmids are very large (>150 kb), low copy number plasmids that are characteristically thermosensitive for conjugative transfer, with transfer occurring optimally between 22°C and 30°C, but being negligible at higher temperatures (Lemoine and Rowbury, 1975; Taylor and Levine, 1980). Another distinguishing feature of IncHI plasmids is that H-pilus production is naturally repressed and does not occur at 37°C (Maher *et al.*, 1993). In contrast, IncHII plasmids are non-thermosensitive for conjugative transfer and constitutively allow production of pili, that are antigenically similar to those encoded by IncHI plasmids (Bradley *et al.*, 1982).

The IncHI group is further subdivided into three groups –IncHI1, IncHI2 and IncHI3– based mainly on DNA sequence studies (Roussel and Chabbert, 1978; Taylor and Brose, 1985; Whiteley and Taylor, 1983). One key feature that distinguishes IncHI1 and IncHI2 plasmids is the observed one-way incompatibility between F and IncHI1 plasmids, which does not occur between F and IncHI2 plasmids. This characteristic IncHI1 phenotype correlates to the presence of a non-functional IncFIA replicon in IncHI1 plasmids, which bears DNA sequence similarity to the RepFIA replicon of the F plasmid (Saul *et al.*, 1988; Taylor *et al.*, 1985). IncHI1 plasmids frequently encode multiple drug and heavy metal resistance genes (Lawley *et al.*, 2000; Parkhill *et al.*, 2001; Sherburne *et al.*, 2000; Wain *et al.*, 2003) and have been implicated as a significant factor in the persistence of typhoid fever worldwide. Plasmid-encoded multiple drug resistance (MDR) in *S.* Typhi, the causative agent of typhoid fever, is always encoded by plasmids of the IncH group (Sherburne *et al.*, 2000; Wain and Kidgell, 2004). Recently, IncHI1 plasmids have been isolated from MDR *S.* Typhi in Asia (Mirza *et al.*, 2000) and India (Shanahan *et al.*, 1998) and also from individuals infected with *S.* Typhi living in Africa (Kariuki *et al.*, 2000) and from travelers returning to North America from South Asia (Harnett *et al.*, 1998).

The complete nucleotide sequences of two IncHI1 plasmids, R27 and pHCM1 have been determined (Parkhill *et al.*, 2001; Sherburne *et al.*, 2000). Plasmid R27 is the prototype IncHI1 plasmid and was isolated from *S.* Typhimurium in the UK during the early 1960's (Sherburne *et al.*, 2000). This 180-kb plasmid contains 210 open reading frames (ORFs), which include a full Tn*10* transposon encoding tetracycline resistance (Lawley *et al.*, 2000; Sherburne *et al.*, 2000). Plasmid pHCM1 was isolated three decades later in Vietnam in 1993 from the MDR *S.* Typhi strain CT18 (Parkhill *et al.*, 2001). The two plasmids, pHCM1 and R27, were determined to share over 168-kb of DNA, with >99% sequence identity. However, plasmid pHCM1 is much larger in size (218-kb) than plasmid R27, due to the acquisition of two distinct regions of DNA, totalling ~50-kb, that plasmid R27 lacks. Significantly, these regions include the genes encoding MDR and the larger of the two regions (35 kb) is located between ORFs R0139 and R0140 in the plasmid R27 sequence. Thus, it would appear that

plasmid R27 is a precursor of plasmid pHCM1 (Parkhill *et al.*, 2001; Wain *et al.*, 2003). A third IncHI1 plasmid, plasmid pSf-R27, was recently discovered in the *S. flexneri* serotype 2a strain 2457T, which was isolated in Tokyo in 1954 (Beloin *et al.*, 2003; Wei *et al.*, 2003). Unlike other IncHI1 plasmids, plasmid pSf-R27 does not encode any drug resistance and is 99.7% identical in DNA sequence to the prototype R27 plasmid (Beloin *et al.*, 2003; Wei *et al.*, 2003).

The regions of similarity among the three IncHI1 plasmids principally encode the core plasmid functions, namely, replication, partitioning and stability, and conjugative transfer (Gilmour *et al.*, 2004). The mosaic genetic organization of these backbone components suggests a complex evolutionary history for IncHI1 plasmids. For example, the genes responsible for conjugative transfer are located in two separate regions of IncHI1 plasmids, termed Tra1 and Tra2. These transfer regions are chimeras composed of both IncF-like and IncP-like elements and encode all the components of the IncHI1 conjugation system (Lawley *et al.*, 2002; Lawley *et al.*, 2003a; Sherburne *et al.*, 2000). Furthermore, the relaxosomal (TraI and TraJ) and coupling (TraG) proteins of IncH plasmids constitute a novel phylogenetic group, indicating that IncH mating-pair formation and relaxosome/coupling determinants have evolved from different lineages (Gilmour *et al.*, 2004).

Replication of IncHI1 plasmids is determined by one of two replicons, RepHI1A or RepHI1B, which are specific to IncHI1 plasmids (Gabant *et al.*, 1993; Gabant *et al.*, 1994). These replicons maintain a plasmid copy number of 1–2 copies per chromosomal origin by an iteron-binding mechanism (Taylor and Brose, 1988). The two IncHI1-specific replicons operate independently of one another and can support active replication of the plasmid. In addition, each replicon independently specifies incompatibility (Newnham and Taylor, 1994). The independence of the two replicons in incompatibility is thought to be due to differences in the repeat sequences of the two replication initiator proteins, RepHIA and RepHIB (Newnham and Taylor, 1994). The two RepHI proteins are only 34.9% similar in amino acid sequence but the organization of their binding sequences is comparable with four direct repeat

sequences upstream and three downstream for RepHIA, and four upstream and four downstream for RepHIB (Newnham and Taylor, 1994). Active partitioning of IncHI1 plasmids is a result of two independent partitioning modules, designated Par1 and Par2, located within the Tra2 region of the plasmid (Lawley and Taylor, 2003). Par1 encodes a Walker-type ATPase and is therefore a member of the type I partitioning family, whereas Par2 encodes an actin-type ATPase, and consequently is classified as a type II partitioning module. Each module is capable of supporting partitioning but Par1 is the major stability determinant (Lawley and Taylor, 2003).

Bacterial plasmids deploy a diverse range of regulatory mechanisms to control their core functions, i.e., replication, partitioning and stability, and conjugative transfer. Coordinate or global regulation of plasmid core determinants is emerging as a widespread phenomenon in large bacterial plasmids (Bingle and Thomas, 2001). The presence of the Par modules in the Tra2 region of IncHI1 plasmids may allow coordinate expression of partitioning and conjugative genes. Similarly, the RepHIA determinant is present immediately upstream of the Tra2 region and may also serve as evidence of coordinate regulation. IncHI1 plasmids also encode several proteins that are homologous to the global DNA-binding proteins: H-NS, TlpA, Hha, and Dam (Beloin *et al.*, 2003; Parkhill *et al.*, 2001; Sherburne *et al.*, 2000). The presence of these proteins indicates that intricate global regulatory networks might control IncHI1 gene expression.

1.8 Bacterial conjugation systems

The bacterial type IV secretion systems (T4SSs) are ancestrally related to bacterial conjugation machines (Christie, 2004; Lawley *et al.*, 2003b). These systems mediate the transfer of DNA and protein substrates across the cell envelopes of Gram-negative and Gram-positive bacteria into phylogenetically diverse prokaryotic and eukaryotic target cells (Cascales and Christie, 2003; Grohmann *et al.*, 2003). The conjugation machines are a large subfamily of T4SSs and enable bacteria to adapt to changing environments through

acquisition of fitness traits. This form of horizontal gene transfer has contributed substantially to genetic diversity and bacterial evolution. The discovery of conjugal transfer in the 1940's revolutionized microbial genetics and has been widely exploited in the laboratory to transfer plasmids and selectable markers between bacterial strains (Lybarger and Sandkvist, 2004). However, in the natural environment conjugation is the primary mechanism for the widespread transmission of antibiotic resistance genes and virulence factors among pathogenic bacteria. Thus conjugation is of the upmost clinical importance (Ochman *et al.*, 2000).

T4SSs are multi-subunit, cell-envelope-spanning structures, composed of a secretion channel and often a pilus or another surface filament or adhesion protein(s) (Christie, 2004; Lawley *et al.*, 2003b). In Gram-negative bacteria the T4SS spans both membranes, and is likely to resemble a transenvelope channel, through which substrates pass, sequestered from periplasmic proteases or nucleases. To date no high-resolution images exist for any type IV secretion apparatus (T4SA), analogous to those of the needle complexes of TTSSs (Marlovits *et al.*, 2004). However, T4SSs do elaborate easily visible surface structures (Kalkum *et al.*, 2004; Lawley *et al.*, 2003b). The conjugative pili of F-like and IncH, IncT, and IncJ plasmids are visible as long flexible tube-like structures (Lawley *et al.*, 2003b; Maher *et al.*, 1993), and mediate efficient transfer in both liquid and solid media. In contrast, plasmids of the IncP, IncN and IncW incompatibility groups elaborate shorter brittle pili that are rarely detected on intact cells, and only mediate efficient DNA transfer on solid media (Eisenbrandt *et al.*, 2000; Kalkum *et al.*, 2004). The surface-exposed pili serve to establish intimate contact between donor and recipient cells and are a component of the mating pair formation (Mpf) system (Schroder and Lanka, 2005).

The Mpf system consists of at least 10 conserved proteins and is essential for production of exocellular pili and the formation of the membrane-spanning protein complex, which serves as a conduit for protein and DNA substrates (Schroder and Lanka, 2005). The most extensively studied Mpf system is that of the plant pathogen, *Agrobacterium tumefaciens. A.*

tumefaciens elaborates a model conjugation machine from 11 Mpf subunits, VirB to VirB11, and the VirD4 coupling protein, to deliver oncogenic transferred DNA (T-DNA) directly into plant cells (Christie *et al.*, 2005). There are three different functional groups of Mpf proteins: (i) exocellular proteins that form the mating pilus, (ii) mating channel components, and (iii) cytoplasmic membrane ATPases (Christie and Vogel, 2000). In *A. tumefaciens* the core secretion channel complex is composed of the VirB8, VirB9 and VirB10 proteins and the exocellular pilus is mainly composed of VirB2 subunits (Fig. 1.13; Schroder and Lanka, 2005). The cytoplasmic membrane ATPases, VirB11 and VirB4, together with the coupling protein VirD4, energises the transport of the T-DNA through the secretion channel (Fig. 1.13).

Coupling proteins (CPs) are NTP-binding proteins that are found in every conjugation system and in most other T4SSs. In conjugation, the CP is required for conjugative DNA transfer, but not for pilus biosynthesis or Mpf. CPs function to recruit processed DNA substrates to the conjugation apparatus, through interactions with the relaxosome components, and thus are the basis for the substrate specificity of T4SSs (Hamilton *et al.*, 2000; Moncalian *et al.*, 1999). The crystal structure of the TrwB CP of plasmid R338 has been elucidated, and shows that CPs form homohexamer ring structures, reminiscent of ring helicases and F1-ATPase (Gomis-Ruth *et al.*, 2001). Structural studies also determined that the monomeric, cytoplasmic domain of the CP is sufficient for binding nucleotides as well as DNA (Moncalian *et al.*, 1999; Schroder and Lanka, 2003), but that binding to the relaxase substrate requires the presence of the N-terminal membrane anchor, probably because oligomerization of the CP is essential for relaxase binding (Schroder and Lanka, 2003).

The processing of substrate DNA for conjugative transfer is a widely conserved reaction among bacteria. A relaxase and one or more auxiliary factors initiate processing by binding to the origin of transfer (*oriT*) sequence, forming the relaxosome. The relaxase then catalyses the cleavage of the DNA strand destined for transfer (T-strand) at the *nic* site located within the *oriT*. This transesterification reaction results in the relaxase remaining covalently

Fig. 1.13. Schematic model of the type IV secretion apparatus. The various protein subunits are named according to the VirB/D4 secretion system of *A. tumefaciens.* The core Mpf complex (yellow) is connected to the exocellular pilus (pink) by the VirB7 lipoprotein. The coupling protein (green) recruits the relaxase-T-strand substrate to the Mpf complex and together with the other cytoplamsic ATPases (blue) energises the transport of the substrate DNA into the recipient cell via the type IV secretion apparatus.

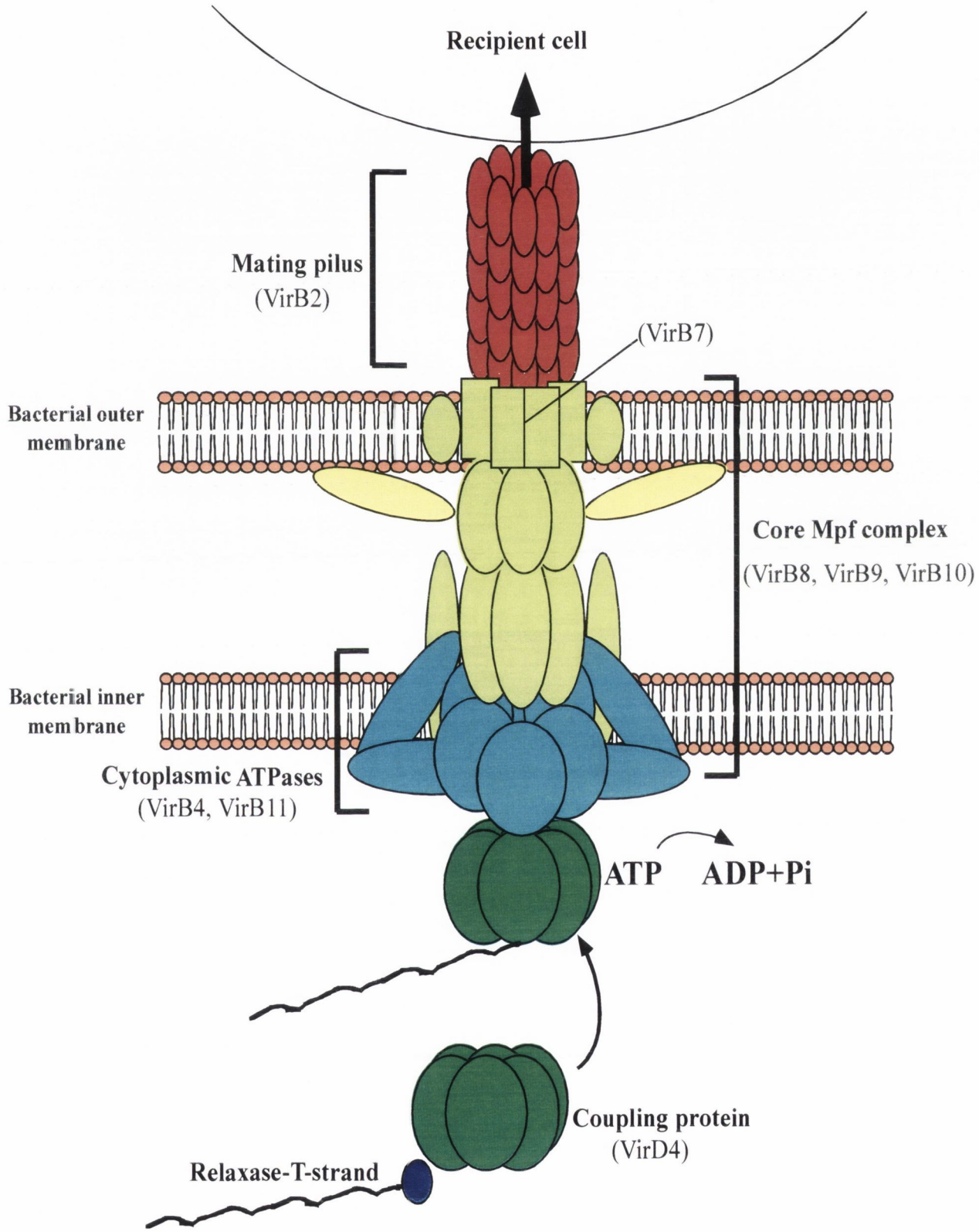
Recipient cell
Mating pilus
(VirB2)
(VirB7)
Bacterial outer membrane
Core Mpf complex
(VirB8, VirB9, VirB10)
Bacterial inner membrane
Cytoplasmic ATPases
(VirB4, VirB11)
ATP
ADP+Pi
Coupling protein
(VirD4)
Relaxase-T-strand

attached to the 5′-end of the T-strand via a phosphodiester bond (Pansegrau and Lanka, 1996). The relaxase-T-strand substrate is then targeted to the Mpf complex by the CP and is secreted unidirectionally in the 5′ to 3′ direction into the recipient cell. Conjugative transfer is probably coupled to replication of the plasmid by a rolling circle-type replication. Following transfer of a complete copy of the T-strand into the recipient cell, the relaxase recognizes the reconstituted *nic* site and undergoes a second transesterification reaction, resulting in reconstitution of the T-strand (Llosa *et al.*, 2002; Pansegrau and Lanka, 1996). In addition to the relaxase-T-strand substrate, it is now firmly established that conjugation machines also transfer proteins that are non-covalently associated with ssDNA, such as the VirE2, SSB and VirF proteins of the *A. tumefaciens* system (Vergunst *et al.*, 2000). Moreover, although the conjugation machineries comprise the largest subfamily of T4SSs, many important pathogens use T4SSs primarily for delivery of proteins rather than nucleic acids (Burns, 2003; Ding *et al.*, 2003; Nagai and Roy, 2003). For example, *Helicobacter pylori* uses a T4SS to inject CagA into gastric epithelial cells (Odenbreit *et al.*, 2000), *Legionella pneumophila* employs a T4SS to evade the immune system upon uptake by macrophages, and *Bordetella pertussis* secretes the pertussis holotoxin into the extracellular environment through a T4SS (Farizo *et al.*, 2000).

1.9 DNA damage response

Exposure of a bacterial cell to DNA-damaging agents (such as UV and ionizing radiation and a variety of chemicals) results in a diverse set of physiological changes termed the 'SOS response'. This phrase was first coined by M. Radman in the mid-1970s and embodies the pleiotropic response used by the bacterial cell when it is in distress (Walker, 1996). The SOS response results in the induction of over 30 unlinked genes (many of which are involved in DNA repair and mutagenesis), which help protect the cell against the effects of DNA-damaging agents (Walker, 1996). Although the response, in its broadest sense, represents all damage-inducible genes, it has become synonymous with a dual-controlling regulatory cascade system involving the RecA and LexA proteins (Brent and Ptashne, 1981; Little *et al.*,

1980; Little *et al.*, 1981). However, more recent studies have shown that in fact many other proteins are induced by DNA damage that are not directly regulated by the classical RecA/LexA system (Koch and Woodgate, 1998). Indeed, transcriptional profiling of *E. coli* treated with the DNA damaging-agent mitomycin C revealed that over 1000 genes were differentially expressed in response to DNA damage (Khil and Camerini-Otero, 2002). This study confirmed induction of the classical SOS genes, but also enabled the expansion of the knowledge base to include novel classical SOS genes, plus additional genes whose transcription is influenced by DNA damage in a LexA-independent manner (Khil and Camerini-Otero, 2002). In addition, this global analysis observed the induction of other stress response pathways in response to DNA damage, such as the osmotic protection and oxidative stress regulatory pathways. Therefore, the classical SOS response is only one of many cellular responses induced upon DNA damage (Fry *et al.*, 2005; Khil and Camerini-Otero, 2002).

As mentioned above, expression of genes belonging to the classical SOS regulatory network is controlled by a complex circuitry involving the RecA and LexA proteins (Walker, 1996). The basic regulatory mechanism is fairly well elucidated and is summarized in Fig. 1.14. In an uninduced cell, the product of the LexA gene acts as repressor of the SOS genes, including the *recA* and *lexA* genes, by binding to a 20-bp site (commonly referred to as the SOS box) found in the 5′-end of these genes (Fig. 1.14; Lewis *et al.*, 1994). Generation of single-stranded DNA (ssDNA) *in vivo* is the ultimate signal for SOS induction. The binding of RecA to these regions of ssDNA in the presence of nucleoside triphosphate results in the formation of a nucleoprotein filament and converts RecA to an activated form (often referred to as RecA*). The interaction of this nucleoprotein filament [stabilized by DinI (Lusetti *et al.*, 2004)] with LexA stimulates proteolytic self-cleavage of the LexA repressor and the subsequent derepression of the SOS regulon (Fig. 1.14; Walker, 1996; Yasuda *et al.*, 1998). Consequently, the products of the SOS genes mediate DNA repair and recombination in the cell. As the cell begins to recover, the inducing signal (ssDNA) is eliminated, RecA is no longer activated, and the intracellular pool of intact LexA increases until homeostatic levels

Fig. 1.14. Schematic model of the SOS response. Exposure of a bacterium to agents or conditions that damage DNA results in the induction of over 30 unlinked genes, which is known as the SOS response. In an uninduced cell, the LexA repressor protein binds to a 20-bp promoter sequence known as the SOS box, present at 5′-end of SOS genes. Derepression of the genes occurs when the RecA protein binds to single-stranded DNA generated by DNA damage. The formation of a RecA/ssDNA nucleoprotein filament converts RecA to an activated form and stimulates proteolytic self-cleavage of the LexA repressor. Consequently, the SOS genes are expressed and their products mediate DNA repair and recombination in the cell.

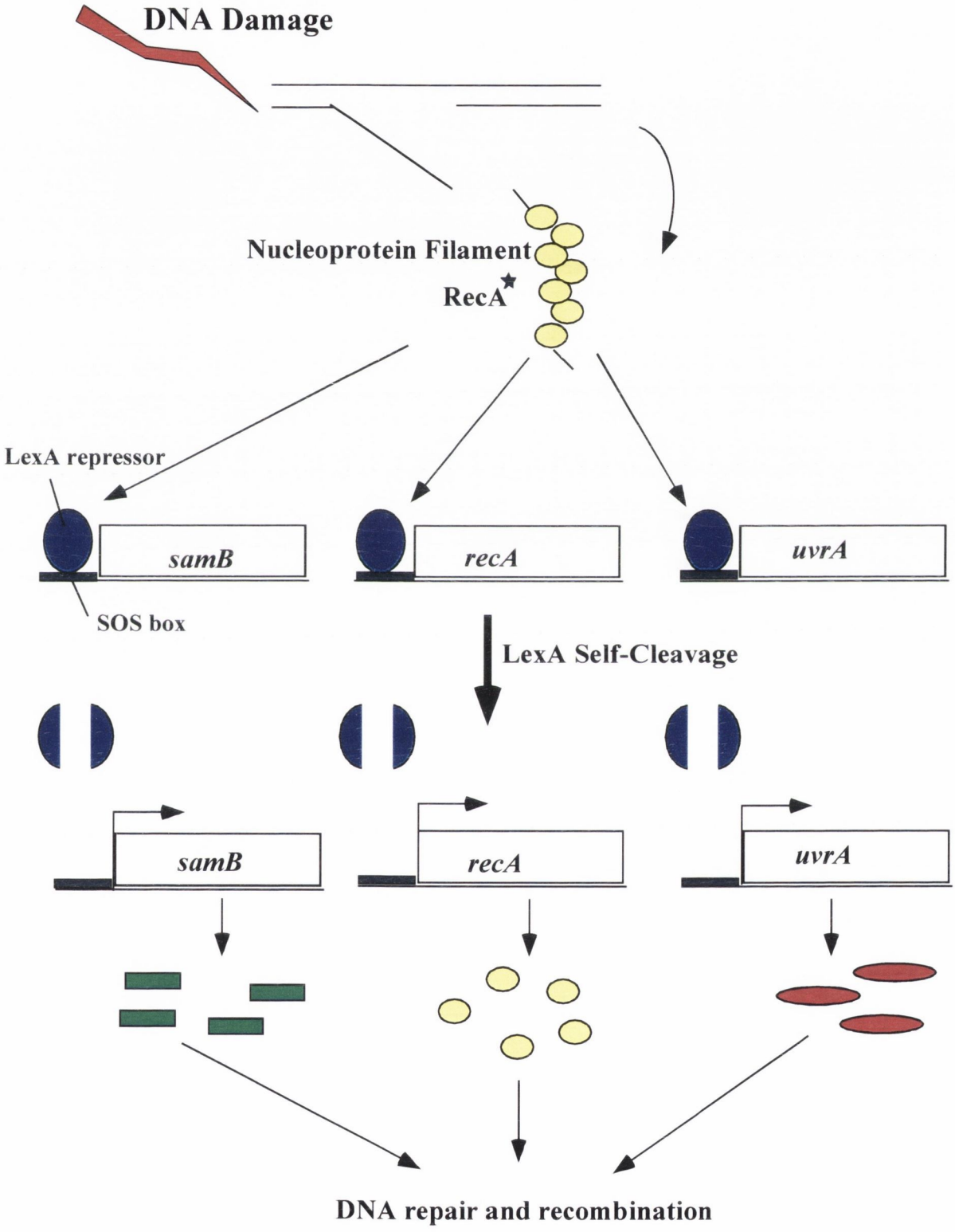
DNA Damage
Nucleoprotein Filament
RecA
LexA repressor
samB
recA
uvrA
SOS box
LexA Self-Cleavage
samB
recA
uvrA
DNA repair and recombination

are reached. Thus, the SOS regulon is repressed and the cell returns to its 'wild-type' physiological state (Walker, 1996).

The SOS response can be expressed to varying degrees in the cell, the extent of the response depending on several factors, most importantly the varying affinity of LexA for different SOS boxes. The SOS boxes in the *lexA, uvrA, uvrB* and *uvrD* genes bind LexA more weakly than does the operator in the *recA* gene, whereas the SOS boxes in the *sulA* and *umuDC* genes bind LexA more tightly (Walker, 1996). Thus, the genes that have low affinity for LexA are fully induced in response to a weak SOS-signal, whereas genes that bind LexA most tightly are only fully induced in response to a potent SOS-signal. This feature of the regulatory system allows cells to utilize certain SOS-regulated functions without a commitment to a full-fledged SOS response (Walker, 1996). In addition, the expression of several SOS-regulated genes is subject to further transcriptional control by other regulatory networks. For example, induction of the SOS genes *yebG* and *sbmC* requires the nucleoid-associated protein H-NS, and also cAMP and RpoS, respectively (Oh and Kim, 1999; Oh *et al.*, 2001).

Another global regulator implicated in the SOS regulatory circuit is deoxyadenosine methyltranferase (Dam), which is part of the *dam*-directed mismatch repair system (Janion, 2001). A deficiency of Dam methylase has been shown to cause induction of the SOS response in both *E. coli* and *S. enterica* (Peterson *et al.*, 1985; Torreblanca and Casadesus, 1996). More recent studies revealed the *Salmonella* prophage ST64B excises at a high rate in *dam* mutants due to increased expression of the SOS regulon and the loss of repression exerted by Dam on the phage genes (Alonso *et al.*, 2005a). Previous studies have also shown that the SOS response contributes to increased excision of other lysogenic phages such as the λ phage in *E. coli* (Waldor and Friedman, 2005), the CTXϕ phage in *Vibrio cholerae* (Quinones *et al.*, 2005), P22 in *S. enterica* (Bunny *et al.*, 2002), and also the pathogenicity island SapIbov1 of *Staphylococcus aureus* (Ubeda *et al.*, 2005). Derepression of phages λ and ϕ80 is mediated through activated RecA, which stimulates autocleavage of their CI repressors, rendering them inactive (Eguchi *et al.*, 1988; Little, 1993). In contrast the CTXϕ

repressor RstR does not appear to undergo autoproteolysis, but instead requires LexA to fully repress the phage genes (Quinones *et al.*, 2005). Similarly, LexA is required to prevent induction of three *S. enterica* prophages (Gifsy-1, Gifsy–2 and Fels-2) by repressing their cI antirepressor gene, *tum* (Bunny *et al.*, 2002). Thus, as a consequence of DNA damage, RecA* induces the lytic cycle of several phages, consequentially enhancing their frequency of transfer (Burrus and Waldor, 2003). Importantly, the SOS response can be induced by several routinely used antibiotics such as ciprofloxacin. Therefore, use of certain antimicrobial agents can stimulate horizontal dissemination of antibiotic resistance genes carried on these phages and related elements (Burrus and Waldor, 2003).

The SOS response, however, does not enhance horizontal transfer of all genetic elements, and is undoubtedly very disadvantageous for conjugative plasmids. As previously mentioned, generation of ssDNA is the ultimate signal for SOS induction. Therefore, it is not surprising that conjugal transfer of ssDNA between bacterial cells elicits a strong SOS response (Althorpe *et al.*, 1999). However, many transmissible plasmids have evolved to permit transfer of ssDNA without generating an SOS signal by expressing factors that both inhibit the bacterial SOS response and also help establish the incoming plasmid in the recipient cell (Althorpe *et al.*, 1999). The genes coding for these factors are highly conserved, and are located in the leading region of many enterobacterial plasmids, thus ensuring early transfer and expression of these genes during conjugation. Examples include the SOS inhibition gene (*psiB*), the anti-restriction gene (*ardA*), and the *ssb* gene all located in the leading regions of several conjugative plasmids, such as the IncI1 plasmid Collb-P9 (Althorpe *et al.*, 1999; Bates *et al.*, 1999).

1.10 Overview

Members of the H-NS protein family are widespread among Gram-negative bacteria and are known to influence global gene expression. *S. flexneri* serotyype 2a strain 2457T expresses three H-NS-like proteins, namely H-NS and StpA, and the recently identified Sfh protein.

The aim of this study was to characterize the novel H-NS-like protein Sfh and to define its role *in vivo*. The data presented reveals a significant role for Sfh in pSf-R27 plasmid biology and highlights the potential influence of Sfh on virulence gene expression in the two pathogens, *S. flexneri* and *S.* Typhimurium. In addition, a novel role for Sfh in plasmid pSf-R27 conjugation was elucidated and the unique regulation of growth phase-dependent expression of the *sfh* gene was examined.

Chapter 2

Materials and Methods

2.1 Chemicals and growth media

2.1.1 Chemicals and reagents

The supplier for each chemical or reagent used in this study is named in parenthesis after the product. DNA restriction and modifying enzymes were obtained from New England Biolabs or Roche Molecular Biochemicals. Custom automated sequencing was performed by GATC Biotech. In addition, several molecular biology kits were used during this study. The basic principle of each kit is briefly described in the appropriate sections below, without giving an exhaustive protocol.

2.1.2 Growth media

Materials for preparing growth media were obtained from Difco or Oxoid. All media were sterilized by autoclaving at 120°C for 20 min prior to use, or storage at room temperature. Additional solutions not suitable for autoclaving, e.g., amino acid or antibiotic solutions, were sterilized by filtration through 0.2-μm Acrodisc Filters (PALL). All quantities listed below are for the preparation of 1 litre of medium in Water Analar^{TM} (BDH, 0.1 $\mu S.mm^{-1}$). Media were supplemented with the appropriate antibiotics as required. Agar media were allowed to cool to 50°C before the addition of the appropriate antibiotic.

2.1.2.1 L-broth and L-agar plates

L agar plates were used throughout this study for reviving bacterial strains from frozen stocks, general culturing of strains, and selection of transformants, transductants and transconjugants. Bacterial strains were routinely grown in Lennox (L) broth unless otherwise stated.

L-broth: 10 g Oxoid tryptone, 5 g Yeast extract, 5 g NaCl

L-agar: 10 g Oxoid tryptone, 5 g Yeast extract, 5 g NaCl, 15 g agar

2.1.2.2 L-Salicin agar plates

L-salicin agar plates were used as an aid to confirm the *hns* status of bacteria by monitoring phospho-β-glucosidase activity. *hns*$^{-}$ strains are derepressed for the expression of the *bgl*

operon and consequent production of phospho-β-glucosidase, an enzyme which catabolises aromatic β-glucosides such as salicin. Thus, *hns*$^{-}$ colonies are yellow in colour when grown on salicin-containing plates in the presence of the pH indicator bromothymol blue. In contrast colonies where the *bgl* operon is silenced (*hns*$^{+}$) are blue in colour (Free *et al.*, 2001).

L-salicin agar: 10 g Oxoid tryptone, 5 g Yeast extract, 5 g NaCl, 15 g agar

After autoclaving 5 g salicin and 5 ml bromothymol blue stock solution (2% (v/v) bromothymol blue, 50% (v/v) ethanol and 0.2-M NaOH) was added.

2.1.2.3 Congo Red agar plates

Congo red agar plates were used to indicate the presence of the LVP in colonies of *S. flexneri* strain 2457T growing on agar plates. The LVP of *S. flexneri* is prone to site-specific integration into the chromosome leading to a down-regulation of virulence gene expression (Colonna *et al.*, 1995). Colonies containing the intact LVP appear red on Congo Red agar due to the binding of the dye by plasmid-borne contact haemolysin. Colonies that have lost or contain an integrated LVP appear white on congo red agar.

Congo Red agar: 30 g Tryptic Soy broth, 15 g agar, 100 mg Congo Red

2.1.2.4 MacConkey Lactose agar plates

MacConkey Lactose agar plates were used to indicate the levels of β-galactosidase activity of bacterial colonies. A constituent of MacConkey base is phenol red, a pH indicator, which turns red under acidic conditions. β-galactosidase-expressing colonies are a red colour due to the production of acidic metabolic products during the fermentation of lactose. In contrast colonies not expressing, or expressing very low levels of β-galactosidase are white or a pale pink colour.

MacConkey lactose agar: 40 g Difco MacConkey agar base, 10 g Lactose, 15 g agar

2.1.2.5 Motility agar plates

Motility agar was used to prepare swarm plates for the measurement of bacterial motility as outlined in Macnab (1986). The centre of each swarm plate was inoculated with equal numbers of bacteria and incubated at 37°C for 8 h. The distance traveled per unit time by bacteria on a swarm plate was a measure of chemotaxis and motility.

Motility agar: 3 g agar, 10 g Bacto tryptone and 5 g NaCl

2.1.2.6 Minimal medium 5.8

Minimal medium 5.8 (MM 5.8) is a low pH, minimal medium previously described by Kox *et al.* (2000). It is used to simulate the conditions experienced by bacteria inside a macrophage and to activate transcription of macrophage-induced genes. The *S.* Typhimurium strain SL1344 used in this study is a histidine auxotroph and therefore, histidine was added to the MM 5.8 to support growth.

MM 5.8: 1 g Casamino acids, 1-mM KH_2PO_4, 0.5-mM K_2SO_4, 5-mM KCl, 7.5-mM $(NH_4)_2SO_4$, 12.285 g bis Tris, 11.2 ml glycerol, 50 ml 1-M Tris-HCl pH 5.8.

After autoclaving 10 µl of 1-M $MgCl_2$, 0.5-mM histidine and 2g glucose were added.

2.1.2.7 SOC medium

SOC medium was used following transformation or electroporation of bacterial strains to increase the efficiency of transformation.

SOC medium: 20 g Tryptone, 5 g Yeast extract, 0.5 g NaCl

After autoclaving 0.95 g $MgCl_2$, 1.2 g $MgSO_4$ and 1.8 g glucose were added.

2.1.3 Antibiotics and X-Gal

All stock antibiotic solutions were stored in aliquots at –20°C and those prepared in water were sterilized by filtration through 0.2-µm Acrodisc Filters (PALL). Carbenicillin, kanamycin, naladixic acid, spectinomycin and streptomycin were prepared as 50 mg ml^{-1}

stock solutions in Water Analar™ (BDH, 0.1 μS.mm^{-1}) and used at a final concentration of 50 μg ml^{-1}. Gentamycin was prepared as a 15 mg ml^{-1} stock solution in Water Analar™ (BDH, 0.1 μS.mm^{-1}) and used at a final concentration of 15 μg ml^{-1}. Tetracycline was prepared as a 10 mg ml^{-1} stock solution in 100% ethanol and used at a final concentration of 10 μg ml^{-1}. Chloramphenicol was prepared as a 25 mg ml^{-1} stock solution in 100% ethanol, and used at a final concentration of 25 μg ml^{-1}. Rifampicin was prepared fresh on day of use as a 50 mg ml^{-1} stock solution in 100% methanol and used at a final concentration of 50 μg ml^{-1}.

X-gal (5-bromo-4-chloro-3-indoyl-β-D-galactoside), a chromogenic substrate for β-galactosidase was prepared as a 20 mg ml^{-1} stock solution in *N, N*-dimethyl formamide and stored in the dark at –20°C. X-gal was used in agar plates at a final concentration of 20 μg ml^{-1}.

2.2 Bacterial strains and culture conditions

2.2.1 Bacterial strains

All bacterial strains used in this study were derivatives of *S. flexneri* serotype 2a strain 2457T, *S.* Typhimurium strains SL1344 and LT2, and *E. coli* strain K-12. These are listed in Table 2.1 together with source and genotype. Bacterial strains were maintained as permanent stocks in 7.7% (v/v) DMSO (dimethyl sulphoxide) or 15% (v/v) glycerol in L-broth and stored at –70°C.

2.2.2 Bacterial culture conditions

Bacterial cultures were routinely grown aerobically in liquid medium at 30°C or 37°C with shaking, except where otherwise stated. Overnight cultures were grown by inoculating single colonies into 3 ml of L-broth with antibiotic selection in sterile test-tubes and incubating at the required temperature overnight. Exponential and stationary cultures were grown by inoculating fresh media to an optical density (OD) of 0.05, with overnight cultures and

Table 2.1. Strains used in this study

Strain	Relevant characteristics[a]	Reference / source
S. flexneri serotype 2a 2457T		
BS184	*mxiC*::MudI*1734*, Km^R, pSf-R27	Maurelli *et al.*, 1984
BS185	BS184 *hns205*::Tn*10*, Tc^R, pSf-R27	Maurelli *et al.*, 1984
CJD1199	BS184 Δ*stpA*::Tc^R, pSf-R27	Porter, 1998
CJD1216	CJD1199 *hnrG*::*bla hns205*::Tn*10*, pSf-R27	Porter, 1998
CJD1650	BS184 pSf-R27Δ*sfh*::$Gent^R$	Deighan *et al.*, 2003
CJD1651	CJD1199 pSf-R27Δ*sfh*::$Gent^R$	This work
CJD1652	BS185 pSf-R27Δ*sfh*::$Gent^R$	This work
MD1	BS184 pSf-R27$Gent^R$	This work
MD2	BS184 Nal^R	This work
MD3	MD1 Rif^R	This work
MD4	BS185 pSf-R27$Gent^R$	This work
MD5	MD4 Rif^R	This work
MD6	CJD1199 pSf-R27$Gent^R$	This work
MD7	MD6 Rif^R	This work
MD8	CJD1650 Rif^R	This work
MD9	CJD1651 Rif^R	This work
MD10	CJD1652 Rif^R	This work
S. Typhimurium		
CJD671	LT2 *spvB*::MudJ, Km^R	O' Byrne and Dorman, 1994b
MD13	SL1344 pSf-R27$Gent^R$	This work
MD14	SL1344 pSf-R27Δ*sfh*::$Gent^R$	This work
MD15	SL1344 Nal^R	This work
SL1344	*rpsL hisG*	Hoiseth and Stocker, 1981
SL1344 *hns*	SL1344 *hns*::Km^R	J. Hinton
TH6232	Δ*hin7517*::FRT *fljBA* off, $FliC^+$	K. T. Hughes
TH6233	Δ*hin7518*::FRT *fljBA* on, $FliC^-$	K. T. Hughes

Table 2.1 *continued*

Strain	Relevant characteristics[a]	Reference/source
E. coli K-12		
DH5α	*supE44* Δ*lacU169*(ϕ*80lacZ*Δ*M15*) *hsdR17 recA1 endA1 gyrA96 thi-1relA1*	Hanahan, 1983
JT4000	Δ*lon-510*	Ebel *et al.*, 1994
MC4100	$F^- \lambda^-$ *araD139* Δ(*argF-lac*)*U169 rpsL150 relA1 flbB5301 deoC ptsF25 rbsR*	Casadaban, 1976
MD11	MC4100 pSf-R27Gent^R	This work
MD16	JT4000 *hns-206*::Ap^R	This work
MD11	SG20250 *hns-206*::Ap^R	This work
PD32	MC4100 *hns-206*::Ap^R	Dersch *et al.*, 1993
SG20250	*lon*$^+$ Δ*lacU169*	Gottesman, 1985
XL-1 Blue	*recA1 endA1 gyrA96 thi-1 hsdR17 supE44 relA1 lac* [F′*proAB lacI*^{q}*Z*ΔM15Tn*10*(Tc^R)]	Stratagene

[a]Antibiotic resistance markers are abbreviated as follows: Tc^R, resistance to tetracycline; resistance to ampicillin; Km^R, resistance to kanamycin; Gent^R, resistance to gentamycin; resistance to naladixic acid; Rif^R, resistance to rifampicin.

monitoring growth to logarithmic or stationary phase by spectrophotometry. Cultures of 3–5 ml were typically grown in test tubes whilst larger cultures were grown in conical flasks of appropriate size to the volume of medium. Every effort was made to ensure identical conditions of growth and harvesting of bacteria for comparative experiments. All broth cultures of *S. flexneri* were inoculated from agar plates containing X-gal or Congo Red to ensure that colonies were not used in which the virulence genes had undergone re-arrangement or integration of the large virulence plasmid had occurred. All broth cultures of *hns* mutants were inoculated from agar plates kept at 4°C for no longer than 5 days to minimize the chance of *hns*$^-$ strains acquiring secondary mutations. In addition, colony morphology, growth rates, and *bgl* phenotypes of *hns*$^-$ strains were strictly monitored.

2.3 Eukaryotic cell lines and growth conditions

2.3.1 Eukaryotic cell lines

The murine macrophage-like cell line J774-A.1 and the epithelial cell lines CHO-K1 and CACO-II were used throughout this study. All cell lines were obtained from the American Type Culture Collection (ATCC) and permanent stocks maintained in 5% (v/v) DMSO and stored in liquid nitrogen.

2.3.2 Eukaryotic cell growth conditions

Murine macrophage-like J774-A.1 cells were maintained in Dulbecco's Modified Eagle's Medium supplemented with 10% (v/v) heat-inactivated foetal bovine serum. CHO-K1 and CACO-II epithelial cells were maintained in Dulbecco's Modified Eagle's Medium with F12 Nutrient mix supplemented with 10% (v/v) heat-inactivated foetal bovine serum. When required 100 U penicillin and 100 μg ml^{-1}streptomycin (Sigma) were added to the growth medium. Cells were routinely grown in 75-cm^2 tissue culture flasks at 37°C in a 5% CO_2 incubator.

2.4 Plasmids, bacteriophage and oligonucleotides

2.4.1 Plasmids

Plasmids used in this study are listed in Table 2.2 together with genotype and source. Any details of plasmid construction will be described in the appropriate results chapters.

2.4.2 Bacteriophage

The bacteriophage used in this study were derivatives of bacteriophage P1 and were routinely stored at 4°C in the dark in 5 ml volumes supplemented with chloroform.

2.4.3 Oligonucleotides

The sequences and nomenclature of all oligonuleotides used in this study are listed in Table 2.3. Oligonucleotides were purchased from MWG-Biotech, Germany.

2.5 Transduction with bacteriophage P1

Throughout this study the temperate bacteriophage P1 *cml cI.100* (Sternberg and Maurer, 1991) was used to transduce bacterial DNA from a donor to a recipient *E. coli* strain. Bacteriophage P1 *cml cI.100* encodes the temperature-sensitive Clr repressor, which is stable at 30°C and prevents lytic growth, but is unstable at 42°C. Hence, the transition from lysogeny to lytic growth can be induced by a transition in growth temperature from 30°C to 42°C. For phage P1, between 110-kb and 115-kb of bacterial DNA (~2.3% of the *E. coli* genome) can be encapsidated into phage particles during lytic growth of the phage in the donor cell. Transducing particles represent between 0.3% and 6% of total phage particles in any phage P1 lysate and comprise less than 5% phage DNA. When a transducing particle attaches to a recipient bacterium, the DNA within the bacteriophage head is injected into the cell and is available for crossing over to the chromosome by homologous recombination.

Table 2.2 Plasmids used in this study

Plasmid	Relevant characteristics[a]	Source/Reference
pACYC184	p15A replicon, Cm^R Tc^R	New England Biolabs
pAF201	*hns* gene in plasmid pACYC184	Free, 1995
pBluescript II KS	pMB1 replicon, Ap^R	Stratagene
pBluescript-IF	RO139-RO140 intergenic DNA fragment of pSf-R27 cloned into plasmid pBluescript II KS	This work
pBluescript-IFGent	*aac* cloned into plasmid pBluescript-IF	This work
pBR322	pMB1/f1 replicon, Ap^R	New England Biolabs
pKOBEGA	pSC101 *ts* (replicates at 30°C), *araC*, arabinose-inducible λ *redγβα* operon, Ap^R	Chaveroche *et al.*, 2000
pPD101	pSC101 replicon, Cm^R	Dersch *et al.*, 1994
pPDsfh	*sfh* gene in plasmid pPD101	This work
pQF50	*lacZ* promoterless trap vector, Ap^R	Farinha and Kropinski, 1990
pQFhilD	539-bp *hilD* promoter region cloned upstream of promoterless *lacZ* gene in plasmid pQF50	This work
pQF(R:100)	327-bp *spvR* promoter region cloned upstream of promoterless *lacZ* gene in plasmid pQF50	Sheehan and Dorman, 1998
pQFsipB	468-bp *sipB* promoter region cloned upstream of promoterless *lacZ* gene in plasmid pQF50	This work
pQFsseA	530-bp *sseA* promoter region cloned upstream of promoterless *lacZ* gene in plasmid pQF50	Carroll, 2003
pQFssrA	645-bp *ssrA* promoter region cloned upstream of promoterless *lacZ* gene in plasmid pQF50	Carroll, 2003
psfh-gfp	587-bp *sfh* promoter region cloned upstream of promoterless *gfp* gene in plasmid pZep08	This work
pSf-R27	RepHI1A and RepHI1B replicons, no antibiotic resistance genes	Beloin *et al.*, 2003
pSf-R27Gent^R	pSf-R27 tagged with *aac* gene of *Streptomyces lividans* conferring gentamycin resistance, $Gent^R$	This work

***Table 2.2** continued*

Plasmid	Relevant characteristics[a]	Source/Reference
pSf-R27Δ*sfh*::Gent^R	*sfh* gene of plasmid pSf-R27 deleted and replaced with *aac* gene of *Streptomyces lividans* conferring gentamycin resistance, Gent^R	Deighan *et al.*, 200
ptraJ-gfp	604-bp *traJ* regulatory region cloned upstream of promoterless *gfp* gene in plasmid pZep08	This work
pUCA/T	2.8 kb AT-rich fragment encompassing *ssrA–ssaB* promoter region cloned into plasmid pUC18	This work
pUC18	ColE1 replicon, Ap^R	Yanisch-Perron *et* 1985
pYCsfh	*sfh* gene in plasmid pACYC184, Cm^R	Beloin *et al.*, 2003
pZep08	*gfp* promoterless trap vector. Cm^R Km^R	Hautefort *et al.*, 19
p18rrnA	*rrnA* internal region gene in plasmid pSPT18	Deighan *et al.*, 20C
p18sfh	*sfh* gene in plasmid pSPT18	Deighan *et al.*, 20C
p671	Plasmid pSLT from CJD671, *spvB*::MudJ, Km^R	O' Byrne and Dorr 1994b

[a]Antibiotic resistance markers are abbreviated as follows: Cm^R, resistance to chloramphenicol; resistance to ampicillin; Km^R, resistance to kanamycin; Gent^R, resistance to gentamycin.

Table 2.3 Oligonucleotides used in this study

Primers	Sequence[a]
A/T-F	5′-GTC GGT ACC GCA AGT TAA AGC CAG GTG-3′
A/T-R	5′-GTC GCA TGC CGC CAG GTC GTA GAG T-3′
dnaE-F	5′-CCT GCG GGT GCA CAG-3′
dnaE-R	5′-AGC AGT TCG TTG TGA ACG-3′
fliF-F	5′-AGT TCA GCG AGC AGG TGA AT-3′
fliF-R	5′-GTA CCA CGG CGC TAA TTT GT-3′
flgA-F	5′-GAC GGT TCC ACT CAC GAT TT-3′
flgA-R	5′-ATC CGT CAG ATT CAG GAT GC-3′
flgA-RBS	5′-GGC GAT GAA CGG AGC G-3′
flgB-FBS	5′-GTC CAC GCA CCA TCA CC-3′
flgD-F	5′-CCG GAA AAG CTG GTT TAT GA-3′
flgD-R	5′-AGA CAT ACG CGC CTC CTT TA-3′
flgH-F	5′-GCG CTT CAC GCT TAC C-3′
flgH-R	5′-CTG TAA CAC AAT CGT GAG C-3′
flgM-F	5′-GCA TTG ACC GTA CCT CAC-3′
flgM-R	5′-CTC ACC GTT ACG GAT AGC C-3′
flgN-F	5′-CCA GAT GAC CAC CGT CC-3′
flgN-R	5′-CCT GCC AGC GCT CTG C-3′
hilD-F	5′-CGC CCA TGG CGA TGT CTG TCG TTC TCG-3′
hilD-R	5′-CGC GGA TCC GAG CAC CAA CAT CCC AGG-3′
hns-For	5′- CCA ATA TAT AAG TTT GAG ATT ACT ACA-3′
hns-Rev	5′- TTA AGC AAG TGC AAT CTA CAA AAG A-3′
hns-RTF	5′-CCG TAC TCT TCG TGC GC-3′
hns-RTR	5′-CCG GAC GCT GAG CAC G-3′
hns-205N	5′-TGG GAA TTC CTT ACA TTC CTG GC-3′
htdA-BSF	5′-GGT TGA TTC AGG TCG AAC C-3′
htdA-BSR	5′-GGG ATT CTC GAC CAG GAC-3′
htdA-FRT	5′-GCA ACT CAC TAA TAC ACG G-3′

Table 2.3 continued

Primers	Sequence[a]
htdA-RRT	5′-GTA TTG TAT CAA TTG GAG CC-3′
IS10-L	5′-CGC GGA TCC GAT ATC AGA CGA GTC AAC AAG-3′
lexA-F	5′-GCT ATG CCA CCG ACG C-3′
lexA-R	5′-CGA CAA GCG GTA ATC CG-3′
MD5	5′-CAC ATC ATC ACT GTG AGT GAC-3′
MD6	5′-CGT CGA TAT CGC TCC AGG C-3′
MD9	5′-CCG CTC GAG GCT TCA CAA CAG GAA TTA GCT G-3′
MD10	5′-CGG AAT TCG CTC CGC ATA ATA CGG ATG C-3′
MD11	5′-GCG TGC ATG CAT GTC TCC CCT GCT CGC GCG CAG-3′
MD11A	5′-GCG TGC ATG CTA ACG TGT TGC CCC AGC AAT CAG-3′
recA-F	5′-GGC GGC AGC ACT GGG-3′
recA-R	5′-GGC AAT CAC CTG CAG CG-3′
rplT-FRT	5′-CAA GCC AAA GGC TAC TAC GG-3′
rplT-RRT	5′-ACG GTC GAT TTC AAC AGA GG-3′
ruvA-F	5′-GTG CTG CTG GAG ACA GG-3′
ruvA-R	5′-GGA GAG GAT CGC CAG C-3′
R27dam-FRT	5′-CCG TTC TCA GTA AGC AC-3′
R27dam-RRT	5′-CGC AGC ACG TAG TAA TCC-3′
R27hha-BSF	5′-GTT CCA GGA ACG CAG CC-3′
R27hha-BSR	5′-CGA TGG TCA TAT GCC CCG-3′
R27hha-For	5′- CTT CTT TCG ACA CAC TGG-3′
R27hha-Rev	5′- CTG ACG GACCAG TGT CC-3′
R27hha-RTF	5′-GCA GGT ATA GCA TCA CTG G-3′
R27hha-RTR	5′-CTG ACG GAC CAG TGT CC-3′
R27tlpA-FRT	5′-GAT GAA CGG GGA TGA AC-3′
R27tlpA-RRT	5′-GGC CGC CAG CAT CTC C-3′
samB-F	5′-CCA CGA CGC GAC ATT CC-3′
samB-R	5′-GCC ATA TGT TTG TCA GGT G-3′
sipB-F	5′-CGC AGA TCT CCC TCA AGA TAT GAT GGA C-3′

Table 2.3 continued

Primers	Sequence[a]
sipB-R	5′-CGC GGT ACC CCT CAG CGA GGC GCG G-3′
sfh-BSF	5′-GCA GCA AAC GTT AAG AAC GC-3′
sfh-BSR	5′-CCA GCA GTT CTT CAA GGA TC-3′
sfh-For2	5′-GGT CAT ATG TCC GGA GC-3′
sfh-Rev2	5′-CCG GCT TCA AGT TGT TCG-3′
sfh-FG	5′-CTG CCC GGG CAC TTT ATG AAC GGC TCG-3′
sfh-RG	5′-CTG TCT AGA CCA GCA GTT CTT CAA GG-3′
sfh-FRT	5′-GTA CTC TTC GTG CGC AG-3′
sfh-RRT	5′-CAG GGC GCG GTT CGC G-3′
sfh-500	5′-GTC GGA TCC ACT TTA TGA AC-3′
sfh+780	5′-GAT AAA GCT TAC TAC AAA GTA G-3′
spvA-FBS	5′-GCG CTG GCT CAC GCC-3′
spvA-RBS	5′-GGC CAT GAC ATA TTG GCG-3′
spvR-FBS	5′-CCC GGT CGT ACA TCG G-3′
spvR-RBS	5′-CCC TGC TCA GCG GGG-3′
ssb-F	5′-GGA CCC GGA AGT ACG C-3′
ssb-R	5′-CGG GTA CGC AAT TGA CC-3′
sseA-FBS	5′-CCC GGT TAG AAG ATT TGC TGC-3′
sseA-RBS	5′-CGA TAT TCA CTA AAC GCA GCC-3′
ssrA-FBS	5′-GCC AGC ATG AAT CCC TC-3′
ssrA-RBS	5′-CCT GAT TAC TAA AGA TGT TTG-3′
traH-BSF	5′-CGT GGT AGC TGT ATC CC-3′
traH-BSR	5′-CCT CTC AAT GTG ATT CCG-3′
traH-FRT	5′-GCT GAA GAA CTG ATC ACC-3′
traH-RRT	5′-CGA CAT GTG ACT AGG TGG-3′
traJ-BSF	5′-TCA CAT CAT GGA TCG GGC-3′
traJ-BSR	5′-GTC GGT GTT CTG GAA CC-3′
traJ-PFgfp	5′-GGA CCC CGG GCA CAA TAG AAG ATT CGG CG-3′
traJ-PRgfp	5′-GGA CTC TAG AGT CGG TGT TCT GGA ACC-3′

Table 2.3 *continued*

Primers	Sequence[a]
traJ-FRT	5′-GGC TGC GGA TAA TTC TGC-3′
traJ-RRT	5′-GCT TAT AGT CAT TAA TCA GG-3′
umuD-F	5′-GAC CTA CAG AGT TGC GCG-3′
umuD-R	5′-CGT TCC GTG AGC TAT CC-3′
virF-F	5′-CGG GAG AAT CGT CAA TGC-3′
virF-R	5′-AAG CGA ACC TTT ATA TCT-3′
virB-F	5′-GTG GCC TTT TTG CTA TTG G-3′
virB-R	5′-CCA GTC GTT GCA CAA ATC C-3′

[a] Restriction enzyme cleavage sites are underlined

2.5.1 Generation of bacteriophage P1 *cml cI.100* lysogens

Phage P1 *cml cI.100* lysogens of the required donor strain were made by incubating 100 µl of an overnight L-broth of the appropriate donor strain with 100 µl of the phage P1 *cml cI.100* lysate stock (grown on wild-type *E. coli* strain MC4100). To aid phage adsorption to bacterial cells 5-mM $CaCl_2$ was added and the mixture was incubated for 30 min at 30°C with aeration. This was then plated onto L-agar plates supplemented with chloramphenicol (25 µg ml^{-1}) and incubated overnight at 30°C. Bacteriophage P1 *cml cI.100* harbours a Tn*9* transposon encoding chloramphenicol resistance. Thus lysogens can be identified as chloramphenicol-resistant colonies.

2.5.2 Preparation of a P1 *cml cI.100* lysate

A high titre lysate was prepared from the desired lysogen by a procedure detailed in Silhavy *et al.* (1984). L-broth (10 ml) was inoculated with 50 µl of an overnight culture of the lysogen (grown at 30°C with selection). This was incubated for 90 min at 30°C with aeration (OD_{600nm} of ~0.1), and induction of the P1 lysogen achieved by incubation in a 42°C waterbath for 20 min. The culture was further incubated at 37°C for 90 min to allow completion of the lytic cycle, resulting in bacterial lysis and release of phage. To this 100 µl chloroform was added and cellular debris pelleted at 4,750 ×*g* for 10 min. The supernatant fraction containing the high titre lysate was then transferred to a 13-ml Sarstedt tube and the lysate maintained sterile by the addition of 100 µl chloroform and stored at 4°C.

2.5.3 Transduction with P1 *cml cI.100*

Phage P1 *cml cI.100* lysates (approximately 10^9–10^{10} bacteriophage ml^{-1}) were used to transduce genetic markers according to Silhavy *et al.* (1984). The recipient strain was grown overnight in 5 ml of L-broth at 37°C. Cells were pelleted at 4,750 ×*g* for 10 min, and resuspended in 2.5 ml 10-mM $MgSO_4$, 5-mM $CaCl_2$. Recipient cells and donor phage lysates were added to 5 tubes in the following ratios:

Tube no.	Volume recipient cells	Volume P1 *cml cI.100* lysate
1	100 µl	-
2	100 µl	10 µl
3	100 µl	50 µl
4	100 µl	100 µl
5	-	100 µl

The tubes were incubated in a 37°C waterbath for 30 min to allow phage adsorption to cells. To these tubes 100 µl 1-M sodium citrate was then added followed by 1 ml of pre-warmed L-broth. The cells were then incubated at 37°C for 1 h to allow phenotypic expression of the transduced marker. Sodium citrate chelates Ca^{2+} and Mg^{2+} ions, thus preventing loss of transductants by further superinfection with viral particles. Cells were then pelleted by centrifugation at 16,000 ×*g* for 2 min, resuspended in 100 µl L-broth and spread onto selection plates containing 10-mM sodium citrate for overnight incubation at 37°C. Plates corresponding to tubes 1 and 5 control for recipient cells and phage lysate contamination respectively. Transductants from plates 2–4 inclusive were single colony purified twice at 37°C, then tested for the presence of a stable lysogen by streaking onto L-agar plates with chloramphenicol and incubating at 30°C.

2.6 Conjugal transfer of plasmid DNA

Bacterial conjugation is a special type of DNA replication (rolling-circle replication) during which one strand of a conjugative plasmid is transferred from a donor to a recipient bacterium using a specialized T4SS. The host-encoded replisome is then responsible for complementary strand synthesis of both the transferred and retained DNA strands (Lawley *et al.*, 2002; Llosa *et al.*, 2002). Conjugative plasmids belonging to the incompatability group HI1 (IncHI1) are large low-copy plasmids that are capable of self-transmission between *Enterobacteriaceae* and other Gram-negative bacteria. This conjugation is thermosensitive with optimum transfer occurring between 22°C and 30°C, but repressed at higher temperatures (Taylor and Levine,

1980). Throughout this study conjugation was used to transfer IncHI1 plasmid plasmid pSf-R27 and its mutant derivatives between strains of *S. flexneri*, *S.* Typhimurium and *E. coli* K-12.

Conjugation assays were performed by a method similar to that detailed in Taylor and Levine (1980). Donor and recipient strains were grown overnight without shaking at either 30°C or 37°C in L-broth. To 500 µl of L-broth, 1 ml of recipient culture and 200 µl of donor culture were added and the mating mixture incubated without shaking in a water bath at either 30°C or 37°C. After 24 h incubation, the mating mixture was plated onto media selecting for transconjugants and donors, and the mating frequency calculated as the number of transconjugants per donor cell. Assays were performed in duplicate and the data expressed as the means of two measurements. Experiments were performed on at least five independent occasions.

2.7 Transformation of bacterial cells with plasmid DNA

Plasmid DNA was transformed by two different methods as described in Ausubel *et al.* (1990). Recipient cells were either made competent by treatment with calcium chloride coupled with a heat-shock uptake of plasmid DNA, or were transformed by electroporation, a high-voltage electroshock treatment. Greater transformation efficiencies can be achieved with electroporation (up to 10^{10} transformants μg^{-1} DNA; Ausubel *et al.*, 1990) than can be obtained with the $CaCl_2$ method (typically 5×10^6 transformants μg^{-1} DNA; Sambrook, 1989). The $CaCl_2$ method was used for routine transformation of *E. coli* or *S.* Typhimurium with plasmid DNA or ligation mixes. Electroporation was used for transformation of *S. flexneri* cells as virulence gene deletion or rearrangement can occur as a result of $CaCl_2$ transformation into this strain (Porter and Dorman, 1997b).

2.7.1 Preparation of calcium chloride-competent cells

An overnight culture of the strain to be made competent for transformation was used to inoculate 100 ml of L-broth and grown to an OD_{600nm} ~ 0.3. The cells were pelleted by centrifugation at 5,858 ×*g* for 10 min, and the bacterial pellet resuspended in 100 ml of ice-cold $CaCl_2$ solution (60-mM $CaCl_2$, 15% glycerol, 10-mM PIPES, pH 7). After incubation on ice for 30 min, cells were again harvested as described above, and resuspended in 50 ml ice-cold $CaCl_2$ solution. Following another 30-min incubation on ice, cells were again collected and resuspended in 2 ml ice-cold $CaCl_2$ solution. At this stage cells were distributed into 200 µl aliquots and used directly, or snap-frozen on dry ice and stored at –70°C.

2.7.2 Transformation of calcium chloride-competent cells

DNA (0.1–1 µg), to be transformed in a volume not exceeding 10 µl, was added to the 200 µl aliquot of competent cells and left on ice for 30 min, thus allowing the DNA to contact the bacterial surface. The tubes were then placed in a 42°C water bath for 2 min before returning to ice for 2 min. This heat-shock treatment allows uptake of the plasmid DNA through the $CaCl_2$-induced competent bacterial membrane by an unknown mechanism (Mandel and Higa, 1970). To the culture 1 ml of SOC broth was added and this then incubated at 37°C for 1 h to allow phenotypic expression of the plasmid-borne antibiotic resistance marker. Subsequently, 10 µl and 100 µl samples of the transformation mix were plated onto appropriate selection plates. Cells to which no DNA had been added were treated in the same way and thus served as a control for contamination. Following overnight incubation at 37°C, single colony transformants were purified on fresh selective agar plates.

2.7.3 Preparation of electrocompetent cells

Typically 100 µl of an overnight culture of the strain to be made electrocompetent for transformation was used to inoculate 100 ml of L-broth and grown to an OD_{600} ~ 0.4. The cells were pelleted by centrifugation at 5,858 ×*g* for 10 min and the bacterial pellet resuspended in 100 ml of sterile, ice-cold Water Analar™ (BDH, 0.1 $\mu S.mm^{-1}$). After 30 min incubation on ice, cells were again pelleted and resuspended in 100 ml cold Water Analar™

(BDH, 0.1 $\mu S.mm^{-1}$), and further incubated on ice for 30 min. Following another centrifugation step, cells were resuspended in 50 ml of ice-cold 10% (v/v) glycerol, incubated on ice for 20 min, pelleted, and finally resuspended in 2 ml of cold 10% (v/v) glycerol. Aliquots (45 µl) were used directly or snap frozen on dry ice and stored at –70°C.

2.7.4 Transformation of electrocompetent cells

The DNA to be electroporated (50–200 ng in 2 µl sterile water) was added to the 45 µl aliquot of electrocompetent cells and incubated on ice for 2 min. The mixture was then transferred to a pre-chilled electroporation cuvette (EquiBio, 2 mm gap width). The cuvette was placed in the Gene Pulser chamber (Bio-Rad) and an electroshock delivered. To the cuvette 1 ml of pre-warmed SOC broth was added and the contents transferred to a sterile tube and incubated at 37°C with aeration for 1 h. This incubation allows phenotypic expression of the antibiotic resistance marker. Subsequently, 10 µl and 100 µl of the transformation mix were plated onto appropriate selection plates. Cells to which no DNA had been added were treated in the same way and thus served as a control for contamination. Following overnight incubation at 37°C, transformants were single colony purified.

2.8 Assays based on spectrophotometry

2.8.1 Monitoring bacterial growth

The growth of bacterial cultures was monitored by measuring the optical density of the culture at a wavelength of 600 nm (OD_{600nm}). For routine measurement of OD_{600nm}, including estimation of cell quantity for β-galactosidase assays (Section 2.8.2), 0.1–1 ml of the culture was transferred into a plastic disposable cuvette (Greiner), and brought to a final volume of 1 ml with L-broth or MM 5.8 broth as necessary. The OD_{600nm} value was measured in a spectrophotometer against a cuvette containing only L-broth or MM 5.8 broth as a blank. This value was linear in the range 0.1–0.8 and was multiplied by the dilution factor if necessary.

2.8.2 Assay of β-galactosidase activity

Transcriptional levels were routinely quantified by the β-galactosidase assay in which the *lac* genes are placed under the regulatory control of the promoter of a target gene. The transcriptional activity of the promoter are reflected in levels of the stable β-galactosidase enzyme, the product of the *lacZ* gene (Miller, 1992). In bacterial cells β-galactosidase cleaves the β-galactoside linkage of lactose, resulting in the formation of galactose and glucose. The resulting products, glucose and galactose then enter the glycolytic pathway. Several synthetic substrates such as ONPG (*o*-nitrophenyl-β-D-galactopyranoside) and X-gal contain the β-galactoside linkage and thus can be hydrolyzed by β-galactosidase. In the case of ONPG, which is colourless, cleavage results in the production of galactose, and *o*-nitrophenol, which is intensely yellow. Therefore, assaying the concentration of *o*-nitrophenol reports on the cellular level of β-galactosidase, which is determined by the activity of the target promoter.

The β-galactosidase assay used in this study was a modified, scaled-down version of the protocol of Miller (1992). The bacterial culture (75 µl) to be assayed was transferred in duplicate into tubes containing 675 µl Z-buffer, 50 µl $CHCl_3$ and 25 µl of 0.1% SDS. Tubes were vortexed briefly to enhance permeabilisation, and then incubated for 5 min at 28°C before addition of 150 µl of ONPG [4 mg ml^{-1} in Water Analar™ (BDH, 0.1 µS.mm^{-1})]. Incubation was continued until a straw yellow colour (*o*-nitrophenol) was obtained (typically corresponding to an OD_{420nm} reading ~ 0.1–0.6). The reaction was stopped with the addition of 375 µl 1-M Na_2CO_3, and the tubes were at 16,000 ×*g* for 10 min to pellet cellular debris. Of the supernatant fraction 1 ml was transferred into a plastic cuvette and the OD_{420nm} determined. The amount of β-galactosidase activity was expressed in arbitrary Miller units calculated as follows:

$$\text{Activity (Miller units)} = \frac{750 \times OD_{420nm}}{t \times v \times OD_{600nm}}$$

t = Reaction time in min (from addition of ONPG to addition of Na_2CO_3)

v = Volume of cells added in ml

Each assay was performed in duplicate, and the mean values were determined from at least 3 independent experiments. Standard deviations were typically less than 10%.

Z buffer: 60-mM $Na_2HPO_4.2H_2O$, 40-mM $NaH_2PO_4.2H_2O$, 50-mM β-mercaptoethanol, 10-mM KCl, 1-mM $MgSO_4.7H_2O$ in Water Analar™ (pH 7)

2.8.3 Determination of nucleic acid concentration

The concentrations of DNA and RNA samples were determined spectrophotometrically by measuring the absorbance at 260 nm. Samples were diluted (typically 1:300) in diethylpyrocarbonate (DEPC) treated-Water Analar™ (BDH, 0.1 $\mu S.mm^{-1}$), placed into a quartz cuvette and the A_{260nm} measured. The quartz cuvette was washed twice with DEPC-treated Water Analar™ (BDH, 0.1 $\mu S.mm^{-1}$) between samples, and each sample was measured in duplicate. The concentration of nucleic acid was then determined according to the following formulae:

A_{260nm} value of 1 corresponds to - 50 $\mu g\ ml^{-1}$ of double-stranded DNA

40 $\mu g\ ml^{-1}$ of single-stranded DNA or RNA

The purity of DNA or RNA was assessed by measuring the A_{280nm}. For pure DNA, uncontaminated by proteins or residual phenol, the ratio of A_{260nm} to A_{280nm} is 1.8, while for RNA uncontaminated by proteins or residual phenol, the ratio of A_{260nm} to A_{280nm} is 2 (Sambrook, 1989).

2.8.4 Determination of protein concentration by the Bradford assay

Protein concentration was determined using a Bio-Rad Protein Assay, which is based on the method of Bradford (1967) and measures the differential colour change (shift in absorbance from 465 to 595 nm) of Coomassie Brilliant Blue G-250 upon protein binding. The concentrations of His-tagged purified Sfh, StpA and H-NS and protein cell lysates were

determined by measuring several serial dilutions of the protein or lysate of interest. The resulting OD_{595nm} measurements were compared to a standard curve determined by measuring several known concentrations of lysozyme, which has a similar molecular mass as Sfh, StpA and H-NS.

2.9 Flow cytometric analysis

Throughout this study flow cytometric analysis was used to monitor gene expression using a green fluorescent protein (GFP)-based assay, in which the *gfp* gene is placed under the regulatory control of the promoter of a target gene. The GFP protein from *Aequoria victoria* (the Pacific crystal jellyfish) is naturally fluorescent without any exogenous cofactor or substrate, when viewed under ultraviolet light (Chalfie *et al.*, 1994). Therefore, assaying the level of fluorescence by flow cytometry, reports on the cellular level of GFP, which is determined by the activity of the target promoter.

The GFP assay used in this study was based on that detailed in Hautefort *et al.* (1997). The bacterial culture (100 µl) to be assayed was harvested in duplicate and immediately fixed at room temperature in 1 ml 4% (w/v) formaldehyde (Sigma) freshly prepared in PBS and then stored at 4°C in the dark until analysis. For flow cytometric analysis, samples were diluted to a concentration of approximately 10^6 bacteria per ml, transferred into flow cytomter tubes and analysed with an EPICS-XL flow cytometer (Beckman Coulter). Approximately 10,000 bacteria were collected per sample and the relative GFP fluorescence expressed as the mean fluorescence of the populations after analysis with EXPO-32 software (Beckman Coulter). Each assay was performed in duplicate, and the mean values were determined from at least 3 independent experiments.

2.10 Isolation of RNA, plasmid DNA and chromosomal DNA

2.10.1 Isolation of RNA

RNA is a chemically unstable molecule and prone to digestion by ubiquitous RNases which require no cofactors to function, and can maintain activity even after autoclaving or boiling (Sambrook, 1989). For these reasons certain precautions were used when isolating or handling RNA. These included wearing gloves, using RNase-free tips and tubes (Orange Scientific), and separate designated electrophoresis tanks. All solutions were prepared with DEPC-treated Water Analar^{TM} (BDH, 0.1 $\mu S.mm^{-1}$), which inactivates RNases by covalent modification (1 ml DEPC L^{-1} Water Analar^{TM}, mixed overnight then autoclaved). In addition, where possible, all steps in the isolation of bacterial RNA were performed quickly, and on ice.

Total RNA for use in Northern blotting, Reverse Transcription PCR (RT-PCR) and microarray analysis was isolated using Tri Reagent^{TM} (Sigma). Tri Reagent^{TM} (Sigma) is a quick and convenient reagent for use in simultaneous isolation of RNA, DNA and protein and is based on the method of Chomczynski (1993). Total RNA extracts were prepared by harvesting 6 OD_{600nm} units of bacteria and RNA isolated using Tri Reagent^{TM} (Sigma) according to the guidelines provided. Briefly, the reagent is a mixture of guanidine thiocyanate and phenol in a mono-phase solution that effectively dissolves RNA, DNA and protein on homogenization. Following the addition of chloroform (300 µl) to the reagent (1.5 ml), the mixture is centrifuged at 16,000 ×*g* for 15 min, which allows separation into three phases: an aqueous phase (containing RNA), the interphase (containing DNA) and an organic phase (containing protein). Total RNA was isolated from the aqueous (top) layer by precipitation with isopropanol (750 µl) and washed with 70% (v/v) ice-cold ethanol. Following resuspension in 100 µl DEPC-treated Water Analar^{TM} (BDH, 0.1 $\mu S.mm^{-1}$), RNA was then DNase treated using the DNA-*free*^{TM} kit (Ambion Inc.) to ensure no DNA contamination. RNA concentration and purity was assessed by A_{260nm} and A_{280nm} measurements as described in Section 2.8.3.

2.10.2 Small-scale isolation of plasmid DNA

The Wizard Plus *SV* Miniprep Kit (Promega) was routinely used to extract plasmid DNA from 3 ml of cultures according to the guidelines provided. The procedure is based on a modified alkaline lysis method of Isch-Horowicz and Burke (1981), where bacteria are lysed and proteins denatured (SDS) in the presence of protease inhibitors. RNA is then degraded (RNase), and chromosomal and plasmid DNA denatured (NaOH). The lysis mixture is then neutralised with salts, causing protein and chromosomal DNA precipitation. Plasmid DNA rapidly re-anneals and debris is pelleted by centrifugation. The supernatant fraction containing plasmid DNA is washed and desalted through a mini-column, and eluted in 100 µl Water Analar^{TM} (BDH, 0.1 $\mu S.mm^{-1}$).

2.10.3 Large-scale isolation of plasmid DNA

The QIAGEN midi-plasmid purification kit was used to extract plasmid DNA from 100 ml overnight bacterial cultures, according to the guidelines provided. Purification is based on a modified alkaline lysis procedure similar to that described in Section 2.10.2, followed by binding of plasmid DNA to a column-based anion-exchange resin under low salt and pH conditions. A medium salt wash removes RNA, proteins, and other impurities, and the plasmid DNA is eluted with a high-salt buffer. The DNA is then precipitated with isopropanol, desalted, and resuspended in 100 µl Water Analar^{TM} (BDH, 0.1 $\mu S.mm^{-1}$).

2.10.4 Purification of genomic DNA

Purification of genomic DNA for Southern blot analysis and PCR was performed using the AGTC Bacterial Genomic DNA Purification Kit (Edge Biosystems). A 5 ml sample of an overnight culture was used for DNA extraction according to the guidelines provided. Briefly, the procedure involves conversion of bacteria to sphaeroplasts (spherical cells from which most of the cell wall is removed) by incubation in a Tris-buffered solution containing lysozyme (cleaves peptidoglycan), sucrose (osmotic stress), and EDTA (chelates divalent metal ions, which are necessary cofactors for protease and DNase activity). Efficient lysis is then achieved by heating to 65°C in the presence of SDS (protein denaturant) and NaCl

(osmotic shock) supplemented with RNase. Latex beads are added that bind and clump denatured proteins and cellular debris. The mixture is centrifuged (debris pellets) and genomic DNA is extracted from the supernatant fraction by precipitation with isopropanol. Genomic DNA is desalted, dried and uniformly resuspended in a final volume of 100 µl Water Analar™ (BDH, 0.1 µS.mm^{-1}).

2.11 Manipulation of DNA *in vitro*

2.11.1 Restriction endonuclease cleavage of DNA

Typically 0.5–2.0 µg of plasmid DNA or purified PCR product was cut with 10 U of restriction enzyme in a 50 µl volume containing the reaction buffer supplied with the enzyme. For double digests involving simultaneous cleavage of DNA by two endonucleases, a suitable buffer was chosen in which both enzymes had >75% activity. Alternatively, double digests were performed sequentially in suitable buffers with ethanol precipitation and/or purification (Section 2.11.2) of the DNA between digestions. Reactions were incubated at 37°C for 1–2 h unless otherwise recommended.

2.11.2 Purification of linear DNA

Linear DNA fragments (PCR products or cleaved DNA) were purified for cloning using the Wizard PCR Prep DNA purification system (Promega). The linear DNA fragments were purified directly, or from an agarose gel slice. For this, the DNA was electrophoresed through a 1× TAE agarose gel containing 1 µg ml^{-1} of ethidium bromide. The desired DNA fragment was cut out using a surgical blade and purified following the guidelines supplied. Briefly, the procedure entails mixing DNA (from PCR reactions or a gel slice) in a buffer that provides the ions and environment where DNA is selectively bound with high affinity to a silica-based resin. The resin is then trapped in a mini-column and macromolecules, primers, salts and other impurities removed by washing with 80% isopropanol. The resin is dried and DNA is eluted in 30–100 µl Water Analar™ (BDH, 0.1 µS.mm^{-1}).

2.11.3 Ethanol precipitation of DNA/RNA

Unless otherwise stated ethanol precipitation of DNA/RNA samples was performed as follows: 0.1 volumes of 3-M sodium acetate (pH 5.2) and 2.5 volumes of 100% ethanol were added to the nucleic acid suspension. The contents of the tube were incubated on ice for 30 min before centrifugation 16,000 ×*g* for 30 min. The pellet was then washed in 500 µl of 70% (v/v) ethanol and resuspended in a suitable volume of Water Analar™ (BDH, 0.1 $\mu S.mm^{-1}$).

2.11.4 Ligation of DNA molecules

T4 DNA ligase catalyses the ATP-dependent formation of phosphodiester bonds between adjacent 5′-phosphoryl and 3′-hydroxyl ends in double-stranded DNA. Bacteriophage T4 DNA ligase supplied with the Rapid DNA ligation Kit (Roche Molecular Biochemicals) was routinely used to clone digested insert DNA into appropriately digested vectors according to the manufacturer's directions. Reactions were performed by incubating an estimated molar ratio of purified vector:insert DNA (1:3 for sticky ends, 1:5 for blunt ends) in a 20 µl volume with 1 µl of T4 DNA ligase. (DNA quantity was estimated by electrophoresing through a 1× TAE agarose gel and comparing band intensity to known standards). The mixture was incubated at room temperature for 20 min and typically a 10 µl sample was directly transformed into appropriate calcium-chloride competent cells.

2.12 Polymerase Chain Reaction

The polymerase chain reaction (PCR) was used for the amplification of DNA for preparation/confirmation of fragments during cloning strategies, and for generating probes for electrophoretic mobility shift assays or Southern blot analyses. The PCR method is based on the ability of a thermostable DNA polymerase to amplify DNA, primed from oligonucleotides annealed to denatured single-stranded templates (Saiki *et al.*, 1988). The procedure involves thermal denaturation of the DNA template, allowing two specific oligonucleotides to hybridize to complementary sequences on opposite strands of the DNA, flanking the sequence

to be amplified. The annealed primers are orientated with their 3′-ends facing each other, such that DNA polymerase in the presence of dNTPs and Mg^{2+} will extend across the region of the original DNA template between the primers. Each synthesized strand is complementary to one of the primers, and can serve as template in further cycles of annealing and extension. The denaturation, annealing and extension steps are repeated for 25–35 cycles resulting in exponential amplification of the DNA region of interest.

2.12.1 Amplification of DNA

Two different thermostable polymerases were used in this study. *Taq* DNA polymerase (New England BioLabs) is a highly processive 5′–3′-DNA polymerase purified in recombinant form, free of endo- or exo-nucleases (Sambrook and Russell, 2001). *Taq* polymerase lacks a 3′–5′ exonuclease activity (proof-reading) and was routinely used for PCR when it was unimportant if the product contained mutations, for example when checking plasmids for cloned inserts. *Pfx* polymerase (Gibco BRL) is also a highly processive 5′–3′-DNA polymerase, free of endo- or exo-nucleases. *Pfx* harbours a 3′–5′ proof-reading exonuclease activity resulting in a reduced error rate of nucleotide misincorporation. *Pfx* polymerase was used for the amplification of probes for electrophoretic mobility shift assays, and for amplification of DNA fragments for cloning purposes.

PCR reactions were carried out by mixing 5 µl 10 × *Pfx* buffer, 0.2 mM of each dNTPs, 100 pmol of each oligonucleotide, 1 U of *Pfx* polymerase, 1–3 mM $MgSO_4$, 10–100 ng template DNA, and Water Analar™ (BDH, 0.1 $\mu S.mm^{-1}$) to a final volume of 50 µl in a 500 µl thin-walled PCR tube (Stratagene). PCR reactions using *Taq* DNA polymerase were performed as above, with the exception that 5 µl 10 × *Taq* buffer (includes 1.5-mM $MgCl_2$) and 1 U *Taq* polymerase were used. Reactions were set-up on ice and immediately placed into the Peltier Thermal Cycler. One tube contained no template DNA and served as a negative control. Routinely the reaction cycles were as follows:

1. 94°C, 2 min [denaturation]
2. oligo annealing temperature[a], 30 sec
3. 72°C, 1 min [extension[b]]
4. 94°C, 1 min [denaturation]
5. steps 2–4 above repeated, 30 cycles
6. 72°C, 10 min [final extension and renaturation]

[a]The annealing temperature was typically set at 4°C below the theoretical melting temperature (Tm) of the oligonucleotides being used. The Tm was calculated using the formula Tm = 2 × (A+T) + 4 × (G+C), where A, T, G and C refer to the base composition of the oligonucleotide (Sambrook and Russell, 2001).

[b]Extension time depended on expected length of PCR product (~1 min per kb).

DNA sequences were amplified from purified chromosomal or plasmid DNA (Section 2.10). PCR amplification was also carried out using template DNA from a cell lysate. Here, a single colony was scrapped from the agar plate with a plastic tip and resuspended in 100 µl Water Analar™ (BDH, 0.1 $\mu S.mm^{-1}$), boiled for 5 min, and 2 µl used for each PCR reaction.

2.13 Reverse Transcription Polymerase Chain Reaction

Reverse transcription polymerase chain reaction (RT-PCR) was used to determine the relative level of abundance and stability of RNA transcripts of specific genes of interest. RT-PCR analyses was performed using the Onestep RT-PCR kit (Qiagen), following the guidelines supplied. The kit contains optimized components that allow both reverse transcription and PCR amplification to be performed sequentially in the one tube. Reverse transcription is based on the ability of the enzyme, reverse transcriptase, to synthesis a DNA strand that is complementary to an RNA template. Subsequently, the newly synthesized complementary DNA (cDNA) acts as template for PCR as described in Section 2.12.1.

2.13.1 cDNA synthesis and amplification

The Onestep RT-PCR enzyme mix contains two reverse transcriptases, Omniscript and Sensiscript, which allow the reverse transcription of RNA amounts greater and less than 50 ng, respectively. The enzyme mix also contains a HotStar *Taq* DNA polymerase, which is completely inactive during the reverse transcriptase reaction. Following the reverse transcriptase step, RT-PCR reactions are heated to 95°C for 15 min to activate HotStar *Taq* DNA polymerase and simultaneously inactivate the reverse transcriptases.

RT-PCR reactions were carried out by mixing 5 µl 5 × Onestep RT-PCR buffer, 0.2 mM of each dNTPs, 30 pmol of each oligonucleotide, 2 µl of Onestep RT-PCR enzyme mix, 1.2 µg DNA-free RNA (Section 2.10.1) as template and RNase-free water to a final volume of 25 µl in a 500-µl thin-walled PCR tube (Stratagene). Reactions were set-up on ice and immediately placed into the Peltier Thermal Cycler. One tube contained no template RNA and served as a negative control. Routinely the reaction cycles were as follows:

1. 50°C, 30 min [reverse transcription]
2. 95°C, 15 min [activation DNA polymerase, inactivate reverse transcriptases]
3. 94°C, 30 sec [denaturation]
4. oligo annealing temperature[a], 30 sec
5. 72°C, 1 min [extension[b]]
5. steps 3–4 above repeated, 20 cycles[c]
6. 72°C, 10 min [final extension and renaturation]

[a]The annealing temperature was typically set at 4°C below the theoretical melting temperature (Tm) of the oligonucleotides being used. The Tm was calculated using the formula Tm = 2 × (A+T) + 4 × (G+C), where A, T, G and C refer to the base composition of the oligonucleotide (Sambrook and Russell, 2001).

[b]Extension time depended on expected length of PCR product (~1 min per 500 bp).

[c] Range of cycles was performed for each transcript of interest to optimize RT-PCR reaction and avoid saturation.

The RT-PCR products were electrophoresed through 1 × TAE agarose gels containing 1 μg ml^{-1} of ethidium bromide and then quantified by densitometry using Quantity-One software (BioRad, Hercules Ca.)

2.13.2 RNA stability assay

The stability of *sfh* mRNA was determined based on a method described previously, which utilizes the antibiotic rifampicin to inhibit transcription (Deighan *et al.*, 2000). Briefly, cells were cultured to exponential phase (OD_{600nm} = ~ 0.2) or early stationary phase (OD_{600nm} = ~ 1.5) and treated with rifampicin (250 μg ml^{-1}) to inhibit transcription. Total RNA was then isolated (Section 2.10.1) in a time-course experiment and *sfh* mRNA stability followed by RT-PCR (Section 2.13.1) using the primer pair sfh-FRT and sfh-RRT (Table 2.3). Experiments were performed on at least three independent occasions.

2.14 Gel electrophoresis

2.14.1 Agarose gel electrophoresis

Electrophoresis through agarose gels was routinely used in this study to separate DNA molecules for size and concentration analysis and for purification of DNA fragments. The size and the percentage of the gel depended on the number of samples and the resolution required. Two different sizes were typically used, mini- (5.9 × 8.3 cm) and midi- (11.0 × 15.0 cm) gels, requiring 20 and 100 ml of TAE-agarose gel solution respectively. The gel solution was prepared from electrophoresis grade agarose (Roche Molecular Biochemicals) and the required volume of 1 × TAE (40-mM Tris, 1-mM EDTA, 0.114% (v/v) glacial acetic acid) and heated to 100°C. Ethidium bromide was added just prior to pouring, giving a final concentration in the gel of 1 μg ml^{-1}. Ethidium bromide intercalates the DNA and fluoresces

strongly in long wavelength UV light. Samples were mixed with Promega's Blue/Orange 6 × loading dye (10-mM Tris pH 7.5, 15% Ficoll® 400, 0.03% bromophenol blue, 0.03% xylene cyanol FF, 0.4% orange G, and 50-mM EDTA) and loaded alongside a known DNA size ladder. Gels were typically run at 50–100 V and recorded by photography using a UVP camera coupled to a thermal imaging system.

2.14.2 SDS-PAGE

Proteins were separated by discontinuous 12% polyacrylamide gel electrophoresis as described in Sambrook (1989). The discontinuous buffer system uses buffers of different pH and composition in the stacking and separating gels. Consequently protein migration through the large pores in the stacking gel (5% acrylamide) is fast and the proteins become concentrated into a narrow band. However, migration through the narrow pores of the separating gel (12% acrylamide) is according to size. Both gels were prepared with 0.1% SDS. Since most proteins bind SDS in a constant weight ratio, this leads to identical charge densities for denatured proteins, and allows proteins to migrate according to size, not charge.

Gel plates were cleaned before use and a 12% separating gel prepared by mixing 2 ml Protogel (National Diagnostics), 1.25 ml of 1.5-M Tris-HCl (pH 8.8), 50 µl 10% SDS, and 1.7 ml of Water Analar™. Polymerization was catalyzed by the addition of 50 µl 10% (w/v) ammonium persulphate and 5 µl of TEMED. The solution was then poured between the plates until 1 cm below the tip of the comb and immediately overlaid with 200 µl ethanol (excludes oxygen) and allowed to polymerize for 30 min. The 5% stacking gel was made by the mixing of 0.833 ml Protogel (National Diagnostics), 1.25 ml 0.5-M Tris-HCl (pH 6.8), 50 µl 10% SDS and 2.87 ml of Water Analar™. The gel was electrophoresed in 1 x Tris-glycine running buffer (25-mM Tris-HCl, 250-mM glycine (pH 8.3), 0.1% (w/v) SDS). Prior to loading, protein samples (Section 2.14.3) were denatured at 95°C for 10 min and then centrifuged at 16,000 ×*g* for 1 min. Electrophoresis was performed at 150 V for 60–90 min in the Mini-Protean system (Bio-Rad).

2.14.3 Preparation of total cellular extracts

Total protein extracts for SDS-PAGE and Western immunoblot analysis were prepared as described below. The OD_{600nm} of each culture was measured. A volume of cells, which corresponded to 2 ml of culture per 1 OD_{600nm} unit, was harvested. The pellet was washed in PBS and snap-frozen on dry ice. The pellets were then resuspended in 50 µl B-PER reagent (Pierce) supplemented with lysozyme (500 µg ml^{-1}) and DNase I (100 U ml^{-1}) and left at room temperature for 15 min. Protein concentration of the lysates was determined using the Bradford assay (Section 2.8.4). To samples 50 µl of 2 × SDS loading buffer (150-mM Tris-HCl (pH 6.8), 1.2% (w/v) SDS, 30% (v/v) glycerol, 15% (v/v) β-mercaptoethanol) were then added and samples boiled at 95°C for 10 min. Typically 10 µl of this protein extract was used for immuno-detection in Western immunoblot analyses.

2.14.4 Staining of proteins

Gels were washed in Water Analar™ (BDH, 0.1 $\mu S.mm^{-1}$) prior to staining with GelCode Blue Stain Reagent (Pierce) for 1 h according to the guidelines supplied. Gels were then destained in Water Analar™ (BDH, 0.1 $\mu S.mm^{-1}$). This stain uses the colloidal properties of Coomassie G-250 for protein binding and staining, but has no affinity for the polymerized gel, thus protein bands appear blue against a clear background.

2.15 Western immunoblot analysis

Western immunoblotting is a sensitive technique whereby proteins (antigens) are solubilised with SDS and 2-β–mercaptoethanol (Section 2.14.3) and separated by SDS-PAGE (Section 2.14.2), before being irreversibly transferred to a nitrocellulose membrane (Section 2.15.1). The membrane is incubated with an antigen-specific primary antibody, and the antigen–antibody complexes detected with a secondary antibody and revealed by a chemiluminescent assay (Section 2.15.2).

2.15.1 Transfer of proteins to nitrocellulose membrane

Following SDS-PAGE (Section 2.14.2), gels were electroblotted to 0.2-mm PROTAN nitrocellulose membrane (Schleicher and Schuell) using a Mini Trans-blot electrophoretic transfer cell (Bio-Rad) filled with transfer buffer (25-mM Tris, 192-mM glycine, 20% (v/v) methanol) at 80 V for 2 h at 4°C. Equal protein loading and consistent transfer to the nitrocellulose membrane were confirmed by staining the membrane with Ponceau S solution (2 g Ponceau S (Sigma), 1 ml glacial acetic acid) for 5 min followed by extensive washing with Water Analar™ (BDH, 0.1 $\mu S.mm^{-1}$).

2.15.2 Detection of bound antigens

Nitrocellulose membranes were blocked for 1 h in blocking buffer [5% (w/v) nonfat dry milk, in phosphate-buffered saline (PBS)]. Anti-StpA (1:1000), anti-Sfh (1:1000), anti-H-NS (1:1000, a generous gift from from E. Bremer, University of Konstanz, Germany), anti-FliC (1:1000, Becton Dickinson) or anti-RpoS (1:3000, a generous gift from R. Hengge, University of Berlin, Germany) antisera were diluted appropriately in blocking buffer and incubated with the membrane for 1 h at room temperature. The membrane was washed 3 × 10 min with PBS and then incubated in blocking buffer containing horseradish-peroxidase (HRP)-conjugated anti-rabbit IgG (Cell Signalling) for 1 h. The blot was washed as before, and in the presence of a suitable chemiluminescent substrate (Pierce SuperSignal), the HRP-mediated enzymatic reaction results in a luminescent signal that visualizes the antigen-antibody complex, which can by detected by autoradiography (Section 2.18). Typical exposures were from 30 sec to 15 min.

2.15.3 Protein stability assay

The stability of Sfh protein was determined using a method described previously, which utilizes the antibiotic spectinomycin to inhibit translation (Geuskens *et al.*, 1992; Johansson and Uhlin, 1999; Johansson *et al.*, 2001). Briefly, cells were cultured to exponential phase (OD_{600nm}= ~0.3) or early stationary phase (OD_{600nm}= ~0.5) and treated with spectinomycin (200 $\mu g\ ml^{-1}$) to inhibit translation. Protein samples were then isolated (Section 2.14.3) in a

time-course experiment and Sfh protein stability monitored by Western blotting (Section 2.15). Experiments were performed on at least three independent occasions.

2.16 Northern blotting

The principle of Northern blotting is that a transcript within immobilized RNA can be quantified after hybridization with a specific probe. This technique was used to investigate the relative level of abundance of the *sfh* RNA transcript as a function of growth phase and the presence or absence of StpA and H-NS. The procedure involves resolution of an RNA sample by denaturing gel electrophoresis (Section 2.16.1) and then transfer of the resolved RNA to nylon membrane (Section 2.16.2). The membrane is hybridized with a transcript-specific Dioxigen (DIG)-labelled riboprobe (Section 2.16.3) and then the RNA-riboprobe complex detected by a chemiluminescent assay (Section 2.16.4).

2.16.1 Denaturing electrophoresis of RNA

RNA molecules can contain a high degree of secondary structure and are consequently electrophoresed under denaturing conditions. In this study, formaldehyde was used as the denaturant for agarose gel electrophoresis. Electrophoresis was done using pre-cast denaturing 1.25% Reliant agarose gels (FMC). Samples of total RNA (5 μg), prepared as described in Section 2.10.1, were denatured prior to loading in 3 volumes of denaturing solution (50% formamide, 1 × MOPS) at 70°C for 5 min, transferred to ice for 5 min, then loaded with 2 μl of Promega's Blue/Orange 6 × loading dye. Gels were run in 1 × 4-morpholinepropanesulphonic acid (MOPS) buffer at 100 V for 1–3 h.

10 × MOPS: 41.85 g MOPS, 6.8 g Sodium acetate.3 H_2O, 20 ml 0.5-M Na_2EDTA, made to 1 L with DEPC-treated Water Analar™ (BDH, 0.1 $\mu S.mm^{-1}$), pH 7.0

2.16.2 Transfer of resolved RNA to nylon membrane

After electrophoresis the resolved RNA was transferred to 0.45 μm Biodyne B nylon membrane (PALL) by overnight capillary transfer according to the method outlined in Sambrook (1989). RNA was immobilized on the membrane after transfer by UV-crosslinking.

2.16.3 DIG riboprobe synthesis

RNA probes (riboprobes) for use in Northern blot analysis were synthesized from plasmids p18sfh and p18rrnA (Table 2.2) by *in vitro* transcription using the DIG RNA Labelling Kit (Roche Molecular Biochemicals) following the guidelines supplied. The fragment of DNA corresponding to the probe of interest was cloned into vector pSPT18 (Roche Molecular Biochemicals). This plasmid has T7 and SP6 phage promoters either side of the multiple cloning site. The plasmid was then linearised appropriately (defines length of probe), such that following T7-based transcription an antisense probe to the RNA transcript of interest is synthesized. The reaction is carried out in the presence of DIG-dUTP as a component of the dNTP mix, which is incorporated into the riboprobe. Typically 1 μl of riboprobe was used per 10 ml hybridisation solution.

2.16.4 Hybridization and detection of DIG probe

Hybridization and detection of DIG-labelled RNA or DNA probes (used for Southern blotting, Section 2.17) were carried out following the detailed instructions in the DIG Systems User's Guide for Filter Hybridization (1995). Briefly, the procedure involves overnight incubation of the probe with the nylon membrane at 68°C. Non-specific hybridized probe is removed by a series of stringency washes (decreasing salt concentration, increasing temperature). Following 30-min incubation with blocking solution (DIG Wash and Block Buffer Set, Roche Molecular Biochemicals), the membrane is then incubated with an anti-DIG alkaline phosphatase (AP)-antibody conjugate (anti-DIG-AP-conjugate, Roche Molecular Biochemicals), which recognizes the immobilised DIG moiety that is incorporated into the probe. In the presence of a suitable chemiluminescent substrate (CDP-Star, Roche

Molecular Biochemicals), the AP-mediated enzymatic dephosphorylation reaction results in a luminescent signal that visualizes hybridized molecules by autoradiography (Section 2.18).

2.17 Southern blotting

The basic principle of Southern blotting (Southern, 1975) involves separation of DNA by agarose gel electrophoresis, which is then denatured *in situ* and transferred to a nylon membrane (Section 2.17.1). Immobilised DNA is hybridised with a Digoxigenin-(DIG) labelled probe (Section 2.17.2) that can be detected by a chemiluminescent immunoassay (Section 2.16.4). This sensitive technique was used to confirm the genetic location of the *sfh* locus and the genetic structure of *sfh* mutants of *S. flexneri* and *S.* Typhimurium following conjugative transfer of plasmid pSf-R27Δ*sfh*::Gent^R.

2.17.1 Electrophoresis, denaturation and transfer of DNA to nylon membrane

Total genomic DNA was isolated from bacterial strains as described in Section 2.10.4 and ~3 μg of undigested DNA was separated by electrophoresis (Section 2.14.1) through a 0.8% midi-sized agarose gel at 40 V for 16 h. The resolved DNA was then depurinated *in situ* (250-mM HCl, 10 min), denatured (1.5-M NaCl, 0.5-M NaOH, 45 min), and neutralised [1.5-M NaCl, 1.5-M Tris-HCl (pH 7.4), 45 min], prior to overnight capillary transfer to Biodyne B nylon membrane (PALL), according to the method outlined in Sambrook (1989). The *in situ* treatment of the DNA allows transfer to proceed more efficiently by cleaving larger fragments, and makes detection more sensitive by denaturing double-stranded DNA. DNA was immobilised on the membrane by UV-crosslinking.

2.17.2 DIG DNA probe synthesis

A DIG-labelled probe was synthesized by PCR (Section 2.12) using the PCR DIG Labelling Mix (Roche Molecular Biochemicals). The mix contains 2 mM-dATP, 2 mM-dCTP, 2-mM dGTP, 1.9-mM dTTP and 0.1-mM DIG-11-dUTP. Of this 5 μl was added to a 50 μl volume PCR reaction instead of standard dNTP mix. The PCR products synthesized incorporate the

DIG-labelled nucleotides. The labelled probes were purified from an agarose gel slice as described in Section 2.11.2, and eluted in a 50 µl volume. Typically 10 µl was used per 10 ml hybridization solution. Hybridization and detection of probe bound to immobilised targets, was carried out as outlined in Section 2.16.4 with the exception that probe was denatured by heating to 95°C for 10 min and then incubated on ice for 10 min prior to use.

2.18 Autoradiography

In this study autoradiography was used to visualize and quantitate on X-ray film non-radioactive chemiluminescent emissions derived from alkaline phosphatase or horseradish peroxidase cleavage of chromogenic reagents (Western, Southern, and Northern blots). In each case X-OMAT UV film (KODAK) was used. When chemiluminescent photon emissions strike a silver halide crystal (X-Ray film is coated with silver halides suspended in gelatin), the crystal absorbs energy and releases an electron. This electron is attracted to a positively charged silver ion forming an atom of metallic silver. After an appropriate time the film was placed into a tray containing diluted Kodak LX-24 X-Ray developer for 3 min, a chemical solution which amplifies the signal by reducing exposed silver halide crystals to metallic silver. The film was washed briefly in water and then fixed in Kodak Industrex liquid fixer for a further 3 min. The fixer serves to convert any silver halide that was not reduced into soluble silver thiosulphate. Developed films were rinsed in a large volume of water and allowed to dry. For quantitative analysis of signal intensity (Northern and Western blotting) several exposures of varying times were taken.

2.19 Bioinformatic analyses

2.19.1 Analysis of DNA curvature

H-NS-like proteins have been reported to show specificity for interacting with curved DNA (Sonnenfield *et al.*, 2001). It was of interest to determine if the various promoters under study

were intrinsically curved. *In silico* curvature analysis of *flgA–flgB*, *hilD, htdA, sfh, sipB, spvA, spvR, sseA*, *ssrA, traH* and *traJ* regulatory regions were performed with the BEND-IT program (http://www.icgeb.org/dna/bend_it.html). The curvature is calculated using the BEND-IT algorithm (Goodsell and Dickerson, 1994) and expressed as degrees per helical turn (10.5°/helical turn = 1°/bp). Curved and straight motifs have a value above or below 5°/helical turn, respectively.

2.19.2 Analysis of RNA structure

The secondary structure of *sfh* mRNA was predicted by the RNA-folding program, Mfold (Mathews *et al.*, 1999; Zuker, 2003) (http://www.bioinfo.rpi.edu/applications/mfold/old/rna/).

2.19.3 Analysis of protein structure

Several computer programs were used to analyse the structure of the TraJ protein. The molecular mass and pI value of TraJ were predicted using the Compute pI/Mw tool (http://ca.expasy.org/tools/pi_tool.html) and functional motifs were identified using Prosite (http://ca.expasy.org/tools/scanprosite), both of which are available on the EXPASY Molecular biology server.

2.19.4 Analysis of protein sequences

The Blast algorithm (Altschul *et al.*, 1990) (http://www.ncbi.nlm.nih.gov/BLAST/) was used to retrieve H-NS-like protein sequences from the genomic databases based on their amino acid sequence similarity to the *E. coli* H-NS protein sequence. Proteins with ≥40% amino acid sequence identity to the *E. coli* H-NS protein were used to construct a cladogram with the Blast Tree View program (Page, 1996).

2.20 Electrophoretic Mobility Shift Assay

The association of recombinant Sfh, H-NS, and StpA proteins (Beloin *et al.*, 2003) with the various promoters under study was investigated using a competitive gel retardation assay

(Bertin *et al.*, 1999). PCR fragments of the various promoters were amplified using *Pfx* polymerase (Gibco-BRL) and purified from agarose gel slices as detailed in Section 2.11.2. Plasmid pBR322 was digested into several fragments with *Taq*1 and *Ssp*I restriction enzymes. One restricted fragment is 217 bp and contains the sequence of the curved *bla* promoter, to which H-NS-like proteins are known to bind (Bracco *et al.*, 1989). The PCR probes and digested plasmid pBR322 were incubated with increasing amounts of purified protein in the range 0–2 μM in a reaction buffer containing 40-mM HEPES (pH 8), 100 mM potassium glutamate, 10-mM magnesium aspartate, 0.022% NP40, 0.1 μg ml^{-1} BSA, and 10% glycerol. The reactions were incubated at room temperature for 15 min and then electrophoresed through 3% (w/v) molecular screening agarose (Roche Molecular Biochemicals). After migration the gels were stained with 1 μg ml^{-1} ethidium bromide and recorded by photography using a UVP camera coupled to a thermal imaging system.

2.21 DNA microarray analysis

DNA microarray analysis was carried out to determine if horizontal transfer of the *sfh* gene on plasmid plasmid pSf-R27 into *S.* Typhimurium could alter gene expression in trans-conjugants. Type 1 DNA microarray analysis (direct comparison of two RNA/DNA samples on the one array) was performed as described previously (Thomson *et al.*, 2004). The PCR product *Salmonella* serovar Typhi CT18 genome array used in this study was provided by J. Wain (Wellcome Trust Sanger Institue, Cambridge, U.K.) and is based on that outlined in Thomson *et al.* (2004). Briefly, the procedure involves isolation of DNA or RNA from control and test strains, which is then fluorescently labelled with Cy3 or Cy5 dyes. In the case of RNA samples, labelling occurs during reverse transcription into cDNA. The DNA is hybridized to the array and detected in a GenePix scanner. Finally results are normalized and imported into the GeneSpring software program for analysis.

2.21.1 Microarray slides

DNA microarrays were printed on amine-binding slides (Codelink™ Activated Slides, Amersham Pharmacia) at room temperature. Each slide contains two arrays, which consist of 48 blocks (each block is 16 × 16) of printed PCR products. After printing, slides are incubated in a humid chamber (70–80%) at room temperature for 24–72 h to drive the covalent reaction between reactive groups on the slide and the 5′-amino groups on the DNA. Slides are then incubated with gentle agitation in 1 % (w/v) ammonium hydroxide for 5 min before being washed for 5 min in 0.1 % SDS and then transferred to boiling water for 2 min to denature the DNA. Once denatured, slides are placed in ice-cold ddH_2O and briefly rinsed in room-temperature ddH_2O followed by centrifugation at 300 ×*g* for 5 min to dry.

2.21.2 RNA isolation

Total RNA extracts were prepared by inoculating 2-litre flasks containing 200 ml volumes of L-broth with 1:100 volumes of overnight cultures of strain SL1344, SL1344(pSf-R27Gent^R) or SL1344(pSf-R27Δ*sfh*::Gent^R) grown without antibiotic selection. Cultures were grown at 37°C with shaking until they reached OD_{600nm}= ~0.6 (exponential phase) or OD_{600nm}= ~2.0 (stationary phase) and then 6 OD_{600nm} units harvested. Total RNA was isolated as described in section 2.10.1. The RNA was quantified (Section 2.8.3), precipitated, and resuspended at a concentration of 1.2 μg μl^{-1} in DEPC-treated ddH_2O. Total RNA extracts were isolated from cultures grown on three independent occasions (RNA for three biological replicates).

The stability of plasmids pSf-R27Gent^R and pSf-R27Δ*sfh*::Gent^R in *S.* Typhimurium strain SL1344 was measured to determine if any segregation-associated plasmid loss took place during the growth conditions used for microarray analysis. Plasmid stability was determined by inoculating 2-litre flasks containing 200 ml volumes of L broth with 1:100 volumes of overnight cultures of strain SL1344(pSf-R27Gent^R) or SL1344(pSf-R27Δ*sfh*::Gent^R) grown without antibiotic selection. The ratio of plasmid-bearing and plasmid-free cells was determined by selective plating at time zero and after 24 h growth at 37°C. Plates were

incubated for 24 h and then scored for colony forming units. Experiments were performed in duplicate on at least three independent occasions.

2.21.3 cDNA synthesis and labelling

In a sterile microfuge tube 16 μg of RNA was incubated with 5 μg of random hexamer primers in a total volume of 15.4 μl using DEPC-treated ddH_2O. To facilitate annealing of the primers to the RNA the mixture was heated to 70°C for 10 min and then cooled on ice, after which 14.6 μl of the following reaction mix was added: 6 μl 5 × buffer, 3 μl 0.1-M DTT, 0.6 μl dNTP mix, 3 μl dCTP-Cy5 or dCTP-Cy3 (Amersham Pharmacia), and 2 μl SuperScript™ II (Invitrogen). Following a 2-h incubation in the dark at 42°C, 1.5 μl 1-M NaOH was added and samples heated to 70°C for 20 min to hydrolyse the RNA. To this 1.5 μl 1-M HCl was then added to neutralize the samples and the resulting labelled cDNA purified using an Autoseq™ G-50 column (Amersham) according to the guidelines provided.

The above describes the reverse transcription and Cy5/Cy3 labelling of enough RNA for one array. Microarrays were carried out in quadruplicate and dye-swap experiments performed for all hybridizations (to correct for any bias in dye incorporation). In each case, SL1344(pSf-R27Gent^R) cDNA was used as the reference strain. Therefore, RNA from each biological replicate resulted in enough Cy5- and Cy3-labelled cDNA for 4 arrays (2 arrays for each dye).

2.21.4 Hybridization and washing of arrays

The hybridization mix for a single array was set up as follows. Of eluted labelled test cDNA 33 μl was added to 33 μl of the oppositely labelled eluted control cDNA, ethanol precipitated and resuspended in 30 μl hybridization buffer (5 × SSC, 6 × Denhardt's solution, 0.12% (w/v) Sarkosyl™, 48% (v/v) formamide and 60-mM Tris-HCl, pH 7.6). To this 2 μl of tRNA (Sigma) and 4 μl of ddH_2O were added. Samples were incubated at 100°C for 5 min then cooled to room temperature for 10 min. Samples were then subjected to centrifugation in a microfuge at 16,000 ×*g* for 5 min. To set up the hybridizations, a piece of filter paper (20 mm

x 70 mm) was moistened with 1.5 ml 15 × SSC and placed at the bottom of the chamber to maintain the correct humidity inside the hybridization chamber (Die-Tech). Samples for hybridization were then applied to the centre of a 25 mm × 60 mm glass cover-slip placed on a flat surface. The array slide was inverted so that the DNA side was facing downwards and then lowered very gently onto the coverslip ensuring even distribution of the solution across the array and taking care to exclude air bubbles. The array slides were placed into the hybridization chambers and the chamber lids securely fastened. The chambers placed at 49°C overnight. The following day hybridization chambers were opened and the arrays washed as follows. Arrays were washed in 2 × SSC at room temperature for 5 min, washed twice with agitation in wash solution [0.1 × SSC in 0.1% (w/v) SDS] at 65°C for 10 min and finally washed twice with agitation in 0.1 × SSC at 65°C for 10 min to remove any traces of SDS. Slides were then dried by centrifugation at 300 ×*g* for 2 min at room temperature.

In this study all RNA samples were hybridized to microarrays in quadruplicate and three biological replicates were performed.

2.21.5 Scanning of microarray slides and data handling

After hybridization, microarray slides were scanned using a GenePix 4000B scanner (Axon Instruments, Inc.). Fluorescent spot intensities and local background data were quantified using the GenePix 3.0 software package (Axon Instruments, Inc.). Data were filtered using the custom designed filterlist.bat program (M. Fookes, Wellcome Trust Sanger Institute, Cambridge, U.K.) and imported into the microarray analysis program GeneSpring 7.0 (Silicon Genetics). Intensity-dependent Lowess (locally weighted line or regression) normalization was performed on the data to compensate for unequal dye incorporation. The final readouts were mean Lowess–normalized Cy5/Cy3 ratio intensities for up to 24 data points per gene (i.e., four slides per biological replicate, duplicate features per slide). Only genes whose expression ratio showed at least a 2-fold difference [false discovery rate (FDR) ≤0.05%] were considered as being statistically significant.

2.22 Cell culture

Cell culture was performed to determine the effect of plasmids pSf-R27Gent^R and pSf-R27Δ*sfh*::Gent^R on *S.* Typhimurium virulence *in vivo*. Both invasion (Section 2.22.1) and survival (Section 2.22.2) of *Salmonella* bacteria in epithelial and macrophage cells, respectively was examined. Since the plasmid-bearing strains were gentamycin resistant, amikacin rather than gentamycin was used to kill extracellular bacteria in cell-culture assays. Amikacin has been shown to be as effective as gentamycin at killing extracellular bacteria without damaging eukaryotic cells (Fleiszig *et al.*, 2001).

2.22.1 Epithelial cell invasion assays

Typically, epithelial cells (CHO-K1 or CACO-II) were seeded 72 h prior to infection in 12-well plates at a density of 2×10^5 cells per well in culture medium [Dulbecco's Modified Eagle's Medium with F12 Nutrient mix supplemented with 10% (v/v) heat-inactivated foetal bovine serum]. Bacteria from overnight L-broth cultures were harvested and resuspended in pre-warmed antibiotic-free culture medium and added to either CHO-K1 or CACO-II monolayers at a multiplicity of 100:1. Plates were centrifuged at 582 ×*g* for 5 min and then incubated at 37°C in 5% CO_2 for 1 h to allow invasion to occur. The culture medium was then aspirated and cells washed three times with PBS. The monolayers were then incubated in fresh culture medium containing amikacin (400 μg ml^{-1}) for 1 h to kill extracellular bacteria. The CHO-K1 monolayers were washed three times with PBS and then lysed with PBS containing 0.5 % (v/v) Triton X-100 (Sigma) to release the intracellular bacteria. An additional step was required to lyse the CACO-II monolayers. CACO-II monolayers were washed three times with PBS, incubated in trypsin-EDTA solution (Sigma) for 10 min at 37°C (to degrade protein matrix to produce a single-cell suspension) and then lysed with PBS containing 0.5 % (v/v) Triton X-100 (Sigma) to release the intracellular bacteria. Bacterial suspensions were serially diluted and spread onto L-agar plates and also L-agar plates supplemented with gentamycin (15 μg ml^{-1}) to ensure no plasmid loss during the assay. Plates were incubated for 24 h and then scored for colony forming units.

2.22.2 Macrophage survival assays

Typically, cells were seeded 72 h prior to infection in 12-well plates at a density of 2×10^5 cells per well in culture medium [Dulbecco's Modified Eagle's Medium with F12 Nutrient mix supplemented with 10% (v/v) heat-inactivated foetal bovine serum]. Bacteria from overnight L-broth cultures were harvested and resuspended in pre-warmed antibiotic-free culture medium and added to the monolayers at a multiplicity of 100:1. Plates were centrifuged at 582 ×*g* for 5 min and then incubated at 37°C in 5% CO_2 for 1 h to allow phagocytosis of the *Salmonella* to occur. The culture medium was then aspirated. The monolayers were washed three times with PBS and incubated in fresh culture medium containing amikacin (400 μg ml^{-1}) for 1 h to kill extracellular bacteria. The amikacin–containing medium was aspirated and cells washed three times with PBS. The monolayers were then either lysed with PBS containing 0.5 % (v/v) Triton X-100 (Sigma) or incubated in fresh culture medium containing a minimum concentration of amikacin (80 μg ml^{-1}) and lysed 4, 6 or 8 h post-infection. After incubation, cells were washed three times with PBS and lysed with PBS containing 0.5 % (v/v) Triton X-100 (Sigma) to release the intracellular bacteria. Cell lysates were serially diluted and spread onto L-agar plates and also L-agar plates supplemented with gentamycin (15 μg ml^{-1}) to ensure no plasmid loss during the assay. Plates were incubated for 24 h and then scored for colony forming units.

2.23 Oxidative stress assay

Oxidative stress assays were performed to quantify the sensitivity of *Salmonella* cells to oxidative damage. Hydrogen peroxide is typically used *in vitro* to test bacterial survival under conditions of oxidative stress, as it is similar to that experienced by *Salmonella* during intracellular survival in macrophages. Assays were performed as follows.

Overnight cultures were pelleted by centrifugation at 16,000 ×*g* for 2 min and resuspended in PBS or PBS containing 20-mM H_2O_2. Bacterial suspensions were incubated at 37°C for either 1 or 2 h and then serially diluted and spread onto L-agar plates. Colony forming units

were calculated and the percentage survival of each strain was determined relative to the PBS control for that strain. Each assay was performed in duplicate, and the mean values were determined from at least 3 independent experiments.

2.24 Ultraviolet survival assay

Ultraviolet (UV) survival assays were used to quantify bacterial tolerance to ultraviolet radiation. Exposure of a bacterial cell to DNA-damaging agents (such as UV and ionizing radiation and a variety of chemicals) results in a diverse set of physiological changes termed the SOS response. The SOS response results in the induction of over 30 unlinked genes (many of which are involved in DNA repair and mutagenesis), which help protect the cell against the effects of DNA-damaging agents (Walker, 1996). Thus mutant strains, which express increased levels of the SOS regulon, are more tolerant to ultraviolet radiation than wild-type strains. This tolerance was tested as follows.

Overnight bacterial cultures were transferred into sterile 55-mm diameter Petri dishes and placed into a UV chamber (GS GENE LINKER^{TM}, Bio-Rad). The cultures were irradiated with various doses (0–12 J m^{-2}) of 254 nm UV and then serially diluted and spread onto four L-agar plates per UV dose. Plates were incubated in the dark for 24 h and then scored for colony forming units. Each assay was performed in duplicate, and the mean values were determined from at least 3 independent experiments.

2.25 Relative fitness assay

The introduction of conjugative plasmids into a bacterium cell by horizontal transfer can confer a physiological or energetic cost, that influences the fitness of the bacterium (Dahlberg and Chao, 2003). Fitness can be defined as the average contribution of one genotype to the next generation or to succeeding generations, compared to that of other genotypes (Lenski, 1991). Thus, the cost to a cell of carrying a conjugative plasmid can be determined by

calculating the relative fitness of plasmid-free and plasmid-bearing strains by direct competition in the same environment. Competitive fitness assays were performed as follows.

Bacterial cultures were founded with 10^5 cells of each competitor, which were preconditioned in L-broth for 24 h. The ratio of the two competing strains was determined at time zero and after 24 h growth at 37°C by selective plating. To ensure no plasmid-loss took place during the competition experiment, cultures were also spread onto plates selecting for the plasmid. Plates were incubated for 24 h and then scored for colony forming units. Relative fitness (W) was expressed as the ratio of the Malthusian parameters of the two strains being compared (Dahlberg and Chao, 2003) and calculated according to the formula:

$$Wij = \frac{\log_2 (N_i(1) / N_i(0))}{\log_2 (N_j(1) / N_j(0))}$$

$N_i(0)$ and $N_i(1)$ = initial and final density of test strain, respectively

$N_j(0)$ and $N_j(1)$ = initial and final density of common competitor strain, respectively

Each assay was performed in duplicate, and the mean values were determined from at least 3 independent experiments.

Chapter 3

Expression of the *sfh* gene is regulated at the level of transcription, translation and protein stability

3.1 Introduction

3.1.1 *Shigella flexneri* H-NS-like proteins

S. flexneri serotype 2a strain 2457T expresses three members of the H-NS protein family, namely H-NS and StpA and the more recently identified Sfh protein (*Shigella flexneri* H-NS-like protein) (Beloin *et al.*, 2003). Unlike the *hns* and *stpA* genes, the *sfh* gene is not located on the chromosome, but on a large ~165-kb plasmid, pSf-R27, that is 99.7% identical in DNA sequence to the prototype IncHI1 plasmid, pSf-R27. Sfh has 59% and 61% amino acid sequence identity to H-NS and StpA, respectively (Beloin *et al.*, 2003). Members of the H-NS protein family have the same overall domain structure with an N-terminal oligomerization domain connected by a flexible linker region to a C-terminal nucleic acid-binding domain (Dorman *et al.*, 1999; Ueguchi *et al.*, 1996; Williams *et al.*, 1996). Consequently, the Sfh protein, like H-NS and StpA is capable of forming homodimers and each protein can form heterodimers with both of its homologues (Deighan *et al.*, 2003; Free *et al.*, 2001; Johansson *et al.*, 2001). This has led to speculation that the properties of these homomeric and heteromeric complexes could vary depending on their protein subunit composition (Dorman *et al.*, 1999; Johansson and Uhlin, 1999).

The three H-NS-like proteins, H-NS, StpA and Sfh all have distinct growth-phase expression profiles. Thus their cellular levels are dynamically linked to the growth phase of the bacterium. In rich growth media, StpA expression is abundant only in early exponential phase, whereas H-NS levels remain relatively constant at all stages of growth (Deighan *et al.*, 2000; Deighan *et al.*, 2003; Free and Dorman, 1995). In contrast, Sfh expression is only induced in early stationary phase, while correspondingly *sfh* mRNA levels rapidly decrease as the culture grows towards stationary phase (Deighan *et al.*, 2003). The inconsistency in *sfh* mRNA and Sfh protein profiles suggests that there is a post-transcriptional aspect to *sfh* growth-phase regulation, distinguishing it from both H-NS and StpA (Deighan *et al.*, 2003). Like H-NS and StpA, Sfh can negatively autoregulate transcription of its own gene and all three proteins can negatively cross-regulate expression of each other's genes (Deighan *et al.*,

2003; Zhang *et al.*, 1996). Expression of H-NS and StpA is also regulated by temperature, with enhanced transcription of the *hns* and *stpA* genes stimulated during cold shock and an increase in growth temperature, respectively (Free and Dorman, 1997; La Teana *et al.*, 1991).

3.1.2 Riboregulation

Regulation of gene expression in prokaryotes occurs not only at the transcriptional level, but also at a number of post-transcriptional steps, including mRNA translation and mRNA decay. Previous studies in *E. coli* have demonstrated that extensive variation exists in the rate of translation and decay of individual mRNAs, and that specific features of the mRNA sequence as well as transcript secondary structure can be important determinants of such variation (Coburn and Mackie, 1999; Grunberg-Manago, 1999). Additionally, the half-lives and translation efficiencies of some mRNAs depend on the physiological state of the cell, as influenced by genetic and environmental factors. Recently, many small non-coding RNAs (ncRNAs) have been identified as crucial post-transcriptional regulatory elements in prokaryotes that influence the stability or translation of various target mRNAs (Gottesman, 2005).

More than 60 ncRNAs have been confirmed in *E. coli*, which is ~1–2% of the number of *E. coli* protein-coding genes (Gottesman, 2005). At least 20 of these belong to the largest class of ncRNAs, which is defined by a strong association and dependence upon the RNA chaperone Hfq (Zhang *et al.*, 2003). These ncRNAs regulate gene expression by base-pairing with their target mRNAs, consequently changing the translation or stability of the mRNA. Bacterial ncRNAs are very small, with an average length of only 80–100 nt. They frequently begin with a sequence that can fold into a stable stem-loop, and transcription terminates with a Rho-independent transcription terminator, a stem-loop that also helps to stabilize the molecule (Gottesman, 2005). Expression of these regulatory ncRNAs is highly regulated in prokaryotes, and they are frequently controlled by global stress response regulatory systems. For instance, OxyS is part of the OxyR-regulated transcriptional response to oxidative stress (Altuvia *et al.*, 1997), RhyB is regulated by the FUR repressor, a global regulator of iron-

acquisition genes (Masse and Gottesman, 2002), and Spot 42 synthesis is regulated by cAMP and cAMP-receptor protein (CRP) (Moller *et al.*, 2002).

As mentioned above these regulatory ncRNAs require the Sm-like protein Hfq to function. The homohexameric Hfq protein most likely functions as an RNA chaperone that increases RNA unfolding and promotes annealing between the ncRNA and its target mRNA. Hfq interacts strongly with the small ncRNAs at single-stranded AU-rich regions, with a preference for binding next to a structured (stem-loop) region (Valentin-Hansen *et al.*, 2004). Hfq also binds to AU-rich regions in the target mRNAs. Subsequently the ncRNA and the target mRNA base-pair, generally at the 5′-end of the message, often occlude the ribosome-binding site (RBS) and/or the translation initiation codon. The base-pairing is usually imperfect and sometimes includes several short (8–9 nt) regions of pairing. The result of this pairing can have multiple regulatory outcomes such as inhibition of translation, mRNA degradation, stimulation of translation, and stabilization of mRNA (Gottesman, 2005).

Multiple lines of evidence suggest that RNase E is the endoribonuclease responsible for mediating degradation of the mRNA targets of bacterial ncRNAs. RNase E is an essential bacterial nuclease that does not have a consensus target sequence (Lin-Chao *et al.*, 1994), but shows specificity for AU-rich single-stranded RNA. Since RNase E cleavage sites and Hfq-binding sites are similar (Moll *et al.*, 2003), it is thought that Hfq and RNase E might compete at some sites (Folichon *et al.*, 2003; Moll *et al.*, 2003). RNase E has been shown not only to degrade the target mRNA, but also the regulatory RNA, and therefore it appears ncRNAs act stoichiometrically rather than catalytically. In addition, RNase E is the scaffold for a protein complex called the degradasome, which includes polynucleotide phosphorylase, RNA helicase B, and also the metabolic protein, enolase (Carpousis, 2002). The degradasome contributes to small ncRNA-directed mRNA degradation (Masse *et al.*, 2003), and enolase has been recently shown to be essential for the degradation of one target of a small RNA (Repoila *et al.*, 2003).

Another outcome resulting from the base-pairing of ncRNAs with their target mRNA is the stimulation of translation and mRNA stability. Stimulation of translation by small ncRNAs is, thus far, unique to prokaryotes (Gottesman, 2005). The only current example is the stimulation of *rpoS* translation by two different small ncRNAs, DsrA and RprA. Both ncRNAs are known to base-pair to the same region of the *rpoS* transcript, which is ~70 nt upstream of the translation initiation codon. This 5′-region of the *rpoS* transcript can fold into an inhibitory stem loop that consequently inhibits ribosome binding. Thus, base-pairing of DsrA or RprA to *rpoS* abrogates the formation of this *cis*-inhibitory RNA structure (Repoila *et al.*, 2003). DsrA and RprA are synthesized in response to different environmental conditions – low temperature (<30°C) (Repoila *et al.*, 2003; Sledjeski *et al.*, 1996) and cell surface stress (Majdalani *et al.*, 2001; Majdalani *et al.*, 2002), respectively. In addition, to its positive effect on *rpoS* expression DsrA also negatively regulates *hns* expression by base-pairing to two different regions of the *hns* transcript, just beyond the translation initiation codon and immediately before the *hns* stop codon. Consequently the *hns* mRNA is circularized, leading to a sharp increase in the rate of *hns* mRNA turnover (Lease and Belfort, 2000). DsrA is capable of performing disparate functions by forming alternative structures in complexes with its target mRNAs. The structure of DsrA is proposed to consist of three stem-loops (Sledjeski and Gottesman, 1995). Stem-loop 1 is involved in base-pairing with *rpoS* mRNA. In contrast, stem-loop 1 remains intact when DsrA is base-pairing with *hns* mRNA, while stem-loop 2 is melted out (Lease and Belfort, 2000).

3.1.3 Regulated proteolysis

In recent years, the relevance of controlled proteolysis for gene regulation and stress survival of bacteria has been increasingly recognized. Controlled protein degradation is responsible for the rapid turnover of specific regulatory proteins and the clearing of abnormal proteins from the cytoplasm (Gottesman, 1996, 2003). Most intracellular selective proteolysis is initiated by oligomeric adenosine triphosphate (ATP)-dependent proteases, such as Lon, ClpXP, ClpAP, and HflB. In *E. coli*, the Clp proteases together with the Lon protease are responsible for at least 70% of protein degradation (Maurizi, 1992). Of the ATP-dependent

proteases, Lon appears to be one of the best conserved. It is found in a wide-range of prokaryotes including *Bacillus subtilis, Caulobacter* and *Myxococcus* and is also present in the mitochondria of eukaryotic cells (Gottesman, 1996, 2003). The Lon protease is a tetrameric protein made up of four identical subunits and within each subunit there is an active serine protease site and a single consensus ATP-binding site (Amerik *et al.*, 1991; Chin *et al.*, 1988; Goldberg *et al.*, 1994). In contrast, the ClpXP and ClpAP proteases consist of multimers of the ClpP protease and a hexamer of the ClpX or ClpA ATPase, respectively (Gottesman *et al.*, 1990; Wojtkowiak *et al.*, 1993). Thus, the protease active site and the ATP-binding site reside in separate subunits of Clp proteases (Hwang *et al.*, 1988; Katayama *et al.*, 1988; Woo *et al.*, 1989). The Clp ATPase subunits (ClpA and ClpX) have chaperone activity and are responsible for the distinct substrate specificities of their respective proteases (Gottesman, 1996).

The Clp and Lon ATP-dependent proteases degrade two major types of substrates within the bacterial cell (Gottesman, 1996, 2003). The first type of substrate consists generally of non-functional or abnormal proteins such as misfolded and mutant proteins, proteins synthesized with wrong amino acids, and truncated proteins (Goldberg and St John, 1976; Gottesman, 1989; Gottesman *et al.*, 1997; Wickner *et al.*, 1999). This quality control activity ensures that non-functional proteins are eliminated from the bacterial cell. The other class of substrates subject to Lon and Clp protein degradation are specific short-lived regulatory proteins (Gottesman, 1996). These natural protein targets tend to be key regulators of stress responses, the cell cycle and cell differentiation, and therefore their function is required for only a limited time within the growth cycle or in response to specific environmental conditions. As a consequence, regulation of these proteins by proteolysis has a major impact on cellular physiology (Jenal and Hengge-Aronis, 2003). One of the most prominent examples is the controlled degradation of the alternative sigma factor, RpoS.

RpoS (σ^S) is the master regulator of the general stress response. RpoS expression varies dramatically with growth phase and other environmental conditions. These changes in RpoS

levels are primarily mediated through changes in translation and stability of the protein (Lange and Hengge-Aronis, 1994). In exponentially growing cells, there is very little σ^s because of low synthesis and rapid degradation. However, when cells enter stationary phase, the half-life of σ^s increases dramatically and consequently RpoS levels increase and the general stress response is induced (Lange and Hengge-Aronis, 1994; Schweder *et al.*, 1996; Takayanagi *et al.*, 1994). Degradation of σ^s during exponential growth depends on the ClpXP protease (Schweder *et al.*, 1996) and the response regulator RssB. In its phosphorylated form, RssB acts as a proteolytic recognition factor (Mika and Hengge, 2005) that binds to σ^s and targets it to the ClpXP protease (Becker *et al.*, 1999; Zhou *et al.*, 2001). Multiple signals have been integrated into the control of σ^s proteolysis and as a result σ^s can be stabilized instantaneously in response to several stress conditions, e.g., starvation, sudden decreases in pH, or high temperature (Hengge-Aronis, 2002a, b). Thus, controlled proteolysis represents an efficient regulatory mechanism that allows rapid changes in σ^s levels and therefore in gene transcription (Gottesman, 1996).

Another known substrate for the ClpXP protease is the nucleoid-associated protein Dps (Flynn *et al.*, 2003). Dps accumulates to substantial levels in cells exposed to starvation or oxidative stress and its degradation is differentially controlled by stress signals. Like RpoS, Dps is stabilized by starvation, but in contrast to RpoS degradation, Dps proteolysis is inhibited by oxidative stress and is independent of the recognition factor RssB (Hengge and Bukau, 2003). However, it is speculated that there is as yet an unknown specific recognition factor or targeting factor for Dps, whose activity could be modulated by growth-phase-specific signals. In addition another Clp protease, ClpAP, was shown to have an indirect role in maintaining ongoing Dps synthesis in long-term stationary phase cells (Stephani *et al.*, 2003). Recently, another nucleoid-associated protein, YmoA, was also shown to be subject to conditional proteolysis in *Yersinia pestis*. YmoA is a repressor of the *Y. pestis* TTSS and is highly unstable during growth at 37°C but stable at lower temperatures. This thermoregulated proteolysis of YmoA is dependent on both the ClpXP and Lon ATP-dependent proteases (Jackson *et al.*, 2004).

Finally there is another set of targets for controlled proteolysis, which fall into a category between the non-functional abnormal proteins and the naturally unstable proteins (Gottesman and Maurizi, 1992). These proteins are part of multi-protein complexes, which in their normal context can be quite stable. However, if the stoichiometry of synthesis is perturbed due to mutation or overproduction of a subunit, rapid degradation of the excess uncomplexed proteins occurs. In other instances, changes in the availability of a partner may lead to regulated destruction of a protein (Gottesman, 1996). The latter is exemplified by the controlled degradation of the two nucleoid-associated proteins, StpA and HU. StpA is subject to Lon degradation when it forms monomers or homodimers. However, heteromerization of StpA with its homologous protein H-NS protects StpA from proteolysis (Johansson and Uhlin, 1999; Johnson *et al.*, 2002). Similarly, when the β-subunit of HU forms a heterodimeric complex with the α-subunit of the protein, it is also protected from degradation by the Lon protease (Bonnefoy *et al.*, 1989)

Previous studies revealed that the *sfh* mRNA and protein profiles do not correspond, indicating that *sfh* expression is controlled at both the transcriptional and post-transcriptional level (Deighan *et al.*, 2003). The aim of this study was to elucidate the underlying mechanism controlling the post-transcriptional aspect of growth-phase-dependent expression of the *sfh* gene. Since H-NS and StpA negatively cross-regulate *sfh* expression, it was also of particular interest to determine the contributions of these proteins to the disparate *sfh* mRNA and protein profiles. Furthermore, this study aimed to determine the expression profile of the *sfh* gene in response to various environmental cues such as temperature.

3.2 Results

3.2.1 Genetic confirmation of the *sfh* mutation

The *S. flexneri sfh* knockout mutant strain CJD1650 (Beloin *et al.*, 2003) was constructed by an allelic replacement technique based on the method of Datsenko and Wanner (2000). The entire *sfh* open reading frame of plasmid pSf-R27 was deleted and replaced with the *aac* gene of *Streptomyces lividans* which codes for gentamycin-3-acetyltransferase, that confers resistance to apramycin and gentamycin (Brau *et al.*, 1984). Essentially, a 2,295-bp linear DNA fragment was produced by PCR in two stages (Fig. 3.1). This amplimer (500-Gent-500) had the 500-bp upstream and 500-bp downstream regions of the *sfh* coding sequence at either end of the 1,295-bp *aac* gene of *Streptomyces lividans*. The linear 2,295-bp DNA fragment was purified and transformed into wild-type strain BS184/pKOBEGA by electroporation (Fig. 3.1). The pKOBEGA plasmid (Table 2.2) harbours a thermosensitive replicon and the λ phage *redγβα* operon under the control of the P_{BAD} promoter (Chaveroche *et al.*, 2000). The Exo, Bet and Gam proteins necessary for homologous recombination reaction were induced during preparation of the BS184/pKOBEGA electrocompetent cells by the addition of 0.02% L-arabinose when the culture reached an OD_{600}nm of 0.2. Growth at 30°C was continued until the culure reached an OD_{600}nm of ~1. Positive clones were selected by growth on L-agar plates containing kanamycin (50 μg ml^{-1}) and gentamycin (15 μg ml^{-1}) at 37°C for 36 h (Beloin et al., 2003). They were single-colony purified four times, and then tested for the loss of the thermosensitive pKOBEGA plasmid. To ensure the *sfh* gene was deleted and the *aac* cassette had correctly inserted into plasmid pSf-R27, positive clones were confirmed by PCR analyses using internal and external primers (Beloin et al., 2003). One of the positive clones harbouring the *sfh* mutant plasmid pSf-R27Δ*sfh*::$Gent^R$ was designated strain CJD1650 (Beloin et al., 2003).

In this study, the Δ*sfh*::$Gent^R$ allele was confirmed to be a complete null mutant for the *sfh* gene by both Southern and Western blotting (Fig. 3.2). Total genomic DNA was isolated from strains BS184 (strain 2457T *mxiC*::MudI*1734,* hereinafter referred to as wild-type

strain), BS185 (*hns*205::Tn*10* truncation mutant), CJD1199 (Δ*stpA*::Tc^R deletion mutant) and CJD1650 (Δ*sfh*::Gent^R deletion mutant). Undigested total DNA from these strains was then electrophoresed on agarose gels and probed for the plasmid pSf-R27 *hha*-like gene and the *sfh* gene. As expected the *sfh*-specific probe detected a homologue in the wild-type strain and in the *hns* and *stpA* mutants, but no hybridization occurred with the *sfh* mutant (Fig. 3.2). Importantly, the *hha*-like probe hybridized to all four strains, and thus the absence of the *sfh* gene in strain CJD1650 is not due to the absence of plasmid pSf-R27Δ*sfh*::Gent^R (Fig. 3.2). To confirm that no Sfh protein is produced by the *sfh* mutant, total protein samples were isolated from stationary phase L-broth cultures of the wild-type strain, strain BS184 and its isogenic *hns, stpA* and *sfh* mutants and analysed by Western immunoblotting (Fig. 3.2). The results clearly established the presence of Sfh in the wild-type and *hns* and *stpA* mutant backgrounds, but the absence of the Sfh protein in the Δ*sfh*::Gent^R knockout mutant (Fig. 3.2).

The growth rates of wild-strain strain, strain BS184 and its *hns, stpA* and *sfh* mutant derivatives were compared in L-broth medium at 37°C by measuring the optical density of the culture at 600 nm over a 7 h time course (Fig. 3.3). The generation time for the wild-type strain and the *sfh* and *stpA* mutants during the exponential phase of growth was 28 min, whereas the *hns* mutant grew considerably slower with a doubling time of 37 min (Fig. 3.3). Therefore, there is no growth defect associated with the Δ*sfh*::Gent^R knockout mutant.

3.2.2 Construction of a *sfh* transcriptional reporter plasmid

The cellular levels of nucleoid-associated proteins, especially H-NS-like proteins, is subject to complex and multifactorial control. Transcription of the *hns* and *stpA* genes is influenced by several environmental factors such as temperature, osmolarity and growth phase (Dorman and Deighan, 2003; Dorman, 2004; Schroder and Wagner, 2002). In addition, numerous nucleoid-associated proteins regulate expression of these genes, including H-NS and StpA, which negatively autoregulate transcription of their own genes and also negatively crossregulate of each other's genes expression (Deighan *et al.*, 2003; Zhang *et al.*, 1996).

Fig. 3.1. Construction of the *sfh* deletion mutant plasmid pSf-R27Δ*sfh*::Gent^R. Schematic representation of the allelic replacement technique used to exchange the entire *sfh* open reading frame of plasmid pSf-R27 with the *aac* gene of *Streptomyces lividans*. The *aac* gene product, gentamycin-3-acetyltransferase, confers resistance to apramycin and gentamycin (Apr/Gent). Details of the replacement technique are described in Section 3.2.1. One of the positive transformants harbouring the *sfh* deletion mutant plasmid pSf-R27Δ*sfh*::Gent^R was designated strain CJD1650 (Beloin et al., 2003).

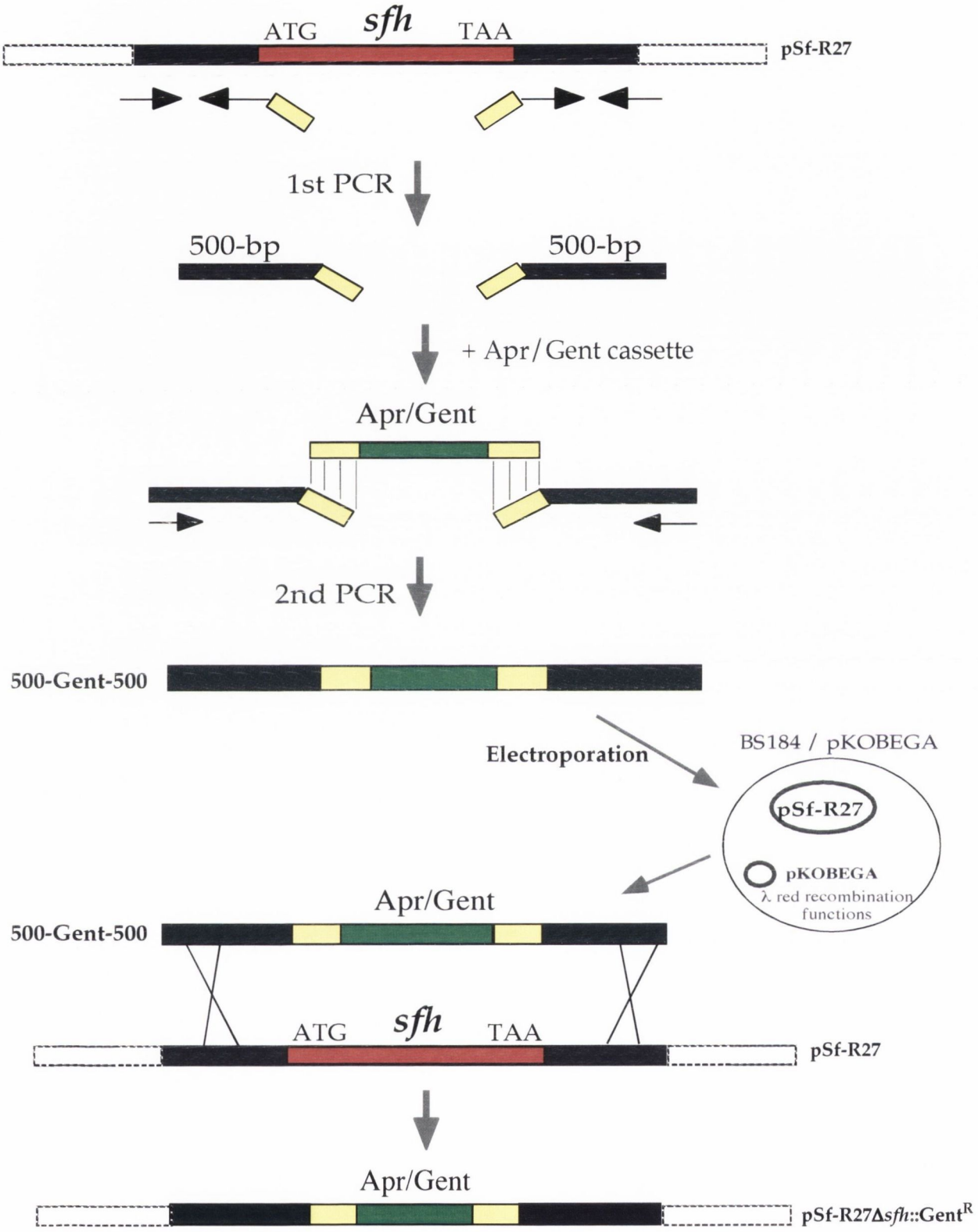
ATG
sfh
TAA
pSf-R27
1st PCR
500-bp
500-bp
+ Apr/Gent cassette
Apr/Gent
2nd PCR
500-Gent-500
Electroporation
BS184 / pKOBEGA
pSf-R27
pKOBEGA
λ red recombination functions
Apr/Gent
500-Gent-500
ATG
sfh
TAA
pSf-R27
Apr/Gent
pSf-R27Δsfh::Gent^R

Fig. 3.2. Genetic confirmation of the *sfh* mutation. (A) Southern blot confirming the Δ*sfh*::Gent^R allele is a complete null mutant for the *sfh* gene. Undigested total DNA from strains BS184 (wild-type), CJD1650 (*sfh*), CJD1199 (*stpA*) and BS185 (*hns*) was probed for the presence of the *sfh* and *hha*-like genes located on the high molecular mass plasmid pSf-R27. An asterisk indicates the position of the wells on the gel. (B) Western blot confirming the absence of the Sfh protein in strain CJD1650. Protein samples were harvested from stationary L-broth cultures of strains BS184 (wild-type), CJD1650 (*sfh*), CJD1199 (*stpA*) and BS185 (*hns*) and probed with anti-Sfh antibodies.

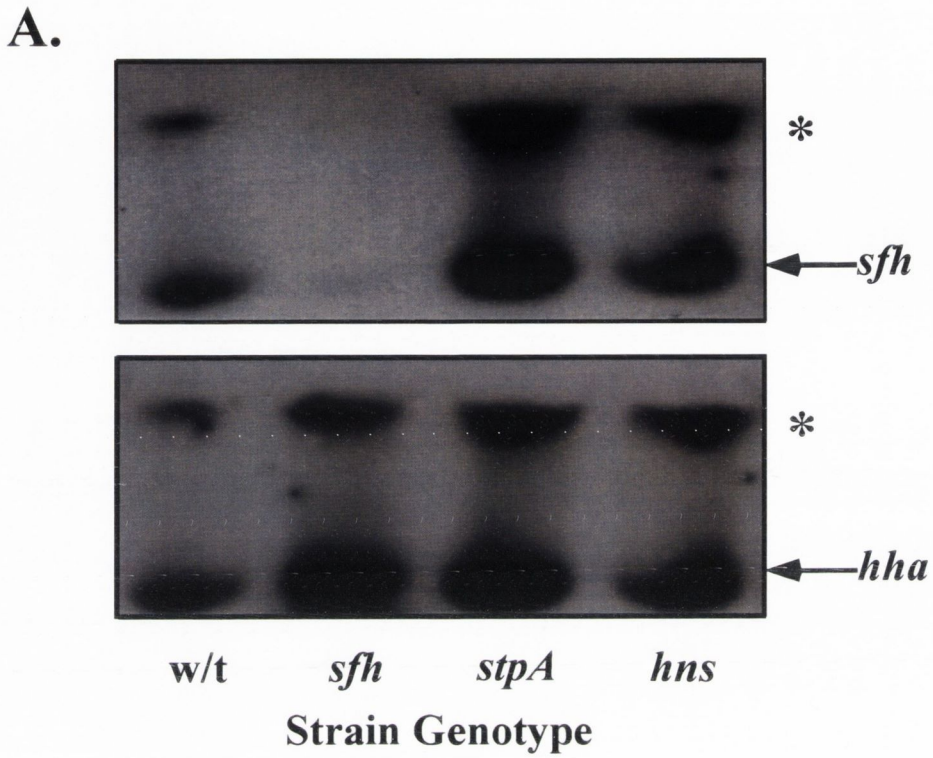
A.
*
sfh
*
hha
w/t
sfh
stpA
hns
Strain Genotype
B.
Sfh
w/t
sfh
stpA
hns
Strain Genotype

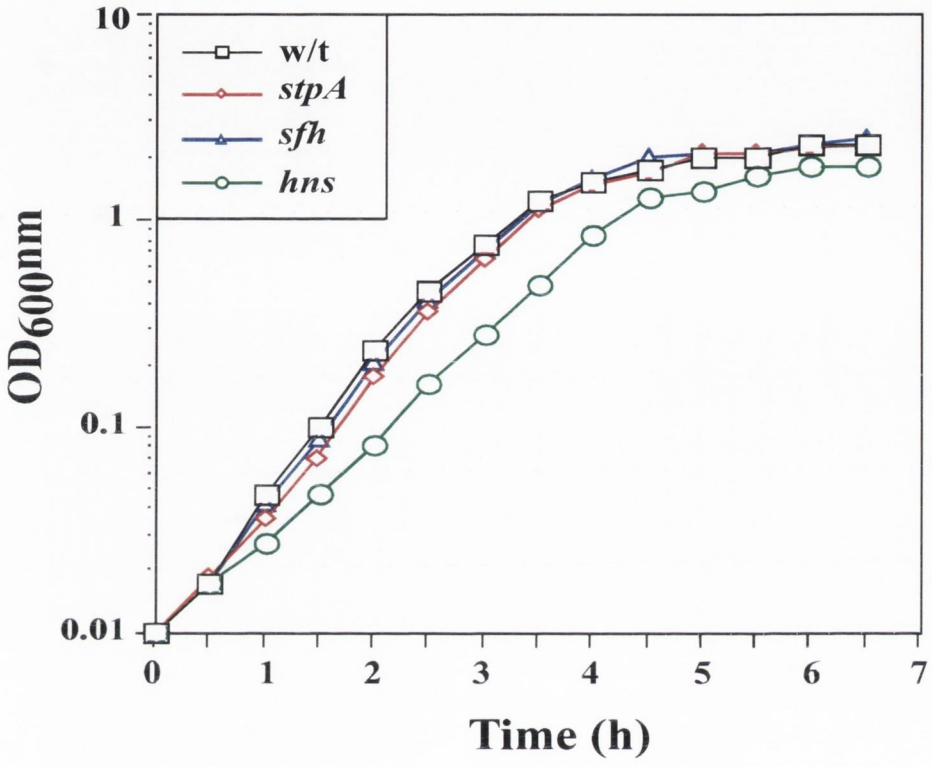

Fig. 3.3. Growth curves of wild-type and mutant strains in L-broth.

Growth curves of strains BS184 (wild-type), CJD1650 (*sfh*), CJD1199 (*stpA*), and BS185 (*hns*) in L-broth at 37°C. Overnight cultures were diluted to an OD_{600}nm of 0.01, and bacterial growth monitored by measuring OD_{600}nm at regular intervals post inoculation. The OD_{600}nm values were then plotted against time. These growth curves are representative of three independent experiments.

Despite identification of the *sfh* transcription start by Deighan *et al.* (2003), no study has investigated *sfh* promoter activity throughout the growth cycle. For this reason, an *sfh–gfp* transcriptional fusion was constructed to monitor *sfh* gene transcription during growth in rich media.

The transcriptional start of the *sfh* monocistronic gene was previously identified as a G residue located 40-bp upstream of the translation initiation codon (Deighan *et al.*, 2003). With this in mind, a 587-bp DNA fragment encompassing the *sfh* regulatory region was amplified by PCR using the oligonucleotides sfh-FG and sfh-RG (Table 2.3) and cloned into the *gfp* reporter plasmid pZep08 to generate plasmid psfh-gfp (Fig. 3.4). The amplimer and vector pZep08 were both digested with restriction endonucleases *Xba*I and *Sma*I to allow ligation of the *sfh* promoter upstream of the promoterless *gfp* gene in plasmid pZep08. To confirm correct insertion of the *sfh* promoter into the vector, plasmid DNA was isolated from clones and sequenced.

3.2.3 *sfh* promoter activity is subject to growth phase and negative autoregulation

Transcriptional activity of the *sfh* promoter was examined throughout the growth cycle in rich broth (L-broth) by flow cytometric analysis utilizing the newly constructed plasmid psfh-gfp (Section 3.2.2). The plasmid-borne *sfh–gfp* transcriptional fusion was transformed into the wild-type *S. flexneri* strain BS184, and its *sfh* isogenic mutant, CJD1650. Samples for flow cytometric analysis were harvested at intervals throughout the growth curve from 37°C L-broth cultures of strains BS184 and CJD1650. The results of the transcriptional assays revealed there is a burst of *sfh* expression immediately after subculture (early exponential phase) and thereafter a steep decline in promoter activity until *sfh* expression levels plateau in stationary phase (Fig. 3.5). These data clearly illustrate that *sfh* gene expression is subject to growth phase-dependent regulation. In addition, it was observed that *sfh* gene expression was elevated in the *sfh* mutant compared to the wild-type strain throughout the growth curve (Fig.

3.5), verifying previous reports that Sfh negatively autoregulates its own expression (Deighan *et al.*, 2003).

Since H-NS-like proteins are known to bind preferentially intrinsically curved DNA (Bracco *et al.*, 1989; Owen-Hughes *et al.*, 1992; Yamada *et al.*, 1990), the intrinsic curvature of the *sfh* promoter was analysed *in silico* using the BEND-IT computer program (http://www.icgeb.org/dna/bend_it.html). The curvature propensity plot of the *sfh* regulatory region revealed that it possessed a large region of curvature (nt –250 to –100 with respect to the transcription start site of the *sfh* gene), consistent with the model in which Sfh negatively autoregulates its own expression (Fig. 3.6). Electrophoretic mobility shift assays (EMSAs) were then used to confirm the interaction of Sfh with its own promoter's regulatory region (Fig. 3.6). A 438-bp DNA fragment encompassing the *sfh* regulatory region (nt –327 to +111 with respect to the transcription initiation site of the *sfh* gene) was amplified by PCR, using the primer pair sfh-BSF and sfh-BSR (Table 2.3). The *sfh* promoter amplimer was added to plasmid pBR322 that was digested with the restriction endonucleases *Taq*1 and *Ssp*I into 8 fragments. The 8 restricted pBR322 DNA fragments act as excess competitor DNA in the EMSA. One of the pBR322 DNA restriction fragments is 217-bp, and contains the intrinsically curved promoter region of the β-lactamase (*bla*) gene, which is known to bind H-NS-like proteins (Bracco *et al.*, 1989; Owen-Hughes *et al.*, 1992; Yamada *et al.*, 1990). The DNA mixture was then incubated with increasing concentrations of purified Sfh, and resolved by electrophoresis through 3% molecular screening agarose. The electrophoretic mobility of the *sfh* promoter fragment was reduced specifically by Sfh in a concentration-dependent manner (Fig. 3.6). Sfh also shifted the mobility of the *bla*-positive control band. Taken together, these data clearly show that Sfh negatively autoregulates its own expression.

3.2.4 Post-transcriptional aspect to *sfh* growth phase-dependent regulation

The expression of the *sfh* gene was studied at the transcriptional and translational level in the wild-type strain, BS184 during growth in L-broth medium at 37°C. Transcription was studied

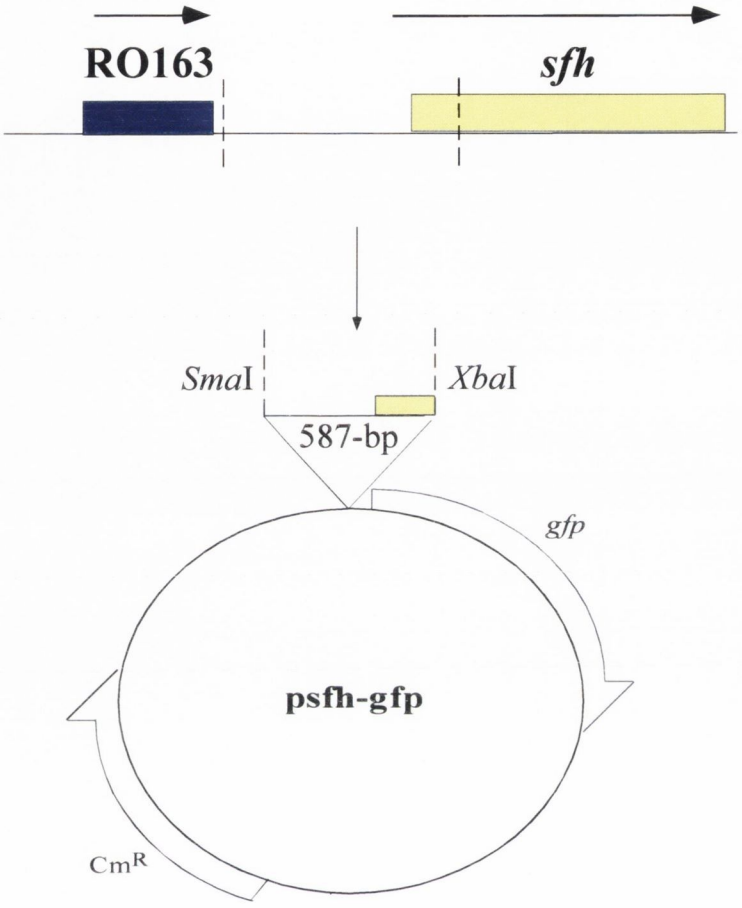

Fig. 3.4. Construction of a *sfh* promoter fusion plasmid. A 587-bp DNA fragment incorporating the 5′-region of the *sfh* gene, and the *sfh* regulatory region was amplified by PCR and ligated into plasmid pZep08 upstream of the promoterless *gfp* gene to generate plasmid psfh-gfp.

Fig. 3.5. Transcriptional activity of the *sfh* promoter. (A) Graph shows *sfh* promoter activity in wild-type strain BS184 and its *sfh* mutant derivative. Strains BS184 (w/t) and CJD1650 (*sfh*) containing plasmid psfh-gfp or pZep08 (plasmid vector control) were grown in L-broth at 37°C. Samples of culture were harvested at various time points throughout the growth curve to analyse *sfh–gfp* expression. The labelling above each data point (a – h) refers to the stage of the growth curve (B) when the samples were extracted. The data represent an average of at least three independent experiments and error bars represent standard deviations. (B) Graph shows the growth curve of wild-type strain BS184 in L-broth at 37°C.

A.

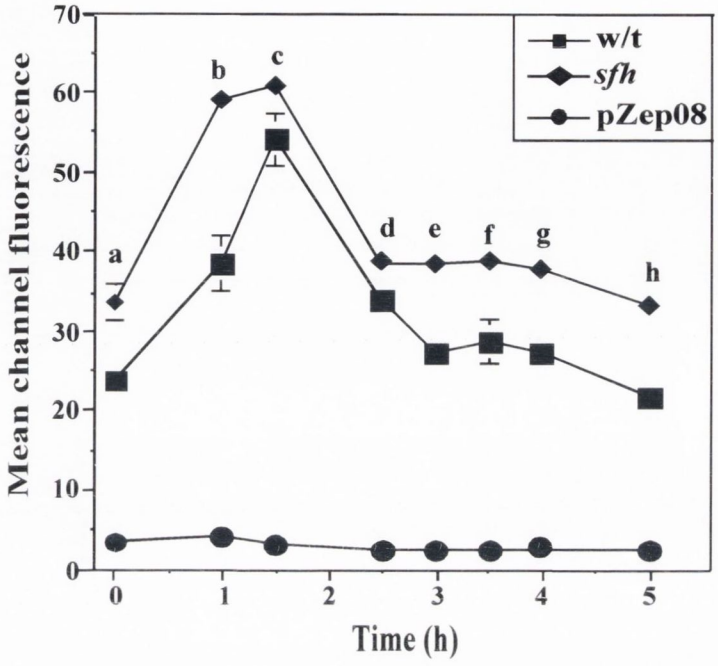
Mean channel fluorescence
Time (h)
w/t
sfh
pZep08
a
b
c
d
e
f
g
h

B.

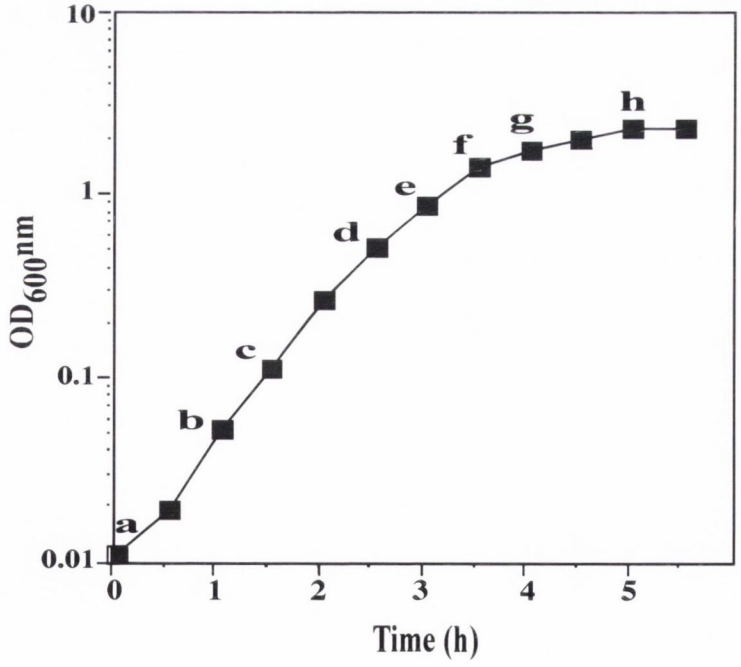
OD600nm
Time (h)
a
b
c
d
e
f
g
h

Fig. 3.6. Direct interaction of Sfh with the *sfh* promoter region.

(A) DNA curvature analysis of the *sfh* promoter region. Graph shows the predicted intrinsic curvature of the *sfh* regulatory region using the computer program BEND-IT. Curvature is expressed as degrees per helical turn and plotted against the position on the promoter sequence, with +1 corresponding to the *sfh* transcription initiation start site. Curved and straight motifs have a value above or below 5 degrees per helical turn, respectively. Regions of intrinsic curvature are arrowed. (B) Competitive gel retardation assay showing the specific binding of Sfh to the *sfh* promoter region. A 438-bp DNA fragment encompassing the *sfh* regulatory region (nt –327 to +111 with respect to the transcription initiation site of the *sfh* gene) was amplified by PCR using the primer pair sfh-BSF and sfh-BSR (Table 2.3). The plasmid pBR322 was digested with restriction endonucleases *Taq*I and *Ssp*I, and the resulting DNA fragments mixed with the 438-bp amplimer of the *sfh* promoter region. The DNA mixtures were incubated with increasing concentrations of Sfh in the range 0 μM to 2 μM. An arrow and an asterisk indicate the position of the *sfh* and *bla* promoter fragments, respectively. The curved *bla* promoter is a positive control known to bind H-NS-like proteins. The positions of the 600-bp and 400-bp molecular size markers are also indicated.

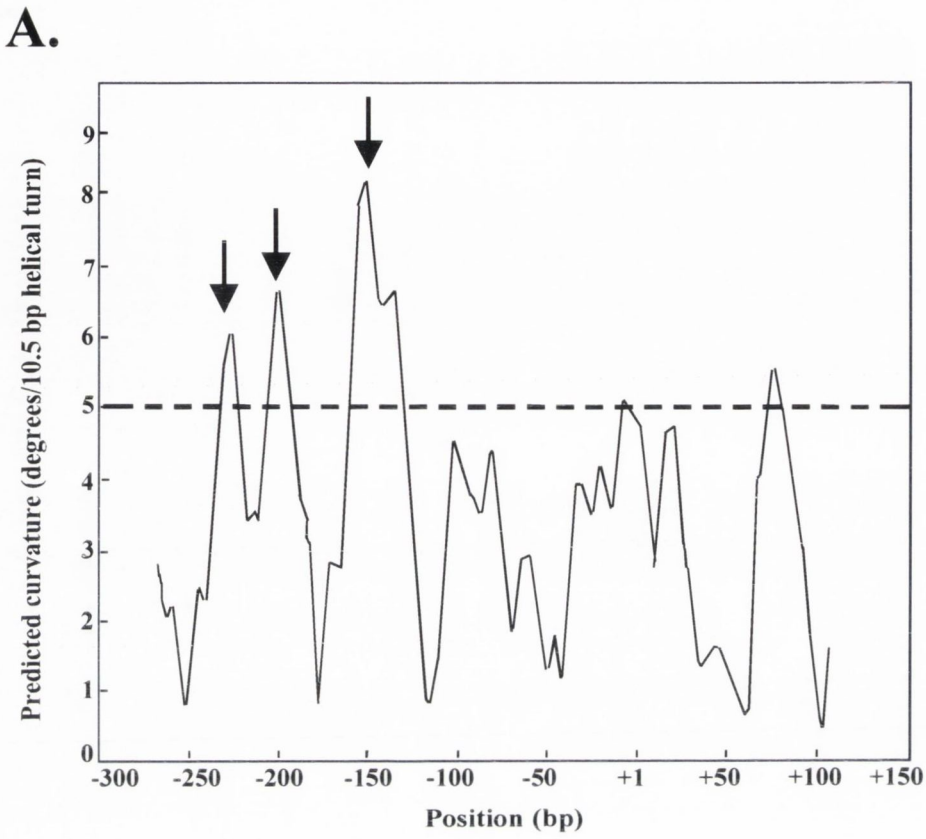
A.
Predicted curvature (degrees/10.5 bp helical turn)
0
1
2
3
4
5
6
7
8
9
-300
-250
-200
-150
-100
-50
+1
+50
+100
+150
Position (bp)

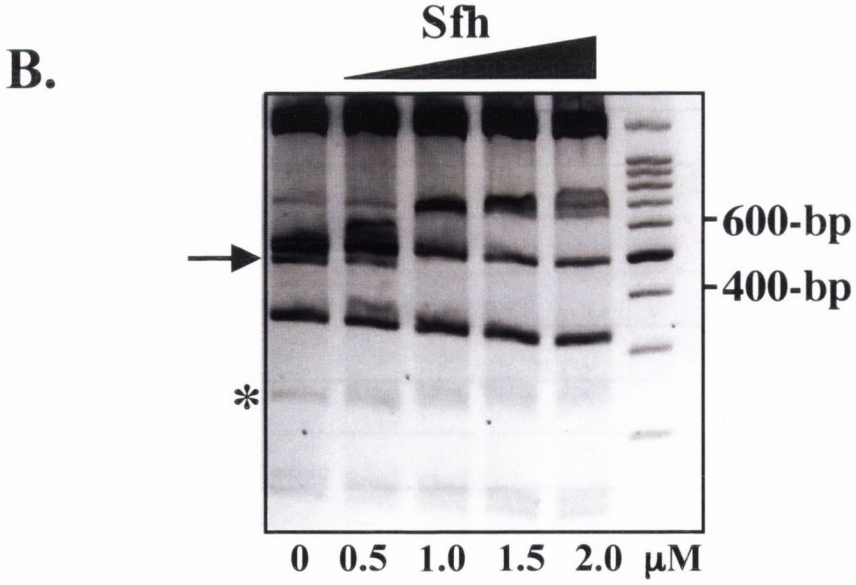
B.
Sfh
600-bp
400-bp
*
0
0.5
1.0
1.5
2.0
μM

by quantitative Northern blotting and Sfh protein levels were monitored by Western blotting. Total RNA and protein samples were isolated from an L-broth culture of strain BS184 at fixed OD_{600} values throughout the growth curve. In agreement with a previous report (Deighan *et al.*, 2003), the expression pattern of *sfh* mRNA was found to be the reciprocal of that displayed by the Sfh protein (Fig. 3.7). The results showed *sfh* mRNA to be abundant in early exponential phase but virtually undetectable from mid-exponential phase growth onwards (Fig. 3.7). These data correlate with the transcriptional profile of the *sfh* promoter obtained by flow cytometry (Fig. 3.5). Consistent with previous findings (Mukhopadhyay *et al.*, 2000), expression of the 16S *rrnA* rRNA was largely unaffected by growth phase (Fig. 3.7), thus allowing it to be used as a loading control in these experiments. The size of the *sfh* transcript (~500 bp) is consistent with it being monocistronic and its level is 5-fold higher in early exponential phase than in cells grown to stationary phase (Fig. 3.7). In contrast, Sfh protein levels are barely discernible in the exponential phase of growth but dramatically increase at the onset of stationary phase (Fig. 3.7). Remarkably, 30 min after bacteria enter the stationary phase of growth, the cellular levels of Sfh protein increase 4-fold (Fig. 3.7). Taken in aggregate these data highlight the inconsistencies in the *sfh* mRNA and Sfh protein expression profiles. The reciprocal expression of *sfh* mRNA and Sfh protein indicates that there must be a post-transcriptional aspect to *sfh* growth phase-dependent regulation, either at the level of the *sfh* message and/or Sfh protein.

3.2.5 Sfh protein stability

The inconsistency of *sfh* mRNA and protein expression profiles could be a result of differential turnover of the Sfh protein though the growth cycle. To assess this possibility, the stability of the Sfh protein was monitored in the wild-type *Shigella* strain BS184. Growing cultures corresponding to early exponential and early stationary phase (which represent when Sfh protein levels are minimum and maximum in the cell, respectively) were treated with the antibiotic spectinomycin to inhibit translation. Protein samples were then isolated in a time-course experiment and Sfh protein stability followed by quantitative Western blotting.

Intriguingly, the results showed that the Sfh protein remained stable throughout the course of the experiment (45 min), in both the exponential and stationary phase cultures (Fig. 3.8). As a positive control for proteolysis, protein samples were also probed with anti-RpoS antibodies. In this case the addition of spectinomycin to the cultures, to prevent *de novo* protein synthesis, revealed the rapid turnover of RpoS, in agreement with previous studies (Lange and Hengge-Aronis, 1994). Evidently, these data demonstrate that Sfh protein stability is equivalent throughout the growth cycle and thus *sfh* growth phase-dependent expression cannot be protease-dependent, i.e., controlled at the protein level.

Since H-NS is known to protect StpA from Lon proteolysis (Johansson and Uhlin, 1999; Johansson *et al.*, 2001), it was of interest to monitor the effect of *hns* and *stpA* mutations on Sfh protein stability. As before, the stability of Sfh was determined during the early exponential and early stationary phases of growth in the various mutants. Surprisingly, the results obtained for the *stpA* mutant were identical to those obtained for the wild-type strain (Fig. 3.9), i.e., Sfh remained stable throughout the course of the experiment, regardless of the growth phase. Therefore, StpA does not influence Sfh protein stability. In contrast, Sfh was rapidly degraded in the *hns* and *hns stpA* (CJD1216–*hns*205::Tn*10* Δ*stpA*::Tc^R) mutant backgrounds at both stages of growth (Fig. 3.9). Quantitative analysis of the level of Sfh at the different time points was used to estimate the half-life of Sfh. Comparisons of the exponential and stationary phase data show that the half-lives of Sfh increase during stationary phase in both the *hns* and *hns stpA* mutant backgrounds due to corresponding decreases in the rate of Sfh degradation (Fig. 3.9). These results suggest H-NS but not its homologous protein StpA is required for the stabilization of Sfh. These findings are reminiscent of those from previous studies, which showed H-NS is required to protect StpA from Lon-mediated proteolysis (Johansson *et al.*, 2001). H-NS prevents proteolysis of StpA by forming heteromeric complexes with its homologous protein.

In light of this, experiments were designed to elucidate whether or not Lon was the protease responsible for the turnover of Sfh in the absence of H-NS. The intention was to perform Sfh

Fig. 3.7. Growth phase-dependent expression of the *sfh* gene.

(A) Northern and (B) Western blot analysis of *sfh* gene expression in wild-type strain BS184 cultured in L-broth at 37°C. Total RNA and protein samples were extracted at various time points throughout the growth curve. The labelling above each lane refers to the stage of the growth curve when the samples were extracted as depicted in (C). Protein and RNA samples were probed with anti-Sfh antibodies and a *sfh*-specific riboprobe, respectively. As a control for RNA stability and loading, total RNA was also hybridized with an *rrnA*-specific riboprobe. The positions of migration of the molecular size markers are indicated. (C) Graph shows growth curve of wild-type strain BS184 in L-broth at 37°C. (D) Densitometric analyses of data in (A) and (B). Transcript levels are expressed as a relative percentage of the *sfh* mRNA content of cells at OD_{600} = 0.1 (sample a), the value of which was taken as 100%. Protein levels are expressed as a relative percentage of the Sfh protein content of cells at OD_{600} = 2.0 (sample f), the value of which was taken as 100%. The data shown for the relative percentage transcript and protein levels are the average of three independent experiments and representative gels are shown.

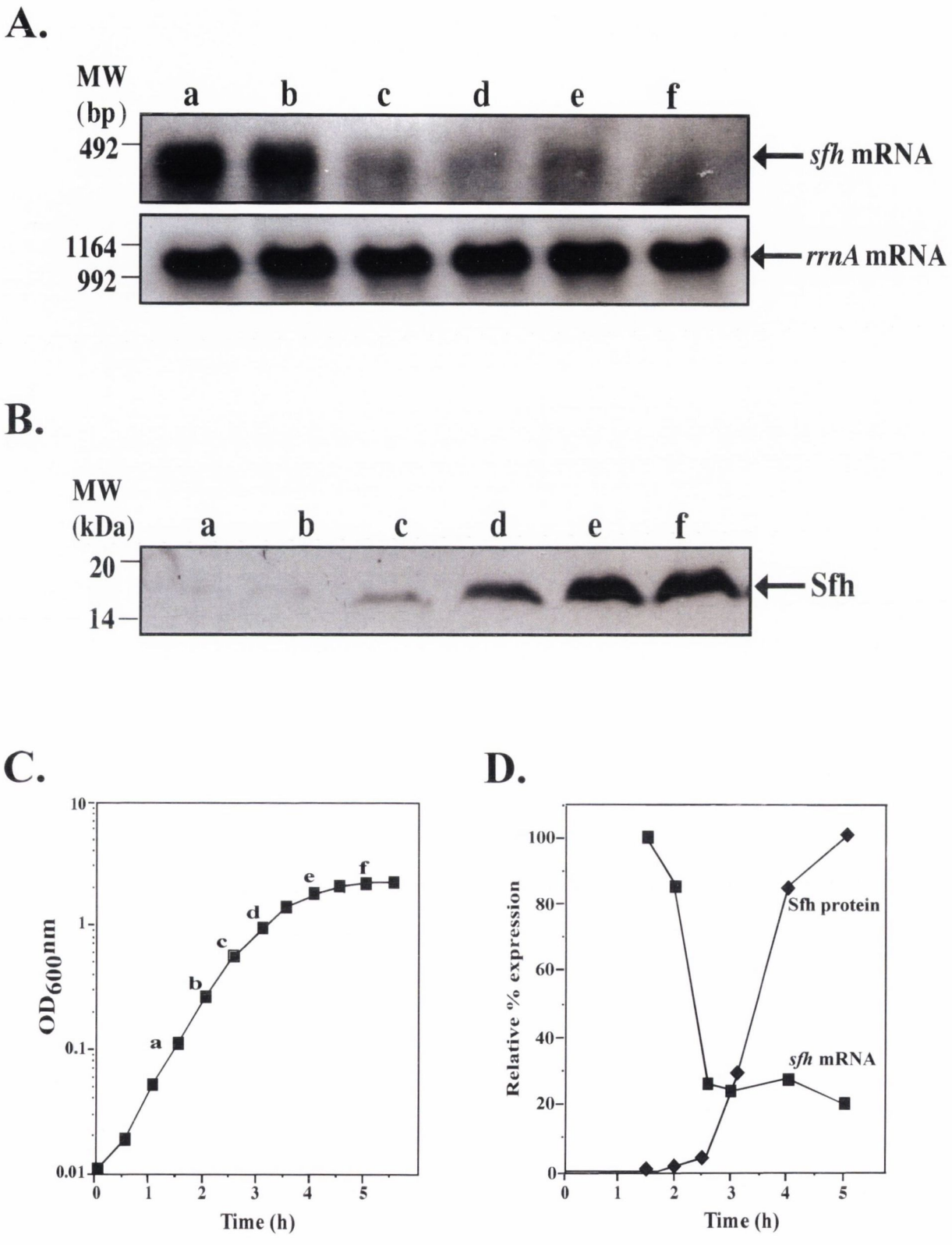
A.
MW
(bp)
492
1164
992
a
b
c
d
e
f
sfh mRNA
rrnA mRNA
B.
MW
(kDa)
20
14
a
b
c
d
e
f
Sfh
C.
OD600nm
10
1
0.1
0.01
a
b
c
d
e
f
0
1
2
3
4
5
Time (h)
D.
Relative % expression
100
80
60
40
20
0
Sfh protein
sfh mRNA
0
1
2
3
4
5
Time (h)

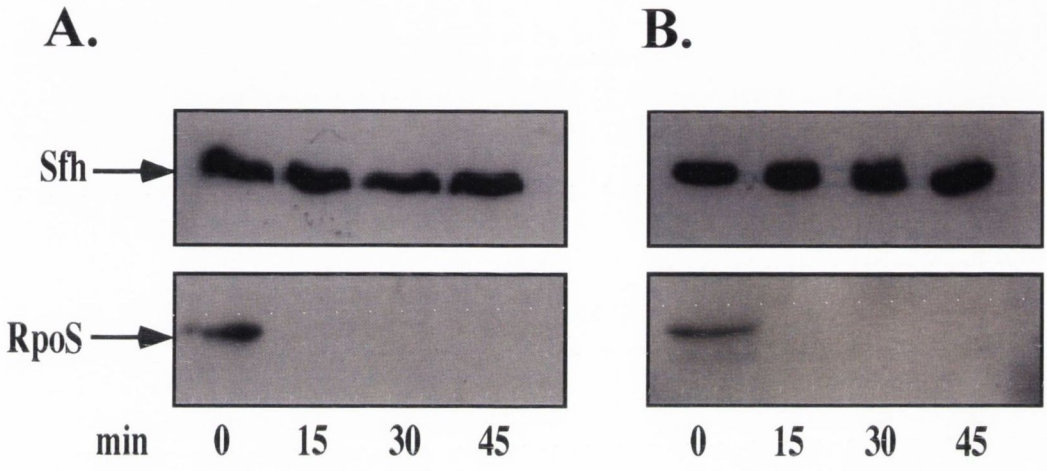

Fig. 3.8. Sfh protein stability. Western blot analysis of Sfh protein stability in (A) exponential and (B) stationary phase of growth. Wild-type strain BS184 was grown in L-broth at 37°C until exponential phase (OD_{600} ~0.3) or early stationary phase (OD_{600} ~1.5) and protein synthesis subsequently inhibited by the addition of spectinomycin (200 μg ml^{-1}) to the cultures. Protein samples were removed at the indicated time (min) before (0) or after (15, 30, 45) spectinomycin treatment. Protein samples were probed with anti-Sfh antibodies (upper panels) and also with anti-RpoS antibodies (lower panels), which act as a positive control for proteolysis.

Fig. 3.9. Sfh protein is unstable in *hns* mutants. Western blot analysis of Sfh protein stability in the (A) exponential phase, and (B) the stationary phase of growth. Wild-type strain BS184 and its *hns, stpA,* and *hns stpA* mutant derivatives were grown in L-broth at 37°C until exponential phase (OD_{600} ~ 0.3) or early stationary phase (OD_{600} ~ 1.5). Protein synthesis was subsequently inhibited by the addition of spectinomycin (200 μg ml^{-1}) to the cultures. Protein samples were removed at the indicated time in min before (0) or after (15, 30, 45) spectinomycin treatment and probed with anti-Sfh antibodies. (C) Graph shows quantitative determination of Sfh in (A), plotted as a function of time. (D) Graph shows quantitative determination of Sfh in (B), plotted as a function of time.

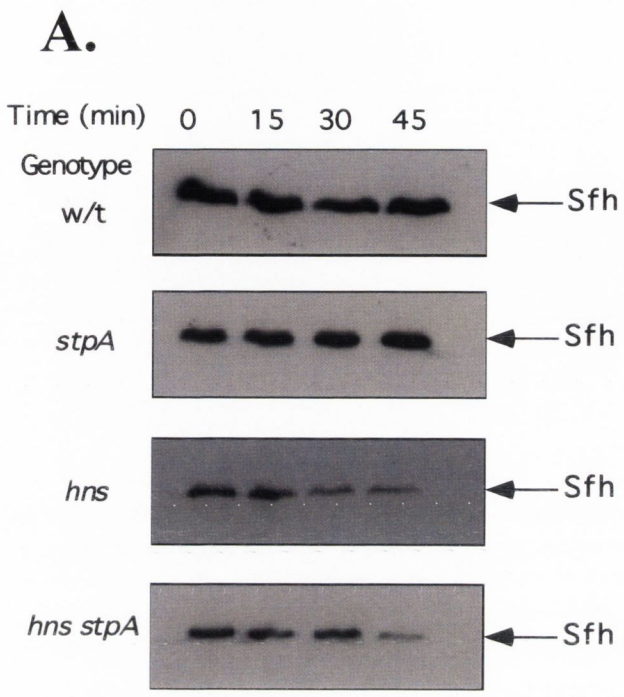
A.
Time (min) 0 15 30 45
Genotype
w/t
stpA
hns
hns stpA
Sfh
Sfh
Sfh
Sfh

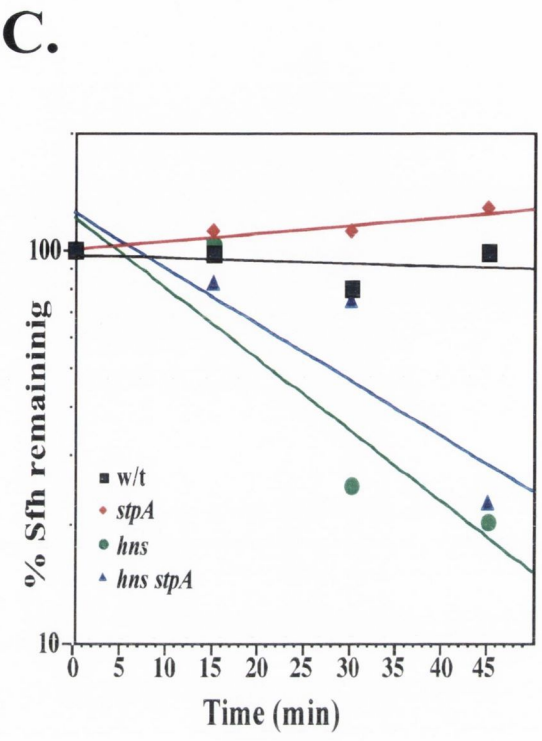
C.
100
10
% Sfh remaininig
w/t
stpA
hns
hns stpA
0 5 10 15 20 25 30 35 40 45
Time (min)

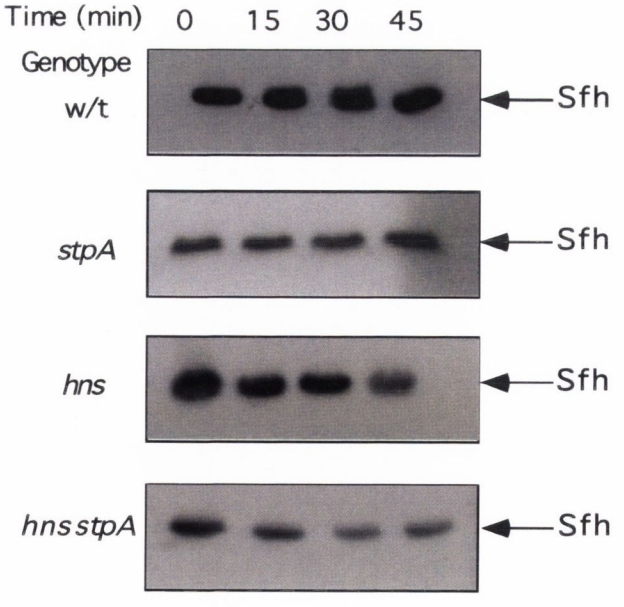
B.
Time (min) 0 15 30 45
Genotype
w/t
stpA
hns
hns stpA
Sfh
Sfh
Sfh
Sfh

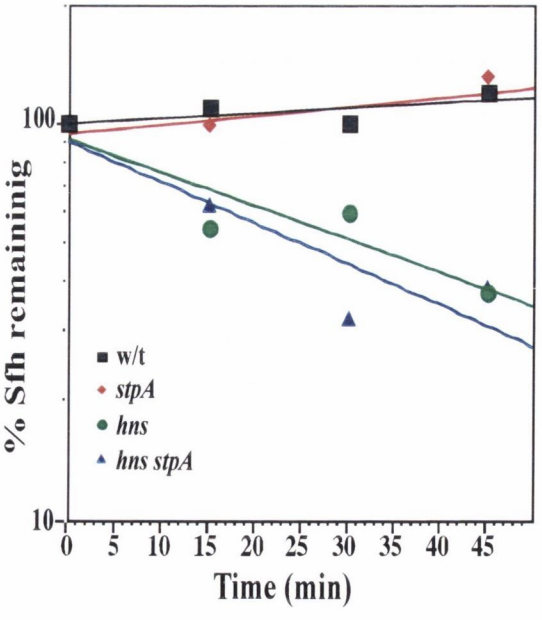
D.
100
10
% Sfh remaininig
w/t
stpA
hns
hns stpA
0 5 10 15 20 25 30 35 40 45
Time (min)

protein stability assays in a *lon, hns,* and *lon hns* mutant background, the results of which would either confirm or refute the hypothesis that Sfh is subject to Lon proteolysis. One would expect Sfh to be stable in the *lon* single mutant as this strain still expresses H-NS, but unstable in the *hns* mutant due to the lack of H-NS. Critically, if Lon is the protease mediating Sfh turnover, then Sfh should be stable in an *hns lon* mutant background, despite the absence of H-NS. This experimental approach fundamentally required *lon*, *hns,* and *lon hns* double mutant strains that expressed Sfh. Unfortunately every attempt to construct a *lon* mutant in *Shigella* was unsuccessful. Instead an *E. coli lon* mutant was utilized, and a *lon hns* double mutant was then generated by P1 transduction (Table 2.1). Since *E. coli* does not express Sfh, the *Shigella* plasmid pSf-R27Gent^R (see Section 3.2.9) had to be conjugated into the *E. coli* mutants before Sfh protein stability assays could be performed. The plasmid pSf-R27Gent^R was successfully conjugated into the *E. coli* wild-type and *hns* mutant strains, but could not be conjugated into the *lon* single or *lon hns* double mutant (data not shown). These data suggest Lon is essential for the correct expression of the H-pilus receptor on the recipient cell, which is currently unknown.

Using a different experimental approach, Sfh was expressed *in trans* from either the low-copy number plasmid pPDsfh (Table 2.2) or the medium-copy number plasmid, pYCsfh (Table 2.2) in the various *E. coli* mutant backgrounds. However, the results of subsequent protein stability assays revealed Sfh was stable in an *E. coli hns* mutant background, regardless of what expression vector was used, i.e., pPDsfh or pYCsfh (data not shown). The apparent anomaly in the *E. coli* results is most likely due to the increased cellular levels of Sfh when it is expressed *in trans* from multicopy plasmids compared to *in situ*. Consequently, Sfh might not require H-NS to protect it from degradation. This hypothesis is strengthened by the observation that during stationary phase, when Sfh protein levels are maximal in the cell, the rate of Sfh turnover in *hns* mutants is slower than in exponential phase (Fig. 3.9).

3.2.6 *sfh* mRNA stability

Cellular *sfh* mRNA levels are maximal during the early exponential phase of growth, when correspondingly, Sfh protein levels are at their lowest. This paradoxical observation could be due to changes in *sfh* mRNA stability though the growth cycle. For this reason, the stability of the *sfh* message was monitored in both the exponential and stationary phase of growth in the wild-type strain BS184. L-broth cultures corresponding to early exponential and early stationary phase (which represent when Sfh protein levels are minimum and maximum in the cell, respectively) were treated with rifampicin, an antibiotic that blocks transcription. Total RNA was then extracted in a time-course experiment and *sfh* mRNA stability followed by reverse transcription PCR (RT-PCR) (Fig. 3.10). As an internal control, the stability of the *hns* message was monitored, and its half-life found not to differ appreciably between the exponential and stationary phases of growth (Fig. 3.10). In contrast, the results of RT-PCR analysis revealed *sfh* mRNA to be more stable in exponentially growing cells than in stationary phase (Fig. 3.10). The half-lives of the *sfh* messages were determined to be ~3.2 min and 2.4 min during the exponential and stationary phases of growth, respectively (Fig. 3.10). These results imply that *sfh* growth phase-dependent expression is not controlled through differential *sfh* mRNA stability, as the *sfh* message is more stable in exponential phase, when there is virtually no Sfh protein. Since neither changes in *sfh* mRNA nor Sfh protein stability can account for growth-phase-dependent expression of the *sfh* gene, it can be deduced that *sfh* gene expression must be post-transcriptionally regulated at the translational level, i.e., the ability of the cell to translate the *sfh* mRNA. Furthermore, the *sfh* message has a long 5′ untranslated region (UTR) (Deighan *et al.*, 2003), a common feature of transcripts subject to translation control via riboregulation (Gottesman, 2004).

3.2.7 *sfh* mRNA structure

To determine if the structure of the *sfh* message could influence its translation efficiency, the secondary structure of the transcript was predicted using the RNA-folding program MFOLD (http://www.bioinfo.rpi.edu/applications/mfold/old/rna/). Significantly, the folded structure

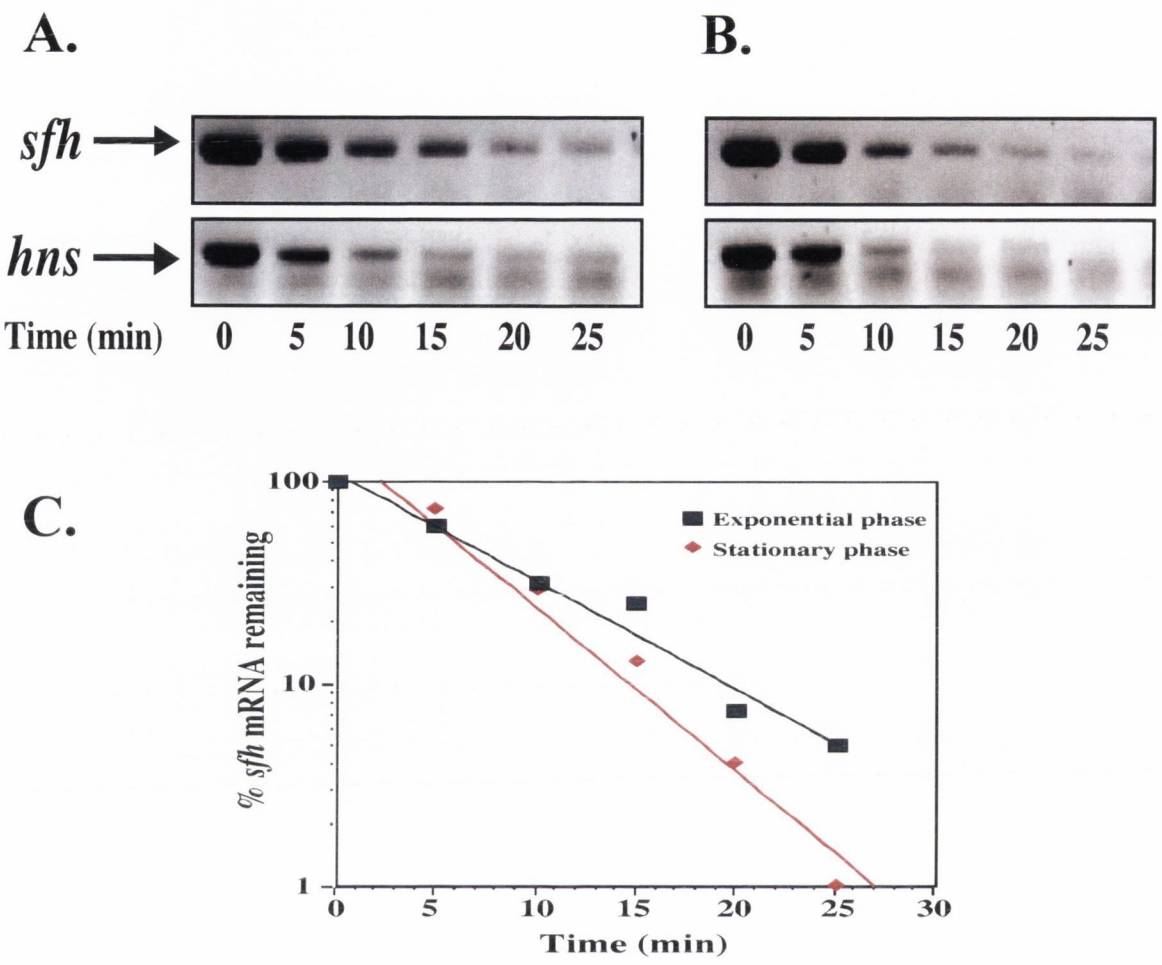

Fig. 3.10. *sfh* mRNA stability. RT-PCR analysis of *sfh* mRNA stability in the (A) exponential phase and (B) the stationary phase of growth. Wild-type strain BS184 was grown in L-broth at 37°C until early exponential phase (OD_{600} ~0.2) or early stationary phase (OD_{600} ~1.5) and transcription subsequently inhibited by the addition of rifampicin (250 μg ml^{-1}) to the cultures. Total RNA samples were extracted at the indicated time (min) before (0) or after (15, 30, 45) rifampicin treatment. mRNA stability was then analysed by RT-PCR analysis with *sfh*-specific primers and also with *hns*-specific primers as a control. (C) Graph shows quantitative determination of *sfh* mRNA in (A) and (B), plotted as a function of time.

revealed the Shine-Dalgarno (SD) sequence of the *sfh* transcript is partially sequestered in a 5′ terminal stem-loop, which would consequently impede translation (Fig. 3.11). Therefore, in order for efficient translation to occur, one can assume that the stem-loop undergoes a structural change that allows ribosomes access to the SD sequence. However, since the stem-loop is very stable (ΔG −18.7), this conformational change is thermodynamically very unfavourable. Recently several riboregulators such as DsrA and RprA have been identified that enhance translation of target mRNAs via specific RNA:RNA interactions (Repoila *et al.*, 2003). The data obtained in this study strongly suggest that a stationary phase-dependent factor, perhaps a riboregulator or an RNA chaperone, facilitates unfolding of the 5′ terminal stem-loop of the *sfh* transcript and that, therefore, *sfh* mRNA is specifically translated only during stationary phase. The proposed model would account for the observed lack of Sfh protein in early exponential phase, albeit that cellular levels of *sfh* mRNA are maximal. However, the results do not discount another hypothesis, in which an exponential phase-dependent factor binds to the *sfh* transcript and prevents its translation. Subsequently, as the cell enters the stationary phase of growth, the inhibitory factor no longer prevents translation (either it is no longer expressed or its negative influence is counteracted) and consequently Sfh protein levels rapidly increase.

3.2.8 H-NS and StpA are not involved in *sfh* growth phase-dependent expression

Both H-NS and StpA have been previously shown to negatively cross-regulate *sfh* gene expression (Deighan *et al.*, 2003) and thus could also contribute to *sfh* post-transcriptional regulation. Furthermore, both proteins have been shown to have RNA chaperone activity, in particular StpA (Brescia *et al.*, 2004; Zhang *et al.*, 1996). In addition, the expression profile of StpA is the exact opposite of Sfh, i.e., StpA is only expressed during the exponential phase of growth (Deighan *et al.*, 2000; Free and Dorman, 1997). These data correlate with the second model above, in which StpA would be the inhibitory factor that prevents *sfh* mRNA translation during the exponential phase of growth. For this reason, the effect of *stpA* and *hns* mutations on *sfh* promoter activity was monitored through the growth cycle. Plasmid psfh-

gfp (Table 2.2) was transformed into the wild-type *S. flexneri* strain BS184, and its *stpA, hns* and *hns stpA* isogenic mutants. Samples for flow cytometric analysis were harvested from early exponential, mid-exponential and stationary phase L-broth cultures of the various strains. Consistent with previous data obtained in this study, the *sfh–gfp* transcriptional fusion displayed growth phase-dependent regulation, being maximally expressed in early exponential phase and repressed ~2-fold thereafter in the wild-type strain (Fig. 3.12). The results of the transcriptional assays also revealed that, whereas in a *stpA* mutant *sfh–gfp* expression was only slightly elevated, in an *hns* mutant *sfh–gfp* expression was strongly derepressed irrespective of growth phase (Fig. 3.12). When the *hns stpA* mutations were combined in the same cell there was no enhancement of *sfh–gfp* expression levels compared those in an *hns* single mutant (Fig. 3.12). The observed minor effect of StpA and in contrast the strong repressive effect of H-NS on *sfh* transcription is in agreement with previous studies (Deighan *et al.*, 2003).

Since the *sfh* regulatory region had already been shown to possess a large region of curvature (Fig. 3.6), the ability of purified H-NS and StpA to interact with the *sfh* promoter region was also examined by competitive EMSAs (Fig. 3.13). A 438-bp DNA fragment encompassing the *sfh* regulatory region (nt –327 to +111 with respect to the transcription initiation start site of the *sfh* gene) was added to *Taq*1–*Ssp*I-digested pBR322 DNA, incubated with increasing equimolar concentrations of purified StpA or H-NS, and resolved by electrophoresis through 3% molecular screening agarose. The electrophoretic mobility of the *sfh* promoter fragment was reduced specifically by StpA and H-NS in concentration-dependent manners (Fig. 3.13). StpA and H-NS also shifted the mobility of the *bla* promoter positive control band. Taken together, these data confirm previous reports that H-NS and StpA can negatively cross-regulate *sfh* gene expression (Deighan *et al.*, 2003).

To investigate further the role of H-NS and StpA in *sfh* gene regulation, expression of the *sfh* gene was studied at the transcriptional and translational level in the wild-type strain BS184 and its *hns*, *stpA,* and *hns stpA* mutant derivatives. Transcription was studied by quantitative

Fig. 3.11. Proposed secondary structure of *sfh*. (A) The predicted secondary structure of *sfh* mRNA using the RNA-folding program, MFOLD. The Shine-Dalgarno sequence and translation initiation codon are highlighted with a red and black arrow, respectively. (B) The complete nucleotide sequence of *sfh* mRNA. The shaded sequence corresponds to the magnified area of the *sfh* secondary structure in (A). The Shine-Dalgarno and translation initiation start site are highlighted in red and bold respectively, and the 5′-untranslated region is in lower case.

A.

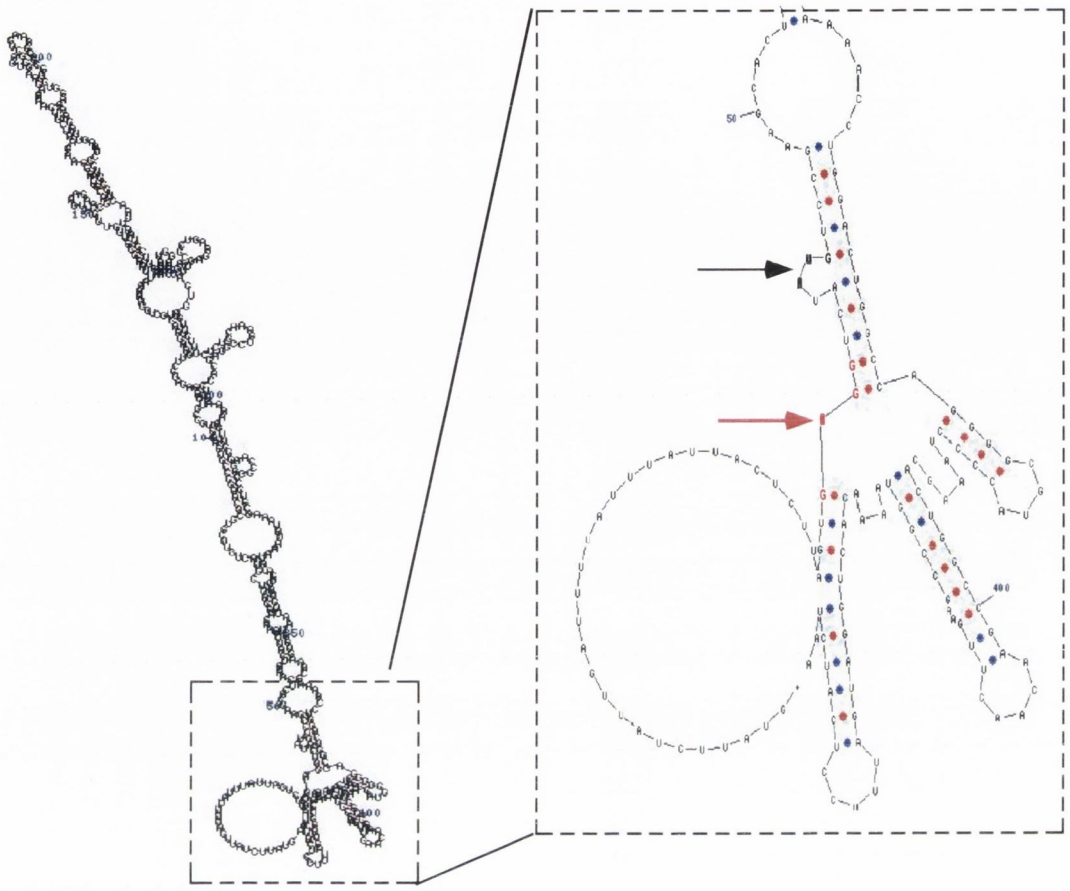

B.

guauucuauugauuuuauuuauuacucuuagu gaggucau **AUG** UCCGAAGCACUCAAAUCAU
UAAACAACAUUCGUACUCUUCGUGCGCAGGGCCGUGAACUGCCGUUAGA
GAUCCUUGAAGAACUGCUGGAAAAAUUAAGCGUUGUUGUUGAAGAACGA
CGUCAGGAAGAAUCUUCAAAAGAAGCUGAGCUGAAAGCGCGUCUGGAGA
AGAUUGAAUCCCUGCGUCAAUUAAUGCUUGAAGAUGGAAUUGACCCUGA
AGAGUUACUGAGUUCUUUCUCUGCAAAGUCCGGAGCACCUAAAAAAGUU
CGCGAACCGCGCCCUGCGAAAUAUAAAUACACUGAUGUUAAUGGUGAAA
CGAAAACCUGGACUGGCCAGGGGCGUACCCCUAAAGCACUGGCCGAACAA
CUUGAAGCCGGUAAAACACUGGAUGAUUUCCUCAUCUAA

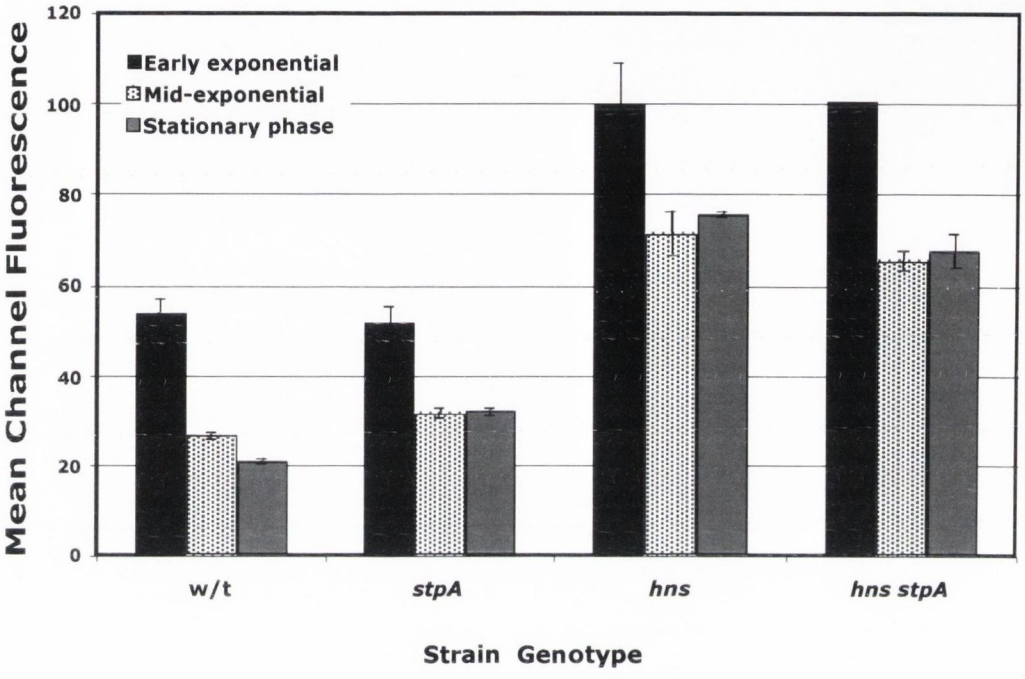

Fig. 3.12. Effect of *stpA* and *hns* mutations on *sfh* promoter activity.

Histograms show the activity of a plasmid-borne *sfh-gfp* transcriptional fusion in wild-type strain BS184 and its *hns*, *stpA*, and *hns stpA* mutant derivatives grown in L-broth at 37°C. Assays were performed on samples harvested from early exponential (OD_{600} = 0.1), mid-exponential (OD_{600} = 0.6), and early stationary (OD_{600} = 1.5) phase cultures. The data represent averages of at least three independent experiments and error bars represent standard deviations.

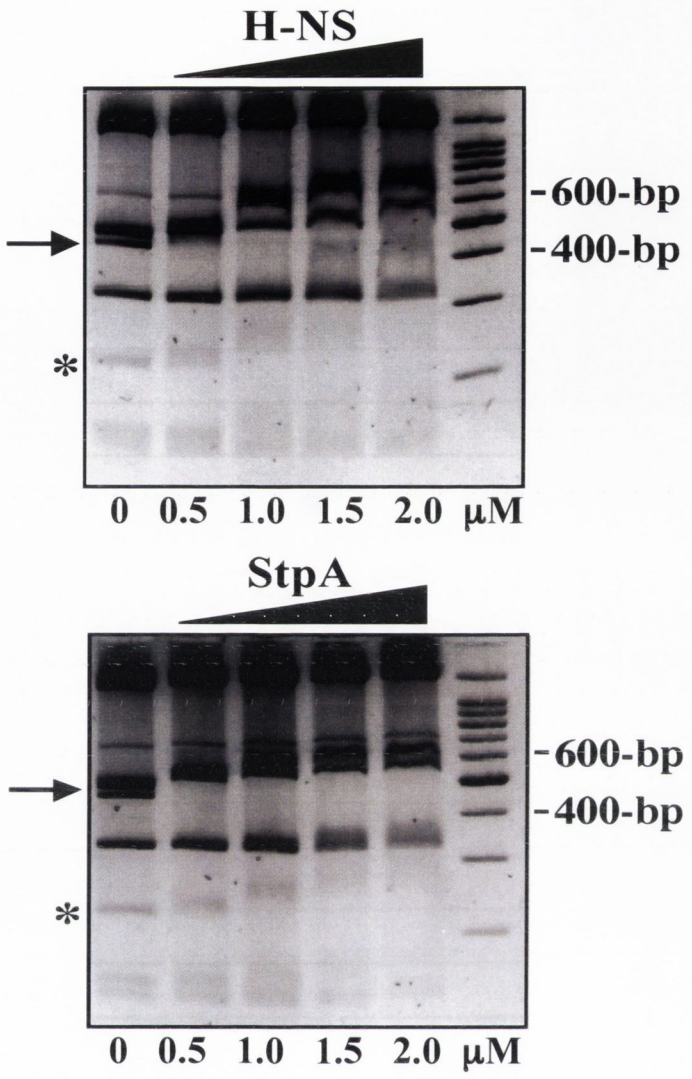

Fig. 3.13. Direct interaction of H-NS and StpA with the *sfh* promoter region.

Competitive gel retardation assays showing the specific binding of H-NS and StpA to the *sfh* promoter region. The plasmid pBR322 was digested with restriction endonucleases *Taq*1 and *Ssp*I, and the resulting DNA fragments mixed with a 438-bp amplimer of the *sfh* promoter region. The DNA mixtures were incubated with increasing equimolar concentrations of H-NS or StpA, in the range 0 μM to 2 μM. An arrow and an asterisk indicate the position of the *sfh* and *bla* promoter fragments, respectively. The curved *bla* promoter is a positive control known to bind H-NS-like proteins. The positions of the 600-bp and 400-bp molecular size markers are also indicated.

Northern blotting and translation by quantitative Western blotting. Total RNA and protein samples were isolated from cultures at fixed OD_{600} values throughout the growth curve. In agreement with previous data, the expression pattern of *sfh* mRNA in wild-type strain BS184 (Fig. 3.14) was found to be the reciprocal of that displayed by the Sfh protein (Fig. 3.15). The contributions of StpA and H-NS to *sfh* gene expression was clear in the *stpA* and *hns* mutant backgrounds. The levels of *sfh* mRNA were elevated slightly in a *stpA* mutant, whereas *sfh* mRNA levels were markedly enhanced ~2.5-fold in a *hns* mutant during exponential growth (Fig. 3.14). Interestingly, when the *hns* and *stpA* mutations were combined in the same cell, *sfh* mRNA levels were further elevated (~ 5.5-fold) compared to wild-type levels (Fig. 3.14). Consistent with the observed increase in *sfh* mRNA levels, Sfh protein levels were correspondingly elevated ~5-fold in an *hns* mutant and ~6-fold in a *stpA hns* double mutant (Fig. 3.15). Taken in aggregate these results confirm that both H-NS and StpA negatively cross-regulate *sfh* expression. However, growth phase-dependent regulation of *sfh* was still observed in all the mutant backgrounds and thus H-NS and StpA are transcriptional repressors of *sfh* expression but are not involved in the growth-phase regulation of the *sfh* gene.

3.2.9 Construction of a pSf-R27 plasmid derivative expressing gentamycin resistance

Unlike other IncHI1 plasmids, plasmid pSf-R27 does not harbour any antibiotic resistance genes (Wei *et al.*, 2003). Thus to move the plasmid pSf-R27 into a new genetic background by conjugative transfer it was necessary to tag the plasmid with a resistance marker that would allow it to be selected for in conjugal matings. The plasmid pSf-R27 was tagged with the antibiotic resistance gene *aac* from *Streptomyces lividans.*

The *aac* gene encodes gentamycin-3-acetyltransferase, which confers resistance to apramycin and gentamycin (Brau *et al.*, 1984). The *aac* gene was cloned into plasmid pSf-R27 at a genetically silent intergenic region between two R27 genes of unknown function (RO139 and RO140) by homologous recombination using an allelic replacement technique (Datsenko and Wanner, 2000). Using PCR, an *Xho*I-*Eco*RI (1.4-kb) DNA fragment containing the

intergenic region between genes RO139 and RO140 and a *Sph*I-*Sph*I (1.2-kb) DNA fragment containing the *aac* cassette were amplified with the primer pairs MD9–MD10 and MD11–MD11A, respectively (Fig. 3.16). The intergenic amplimer was digested with restriction endonucleases *Xho*I and *Eco*RI and ligated into similarly restricted plasmid pBluescript, generating vector pBluescript-IF (Table 2.2). The *aac* cassette amplimer and vector pBluescript-IF were then both digested with restriction endonuclease *Sph*I to allow ligation within the cloned intergenic region to generate vector pBluescript-IFGent^{R} (Table 2.2), which was subsequently digested with restriction endonucleases *Xho*I and *Eco*RI (Fig. 3.16).

The resulting linear 2.6-kb DNA fragment (encompassing the *aac* cassette flanked either side by ~700 bp of DNA corresponding to the intergenic region) was purified and transformed into wild-type strain BS184/pKOBEGA by electroporation (Fig. 3.16). The pKOBEGA plasmid (Table 2.2) harbours a thermosensitive replicon and the λ phage *redγβα* operon under the control of the P_{BAD} promoter (Chaveroche *et al.*, 2000). The Exo, Bet and Gam proteins necessary for homologous recombination reaction were induced during preparation of the BS184/pKOBEGA electrocompetent cells by the addition of 0.02% L-arabinose when the culture reached an OD_{600}nm of 0.2. Growth at 30°C was continued until the culure reached an OD_{600}nm of ~1. Positive clones were selected by growth on L-agar plates containing kanamycin (50 μg ml^{-1}) and gentamycin (15 μg ml^{-1}) at 37°C for 36 h. They were single-colony purified four times, and then tested for the loss of the thermosensitive pKOBEGA plasmid.

To ensure correct insertion of the *aac* cassette into plasmid pSf-R27, positive clones were confirmed by PCR analyses using internal and external primers (Fig. 3.16). One of the positive clones, designated plasmid pSf-R27Gent^{R,} was then conjugated into a fresh strain BS184 genetic background and also into *hns* and *stpA* mutant backgrounds as described previously (Taylor and Levine, 1980).

Fig. 3.14. Effect of *hns* and *stpA* mutations on *sfh* mRNA expression profile.

(A) Northern blot analysis of the *sfh* mRNA content of wild-type strain BS184 and its *hns*, *stpA*, and *hns stpA* mutant derivatives grown in L-broth at 37°C. Total RNA was extracted at fixed OD_{600} values throughout the growth curve and probed with a *sfh*-specific riboprobe. As a control for RNA integrity and loading, total RNA was also hybridized with an *rrnA*-specific riboprobe. The labelling above each lane refers to the stage of the growth curve when the samples were extracted, namely, (a) early exponential phase (OD_{600} = 0.1), (b) mid-exponential phase (OD_{600} = 0.6), and (c) early stationary phase (OD_{600} = 1.5). The positions of migration of the molecular size markers are indicated. (B) Histograms showing densitometric analyses of the data in (A). The relative transcript levels are expressed as a percentage of the *sfh* mRNA content of strain BS184 cells at OD_{600} = 0.1 (early exponential phase), the value of which was taken as 100%. The data shown are averages of at least three independent experiments and a representative blot is shown.

A.

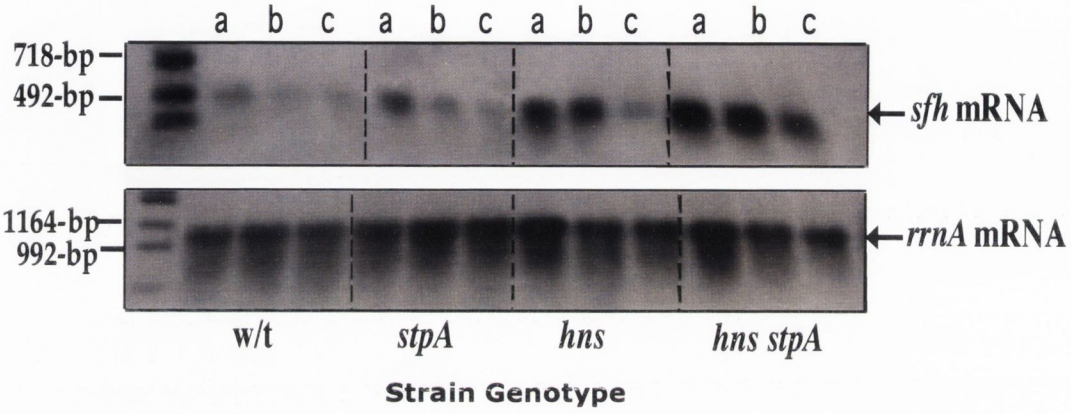
a b c a b c a b c a b c
718-bp
492-bp
sfh mRNA
1164-bp
992-bp
rrnA mRNA
w/t
stpA
hns
hns stpA
Strain Genotype

B.

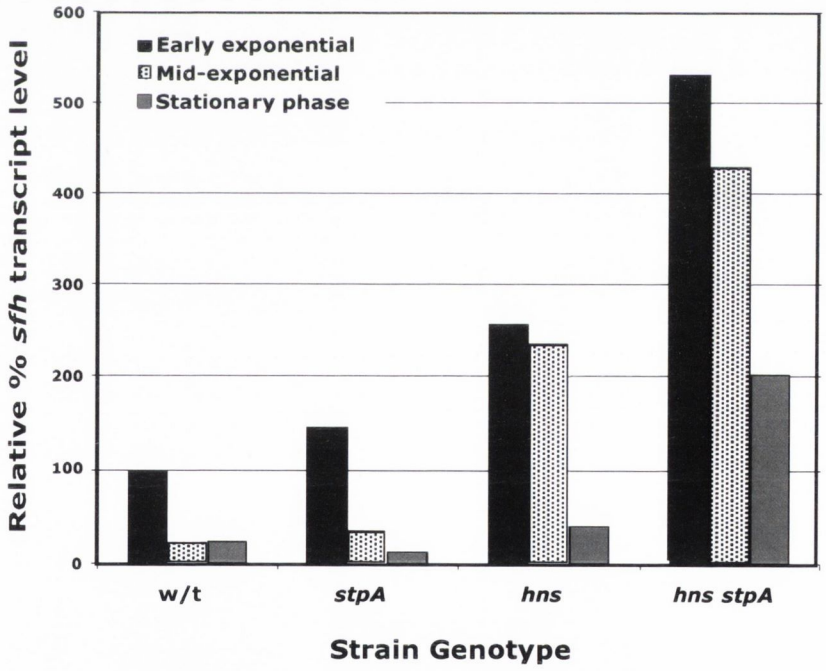
Relative % sfh transcript level
600
500
400
300
200
100
0
Early exponential
Mid-exponential
Stationary phase
w/t
stpA
hns
hns stpA
Strain Genotype

Fig. 3.15. Effect of *hns* and *stpA* mutations on Sfh expression profile.

(A) Western blot of the Sfh content of wild-type strain BS184 and its *hns*, *stpA*, and *hns stpA* mutant derivatives grown in L-broth at 37°C. Total protein samples were harvested at fixed OD_{600} values throughout the growth curve and probed with anti-Sfh antibodies. The labelling above each lane refers to the stage of the growth curve when the samples were harvested, namely, (a) early exponential phase (OD_{600} = 0.1), (b) mid-exponential phase (OD_{600} = 0.6) and (c) early stationary phase (OD_{600} = 1.5). (B) Histograms showing densitometric analyses of the data in (A). The relative percentages of protein are expressed as a percentage of the Sfh content of strain BS184 cells at OD_{600} = 1.5 (early stationary), the value of which was taken as 100%. The data shown are averages of at least three independent experiments and a representative blot is shown.

A.

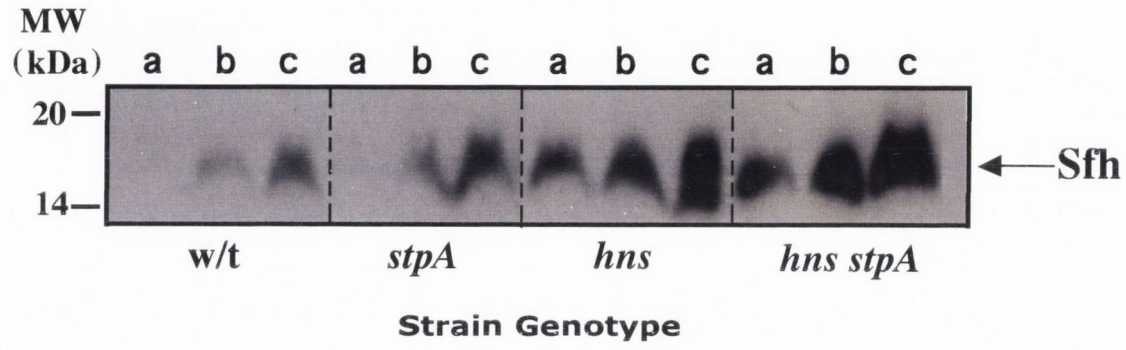
MW
(kDa)
a b c a b c a b c a b c
20
14
Sfh
w/t
stpA
hns
hns stpA
Strain Genotype

B.

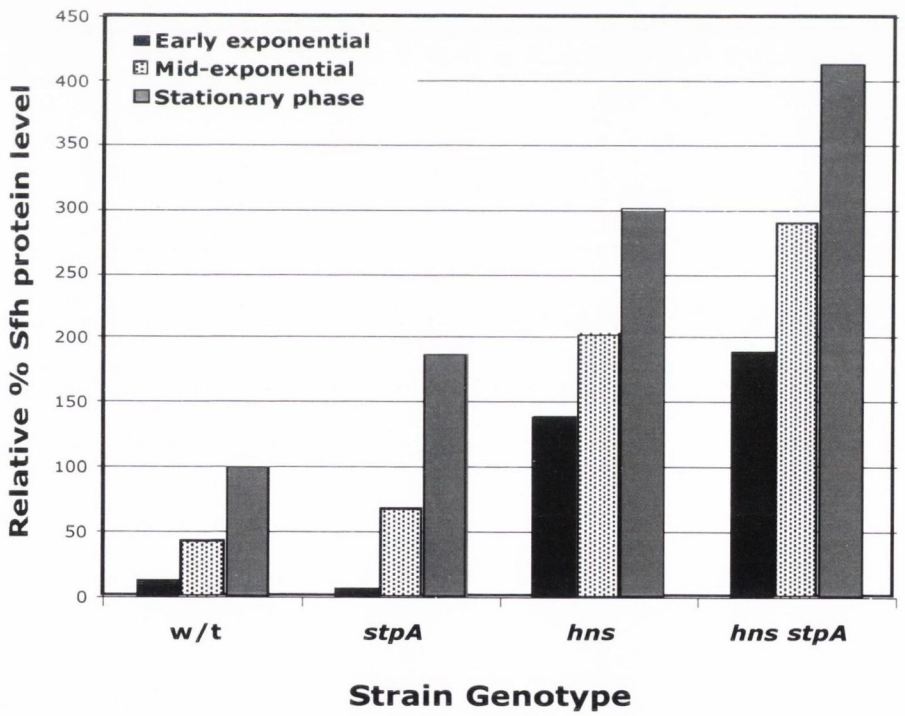
Early exponential
Mid-exponential
Stationary phase
Relative % Sfh protein level
450
400
350
300
250
200
150
100
50
0
w/t
stpA
hns
hns stpA
Strain Genotype

Fig. 3.16. Construction of a pSf-R27 plasmid derivative expressing gentamycin resistance. (A) Schematic representation of the allelic replacement technique used to clone the *Streptomyces lividans aac* gene into a genetically silent intergenic region between two R27 plasmid genes of unknown function (RO139 and RO140). The *aac* gene product, gentamycin-3-acetyltransferase, confers resistance to apramycin and gentamycin (Apr/Gent). Details of the replacement technique are described in Section 3.2.9. (B) PCR analyses confirming the correct insertion of the *aac* gene into plasmid pSf-R27Gent^R. Plasmid DNA was isolated from positive transformants and used as template in PCR reactions, with internal and external primers to the region exchanged as indicated in the diagram. DNA fragment A was amplified with the internal primers MD9–MD10 and confirms the presence of the entire region exchanged. DNA fragments B and C were amplified with the internal and external primers MD5–MD11A and MD11–MD6, respectively and confirm the correct insertion of the *aac* gene into plasmid pSf-R27. One positive transformant that was shown to have the correct insertion of the *aac* gene was designated pSf-R27Gent^R.

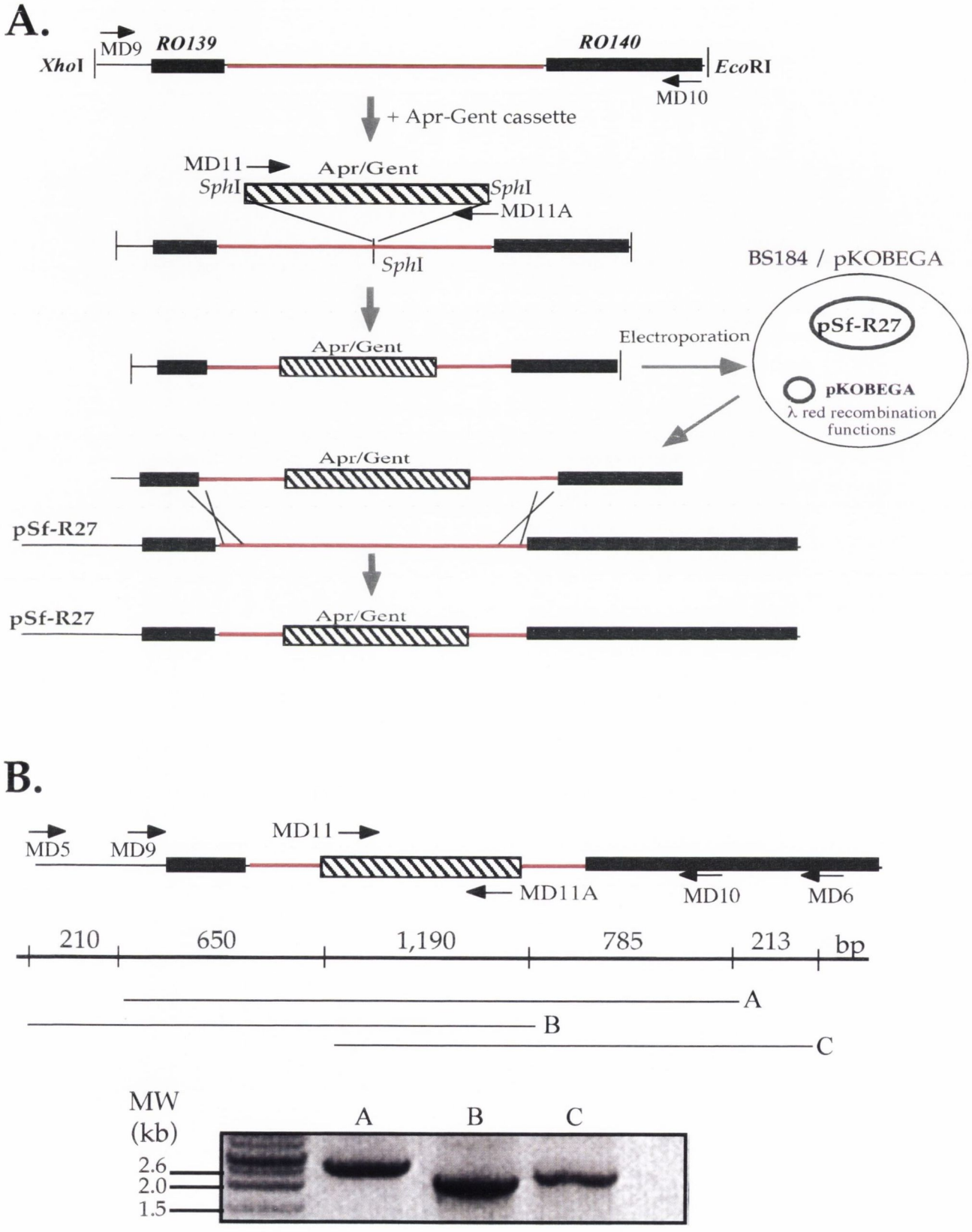
A.
MD9
RO139
RO140
XhoI
EcoRI
MD10
+ Apr-Gent cassette
MD11
Apr/Gent
SphI
SphI
MD11A
SphI
BS184 / pKOBEGA
Electroporation
pSf-R27
pKOBEGA
λ red recombination functions
Apr/Gent
Apr/Gent
pSf-R27
pSf-R27
Apr/Gent
B.
MD5
MD9
MD11
MD11A
MD10
MD6
210
650
1,190
785
213
bp
A
B
C
MW
(kb)
2.6
2.0
1.5
A
B
C

3.2.10 *sfh* growth-phase-dependent expression is independent of plasmid pSf-R27Gent^R

The results of above studies have demonstrated that growth-phase-dependent expression of the *sfh* gene is controlled post-transcriptionally at the translational level by an unknown factor. To determine if this factor was *Shigella*- or plasmid pSf-R27-specific, *sfh* gene expression was monitored in the wild-type *E. coli* stain MC4100 with and without plasmid pSf-R27Gent^R. Plasmid pSf-R27Gent^R encoding the *sfh* gene was transferred into the wild-type *E. coli* strain MC4100 by conjugation and the newly constructed strain, designated MC4100(pSf-R27 Gent^R), confirmed by PCR and Western blot analyses (data not shown). The reporter plasmid psfh-gfp (Table 2.2) was then transformed into the wild-type strain MC4100 and its plasmid-bearing derivative MC4100(pSf-R27Gent^R). Samples for flow cytometric analysis were harvested at intervals from 37°C L-broth cultures of strains MC4100 and MC4100(pSf-R27 Gent^R) throughout the growth curve. The flow cytometry results revealed that the transcriptional profiles of the *sfh* gene in *E. coli* and *Shigella* are virtually indistinguishable (Fig. 3.17 and 3.5). Intriguingly, *sfh–gfp* expression levels were markedly higher (~3-fold) in strain MC4100(pSf-R27Gent^R) than in the wild-type strain MC4100 during the stationary phase of growth (Fig. 3.17). These results imply that plasmid pSf-R27Gent^R might encode a positive regulator of *sfh* expression.

Expression of the *sfh* gene was also monitored at the translational level in strain MC4100(pSf-R27Gent^R) at various intervals throughout the growth curve by quantitative Western blotting (Fig. 3.17) The expression profile of Sfh obtained was very similar to that observed in *Shigella*, with low levels of Sfh detected during the exponential phase of growth and a dramatic induction in Sfh seen as the cell entered stationary phase (Fig. 3.17). To eliminate the possibility that plasmid pSf-R27Gent^R encodes the factor mediating *sfh* growth phase-dependent regulation, Sfh was expressed *in trans* from the multicopy plasmid pYCsfh. Total protein samples for Western immunoblotting were then harvested from exponential and stationary phase L-broth cultures of strain MC4100 harbouring either plasmid pYCsfh or pSf-R27Gent^R. Comparison of the results obtained clearly illustrate that Sfh expression is still growth phase regulated in the absence of plasmid pSf-R27Gent^R (Fig. 3.18). Collectively,

these data reveal that the factor controlling *sfh* growth phase-dependent expression is not specific to *Shigella* or encoded by plasmid pSf-R27Gent^R. The results indicate that the factor is more universal and therefore probably encoded by a chromosomal gene.

3.2.11 Thermal regulation of Sfh expression

H-NS and StpA expression have been shown previously to be regulated by temperature, with enhanced transcription of the *hns* and *stpA* genes being stimulated during cold shock (an abrupt decrease in the the temperature of the growth medium from 37°C to 4°C) and heat shock (an abrupt increase in the the temperature of the growth medium from 30°C to 42°C), respectively (Free and Dorman, 1997; La Teana *et al.*, 1991). Quantitative Western blotting was used to investigate whether heat (Fig. 3.19) and/or cold shock (Fig. 3.20) affected Sfh expression. To examine Sfh expression in response to heat shock, wild-type *Shigella* strain BS184 was grown in L-broth at 30°C until early exponential phase and then the culture split in two. One half was allowed to continue growing at 30°C, while the other half was incubated at 42°C. Total protein samples were then harvested in a time-course experiment and Sfh expression followed by Western immunoblotting. The results revealed Sfh expression was non-responsive to the heat shock (Fig. 3.19). In both the starting culture (30°C) and the heat-shock culture (42°C), Sfh levels were relatively equal and the normal growth-phase regulation of Sfh was observed (Fig. 3.19). As a positive control for heat shock, protein samples were also probed with anti-StpA antibodies. In this case the heat shock led to a very strong sustained increase in StpA after 60 min and no enhanced StpA expression was seen in the 30°C control culture (Fig. 3.19).

The effect of cold shock on Sfh expression was also monitored by Western immunoblotting (Fig. 3.20). This time the starting culture was grown at 37°C and then split into two aliquots. One aliquot was allowed to continue growing at 37°C, while the other aliquot was incubated at 4°C. This cold-shock treatment resulted in an immediate halt to bacterial growth. The cellular Sfh protein content appeared to be unaffected by the cold-shock treatment, whereas

3.2.10 *sfh* growth-phase-dependent expression is independent of plasmid pSf-R27Gent^R

The results of above studies have demonstrated that growth-phase-dependent expression of the *sfh* gene is controlled post-transcriptionally at the translational level by an unknown factor. To determine if this factor was *Shigella*- or plasmid pSf-R27-specific, *sfh* gene expression was monitored in the wild-type *E. coli* stain MC4100 with and without plasmid pSf-R27Gent^R. Plasmid pSf-R27Gent^R encoding the *sfh* gene was transferred into the wild-type *E. coli* strain MC4100 by conjugation and the newly constructed strain, designated MC4100(pSf-R27 Gent^R), confirmed by PCR and Western blot analyses (data not shown). The reporter plasmid psfh-gfp (Table 2.2) was then transformed into the wild-type strain MC4100 and its plasmid-bearing derivative MC4100(pSf-R27Gent^R). Samples for flow cytometric analysis were harvested at intervals from 37°C L-broth cultures of strains MC4100 and MC4100(pSf-R27 Gent^R) throughout the growth curve. The flow cytometry results revealed that the transcriptional profiles of the *sfh* gene in *E. coli* and *Shigella* are virtually indistinguishable (Fig. 3.17 and 3.5). Intriguingly, *sfh–gfp* expression levels were markedly higher (~3-fold) in strain MC4100(pSf-R27Gent^R) than in the wild-type strain MC4100 during the stationary phase of growth (Fig. 3.17). These results imply that plasmid pSf-R27Gent^R might encode a positive regulator of *sfh* expression.

Expression of the *sfh* gene was also monitored at the translational level in strain MC4100(pSf-R27Gent^R) at various intervals throughout the growth curve by quantitative Western blotting (Fig. 3.17) The expression profile of Sfh obtained was very similar to that observed in *Shigella*, with low levels of Sfh detected during the exponential phase of growth and a dramatic induction in Sfh seen as the cell entered stationary phase (Fig. 3.17). To eliminate the possibility that plasmid pSf-R27Gent^R encodes the factor mediating *sfh* growth phase-dependent regulation, Sfh was expressed *in trans* from the multicopy plasmid pYCsfh. Total protein samples for Western immunoblotting were then harvested from exponential and stationary phase L-broth cultures of strain MC4100 harbouring either plasmid pYCsfh or pSf-R27Gent^R. Comparison of the results obtained clearly illustrate that Sfh expression is still growth phase regulated in the absence of plasmid pSf-R27Gent^R (Fig. 3.18). Collectively,

these data reveal that the factor controlling *sfh* growth phase-dependent expression is not specific to *Shigella* or encoded by plasmid pSf-R27Gent^R. The results indicate that the factor is more universal and therefore probably encoded by a chromosomal gene.

3.2.11 Thermal regulation of Sfh expression

H-NS and StpA expression have been shown previously to be regulated by temperature, with enhanced transcription of the *hns* and *stpA* genes being stimulated during cold shock (an abrupt decrease in the the temperature of the growth medium from 37°C to 4°C) and heat shock (an abrupt increase in the the temperature of the growth medium from 30°C to 42°C), respectively (Free and Dorman, 1997; La Teana *et al.*, 1991). Quantitative Western blotting was used to investigate whether heat (Fig. 3.19) and/or cold shock (Fig. 3.20) affected Sfh expression. To examine Sfh expression in response to heat shock, wild-type *Shigella* strain BS184 was grown in L-broth at 30°C until early exponential phase and then the culture split in two. One half was allowed to continue growing at 30°C, while the other half was incubated at 42°C. Total protein samples were then harvested in a time-course experiment and Sfh expression followed by Western immunoblotting. The results revealed Sfh expression was non-responsive to the heat shock (Fig. 3.19). In both the starting culture (30°C) and the heat-shock culture (42°C), Sfh levels were relatively equal and the normal growth-phase regulation of Sfh was observed (Fig. 3.19). As a positive control for heat shock, protein samples were also probed with anti-StpA antibodies. In this case the heat shock led to a very strong sustained increase in StpA after 60 min and no enhanced StpA expression was seen in the 30°C control culture (Fig. 3.19).

The effect of cold shock on Sfh expression was also monitored by Western immunoblotting (Fig. 3.20). This time the starting culture was grown at 37°C and then split into two aliquots. One aliquot was allowed to continue growing at 37°C, while the other aliquot was incubated at 4°C. This cold-shock treatment resulted in an immediate halt to bacterial growth. The cellular Sfh protein content appeared to be unaffected by the cold-shock treatment, whereas

Fig. 3.17. *sfh* gene expression is growth phase regulated in *E. coli*. (A) Graph shows *sfh* promoter activity in wild-type *E. coli* strain MC4100 with and without plasmid pSf-R27Gent^R. Strains MC4100 (w/t) and MC4100 harbouring plasmid pSf-R27Gent^R (w/t pSf-R27Gent^R) were grown in L-broth at 37°C containing either plasmid psfh-gfp or pZep08 (plasmid control). Samples of culture were harvested at various time points throughout the growth curve to analyse *sfh–gfp* expression. The labelling above each data point (a – h) refers to the stage of the growth curve when the samples were extracted as depicted in (B). The data represent averages of at least three independent experiments and error bars represent standard deviations. (B) Graph shows growth curve of strain MC4100(pSf-R27Gent^R) in L-broth at 37°C. (C) Western blot analysis of Sfh protein levels in strain MC4100(pSf-R27Gent^R) grown in L-broth at 37°C. Total protein samples were harvested at various time points throughout the growth curve and probed with anti-Sfh-specific antibodies. The labelling above each lane refers to the stage of the growth curve when the samples were extracted as depicted in (B). The positions of the molecular size markers are indicated. The experiment was repeated on three independent occasions and a representative blot is shown.

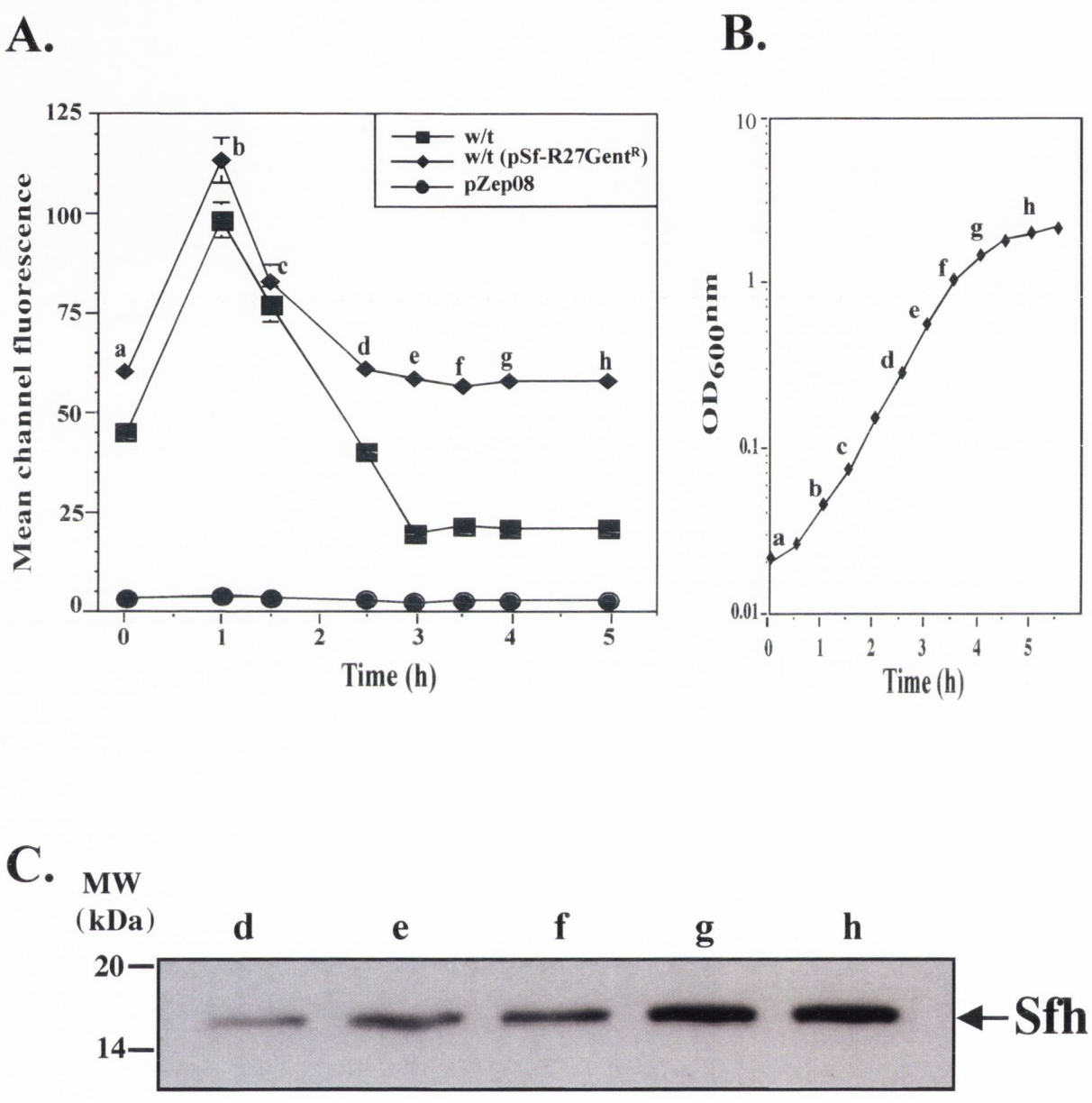
A.
B.
C.
Mean channel fluorescence
Time (h)
w/t
w/t (pSf-R27Gent^R)
pZep08
OD600nm
MW
(kDa)
20
14
Sfh

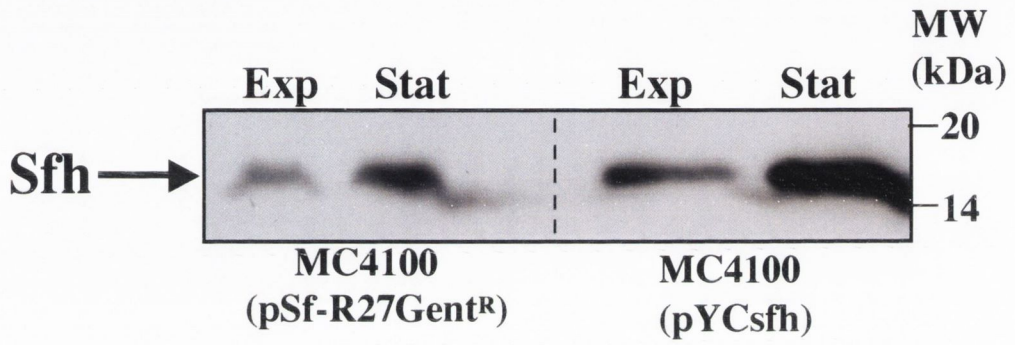

Fig. 3.18. Sfh growth-phase expression is independent of pSf-R27Gent^R. Western blot analysis of Sfh protein levels in *E. coli* strain MC4100 harbouring either plasmid pSf-R27Gent^R or pYCsfh. Strains were grown in L-broth at 37°C and total protein samples harvested during the exponential phase (OD_{600} = 0.6) and stationary phase (OD_{600} = 2.0) of growth. Total protein samples were probed with anti-Sfh specific antibodies. The positions of the molecular size markers are indicated. The experiment was repeated on three independent occasions and a representative blot is shown.

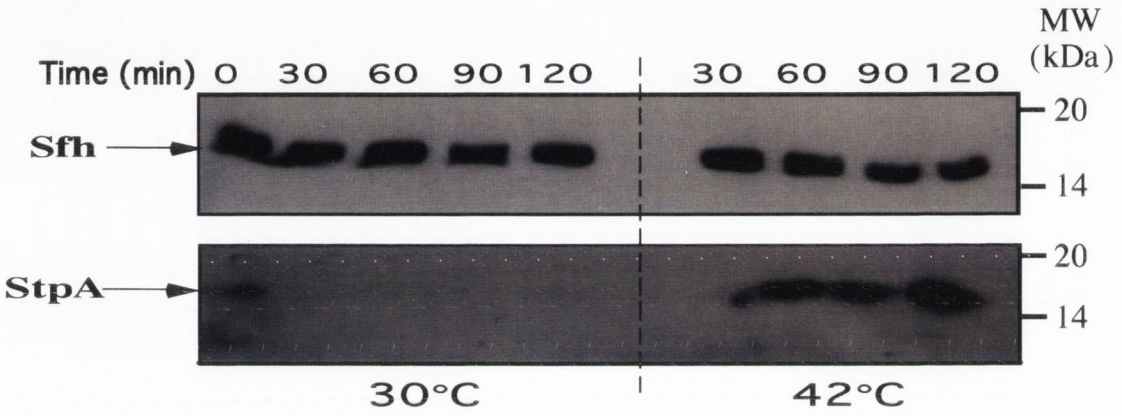

Fig. 3.19. Effect of heat shock on Sfh expression. Western blot analysis of Sfh expression in response to heat shock. Wild-type strain BS184 was grown in L-broth at 30°C until the early exponential phase of growth (OD_{600} ~ 0.3) and then the culture split in two. One half was allowed to continue growing at 30°C, while the other half was heat-shocked and incubated at 42°C. Total protein samples were harvested at the indicated time (min) before (0) or after (30, 60, 90, 120) heat-shock treatment and probed with anti-Sfh antibodies. As a control for heat shock, protein samples were also probed with anti-StpA specific antibodies. The positions of the molecular size markers are indicated. The experiment was repeated on three independent occasions and a representative blot is shown.

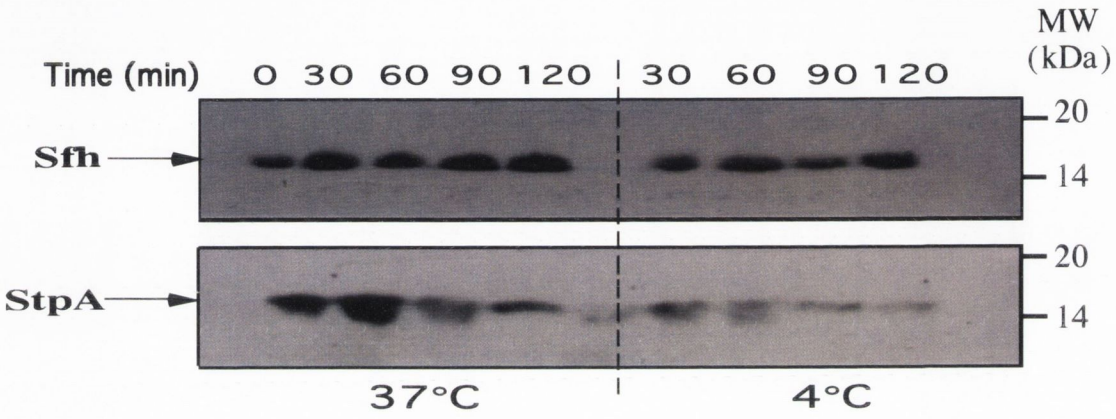

Fig. 3.20. Effect of cold shock on Sfh expression. Western blot analysis of Sfh expression in response to cold shock. Wild-type strain BS184 was grown in L-broth at 37°C until the early exponential phase of growth (OD_{600} ~ 0.3) and then the culture split in two. One half was allowed to continue growing at 37°C, while the other half was cold-shocked and incubated at 4°C. Total protein samples were harvested at the indicated time (min) before (0) or after (30, 60, 90, 120) cold-shock treatment and probed with anti-Sfh and anti-StpA antibodies. The positions of the molecular size markers are indicated. The experiment was repeated on three independent occasions and a representative blot is shown.

the cellular StpA content decreased by 6-fold following the cold-shock stress (Fig. 3.20). In agreement with previous data, H-NS expression was induced by cold shock (data not shown). It can be concluded from the above results that unlike H-NS and StpA, Sfh expression appears to be more or less unaffected by either heat shock or cold shock.

Quantitative Western blot analysis was also used to monitor expression of all three *S. flexneri* H-NS-like proteins in response to temperature of the growth medium (Fig. 3.21). Total protein samples were harvested at various intervals throughout the growth cycle from L-broth cultures of wild-type strain BS184 grown at either 25°C or 37°C. Consistent with previous data (Free and Dorman, 1997; Sonden and Uhlin, 1996), StpA expression was significantly higher in the 37°C grown culture than in the 25°C culture (Fig. 3.21). In the case of H-NS expression, there was dramatically less H-NS present in the 25°C culture during exponential growth compared to the level of H-NS in 37°C culture (Fig. 3.21). In contrast, Sfh protein levels were elevated in the culture grown at the lower temperature of 25°C than in the 37°C culture (Fig. 3.21). These results clearly show that H-NS, StpA, and Sfh are differentially expressed depending on the temperature of the growth medium and that all three H-NS-like proteins have distinct and unique expression profiles in rich broth at 25°C and 37°C.

3.3 Discussion

In recent years the family of known H-NS-like proteins in Gram-negative bacteria has expanded rapidly, largely resulting from the pace of complete bacterial genome sequencing (Tendeng and Bertin, 2003). Sequencing studies have also highlighted that, although some bacteria contain only one *hns* gene, many others contain multiple *hns*-related genes, as is the case for *S. flexneri* serotype 2a strain 2457T. This bacterium harbours three *hns*-like genes, namely, *hns* and *stpA,* and also the novel *hns*-like gene, *sfh* (Beloin *et al.*, 2003). Expression of the chromosomal genes *hns* and *stpA* is tightly controlled by complex regulatory networks, which involve several *trans*-acting factors and environmental cues (Dorman, 2004). The aim of this study was to analyse in detail the expression profile of the *sfh* gene during growth in rich medium and to determine the environmental and cellular factors that influence *sfh* gene expression.

Expression of the *sfh* gene was studied at both the transcriptional and translational level through the growth cycle in rich medium (Fig. 3.5 and 3.7). Like its homologues, *hns* (Dersch *et al.*, 1993; Free and Dorman, 1995) and *stpA* (Free and Dorman, 1997; Sonden and Uhlin, 1996), *sfh* gene expression was revealed to be growth-phase regulated. At the transcriptional level, *sfh* gene expression was monitored by flow cytometry using a *sfh–gfp* transcriptional fusion (Fig. 3.5) and by quantitative Northern blotting (Fig. 3.7). The transcriptional profiles obtained for the *sfh* promoter and *sfh* mRNA correlated, and revealed that there is a burst of *sfh* gene expression immediately after subculture (early exponential phase) and thereafter a sharp decline in *sfh* gene expression (Fig. 3.5 and 3.7). Furthermore, *sfh* gene expression was observed to be elevated in the *sfh* mutant compared to the wild-type strain (Fig. 3.5), verifying previous reports that Sfh negatively autoregulates its own expression (Deighan *et al.*, 2003). Consistent with this, purified Sfh preferentially bound to the *sfh* regulatory region in a competitive gel retardation assay (Fig. 3.6). Significantly, despite increased *sfh* gene expression in the absence of Sfh, the overall transcriptional regulatory profiles of the *sfh* gene in the wild-type and *sfh* mutant strains were identical, i.e., *sfh* gene expression was still growth-phase regulated (Fig. 3.5). Therefore, it must be

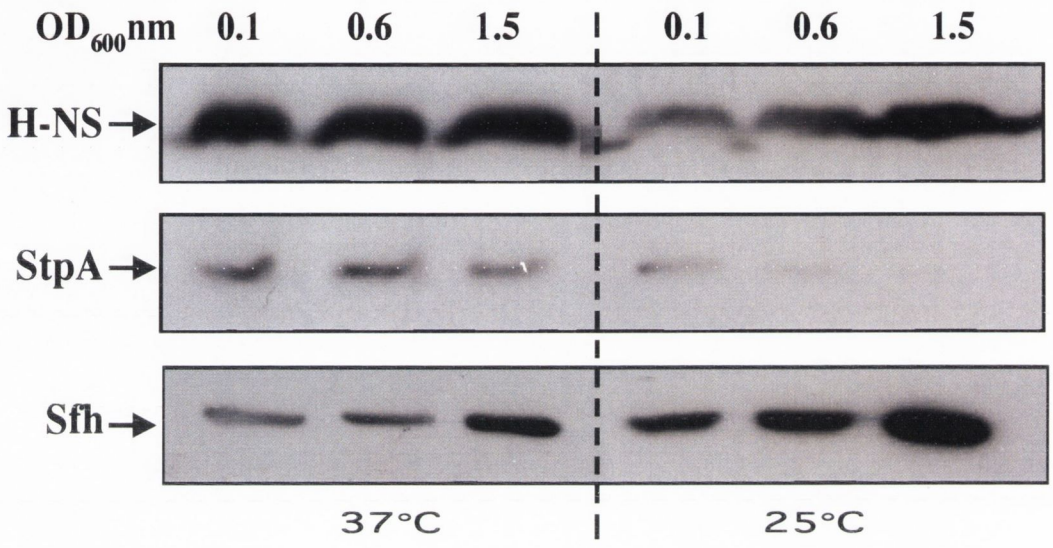

Fig. 3.21. Thermal regulation of Sfh, H-NS, and StpA expression. Western blot analysis of Sfh, H-NS, and StpA expression in wild-type strain BS184 grown in L-broth at 25°C and 37°C. Total protein samples were harvested at fixed OD_{600} values throughout the growth curve corresponding to the early exponential phase (OD_{600} = 0.1), mid-exponential phase (OD_{600} = 0.6), and early stationary phase (OD_{600} = 1.5) of growth. Total protein samples were probed with anti-H-NS-, anti-StpA- and anti-Sfh-specific antibodies as indicated. The experiment was repeated on three independent occasions and representative blots are shown.

concluded that Sfh negatively autoregulates its own expression, but does not influence *sfh* gene growth phase-dependent expression. Instead the results suggest that either transcription of the *sfh* gene is induced by a *trans*-acting factor expressed during early exponential phase or that it is repressed by a factor expressed during the stationary phase of growth, which following subculture is diluted, resulting in increased *sfh* transcriptional activity. Interestingly, the nucleoid-associated proteins FIS and LRP are both specifically expressed during the early exponential phase of growth in rich media (Azam *et al.*, 1999) and positively regulate *hns* and *stpA* gene expression, respectively (Falconi *et al.*, 1996; Zhang *et al.*, 1996). In addition, their consensus binding-sites are very AT-rich (McLeod and Johnson, 2001), a feature consistent with the *sfh* regulatory region (Fig. 3.6). Furthermore, *sfh* gene expression is negatively cross-regulated by H-NS and StpA (Fig. 3.12, 3.14 and 3.15) and FIS and Lrp are known to antagonize H-NS-mediated repression at several promoters such as those of the *fimB* (Kawula and Orndorff, 1991), *ompC* (Suzuki *et al.*, 1996) and *rrnB* genes (Tippner *et al.*, 1994).

Using Western immunoblotting the expression profile of the Sfh protein was found to be the reciprocal of that displayed by the *sfh* mRNA (Fig. 3.7). Sfh protein levels were observed to be very low during exponential growth, but dramatically increased ~4-fold at the onset of stationary phase (Fig. 3.7). Therefore, the three *Shigella* H-NS-like proteins –H-NS, StpA, and Sfh– all have distinct growth-phase expression profiles in rich broth. H-NS protein levels remain relatively constant throughout the growth cycle (Free and Dorman, 1995), whereas StpA (Free and Dorman, 1997) and Sfh (Fig. 3.7) are only abundant in early exponential phase and stationary phase, respectively. The differential expression of Sfh, StpA, and H-NS provides *Shigella* with the capacity to vary the composition of its H-NS-like proteins as a function of growth phase. Consequently, the formation of homomeric and heteromeric protein complexes *in vivo* will alter, as the different H-NS-like proteins become the dominant species. This scenario is analogous to the differential growth-phase expression of the two subunits, α and β, of the nucleoid-associated protein HU (Claret and Rouviere-Yaniv, 1997). The differential growth-phase expression of the two subunits results in the formation of three

different HU protein complexes *in vivo* (Claret and Rouviere-Yaniv, 1996, 1997). Throughout the growth curve, the composition of HU varies from homomeric $HU\alpha_2$ complexes (early exponential phase), to heteromeric $HU\alpha\beta$ complexes (mid to late exponential phase), to homomeric $HU\beta_2$ complexes (stationary phase) (Claret and Rouviere-Yaniv, 1997). The different HU complexes have distinct effects on cellular physiology (Claret and Rouviere-Yaniv, 1997) and support a model that the properties of different H-NS-like protein complexes could also vary depending on their subunit composition. Moreover, the hypothesis is further strengthened by a recent study that revealed that mutants deficient in either IHFα, IHFβ, or both IHFα and IHFβ do not have equivalent effects on gene expression (Mangan *et al.*, 2006). Significantly, Mangan *et al.* (2006) revealed that there are three overlapping IHF regulons in *S.* Typhimurium due to the formation of three different IHF complexes ($IHF\alpha_2$ $IHF\beta_2$ $IHF\alpha\beta$), all of which have common and unique regulatory properties (Mangan *et al.*, 2006).

The disparate expression profiles of *sfh* mRNA and protein (Fig. 3.7) indicate that *sfh* growth-phase-dependent expression is regulated not only at the level of transcription, but also post-transcriptionally at either the level of the *sfh* message and/or the Sfh protein. Analysis of Sfh protein stability in a wild-type background revealed that the Sfh protein is extremely stable (Fig. 3.8), like its homologous proteins H-NS and StpA (Johansson and Uhlin, 1999). Notably, no differential turnover of the Sfh protein was detected throughout the growth cycle (Fig. 3.8). Thus *sfh* growth-phase-dependent expression is not post-transcriptionally regulated at the protein level. The stability of the *sfh* message was also analysed throughout the growth cycle (Fig. 3.10). The results obtained revealed that the *sfh* transcript was more stable in the exponential phase ($t_{1/2}$ ~3.2 min) rather than in the stationary phase ($t_{1/2}$ 2.4 min) of growth. These data do not explain the paradoxical *sfh* mRNA and protein expression profiles, as the *sfh* message is more stable in exponential phase, when there is virtually no Sfh protein in the cell (Fig. 3.10). If *sfh* growth-phase-dependent expression was controlled by differential *sfh* mRNA stability, then one would expect *sfh* mRNA to be unstable in

exponential phase, as this would account for the lack of Sfh protein despite maximal cellular levels of *sfh* mRNA.

Since neither changes in *sfh* mRNA nor protein stability can account for *sfh* growthphase expression, it can be deduced that *sfh* expression must be post-transcriptionally regulated at the translational level. The predicted secondary structure of the *sfh* mRNA (Fig. 3.11) revealed that the long 5′-UTR of the *sfh* message formed a very stable stem-loop, which partially sequestered the SD sequence. These findings are reminiscent of those obtained from studies on the *rpoS* transcript. The 5′-region of the *rpoS* transcript forms a *cis*-inhibitory stem-loop that occludes its SD sequence and thus prevents translation of the message (Repoila *et al.*, 2003). In response to various environmental stress conditions, two ncRNAs –DsrA and RprA– can activate translation of the *rpoS* transcript by base-pairing to the 5′-region of the *rpoS* transcript, thus preventing the formation of the *cis*-inhibitory RNA structure (Repoila *et al.*, 2003).

In light of these data, it is proposed that the *sfh* message folds into a *cis*-inhibitory secondary structure that hinders efficient translation of the transcript. At the onset of stationary phase, expression of an unknown factor is induced, perhaps a riboregulator or an RNA chaperone, which facilitates the unfolding of the 5′-terminal stem-loop of the *sfh* transcript. Consequently translation of *sfh* mRNA is stimulated, resulting in elevated Sfh protein levels during the stationary phase of growth.

Previous studies have shown that a large class of riboregulators require the Hfq RNA chaperone protein to function (Zhang *et al.*, 2003). Hfq preferentially binds to RNA at single-stranded AU-rich regions, which are next to a structured (stem-loop) region (Valentin-Hansen *et al.*, 2004). Intriguingly, the 5′-terminal stem-loop of the *sfh* transcript is preceded by a single-stranded AU-rich RNA region (Fig. 3.11). These findings are consistent with a model in which a riboregulator stimulates *sfh* mRNA translation during the stationary phase of growth. Given the limited, usually discontinuous base-pairing between ncRNAs and their

mRNAs targets, it is very difficult to predict ncRNAs that might target *sfh* mRNA. One possible candidate is the small ncRNA, SraD, as its expression is triggered during the transition from exponential to stationary phase (Rasmussen *et al.*, 2005). Recently SraD was shown, in conjunction with Hfq, to destabilize the *ompA* transcript when rapidly growing cells enter stationary phase (Rasmussen *et al.*, 2005). One interesting possibility is that SraD might bind to *sfh* mRNA and stimulate translation of this transcript rather than enhancing its degradation, as for *ompA* mRNA.

However, taken in aggregate, the results do not discount a second hypothesis, which is closely related to the above one. The alternative model proposed is that during the exponential growth phase an unknown inhibitory factor binds to the *sfh* transcript and thus prevents its translation. Subsequently, as the cell enters the stationary phase of growth, the inhibitory factor no longer prevents translation of *sfh* mRNA (either it is no longer expressed or its negative influence is counteracted) and thus Sfh protein levels rapidly increase. This model is supported by the observation that *sfh* mRNA is more stable in exponential phase than in stationary phase. It is possible that binding of the inhibitory factor not only hinders translation of the *sfh* transcript, but also helps stabilize the message. Previous reports have shown that one consequence of Hfq binding to ncRNAs is protection of the ncRNA against RNase E digestion. Since Hfq binding sites and RNase E cleavage sites share sequence similarity, it is thought that Hfq-binding blocks cleavage by occluding RNase E cleavage sites (Folichon *et al.*, 2003; Moll *et al.*, 2003). As stated previously, the 5′-region of *sfh* mRNA is AU-rich and therefore is likely to be targeted by RNase E.

The characteristics of the unknown inhibitory factor interacting with the *sfh* message in the above model are reminiscent of the StpA protein. StpA is a potent RNA chaperone (Zhang *et al.*, 1996) and is specifically expressed during the exponential phase of growth (Free and Dorman, 1997). Moreover, both StpA and H-NS are known to be involved in the *sfh* regulatory network (Deighan *et al.*, 2003). For this reason, the contributions of StpA and H-NS to *sfh* growth-phase-dependent regulation were investigated at both the transcriptional and

translational level (Fig. 3.12, 3.14 and 3.15). In agreement with previous findings, *sfh* expression was derepressed in *stpA* and *hns* mutants (Fig. 3.12, 3.14 and 3.15). When the *hns* and *stpA* mutations were combined in the same cell, *sfh* mRNA and protein levels were elevated about 6-fold compared to wild-type levels (Fig. 3.14 and 3.15). Moreover, both StpA and H-NS were shown to specifically bind to the *sfh* regulatory region in competitive gel retardation assays (Fig. 3.13). Significantly, however, *sfh* gene expression was still growth phase-dependent in all the different *stpA* and *hns* mutant backgrounds (Fig. 3.12, 3.14 and 3.15). Since the strong repressive effect of H-NS and StpA on *sfh* gene expression was irrespective of growth phase, it must be concluded that H-NS and StpA negatively cross-regulate *sfh* gene expression, but importantly do not influence the growth-phase regulation of the *sfh* gene. The results of this study also eliminated the possibility that the factor mediating *sfh* growth-phase-dependent expression was *Shigella*- or plasmid pSf-R27-specific. The expression pattern of Sfh in *E. coli* (Fig. 3.17), a new genetic background, was shown to be very similar to that observed in *Shigella* (Fig. 3.7) and *sfh* gene expression was still growth-phase regulated in the absence of plasmid pSf-R27 (Fig. 3.17 and 3.18).

Previously, three-way interactions have been demonstrated between the H-NS-like proteins Sfh, H-NS, and StpA (Deighan *et al.*, 2003). Thus, Sfh can form either homomeric (Sfh:Sfh) or heteromeric (Sfh:StpA, Sfh:H-NS) protein complexes in the cell. However, the results of Sfh protein stability assays suggest that the formation and ratio of the different Sfh protein complexes *in vivo* is strictly controlled by regulated proteolysis (Fig. 3.9). Sfh was degraded relatively rapidly in strains lacking H-NS (Fig. 3.9), while in contrast it remained stable irrespective of the presence or absence of StpA (Fig. 3.9). Taken together these data indicate that Sfh is protected from proteolysis in the presence of H-NS but not StpA. Consequently, it can be concluded that there are very low levels of Sfh monomers and homodimers *in vivo* because they would be degraded rapidly and that Sfh must be present mainly *in vivo* in heteromeric complexes with H-NS. This hypothesis is fully supported by earlier studies in *E. coli* on the proteins StpA, H-NS, and HU (Bonnefoy *et al.*, 1989; Johansson and Uhlin, 1999; Johansson *et al.*, 2001). It was shown that StpA was protected from Lon protease degradation

by the formation of heteromeric protein complexes with H-NS (Johansson and Uhlin, 1999; Johansson *et al.*, 2001). Protection against Lon degradation was also observed for the β-subunit of HU when it formed heteromeric complexes with the α-subunit (Bonnefoy *et al.*, 1989). Significantly, Sfh protein degradation in a *hns* background was irrespective of growth phase (Fig. 3.9) and thus is not growth-phase regulated. The data presented demonstrate that the stoichiometry of the three proteins Sfh, H-NS and StpA is regulated by proteolysis and strengthens the hypothesis of the physiological relevance of different H-NS-like protein complexes in the modulation of gene expression.

The protease mediating Sfh degradation in the absence of H-NS has not yet been identified. However, since Lon mediates StpA degradation in *hns* mutants, this suggests strongly that the Lon protease might also be mediating the differential turnover Sfh. The proposed Lon protease cleavage site is $\phi X_{3-4}LS(L,X)X_5SX\phi$, in which ϕ represents a hydrophobic side chain (Gottesman and Maurizi, 1992). In the StpA protein, the first residue of the Lon consensus cleavage site, ϕ, was determined to be at amino acid 21 (Johansson and Uhlin, 1999). Protein sequence alignment of the three *Shigella* H-NS-like proteins identified the amino acid at position 21 to be phenylalanine in StpA, cysteine in H-NS, and leucine in Sfh. In *E. coli*, the conversion of the phenylalanine residue at position 21 of StpA to a cysteine results in the inability of the Lon protease to degrade the $StpA_{F21C}$ protein (Johansson and Uhlin, 1999). The amino acid substitution results in a polar instead of a hydrophobic amino acid at the first residue of the Lon cleavage site in StpA and therefore Lon is unable to cleave the protein. Like StpA, Sfh has a hydrophobic amino acid (leucine) at position 21, whereas H-NS has the polar amino acid cysteine and consequently is not subject to Lon degradation. These data support the hypothesis that Lon is the protease mediating Sfh degradation. However, further experimentation will be required to determine if this is the case.

Previous studies have shown that H-NS and StpA expression are regulated by temperature, with enhanced transcription of the *hns* and *stpA* genes being stimulated during cold shock and heat shock, respectively (Free and Dorman, 1997; La Teana *et al.*, 1991). Consistent with

Fig. 3.22. Model summarizing the *trans*-acting factors that regulate *sfh* growth phase-dependent expression. During exponential growth, transcription of the *sfh* gene is induced either by the presence of a transcriptional activator or by the absence of a stationary growth phase-specific repressor (illustrated by yellow square), resulting in high *sfh* mRNA levels in the cell. However, *sfh* mRNA is not efficiently translated because it either folds into an inhibitory secondary structure or a *trans*-acting factor (illustrated by blue circle) directly binds to the *sfh* message and blocks translation. At the onset of stationary phase, due to the absence of the exponential phase inhibitory factor or the presence of a translation stimulatory factor (illustrated by blue circle) *sfh* mRNA is translated, leading to high levels of Sfh protein in the cell. Subsequently, Sfh binds to and negatively autoregulates the *sfh* gene. In addition, its homologous proteins H-NS and StpA also negatively influence *sfh* gene expression. The positional binding of Sfh, StpA and H-NS to the regulatory region of the *sfh* gene is purely illustrative and does not infer any relative specificity of their binding sites within the *sfh* promoter region. Sfh forms either homomeric or heteromeric protein complexes with StpA and H-NS. Sfh homomeric and Sfh:StpA heteromeric complexes are subject to controlled proteolysis. Thus, Sfh must be present *in vivo* in mainly heteromeric complexes with H-NS.

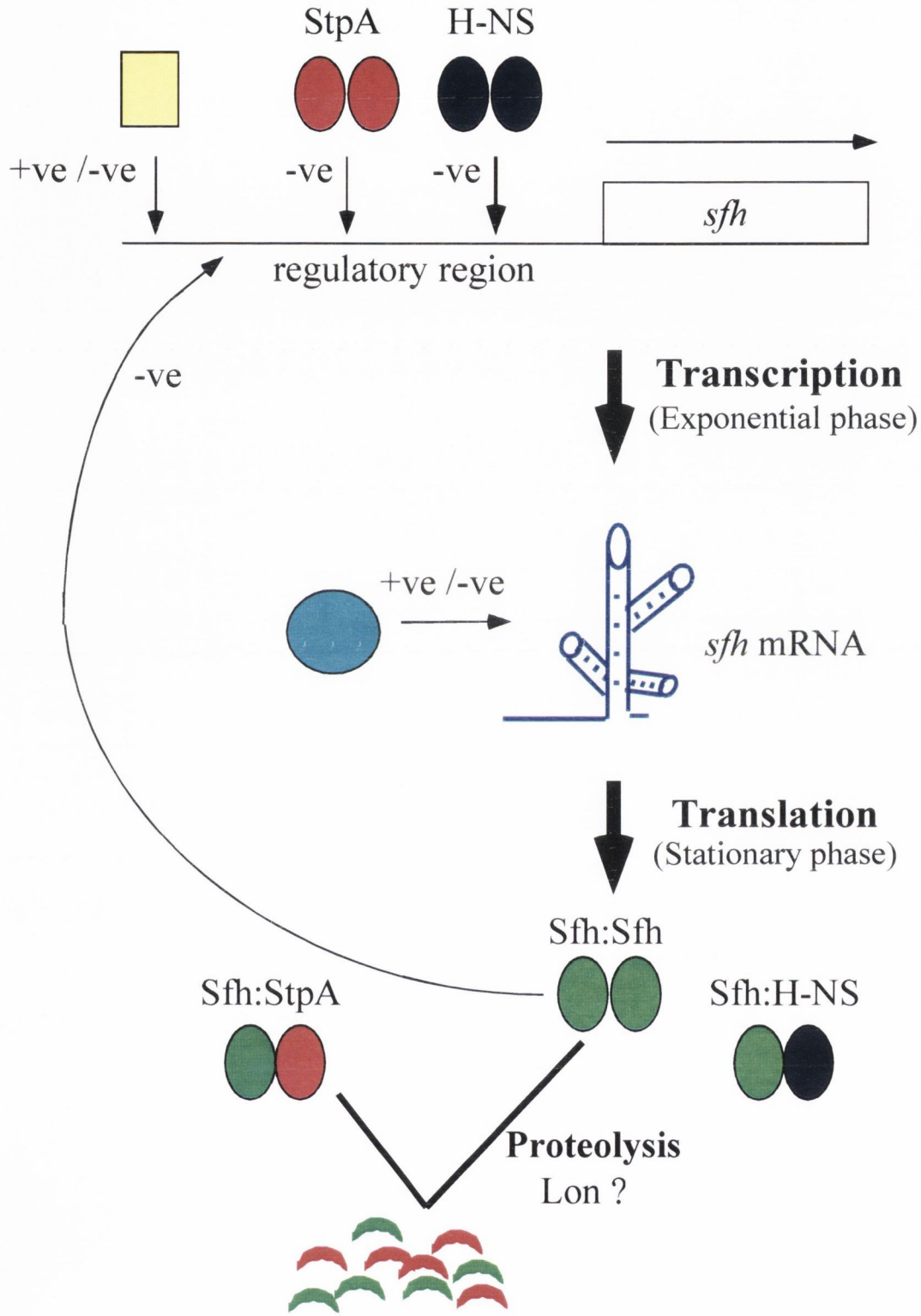
StpA
H-NS
+ve /-ve
-ve
-ve
sfh
regulatory region
-ve
Transcription
(Exponential phase)
+ve /-ve
sfh mRNA
Translation
(Stationary phase)
Sfh:Sfh
Sfh:StpA
Sfh:H-NS
Proteolysis
Lon ?

these findings, the data in this study showed that heat shock results in a strong sustained increase in StpA expression (Fig. 3.19) and that H-NS expression is induced by cold shock (data not shown). In contrast, Sfh expression was more or less unaffected by either heat or cold shock (Fig. 3.19 and 3.20). However, an effect of temperature on Sfh expression was evident when the temperature of the growth medium was altered (Fig. 3.21). Quantitative Western blotting revealed that Sfh protein levels are markedly higher in a culture grown at 25°C than in one grown at 37°C (Fig. 3.21). In agreement with previous reports, StpA and H-NS expression were downregulated at the lower growth temperature (Free and Dorman, 1997; Lease *et al.*, 1998; Lease and Belfort, 2000; Sonden and Uhlin, 1996). The low levels of H-NS at 25°C can be directly attributed to the dramatic increase (~30-fold) in DsrA at low temperatures, which results in a sharp increase in *hns* mRNA turnover (Repoila and Gottesman, 2001). However, the increase in Sfh protein levels at 25°C is probably not due to a positive effect of DsrA on *sfh* expression, but rather can be attributed to the low levels of H-NS and StpA, which consequently would result in derepression of *sfh* expression.

The data presented in this study reveal the complex growth-phase regulation of *sfh* gene expression, which is controlled by several *trans*-acting transcriptional and translational factors, as summarized in Fig 3.22. Intriguingly, Sfh, StpA, and H-NS all have distinct growth-phase expression profiles, are subject to differential proteolysis, and are expressed differentially in response to temperature. This dynamic situation provides *Shigella* with the capacity to vary the stoichiometry of its H-NS-like proteins in response to various stress conditions. These data are consistent with the model that different H-NS-like protein complexes have distinct biological properties that potentially could modulate different subsets of genes in response to environmental change. Defining the precise roles of the different H-NS-like protein complexes and deciphering the exact mechanism underlying the translational block of *sfh* mRNA during the exponential phase of growth awaits further experimentation.

Chapter 4

Conjugative transfer of plasmid pSf-R27 is modulated by chromosome- and plasmid-encoded H-NS-like proteins

4.1 Introduction

Plasmids belonging to the incompatibility group HI1 (IncHI1) are low-copy number, high molecular mass, covalently closed, circular replicons that are capable of self-transmission between *Enterobacteriaceae* and other Gram-negative bacteria. This conjugation is thermosensitive with transfer being optimal between 22°C and 30°C, but repressed at higher temperatures (Taylor and Levine, 1980). Electron microscopic analysis of cells grown at 37°C, which harboured the IncHI1 plasmid R27, revealed the absence of H-pili on the cell surface (Maher *et al.*, 1993). Pili are required to bring the recipient and donor cells into close proximity, and therefore a lack of pili would result in no conjugative transfer. However, the molecular basis of the thermosensitivity of IncHI1 transfer has not yet been elucidated.

The prototype IncHI1 plasmid R27 and the *S.* Typhi IncHI1 plasmid pHCM1 have been sequenced and analysed (Parkhill *et al.*, 2001; Sherburne *et al.*, 2000). Sequence analysis revealed that the genes responsible for IncHI1 conjugation are located in two separate regions of the plasmid, termed Tra1 and Tra2, which are separated by 64 kb (Parkhill *et al.*, 2001; Sherburne *et al.*, 2000). These transfer regions are chimaeras composed of both IncF-like and IncP-like elements and encode all the components of the IncHI1 conjugation system (Lawley *et al.*, 2002; Sherburne *et al.*, 2000). Since mutations in either Tra1 or Tra2 abolish transfer, both regions are essential for conjugation (Lawley *et al.*, 2002; Lawley *et al.*, 2003a; Rooker *et al.*, 1999). All conjugative systems consist of two distinct protein complexes, namely, the membrane-associated mating pair formation (Mpf) complex, and the cytoplasmic relaxosome, both of which are linked together by a coupling protein (Llosa *et al.*, 2002). The Tra1 region of IncHI1 plasmids encodes the relaxosome components, the coupling protein and a few Mpf proteins of the conjugative apparatus, while the Tra2 region mostly encodes the Mpf proteins (Fig. 4.1; Lawley *et al.*, 2002; Lawley *et al.*, 2003a).

The Tra1 region of IncHI1 plasmids contains 14 open reading frames (ORFs) and is organized into three operons, which are separated by two intergenic regions of DNA that are 757 bp and 400 bp in size (Fig. 4.1; Alonso *et al.*, 2005b; Lawley *et al.*, 2002). The origin of

transfer (*oriT*) is located in the 757-bp intergenic region between the genes *traH* and *trhR*. The five genes located in two operons (R and F operons) immediately downstream of the *oriT* region are involved in H-pilus biosynthesis (Fig. 4.1) and three of them (*trhF, trhH and trhG*) encode proteins with amino acid sequence similarity to Mpf proteins from IncF plasmids (Lawley *et al.*, 2002). Upstream of the *oriT* region are four ORFs (*traH, traI, traG, traJ*) required for plasmid transfer, but not for H-pilus production, which are dispersed among several non-conjugative transfer genes (Fig. 4.1; Lawley *et al.*, 2002). The *traI* gene encodes the major component of the IncHI1 relaxosome. The TraI protein contains three relaxase motifs that are characteristic of relaxases from the IncP lineage, but overall TraI shares no homology to any known relaxases (Lawley *et al.*, 2002). The IncHI1-coupling protein, TraG, is also encoded by a Tra1 gene (Fig. 4.1). TraG contains the nucleoside triphosphate (NTP)-binding domains, the so-called Walker A and Walker B motifs, and shares only a low level of sequence identity with previously identified coupling proteins (Lawley *et al.*, 2002). Site-directed mutagenesis of the TraG NTP-binding Walker regions demonstrated that these motifs were essential for plasmid R27 conjugation (Gunton *et al.*, 2005). In addition, Gunton *et al.* (2005) determined that the four periplasm-spanning residues of TraG are essential for its interaction with the Mpf protein TrhB (Gunton *et al.*, 2005).

The Tra2 region of plasmid R27 contains 24 genes, organized into three operons, designated the AC, AN, and Z operons (Fig. 4.1; Alonso *et al.*, 2005b). The AC and AN operons are transcribed in the same direction and encode 11 Mpf proteins that are essential for conjugative transfer. The products of nine genes (*trhA, trhL, trhE, trhK, trhB, trhV, trhC, trhP* and *trhW*) are required for H-pilus biosynthesis (Fig. 4.1). Most of the Tra2 Mpf proteins share sequence similarity to IncF Mpf proteins (Lawley *et al.*, 2003a; Rooker *et al.*, 1999). The TrhC protein has been found to localize to the cytoplasmic membrane and its expression is temperature sensitive, with optimal expression occurring at the permissive temperature for IncHI1 conjugation (Gilmour *et al.*, 2001). Interestingly, the Mpf protein TrhK has a marked level of amino acid sequence similarity to the HrcC/HrpH secretin family present in the TTSS of organisms such as *Pseudomonas fluorescens* (Lawley *et al.*, 2003a). In addition to the

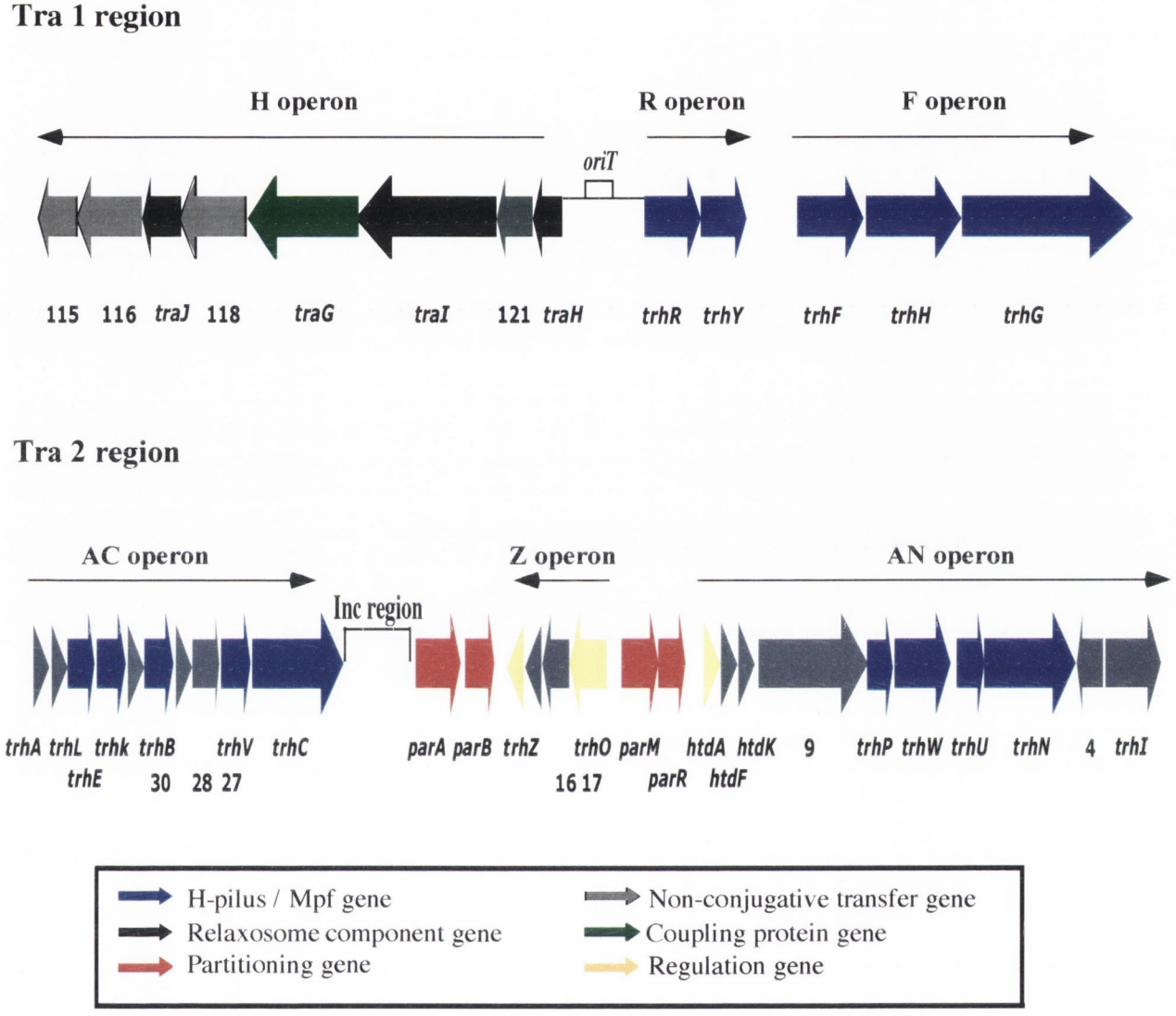

Fig. 4.1. Schematic map of the Tra1 and Tra2 regions of IncHI1 plasmids. Horizontal arrows indicate the proposed transcriptional units and the Inc region is a 3-kb intergenic region involved in IncHI1 plasmid incompatibility. The partitioning genes *parA, parB, parM,* and *parR* are not in an operon. Figure adapted from Alonso *et al.* (2005).

essential Mpf genes, three Tra2 genes –*trhO, trhZ* and *htdA*– modulate plasmid R27 transfer frequency. Transposon mutagenesis demonstrated that the TrhO and TrhZ proteins positively regulate conjugative transfer, whereas the HtdA protein is a strong repressor of plasmid R27 conjugation (Lawley *et al.*, 2003a; Whelan *et al.*, 1994). The remaining Tra2 operon, the Z operon, encodes entry exclusion proteins and is flanked on either side by partitioning genes (Fig. 4.1; Alonso *et al.*, 2005b).

One of the hallmarks of IncHI1 plasmids is their unusual temperature-dependent conjugative transfer. To date the mechanism underlying this phenomenon has not been elucidated. Efforts to isolate a mutant of the prototype R27 plasmid that displays temperature-independent transfer have been unsuccessful, implying that there might be more than one mechanism thermally regulating IncHI1 plasmid transfer. It is possible that IncHI1 plasmid thermosensitive transfer is regulated by *tra* mRNA or protein instability, the loss of requisite protein-protein interactions, or differential binding of a repressor or activator through a range of temperatures, consequently only permitting IncHI1 transfer at low temperatures. Interestingly, sequence analysis of several IncHI1 plasmids identified homologues to the nucleoid-associated proteins, H-NS, TlpA, and Hha (Parkhill *et al.*, 2001; Sherburne *et al.*, 2000; Wei *et al.*, 2003). It is notheworthy that all these proteins have been implicated in the thermal regulation of other temperature-dependent expression systems such as the *Salmonella* and *Shigella* virulence genes (Dorman *et al.*, 2001; Rhen and Dorman, 2005). Furthermore, a plethora of nucleoid-associated proteins, including H-NS, Hha, IHF and Lrp, regulate conjugative transfer of the F plasmid (Will *et al.*, 2004) and F-like plasmids, such as R100 (Camacho *et al.*, 2005a; Dempsey and Fee, 1990; Nieto *et al.*, 1998), pRK100 (Starcic *et al.*, 2003; Starcic-Erjavec *et al.*, 2003), and the *Salmonella* virulence plasmid, pSLT (Camacho and Casadesus, 2002, 2005; Camacho *et al.*, 2005b).

The aim of this study was to examine the role, if any, of the three *Shigella* H-NS-like proteins Sfh, H-NS, and StpA in the temperature-dependent regulation of plasmid pSf-R27

conjugative transfer. At the time that this work was carried out no reports of H-NS-like proteins modulating plasmid R27 transfer had been published.

4.2 Results

4.2.1 Construction of *sfh hns* and *sfh stpA* double mutants

Double mutant strains, CJD1651 (*sfh stpA*) and CJD1652 (*sfh hns*), were constructed by conjugating the plasmid pSf-R27 harbouring the Δ*sfh*::Gent^R allele (pSf-R27Δ*sfh*::Gent^R) into the *hns*::Tn*10* (BS185) and Δ*stpA*::Tc^R (CJD1199) mutant backgrounds as described previously (Taylor and Levine, 1980). Transconjugants were selected and twice single-colony purified on L–agar plates containing tetracycline (15 μg ml^{-1}) and gentamycin (15 μg ml^{-1}).

The double mutant strains were confirmed to be complete null mutants for the *sfh* gene by both Southern and Western blotting (Fig. 4.2). Total genomic DNA was isolated from strains BS184 (wild-type), BS185 (*hns*), CJD1199 (*stpA*), CJD1650 (*sfh*), CJD1216 (*hns stpA*), CJD1651 (*sfh stpA*), and CJD1652 (*sfh hns*). Undigested total DNA from these strains was then electrophoresed on agarose gels and probed for the *hha*-like gene of the plasmids pSf-R27Gent^R and pSf-R27Δ*sfh*::Gent^R and for the *sfh* gene. As expected the *sfh*-specific probe detected a homologue in the wild-type strain and in the *hns* and *stpA* single and double mutants, but no hybridization occurred with the *sfh* single and double mutants (Fig. 4.2). Importantly, the *hha*-like probe hybridized to all strains, showing that the absence of the *sfh* gene in the double mutant strains CJD1651 and CJD1652 is not due to the absence of plasmid pSf-R27Gent^R (Fig. 4.2).

To confirm that strains CJD1651 and CJD1652 produced no Sfh protein, in addition to StpA and H-NS respectively, total protein samples were isolated from L-broth cultures of the wild-type strain BS184 and its isogenic *hns, stpA,* and *sfh* double mutants and analysed by Western immunoblotting (Fig. 4.2). The results showed the presence of Sfh in the wild-type and *hns stpA* mutant backgrounds, but the absence of the Sfh protein in the two *sfh* double mutant strains (Fig. 4.2). Furthermore, the results confirmed that the *sfh stpA* and *sfh hns* mutants were depleted for the StpA and H-NS proteins, respectively.

Surprisingly, every attempt to construct a *sfh hns stpA* triple mutant proved unsuccessful. When the plasmid pSf-R27Δ*sfh*::Gent^R was conjugated into the *hns stpA* (CJD1216) double mutant background, either no transconjugants were detected or those that were isolated had a *hns*$^+$ genotype. This was because strain CJD1216 has a full Tn*10* insertion in the *hns* gene, and this had precisely excised in the transconjugants. PCR analysis confirmed the presence of the Tn*10* insertion in strain CJD1216 and its absence in the transconjugants (Fig. 4.3). Moreover, Western immunoblotting verified that the transconjugants produced full length H-NS (Fig. 4.3). Since *E. coli* only expresses two H-NS-like proteins, H-NS and StpA, and *hns stpA* double mutants are viable, it must be deduced that the plasmid pSf-R27 encodes a toxic factor, which is repressed in the presence of one or more H-NS-like proteins. However, in their absence overexpression of this factor is lethal to the cell.

The growth rates of wild-strain strain BS184 and its *hns, stpA,* and *sfh* single and double mutant derivatives were compared in L-broth medium at 37°C by measuring the optical density of the culture at 600 nm over a 7-h time course (Fig. 4.4). The generation time for the wild-type strain and its *sfh* and *stpA* mutants during the exponential phase of growth was 28 min, whereas that of the *hns* mutant was 37 min (Fig. 4.4). A strain combining the *sfh* and *stpA* mutations had only a slightly longer doubling time compared to the parental strain BS184 (29 min). In contrast, the *hns sfh* double mutant strain grew markedly slower with a doubling time of 47 min (Fig. 4.4). These single and double mutants were used to examine the role of H-NS-like proteins, if any, in plasmid pSf-R27 thermosensitive conjugation.

4.2.2 Role for Sfh, StpA and H-NS in plasmid pSf-R27 conjugation

H-NS is a known regulator of several temperature-dependent expression systems, which are mainly associated with bacterial virulence, such as the *E. coli hly* (Nieto *et al.*, 2000) and *pap* operons (van der Woude *et al.*, 1996), and the *Salmonella* and *Shigella* virulence systems (Beloin and Dorman, 2003; Dorman *et al.*, 2001; Rhen and Dorman, 2005). All these systems are repressed by H-NS at low temperatures, but their expression is permitted at 37°C, the

Fig. 4.2. Genetic confirmation of *sfh* double mutant strains. (A) Southern blot confirming the absence of the *sfh* gene in the *sfh stpA* and *sfh hns* double mutant strains CJD1651 and CJD1652, respectively. Undigested total DNA from strains BS184 (wild-type), CJD1650 (*sfh*), CJD1199 (*stpA*), BS185 (*hns*), CD1216 (*hns stpA*), CJD1651 (*sfh stpA*), and CJD1652 (*sfh hns*) was probed for the presence of *hha*-like gene located on the high molecular mass plasmids pSf-R27Gent^R and pSf-R27Δ*sfh*::Gent^R and for the *sfh* gene. An asterisk indicates the position of the wells on the gel. (B) Western blot confirming the absence of the Sfh protein in strains CJD1651 and CJD1652. Protein samples were harvested from L-broth cultures of strains BS184 (wild-type), CD1216 (*hns stpA*), CJD1651 (*sfh stpA*), and CJD1652 (*sfh hns*), and probed with anti-Sfh-, anti-StpA- and anti-H-NS-specific antibodies as indicated.

A.

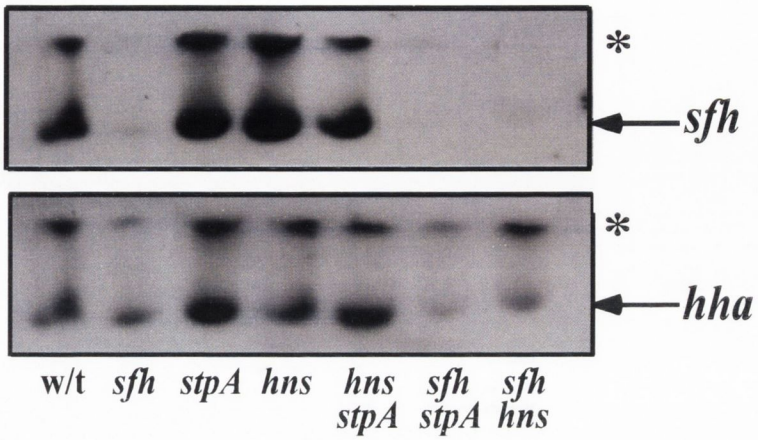
*
sfh
*
hha
w/t
sfh
stpA
hns
hns stpA
sfh stpA
sfh hns
Strain Genotype

B.

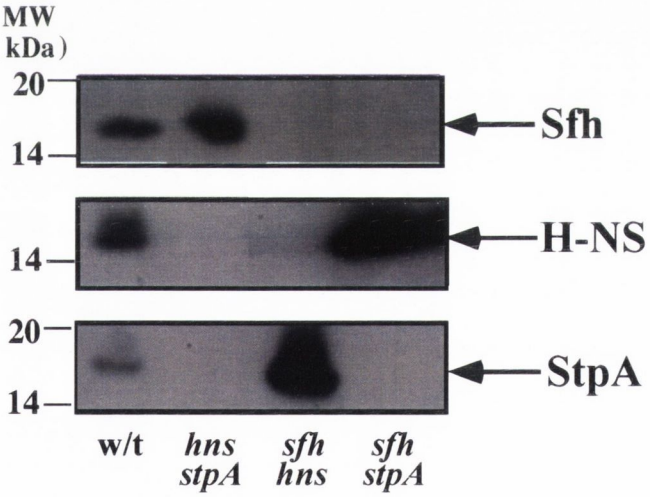
MW (kDa)
20
14
Sfh
14
H-NS
20
14
StpA
w/t
hns stpA
sfh hns
sfh stpA
Strain Genotype

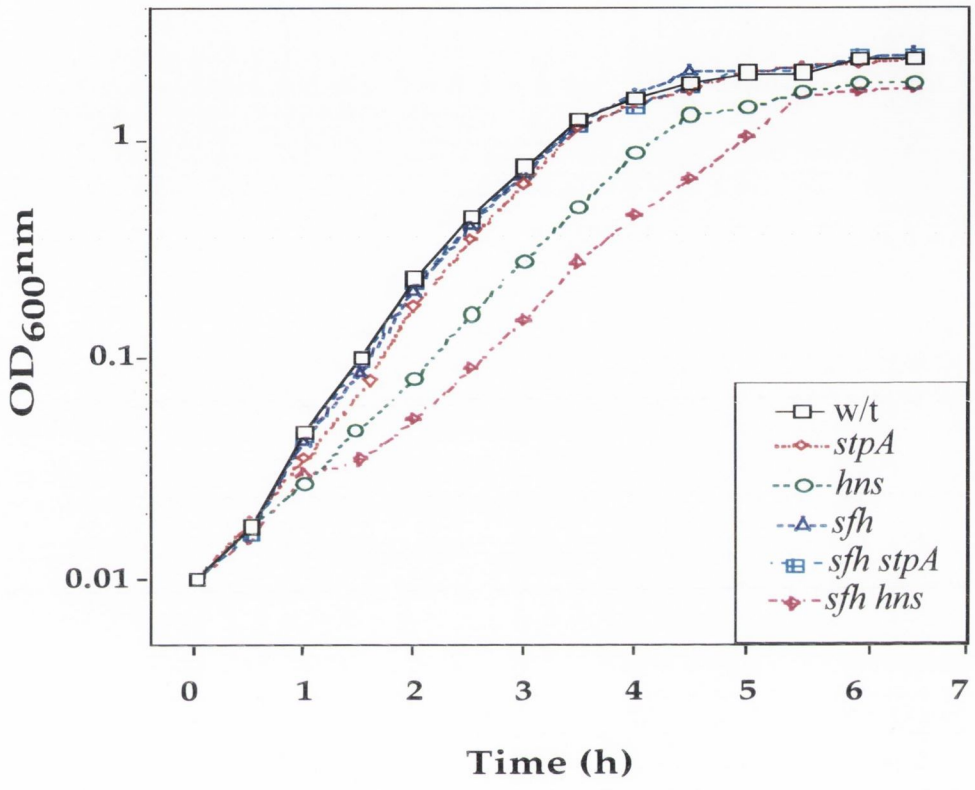

Fig. 4.4. Growth curves of *sfh* double mutant strains. Growth curves of wild-type strain BS184 and its *sfh*, *hns*, and *stpA* single and double mutant derivatives in L-broth at 37°C. Overnight cultures were diluted to an OD_{600}nm of 0.01, and bacterial growth monitored by measuring OD_{600}nm at regular intervals post inoculation. The OD_{600}nm values were then plotted against time. These growth curves are representative of three independent experiments.

physiological temperature for human infection. In contrast, the thermoregulation of IncHI1 plasmid conjugation is the reverse, namely, conjugation is repressed at temperatures above 30°C (Taylor and Levine, 1980). Nevertheless, since plasmid pSf-R27 encodes the H-NS-like protein, Sfh and members of the H-NS protein family are known thermoregulators, it was of interest to determine if Sfh, StpA or H-NS could influence the thermosensitive transfer of plasmid pSf-R27.

To test this hypothesis, conjugal transfers of plasmid pSf-R27Gent^R from the wild-type strain MD1 (BS184 Rif^R) and its *stpA* and *hns* single and double mutant derivatives into the wild-type strain MD2 (BS184 Nal^R) were compared. In addition, conjugal transfers of plasmid pSf-R27Δ*sfh*::Gent^R from the *sfh* mutant strain (CJD1650 Rif^R) and its *stpA* and *hns* double mutant derivatives into the wild-type strain MD2 (BS184 Nal^R) were compared. Conjugal matings were performed at both the permissive (30°C) and non-permissive (37°C) temperatures for IncHI1 plasmid conjugation. Matings were incubated for 24 h and transfer frequencies calculated as the number of transconjugants per donor cell. Consistent with IncHI1 plasmid conjugation, transfer of plasmid pSf-R27Gent^R was thermosensitive, being transferred from the wild-type strain into the recipient at 30°C, but not at 37°C (Table 4.1). Moreover, at 37°C no conjugative transfer was detected from any of the *sfh, stpA,* and *hns* mutant strains (data not shown). Since conjugation is still temperature-dependent in the absence of Sfh, StpA and H-NS, it must be concluded that none of the *Shigella* H-NS-like proteins are involved in the regulatory pathway controlling plasmid pSf-R27 thermosensitive transfer.

At 30°C, the conjugal transfer of plasmid pSf-R27Gent^R from the mutant strains was repressed compared to that observed for the wild-type strain (Table 4.1). In an *hns* mutant the conjugation frequency of plasmid pSf-R27Gent^R decreased ~100-fold compared to that of the wild-type strain, whereas a single mutation in *stpA* repressed transfer to a far lesser extent (Table 4.1). The effect of *stpA* and *hns* mutations on transfer of plasmid pSf-R27Δ*sfh*::Gent^R was also investigated. Both double mutant strains (*sfh hns, sfh stpA*) displayed reduced

transfer frequency of plasmid pSf-R27Δ*sfh*::Gent^R, with the most marked reduction in transfer occurring with the *sfh hns* strain (Table 4.1). Taken in aggregate these data show a novel role for all three H-NS-like proteins Sfh, H-NS and StpA, in the modulation, but not the thermal regulation of plasmid pSf-R27 conjugation.

4.2.3 Sfh represses *tra* gene expression

To ascertain whether Sfh was modulating plasmid pSf-R27 conjugative transfer at the level of transcription, RT-PCR analyses of nine randomly chosen pSf-R27 transfer genes was performed (Fig. 4.5). For a broadly based study, the genes chosen were from both the Tra1 and Tra2 regions of plasmid pSf-R27 with the exception of the Z operon and the partitioning genes (Fig. 4.1) and encompassed genes coding for regulatory (*htdA*; AN operon), Mpf (*trhR*; R operon/ *trhF*; F operon/ *trhB, trhV*; AC operon), relaxosome proteins (*traH, traJ*; H operon), and non-conjugative transfer genes (R0121, R0116; H operon).

Total RNA was extracted from L-broth cultures of the wild-type strain BS184 and its *sfh* mutant derivative grown at 37°C and used as template for RT-PCR. As an internal control for RNA integrity and loading, RT-PCR analyses of *rplT* transcription was also performed (the *rplT* gene encodes the 50S ribosomal subunit protein L20), and its expression found not to markedly alter between the wild-type and *sfh* mutant background (Fig. 4.5). In contrast, the results of RT-PCR analyses revealed that transcription of several *tra* genes located in the Tra1 region (*traH,* R0121, *traJ,* R0116) and in the Tra2 region (*trhV, trhB, htdA*) of plasmid pSf-R27 was elevated in the *sfh* mutant (Fig. 4.5), suggesting that Sfh is a repressor *tra* gene expression. However, not all *tra* genes displayed altered expression in the *sfh* mutant; transcription of the Mpf genes, *trhF* and *trhR,* was unaffected by the absence of Sfh (Fig. 4.5). Notably, these genes are in different Tra1 operons (R and F operons) than those genes (*traH, traJ, R0118, R0121*; H operon) that displayed a response to Sfh (Fig. 4.1).

Table 4.1. Effect of *hns* and *stpA* mutations on plasmids pSf-R27Gent^R and pSf-R27Δ*sfh*:::Gent^R conjugation

Genotype of donor strain	Conjugation frequency[a]	Relative conjugation from mutant to w/t strain (%)
w/t	8.09×10^{-5}	100
sfh	3.2×10^{-5}	39.5
hns	8×10^{-7}	1
hns sfh	1.9×10^{-6}	2.3
stpA	4.99×10^{-5}	62
stpA sfh	2.3×10^{-5}	28.5

[a] Transconjugants /donor cell after 24 h matings at 30°C. Recipient was MD2 (w/t Nal^R) in all crosses. Experiment was performed on four independent occasions and a representative experiment is presented.

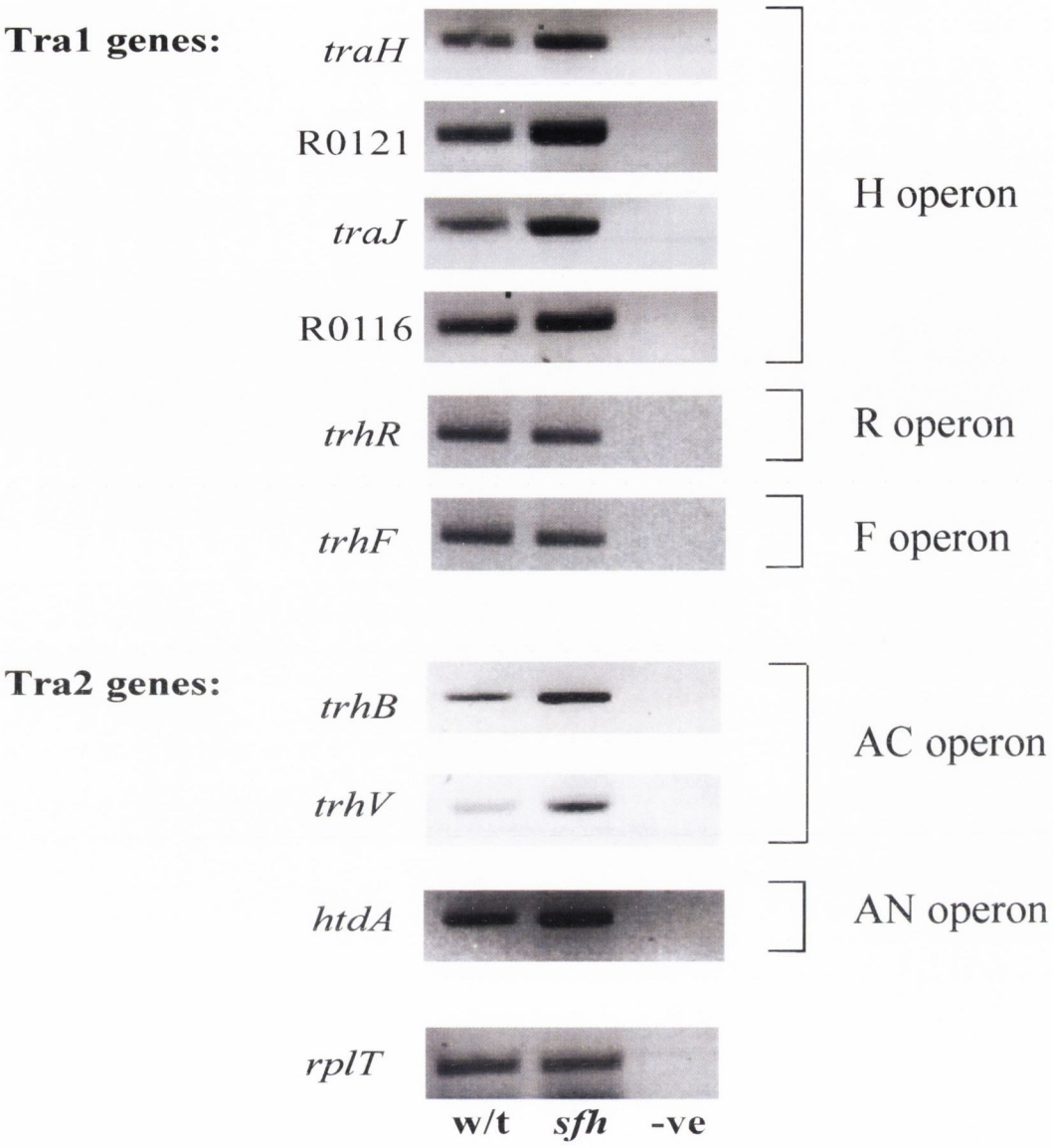

Fig. 4.5. Effect of Sfh on *tra* gene transcription. RT-PCR analyses of selected *tra* genes, located in the Tra1 and Tra2 regions of IncHI1 plasmids, in the presence and absence of Sfh. Genes located within the same Tra operon are grouped. Total RNA was extracted from log phase (OD_{600}~0.6) L-broth cultures, grown at 37°C, of the wild type strain BS184 and its *sfh* mutant derivative, DNase treated, and used as template for RT-PCR. As a control for RNA integrity and loading, RT-PCR analyses of *rplT* transcription was also performed. The experiment was repeated on at least three independent occasions and representative gels are shown.

These data indicate that Sfh is a transcriptional repressor of several specific *tra* operons located in both the Tra1 and Tra2 regions of plasmid pSf-R27. Notably, some of the *tra* operons regulated by Sfh have a mosaic-like organization and include both conjugative (Mpf, relaxosome and regulatory) and non-conjugative genes (Fig. 4.1; (Lawley *et al.*, 2002; Lawley *et al.*, 2003a; Sherburne *et al.*, 2000). Consistent with this, expression of the genes R0121 and R0116, which are known not to be essential for conjugative transfer (Lawley *et al.*, 2002) was derepressed in the *sfh* mutant to a similar extent as the essential conjugation genes, *traH* and *traJ* (Fig. 4.5). Collectively, the results imply that the observed influence of the three *Shigella* H-NS-like proteins on plasmid pSf-R27 conjugal transfer is probably mediated via transcriptional regulation of the *tra* genes.

4.2.4 Effect of *sfh*, *hns*, and *stpA* mutations on *htdA* gene expression

The *htdA* gene is located in the Tra2 region of IncHI1 plasmids (Fig. 4.1) and encodes a 19.9-kDa protein that is required for full repression of conjugation (Whelan *et al.*, 1994). Previous reports have shown that *htdA* mutants are derepressed for conjugation, with an observed 6,000-fold increase in transfer frequency due to a concomitant significant induction of H-pilus production in the mutant (Lawley *et al.*, 2003a; Whelan *et al.*, 1994). Preliminary RT-PCR analyses revealed that *htdA* gene expression is elevated in a *sfh* mutant background at 37°C (Fig. 4.5). To investigate further the role of H-NS-like proteins in *htdA* gene expression, RT-PCR analyses of *htdA* transcripts was performed at both 30°C and 37°C in a wild-type and in *sfh*, *hns,* and *stpA* mutant background.

The results revealed that *htdA* gene expression is 2-fold higher in wild-type cells grown at 30°C than at 37°C (Fig. 4.6), which is consistent with the repressive role of HtdA in IncHI1 plasmid conjugation. In agreement with previous data obtained in this study, *htdA* mRNA levels were slightly elevated in the *sfh* mutant compared to the wild-type strain at both 30°C and 37°C (Fig. 4.6). Quantitative analysis of *htdA* mRNA levels in the different strains revealed a marked enhancement of *htdA* mRNA in strains lacking H-NS (Fig. 4.6).

Intriguingly, the negative influence of H-NS on *htdA* gene expression was most notable at 37°C, and the combination of the *sfh* and *hns* mutations in the same cell resulted in a further ~2-fold enhancement of *htdA* mRNA levels compared those in an *hns* single mutant (Fig. 4.6). In contrast, combining the *hns* and *stpA* mutations in the same cell had no such additive effect. Moreover, *htdA* gene expression was relatively unaffected in a *stpA* single mutant (Fig. 4.6). These data suggest that StpA does not influence *htdA* gene expression, whereas its paralogues, Sfh and especially H-NS, are transcriptional repressors of the *htdA* gene.

As mentioned above, H-NS strongly represses *htdA* gene expression at 37°C, albeit that the repressive effect of H-NS on gene transcription is usually negated at this growth temperature. Therefore, it was possible that the observed repressive effect of H-NS on *htdA* gene transcription was not a direct effect, but rather an indirect effect mediated through a *trans*-acting factor. Since H-NS-like proteins are known to bind preferentially to intrinsically to curved DNA (Bracco *et al.*, 1989; Owen-Hughes *et al.*, 1992; Yamada *et al.*, 1990), the intrinsic curvature of the *htdA* promoter was analysed *in silico* using the BEND-IT computer program. The curvature propensity plot obtained revealed that the *htdA* regulatory region contains several regions of intrinsic curvature (Fig. 4.7), indicating that H-NS, Sfh, and StpA could be directly influencing *htdA* gene expression. To clarify this issue, the ability of the three proteins H-NS, Sfh, and StpA to directly bind to the *htdA* regulatory region was analysed by competitive EMSAs (Fig. 4.7). A 456-bp DNA fragment encompassing the *htdA* regulatory region (nt –386 to +130 with respect to the translation start codon of the *htdA* gene) was amplified by PCR, using the primer pair htdA-BSF and htdA-BSR (Table 2.3). The *htdA* promoter amplimer was then added to *Taq*1–*Ssp*I-digested pBR322 DNA, which acts as competitor DNA in the EMSA. One of the pBR322 DNA restriction fragments contains the intrinsically curved promoter region of the *bla* gene, which is known to bind H-NS-like proteins. The DNA mixture was then incubated with increasing equimolar concentrations of purified Sfh, H-NS, or StpA and resolved by electrophoresis through 3% molecular screening agarose.

Fig. 4.6. Effect of Sfh, H-NS, and StpA on *htdA* gene transcription. (A) RT-PCR analyses of *htdA* gene transcription in wild-type strain BS184 and its *sfh*, *hns,* and *stpA* single and double mutant derivatives at 30°C and 37°C. Total RNA was extracted from log phase (OD_{600}~0.6) L-broth cultures, grown either 30°C or 37°C, of the various strains being tested, DNase treated, and used as template for RT-PCR. As a control for RNA integrity and loading, RT-PCR analyses of *rplT* gene transcription was also performed. (B) Histograms showing densitometric analyses of RT-PCR analyses of *htdA* gene transcription. The densitometric data shown are averages of at least three independent experiments in which RT-PCR samples from L-broth cultures, grown at 30°C and 37°C, of the various strains being tested were run on the same gel (data not shown). The relative transcript levels are expressed relative to the *htdA* mRNA content of strain BS184 cells grown at 30°C, the value of which was taken as 1.

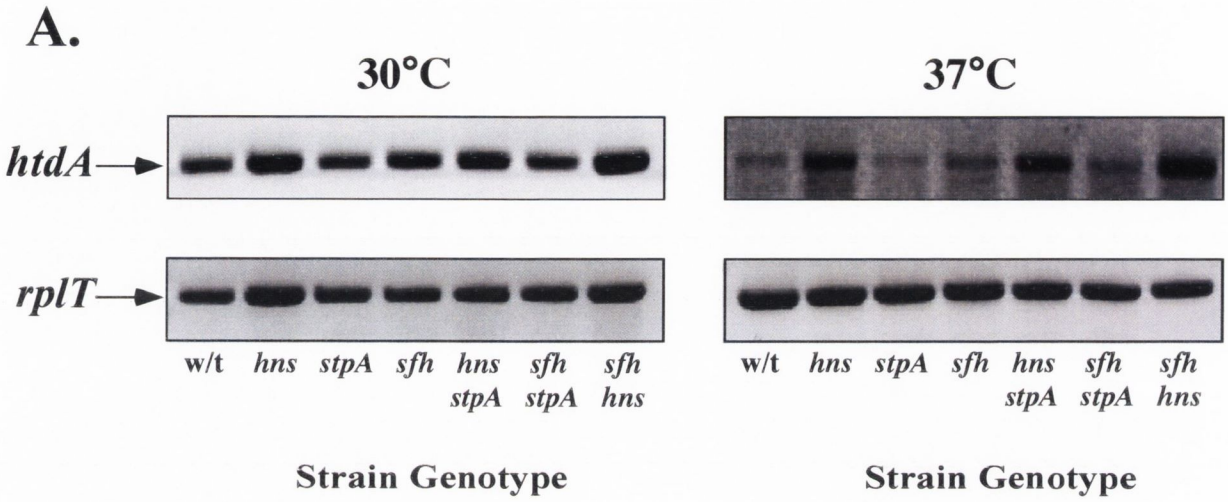
A.
30°C
37°C
htdA
rplT
w/t
hns
stpA
sfh
hns stpA
sfh stpA
sfh hns
Strain Genotype
Strain Genotype

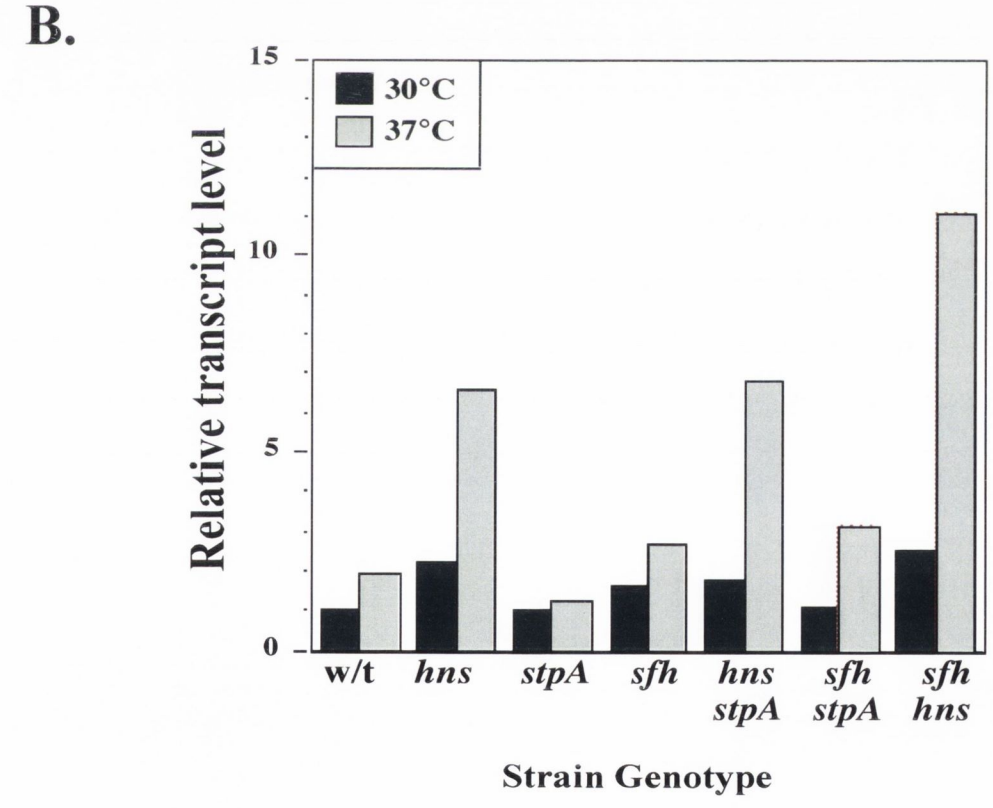
B.
Relative transcript level
30°C
37°C
15
10
5
0
w/t
hns
stpA
sfh
hns stpA
sfh stpA
sfh hns
Strain Genotype

Fig. 4.7. Direct interaction of Sfh, H-NS, and StpA with the *htdA* promoter region. (A) DNA curvature analysis of the *htdA* promoter region. Graph shows the predicted intrinsic curvature of the *htdA* regulatory region using the computer program BEND-IT. Curvature is expressed as degrees per helical turn and plotted against the position on the promoter sequence, with +1 corresponding to the *htdA* translation initiation codon. Curved and straight motifs have a value above or below 5 degrees per helical turn, respectively. Regions of intrinsic DNA curvature are arrowed. (B) Competitive gel retardation assay showing the specific binding of Sfh, H-NS and StpA to the *htdA* promoter region. A 456 bp DNA fragment encompassing the *htdA* regulatory region (nt –386 to +130 with respect to the translation initiation codon of the *htdA* gene) was amplified by PCR using the primer pair htdA-BSF and htdA-BSR (Table 2.3). The plasmid pBR322 was digested with restriction endonucleases *Taq*1 and *Ssp*I, and the resulting DNA fragments mixed with the 456-bp amplimer of the *htdA* promoter region. The DNA mixtures were incubated with increasing equimolar concentrations of Sfh, H-NS, or StpA in the range 0 μM to 2 μM. An arrow and an asterisk indicate the position of the *htdA* and *bla* promoter fragments, respectively. The curved *bla* promoter is a positive control known to bind H-NS-like proteins. The positions of the 600-bp and 400-bp molecular size markers are also indicated.

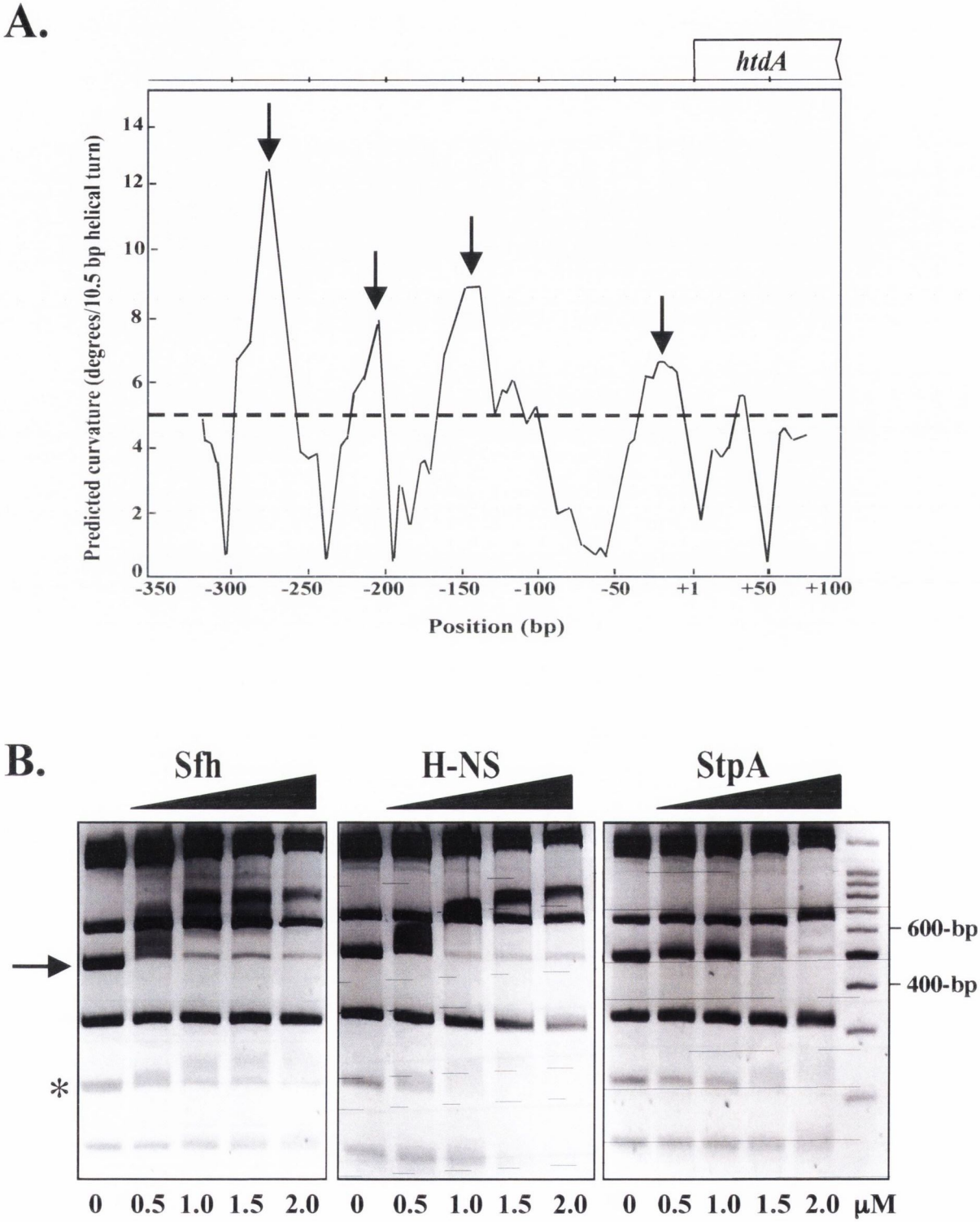
A.
htdA
Predicted curvature (degrees/10.5 bp helical turn)
0
2
4
6
8
10
12
14
-350
-300
-250
-200
-150
-100
-50
+1
+50
+100
Position (bp)
B.
Sfh
H-NS
StpA
600-bp
400-bp
*
0 0.5 1.0 1.5 2.0 0 0.5 1.0 1.5 2.0 0 0.5 1.0 1.5 2.0 μM

The electrophoretic mobility of the *htdA* promoter fragment was reduced specifically by all three *Shigella* H-NS-like proteins, in concentration-dependent manners (Fig. 4.7). However, it should be noted that the interaction of Sfh and H-NS with the *htdA* promoter fragment was much stronger than that observed for StpA, which only shifted the mobility of the *htdA* DNA band at a protein concentration of ≥1.5 μM. These findings correlate with the RT-PCR results, which showed that StpA does not markedly influence *htdA* gene expression and also illustrate that H-NS and Sfh directly repress *htdA* gene transcription.

4.2.5 Effect of *sfh*, *hns*, and *stpA* mutations on *traJ* gene expression

The *traJ* gene is located in the H operon of the Tra1 region of IncHI1 plasmids (Fig. 4.1) and is predicted to encode a small ~25-kDa basic protein. Previous work on the Tra1 region of plasmid R27 suggested that the *traJ* gene could encode a relaxosome accessory component since transposon mutagenesis revealed that the *traJ* gene was essential for conjugative transfer, but not for H-pilus synthesis, a characteristic feature of relaxosome accessory proteins (Lawley *et al.*, 2002). However, Lawley *et al.* (2002) also discovered that TraJ contains two putative functional motifs, a helix-turn-helix motif and a leucine zipper motif. These motifs are normally associated with DNA binding and protein dimerization, respectively, and suggest that TraJ might be a novel transcriptional regulator of IncHI1 plasmid conjugation. To investigate this further, the amino acid sequence of TraJ was analysed *in silico* using the Prosite program (http://ca.expasy.org/tools/scanprosite). In agreement with previous studies, a putative helix-turn-helix motif was identified in the N-terminus of TraJ between residues 8 and 48. A putative leucine zipper motif, consisting of four heptad repeats, was also identified in the C-terminus of the protein between residues 182 and 203 (Fig. 4.8). No other identifiable functional features of TraJ were found. It possesses no amino acid sequence similarity to any other previously described proteins. Intriguingly, the putative helix-turn-helix motif of TraJ shares amino acid sequence similarity to the helix-turn-helix signature of the AraC Family 1 (Fig. 4.8), supporting the hypothesis that TraJ could be a novel transcriptional regulator. Since members of the AraC protein family are known to

specifically counteract H-NS repression (Egan, 2002), it was of interest to determine if H-NS, Sfh, or StpA could influence *traJ* gene expression. For this reason, RT-PCR analyses of *traJ* transcripts was performed in various *hns, stpA,* and *sfh* mutant backgrounds.

Total RNA was extracted from L-broth cultures of the wild-type strain BS184 and its *hns, stpA,* and *sfh* single and double mutant derivatives grown at either 30°C or 37°C and used as template for RT-PCR. The results of RT-PCR analyses revealed that *traJ* gene expression is not subject to thermal regulation, as the level of *traJ* mRNA was approximately equal in the wild-type strain irrespective of growth temperature (Fig. 4.9).

In contrast, there were discernible differences in *traJ* gene expression at 30°C or 37°C in the mutant backgrounds. At the permissive temperature for conjugation, *traJ* gene expression was strongly derepressed (~5-fold) in *hns* mutants and to a lesser extent (~2-fold) in *sfh* mutants (Fig. 4.9). Surprisingly, the combination of both mutant alleles (*sfh* and *hns*) in the same cell at 30°C resulted in a decrease in *traJ* mRNA levels, compared to those in a *hns* single or *hns stpA* double mutant (Fig. 4.9).

At 37°C, *traJ* transcription in all the strains was generally either relatively equal to its level in the same strain at 30°C, or else markedly downregulated. One exception was the *sfh* mutant, which showed a slight increase in *traJ* gene expression. Moreover, when the *sfh* mutation was combined with the *hns* mutant allele, *traJ* gene expression was further enhanced 2-fold (Fig. 4.9). The repressive effect of H-NS on *traJ* transcription was not evident at 37°C in the *hns* single mutant (Fig. 4.9), indicating H-NS exerts its negative influence on the *traJ* gene mainly at lower temperatures. The results also highlight the possibility that Sfh might be a more effective repressor of the *traJ* gene at 37°C than at 30°C, since the *sfh* and *sfh hns* mutants displayed the strongest upregulation of *traJ* gene expression at the non-permissive temperature (Fig. 4.9). Interestingly, the *stpA* single mutant showed a slight decrease in *traJ* mRNA levels compared to the wild-type strain regardless of growth temperature, implying that StpA might positively regulate *traJ* transcription (Fig. 4.9).

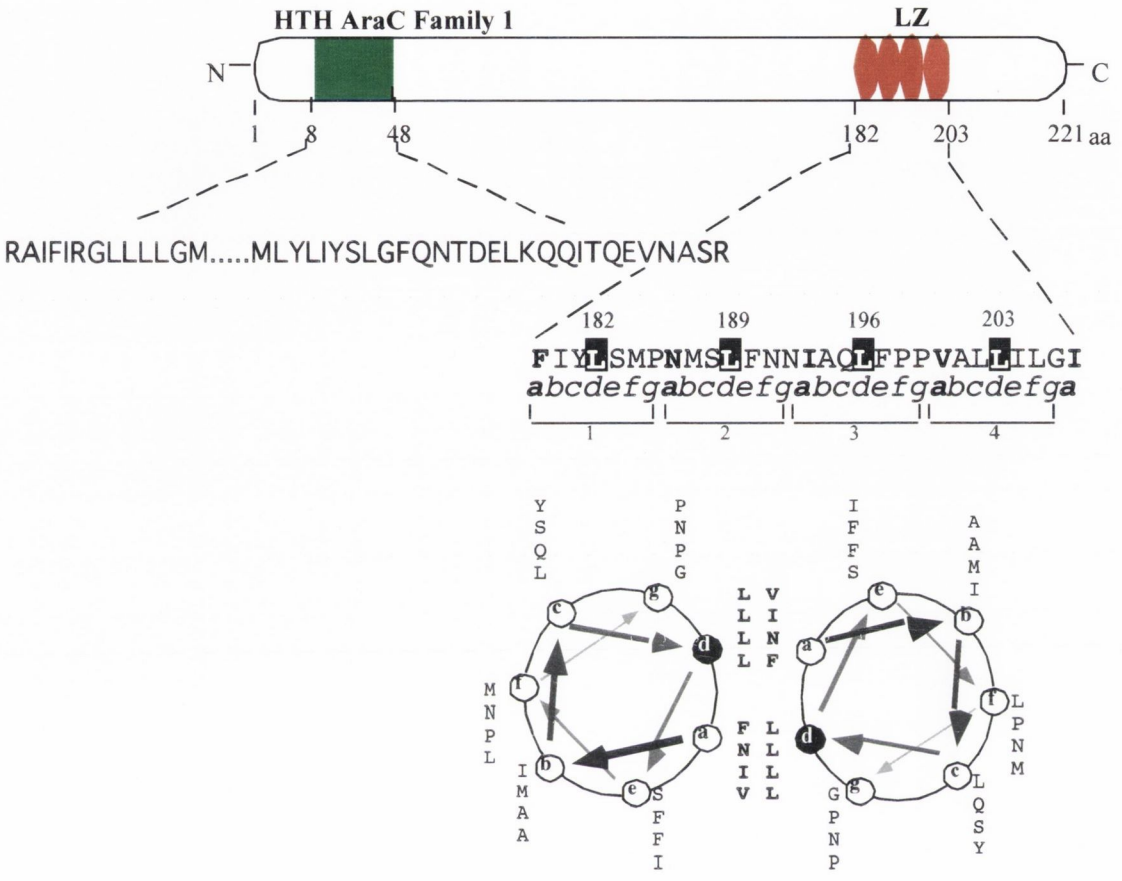

Fig. 4.8. Predicted functional motifs of the TraJ protein. The position of a putative helix-turn-helix (HTH) and leucine zipper (LZ) motif are indicated. The single letter amino acid sequence of the leucine zipper motif with the four-component heptad repeats is shown. The leucine repeat is shaded in black and the repeating positions are indicated by the letters a–g. A helical wheel diagram portrays the predicted homodimer conformation of TraJ. The helix-turn-helix AraC Family 1 signature is also indicated.

Fig. 4.9. Effect of Sfh, H-NS, and StpA on *traJ* gene transcription. (A) RT-PCR analyses of *traJ* gene transcription in wild-type strain BS184 and its *sfh*, *hns*, and *stpA* single and double mutant derivatives at 30°C and 37°C. Total RNA was extracted from log phase (OD_{600}~0.6) L-broth cultures, grown at either 30°C or 37°C, of the various strains being tested, DNase treated, and used as template for RT-PCR. As a control for RNA integrity and loading, RT-PCR analyses of *rplT* gene transcription was also performed. (B) Histograms showing densitometric analyses of RT-PCR analyses of *traJ* gene transcription. The densitometric data shown are averages of at least three independent experiments in which RT-PCR samples from L-broth cultures, grown at 30°C and 37°C, of the various strains being tested were run on the same gel (data not shown). The relative transcript levels are expressed relative to the *traJ* mRNA content of strain BS184 cells grown at 30°C, the value of which was taken as 1.

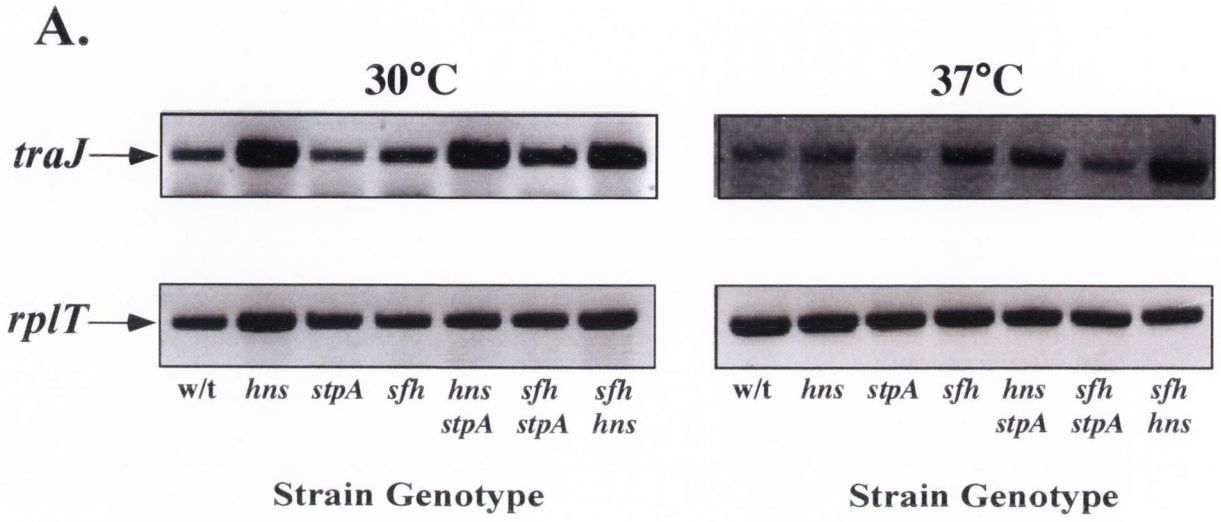
A.
30°C
37°C
traJ
rplT
w/t
hns
stpA
sfh
hns stpA
sfh stpA
sfh hns
Strain Genotype
Strain Genotype

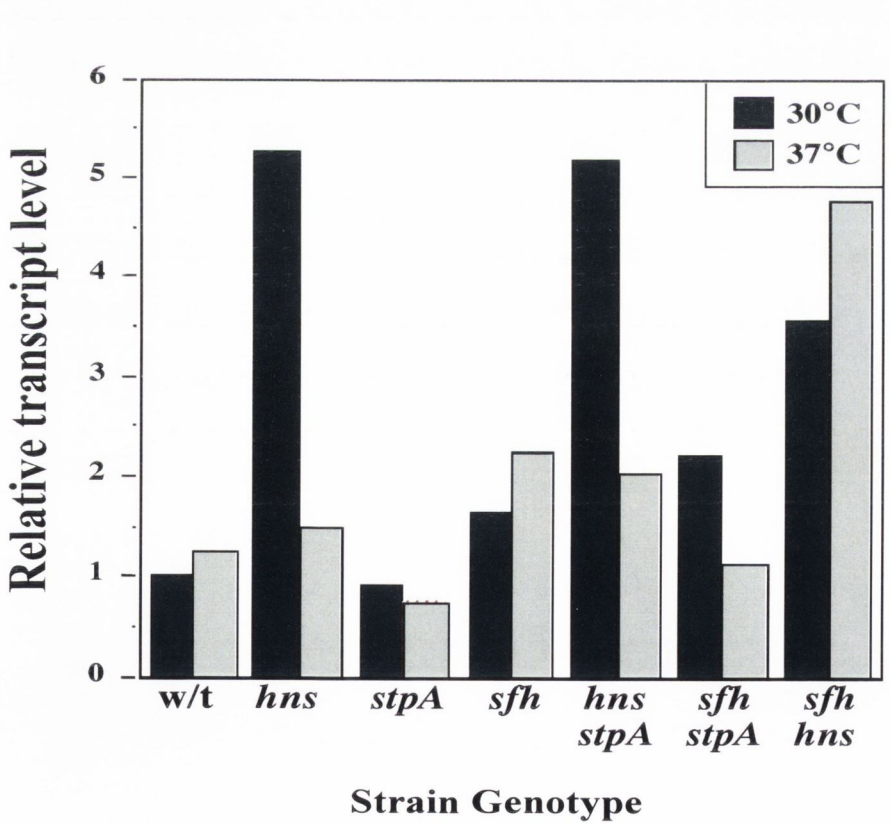
B.
Relative transcript level
0
1
2
3
4
5
6
30°C
37°C
w/t
hns
stpA
sfh
hns stpA
sfh stpA
sfh hns
Strain Genotype

Since H-NS-like proteins are known to bind preferentially to intrinsically curved DNA (Bracco *et al.*, 1989; Owen-Hughes *et al.*, 1992; Yamada *et al.*, 1990), the intrinsic curvature of the DNA upstream of the *traJ* gene was analysed *in silico* using the BEND-IT computer program. The curvature propensity plot obtained revealed that the area contains several regions of curvature (Fig. 4.10), indicating that H-NS, Sfh, and StpA could be directly influencing *traJ* gene expression. To assess this possibility, the ability of H-NS, Sfh, and StpA to directly interact with the *traJ* regulatory region was examined using competitive EMSAs. A 502-bp DNA fragment encompassing the *traJ* regulatory region (nt –401 to +101 with respect to the translation initiation codon of the *traJ* gene) was added to *Taq*1–*Ssp*I-digested pBR322 DNA and then incubated with increasing equimolar concentrations of purified Sfh, H-NS, or StpA. The electrophoretic mobility of the *traJ* DNA fragment was specifically retarded by the three proteins, in concentration-dependent manners (Fig. 4.10). However, StpA only shifted the mobility of the *traJ* band at a protein concentration of ≥1.5 μM, compared to a concentration of ≤0.5 μM for H-NS and Sfh (Fig. 4.10).

Collectively, these data signified that there might be an internal promoter just upstream of the *traJ* gene in the H operon, to which the H-NS-like proteins directly bind thereby regulating *traJ* transcription. For this reason, a 604-bp DNA fragment (nt –503 to +101 with respect to the translation initiation codon of the *traJ* gene) containing the putative *traJ* promoter was cloned upstream of the promoterless *gfp* gene in plasmid pZep08 to generate plasmid ptraJ-gfp (Table 2.2). To confirm that the *traJ* fragment was correctly inserted into the vector, plasmid DNA was isolated from clones and sequenced (data not shown).

Transcriptional activity of the putative *traJ* promoter was examined throughout the growth cycle in L-broth medium by flow cytometric analysis utilizing the newly constructed plasmid ptraJ-gfp. The plasmid-borne *traJ–gfp* transcriptional fusion was transformed into the wild-type *Shigella* strain BS184 and its *sfh, hns, and stpA* mutant derivatives. Samples for flow cytometric analysis were harvested at intervals throughout the growth curve from L-broth cultures, grown at 30°C and 37°C, of the various strains being tested. The results of the

assays revealed that no transcriptional activity could be detected from plasmid ptraJ-gfp under any of the conditions tested (data not shown). The plasmid ptraJ-gfp displayed exactly the same *gfp* expression levels as the negative control plasmid pZep08 (Fig. 4.11). Thus it must be concluded that there is no promoter within 500 bp upstream of the *traJ* gene. In light of this, it seems likely that *traJ* gene expression is driven by a promoter upstream of the *traH* gene, the first gene of the H operon within which the *traJ* gene is located (Fig. 4.1).

4.2.6 Effect of *sfh, hns,* and *stpA* mutations on *traH* gene expression

The *traH* gene is located just downstream of the *oriT* of IncHI1 plasmids and is the first gene of the Tra1 H operon (Fig. 4.1). TraH is thought to function as a relaxosome accessory protein, since *traH* mutants elaborate H-pili, but are defective for conjugative transfer (Lawley *et al.*, 2002). In this study, RT-PCR analyses of *traH* transcription was performed at both 30°C and 37°C in a wild-type and in *hns, stpA,* and *sfh* mutant backgrounds. Surprisingly, the results showed that *traH* gene expression was 2.5-fold higher in wild-type cells grown at 37°C, compared to those grown at 30°C (Fig. 4.12), indicating *traH* gene expression is maximal under non-permissive conditions. These data are consistent with a previous report, which determined that the H operon promoter displayed higher expression at 37°C, than at 30°C (Alonso *et al.*, 2005b). Quantitative analysis of *traH* mRNA levels in the different mutant strains revealed that, at 30°C *traH* expression is dramatically upregulated 9-fold in all the tested *hns* backgrounds (Fig. 4.12). Interestingly, combining the *sfh* or *stpA* mutation with the *hns* mutant allele had no additive effect on *traH* mRNA levels. The repressive effect of Sfh and StpA on *traH* gene expression was only significantly evident at 30°C in the *sfh stpA* double mutant (Fig. 4.12). At the non-permissive temperature, *traH* gene expression was markedly derepressed in all the mutant backgrounds except in the *sfh stpA* double mutant. Intriguingly, strains lacking both Sfh and StpA displayed a slight decrease in *traH* gene expression levels compared to those observed for the wild-type strain at 37°C. Perhaps this is due to increased H-NS levels in the *sfh stpA* double mutant, as neither Sfh nor StpA is present in this strain to negatively cross-regulate *hns* expression. Taken in aggregate,

Fig. 4.10. Direct interaction of Sfh, H-NS, and StpA with the *traJ* promoter region. (A) DNA curvature analysis of the *traJ* promoter region. Graph shows the predicted intrinsic curvature of the *traJ* regulatory region using the computer program BEND-IT. Curvature is expressed as degrees per helical turn and plotted against the position on the promoter sequence, with +1 corresponding to the *traJ* translation initiation codon. Curved and straight motifs have a value above or below 5 degrees per helical turn, respectively. Regions of intrinsic DNA curvature are arrowed. (B) Competitive gel retardation assay showing the specific binding of Sfh, H-NS and StpA to the *traJ* promoter region. A 502-bp DNA fragment encompassing the *traJ* regulatory region (nt –401 to +101 with respect to the translation initiation codon of the *traJ* gene) was amplified by PCR using the primer pair traJ-BSF and traJ-BSR (Table 2.3). The plasmid pBR322 was digested with restriction endonucleases *Taq*1 and *Ssp*I, and the resulting DNA fragments mixed with the 502-bp amplimer of the *traJ* promoter region. The DNA mixtures were incubated with increasing equimolar concentrations of Sfh, H-NS, or StpA in the range 0 μM to 2 μM. An arrow and an asterisk indicate the position of the *traJ* and *bla* promoter fragments, respectively. The curved *bla* promoter is a positive control known to bind H-NS-like proteins. The positions of the 600-bp and 400-bp molecular size markers are also indicated.

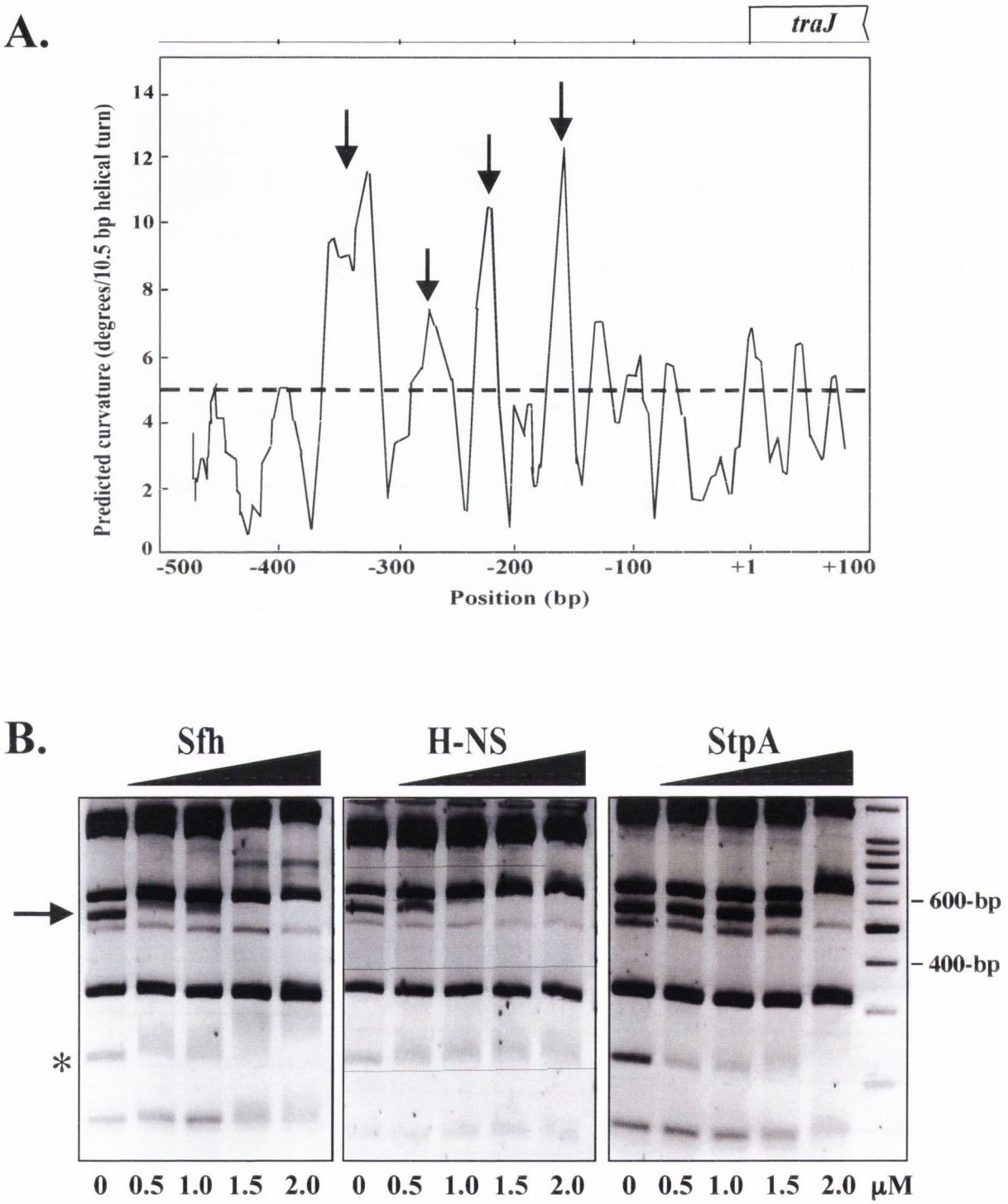
A.
traJ
Predicted curvature (degrees/10.5 bp helical turn)
0
2
4
6
8
10
12
14
-500
-400
-300
-200
-100
+1
+100
Position (bp)
B.
Sfh
H-NS
StpA
600-bp
400-bp
*
0 0.5 1.0 1.5 2.0 0 0.5 1.0 1.5 2.0 0 0.5 1.0 1.5 2.0 μM

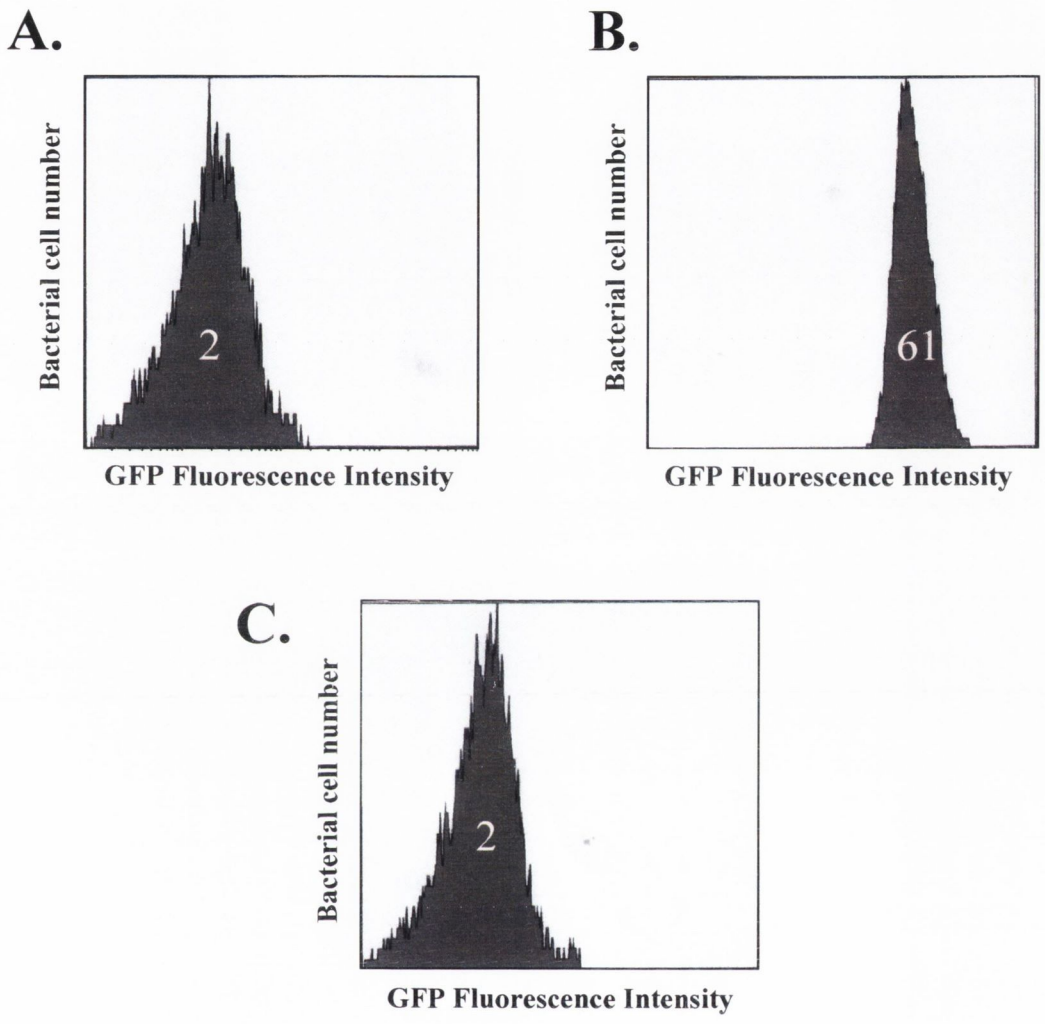

Fig. 4.11. Transcriptional activity of the plasmid ptraJ-gfp.

Sample data showing fluorescence intensity of wild-type BS184 cells harbouring the plasmids (A) pZep08 (-ve control), (B) psfh-gfp (+ve control) and (C) ptraJ-gfp. The mean channel fluorescence of each sample is indicated.

Fig. 4.12. Effect of Sfh, H-NS, and StpA on *traH* gene transcription. (A) RT-PCR analyses of *traH* gene transcription in wild-type strain BS184 and its *sfh*, *hns*, and *stpA* single and double mutant derivatives at 30°C and 37°C. Total RNA was extracted from log phase (OD_{600}~0.6) L-broth cultures, grown either 30°C or 37°C, of the various strains being tested, DNase treated, and used as template for RT-PCR. As a control for RNA integrity and loading, RT-PCR analyses of *rplT* gene transcription was also performed. (B) Histograms showing densitometric analyses of RT-PCR analyses of *traH* gene transcription. The densitometric data shown are averages of at least three independent experiments in which RT-PCR samples from L-broth cultures, grown at 30°C and 37°C, of the various strains being tested were run on the same gel (data not shown). The relative transcript levels are expressed relative to the *traH* mRNA content of strain BS184 cells grown at 30°C, the value of which was taken as 1.

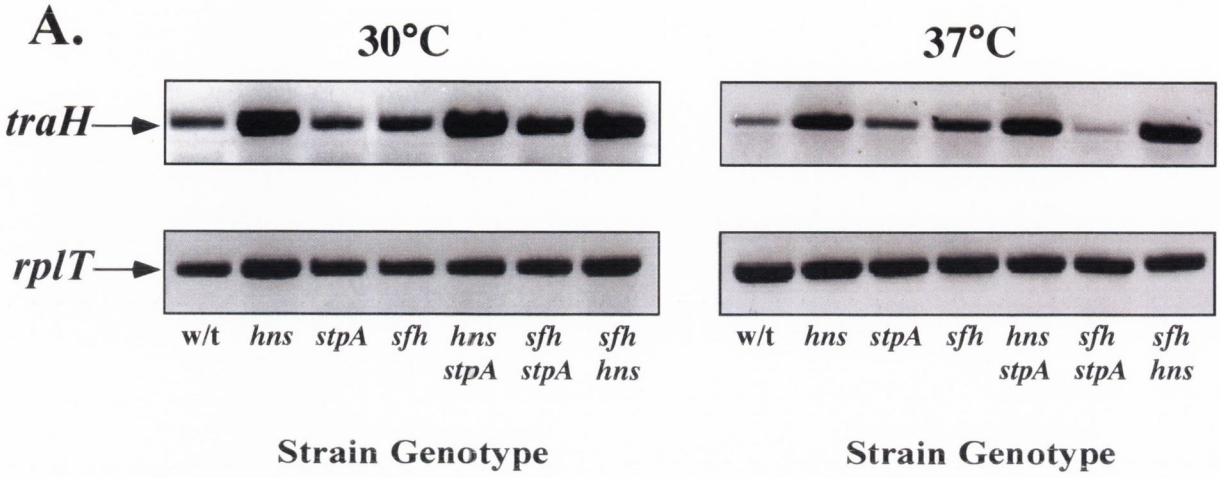
A.
30°C
37°C
traH
rplT
w/t
hns
stpA
sfh
hns stpA
sfh stpA
sfh hns
Strain Genotype
Strain Genotype

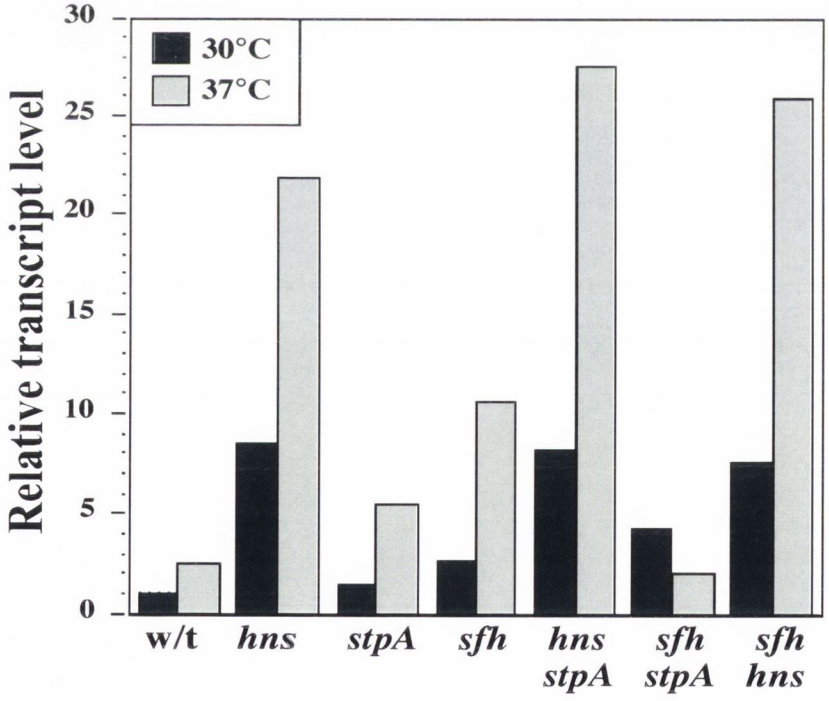
B.
30°C
37°C
Relative transcript level
0
5
10
15
20
25
30
w/t
hns
stpA
sfh
hns stpA
sfh stpA
sfh hns
Strain Genotype

these data clearly show that H-NS is a strong repressor of the *traH* gene irrespective of growth temperature, whereas StpA and Sfh preferentially repress the *traH* gene at 37°C.

Recently, the transcriptional start site for the *traH* gene was elucidated, and analysis of the *traH* regulatory region revealed that it contained several A/T rich regions positioned as tracts (Alonso *et al.*, 2005b). Consistent with these data, this study determined using the BEND-IT computer program that the *traH* promoter region is intrinsically curved (Fig. 4.13). In light of this, the ability of the three *Shigella* H-NS-like proteins to bind to the *traH* regulatory region was investigated using competitive EMSAs. A 536-bp DNA fragment encompassing the *traH* regulatory region (nt –390 to +146 with respect to the transcription start site of *traH*) was added to *Taq*1–*Ssp*I-digested pBR322 DNA and then incubated with increasing equimolar concentrations of purified Sfh, H-NS, or StpA. The electrophoretic mobility of the *traH* promoter region DNA fragment was specifically retarded by the three proteins in concentration-dependent manners (Fig. 4.13). In addition, all three proteins shifted the positive control *bla* promoter band.

4.2.7 *Shigella* H-NS-like proteins regulate plasmid pSf-R27 *hha, tlpA,* and *dam* paralogues

Conjugative transfer of the *E. coli* F plasmid and several other F-like plasmids is controlled by a complex regulatory circuit involving both plasmid- and chromosome-encoded proteins (Will *et al.*, 2004). Notably, nucleoid-associated proteins constitute all of the host-encoded proteins that influence F-like conjugative transfer (Dempsey and Fee, 1990; Nieto *et al.*, 1998; Starcic *et al.*, 2003; Starcic-Erjavec *et al.*, 2003; Will *et al.*, 2004). Since nucleoid-associated proteins often regulate gene expression in a concerted manner, acting either synergistically or antagonistically, it was of interest to determine if the three *Shigella* H-NS-like proteins could influence expression of the plasmid pSf-R27 *hha-*, *tlpA-*, and *dam*-like genes. For this reason, RT-PCR analyses of the plasmid pSf-R27 *hha-*, *tlpA-*, and *dam*-like

genes was performed on total RNA extracted from L-broth cultures of the wild-type strain BS184 and its *hns, stpA*, and *sfh* mutant derivatives grown at 30°C or 37°C.

The results obtained for the plasmid pSf-R27 *tlpA*-like gene revealed that its expression was relatively unaffected in *hns, stpA,* and *sfh* mutants at 30°C, with only slight elevation in *tlpA*-like gene expression (>2-fold) observed in a *hns* single mutant background (Fig. 4.14). In stark contrast, at 37°C *tlpA*-like gene expression was dramatically derepressed ~5-fold in the *hns* and *sfh* mutants, and to a lesser extent (2.5 fold) in the *stpA* mutant (Fig. 4.14). The effect of double mutations on *tlpA*-like gene expression at 37°C was also investigated. All the double mutants displayed a decrease in pSf-R27 *tlpA* mRNA levels compared to those observed for their corresponding single mutants (Fig. 4.14). These data indicate that in the absence of their two homologous proteins, Sfh, H-NS, and StpA might be more effective repressors of *tlpA*-like gene expression, perhaps due to a corresponding increase in their cellular levels. However, the results also support a model in which heteromeric complexes of the different H-NS-like proteins are required for optimal regulation of the *tlpA*-like gene.

Analysis of the results obtained for the plasmid pSf-R27 *hha*-like gene revealed that its expression is thermally regulated (Fig. 4.15). Wild-type cells grown at 30°C were shown to have a 50% reduction in pSf-R27 *hha* mRNA levels compared to those grown at physiological temperature (Fig. 4.15). Interestingly, *hha*-like gene expression was unaffected by the absence of StpA, whereas the *hns* single and *hns stpA* double mutants displayed elevated *hha*-like gene expression levels and a loss of *hha* temperature-dependent expression (Fig. 4.15). In contrast, strains lacking Sfh showed the reverse in *hha* temperature-dependent expression, i.e., pSf-R27 *hha* mRNA levels were higher in the *sfh* mutants grown at 30°C than those grown at 37°C (Fig. 4.15). At the higher growth temperature, pSf-R27 *hha* mRNA levels were reduced in all the *sfh* mutants compared to the wild-type strain (Fig. 4.15), suggesting that Sfh positively regulates *hha*-like gene expression at 37°C.

Fig. 4.13. Direct interaction of Sfh, H-NS, and StpA with the *traH* promoter region. (A) DNA curvature analysis of the *traH* promoter region. Graph shows the predicted intrinsic curvature of the *traH* regulatory region using the computer program BEND-IT. Curvature is expressed as degrees per helical turn and plotted against the position on the promoter sequence, with +1 corresponding to the *traH* transcription start site. Curved and straight motifs have a value above or below 5 degrees per helical turn, respectively. Regions of intrinsic DNA curvature are arrowed. (B) Competitive gel retardation assay showing the specific binding of Sfh, H-NS and StpA to the *traH* promoter region. A 536-bp DNA fragment encompassing the *traH* regulatory region (nt –390 to +146 with respect to the transcription start site of the *traH* gene) was amplified by PCR using the primer pair traH-BSF and traH-BSR (Table 2.3). The plasmid pBR322 was digested with restriction endonucleases *Taq*1 and *Ssp*I, and the resulting DNA fragments mixed with the 536-bp amplimer of the *traH* promoter region. The DNA mixtures were incubated with increasing equimolar concentrations of Sfh, H-NS, or StpA in the range 0 μM to 2 μM. An arrow and an asterisk indicate the position of the *traH* and *bla* promoter fragments, respectively. The curved *bla* promoter is a positive control known to bind H-NS-like proteins. The positions of the 600-bp and 400-bp molecular size markers are also indicated.

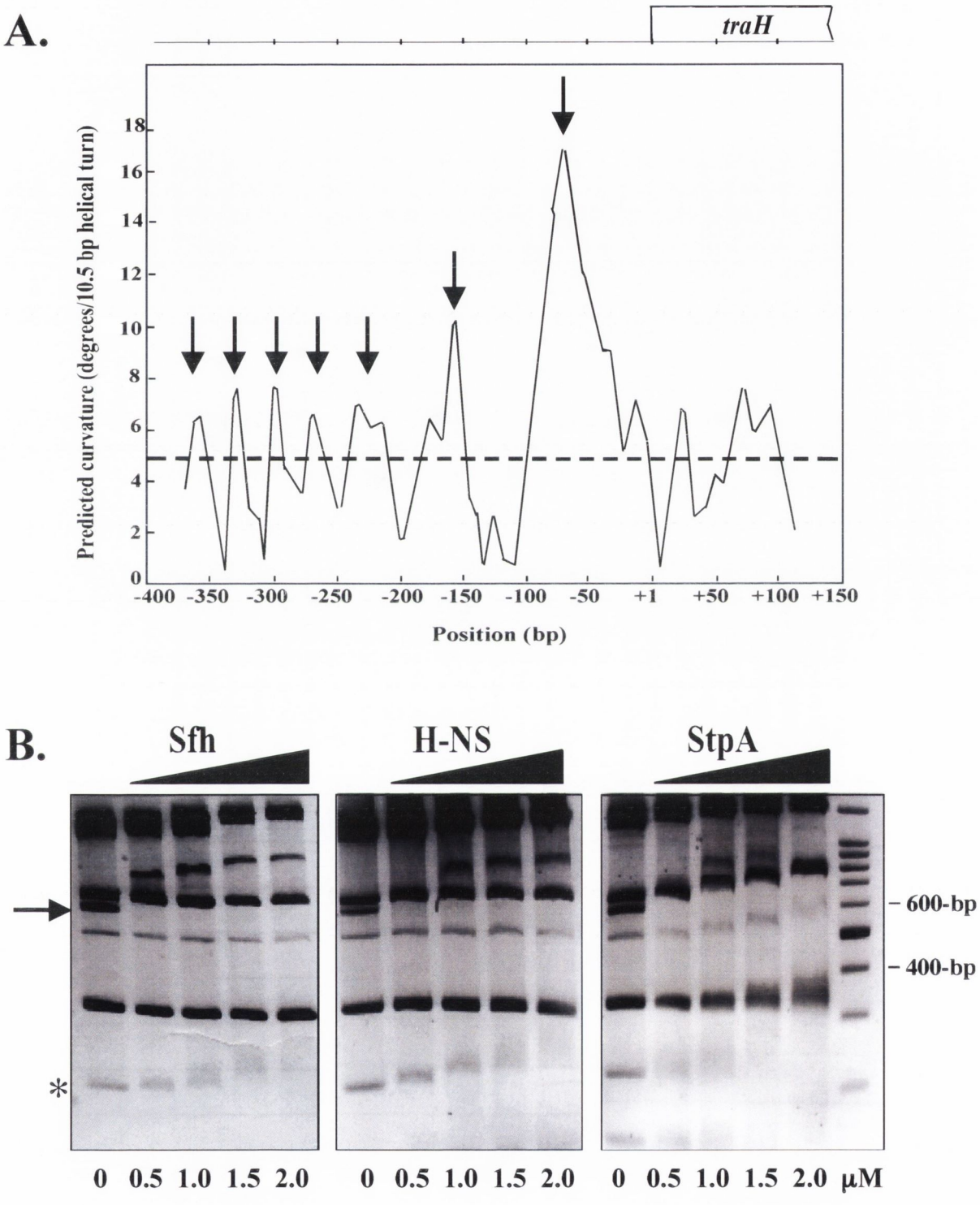
A.
traH
Predicted curvature (degrees/10.5 bp helical turn)
0
2
4
6
8
10
12
14
16
18
-400 -350 -300 -250 -200 -150 -100 -50 +1 +50 +100 +150
Position (bp)
B.
Sfh
H-NS
StpA
600-bp
400-bp
*
0 0.5 1.0 1.5 2.0
0 0.5 1.0 1.5 2.0
0 0.5 1.0 1.5 2.0 μM

Fig. 4.14. Effect of Sfh, H-NS, and StpA on *tlpA*-like gene transcription. (A) RT-PCR analyses of pSf-R27 *tlpA*-like gene transcription in wild-type strain BS184 and its *sfh*, *hns*, and *stpA* single and double mutant derivatives at 30°C and 37°C. Total RNA was extracted from log phase (OD_{600}~0.6) L-broth cultures, grown either 30°C or 37°C, of the various strains being tested, DNase treated, and used as template for RT-PCR. As a control for RNA integrity and loading, RT-PCR analyses of *rplT* gene transcription was also performed. (B) Histograms showing densitometric analyses of RT-PCR analyses of pSf-R27 *tlpA*-like gene transcription. The densitometric data shown are averages of at least three independent experiments in which RT-PCR samples from L-broth cultures, grown at 30°C and 37°C, of the various strains being tested were run on the same gel (data not shown). The relative transcript levels are expressed relative to the pSf-R27 *tlpA* mRNA content of strain BS184 cells grown at 30°C, the value of which was taken as 1.

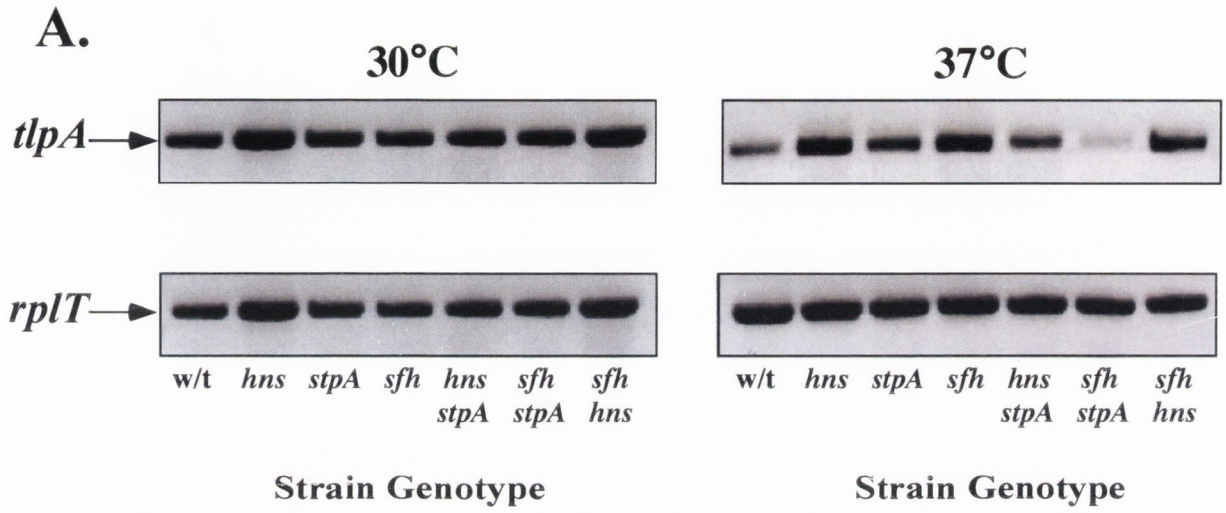
A.
30°C
37°C
tlpA
rplT
w/t
hns
stpA
sfh
hns stpA
sfh stpA
sfh hns
Strain Genotype
Strain Genotype

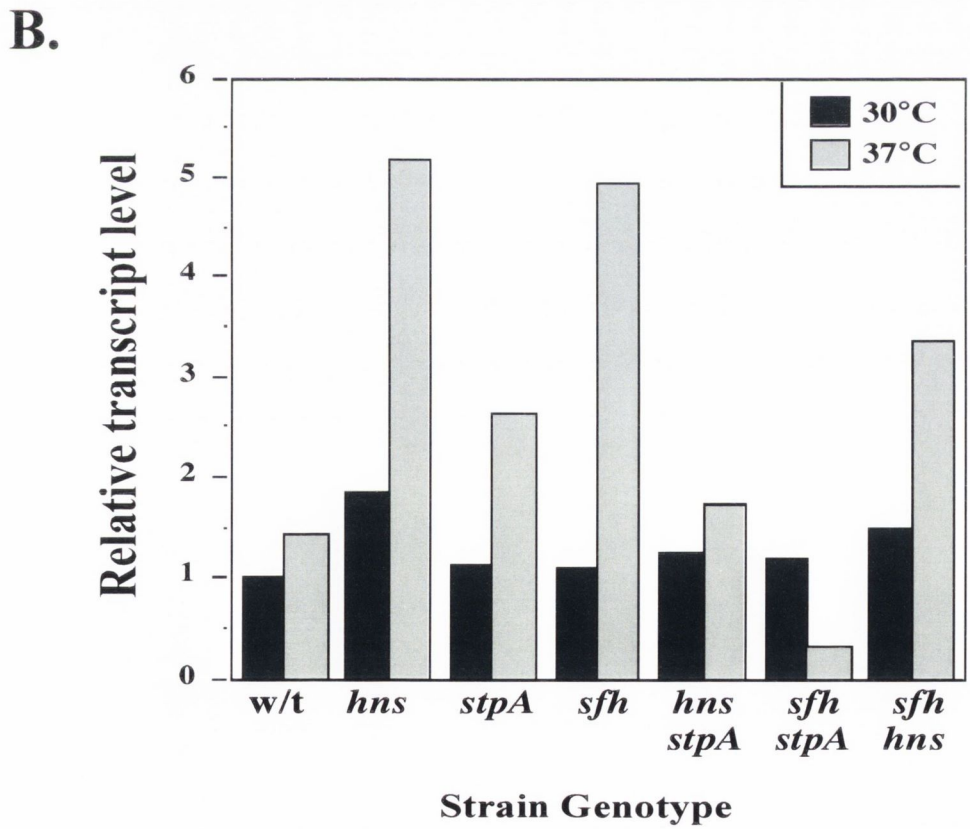
B.
Relative transcript level
0
1
2
3
4
5
6
30°C
37°C
w/t
hns
stpA
sfh
hns stpA
sfh stpA
sfh hns
Strain Genotype

Fig. 4.15. Effect of Sfh, H-NS, and StpA on *hha*-like gene transcription. (A) RT-PCR analyses of pSf-R27 *hha*-like gene transcription in wild-type strain BS184 and its *sfh*, *hns*, and *stpA* single and double mutant derivatives at 30°C and 37°C. Total RNA was extracted from log phase (OD_{600}~0.6) L-broth cultures, grown either 30°C or 37°C, of the various strains being tested, DNase treated, and used as template for RT-PCR. As a control for RNA integrity and loading, RT-PCR analyses of *rplT* gene transcription was also performed. (B) Histograms showing densitometric analyses of RT-PCR analyses of pSf-R27 *hha*-like gene transcription. The densitometric data shown are averages of at least three independent experiments in which RT-PCR samples from L-broth cultures, grown at 30°C and 37°C, of the various strains being tested were run on the same gel (data not shown). The relative transcript levels are expressed relative to the pSf-R27 *hha* mRNA content of strain BS184 cells grown at 30°C, the value of which was taken as 1.

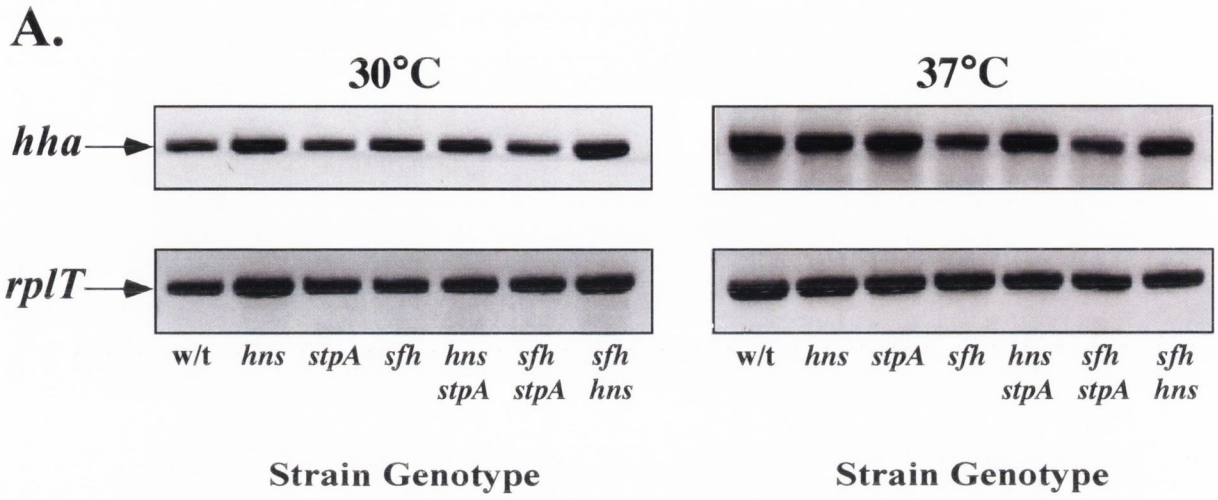
A.
30°C
37°C
hha
rplT
w/t
hns
stpA
sfh
hns stpA
sfh stpA
sfh hns
Strain Genotype
Strain Genotype

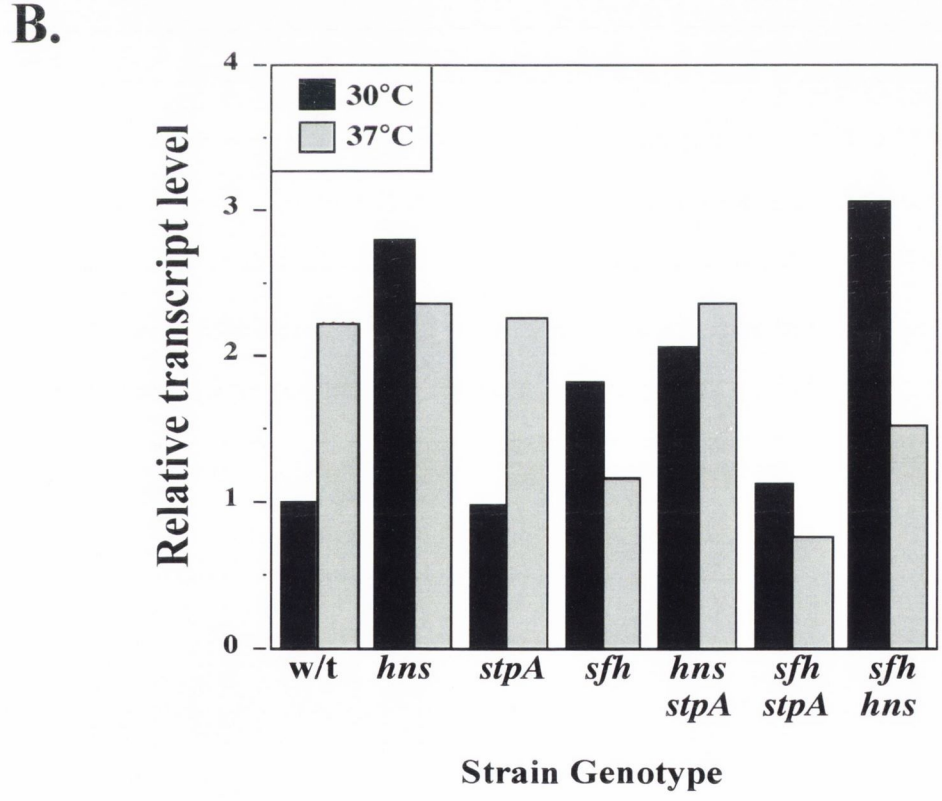
B.
Relative transcript level
30°C
37°C
0
1
2
3
4
w/t
hns
stpA
sfh
hns stpA
sfh stpA
sfh hns
Strain Genotype

Finally, RT-PCR analyses of the *dam*-like gene showed that H-NS is a strong repressor of *dam*-like gene expression irrespective of growth temperature (Fig. 4.16). In contrast, Sfh and StpA only markedly repressed transcription of the *dam*-like gene at 37°C (Fig. 4.16). Quantitative analysis of pSf-R27 *dam* mRNA levels in the different strains highlighted the remarkable reduction of *dam*-like gene expression in the *sfh stpA* double mutant at 37°C. Not only are pSf-R27 *dam* mRNA levels in this mutant lower at 37°C than those observed for the wild-type strain, but they are also dramatically downregulated compared to the pSf-R27 *dam* transcript levels detected in the *sfh* and *stpA* single mutants at this temperature (Fig. 4.16). As mentioned above, this paradoxical observation could either be due to increased H-NS protein levels in the *sfh stpA* mutant or might also indicate that heteromeric H-NS-like complexes are required for optimal control of gene expression.

4.3 Discussion

In recent years the family of known H-NS-like proteins in Gram-negative bacteria has expanded rapidly, and sequencing studies have revealed that some bacterial species contain multiple *hns*-like genes (Tendeng and Bertin, 2003). Often these additional H-NS-like proteins are encoded on mobile genetic elements, as is the case for the *Shigella* H-NS-like protein Sfh which is encoded on the large self-transmissible plasmid pSf-R27 (Beloin *et al.*, 2003). Many of the H-NS-like proteins encoded by plasmids or pathogenicity islands are known to regulate the genetic elements that encode them. Previous reports have shown that the protein KorB encoded by the F-like plasmid pKM101 has two H-NS-like nucleic acid-binding domains in tandem and is a regulator of plasmid gene expression and partitioning (More *et al.*, 1996). The Orf4 protein encoded by the IncM plasmid R446 also has a H-NS-like carboxyl terminus and is required for the regulation of conjugative pili expression during conjugation (Tietze and Tschape, 1994). Together, these data lead to the hypothesis that Sfh could be a regulator of plasmid pSf-R27 genes, in particular the transfer genes. Moreover, since conjugative transfer of IncHI1 plasmids is thermosensitive, the model is further strengthened by the fact H-NS-like proteins are known thermoregulators. The aim of this study was to determine if Sfh, and/or its paralogues H-NS and StpA, could influence the conjugative transfer of the IncHI1 plasmid pSf-R27.

The contributions of the three *Shigella* H-NS-like proteins to plasmid pSf-R27 temperature-dependent transfer was investigated using quantitative conjugation assays (Table 4.1). The conjugative studies revealed that the transfer frequency of plasmid pSf-R27 is reduced over 2-fold in a *sfh* mutant compared to that of a wild-type strain, confirming a role for Sfh in the modulation of plasmid pSf-R27 conjugative transfer (Table 4.1). In addition, conjugative transfer of plasmid pSf-R27 was also repressed in the absence of StpA and H-NS, thus identifying a novel role for these proteins in plasmid pSf-R27 conjugative transfer (Table 4.1). These data suggested the participation of both plasmid- and chromosome-encoded proteins in the regulatory circuit of plasmid pSf-R27. This observation is reminiscent of F-like plasmids, whose conjugative transfer is regulated by a complex network of plasmid- and

Fig. 4.16. Effect of Sfh, H-NS, and StpA on *dam*-like gene transcription. (A) RT-PCR analyses of pSf-R27 *dam*-like gene transcription in wild-type strain BS184 and its *sfh*, *hns*, and *stpA* single and double mutant derivatives at 30°C and 37°C. Total RNA was extracted from log phase (OD_{600}~0.6) L-broth cultures, grown either 30°C or 37°C, of the various strains being tested, DNase treated, and used as template for RT-PCR. As a control for RNA integrity and loading, RT-PCR analyses of *rplT* gene transcription was also performed. (B) Histograms showing densitometric analyses of RT-PCR analyses of pSf-R27 *dam*-like gene transcription. The densitometric data shown are averages of at least three independent experiments in which RT-PCR samples from L-broth cultures, grown at 30°C and 37°C, of the various strains being tested were run on the same gel (data not shown). The relative transcript levels are expressed relative to the pSf-R27 *dam* mRNA content of strain BS184 cells grown at 30°C, the value of which was taken as 1.

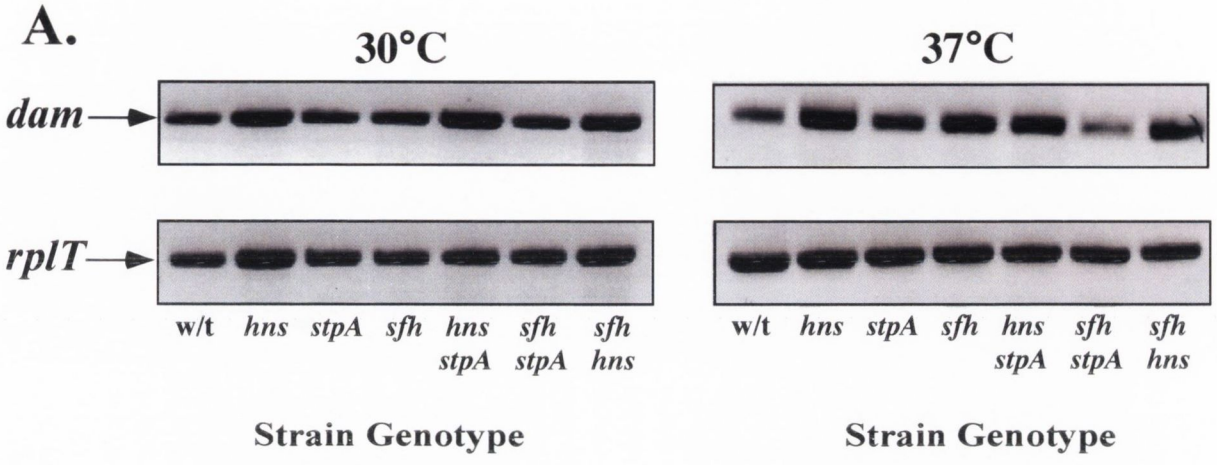
A.
30°C
37°C
dam
rplT
w/t
hns
stpA
sfh
hns stpA
sfh stpA
sfh hns
Strain Genotype
Strain Genotype

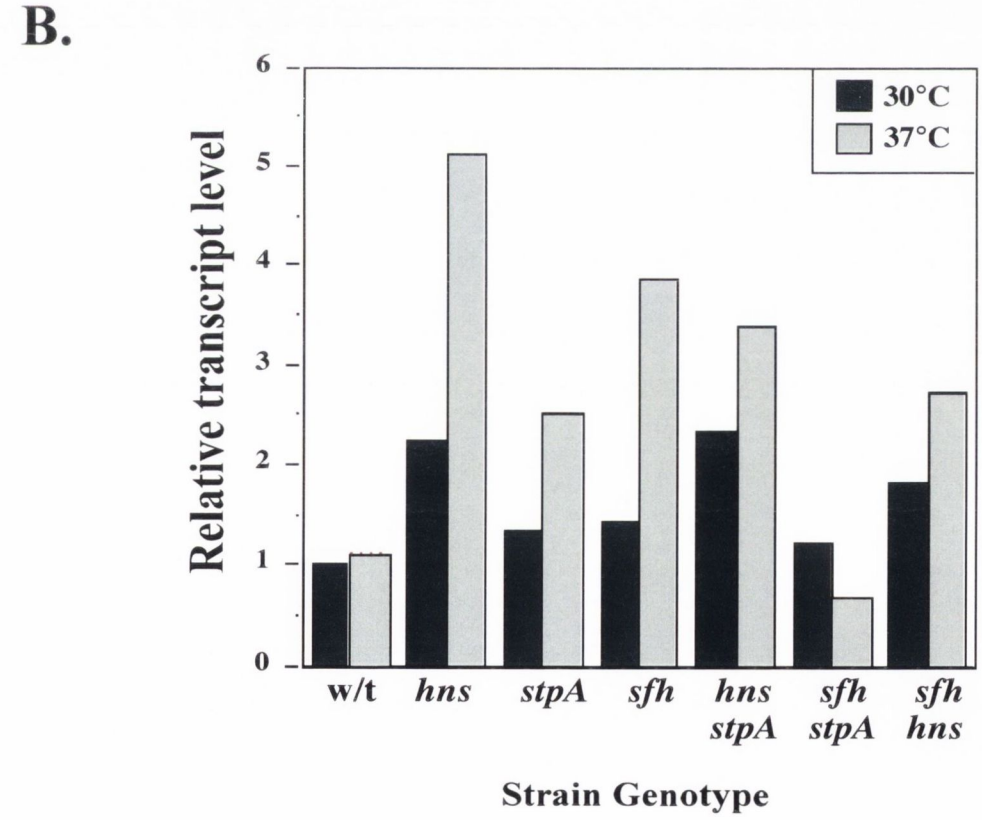
B.
Relative transcript level
0
1
2
3
4
5
6
30°C
37°C
w/t
hns
stpA
sfh
hns stpA
sfh stpA
sfh hns
Strain Genotype

host-encoded genes, including the *hns* gene (Starcic-Erjavec *et al.*, 2003; Will *et al.*, 2004). Conjugation studies were also performed at 37°C, the non-permissive temperature for IncHI1 plasmid conjugative transfer. As expected, no conjugative transfer was detected from the wild-type strain and, moreover, from any of its *sfh, stpA,* and *hns* single and double mutant derivatives (data not shown). Therefore, since conjugation is still temperature-dependent in the absence of Sfh, StpA, and H-NS, it must be concluded that none of the *Shigella* H-NS-like proteins are involved in the regulatory pathway controlling plasmid pSf-R27 thermosensitive transfer.

These data are consistent with a recent report in *E. coli* that showed the transfer frequency of derepressed plasmid R27 (drR27) is still temperature-dependent in the absence of H-NS, and that *hns* mutants display a 2-fold reduction in conjugative transfer of plasmid drR27 at 30°C (Alonso *et al.*, 2005b). However, the data obtained herein showed nearly a 100-fold decrease in plasmid pSf-R27 transfer frequency in a *hns* mutant background (Table 4.1). The apparent discrepancy in fold reduction in transfer frequency is probably because Alonso *et al.* (2005) used the plasmid drR27 in conjugative matings, which has an insertion in the *htdA* gene (Alonso *et al.*, 2005b). RT-PCR data obtained in the present study reveal that H-NS is a repressor of the *htdA* gene (Fig 4.6), which codes for a known repressor of plasmid R27-mediated conjugation (Whelan *et al.*, 1994). In addition, the *htdA* gene is the first gene of the AN operon of the Tra2 region (Fig. 4.1). Thus, an insertional mutation in this gene would more than likely have polar effects. Therefore, the *E. coli* study (Alonso *et al.*, 2005b) did not address the effect of H-NS on plasmid R27-mediated conjugation in its native context and this most likely explains the different transfer frequencies obtained.

Using RT-PCR analyses of mRNA transcripts for all three proteins, Sfh, H-NS, and StpA were shown to influence *tra* gene expression. As mentioned above, H-NS represses transcription of the *htdA* gene, most notably at 37°C (Fig. 4.6). This raises some interesting questions, as H-NS usually represses gene expression at lower temperatures and permits expression at physiological temperature. Sfh was also shown to repress *htdA* gene expression

at 37°C, albeit to a lesser extent (Fig. 4.6). In contrast, StpA did not appear to affect *htdA* gene expression to any marked extent (Fig. 4.6). All three proteins, especially H-NS and Sfh, specifically interacted with the *htdA* regulatory region in competitive EMSAs (Fig. 4.7), indicating that their negative regulatory influence on the *htdA* gene is direct. The three *Shigella* H-NS-like proteins also repressed expression of *tra* genes located in the Tra1 region of plasmid pSf-R27 (Fig. 4.5, 4.9 and 4.12). Again, H-NS was observed to markedly repress *tra* gene expression. Interestingly, *traH* gene expression was derepressed ~9-fold in *hns* mutants, regardless of growth temperature, compared to the level of *traH* gene expression in the wild-type strain at the corresponding temperature (Fig. 4.12). In contrast, H-NS specifically represses *traJ* gene expression at 30°C, whereas its paralogue Sfh appears preferentially to negatively influence *traJ* gene expression at 37°C (Fig. 4.9). Sfh and StpA were also observed preferentially to repress *traH* transcription at the non-permissive temperature for conjugative transfer (Fig. 4.12). These data strongly suggest that all three proteins –H-NS, StpA and Sfh– have unique regulatory properties and are required for the apt expression of the *tra* genes under different environmental conditions.

The transcriptional data presented herein also support a model in which the regulatory properties of homomeric and heteromeric H-NS-like protein complexes vary depending on their subunit composition. At the non-permissive temperature for IncHI1 plasmid transfer, *traH* gene expression was significantly derepressed in all the mutant backgrounds tested, with the exception of the *sfh stpA* double mutant (Fig 4.12). Intriguingly, strains lacking both Sfh and StpA displayed a slight decrease in *traH* transcript levels compared to those observed for the wild-type strain at 37°C (Fig. 4.12). Indeed, this phenomenon was also observed for several other genes, in particular the putative plasmid pSf-R27 regulatory genes *hha, dam,* and *tlpA* (Fig. 4.14, 4.15 and 4.16). Why do *sfh* or *stpA* single mutants derepress transcription of these genes, yet the combination of both mutations in the same cell results in repression of the same gene? It is possible that the effect is due to increased H-NS levels in a *sfh stpA* mutant, as neither Sfh nor StpA is present in the cell to repress *hns* expression. Another

attractive hypothesis is that heteromeric H-NS-like complexes, especially StpA:Sfh complexes, are required for optimal control of plasmid pSf-R27 gene expression.

Surprisingly, RT-PCR analyses of *traH* and *traJ* transcription revealed that the two genes are differentially regulated by the *Shigella* H-NS-like proteins, albeit that they are both transcribed from the same promoter (Fig. 4.9 and 4.12). However, the present study also revealed that the H-NS-like proteins can bind directly upstream of both genes (Fig. 4.10 and 4.13). It is possible that this specific binding is controlled differentially by temperature, which would account for the different expression profiles of the genes in the various mutants. Interestingly, H-NS mediated repression of the F-plasmid transfer-regulatory genes *traM* and *traJ* involves H-NS binding to an extended region of the plasmid, thereby acting as a regional silencer (Will *et al.*, 2004). It is possible that an analogous situation occurs at the H operon of plasmid pSf-R27, which encodes TraH and TraJ.

The RT-PCR data presented herein show that in general the *Shigella* H-NS-like proteins act as transcriptional repressors of *tra* gene expression. These findings are consistent with two previous studies (Alonso *et al.*, 2005b; Forns *et al.*, 2005). Since *tra* gene expression is repressed by H-NS-like proteins, one would expect plasmid pSf-R27 transfer frequency to increase in their absence. However, this was found not to be the case in the present study or by Alonso *et al.* (2005b), but is disputed by another report (Forns *et al.*, 2005). The data obtained herein suggest that *tra* gene expression is controlled at the post-transcriptional level. Thus an increase in *tra* transcript levels would not result in a corresponding increase in Tra protein levels. This model correlates with the general consensus that IncHI1 *tra* gene expression is post-transcriptionally controlled, and accounts for the thermosensitive transfer of IncHI1 plasmids (Alonso *et al.*, 2005b; Forns *et al.*, 2005). Furthermore, not all the *tra* operons were responsive to the absence of Sfh (Fig 4.5). Thus, not all the essential Tra proteins are upregulated in the absence of H-NS-like proteins.

The mechanism underlying IncHI1 thermosensitive transfer has not yet been elucidated. Although H-NS-like proteins do modulate IncHI1 plasmid transfer, no transfer can be detected in their absence at the non-permissive temperature for conjugation. Moreover, every effort to isolate a mutant of the prototype R27 plasmid that displays temperature-independent transfer have been unsuccessful (Alonso *et al.*, 2005b; Lawley *et al.* 2003a; Lawley *et al.* 2002; Forns *et al.*, 2005). These data imply that there might be more than one mechanism thermally regulating IncHI1 plasmid transfer. Paralogues of the regulatory proteins Dam, Hha, and TlpA are all encoded on IncHI1 plasmids (Parkhill *et al.*, 2001; Sherburne *et al.*, 2000). A recent report showed that the Hha-like protein encoded by the prototype R27 plasmid could influence plasmid R27 *tra* gene expression (Forns *et al.*, 2005). Members of the Hha protein family are known to interact directly with H-NS-like proteins (Nieto *et al.*, 2002), consequently modulating their activity (Nieto *et al.*, 2000). Furthermore, Hha:H-NS complexes have been shown to regulate gene expression in a temperature-dependent manner (Madrid *et al.*, 2002a; Madrid *et al.*, 2002b; Nieto *et al.*, 2000) and the Hha homologue RmoA positively regulates transfer of plasmid R100 (Nieto *et al.*, 1998). Dam has also been implicated in the regulation of temperature-dependent expression systems (van der Woude *et al.*, 1996) and Dam methylation acts as a repressor of conjugative transfer of the F (Torreblanca and Casadesus, 1996), pSLT (Camacho and Casadesus, 2002), and R100 (Camacho *et al.*, 2005a) plasmids. The TlpA protein is an autoregulatory repressor, which uses its temperature-sensitive folding equilibrium to regulate gene expression in response to temperature shifts (Hurme *et al.*, 1997). Therefore, the Hha-, Dam-, and TlpA-like proteins encoded by IncHI1 plasmids are prime candidates to control thermosensitive transfer of IncHI1 plasmids.

Importantly, the present study determined by RT-PCR analyses of gene transcription that expression of all three proteins –pSf-R27 Hha, Dam and TlpA– is regulated by the *Shigella* H-NS-like proteins, in some instances in a temperature-dependent manner (Fig. 4.14, 4.15 and 4.16). This observation raises some interesting questions about the regulatory circuit of plasmid pSf-R27 and other IncHI1 plasmids. It appears that regulatory cascades, in which the

H-NS-like proteins act hierarchically, could control plasmid gene expression. The importance of H-NS-like proteins as global repressors of plasmid pSf-R27 was also evident from the unsuccessful attempts to construct a triple *sfh hns stpA* mutant. A previous report has shown that overexpression of the relaxosome components of the broad host-range plasmid R1162 has a toxic effect on the cell (Perwez and Meyer, 1999). In light of this, it is possible that the marked overexpression of plasmid pSf-R27 *tra* genes in strains lacking all three H-NS-like proteins could be the underlying reason for the observed lethality of the triple mutant. Further investigation is required to either refute or confirm this hypothesis, and also to decipher the regulatory network of plasmid pSf-R27.

Chapter 5

Stealth-like role for Sfh in horizontal transfer of plasmid pSf-R27

5.1 Introduction

In recent years, advances in genomic technology have revolutionized molecular biology and led to a rapid increase in bacterial genome sequencing. Perhaps one of the most fundamental changes brought about by the new masses of genome sequence information is the realization that horizontal (or lateral) gene transfer is an important, if not the dominant, force in shaping prokaryotic genomes (Doolittle *et al.*, 2003; Gogarten *et al.*, 2002). In bacteria, self-transmissible plasmids, bacteriophages, and other mobile DNA elements can be exchanged between cells and even across species boundaries. The horizontally acquired DNA sequences can then be incorporated into the chromosome, re-excised, re-inserted, multiplied, and deleted. This genetic flux can provide a mechanism, by which bacteria acquire new genetic properties that allow them to colonize new ecological niches (Gogarten and Townsend, 2005). Indeed, mobile genetic elements, in addition to their core genes, typically carry several different accessory genes that provide their host with a selective advantage, such as antibiotic resistance, virulence factors, or unusual metabolic pathways. Consequently, most medically and economically important bacterial phenotypes are encoded by mobile genetic elements (Frost *et al.*, 2005).

For the past three decades, horizontal transfer of IncHI plasmids has been implicated as a significant factor in the persistence of *S.* Typhi, the causative agent of typhoid fever, by conferring multiple drug resistance (MDR) (Fica *et al.*, 1997). The prototype IncHI1 plasmid R27, which was isolated from *S.* Typhimurium in the early 1960's, has a full Tn*10* insertion that confers tetracycline resistance (Sherburne *et al.*, 2000). DNA sequence analysis of plasmid pHCM1, the IncHI plasmid associated with *S.* Typhi endemics in South East Asia, revealed that it encodes MDR (Fica *et al.*, 1997; Parkhill *et al.*, 2001; Wain *et al.*, 2003). More recently, another IncHI1 plasmid designated pSf-R27 was discovered in *S. flexneri* serotype 2a strain 2457T (Beloin *et al.*, 2003; Wei *et al.*, 2003). The DNA sequence of plasmid pSf-R27 is 99.7% identical to that of plasmid R27 and, like many mobile genetic elements, is very AT-rich (55%) (Wei *et al.*, 2003). Uniquely, plasmid pSf-R27 does not harbour any drug resistance genes (Beloin *et al.*, 2003; Wei *et al.*, 2003), but like all other

IncHI1 plasmids encodes paralogues of several known global transcriptional regulators including H-NS, Dam, Hha, and TlpA. The presence of these genes on IncHI1 plasmids raises the intriguing possibility that horizontal transfer of these regulatory proteins could exert wide-ranging influences on the global gene expression profile of bacteria that receive them.

Interestingly, sequencing studies have identified *hns*-related genes on many other self-transmissible plasmids (Forns *et al.*, 2005; Gilmour and Taylor, 2004; More *et al.*, 1996; Tietze and Tschape, 1994) and within elements such as pathogenicity islands (Mellies *et al.*, 1999; Williamson and Free, 2005) that are thought to have been acquired via horizontal transfer. In light of these data, it was of interest to determine specifically if global gene expression is altered following horizontal transfer of plasmid pSf-R27, both with and without its H-NS-like protein Sfh. It was envisioned that Sfh could possibly influence the transcriptome of transconjugants by either targeting genes in the recipient that are not affected by the chromosomally encoded paralogues, H-NS and StpA, or by forming heteromers with its paralogues, which might have novel regulatory abilities. To test this hypothesis, plasmids pSf-R27Gent^R and pSf-R27Δ*sfh*::Gent^R were introduced into the mouse-virulent *S.* Typhimurium strain SL1344 and the effect of such introduction on the trancriptome of transconjugants elucidated by DNA microarray analysis.

The development of DNA microarrays has transformed gene expression studies by allowing the expression levels of tens of thousands of different genes to be measured simultaneously. DNA microarrays have been used to study gene expression in bacteria (Majtan *et al.*, 2004), yeasts (Beilharz and Preiss, 2004), flies (Gupta and Oliver, 2003), nematodes (Lee *et al.*, 2004), and even higher organisms (Qian *et al.*, 2005; West and van de Rijn, 2006). In the case of bacteria, which have relatively small and fully sequenced genomes, it is possible to analyse the expression of all predicted genes. DNA microarrays consist of either oligonucleotide or PCR products complementary to every gene in a specific genome deposited in an ordered grid onto specially coated microscope slides. The complementary sequences provide hybridization targets for fluorescently labelled nucleic acids representative

of expressed transcripts under a specific condition. Imaging and computational analysis are then used to determine the relative transcript levels of each gene under the specific condition being tested. DNA microarray analysis was employed herein to elucidate the global gene response of *S.* Typhimurium to the horizontal acquisition of plasmids pSf-R27Gent^{R} and pSf-R27Δ*sfh*::Gent^{R}.

5.2 Results

5.2.1 Construction of *S.* Typhimurium strains for microarray analysis

Plasmid pSf-R27Gent^R (pSf-R27 tagged with the *aac* gene of *Streptomyces lividans* conferring gentamycin resistance) and plasmid pSf-R27Δ*sfh*::Gent^R (pSf-R27 harbouring the Δ*sfh*::Gent^R allele) were transferred separately into wild-type *S.* Typhimurium strain SL1344 by conjugation. The newly constructed strains SL1344(pSf-R27Gent^R) and SL1344(pSf-R27Δ*sfh*::Gent^R) were analysed by PCR analyses (Fig. 5.1). The results confirmed the presence of plasmid pSf-R27Gent^R with a functional *sfh* gene in strain SL1344(pSf-R27Gent^R) and the presence of plasmid pSf-R27Δ*sfh*::Gent^R without a functional *sfh* gene in strain SL1344(pSf-R27Δ*sfh*::Gent^R). Importantly, the results also demonstrated the presence of the *spvR* gene in strains SL1344(pSf-R27Gent^R) and SL1344(pSf-R27Δ*sfh*::Gent^R), showing that the *Salmonella* large virulence plasmid (pSLT) is still retained in the transconjugants following the acquisition of plasmid pSf-R27Gent^R or pSf-R27Δ*sfh*::Gent^R.

The introduction of conjugative plasmids into a bacterial cell by horizontal transfer can confer a physiological or energetic cost (Dahlberg and Chao, 2003). In light of this, the growth rate of the transconjugants was measured by cellular density at OD_{600}nm over a 6-h time course (Fig. 5.2). Both strains SL1344(pSf-R27Gent^R) and SL1344(pSf-R27Δ*sfh*::Gent^R) had slightly longer doubling times compared to the parental strain SL1344, with the loss of the *sfh* allele having the more marked effect on growth rate.

The stability of plasmids pSf-R27Gent^R and pSf-R27Δ*sfh*::Gent^R in *S.* Typhimurium was also examined. Strains SL1344(pSf-R27Gent^R) and SL1344(pSf-R27Δ*sfh*::Gent^R) were grown in L-broth without antibiotic selection and bacterial samples taken throughout the growth cycle. Samples were serially diluted and replica-plated onto L-agar plates containing streptomycin (50 μg ml^{-1}) or gentamycin (15 μg ml^{-1}) to determine the total viable count and the number of plasmid-bearing cells, respectively. The results demonstrated that plasmids pSf-R27Gent^R and pSf-R27Δ*sfh*::Gent^R were ~96% and ~94% stable in strain SL1344, respectively.

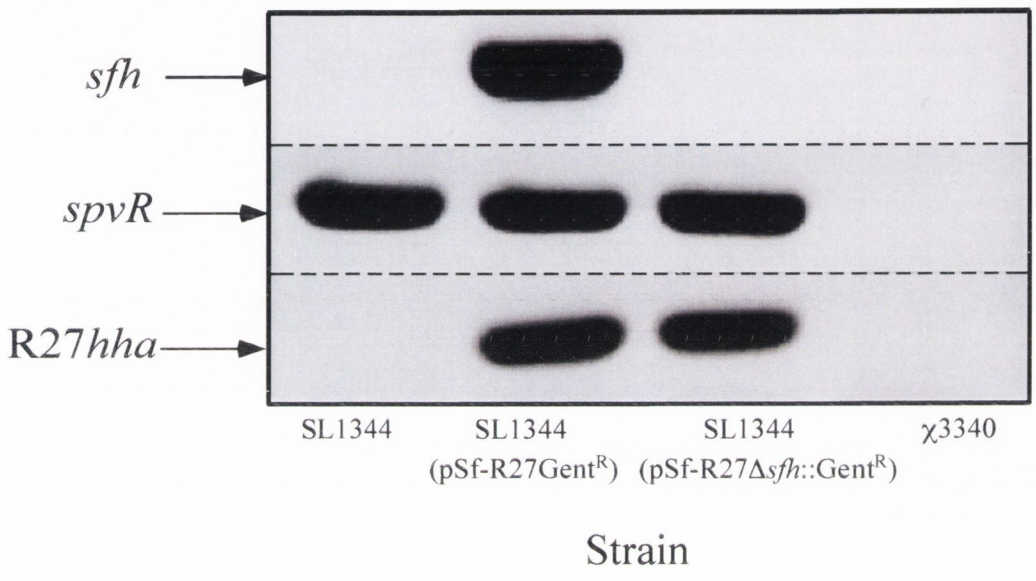

Fig. 5.1 Genetic confirmation of strains SL1344(pSf-R7Gent^R) and SL1344(pSf-R27Δ*sfh*::Gent^R). PCR analysis confirming the presence of plasmids pSf-R27Gent^R and pSf-R27Δ*sfh*::Gent^R in strains SL1344(pSf-R27Gent^R) and SL1344(pSf-R27Δ*sfh*::Gent^R), respectively. Genomic DNA from strains SL1344 (wild-type), SL1344(pSf-R27Gent^R) (*sfh*$^+$), SL1344(pSf-R27Δ*sfh*::Gent^R) (*sfh* mutant), and χ3340 (cured of pSLT) was used to amplify genes known to be present on the large virulence plasmid pSLT (*spvR*) or the plasmid pSf-R27 (*sfh* and R27*hha*).

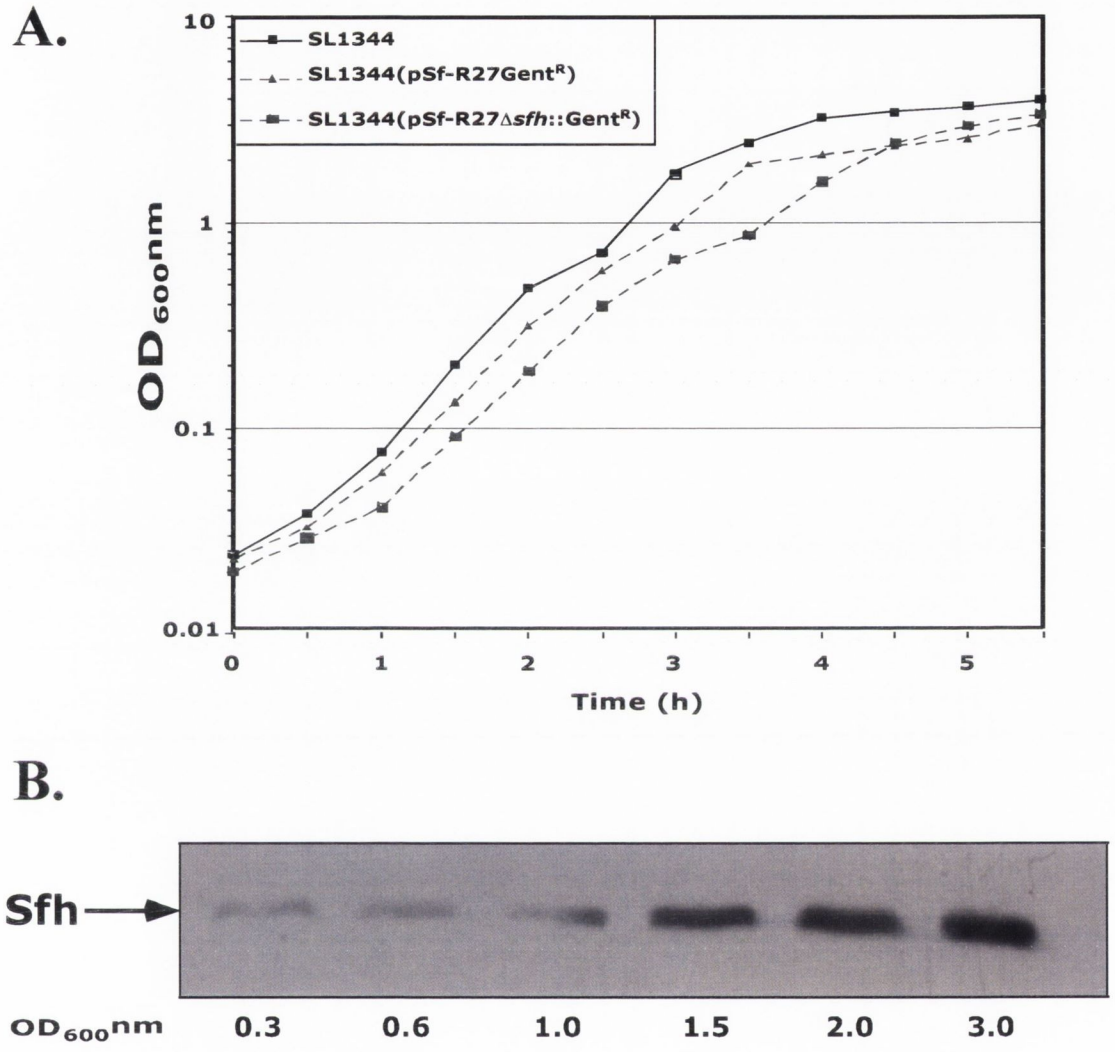

Fig. 5.2. Expression of protein Sfh in *S.* Typhimurium as a function of growth.

(A) The optical densities at 600 nm of L-broth cultures, grown at 37°C, of wild-type strain SL1344, SL1344(pSf-R27Gent^R), and SL1344(pSf-R27Δ*sfh*::Gent^R) were plotted against time. (B) Western blot analysis of Sfh protein levels in strain SL1344(pSf-R27Gent^R) grown in L- broth at 37°C. Total protein samples were harvested at fixed OD_{600}nm values throughout the growth curve as indicated.

To establish the optimum points on the growth curve for transcriptional profiling, the expression profile of Sfh in *S.* Typhimurium was determined by quantitative Western blotting. Strain SL1344 harbouring plasmid pSf-R27Gent^R was grown in L-broth and total protein samples isolated at fixed OD_{600}nm values throughout the growth curve (Fig. 5.2). The expression pattern of Sfh was similar to that previously observed in *Shigella* and *E. coli* (Chapter 3), with Sfh virtually undetectable in exponential phase and with a dramatic induction in protein levels as the culture entered stationary phase (Fig. 5.2). Based on the results obtained from Western blot analysis, two fixed OD_{600}nm values were chosen at which to isolate RNA for transcriptional profiling. Fixed OD_{600}nm values rather than fixed time points were chosen, as the three strains to be used in DNA microarray studies had different growth rates (Fig. 5.2). Thus using fixed OD_{600}nm values ensured that all cells would be at the same stage of the growth cycle for transcriptional profiling. The OD_{600}nm values chosen were 0.6 and 2.0, which represent when Sfh protein levels are minimal and maximal in the cell, respectively (Fig. 5.2).

5.2.2 DNA microarray analysis and data handling

The *S.* Typhi strain CT18 whole genome array used in this study was provided by J. Wain (Wellcome Trust Sanger Institute, Cambridge, U.K.) and is based on that outlined by Thomson *et al.* (2004). The array comprised specific unique PCR products of 4,097 annotated coding sequences from the chromosome and plasmids of *S.* Typhi strain CT18. Also included on the array were 345 PCR products corresponding to all the strain LT-2 specific (relative to strain CT18) loci, plus 2 PCR products representing the plasmid R27-specific genes (relative to plasmid pHCM1). All microarray studies were carried out in the Pathogen Microarray Laboratory at the Wellcome Trust Sanger Institute in Cambridge, England.

Overnight cultures of strain SL1344 and its plasmid-bearing derivatives SL1344(pSf-R27Gent^R) and SL1344(pSf-R27Δ*sfh*::Gent^R) were subcultured into 200 ml L-broth medium

in 2-litre flasks and grown at 37°C without antibiotic selection. Total RNA was extracted from cultures of each strain at OD_{600}nm values equivalent to the mid-exponential (OD_{600}nm ~0.6) and stationary phases (OD_{600}nm ~2.0) of growth. The RNA was then fluorescently labelled during reverse transcription into cDNA and used as template for DNA microarray analysis. Total RNA extracts were isolated from bacterial cultures grown on three independent occasions and thus three biological replicates were performed in the DNA microarray studies. The cDNA samples were hybridized to microarrays in quadruplicate and dye-swap experiments performed for all hybridizations (to correct for any bias in dye incorporation). In each case strain SL1344(pSf-R27Gent^R) cDNA was used as the reference sample.

The transcriptomes of strains harbouring plasmids pSf-R27Gent^R and pSf-R27Δ*sfh*::Gent^R were compared with each other and with that of the parental strain SL1344. Statistically significant microarray data were obtained by filtering with a false discovery rate (FDR) ≤0.05% using the GeneSpring 7.0 software program. Only genes whose expression ratio showed at least a 2-fold difference (FDR ≤0.05%) were regarded as showing a significant response to the presence or absence of plasmids pSf-R27Gent^R and pSf-R27Δ*sfh*::Gent^R. Microsoft Excel files containing all these data are presented as supplementary data on a CD-ROM at the back of this thesis. Genes are listed alphabetically with their expression ratio for each growth phase shown. The expression ratio is a numerical value representing the fold increase or decrease in expression of a specific gene between the test and reference strain being compared. It is calculated by dividing the average expression value for a gene in the test strain by the average expression value for the same gene in the reference strain. Consequently, genes with an expression ratio less than 1.0 were deemed to be activated by Sfh and those with a ratio above 1.0 were repressed by Sfh. Likewise, genes activated by the introduction of plasmid pSf-R27Gent^R into strain SL1344 had an expression ratio below 1.0 and those repressed by the plasmid had a ratio greater than 1.0.

5.2.3 Effect of plasmid pSf-R27Gent^R on the *S.* Typhimurium transcriptome

It was anticipated that the horizontal transfer of plasmid pSf-R27Gent^R into the wild-type *S.* Typhimurium strain SL1344 would result in widespread changes in the global transcriptional profile of this strain. Surprisingly, when the gene expression profile of strain SL1344(pSf-R27Gent^R) was compared with that of the parental strain SL1344, it was evident that the introduction of plasmid pSf-R27Gent^R affected the transcription of only a limited number of *S.* Typhimurium genes (Fig. 5.3). Of the genes which passed the statistical filter set with a FDR $\leq$0.05%, only 68 were differentially expressed 2-fold or more and 28 of these coded for genes of unknown function (Fig. 5.3 and supplementary data). In exponential phase, a restricted group of 51 genes showed $\geq$2-fold changes in expression. The majority of these genes (42) were repressed by the introduction of plasmid pSf-R27Gent^R with only 9 genes being activated (Fig. 5.3). In the stationary phase of growth, a total of 44 genes were differentially expressed; 28 were repressed and 16 upregulated in the presence of plasmid pSf-R27Gent^R (Fig. 5.3).

An overview of the genes affected by plasmid pSf-R27Gent^R was obtained by defining functional categories of the statistically significant genes based on the Kyoto Encyclopedia of Genes and Genomics (KEGG; www.genome.ad.jp/kegg/kegg2.html). From this analysis it was evident that only a small subset of the defined functional categories were notably affected by the introduction of plasmid pSf-R27Gent^R (Fig. 5.4). The results revealed that the genes displaying the greatest response to plasmid pSf-R27Gent^R were those coding for factors involved in chromosome replication and in the expression of ribosome components. In exponential phase nearly half of the genes showing more than a 50% reduction in transcription due to the presence of plasmid pSf-R27Gent^R encoded 30S and 50S ribosomal subunit proteins (Supplementary data). In addition, transcription of the gene coding for the elongation factor G (*fusA*) was downregulated, suggesting perhaps a reduction in translation capacity of strain SL1344(pSf-R27Gent^R) (Supplementary data). These data are consistent with the slightly slower growth rate observed in the plasmid pSf-R27Gent^{R+} strain compared to wild-type strain SL1344 (Fig. 5.2).

Other groups of genes affected by the presence of plasmid pSf-R27Gent^R are those involved in adaptation to stress and also several genes encoding components of the cell membrane, such as flagella and fimbriae. The gene coding for the phase 1 flagellin (*fliC*) was strongly upregulated in response to plasmid pSf-R27Gent^R irrespective of growth phase. In contrast, transcription of the fimbrial genes *fimY* and *stcA* was elevated in exponential phase, but repressed more than 2-fold in the stationary phase of growth (Supplementary data). These data indicate that fimbrial expression in strain SL1344(pSf-R27Gent^R) could be growth phase-dependent.

Interestingly, only two *Salmonella* virulence genes were significantly affected by the introduction of plasmid pSf-R27Gent^R. Both the SPI-2 gene *ssrA* (encodes the histidine kinase of the SsrA/B two-component regulatory system) and the SPI-5 gene *sigD/sopB* (encodes an effector protein secreted by SPI-1 TTSS) were repressed over 2-fold in the stationary phase of growth (Supplementary data). The introduction of plasmid pSf-R27Gent^R into strain SL1344 did not appear to significantly alter the transcription of other known virulence factors, at least under the growth conditions used in this microarray study.

5.2.4 Effect of plasmid pSf-R27Δ*sfh*::Gent^R on the *S.* Typhimurium transcriptome

The effect of deleting the *sfh* gene from plasmid pSf-R27 was elucidated by comparing the gene expression profile of strain SL1344(pSf-R27Δ*sfh*::Gent^R) to that of strain SL1344(pSf-R27Gent^R) and strain SL1344. In stark contrast to the data obtained for plasmid pSf-R27Gent^R, the introduction of plasmid pSf-R27Δ*sfh*::Gent^R into strain SL1344 resulted in altered expression of a wide range of genes (Fig. 5.5). The microarray study revealed 430 genes that were differentially expressed 2-fold or more (FDR ≤0.05%) in the *sfh* mutant (Supplementary data). Analysis of the exponential phase data showed that transcription of 353 genes was altered at least 2-fold and nearly 90% of these were chromosomal, with the majority (245) being upregulated in the absence of Sfh (Fig. 5.5 and supplementary data). In stationary phase, a total of 171 genes displayed ≥2-fold changes in transcription, with 130

Fig. 5.3. Impact of plasmid pSf-R27Gent^R on the transcriptome of strain SL1344. Statistically filtered microarray data (FDR ≤0.05%) from strain SL1344 *vs* strain SL1344(pSf-R27Gent^R) are presented in scatter plots for the exponential and stationary phases of growth. Each gene is represented as a spot, which is coloured according to its expression ratio. Red indicates an increase in expression, yellow indicates no change, and blue indicates a decrease in expression as shown in the scale bar on the right. Spots above and below the lines represent genes whose expression was up- and down-regulated ≤2-fold, respectively, in strain SL1344 compared to SL1344(pSf-R27Gent^R). Spots between the lines represent genes whose expression was not significantly altered by the introduction of plasmid pSf-R27Gent^R.

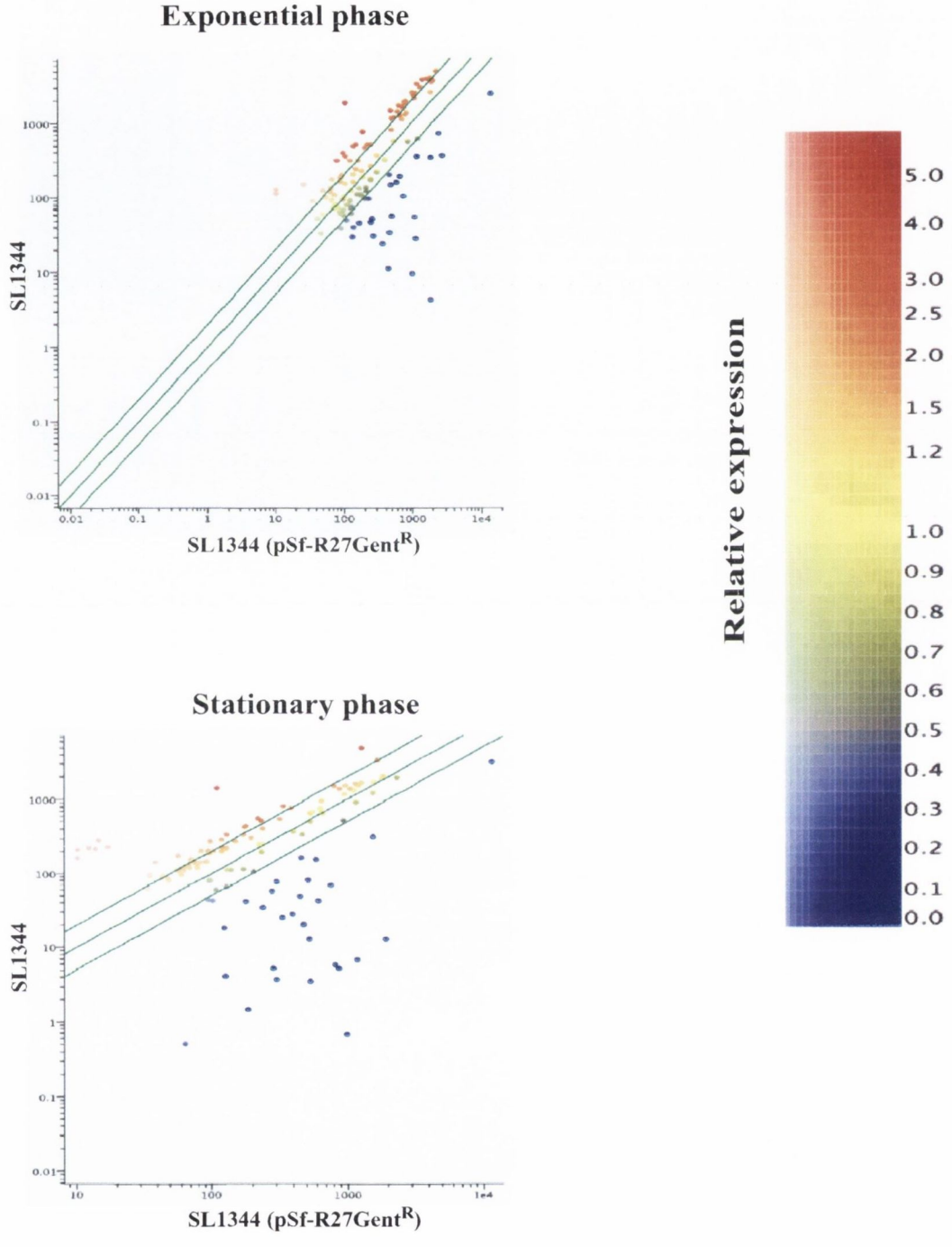
Exponential phase
SL1344
SL1344 (pSf-R27Gent^R)
Stationary phase
SL1344
SL1344 (pSf-R27Gent^R)
Relative expression
5.0
4.0
3.0
2.5
2.0
1.5
1.2
1.0
0.9
0.8
0.7
0.6
0.5
0.4
0.3
0.2
0.1
0.0

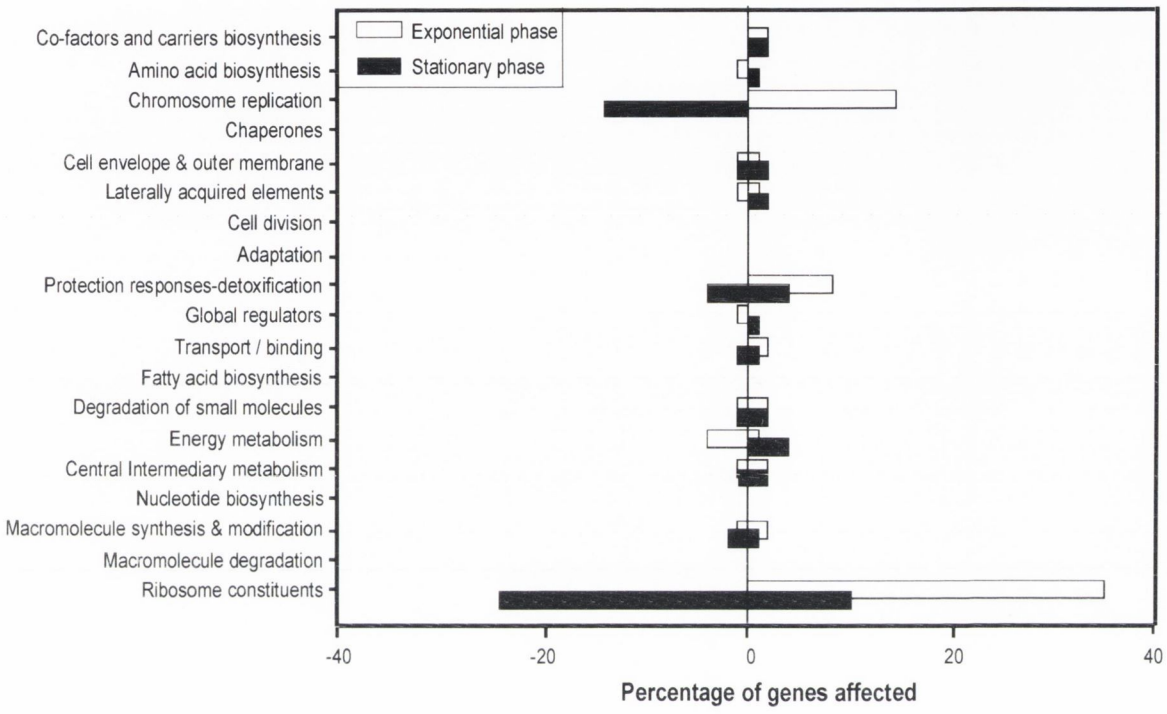

Fig. 5.4. Functional categories of genes affected by plasmid pSf-R27Gent^R.

Genes affected by plasmid pSf-R27Gent^R were grouped into functional categories based on the Kyoto Encyclopedia of Genes and Genomics (KEGG). The histograms represent the percentage of genes affected by the introduction of plasmid pSf-R27Gent^R into *S.* Typhimurium strain SL1344 in exponential (white bars) and stationary phases (black bars) of growth, with each functional category listed on the left.

Fig. 5.5. Impact of plasmid pSf-R27Δ*sfh*::Gent^R on the transcriptome of strain SL1344. Statistically filtered microarray data (FDR ≤0.05%) from strain SL1344(pSf-R27Gent^R) *vs* strain SL1344(pSf-R27Δ*sfh*::Gent^R) are presented in scatter plots for the exponential and stationary phases of growth. Each gene is represented as a spot, which is coloured according to its expression ratio. Red indicates an increase in expression, yellow indicates no change, and blue indicates a decrease in expression as shown in the scale bar on the right. Spots above and below the lines represent genes whose expression was up- and down-regulated ≤2-fold, respectively, in the absence of Sfh. Spots between the lines represent genes whose expression was not significantly altered by the *sfh* mutation.

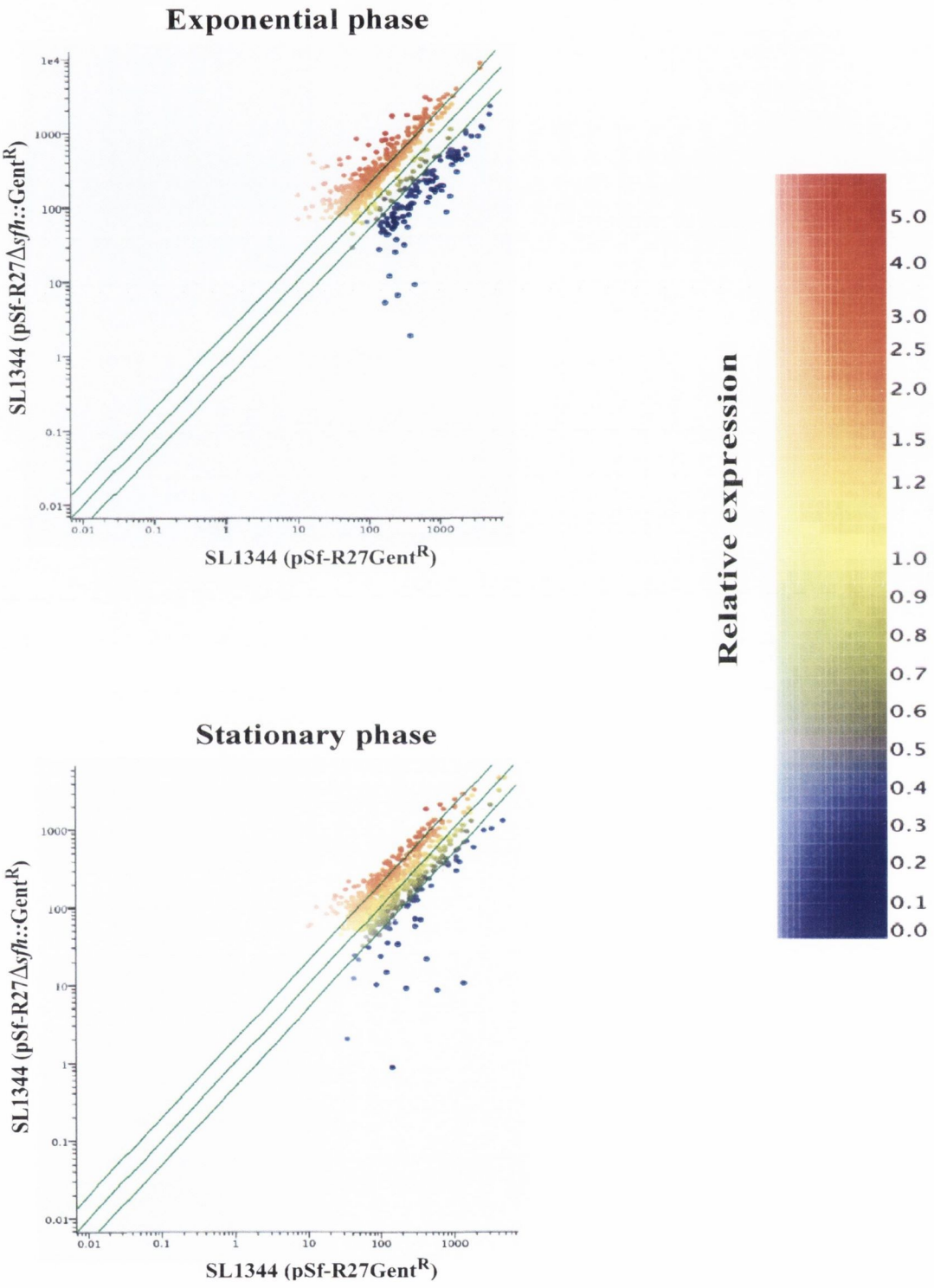
Exponential phase
SL1344 (pSf-R27Δsfh::Gent^R)
SL1344 (pSf-R27Gent^R)
Stationary phase
SL1344 (pSf-R27Δsfh::Gent^R)
SL1344 (pSf-R27Gent^R)
Relative expression
5.0
4.0
3.0
2.5
2.0
1.5
1.2
1.0
0.9
0.8
0.7
0.6
0.5
0.4
0.3
0.2
0.1
0.0

showing increases in expression and 41 displaying decreases (Fig. 5.5). Consistent with the exponential phase data, the majority of genes affected in stationary phase were chromosomal (Supplementary data). Surprisingly, very few pSf-R27 genes were affected by the absence of Sfh. Most of the genes displaying altered expression were involved in the replication, partition, and stability of plasmid pSf-R27, suggesting a role for Sfh in the maintenance of the plasmid in the cell (Table 5.1). Previous work in this study (Chapter 4) revealed that Sfh modulates conjugative transfer of plasmid pSf-R27 by repressing transcription of the *tra* genes. Consistent with these data, transcription of some *tra* genes was activated over 2-fold in strain SL1344(pSf-R27Δ*sfh*::Gent^R). Moreover, transcription of the *dam* paralogue encoded by plasmid pSf-R27 was also activated in the *sfh* mutant, confirming previous results (Chapter 4) that Sfh is involved in its regulatory circuit (Table 5.1). Importantly, these data clearly demonstrate Sfh can influence gene expression both on and beyond the R27-like plasmid that encodes it.

An overview of the statistically significant genes affected by the *sfh* mutation was obtained by defining functional categories of the genes based on the Kyoto Encyclopedia of Genes and Genomics (KEGG; www.genome.ad.jp/kegg/kegg2.html). The analysis clearly illustrates that the introduction of plasmid pSf-R27Δ*sfh*::Gent^R compared to plasmid pSf-R27Gent^R not only affects a greater number of genes, but that these genes also represent a much wider range of functional categories (Fig. 5.6). From the data, functional categories with a high proportion of Sfh-dependent genes were identified. Genes involved in adaptation to stress, such as the SOS response, in metabolism, in motility, or in virulence were most prominent. Examples from these categories were selected for further analysis.

5.2.5 Motility gene expression

The synthesis and function of the *Salmonella* flagellar system requires the expression of more than 50 genes, which are divided among at least 17 operons on the *Salmonella* chromosome (Fig. 1.8). DNA microarray analysis revealed that plasmid pSf-R27Δ*sfh*::Gent^R negatively

influenced the expression of several flagellar genes (*flgH, flgN, flgM*) in exponential phase (Supplementary data). These genes all map to Region 1 of the flagellar regulon, which consists of two divergently transcribed operons located at 26 centisomes on the *Salmonella* chromosome (Macnab, 1996). Importantly, located within one of these operons is the gene coding for the anti-sigma factor FlgM, which is one of the key regulators of flagellar biogenesis (Fig. 5.7). Expression of the remaining flagellar operons did not alter significantly (more than 2-fold) following the introduction of plasmid pSf-R27Δ*sfh*::Gent^R with the exception of the *fliB* operon, which was upregulated in the absence of Sfh (Supplementary data). To determine if Sfh is a positive regulator of Region 1 flagellar genes, RT-PCR analyses was performed on several genes located within this region of the flagellar regulon. Total RNA was extracted from bacterial cultures of strain SL1344(pSf-R27Gent^R) and strain SL1344(pSf-R27Δ*sfh*::Gent^R) and used as template for RT-PCR. Expression of the *fliF* gene was not affected by any extent by the presence or absence of Sfh in the DNA microarray experiment, thus allowing it to be used as a negative control in these experiments. Consistent with the DNA microarray data, analysis of the RT-PCR results showed that flagellar gene expression was repressed in strain SL1344(pSf-R27Δ*sfh*::Gent^R) compared to strain SL1344 harbouring plasmid pSf-R27Gent^R (Fig. 5.7).

To examine in further detail the role of Sfh in the *Salmonella* flagellar regulon, the possibility that Sfh could directly bind to and affect transcription of Region 1 flagellar genes was assessed. H-NS-like proteins do not have a consensus DNA-binding sequence, but instead preferentially bind to intrinsically curved DNA (Bracco *et al.*, 1989; Owen-Hughes *et al.*, 1992; Yamada *et al.*, 1990). Therefore, the intrinsic curvature of the divergently transcribed *flgA* and *flgB* flagellar operons was analysed *in silico* using the BEND-IT computer program (http://www.icgeb.org/dna/bend_it.html). The curvature propensity plot revealed that the regulatory region between the two operons possesses a large area of DNA curvature, supporting the theory Sfh could directly bind to and affect flagellar gene transcription (Fig. 5.8).

Table 5.1. pSf-R27 genes affected by the *sfh* mutation

Gene	Function	pSf-R27Δ*sfh*::Gent^R/pSf-R27Gent^R expression ratio[a]	
		Exponential phase	Stationary phase
m paralogue	Putative DNA modification methylase	2.28	ND
CM1.134c	Putative recombinase	2.88	2.74
CM1.193c	Hypothetical protein	0.39	2.35
CM1.195	Hypothetical protein	0.02	0.04
CM1.250c	Putative periplasmic protein	0.19	0.53
CM1.50	Replication initiation protein	2.01	ND
CM1.97	Putative periplasmic protein	2.18	ND
rB	Putative plasmid partition protein	0.34	ND
rM	Putative plasmid stability/ partition protein	0.34	ND
rR	Hypothetical protein	0.26	ND
n	Transcriptional regulator	0.01	0.02
G	Conjugation coupling protein	ND	8.07
l	Putative conjugative DNA helicase	2.24	1.41

[a]ND = No data

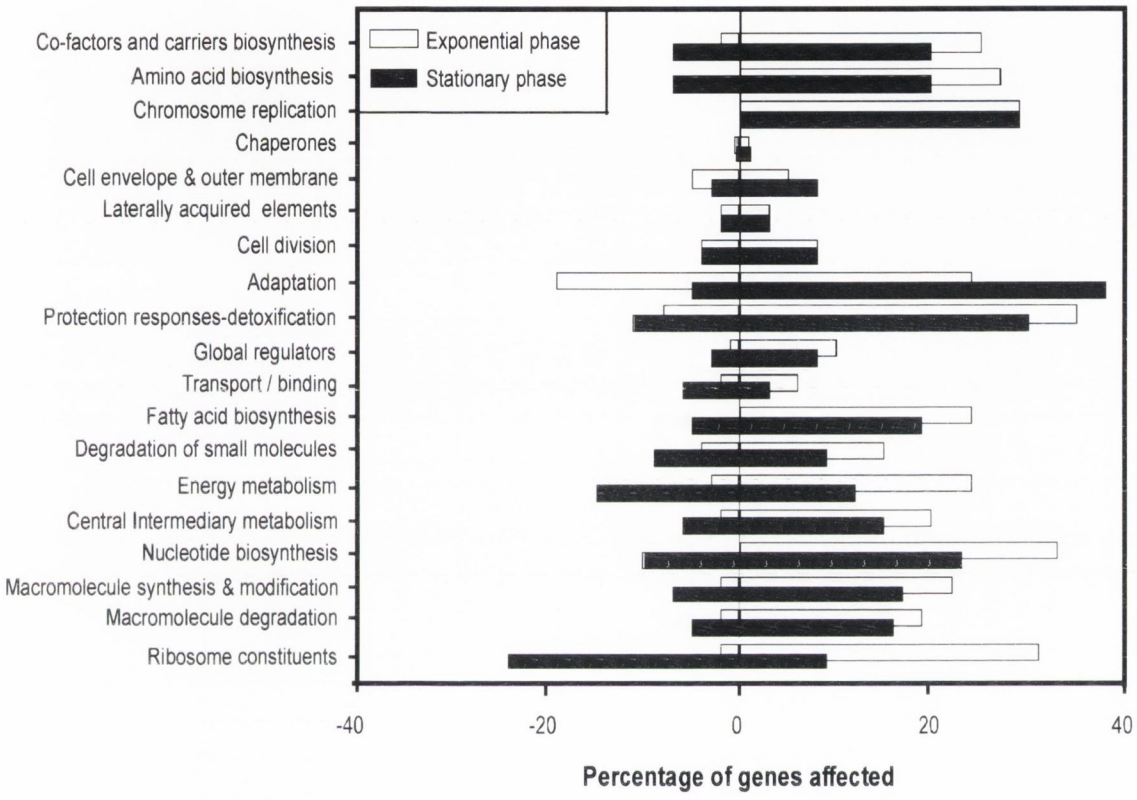

Fig. 5.6. Functional categories of genes affected by plasmid pSf-R27Δ*sfh*::Gent^R.

Genes affected by plasmid pSf-R27Δ*sfh*::Gent^R were grouped into functional categories based on the Kyoto Encyclopedia of Genes and Genomics (KEGG). The histograms represent the percentage of genes affected by the introduction of plasmid pSf-R27Δ*sfh*::Gent^R in exponential (white bars) and stationary phases (black bars) of growth, with each functional category listed on the left.

Fig. 5.7. The effect of deleting the *sfh* gene on flagellar gene expression.

(A) Schematic map of genes belonging to Region 1 of the *Salmonella* flagellar regulon, which includes the *flgM* gene coding for the anti-sigma factor FlgM. Arrows indicate the positions of the various promoters. (B) RT-PCR analyses of flagellar gene transcription in strain SL1344 harbouring pSf-R27Gent^R or pSf-R27Δ*sfh*::Gent^R. Total RNA was extracted from cultures grown to log phase (OD_{600}~0.6) in L-broth at 37°C, DNase treated, and used as template for RT-PCR. To control for loading, RT-PCR analyses of *fliF* transcription was performed, as *fliF* gene expression does not alter to any marked extent in the presence and absence of Sfh. Densitometric analyses of the RT-PCR data are shown on the right for comparison. The transcript levels are expressed relative to each gene's transcript level in strain SL1344 (pSf-R27Gent^R), the value of which was taken as 1. The data shown are averages of at least three independent experiments and representative gels are shown.

A.

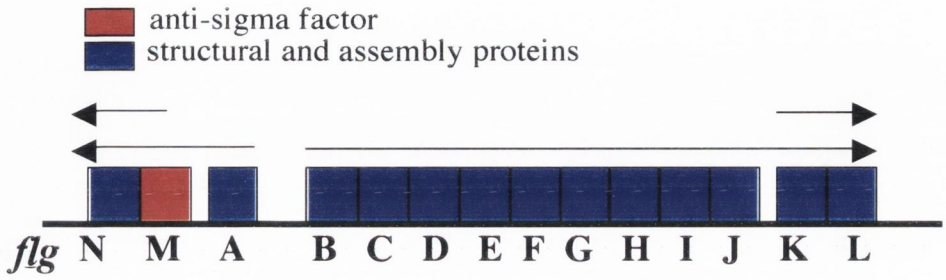
anti-sigma factor
structural and assembly proteins
flg N M A B C D E F G H I J K L

B.

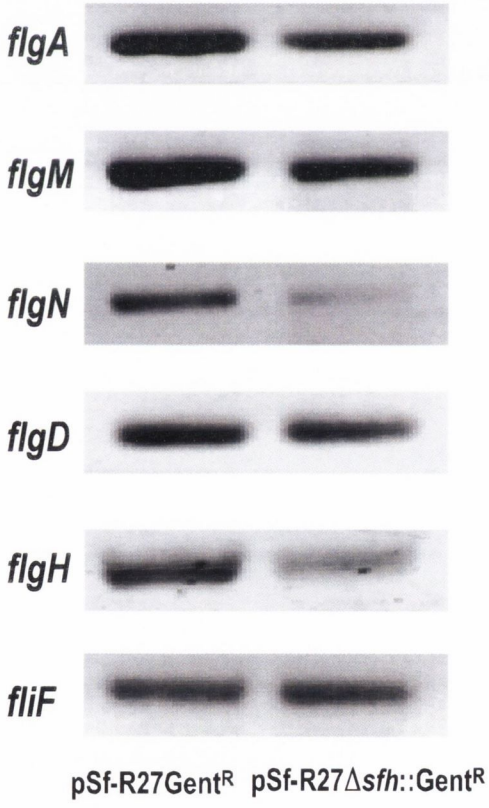
flgA
flgM
flgN
flgD
flgH
fliF
pSf-R27GentR pSf-R27Δsfh::GentR

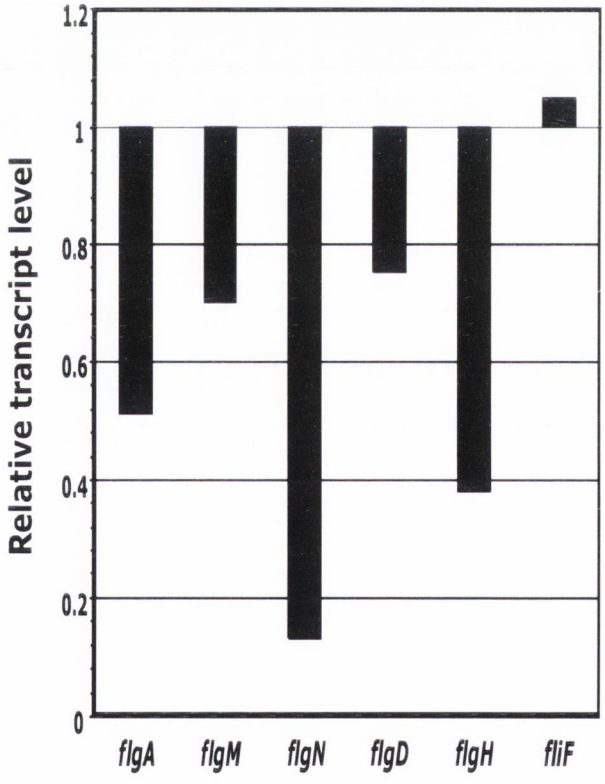
Relative transcript level
1.2
1
0.8
0.6
0.4
0.2
0
flgA flgM flgN flgD flgH fliF

Fig. 5.8. Direct interaction of Sfh and H-NS with the *flgA–flgB* promoter region. (A) DNA curvature analysis of the *flgA–flgB* promoter region. Graph shows the predicted intrinsic curvature of the *flgA–flgB* intergenic regulatory region using the computer program BEND-IT. Curvature is expressed as degrees per helical turn and plotted against the position on the promoter sequence, with +1 corresponding to the *flgA* translation initiation codon. Curved and straight motifs have a value above or below 5 degrees per helical turn, respectively. Regions of intrinsic DNA curvature between the *flgA* and *flgB* genes are arrowed. (B) Competitive gel retardation assay showing the specific binding of Sfh and H-NS to the *flgA–flgB* promoter region. The plasmid pBR322 was digested with restriction endonucleases *Taq*1 and *Ssp*I, and the resulting DNA fragments mixed with a 476-bp PCR amplimer of the *flgA–flgB* promoter region used in the DNA curvature analysis. The DNA mixtures were incubated with equimolar concentrations of Sfh and H-NS in the range 0 μM to 2 μM. An arrow and an asterisk indicate the position of the *flgA–flgB* and *bla* promoter fragments, respectively. The curved *bla* promoter is a positive control known to bind H-NS-like proteins. The positions of the 600-bp and 400-bp molecular size markers are also indicated.

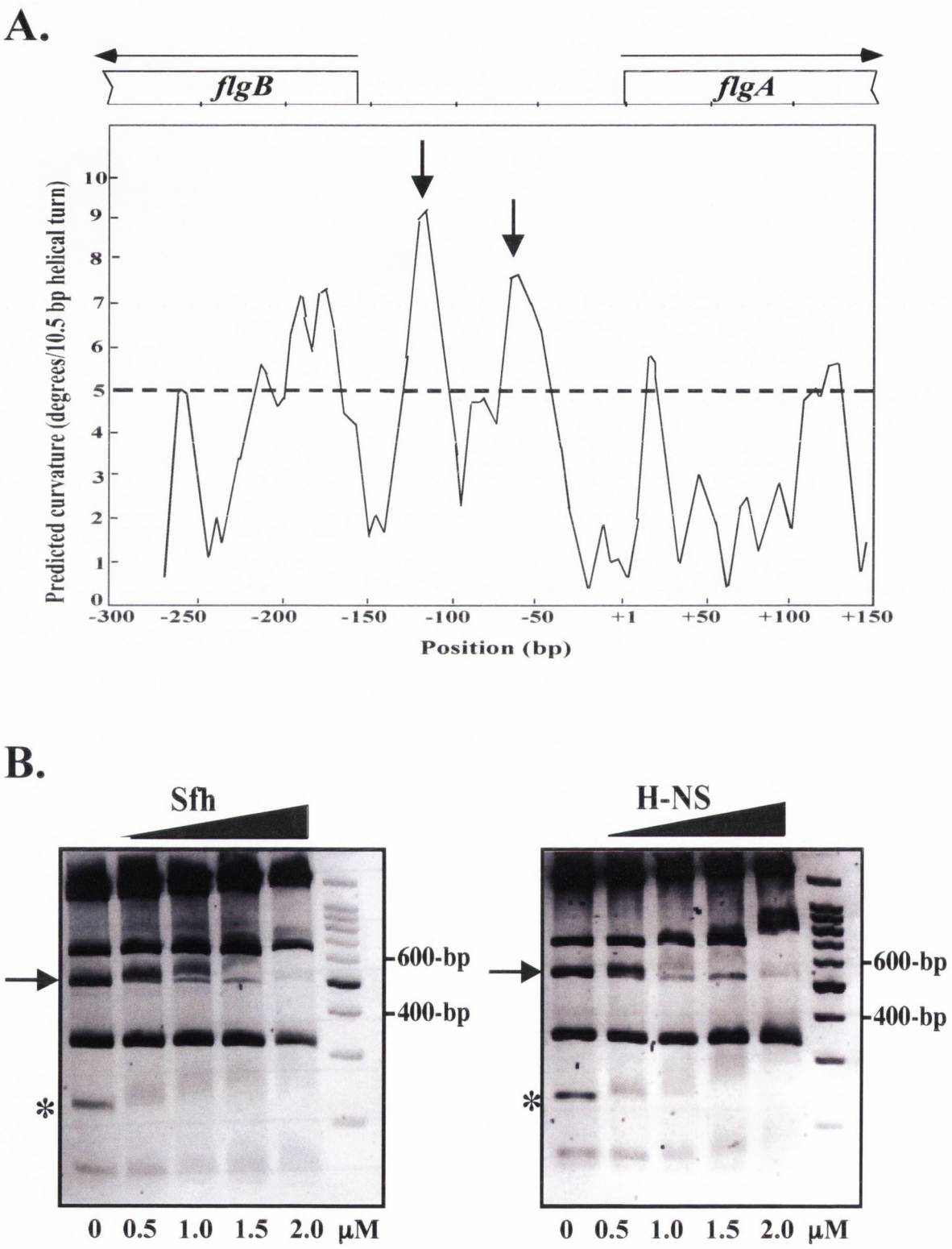
A.
flgB
flgA
Predicted curvature (degrees/10.5 bp helical turn)
0
1
2
3
4
5
6
7
8
9
10
-300
-250
-200
-150
-100
-50
+1
+50
+100
+150
Position (bp)
B.
Sfh
H-NS
600-bp
400-bp
600-bp
400-bp
*
*
0 0.5 1.0 1.5 2.0 μM
0 0.5 1.0 1.5 2.0 μM

To assess this possibility, the interaction of purified Sfh with the *flgA–flgB* promoter region was examined using a competitive gel retardation assay. A 476-bp DNA fragment encompassing the *flgA–flgB* regulatory promoter region (nt –325 to +151 with respect to the translation initiation codon of the *flgA* gene) was amplified by PCR using the primer pairs flgA-RBS and flgB-FBS (Table 2.3). The *flgA–flgB* promoter amplimer was then added to *Taq*1-*Ssp*I-digested pBR322 DNA, which acts as competitor DNA in the EMSA. One of the pBR322 DNA restriction fragments contains the intrinsically curved promoter region of the *bla* gene, which is known to bind H-NS-like proteins. The DNA mixture was then incubated with increasing concentrations of purified Sfh, and resolved by electrophoresis through 3% molecular screening agarose. The electrophoretic mobility of the *flgA–flgB* promoter fragment was reduced specifically by Sfh in a concentration-dependent manner (Fig. 5.6). Sfh also shifted the mobility of the *bla* positive control band. In a parallel experiment, both the *flgA* promoter region and the *bla* control band were shifted specifically by equimolar amounts of the Sfh paralogous protein H-NS (Fig. 5.8).

The above results indicated that the presence or absence of Sfh might alter the motility of *S.* Typhimurium. To test this hypothesis, the effect of the *sfh* mutation on the motility phenotype was established by an agar plate motility test. Equal numbers of bacteria were used to inoculate the centres of semi-solid agar plates and incubated for 8 h at 37°C. The results showed that strain SL1344(pSf-R27Δ*sfh*::Gent^R) was markedly less motile than either strain SL1344 or strain SL1344(pSf-R27Gent^R) (Fig. 5.9). Moreover, full motility was restored when the *sfh* mutation was complemented *in trans* using the multicopy plasmid pYCsfh, which harbours a functional copy of the *sfh* gene (Fig 5.9). This negative effect on motility was reminiscent of the phenotypes of *hns* mutants (Hinton *et al.*, 1992). Consequently, the effect of a *hns* mutation on the motility phenotype was also investigated. In agreement with previous studies, the *hns* mutant was non-motile on semi-solid agar plates but when Sfh was expressed *in trans* using plasmid pYCsfh full motility was restored (Fig. 5.9). Taken in aggregate, these results demonstrate a role for Sfh in the *Salmonella* flagellar regulatory network.

S. Typhimurium possesses two genes (*fliC* and *fljB*) that code for immunologically distinct flagellins (Macnab, 1996). Expression of these genes is subject to phase variation mediated by a DNA inversion switch (Bonifield and Hughes, 2003; Macnab, 1996). Therefore, at any given time only one flagellin protein is expressed on the cell surface. As stated earlier, the introduction of plasmid pSf-R27Gent^R increased transcription of the *fliC* flagellin gene in strain SL1344. To ensure that expression of FliC phase I flagellin protein is genuinely upregulated in strain SL1344(pSf-R27Gent^R), FliC protein levels were determined by SDS-PAGE analysis and Western immunoblotting. Total protein was harvested from bacterial cultures of strain SL1344 and its plasmid-containing derivatives SL1344(pSf-R27Gent^R) and SL1344(pSf-R27Δ*sfh*::Gent^R) grown at 37°C in L-broth. Protein was also extracted from *S.* Typhimurium strains locked On (TH6233) and locked Off (TH6232) for flagellar phase variation, and used as negative and positive controls for FliC expression, respectively. Total protein concentrations were determined by the Bradford assay. Equal amounts of lysate protein were separated by SDS-PAGE and then visualized with Coomassie brilliant blue stain or analyzed by Western blotting using anti-FliC antiserum.

The results demonstrated a dramatic increase in FliC protein levels in the plasmid-containing strains compared to the parental strain SL1344 (Fig. 5.10). The elimination of the *sfh* gene from plasmid pSf-R27 did not alter FliC protein levels. These findings are fully consistent with the results obtained from the DNA microarray analysis (Supplementary data). Interestingly, the anti-FliC antibody cross-reacted with the phase II flagellin protein FljB and revealed that FljB was only detectable in the wild-type strain SL1344 (Fig. 5.10). These results suggest that the increased FliC expression observed in strains SL1344(pSf-R27Gent^R) and SL1344(pSf-R27Δ*sfh*::Gent^R) is due to a lack of phase variation in these strains. Since FliC and FljB levels in strains SL1344(pSf-R27Gent^R) and SL1344(pSf-R27Δ*sfh*::Gent^R) are equivalent, it can be deduced that the decrease in expression of the key flagellar genes located in Region 1 is the most likely explanation for the reduced motility displayed by strain SL1344(pSf-R27Δ*sfh*::Gent^R) (Fig. 5.9).

Fig. 5.9. The effect of deleting the *sfh* gene on *Salmonella* motility. (A) The motilities of strains SL1344, SL1344(pSf-R27Gent^R), SL1344(pSf-R27Δ*sfh*::Gent^R) and the complemented mutant, SL1344 (pSf-R27Δ*sfh*::Gent^R, pYC*sfh*$^+$) were measured on motility agar plates. Equal numbers of bacteria were used to inoculate the centres of semi-solid L-agar plates and incubated at 37°C for 8 h. Motility was measured as the rate of formation of bacteria swarm rings on the plate and is expressed as a percentage of the strain SL1344 value below each Petri dish. (B) The effect of an *hns* knockout mutation on the *Salmonella* motility phenotype and the complementation of this lesion by the Sfh-encoding plasmid pYC*sfh*$^+$.

A.

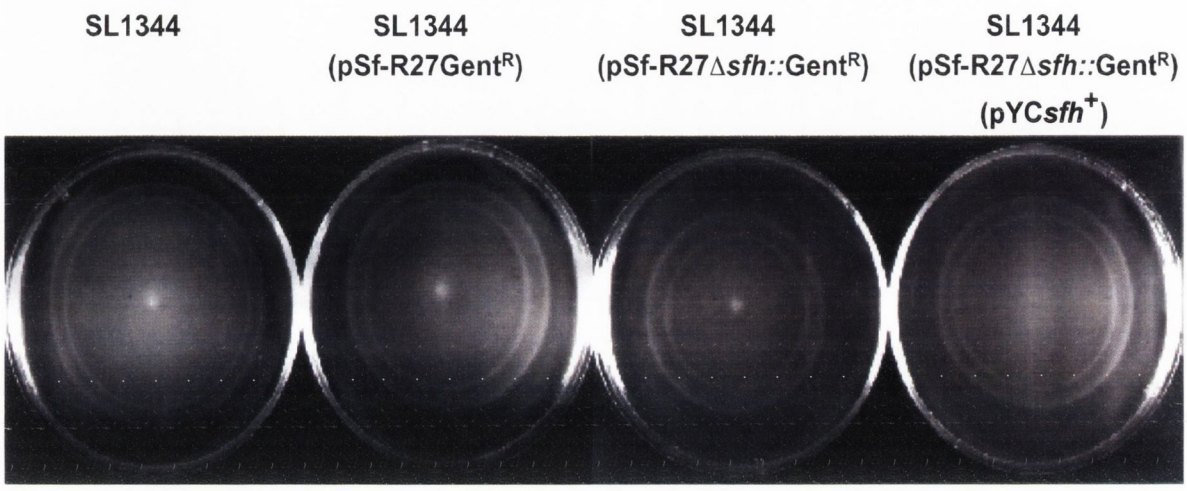
SL1344
SL1344 (pSf-R27Gent^{R})
SL1344 (pSf-R27Δ*sfh::*Gent^{R})
SL1344 (pSf-R27Δ*sfh::*Gent^{R}) (pYC*sfh*$^{+}$)
100%
98%
80%
98%

B.

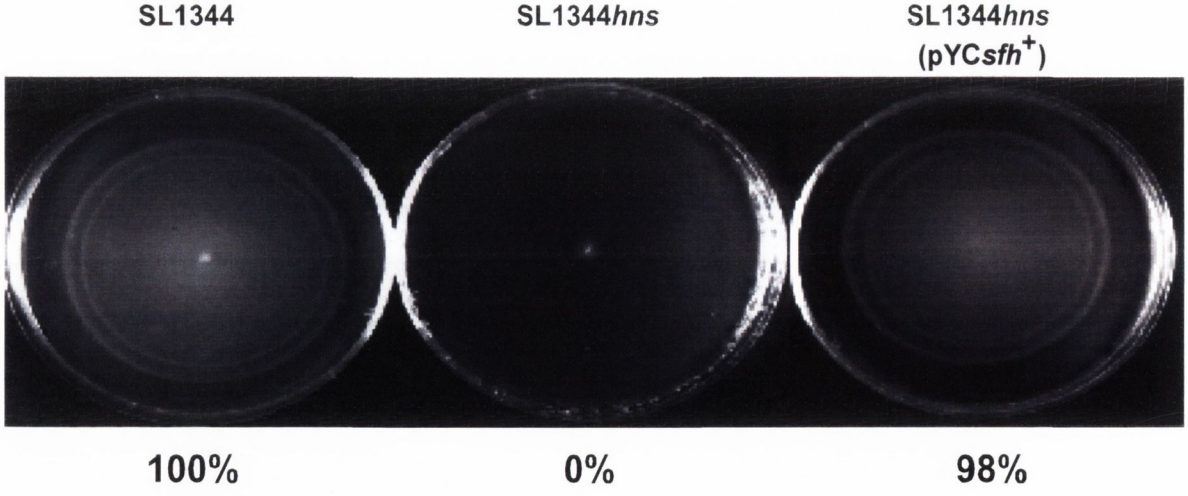
SL1344
SL1344*hns*
SL1344*hns* (pYC*sfh*$^{+}$)
100%
0%
98%

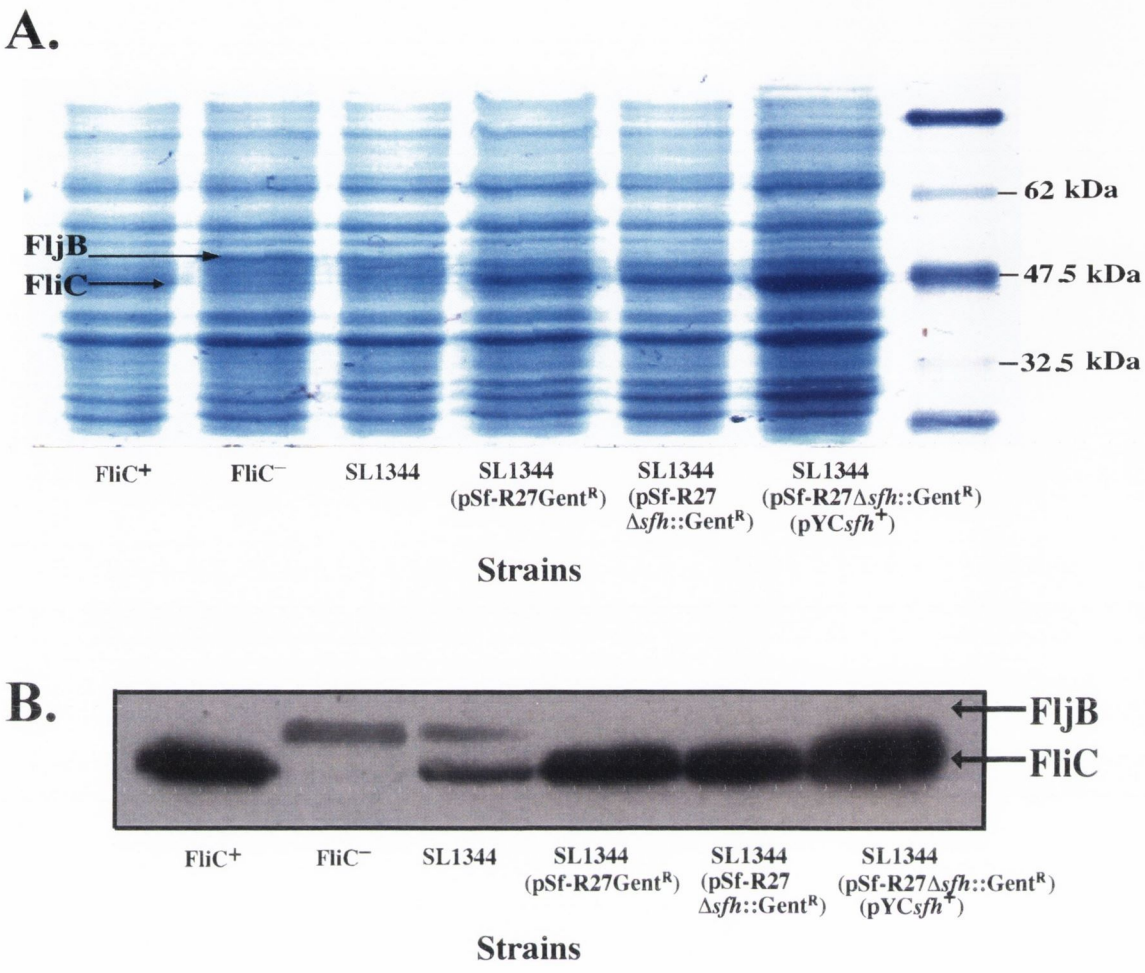

Fig. 5.10. Impact of plasmid pSf-R27Gent^R on flagellin expression. Expression of the phase I flagellin protein FliC was examined by (A) SDS PAGE and (B) Western immunoblotting. Total protein samples were harvested from log phase L-broth cultures of strains SL1344, SL1344(pSf-R27Gent^R), SL1344(pSf-R27Δ*sfh*::Gent^R), and SL1344(pSf-R27Δ*sfh*::Gent^R, pYC*sfh*$^+$) grown at 37°C. Strains TH6233 (locked On, negative control; FliC$^-$) and TH6232 (locked Off, positive control; FliC$^+$) were included for comparison. The experiment was performed on three independent occasions and a representative gel and blot are shown.

5.2.6 Global regulators

S. Typhimurium is capable of adapting to diverse environmental conditions and stresses and, therefore, has evolved sophisticated regulatory networks that can respond quickly and efficiently to changes in growth conditions. Expression of these various regulatory pathways is tightly controlled by an array of transcriptional regulators. The microarray data showed that several known transcriptional regulators, including the two nucleoid-associated proteins HU and Dps, were responsive to the introduction of plasmid pSf-R27Δ*sfh*::Gent^R. Expression of the *dps* gene and the *hupA* and *hupB* genes, which encode Dps and the subunits of the heteromeric HU protein, respectively, were repressed in the absence of Sfh (Supplementary data). Both nucleoid-associated proteins are involved in cellular adaptation to stress. HU contributes to the osmotic stress response of the cell (Manna and Gowrishankar, 1994), while Dps protects the cell from an array of harmful conditions, such as oxidative and thermal stress, acid and alkali shock, gamma and ultraviolet radiation and heavy metal toxicity (Wolf *et al.*, 1999). Several other key regulators that displayed altered expression following the introduction of plasmid pSf-R27Δ*sfh*::Gent^R are also involved in stress-response regulatory circuits. These include NhaR (Na^+/H^+ antiporter regulator), MelR (melibiose operon regulator), LexA (SOS response regulator), and SoxS (activator of the superoxide regulon) (Supplementary data).

5.2.7 DNA damage response

Horizontal transfer of mobile genetic elements such as conjugative plasmids is known to trigger a strong SOS response in the recipient bacterium, especially during interspecies conjugation (Matic *et al.*, 2000). The SOS response results in the induction of over 30 unlinked genes, many of which are involved in DNA repair and mutagenesis (Walker, 1996). Intriguingly, the introduction of plasmid pSf-R27Gent^R into strain SL1344 did not alter expression of any genes belonging to the SOS regulon. In contrast, introduction of plasmid pSf-R27Δ*sfh*::Gent^R into *S.* Typhimurium induced numerous genes involved in the SOS response (Fig. 5.11) and also the *hsdM* and *hsdS* genes of the type I restriction modification

system (Supplementary data). Type 1 restriction modifications systems function to distinguish between foreign DNA and the cell's own genome by protecting the cellular DNA from restriction by modification methylation of adenine or cytosine residues within the specific sequences recognized by the restriction enzymes (Redaschi and Bickle, 1996). Furthermore, several phage genes were also upregulated following the introduction of plasmid pSf-R27Δ*sfh*::Gent^R (Table 5.2). Previous studies have shown that induction of the SOS response stimulates the lytic cycle of several phages, including three *S. enterica* prophages, namely, Gifsy-1, Gifsy–2 and Fels-2 (Bunny *et al.*, 2002). Interestingly, one of the Gisfy-2 phage genes (STM1034) displaying increased expression is homologous to RecA.

To confirm these microarray data, RT-PCR transcriptional analyses were performed on six classic SOS genes – *recA, lexA, ruvA, umuD, samB* and *ssb*. Total RNA was extracted from bacterial cultures of strains SL1344(pSf-R27Gent^R) and SL1344(pSf-R27Δ*sfh*::Gent^R) and used as template for RT-PCR. Expression of the *dnaE* gene was not affected by any extent by the presence or absence of Sfh in the DNA microarray experiment, thus allowing it to be used as a control in these experiments. In agreement with the microarray data, transcript levels of the tested SOS genes were elevated in the absence of Sfh (Fig. 5.11). These results suggested that the upregulation of the SOS regulon in strain SL1344(pSf-R27Δ*sfh*::Gent^R) might enhance its tolerance to DNA-damaging agents compared to strains SL1344 and SL1344(pSf-R27Gent^R).

To test this hypothesis, UV survival assays were performed on bacterial cultures of each strain and the results compared. The data obtained visibly showed that cells harbouring plasmid pSf-R27Δ*sfh*::Gent^R were significantly more resistant to UV than either of the other strains (Fig. 5.12). When cells were irradiated with a UV dose in the range 80 to 100 J/m^2, the *sfh* mutant was observed to be ~10-fold less sensitive to UV irradiation than the other two strains tested (Fig. 5.12). Taken together these results demonstrate a novel role for Sfh in suppression of the classical SOS response.

Fig. 5.11. Sfh supresses the SOS response. (A) Expression profile of selected SOS genes in strain SL1344(pSf-R27Δ*sfh*::Gent^R) relative to their expression in strain SL1344(pSf-R27Gent^R). The SOS genes selected were – the *ssb* gene (encodes single-stranded DNA-binding protein; member of LexA regulon; alkali-inducible), the *uvrA* gene (encodes excision nuclease subunit A; repair of UV damage to DNA; member of LexA regulon), the *dinF* gene (damage inducible gene F – induced by UV and mitomycin C; member of LexA regulon), the *lexA* gene (global repressor for SOS regulon), the *recA* gene (recombination and DNA repair gene; role in cleavage of LexA repressor; member of LexA regulon), the *recN* gene (recombination and DNA repair gene, member of LexA regulon), the *umuD* gene (encodes DNA polymerase V subunit; error-prone repair polymerase; member of LexA regulon), the *ruvA* gene (encodes holliday junction recognition protein ; member of LexA regulon), the *yebG* gene (DNA damage-inducible gene of unknown function, member of LexA regulon; requires H-NS and cAMP for induction), and the *samB* gene (UV-inducible gene of unknown function; related to UmuDC operon; member of LexA regulon). Each gene is represented by a box, which is coloured according to its expression ratio in the exponential and stationary phases of growth. Red indicates an increase in expression, yellow indicates no change, and blue indicates a decrease in expression, as shown in the scale bar on the right. (B) RT-PCR analyses of SOS gene transcription in strain SL1344 harbouring pSf-R27Gent^R or pSf-R27Δ*sfh*::Gent^R. Total RNA was extracted from cultures grown to stationary phase (OD_{600}~2.0) in L-broth at 37°C, DNase treated, and used as template for RT-PCR. To control for loading, RT-PCR analyses of *dnaE* transcription was performed, as *dnaE* gene expression does not alter to any extent in the presence and absence of Sfh. Densitometric analyses of the RT-PCR data are shown on the right for comparison. The relative transcript levels are expressed relative to each gene's transcript level in strain SL1344(pSf-R27Gent^R), the value of which was taken as 1. The data shown are averages of at least three independent experiments and representative gels are shown.

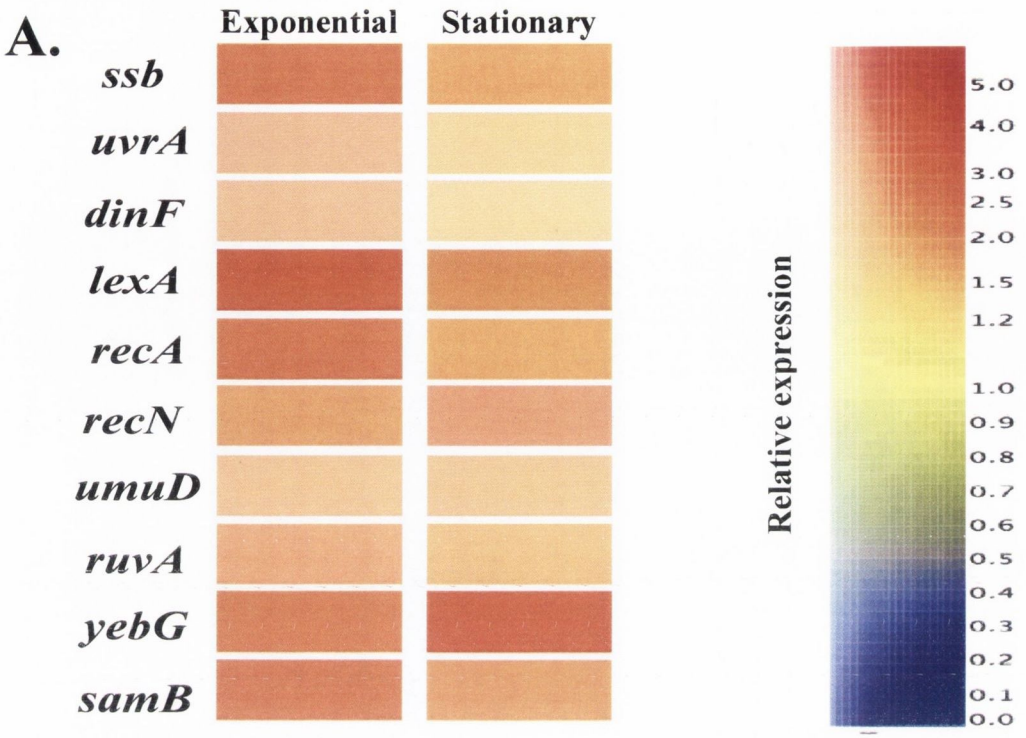
A.
Exponential
Stationary
ssb
uvrA
dinF
lexA
recA
recN
umuD
ruvA
yebG
samB
Relative expression
5.0
4.0
3.0
2.5
2.0
1.5
1.2
1.0
0.9
0.8
0.7
0.6
0.5
0.4
0.3
0.2
0.1
0.0

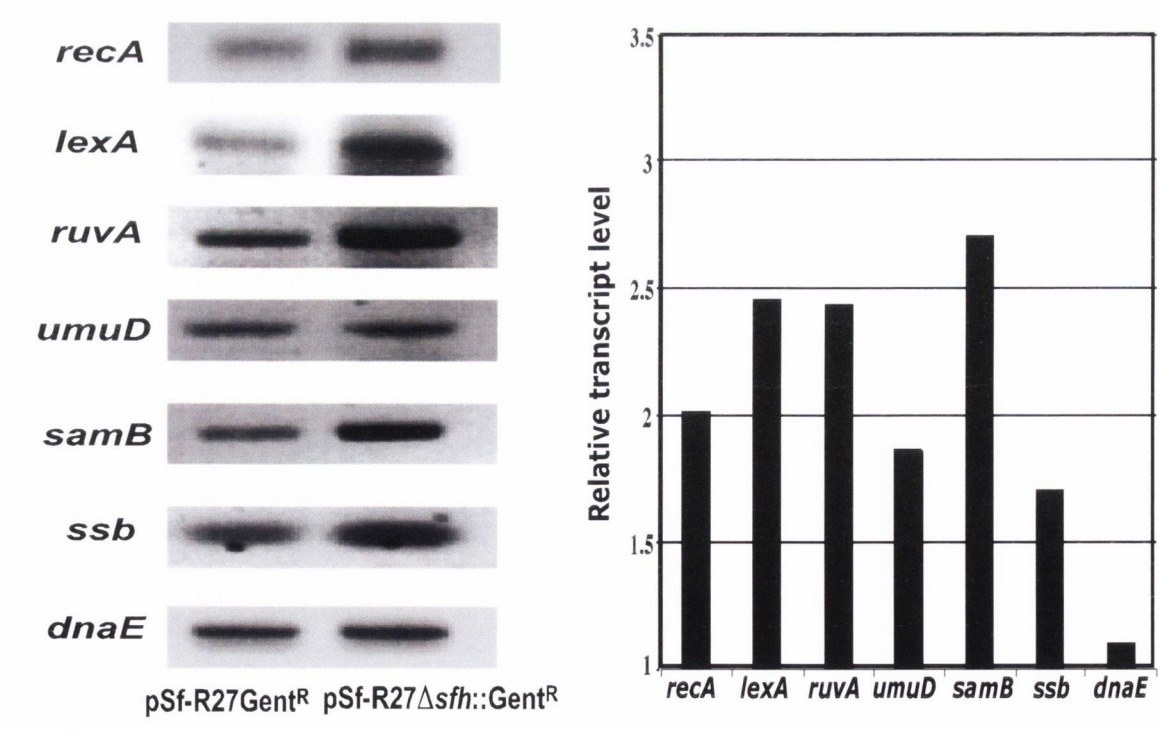
B.
recA
lexA
ruvA
umuD
samB
ssb
dnaE
pSf-R27GentR
pSf-R27Δsfh::GentR
Relative transcript level
3.5
3
2.5
2
1.5
1
recA
lexA
ruvA
umuD
samB
ssb
dnaE

Table 5.2. Phage genes affected by the *sfh* mutation

Gene	Function	pSf-R27Δ*sfh*::Gent^R/pSf-R27Gent^R expression ratio[a]	
		Exponential phase	Stationary phase
STM0906	Fels-1 prophage protein	11.36	5.76
STM1032	Gifsy-2 prophage protein	3.19	ND
STM1033	Gifsy-2 prophage protein, homology to Clp protease	3.04	1.94
STM1034	Gifsy-2 prophage, putative RecA/RadA recombinase	3.24	2.27
STM1035	Gifsy-2 prophage, ATP-binding sugar transporter-like protein	2.87	ND
STM1036	Gifsy-2 prophage, probable minor tail protein	2.67	2.18
STM1037	Gifsy-2 prophage, probable minor tail protein	2.15	ND
STM2235	Putative phage protein	4.44	1.82
STM2238	Putative phage protein	0.39	0.19
STM2598	Gifsy-1 prophage protein	2.42	2.95
STM2601	Gifsy-1 prophage, putative minor capsid protein	1.79	1.36
STM2602	Gifsy-1 prophage,putative DNA packaging protein	1.89	2.77
STM2603	Gifsy-1 prophage, putative head protein	1.58	3.00
STM2604	Gifsy-1 prophage, putative head protein	ND	2.79
STM2605	Gifsy-1 prophage, putative head-tail preconnector protein	1.79	3.13
STM2606	Gifsy-1 prophage, putative head-tail preconnector protein	1.87	2.56
STM2608	Gifsy-1 prophage, putative terminase large chain protein	1.64	2.90

Table 5.2 continued

Gene	Function	pSf-R27Δ*sfh*::Gent^R/pSf-R27Gent^R expression ratio[a]	
		Exponential phase	Stationary phase
STM2609	Gifsy-1 prophage, putative DNA packaging protein	2.15	3.27
STM2706	Fels-2 prophage, putative tail fibre protein	14.78	6.07
STY1027	Putative bacteriophage protein	5.87	ND
STY1042	Putative bacteriophage protein	17.50	6.52
STY4610	Putative phage tail fibre protein	5.30	4.56

[a]ND = No data

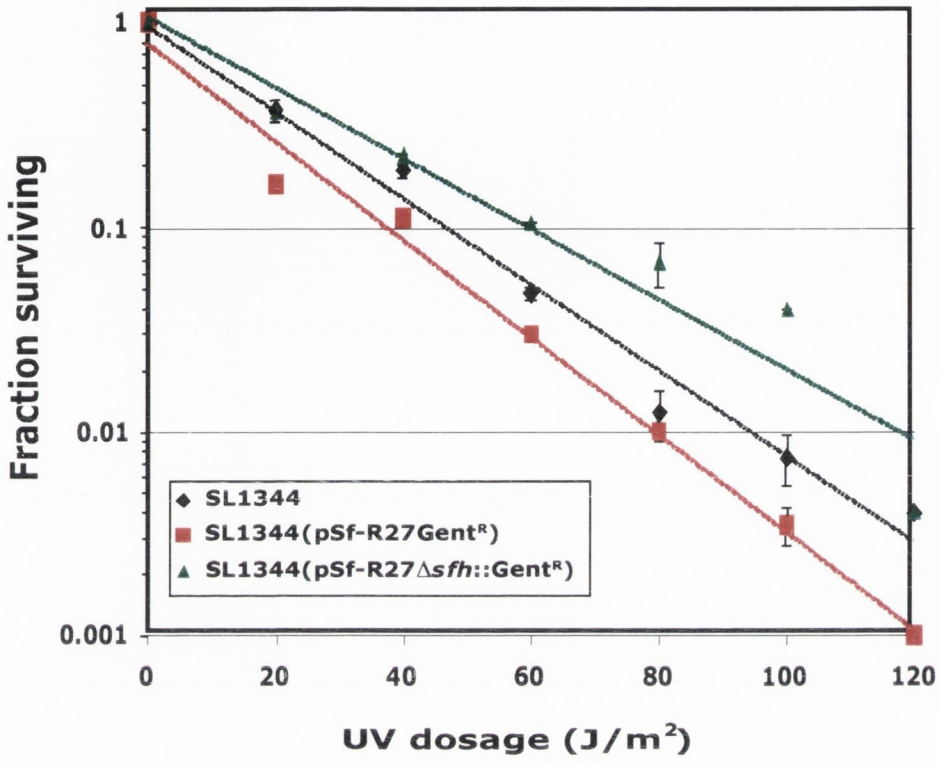

Fig. 5.12. The effect of deleting the *sfh* gene on UV sensitivity. Strains SL1344, SL1344(pSf-R27Gent^R) and the *sfh* mutant strain SL1344(pSf-R27Δ*sfh*::Gent^R) were compared for their resistance to UV irradiation. L-broth cultures of each strain were grown at 37°C to stationary phase and then irradiated with various UV doses as indicated. Numbers of surviving colonies were calculated after 24 h incubation in the dark and plotted against UV dosage (J/m^2). The survival values given are the means of at least four independent experiments and error bars represent standard deviations.

Recent studies have reported that many DNA damage-inducible genes are not directly regulated by the classical RecA/LexA system (Fernandez De Henestrosa *et al.*, 2000; Koch and Woodgate, 1998). Global analysis of the DNA-damage response in *E. coli* revealed the induction of other stress-response pathways, such as the osmotic protection and oxidative stress regulatory pathways (Khil and Camerini-Otero, 2002). In this microarray study, the expression of several genes belonging to different stress-response pathways were observed to be Sfh-dependent (Table 5.3). Many of the stress response genes affected by Sfh are linked to changes in environmental conditions, such as temperature (*cspB*), osmolarity (*osmE, osmY otsB*), and oxygen (*katE, sodA, sodB*). Interestingly, expression of all these genes is critical for the survival of *Salmonella in vivo* and suggests that Sfh could have a role in coordinating the expression of genes required for *Salmonella* pathogenesis.

5.2.8 Virulence gene expression

S. Typhimurium is dependent upon the products of a large number of genes to cause infection (Finlay and Brumell, 2000; Lucas and Lee, 2000; Marcus *et al.*, 2000). Some of these virulence genes are located on the 90-kb *Salmonella* large virulence plasmid, pSLT. However, the majority of virulence genes are located within the five *Salmonella* pathogenicity islands, of which SPI-1 and SPI-2 are the best characterized. Results from DNA microarray analysis showed that virulence genes belonging to all five pathogenicity islands displayed altered expression following the introduction of plasmid pSf-R27Δ*sfh*::Gent^R (Fig. 5.13). The affected genes are involved in most aspects of *Salmonella* virulence and represented all the different SPI functional classes of proteins, namely, regulatory, structural, and effector proteins.

Most of the affected SPI-1 genes showed an increase in expression in exponential phase and all were upregulated in stationary phase (Fig. 5.13). In stark contrast, the loss of Sfh from plasmid pSf-R27 correlated with a strong downregulation of SPI-2 gene expression in exponential phase (Fig. 5.13).

Several *Salmonella* effector proteins translocated into the host cell by either the TTSS of SPI-1 or SPI-2 are encoded outside these pathogenicity islands. For example, genes within SPI-5 have been described previously as being co-regulated with SPI-1 (*sigD*) and SPI-2 (*pipB*) (Knodler *et al.*, 2002). The response of the SPI-5 gene *sigD* to the presence of plasmid pSf-R27Δ*sfh*::Gent^R corresponds with its regulatory relationship to SPI-1 (Fig. 5.13). Unusually, expression of the SPI-5 gene *sigE,* which encodes a molecular chaperone required for SigD secretion (Darwin and Miller, 2000), is downregulated, suggesting a loss of coordinate expression of these two genes.

The pathogenicity island SPI-3 contains at least ten open reading frames, two of which, *mgtC* and *mgB,* encode a transport system that allows the uptake of magnesium under low Mg^{2+}conditions. These genes are required for survival inside macrophage and virulence in the mouse (Blanc-Potard and Groisman, 1997; Blanc-Potard *et al.*, 1999). Interestingly the SPI-3 gene *slsA* was repressed in strain SL1344(pSf-R27Δ*sfh*::Gent^R), a pattern that mirrored the SPI-2 genes, which are required for survival and replication inside macrophage (Fig. 5.13). The genes within the poorly defined SPI-4 island showed a variety of responses to the absence of Sfh (Fig. 5.13).

In addition to virulence genes from all five *Salmonella* pathogenicity islands being affected, the introduction of plasmid pSf-R27Δ*sfh*::Gent^R also resulted in a strong derepression of the *spv* genes encoded on the pSLT virulence plasmid (Supplementary data). Furthermore, genes encoded by the *Salmonella* Fels and Gifsy prophages also displayed increased expression in an *sfh*$^-$ background (Table 5.2). Previous studies have identified virulence genes encoded on these prophages, such as the Gifsy-1 genes *gipA* and *gogB* (Coombes *et al.*, 2005a; Stanley *et al.*, 2000), the Gifsy-2 genes *sodCI* and *gtgE* (Figueroa-Bossi and Bossi, 1999; Ho *et al.*, 2002), and the Fels-1 gene *sodCIII* (Figueroa-Bossi *et al.*, 2001). Virulence studies of *Salmonella* strains cured of Gifsy-1, Gifsy-2, or both lysogenic phage revealed that Gifsy-2 plays an important role in *Salmonella* virulence in mice, most likely by the contribution of SodCI (Fang *et al.*, 1999; Figueroa-Bossi *et al.*, 2001) and GtgE (Ho *et al.*, 2002). All these

Table 5.3. Stress response genes affected by the *sfh* mutation

Gene	Function	pSf-R27Δ*sfh*::Gent^R/pSf-R27Gent^R expression ratio[a]	
		Exponential phase	Stationary phase
cpxP	Extracytoplasmic stress protein	ND	2.86
cspB	Cold-shock protein	ND	2.34
cstA	Carbon starvation protein A	0.32	ND
cutA	Periplasmic divalent cation tolerance protein	4.3	ND
imp	Organic solvent tolerance protein precursor	2.14	1.92
katE	Hydroperoxidase II; catalase	ND	2.35
mscL	Osmotic stress; conductance mechanosensitive channel	0.32	ND
osmE	Osmotic stress; activator of *ntrL* transcription	0.44	1.60
osmY	Osmotic stress; periplasmic protein	1.43	2.30
otsB	Osmotic stress; trehalose phosphatase	2.09	2.46
psiF	Phosphate starvation-inducible protein	0.39	2.07
sodA	Superoxide dismutase (Mn)	4.41	0.41
sodB	Superoxide dismutase (Fe)	0.35	ND
STY0440	Putative peroxidase	2.38	ND
STY1871	Putative heat-shock protein	0.05	0.55

[a]ND = No data

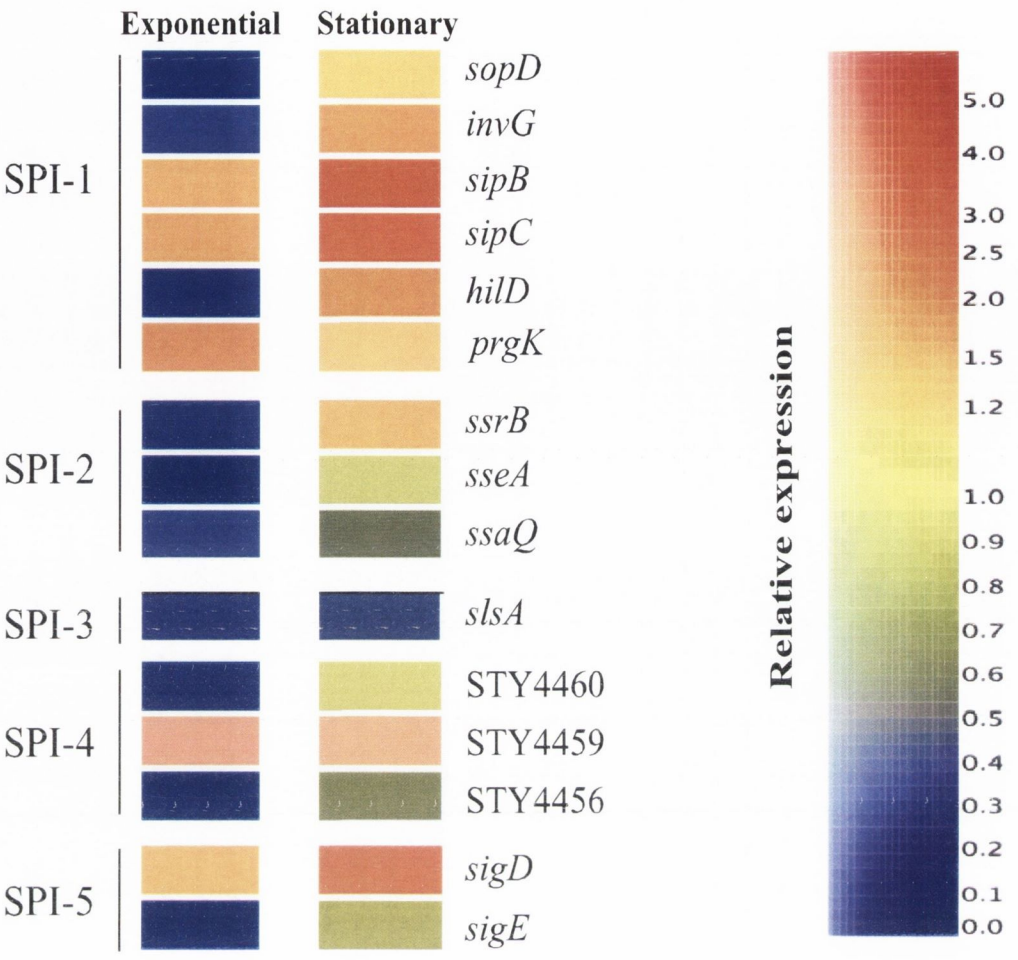

Fig. 5.13. The effect of deleting the *sfh* gene on virulence gene expression. Expression profile of selected virulence genes within the *Salmonella* pathogenicity islands in strain SL1344(pSf-R27Δ*sfh*::Gent^R) relative to their expression in strain SL1344(pSf-R27Gent^R). Each gene is represented by a box, which is coloured according to its expression ratio in the exponential and stationary phases of growth. Red indicates an increase in expression, yellow indicates no change, and blue indicates a decrease in expression as shown in the scale bar on the right. Expression ratios greater than 1.0 indicate genes normally repressed by Sfh, while expression ratios less than 1.0 indicate genes normally activated by Sfh.

data indicate a putative role for Sfh in *Salmonella* virulence gene expression and a more extensive analysis of this hypothesis is provided later in this study (Chapter 6).

5.2.9 Metabolism

The introduction of plasmid pSf-R27Δ*sfh*::Gent^R (but not plasmid pSf-R27Gent^R) resulted in a strong induction of genes involved in the adaptation of *S.* Typhimurium to the intestinal milieu. Genes upregulated included those contributing to anaerobic respiration (nitrite reductase) and fermentation (alcohol dehydrogenase), genes required for utilization of propanediol *(pdu* operon), for uptake and utilization of melibiose (*mel* genes), for adjustment to high osmolarity [for synthesis of osmoprotectant trehalose (*otsB*), and for uptake of compatible solutes (*proP*)] (Supplementary data). The genes coding for the outer membrane porin proteins OmpC, OmpF, and OmpS1 were also induced (Supplementary data). In contrast, genes contributing to aerobic respiration (*cyo* genes) and the gene coding for the large conductance mechano-sensitive channel MscL, that is required when bacteria experience a sudden decrease in osmotic pressure, were repressed (Supplementary data). These data are consistent with a profound shift in cellular metabolism for survival in the high osmolarity and low oxygen growth conditions experienced by *S.* Typhimurium in the mammalian gut and provide another putative link between *Salmonella* virulence and Sfh.

5.2.10 Fitness

Given the dramatic influence of plasmid pSf-R27Δ*sfh*::Gent^R on the *S.* Typhimurium transcriptome, the possibility that the introduction of this plasmid might influence the fitness of the bacterium was tested. The introduction of conjugative plasmids into a bacterial cell by horizontal transfer can confer a physiological or energetic cost, which influences the fitness of the bacterium (Dahlberg and Chao, 2003). The 'fitness cost' associated with plasmids pSf-R27Gent^R and pSf-R27Δ*sfh*::Gent^R was determined by calculating the relative fitness of strain SL1344 and its plasmid-bearing derivatives in direct competition experiments.

Results of the competitive fitness assays revealed that the presence of plasmid pSf-R27Gent^R had a mild negative effect on the fitness of strain SL1344 (Table 5.4). In contrast, the introduction of plasmid pSf-R27Δ*sfh*::Gent^R strongly reduced bacterial fitness, as might be expected in the light of its impact on the global gene expression profile of the cell (Table 5.4). Surprisingly, introduction of the multi-copy plasmid pACYC184 into strain SL1344(pSf-R27Δ*sfh*::Gent^R) caused a further 10-fold decrease in bacterial fitness (Table 5.4). These results are consistent with data obtained from direct competition experiments in *E. coli*, which showed that introduction of plasmid pACYC184 into wild-type strain MC4100 results in a dramatic reduction in fitness (data not shown). Remarkably, when plasmid pACYC184 harbours the *sfh* (pYCsfh) or *hns* (pAF201) gene, its 'fitness cost' is dramatically reduced (Table 5.4). Expression of Sfh *in trans* completely negated the 'fitness cost' associated with plasmid pACYC184, while expression of H-NS *in trans* increased bacterial fitness 5-fold (Table 5.4).

Interestingly, the phenotype of strain SL1344(pSf-R27Δ*sfh*::Gent^R) resembles that of an *hns* mutant, albeit that it contains wild-type H-NS protein levels. This observation led to the hypothesis that H-NS might be less active in strain SL1344(pSf-R27Δ*sfh*::Gent^R) due to a titration effect exerted by the introduced plasmid. The DNA sequence of plasmid pSf-R27 is very AT-rich (55%) and thus its introduction into a bacterium could dramatically increase the potential number of binding sites for H-NS-like proteins. In the absence of Sfh it is possible that H-NS binds to plasmid pSf-R27Δ*sfh*::Gent^R, which results in an overall reduction in H-NS availability (and hence activity) such that sites within the host genome, especially sites of lower affinity, might be occupied less. This model would account for the *hns* mutant phenotype of strain SL1344(pSf-R27Δ*sfh*::Gent^R) and is supported by the fact that both H-NS and Sfh have common binding sites within the regulatory regions of various plasmid pSf-R27 genes (Chapter 4).

To test this hypothesis, an AT-rich plasmid containing a high-affinity H-NS binding site was constructed and transformed into to strain SL1344 to determine if its acquisition correlated

Table 5.4. Relative fitness of strain SL1344 harbouring plasmids

Strain	Relative mean fitness[a]
SL1344	1.02 ± 0.04
SL1344 (pSf-R27Gent^R)	0.83 ± 0.01
SL1344 (pSf-R27Δ*sfh*::Gent^R)	0.22 ± 0.04
SL1344 (pSf-R27Δ*sfh*::Gent^R, pACYC184)	0.02 ± 0.002
SL1344 (pSf-R27Δ*sfh*::Gent^R, pYCsfh)	0.28 ± 0.02
SL1344 (pSf-R27Δ*sfh*::Gent^R, pAF201)	0.10 ± 0.01
SL1344 (pUC18)	0.72±0.03
SL1344 (pUCA/T)	0.47±0.02
SL1344 (pPD101)	1.06±0.02
SL1344 (pPDsfh)	1.15±0.02
SL1344 (pUCA/T, pPD101)	0.77±0.04
SL1344 (pUCA/T, pPDsfh)	0.98±0.02

[a] Fitness relative to the common competitor strain SL1344 Nal^R

with a concomitant decrease in bacterial fitness due to a reduction in H-NS activity. For this reason, an ~2.8-kb AT-rich DNA fragment encompassing the *ssrA–ssaB* promoter region was amplified by PCR using the primers A/T-F and A/T-R (Table 2.3) and cloned into the vector pUC18 to generate plasmid pUCA/T (Fig. 5.14). Importantly, the *ssrA–ssaB* DNA fragment cloned into pUCA/T contains a high-affinity H-NS- and Sfh-binding site (Chapter 6; Fig. 6.11) and does not code for any protein. The 'fitness cost' associated with the AT-rich DNA sequence in pUCA/T was determined by calculating the relative fitness of strain SL1344 and its plasmid-bearing derivatives SL1344(pUC18) and SL1344(pUCA/T) in direct competition experiments. The results show that cells harbouring plasmid pUC18 display a small reduction in fitness compared to strain SL1344, whereas introduction of plasmid pUCA/T into strain SL1344 resulted in more than a 2-fold reduction in bacterial fitness (Table 5.4). Since the AT-rich DNA sequence inserted into plasmid pUCA/T does not code for any proteins, it must be concluded that the elevated 'fitness cost' associated with plasmid pUCA/T (compared to pUC18) corresponds directly with its higher AT content and, moreover, that the presence of a high-affinity H-NS/Sfh-binding site could be titrating H-NS from its chromosomal binding sites.

In light of these data, it was proposed that expression of Sfh *in trans* should alleviate the titration effect, if any, exerted by plasmid pUCA/T, as H-NS and Sfh have a common binding site on the plasmid. For this reason the *sfh* gene was amplified by PCR using the primers sfh-500 and sfh+780 (Table 2.3) and cloned into the low-copy number vector pPD101 to generate plasmid pPDsfh (Fig. 5.15). The sequence of the *sfh* promoter region and ORF in plasmid pPDsfh was confirmed by sequencing. The results of competitive fitness assays revealed that expression of Sfh *in trans* from plasmid pPDsfh completely negated any 'fitness cost' associated with the plasmid pUCA/T (Table 5.4). Remarkably, cells harbouring plasmids pUCA/T and pPDsfh had the same relative fitness as the wild-type strain SL1344 (Table 5.4). The plasmid copy numbers of plasmids pUC18, pUCA/T, pPD101, and pPDsfh were determined in the relative strains under the fitness assay growth conditions and their copy numbers shown to be comparable between strains (data not shown). Thus, the observed

differences in the relative fitness of the tested plasmid-bearing strains cannot be due to changes in plasmid copy number. Taken in aggregate, these data indicate a novel stealth-like role for Sfh in plasmid biology, since Sfh expression always decreases and in some cases even negates the reduction in bacterial fitness associated with plasmid carriage.

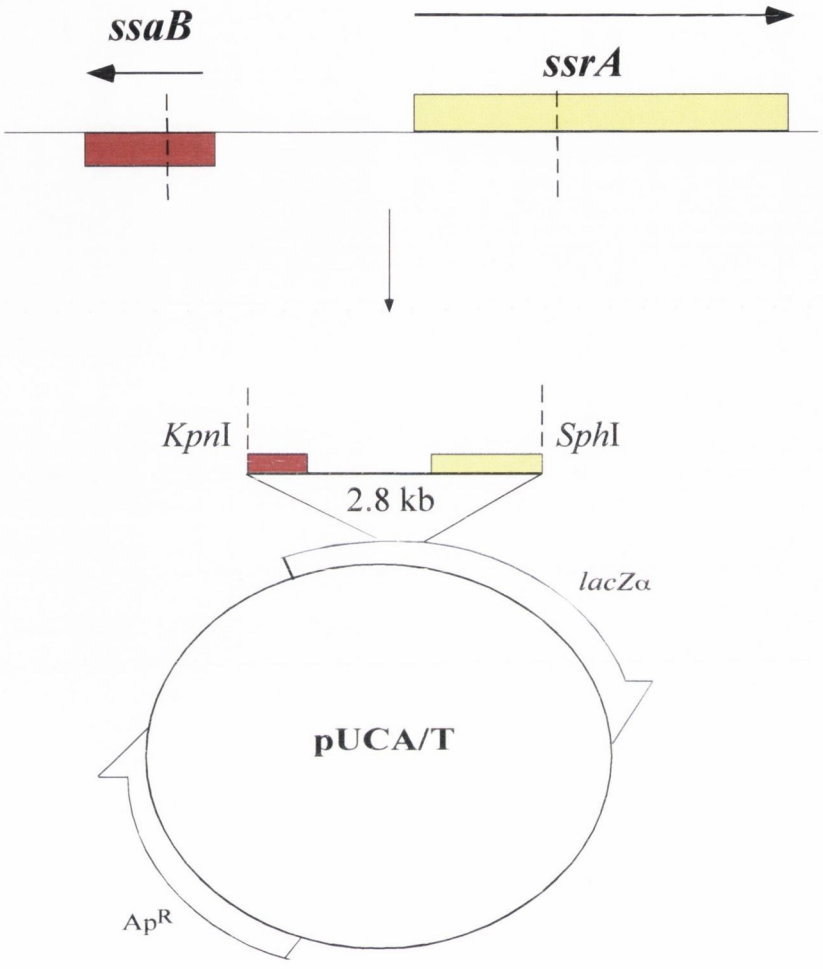

Fig. 5.14. Construction of an AT-rich plasmid. A 2.8-kb section of AT-rich DNA, incorporating the 5′-region of the *ssrA* and *ssaB* genes, and the *ssrA–ssaB* intergenic regulatory region was amplified by PCR and ligated into the multiple cloning site of plasmid pUC18 to generate plasmid pUCA/T.

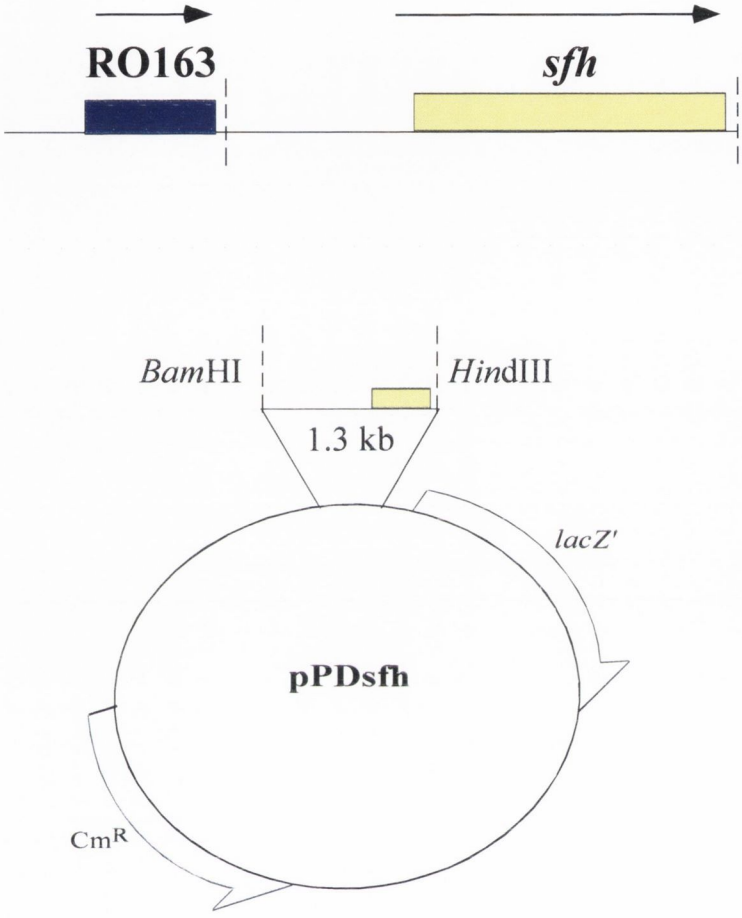

Fig. 5.15. Construction of a low-copy number *sfh* plasmid. A 1.3-kb section of DNA, incorporating the *sfh* regulatory region and open reading frame, was amplified by PCR and ligated into the multiple cloning site of the low-copy number vector pPD101 to generate plasmid pPDsfh.

5.3 Discussion

The presence of genes encoding paralogues of several known transcriptional regulators, e.g., H-NS, Dam, Hha, TlpA, on IncHI1 plasmids raised the intriguing possibility that horizontal transfer of these regulatory proteins could exert wide-ranging influences on the global gene expression profile of transconjugants. Sequencing studies have identified *hns*-related genes on many other self-transmissible plasmids and within elements such as pathogenicity islands that are thought to have been acquired via horizontal transfer. Therefore, it was of particular interest to determine if the transcriptome of transconjugants is affected when an IncHI1 plasmid, with and without a functioning H-NS-like protein, is acquired by horizontal transfer. Moreover, it was important to determine if the expression, and the functional roles of established H-NS-like proteins, are modulated when a new paralogue is acquired by horizontal transfer. To resolve all these issues, the plasmids pSf-R27Gent^R and pSf-R27Δ*sfh*::Gent^R were introduced into the mouse-virulent *S.* Typhimurium strain SL1344 to observe their effects on the transconjugant's transcriptome by DNA microarray analysis.

Surprisingly, introduction of the Sfh-expressing plasmid pSf-R27Gent^R had a very minor influence on the transcriptome of *S.* Typhimurium strain SL1344. Genes displaying the greatest response to plasmid pSf-R27Gent^R were those coding for factors involved in chromosome replication and in the expression of ribosome components. These results are consistent with the slightly slower growth rate observed in the plasmid pSf-R27Gent^{R+} strain compared to strain SL1344 (Fig. 5.2). In addition, several flagellar and fimbrial genes showed altered expression. This was confirmed for the phase I flagellin gene *fliC* at the protein level (Fig. 5.10). In contrast, horizontal transfer of plasmid pSf-R27 lacking a functional *sfh* gene (pSf-R27Δ*sfh*::Gent^R) resulted in widespread changes in the transcriptome across several categories of functional groups of genes (Fig. 5.6). Genes involved in motility, metabolism, virulence, and the response to DNA damage all showed marked changes in expression following the establishment of plasmid pSf-R27Δ*sfh*::Gent^R in strain SL1344. Consistent with members of the H-NS protein family being global transcriptional repressors, most the genes showing altered expression were upregulated in the *sfh*$^-$ background. One

exception was the downregulation of several flagellar genes in strain SL1344(pSf-R27Δ*sfh*::Gent^R), which correlated with a reduction in its motility phenotype (Fig. 5.9).

H-NS-like proteins usually act as transcriptional repressors by binding to the promoter region of interest, although in some rare cases they are known to function as transcriptional activators. Indeed, a previous report demonstrated that H-NS plays a positive role in the regulation of flagellar genes and in the expression of the *Salmonella* motility phenotype (Hinton *et al.*, 1992). Analysis of the *flgA–flgB* regulatory region *in silico* indicated that it possesses several regions of DNA curvature (Fig. 5.8), a structural feature that is characteristic of high-affinity, H-NS-like protein-binding sites. Consistent with these findings, both Sfh and H-NS were shown to bind preferentially to the *flgA–flgB* promoter region in competitive gel retardation assays (Fig. 5.8). Therefore, the observed positive effect on flagellar gene expression is probably due to the direct interaction of members of the H-NS protein family with the *flgA–flgB* regulatory region. Interestingly, horizontal transfer of either plasmid pSf-R27Gent^R or plasmid pSf-R27Δ*sfh*::Gent^R into strain SL1344 resulted in upregulation of the phase I flagellin, FliC, and consequent repression of the phase II flagellin, FljB (Fig. 5.10). These observations raise some interesting questions about the physiological relevance of preferentially expressing FliC. Flagellin is a major pro-inflammatory determinant of *Salmonella* (Zeng *et al.*, 2003) and a recent study demonstrated that cytosolic bacterial flagellin activates caspase-1 and secretion of interleukin 1β via Ipaf, a NACHT-leucine–rich repeat family member (Miao *et al.*, 2006). When *S.* Typhimurium does not express flagellin it can go largely undetected in host cells (Zeng *et al.*, 2003). Therefore, flagellar phase variation is considered generally as a strategy used by *Salmonella* to evade the host immune system. Thus, preferential expression of either flagellin would be considered disadvantageous to the bacterium. Further investigation will be required to resolve this conundrum.

The introduction of plasmid pSf-R27Δ*sfh*::Gent^R (but not plasmid pSf-R27Gent^R) resulted in a strong induction of genes involved in the adaptation of *S.* Typhimurium to the intestinal

milieu. Genes contributing to anaerobic respiration, fermentation, and adjustment to high osmolarity were all upregulated, whereas genes required for aerobic respiration and osmotic down-shock were repressed (Supplementary data). These traits are reminiscent of the phenotypes of *hns* mutants (Dorman, 2004; Rimsky, 2004). The virulence genes of *S.* Typhimurium are sensitive to various environmental conditions including osmotic stress and anaerobiosis. In this study, virulence genes on all five *Salmonella* pathogenicity islands together with the *spv* virulence genes on the pSLT plasmid showed altered transcription in response to the introduction of plasmid pSf-R27Δ*sfh*::Gent^R (Fig. 5.13 and supplementary data). Taken together these data highlight the coordinate expression of *Salmonella* metabolic and virulence genes required for adaptation to the host environment and strongly suggest that horizontal acquisition of Sfh on plasmid pSf-R27 can potentially contribute to these cellular signaling pathways. It should be noted that a connection between nucleoid-associated proteins (including H-NS) and *Salmonella* virulence has been recognized for some time (Kelly *et al.,* 2004; Mangan *et al.,* 2006; Olekhnovich and Kadner, 2006; Rhen and Dorman, 2005; Schechter *et al.,* 2003; Wilson *et al.,* 2001). Only two nucleoid-associated proteins, Dps and HU, displayed altered expression in the *sfh*$^-$ background. Surprisingly, expression of the established chromosomal H-NS-like proteins, H-NS and StpA, was not affected by the introduction of a new paralogue.

Horizontal transfer of mobile genetic elements such as conjugative plasmids is known to trigger a strong SOS response in the recipient bacterium (Matic *et al.*, 2000). Intriguingly, horizontal transfer of plasmid pSf-R27Gent^R did not provoke an SOS response, whereas plasmid pSf-R27Δ*sfh*::Gent^R did (Fig. 5.11). These results suggest that Sfh is required by the plasmid to suppress any SOS signals generated by the incoming foreign DNA. Previous studies have shown that many transmissible plasmids have evolved to permit transfer of ssDNA without generating an SOS signal by expressing factors that both inhibit the bacterial SOS response and also help establish the incoming plasmid in the recipient cell (Althorpe *et al.,* 1999; Bates *et al.,* 1999; Matic *et al.,* 2000). The genes coding for these factors (e.g., *psiB, ardA, ssb*) are highly conserved, and located in the leading region of many

enterobacterial plasmids (Althorpe *et al.*, 1999). Significantly, bioinformatic analysis of plasmid pSf-R27 revealed that this plasmid does not code for any of these factors, strengthening the model in which Sfh suppresses the SOS response. Furthermore, H-NS has been reported to suppress the UV damage repair process in *Shigella* (Palchaudhuri *et al.*, 1998) and is a known regulator of the SOS genes *yebG* and *sbmC* (Oh and Kim, 1999; Oh *et al.*, 2001). In addition, another member of the H-NS protein family, StpA, was identified as part of the classical SOS regulon in *S.* Typhimurium (Benson *et al.*, 2000).

The findings of this study indicate that horizontal transfer of plasmid pSf-R27 lacking a functional *sfh* gene (pSf-R27Δ*sfh*::Gent^R), but not of the wild-type plasmid (pSf-R27Gent^R) has a profound effect on the transconjugant transcriptome. Consequently, acquisition of plasmid pSf-R27Δ*sfh*::Gent^R dramatically reduces the fitness of the recipient bacterium, whereas in comparison plasmid pSf-R27Gent^R has only a minor 'fitness cost' (Table 5.4). These observations raise some interesting questions about how Sfh is able to exert such widespread changes in the global expression profile. The results of the microarray study show that the expression of several transcriptional regulators is altered in the absence of Sfh (Supplementary data) and, thus, it is possible that Sfh could be indirectly modulating global gene expression. It is also possible that in the absence of Sfh, expression of a plasmid pSf-R27-encoded factor is derepressed, which mediates the profound effect on the transconjugant transcriptome. However, the effect of Sfh on flagellar gene expression and virulence gene expression (Chapter 6) was found to be direct. Furthermore, H-NS was also shown to bind to these promoters and the phenotype of strain SL1344(pSf-R27Δ*sfh*::Gent^R) resembles that of an *hns* mutant, albeit that it contains wild-type H-NS protein levels. Collectively these data support a model in which the H-NS protein is less active in strain SL1344(pSf-R27Δ*sfh*::Gent^R) due to a titration effect exerted by the introduced plasmid.

Consistent with this model the DNA sequence of plasmid pSf-R27 is very AT-rich (55%) and, thus, its introduction into a bacterium would dramatically increase the potential number of binding sites for H-NS-like proteins. Moreover, all three H-NS-like proteins, Sfh, H-NS, and

StpA, have been shown to bind to plasmid pSf-R27 (Chapter 4). However, since Sfh is encoded by plasmid pSf-R27, it seems likely that Sfh might have a higher affinity for these sites than the chromosomal proteins H-NS and StpA and thus preferentially occupy them. Therefore, one can envisage that, in the absence of Sfh, H-NS could bind to the plasmid pSf-R27 and repress gene transcription (Fig. 5.16). Consequently, there would be a reduction in overall H-NS availability (and hence activity) such that sites within the host chromosome, especially sites of lower affinity, might be occupied less often, leading to a phenotype that resembles that of an *hns* mutant (Fig. 5.16).

Sfh is known to repress transcription of many plasmid pSf-R27 genes including several transcriptional regulators and conjugation genes (Chapter 4). Thus, one would expect a vast number of plasmid pSf-R27 genes to be induced in the absence of Sfh. Significantly, this was not the case (Table 5.1) and taken together these data suggest that plasmid pSf-R27 gene expression is still repressed in strain SL1344(pSf-R27Δ*sfh*::Gent^{R}). These results strengthen the model in which the absence of Sfh leads to H-NS binding to plasmid pSf-R27, thereby repressing plasmid gene transcription. The proposed above model is based on changes in H-NS activity resulting from variations in available binding sites for H-NS-like proteins in the presence and absence of Sfh. Critically, this study showed that the introduction of plasmid pUCA/T, which harbours a high-affinity H-NS/Sfh-binding site, into strain SL1344 results in a concomitant reduction in bacterial fitness (Table 5.4). Significantly, the results of competitive fitness assays indicate that plasmid pUCA/T exerts a H-NS titration effect that can be negated by expressing Sfh *in trans*. These data strongly suggest that horizontal acquisition of plasmid pSf-R27Δ*sfh*::Gent^{R} correlates with a concomitant decrease in bacterial fitness due to a reduction in H-NS activity in the transconjugant.

However, the results of this study do not discount a second model, which is closely related to the above hypothesis. The alternative model is based on the fact that H-NS-like proteins can form heteromeric complexes with one another and that these protein complexes may have different regulatory properties depending on their subunit composition. It is possible that *in*

vivo Sfh forms a heteromeric complex with either H-NS or StpA, which optimally regulates plasmid pSf-R27 gene expression to minimize the impact or 'fitness cost' of the plasmid on the host transcriptome. In the absence of Sfh, the established H-NS-like protein complexes (homomeric H-NS or homomeric StpA or heteromeric H-NS:StpA) are unable to optimally regulate a key gene or genes within plasmid pSf-R27, subsequently leading to widespread changes in the host transcriptome. This model is strengthened by previous data (Chapter 3) showing that Sfh is protected from proteolysis in the presence of H-NS, but not of StpA. Consequently, it was concluded that Sfh must be present mainly *in vivo* in heteromeric complexes with H-NS. Moreover, transcriptional data obtained for several plasmid pSf-R27 genes suggested that heteromeric H-NS-like protein complexes, especially StpA:Sfh complexes, might be required for optimal control of plasmid pSf-R27 gene expression (Chapter 4). In this hypothesis, one must also consider the possibility that the established H-NS-like protein complexes can achieve optimal plasmid pSf-R27 gene expression without Sfh, but that this requires more protein complexes to bind to the plasmid compared to Sfh homomeric and heteromeric complexes, thus titrating H-NS and StpA away from their chromosomal binding sites.

The maintenance of a plasmid by a bacterium is a heavy metabolic burden and as a result reduces the fitness of the bacterium. Consequently, a bacterium will always try to minimize the 'fitness cost' associated with a plasmid by optimizing global gene expression. In general, plasmid pSf-R27 gene expression was repressed even in the absence of Sfh, suggesting that the plasmid could code for a toxic factor, whose expression would subsequently be lethal or dramatically reduce bacterial fitness. Therefore, the cell employs the chromosomally encoded H-NS-like proteins to repress plasmid pSf-R27 gene expression to minimize the 'fitness cost' of the plasmid, albeit that it results in widespread changes in the host chromosomal gene expression and concomitant reduction in fitness. Indirect evidence that Sfh and its paralogues H-NS and StpA are required to repress a toxic factor encoded by plasmid pSf-R27 comes from attempts to make a triple *hns stpA sfh* knockout mutant (Chapter 4). Every combination of double mutants is viable, but it is impossible to make a triple mutant.

Fig. 5.16. Model summarizing the stealth-like role of Sfh in horizontal transfer of plasmid pSf-R27. (A) Horizontal transfer of plasmid pSf-R27 expressing its H-NS-like protein Sfh (purple circles) has little impact on the transconjugant transcriptome because Sfh binds to plasmid pSf-R27 and represses gene transcription. (B) Horizontal transfer of plasmid pSf-R27 lacking a functional *sfh* gene (pSf-R27Δ*sfh*) has a profound effect on the transconjugant transcriptome because, in the absence of Sfh, H-NS (red circles) binds to the plasmid pSf-R27Δ*sfh* and represses gene transcription. Consequently, there is a reduction in overall H-NS availability (and hence activity) such that H-NS-binding sites within the host genome, especially sites of lower affinity, are occupied less often, leading to a phenotype that resembles that of an *hns* mutant.

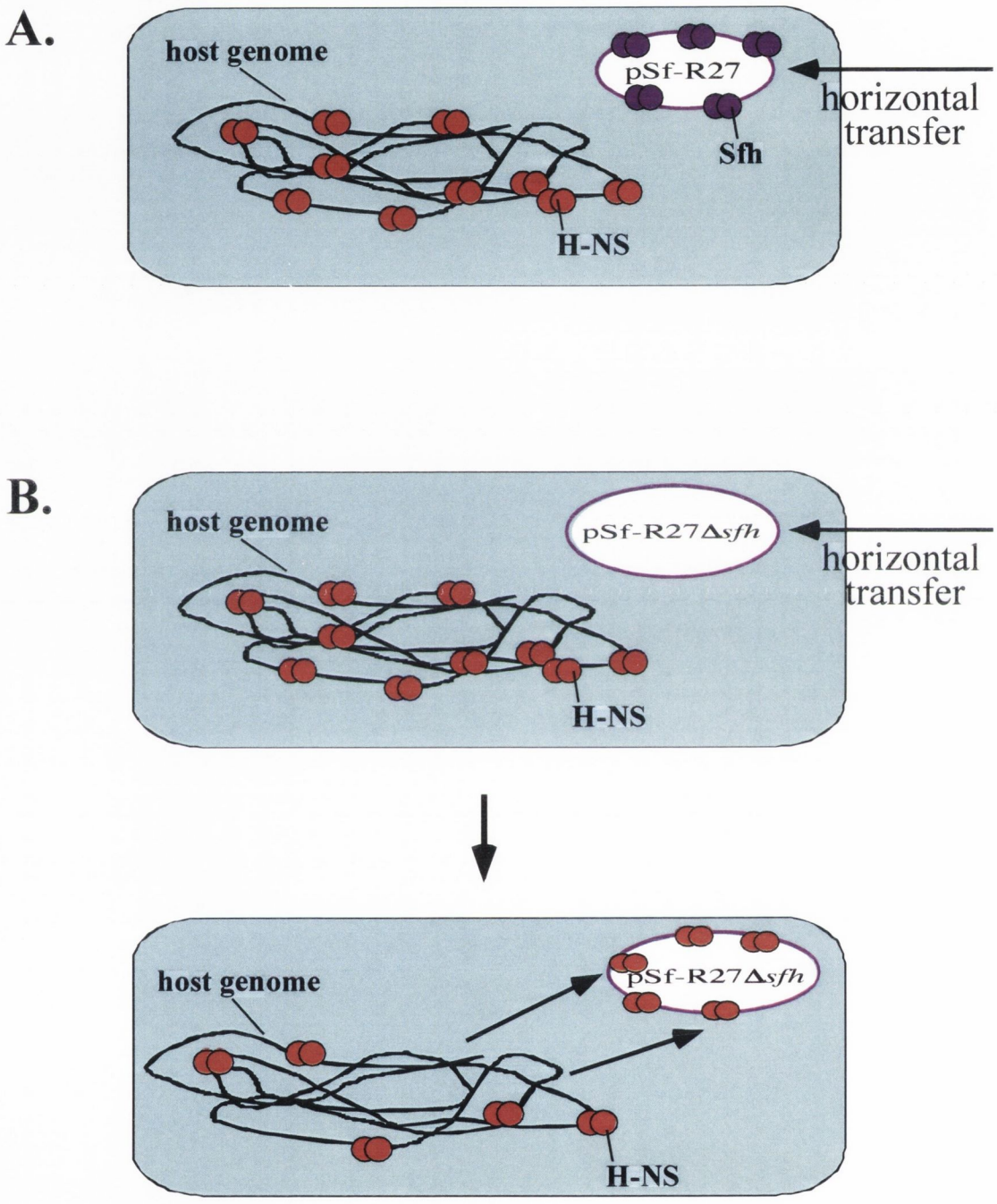
A.
host genome
pSf-R27
horizontal transfer
Sfh
H-NS
B.
host genome
pSf-R27Δsfh
horizontal transfer
H-NS
host genome
pSf-R27Δsfh
H-NS

Collectively the findings of this study show that plasmid pSf-R27 requires its H-NS-like gene *sfh* to minimize the impact of the plasmid on the host transcriptome. The data highlight the importance of Sfh on the 'visibility' of the horizontally acquired plasmid in the recipient bacteria. Sfh essentially acts like a 'stealth gene' allowing plasmid pSf-R27 to disseminate into new hosts virtually without detection at the level of the host transcriptome. In addition, Sfh was shown to reduce the 'fitness cost' associated with several other unrelated plasmids. Given the presence of *hns*-like genes on so many other self-transmissible plasmids and other mobile genetic elements, it is plausible that these genes represent a universal regulatory mechanism used by mobile genetic elements for promiscuous horizontal DNA transfer. Furthermore, this model is strengthened by the high AT-rich content of horizontally acquired genes compared to chromosomal genes, indicating they possess binding sites for H-NS-like proteins. Finally, the study raises the intriguing possibility that horizontal transmission of new regulatory proteins can potentially modulate global regulatory circuits in bacteria.

Chapter 6

Role for Sfh in *Salmonella* and *Shigella* virulence gene expression

6.1 Introduction

6.1.1 *Salmonella* and *Shigella* virulence

S. Typhimurium and *S. flexneri* are Gram-negative facultative intracellular pathogens, which cause gastroenteritis and shigellosis in humans, respectively (Ohl and Miller, 2001; Sansonetti, 2001). Both pathogens rely on a wide range of virulence factors to colonize and replicate within the host, to neutralize host defenses, and to spread by infecting new hosts (Ehrbar and Hardt, 2005). In particular, their ability to cause disease is dependent on TTSSs that translocate discrete sets of bacterial effector proteins into host cells. In *S.* Typhimurium virulence genes are often contained in large clusters called *Salmonella* pathogenicity islands, or SPIs for short. These genetic elements are often found integrated at tRNA loci and are thought to be horizontally acquired (Blanc-Potard *et al.*, 1999). The two largest and most important SPIs, SPI-1 and SPI-2, each encode a TTSS. In contrast, *S. flexneri* expresses only one TTSS, which is encoded within a 31-kb 'entry region' of the large virulence plasmid (LVP) (Sansonetti, 1991a). Like the SPIs, it appears that the LVP was originally acquired by *Shigella* through horizontal transfer.

The expression of a TTSS and other virulence genes is thought to represent a heavy metabolic burden on the bacterial cell that could compromise survival if inappropriately expressed. Therefore, both *Salmonella* and *Shigella* have evolved complex regulatory systems to sense environmental shifts to ensure virulence gene expression is strictly restricted to a given environment, such as the intestinal or the intracellular milieu (Dorman *et al.*, 2001; Jones, 2005; Rhen and Dorman, 2005). These virulence regulatory networks involve both proteins encoded within the virulence genetic element itself and also pleiotropic factors encoded by genes located on the chromosome. One of the most important of these chromosomally encoded regulators is the H-NS protein (Beloin and Dorman, 2003; O'Byrne and Dorman, 1994a). In addition, several other nucleoid-associated proteins including FIS, IHF, and Lrp are known to modulate *Salmonella* and *Shigella* virulence (Akbar *et al.*, 2003; Falconi *et al.*, 2001; Kelly *et al.*, 2004; Mangan *et al.*, 2006; Porter and Dorman, 1997a).

6.1.2 *Shigella* virulence gene regulation

The regulation of *Shigella* virulence gene expression has been extensively studied. Transcription of genes within the 31-kb 'entry region' of the LVP are required for invasion of epithelial cells and are tightly controlled through a regulatory cascade involving both chromosomal and plasmid-encoded regulatory proteins (Maurelli *et al.*, 1985; Sansonetti *et al.*, 1983; Sasakawa *et al.*, 1988). The *virF* and *virB* genes, both located on the LVP, encode the essential regulatory proteins, VirF and VirB, respectively. VirF is an AraC-like transcription factor that activates the *virB* gene and one of the structural genes, *icsA* (Falconi *et al.*, 1998; Nakayama and Watanabe, 1998; Porter and Dorman, 2002). In turn, the VirB protein binds to and activates transcription of all the remaining structural genes (Adler *et al.*, 1989; Beloin *et al.*, 2002; Tobe *et al.*, 1991). In addition, the chromosomally encoded nucleoid-associated proteins H-NS, IHF, and FIS contribute to the regulation of virulence gene expression. The FIS protein positively regulates transcription of the *virF* gene (Falconi *et al.*, 2001), while IHF activates both the *virF* and *virB* regulatory genes and also the *icsA* gene, a VirF-dependent structural gene (Porter and Dorman, 1997a). In contrast, the H-NS protein represses transcription of the virulence genes.

Under non-permissive conditions, H-NS acts as a transcriptional repressor by binding to the promoter regions of the *virF* and *virB* genes, and also to the VirB-dependent structural genes (Beloin and Dorman, 2003; Falconi *et al.*, 1998; Tobe *et al.*, 1993). At temperatures below 32°C, H-NS binds to the *virF* promoter at two sites, which are separated by an intrinsically bent region of DNA (Falconi *et al.*, 1998; Prosseda *et al.*, 1998; Prosseda *et al.*, 2004). Prosseda *et al.* (2004) reported that this intrinsic bend is responsible for the strict thermoregulation of *virF* gene expression. The bend abruptly melts at temperatures above 32°C, unmasking a binding site for the transcriptional activator FIS and also concomitantly displacing the repressor H-NS (Prosseda *et al.*, 2004). Thus, the temperature-dependent DNA conformation transition leads to increased transcription of the *virF* gene and subsequent activation of the *virB* promoter by VirF, and production of VirB (Dorman *et al.*, 2001). The VirB protein has no amino acid sequence similarity to previously described transcriptional

activators, but does closely resemble the plasmid partitioning proteins ParB and SopB (Abeles *et al.*, 1985; Bignell and Thomas, 2001; Watanabe *et al.*, 1990). VirB activates VirB dependent-promoters by oligomerizing along the DNA and displacing H-NS, thus acting as an H-NS antagonist or antirepressor (Mc Kenna *et al.*, 2003; Turner, E.C., and Dorman, C.J., unpublished data).

6.1.3 *Salmonella* virulence gene regulation

The expression of SPI-1 and SPI-2 is highly regulated by *Salmonella* in a temporal and spatial fashion. The SPI-1 island encodes the Inv/Spa TTSS, which is closely related to the Mxi-Spa TTSS of *Shigella* and is required by *S.* Typhimurium for epithelial cell invasion (Hardt *et al.*, 1998b; Mills *et al.*, 1995; Wood *et al.*, 1998). Optimal expression of SPI-1 occurs under conditions which approximate those in the gut lumen, i.e., low oxygen and high osmolarity (Bajaj *et al.*, 1996; Hansen-Wester and Hensel, 2001; Jones *et al.*, 1994). The more recently discovered SPI-2 island is essential for *Salmonella* intracellular survival and replication, and SPI-2 genes are related to the *ysc/lcr/yop* genes of *Yersinia* and the *esc/esp* genes of EPEC (Hansen-Wester and Hensel, 2001). Unlike SPI-1, very little is known about the environmental conditions that influence SPI-2 gene expression. Some studies report that low pH, Mg^{2+} deprivation, and phosphate starvation activates SPI-2, while other studies refute this (Beuzon *et al.*, 1999; Cirillo *et al.*, 1998; Deiwick *et al.*, 1999; Lee *et al.*, 2000; Miao *et al.*, 2002; Rathman *et al.*, 1996). Thus, the environmental conditions that induce SPI-2 is a contentious topic of investigation, but in general SPI-2 genes are preferentially expressed in the intracellular environment of the macrophage (Cirillo *et al.*, 1998; Valdivia and Falkow, 1997).

Although the expression of both *Salmonella* TTSSs is regulated in response to specific environmental factors, the mechanisms of regulation are significantly different. A common theme, however, is the control of gene expression by local regulators encoded by SPI-1 and SPI-2, and the modulation by global regulatory systems encoded by genes outside of the SPIs. For SPI-1, it is clear that HilA, encoded by SPI-1 itself, acts as a key factor in the induction of

invasion gene expression (Bajaj *et al.*, 1995; Bajaj *et al.*, 1996). HilA is a member of the ToxR/OmpR protein family and directly activates the expression of genes coding for both the SPI-1 TTSS machinery and effector proteins. In addition, HilA also indirectly regulates the *sip* operon due to its effect on the expression of the SPI-1-encoded AraC-like transcriptional regulator InvF (Darwin and Miller, 1999a; Kaniga *et al.*, 1994; Lucas and Lee, 2000). Although HilA is a central regulator of invasion within SPI-1, the expression of the *hilA* gene is itself controlled by two additional SPI-1 regulators, namely, HilC and HilD (Eichelberg and Galan, 1999; Johnston *et al.*, 1996; Schechter *et al.*, 1999). Both HilC and HilD are members of the AraC/XylS family of transcriptional regulators and activate *hilA* gene expression by directly binding to the *hilA* promoter (Boddicker *et al.*, 2003; Lucas and Lee, 2000; Olekhnovich and Kadner, 2004; Schechter and Lee, 2001). HilC and HilD can also directly activate virulence gene expression independently of HilA (Akbar *et al.*, 2003). In addition, SPI-1 expression is regulated by an array of proteins encoded outside of SPI-1, including EnvZ/OmpR, HilE, FliZ, Lon, PhoB, PhoP/Q, SirA/BarA, FimY/Z, CsrA, and RtsA (Bajaj *et al.*, 1996; Ellermeier and Slauch, 2003; Goodier and Ahmer, 2001; Lawhon *et al.*, 2003; Lucas and Lee, 2000; Lucas *et al.*, 2000; Takaya *et al.*, 2005). The nucleoid-associated proteins FIS, H-NS, Hha, and HU are also involved in the regulation of SPI-1 gene expression (Fahlen *et al.*, 2001; Schechter *et al.*, 2003; Wilson *et al.*, 2001). FIS is required for full expression of the *hilA* and *invF* regulatory genes and this positive effect is antagonized by H-NS (Wilson *et al.*, 2001). Under low osmolarity conditions H-NS and Hha strongly downregulate *hilA* gene expression by binding to sequences flanking the *hilA* promoter, which strongly suggests they might form a repressive DNA loop (Olekhnovich and Kadner, 2006).

In contrast to SPI-1, the regulation of SPI-2 has not been characterized in detail, but it is known to involve both SPI-2 and chromosomally encoded regulators. The SPI-2-encoded two-component regulatory system SsrA/SsrB is pivotal for the coordinate expression of SPI-2 genes (Ochman *et al.*, 1996; Worley *et al.*, 2000). SsrA belongs to the BvgS family of cytoplasmic membrane sensor proteins and SsrB is the response regulator of the two-component system. Once activated SsrB induces transcription of genes coding for the SPI-2

TTSS, chaperones and effector proteins (Worley *et al.*, 2000). In addition, SsrB also activates genes outside of SPI-2, including at least five genes encoding effectors proteins that are secreted by the SPI-2 TTSS (*sspH2*, *sseI*, *sseJ*, *sifA* and *sifB*) (Beuzon *et al.*, 2000; Miao and Miller, 2000; Worley *et al.*, 2000). The SsrA/B system is itself under the control of two other sensor–regulator systems, EnvZ/OmpR and PhoP/PhoQ, which positively act hierarchically upstream of SsrA/B (Bijlsma and Groisman, 2005; Lee *et al.*, 2000). The active phosphorylated form of OmpR (OmpR-P) directly binds to several sites within the promoter regions of the *ssrA* and *ssrB* genes, and subsequently activates transcription of both genes independently (Feng *et al.*, 2003; Lee *et al.*, 2000). In a more recent study, PhoP was also shown to bind directly to and to induce transcription of the *ssrB* gene (Bijlsma and Groisman, 2005). In addition, the PhoP/Q system was shown to positively regulate SsrA protein levels post-transcriptionally (Bijlsma and Groisman, 2005). Other positive regulators of SPI-2 include SlyA and the nucleoid associated protein FIS which activate transcription of the *ssrA/B* promoters and also several SPI-2 effector promoters (Kelly *et al.*, 2004; Linehan *et al.*, 2005). YdgT is the only known negative modulator of SPI-2 expression. However, it is still not clear whether this effect is direct or indirect (Coombes *et al.*, 2005b). Coombes *et al.* (2005) speculated that YdgT mediates its effect through another negative regulator, in particular H-NS, since H-NS and YdgT are known to form heteromeric complexes (Coombes *et al.*, 2005b; Paytubi *et al.*, 2004).

Like *Shigella, S.* Typhimurium harbours a high molecular weight virulence plasmid. Encoded within an 8-kb region of this plasmid is a cluster of genes termed the *spv* genes (Gulig *et al.*, 1992). The *spv* system consists of five genes designated *spvRABCD* and they are essential for *S.* Typhimurium to cause an efficient systemic infection (Gulig *et al.*, 1992; Gulig *et al.*, 1993). The *spvR* gene encodes a LysR-like positive regulator, which activates both its own expression and that of the structural genes (Coynault *et al.*, 1992). SpvR has been shown to bind to the *spvA* promoter in a hierarchical fashion at two sites, with binding to a proximal site being dependent on binding to a more distal site (Sheehan and Dorman, 1998). In addition to SpvR, many other factors have been implicated in the regulation of *spv* gene

expression. Like other virulence genes, environmental conditions play a part. The *spv* system is not significantly expressed by salmonellae during exponential growth in rich media, but is moderately induced when the bacteria enter the stationary phase of growth (Rhen and Dorman, 2005). The observed induction of *spv* expression *in vitro* as the cells enter stationary phase is dependent on the stationary phase sigma factor RpoS (Chen *et al.*, 1995). Similar to SPI-2, *spv* expression is strongly induced in low pH minimal medium at low divalent cation concentration (Deiwick *et al.*, 1999; Kim and Falkow, 2004), i.e., in a medium that mimics facets of the intravacuolar environment of *S.* Typhimurium. Consistent with this, several studies have shown *spv* gene induction in mice (Heithoff *et al.*, 1997) and following phagocytosis of *S.* Typhimurium by macrophages (Eriksson *et al.*, 2003; Marshall *et al.*, 2000). Other known regulators of the *spv* system include H-NS, IHF, Lrp, and CRP. The nucleoid-associated proteins H-NS and Lrp have been shown to repress *spv* gene expression in stationary phase (Marshall *et al.*, 1999; O'Byrne and Dorman, 1994a), as has the cAMP-receptor protein CRP (O'Byrne and Dorman, 1994b). In contrast, IHF has been shown to positively regulate the *spv* system in a supercoiling-dependent manner (Marshall *et al.*, 1999). Consistent with this, the *spv* promoters are sensitive to alterations in DNA superhelicity, with an increase in negative supercoiling causing a corresponding decrease in *spv* expression (O'Byrne and Dorman, 1994a).

Results from DNA microarray analysis revealed that *Salmonella* virulence gene expression was altered in strain SL1344(pSf-R27Δ*sfh*::Gent^R), compared to that in the wild-type strain SL1344, with and without plasmid pSf-R27Gent^R. Genes belonging to several *Salmonella* pathogenicity islands, in addition to the *spv* genes of the large virulence plasmid, were affected by the *sfh* mutation. These data suggest Sfh could have a role in modulating *Salmonella* virulence expression. The aim of this study was to investigate further the putative role for Sfh in regulating *Salmonella* virulence and also to determine if Sfh can interact with the *Shigella* virulence gene regulatory cascade.

6.2 Results

6.2.1 Impact of Sfh on *Shigella* virulence gene expression

H-NS is known to repress *Shigella* virulence gene expression under non-permissive conditions by repressing transcription of *virF* and *virB,* the gene coding for the master regulator of the *S. flexneri* virulence cascade and an intermediate regulatory gene subject to VirF-dependent activation, respectively (Beloin and Dorman, 2003; Falconi *et al.*, 1998; Tobe *et al.*, 1993). To determine if Sfh could also influence virulence gene expression in *S. flexneri* a *lacZ* reporter gene fusion to the *mxiC* gene, one of the VirB-dependent structural genes on the large virulence plasmid, was used to monitor the effect of *hns*, *stpA,* and *sfh* mutations on virulence gene expression. Samples for β-galactosidase analysis were harvested from L-broth cultures of the various strains being tested grown at 30°C or 37°C. Consistent with *Shigella* virulence expression, the *mxiC–lacZ* fusion displayed thermal regulation, being expressed at 37°C and repressed at 30°C (Fig. 6.1). At 30°C, *mxiC–lacZ* expression was repressed in strains lacking StpA and Sfh but derepressed in the *hns* mutant strain due to the absence of H-NS (Fig. 6.1). The strong repressive effect of H-NS, and in stark contrast the lack of effect of the StpA protein on virulence gene expression, was in agreement with previous studies (Hromockyj *et al.*, 1992; Maurelli and Sansonetti, 1988; Porter and Dorman, 1994; Porter, 1998). At 37°C, the permissive temperature, all three single mutant strains expressed the *mxiC–lacZ* fusion (Fig. 6.1).

The effect of *sfh* double mutations on *mxiC-lacZ* expression was also investigated. As expected, the *mxiC–lacZ* fusion was expressed in all strains at 37°C. In the *sfh stpA* double mutant *mxiC–lacZ* expression was repressed at 30°C due to the presence of H-NS, whereas in the *sfh hns* strain *mxiC–lacZ* expression was dramatically derepressed (Fig. 6.1). The combination of the *sfh* and *hns* mutations in the same cell resulted in a 1.5-fold enhancement of *mxiC–lacZ* expression levels compared those in an *hns* single mutant. Combining *hns* and *stpA* mutations in the same cell had no such additive effect. In contrast *mxiC–lacZ* expression levels were observed to be lower than those in the *hns* single mutant, presumably due to the

negative effect of increased Sfh expression in this strain (Fig. 6.1). Taken in aggregate, the transcriptional data obtained suggested that Sfh, in addition to H-NS, could influence *Shigella* virulence gene expression.

6.2.2 Sfh binds to the promoter regions of the *virF* and *virB* genes

In previous work, H-NS has been shown to bind to the promoter regions of the *virF* and *virB* genes, thereby repressing *Shigella* virulence gene expression under non-permissive conditions (Beloin and Dorman, 2003; Maurelli and Sansonetti, 1988; Tobe *et al.*, 1993). In light of this, the ability of Sfh to bind to these promoter regions was investigated using a competitive EMSA. DNA fragments encompassing the *virF* (nt –325 to +151 with respect to the translation initiation codon of the *virF* gene) and *virB* (nt –325 to +151 with respect to the translation initiation codon of the *virB* gene) regulatory promoter regions were amplified by PCR, using the primer pairs virF-F virF-R and virB-F virB-R, respectively (Table 2.3). DNA fragments from *Taq*1–*Ssp*I digested pBR322 DNA (which acts as competitor DNA in the EMSA) was then mixed with the *virB* or *virF* promoter amplimer. One of the pBR322 DNA restriction fragments contains the intrinsically curved promoter region *bla* gene, which is known to bind H-NS-like proteins (Bertin *et al.*, 1999; Lucht *et al.*, 1994; Zuber *et al.*, 1994). The DNA mixture was then incubated with increasing concentrations of purified Sfh, and resolved by electrophoresis through 3% molecular screening agarose. The electrophoretic mobilities of the *virF* and *virB* promoter fragments were retarded specifically by Sfh in concentration-dependent manners (Fig. 6.2). Sfh also shifted the mobility of the *bla* positive control band. These data indicate that, like H-NS, Sfh can potentially repress expression of the VirB protein and, thus, are consistent with the observed ability of Sfh to repress transcription of the *mxiC–lacZ* fusion.

Fig. 6.1. Effect of Sfh on virulence gene expression in *S. flexneri*.

(A) Schematic map of the 31-kb invasion region of *S. flexneri*. The locations of the promoters of the three operons and the insertion site of the MudI*1734* transcriptional fusion within the *mxiC* gene are indicated. (B) Histograms show the activity of the *mxiC–lacZ* fusion in wild-type strain BS184 and its *stpA, hns, sfh, sfh stpA,* and *sfh hns* mutant derivatives. β-galactosidase assays were performed on strains cultured in L-broth to stationary phase at 30°C (grey bars) and 37°C (black bars). The results are an average of three independent experiments and error bars represent standard deviations.

A.

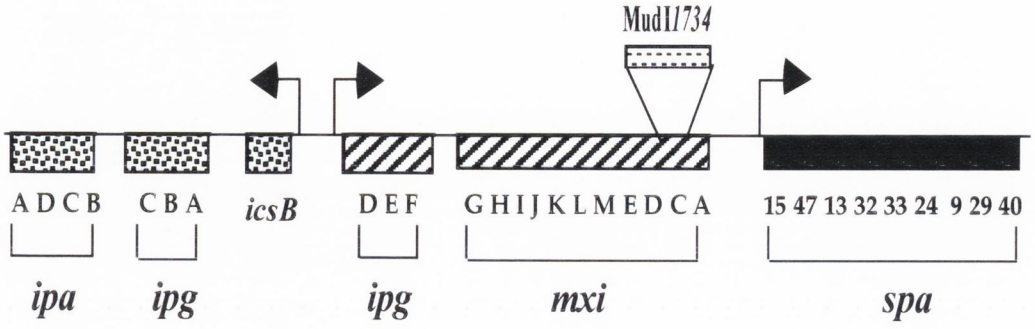
MudI1734
A D C B
C B A
icsB
D E F
G H I J K L M E D C A
15 47 13 32 33 24 9 29 40
ipa
ipg
ipg
mxi
spa

B.

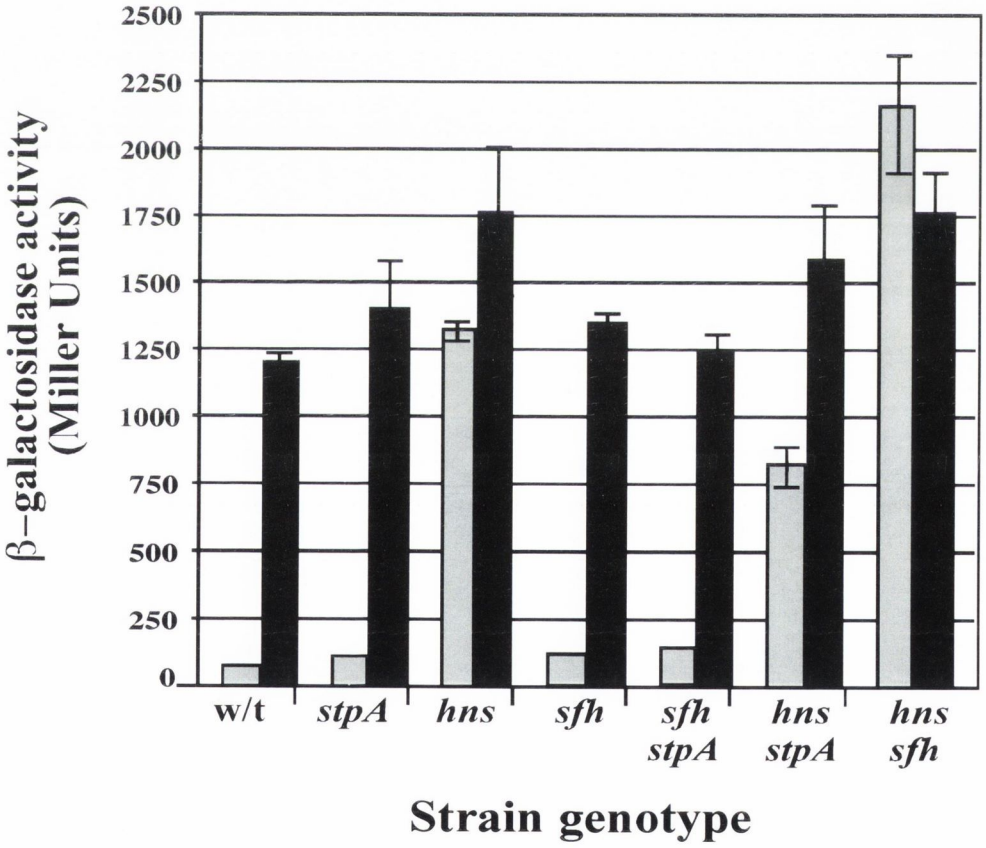
β–galactosidase activity (Miller Units)
2500
2250
2000
1750
1500
1250
1000
750
500
250
0
w/t
stpA
hns
sfh
sfh stpA
hns stpA
hns sfh
Strain genotype

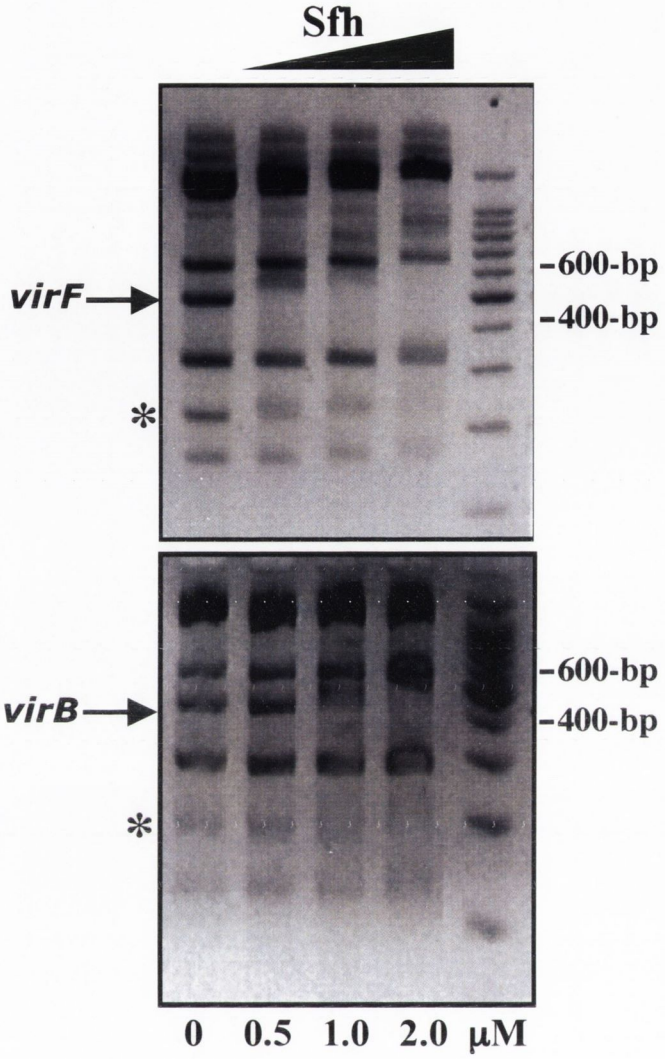

Fig. 6.2. Direct interaction of Sfh with the *virF* and *virB* promoter regions. Competitive gel retardation assays showing the specific binding of Sfh to the *virF* and *virB* promoter regions. The plasmid pBR322 was digested with restriction endonucleases *Taq*1 and *Ssp*I, and the resulting DNA fragments mixed with a 478-bp PCR amplimer of the *virF* promoter region or a 450-bp PCR amplimer of the *virB* promoter region. The DNA mixtures were incubated with increasing concentrations of Sfh in the range 0 μM to 2 μM. Arrows and an asterisk indicate the position of the *virF, virB* and *bla* promoter fragments, respectively. The curved *bla* promoter is a positive control known to bind H-NS-like proteins. The positions of the 600-bp and 400-bp molecular size markers are also indicated.

6.2.3 Cloning of SPI-1 promoters

Preliminary experiments using DNA microarray analysis indicated a potential role for Sfh in *Salmonella* virulence gene expression (Chapter 5). In particular, the data implied Sfh-regulated genes belonging to the two key *Salmonella* pathogenicity islands SPI-1 and SPI-2. To investigate this further, several *lacZ* promoter fusions to SPI-1 genes were constructed. For a comprehensive study, the constructs were designed to encompass regulatory and TTSS structural and effector proteins encoded by the pathogenicity island. Using data from DNA microarray analysis and previous reports on the transcriptional organization of SPI-1, regions of interest thought likely to contain promoters were identified and amplified by PCR. A 539-bp DNA fragment upstream of the *hilD* gene, which potentially contains the promoter for SPI-1 transcriptional regulator, was amplified using primers hilD-F and hilD-R (Table 2.3). Data from DNA microarray analysis also strongly indicated that the intergenic region between the SPI-1 genes *sicA* and *sipB* contained a promoter for SPI-1 secreted effectors. For this reason a 468-bp DNA fragment upstream of the *sipB* gene was amplified using primers sipB-F and sipB-R (Table 2.3). The two DNA fragments mentioned above were cloned into plasmid pQF50 upstream of the promoterless *lacZ* gene to generate plasmids pQFhilD and pQFsipB, respectively (Fig. 6.3). To confirm correct insertion of the DNA fragments into the vector, plasmid DNA was isolated from clones and sequenced. Using these plasmids, along with plasmids pQFssrA and pQFsseA (Table 2.2), SPI-1 and SPI-2 transcriptional activity was assayed to ascertain to what extent Sfh is involved in their gene regulation.

6.2.4 Impact of plasmids pSf-R27Gent^R and pSf-R27Δ*sfh*::Gent^R on SPI-1 gene regulation

Regulation of SPI-1 gene expression is complex and involves both regulatory proteins encoded on the pathogenicity island and also an array of chromosomally encoded proteins and environmental stimuli. Preliminary data from DNA microarray analysis suggested that Sfh, encoded by plasmid pSf-R27Gent^R, could also be part of the SPI-1 regulatory network (Chapter 5). Transcriptional activity of genes belonging to all the SPI-1 functional classes –

regulatory, structural and effector – were affected by the *sfh* mutation. SPI-1 secreted effectors SipB and SipC, in addition to the structural protein PrgK, showed enhanced expression in the absence of Sfh irrespective of growth phase (Fig. 5.13). In contrast, expression of the genes *invG* (encodes a putative structural component of the type III secretory apparatus) and *hilD* (encodes a positive regulator of SPI-1) were Sfh-activated in exponential phase, but Sfh-repressed in stationary phase (Fig. 5.13). However, the *invG* and *hilD* genes only showed a moderate increase in expression during stationary phase of growth in an *sfh*$^-$ background. To confirm these data and a role for Sfh in SPI-1 regulation, gene expression assays were performed utilizing plasmids pQFhilD and pQFsipB (Section 6.2.3). The plasmids were transformed into strains SL1344, SL1344(pSf-R27Gent^R), SL1344(pSf-R27Δ*sfh*::Gent^R) and also the complemented mutant strain SL1344(pSf-R27Δ*sfh*::Gent^R, pYCsfh$^+$). Samples for β-galactosidase analysis were harvested from exponential phase (OD_{600nm} ~0.6) and stationary phase (OD_{600nm} ~2) L-broth cultures grown under conditions identical to those used for DNA microarray analysis.

The results of β-galactosidase analysis showed a dramatic induction of *hilD* gene transcription in the presence of plasmid pSf-R27Gent^R (Fig. 6.4). Consistent with the microarray data, deletion of *sfh* from plasmid pSf-R27 resulted in a decrease in *hilD–lacZ* fusion expression in exponential phase and a slight increase in expression in stationary phase. Complementation of the *sfh* mutation with the multi-copy plasmid pYCsfh$^+$ caused a significant reduction in *hilD* transcription irrespective of growth phase (Fig. 6.4), indicating that Sfh can repress *hilD* transcription under at least some conditions. In all the plasmid-bearing strains, *hilD–lacZ* transcription levels were considerably elevated compared to those observed in the wild-type strain SL1344 (Fig. 6.4). Taken together, the β-galactosidase data suggest that introduction of plasmid pSf-R27Gent^R or plasmid pSf-R27Δ*sfh*::Gent^R into strain SL1344 leads to a significant induction of *hilD* transcription. However, these data are contradictory to those obtained from the microarray study, which showed *hilD* gene expression levels to be comparable in strains SL1344 and SL1344(pSf-R27Gent^R). This inconsistency is probably due to the putative nature of the *hilD* promoter region cloned into the *lacZ* reporter vector

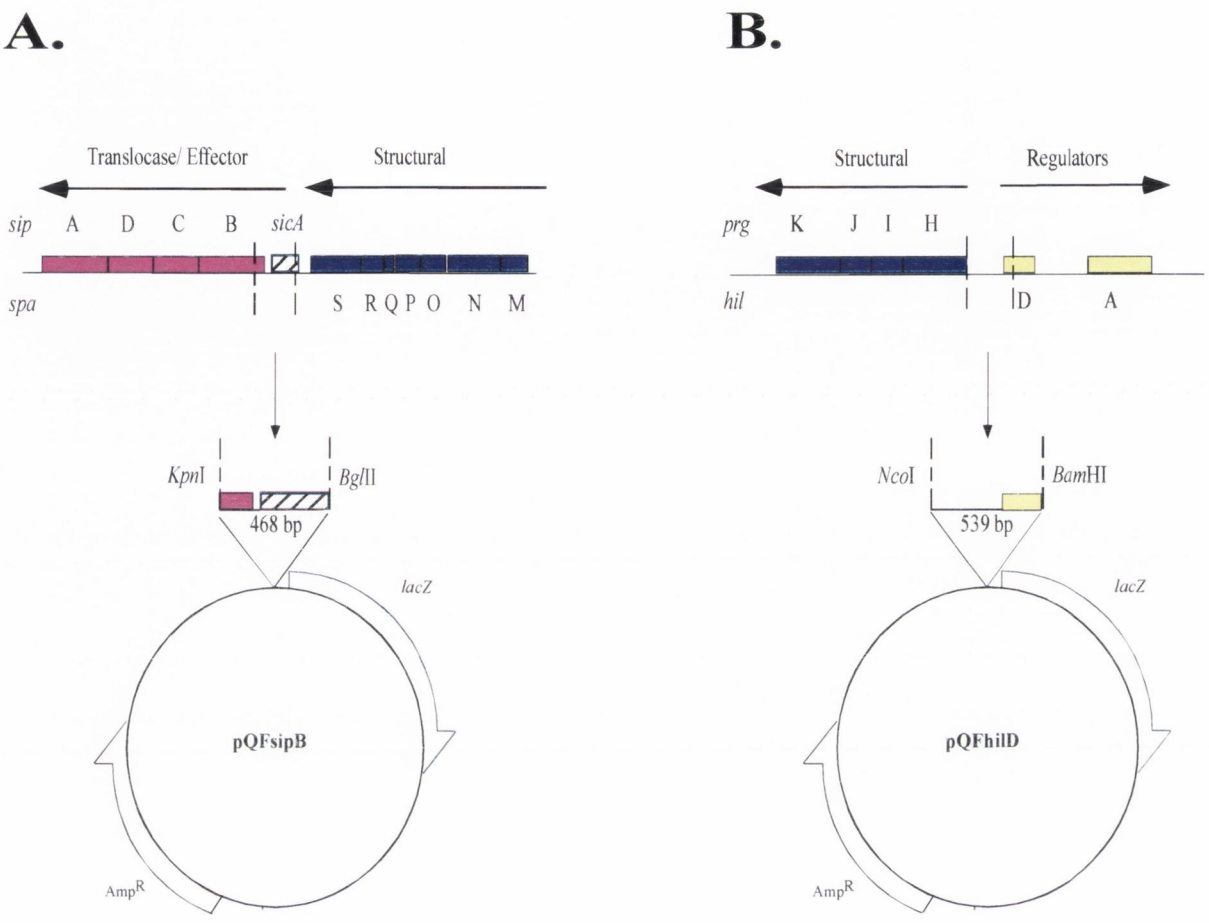

Fig. 6.3. Construction of SPI-1 promoter fusion plasmids. Regions of DNA thought to contain SPI-1 promoters were amplified by PCR and ligated into the multiple cloning site of plasmid pQF50 upstream of the promoterless *lacZ* gene. (A) A 468-bp section of DNA incorporating the 5′-region of the *sipB* gene, the *sipB–sicA* intergenic region, and part of the *sicA* gene was cloned into plasmid pQF50 to generate plasmid pQFsipB. (B) A 539-bp section of DNA incorporating the 5′-region of the *hilD* gene and the upstream *hilD–prgH* intergenic region was cloned into plasmid pQF50 to generate plasmid pQFhilD.

Fig. 6.4. Impact of plasmids pSf-R27Gent^R and pSf-R27Δ*sfh*::Gent^R on SPI-1 promoter fusions. Histograms show the activity of (A) *hilD–lacZ* and (B) *sipB–lacZ* transcriptional fusions in the wild-type strain SL1344 and its plasmid bearing derivatives SL1344(pSf-R27Gent^R), SL1344(pSf-R27Δ*sfh*::Gent^R) and SL1344(pSf-R27Δ*sfh*::Gent^R, pYCsfh$^+$). β–galactosidase assays were performed on strains cultured in L-broth to exponential (grey bars) and stationary phase (black bars) at 37°C. The data represent an average of at least three independent experiments and error bars represent standard deviations.

A.

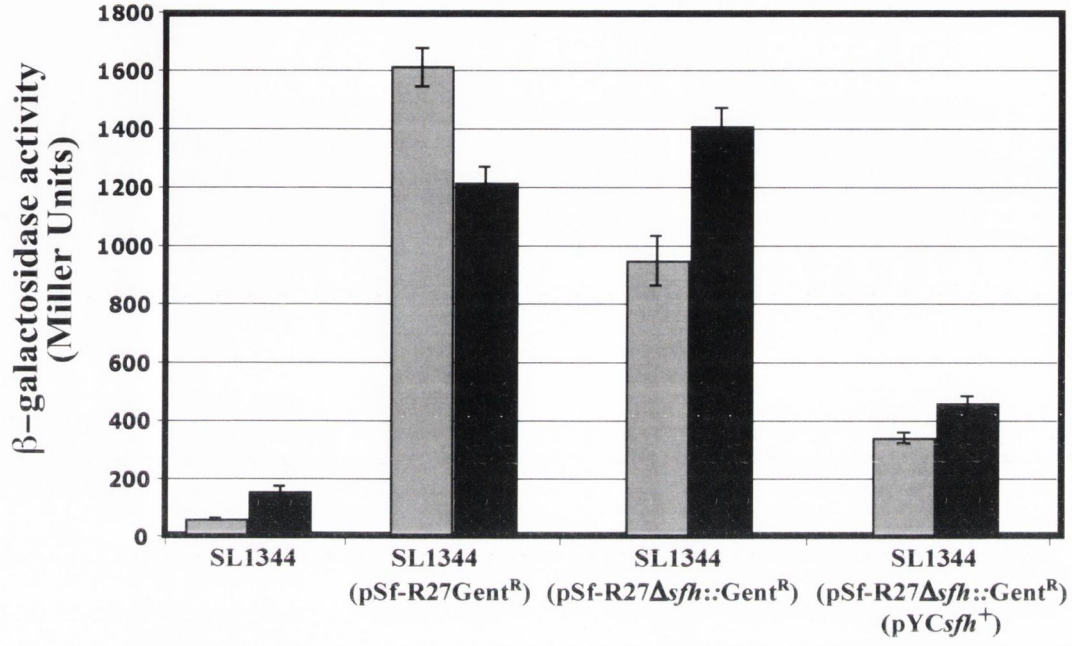
β–galactosidase activity (Miller Units)
1800
1600
1400
1200
1000
800
600
400
200
0
SL1344
SL1344 (pSf-R27Gent^R)
SL1344 (pSf-R27Δ*sfh*::Gent^R)
SL1344 (pSf-R27Δ*sfh*::Gent^R) (pYC*sfh*$^+$)

B.

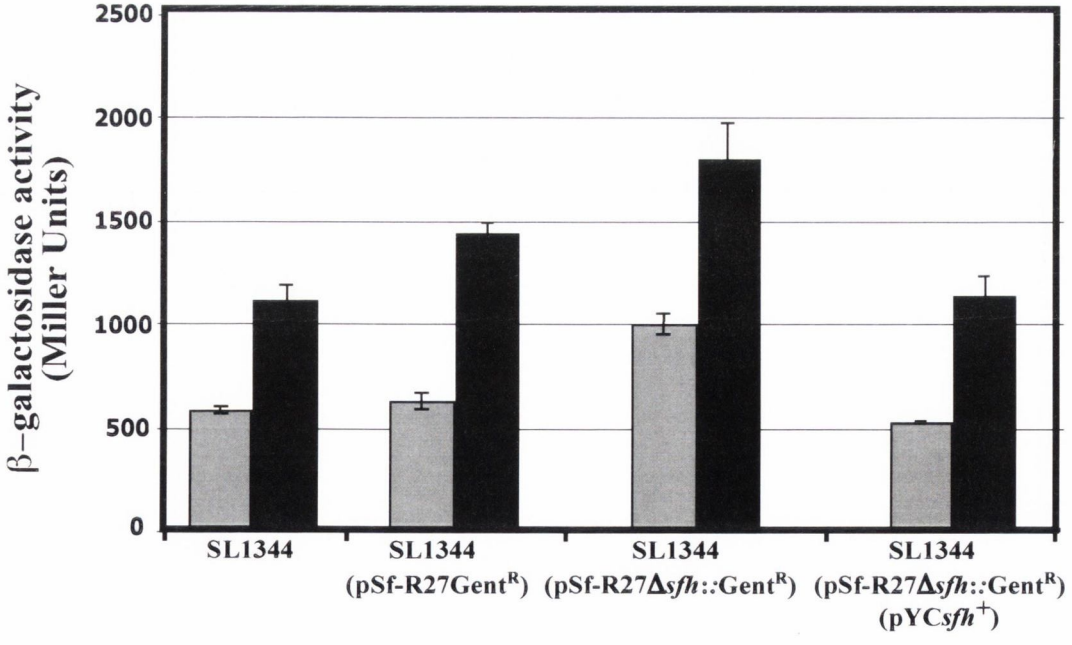
β–galactosidase activity (Miller Units)
2500
2000
1500
1000
500
0
SL1344
SL1344 (pSf-R27Gent^R)
SL1344 (pSf-R27Δ*sfh*::Gent^R)
SL1344 (pSf-R27Δ*sfh*::Gent^R) (pYC*sfh*$^+$)

pQFhilD. In agreement with the microarray data, β-galactosidase analysis determined that transcription of the SPI-I secreted effector gene *sipB* is upregulated in the *sfh* mutant compared to strain SL1344 with and without plasmid pSf-R27Gent^R (Fig. 6.4). Furthermore, expression of Sfh *in trans* from a multi-copy plasmid resulted in ~2-fold reduction in *sipB* transcription, confirming once more the negative regulatory effect of Sfh on the *sipB* gene (Fig. 6.4).

6.2.5 Impact of plasmids pSf-R27 Gent^R and pSf-R27Δ*sfh*::Gent^R on SPI-2 gene regulation

Unlike SPI-1, SPI-2 gene regulation has not been elucidated in detail. The only known regulators of SPI-2 gene expression are SlyA, YdgT and the two-component signal transduction systems SsrA/B, OmpR/EnvZ and PhoP/Q (Bijlsma and Groisman, 2005; Coombes *et al.*, 2005b; Lee *et al.*, 2000; Linehan *et al.*, 2005; Ochman *et al.*, 1996; Worley *et al.*, 2000). DNA microarray analysis revealed that Sfh could influence expression of several genes belonging to SPI-2 (Chapter 5) and, thus, that Sfh could be a novel SPI-2 regulator. SPI-2 genes coding for regulatory, TTSS structural, and effector proteins were among those affected by Sfh (Fig. 5.11). The *ssaQ* gene (encodes a putative structural component of the type III secretory apparatus), the *sseA* gene (encodes a chaperone for SseB and SseD), and the *ssrB* gene (encodes the response regulator of the SsrA/B two-component regulatory system) were all Sfh-activated in exponential phase as determined from DNA microarray analysis (Fig. 5.11). In addition, DNA microarray analysis showed that the SPI-2 regulatory gene *ssrA* (encodes the histidine kinase of the SsrA/B two-component regulatory system) was the only virulence gene significantly affected by the introduction of plasmid pSf-R27Gent^R into strain SL1344 under the growth conditions tested (Supplementary data).

The SsrA/B two-component signal transduction system is central to the induction of SPI-2 gene expression (Cirillo *et al.*, 1998). Consequently, expression from the *ssrA* promoter is considered a good indication of SPI-2 expression in general. To confirm a role for Sfh in SPI-2 regulation, β-galactosidase analyses was performed using *lacZ* transcriptional fusions

to the *ssrA* and *sseA* genes, in the presence and absence of Sfh. Plasmids pQFssrA and pQFsseA were a kind gift from R. Carroll (University of Dublin, Ireland) and harbour the known *ssrA* promoter (Carroll, 2003; Feng *et al.*, 2003) and putative *sseA* promoter cloned upstream of the promoterless *lacZ* reporter gene in the plasmid pQF50, respectively (Table 2.3). The plasmids were transformed into strains SL1344, SL1344(pSf-R27Gent^R), and SL1344(pSf-R27Δ*sfh*::Gent^R). In addition, the *sfh* mutant strain SL1344(pSf-R27Δ*sfh*::Gent^R) was complemented with plasmid pYCsfh$^+$. Samples for β-galactosidase analysis were harvested from exponential phase (OD_{600nm} ~0.6) and stationary phase (OD_{600nm} ~2) L-broth cultures grown under conditions identical to those previously used for DNA microarray analysis.

Consistent with the DNA microarray data, β-galactosidase analysis showed a negative effect of Sfh on *ssrA* gene expression (Fig. 6.5). In the presence of plasmid pSf-R27Gent^R, *ssrA* transcription was repressed in stationary phase, the stage of the growth cycle when SPI-2 expression is normally induced (Fig. 6.5; Hansen-Wester and Hensel, 2001). However, by inactivating the *sfh* gene on plasmid pSf-R27 this repression was alleviated and *ssrA–lacZ* expression levels were restored to levels similar to those in wild-type strain SL1344 without the plasmid pSf-R27Gent^R (Fig. 6.5). Furthermore, expression of Sfh *in trans* from a multi-copy plasmid resulted in a significant reduction of *ssrA* transcription, irrespective of growth phase (Fig. 6.5). Taken together, these data indicate that Sfh is a negative regulator of the key SPI-2 two-component system SsrA/B. β-Galactosidase analysis also confirmed that transcription of the SPI-2 chaperone gene *sseA* is downregulated in the *sfh* mutant compared to strain SL1344 with and without plasmid pSf-R27Gent^R (Fig. 6.5). The *sseA–lacZ* fusion displayed growth phase-dependent regulation, being induced in stationary phase, which is consistent with previous studies (Fig. 6.5). However, when the *sfh* mutation was complemented with the multi-copy plasmid pYCsfh$^+$, *sseA* gene expression was dramatically repressed (Fig. 6.5). This apparent anomaly is probably due to the decrease in expression of the two-component system SsrA/B in strain SL1344(pSf-R27Δ*sfh*::Gent^R, pYCsfh$^+$), which would subsequently cause repression of SPI-2 gene expression, including the *sseA* gene.

Fig. 6.5. Impact of plasmids pSf-R27Gent^R and pSf-R27Δ*sfh*::Gent^R on SPI-2 promoter fusions. Histograms show the activity of (A) *ssrA–lacZ* and (B) *sseA–acZ* transcriptional fusions in the wild-type strain SL1344 and its plasmid bearing derivaives SL1344(pSf-R27Gent^R), SL1344(pSf-R27Δ*sfh*::Gent^R) and SL1344(pSf-R27Δ*sfh*::Gent^R, pYCsfh$^+$). β–galactosidase assays were performed on strains cultured in L-broth to exponential (grey bars) and stationary phase (black bars) at 37°C. The data represent an average of at least three independent experiments and error bars represent standard deviations.

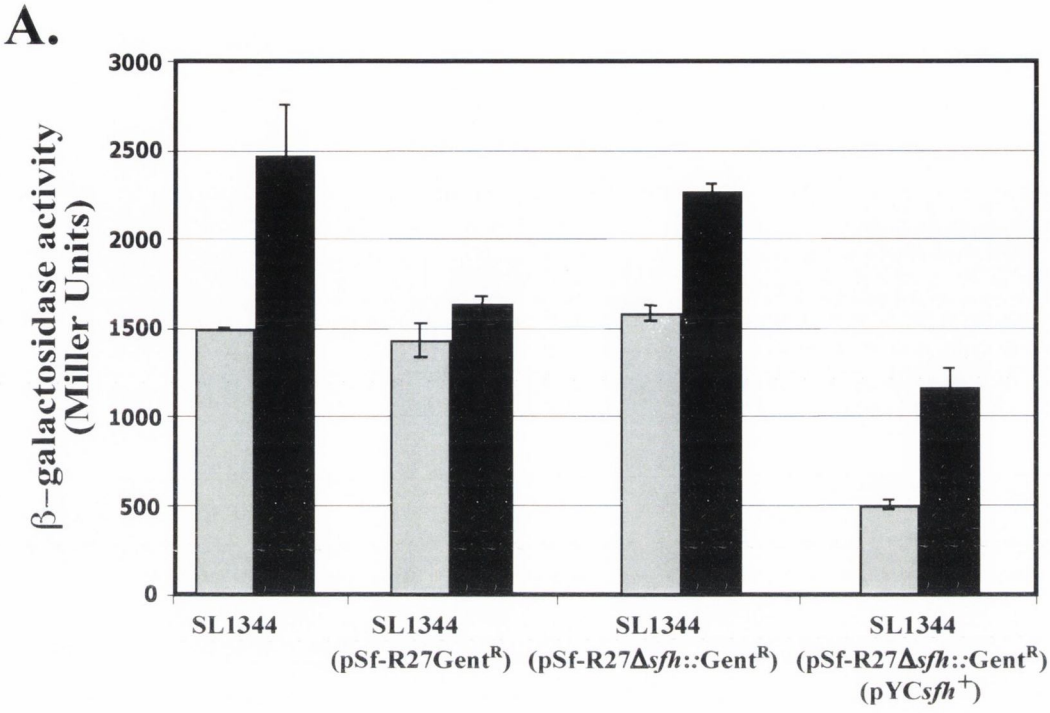
A.
β–galactosidase activity (Miller Units)
3000
2500
2000
1500
1000
500
0
SL1344
SL1344 (pSf-R27Gent^R)
SL1344 (pSf-R27Δsfh::Gent^R)
SL1344 (pSf-R27Δsfh::Gent^R) (pYCsfh^+)

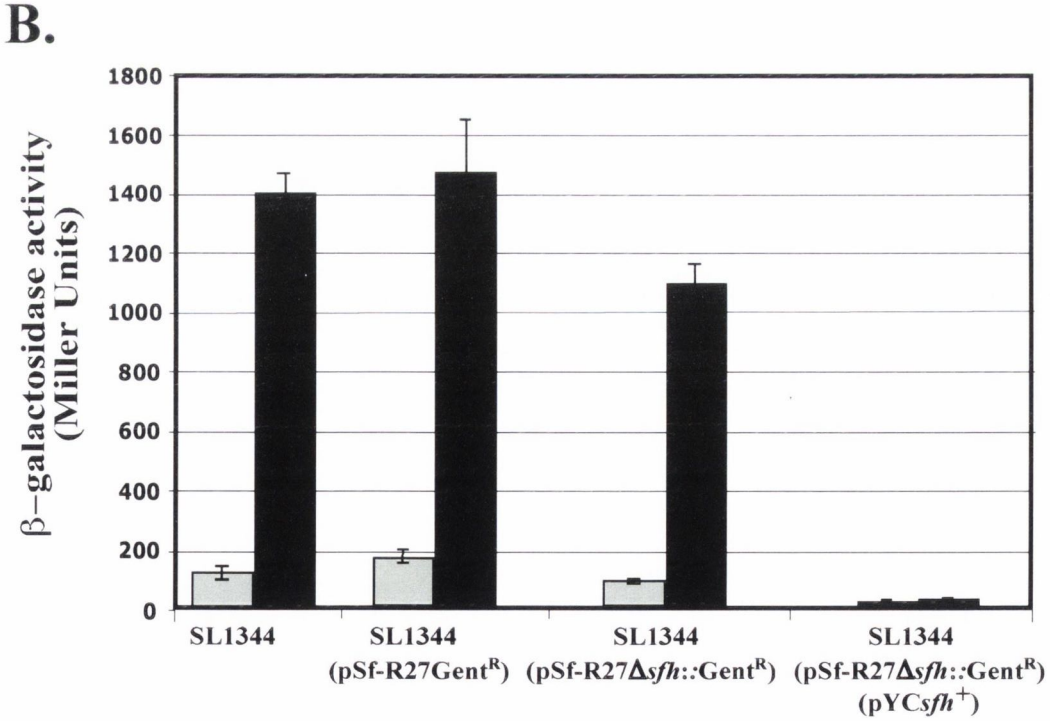
B.
β–galactosidase activity (Miller Units)
1800
1600
1400
1200
1000
800
600
400
200
0
SL1344
SL1344 (pSf-R27Gent^R)
SL1344 (pSf-R27Δsfh::Gent^R)
SL1344 (pSf-R27Δsfh::Gent^R) (pYCsfh^+)

6.2.6 Impact of plasmids pSf-R27Gent^R and pSf-R27Δ*sfh*::Gent^R on the *spv* gene cluster

The *spvRABCD* gene cluster, which is common to the virulence plasmids of many serovars of *Salmonella*, is essential for the development of a systemic infection in mice (Gulig *et al.*, 1992; Gulig *et al.*, 1993). The *spv* cluster is expressed from two main promoters, one situated upstream of the *spvR* gene and the other in front of the *spvA* gene. Several studies have demonstrated that the *spv* genes are poorly expressed by salmonellae growing exponentially in rich media, but are induced in stationary phase (Chen *et al.*, 1995; Coynault *et al.*, 1992; O'Byrne and Dorman, 1994b). Results from DNA microarray analysis indicated that Sfh could be a negative regulator of *spv* gene expression during growth in rich media (Supplementary data). To ascertain whether Sfh was involved in regulating *spv* gene expression, the transcriptional activities of the *spvR* and *spvB* genes were measured using the plasmids p671 and pQF(R:101) in the presence and absence of Sfh (Table 2.2). Plasmid pQF(R:101) harbours the *spvR* promoter upstream of the promoterless *lacZ* reporter gene plasmid pQF50 (Sheehan and Dorman, 1998). The *Salmonella* virulence plasmid p671, isolated from strain CJD671 (Table 2.1), contains a MudJ insertion in the *spvB* gene. This creates a *spvB–lacZ* transcriptional fusion that can be used to monitor *spv* structural gene expression. Both plasmids were transformed separately into strains SL1344, SL1344(pSf-R27Gent^R), SL1344(pSf-R27Δ*sfh*::Gent^R) and SL1344 (pSf-R27Δ*sfh*::Gent^R, pYC*sfh*$^+$). Samples for β-galactosidase analysis were harvested from exponential phase (OD_{600nm} ~0.6) and stationary phase (OD_{600nm} ~2) L-broth cultures grown under conditions identical to those used for DNA microarray analysis.

In agreement with DNA microarray analysis, data obtained from β-galactosidase assays showed an increase in *spv* gene expression in the absence of Sfh (Fig. 6.6). In an *sfh*$^-$ background, transcription from the *spvR* promoter was upregulated in stationary phase. Surprisingly, the introduction of plasmid pSf-R27Gent^R into strain SL1344 did not cause any significant changes in *spvR* gene expression (Fig. 6.6). However, when Sfh was expressed from a multi-copy plasmid there was over a 2-fold reduction in *spvR–lacZ* expression (Fig. 6.6). Because transcription of the *spvABCD* genes is SpvR dependent, it was predicted that

Sfh would also have a negative effect on expression of these genes. Consistent with this, data obtained from the single copy *spvB–lacZ* fusion were nearly identical to those observed with the *spvR–lacZ* transcriptional fusion (Fig. 6.6). Taken together, these results support a role for Sfh in *spv* gene regulation.

6.2.7 Sfh directly binds to *Salmonella* virulence promoters

The expression of a wide range of *Salmonella* virulence genes was altered by the introduction of plasmid pSf-R27Δ*sfh*::Gent^R into strain SL1344. To assess the possibility that this involved a direct effect of Sfh on virulence gene transcription, the interaction of purified Sfh with the promoter regions of the representative SPI-1, SPI-2, and *spv* genes used in the β-galactosidase transcriptional assays above was investigated. Since H-NS-like proteins are known to preferentially bind intrinsically curved DNA (Bracco *et al.*, 1989; Owen-Hughes *et al.*, 1992; Yamada *et al.*, 1990), the intrinsic curvature of the various promoters under investigation was also analysed *in silico* using the BEND-IT computer program (http://www.icgeb.org/dna/bend_it.html). The curvature propensity plots of all the virulence regulatory regions being examined revealed they possessed regions of DNA curvature, supporting the model that Sfh could be directly binding to them and affecting virulence gene transcription (Fig. 6.7 – 6.12).

Firstly, the interaction of purified Sfh with the SPI-1 *hilD* and *sipB* promoters was examined by competitive EMSAs. DNA fragments encompassing either the *hilD* or *sipB* regulatory region were added to *Taq*1-*Ssp*I-digested pBR322 DNA and then incubated with increasing concentrations of purified Sfh. The electrophoretic mobilities of the *hilD* (Fig. 6.7) and *sipB* (Fig. 6.8) promoter fragments were observed to be specifically retarded by Sfh in concentration-dependent manners. In a parallel experiment both the *hilD* and *sipB* promoter regions were shifted specifically by the Sfh paralogous protein H-NS (Fig 6.7 and 6.8). Previous studies have shown the H-NS protein represses *spv* gene expression and that this involves a direct effect at the *spv* promoters (O'Byrne and Dorman, 1994a). This study

Fig. 6.6. Impact of plasmids pSf-R27Gent^R and pSf-R27Δ*sfh*::Gent^R on *spv* promoter fusions. Histograms show the activity of (A) *spvR–lacZ* and (B) *spvB–lacZ* transcriptional fusions in the wild-type strain SL1344 and its plasmid-bearing derivatives SL1344(pSf-R27Gent^R), SL1344(pSf-R27Δ*sfh*::Gent^R) and SL1344(pSf-R27Δ*sfh*::Gent^R, pYCsfh$^+$). β–galactosidase assays were performed on strains cultured in L-broth to exponential (grey bars) and stationary phase (black bars) at 37°C. The data represent an average of at least three independent experiments and error bars represent standard deviations.

A.

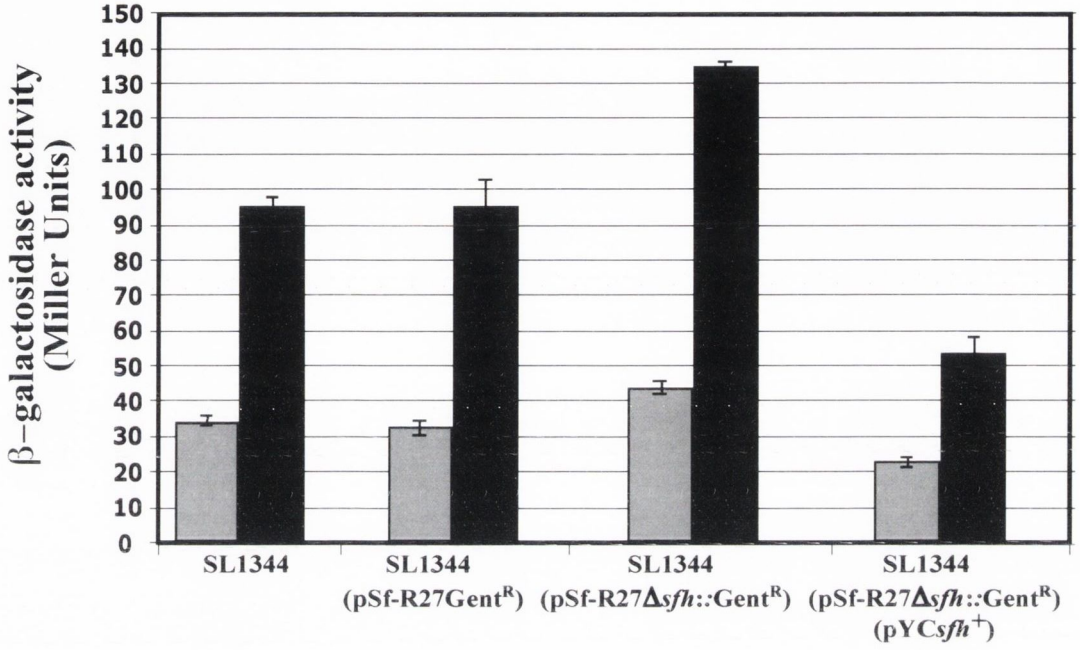
β–galactosidase activity (Miller Units)
150
140
130
120
110
100
90
80
70
60
50
40
30
20
10
0
SL1344
SL1344 (pSf-R27Gent^R)
SL1344 (pSf-R27Δ*sfh*::Gent^R)
SL1344 (pSf-R27Δ*sfh*::Gent^R) (pYC*sfh*$^+$)

B.

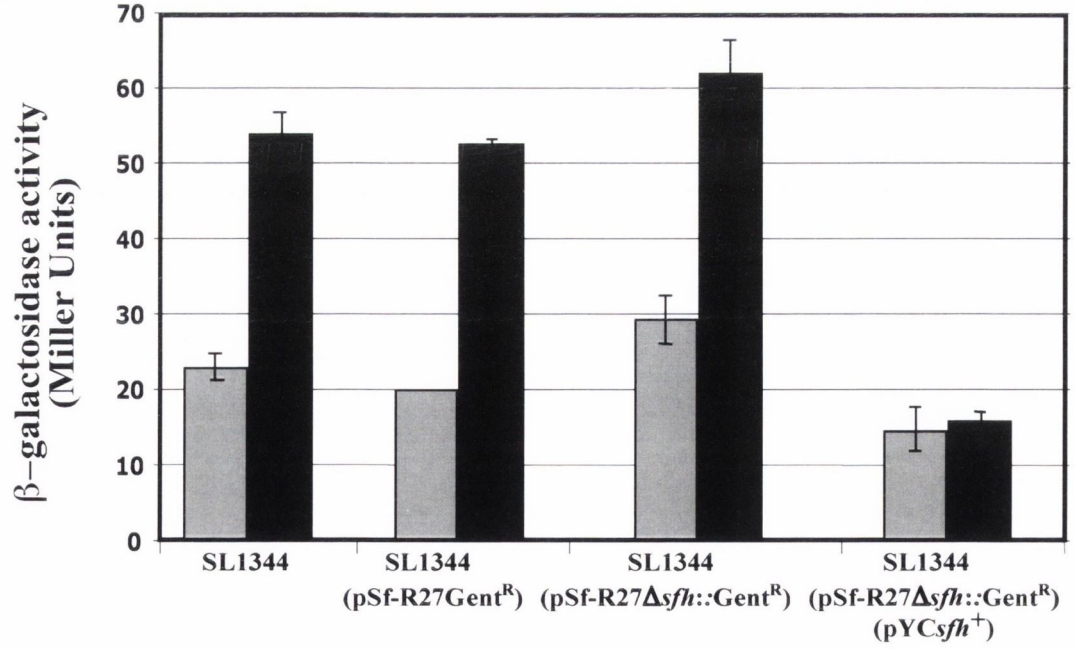
β–galactosidase activity (Miller Units)
70
60
50
40
30
20
10
0
SL1344
SL1344 (pSf-R27Gent^R)
SL1344 (pSf-R27Δ*sfh*::Gent^R)
SL1344 (pSf-R27Δ*sfh*::Gent^R) (pYC*sfh*$^+$)

Fig. 6.7. Direct interaction of Sfh and H-NS with the *hilD* promoter region.

(A) DNA curvature analysis of the *hilD* promoter region. Graph shows the predicted intrinsic curvature of the *hilD* regulatory region using the computer program BEND-IT. Curvature is expressed as degrees per helical turn and plotted against the position on the promoter sequence, with +1 corresponding to the *hilD* translation initiation codon. Curved and straight motifs have a value above or below 5 degrees per helical turn, respectively. Regions of intrinsic DNA curvature are arrowed. (B) Competitive gel retardation assays showing the specific binding of Sfh and H-NS to the *hilD* promoter region. A 539-bp DNA fragment encompassing the *hilD* regulatory region (nt –303 to +236 with respect to the translation initiation codon of the *hilD* gene) was amplified by PCR using the primer pair hilD-F and hilD-R (Table 2.3). The plasmid pBR322 was digested with restriction endonucleases *Taq*1 and *Ssp*I, and the resulting DNA fragments mixed with the 539-bp amplimer of the *hilD* promoter region. The DNA mixtures were incubated with increasing concentrations of Sfh or H-NS in the range 0 μM to 2 μM. An arrow and an asterisk indicate the position of the *hilD* and *bla* promoter fragments, respectively. The curved *bla* promoter is a positive control known to bind H-NS-like proteins. The positions of the 600-bp and 400-bp molecular size markers are also indicated.

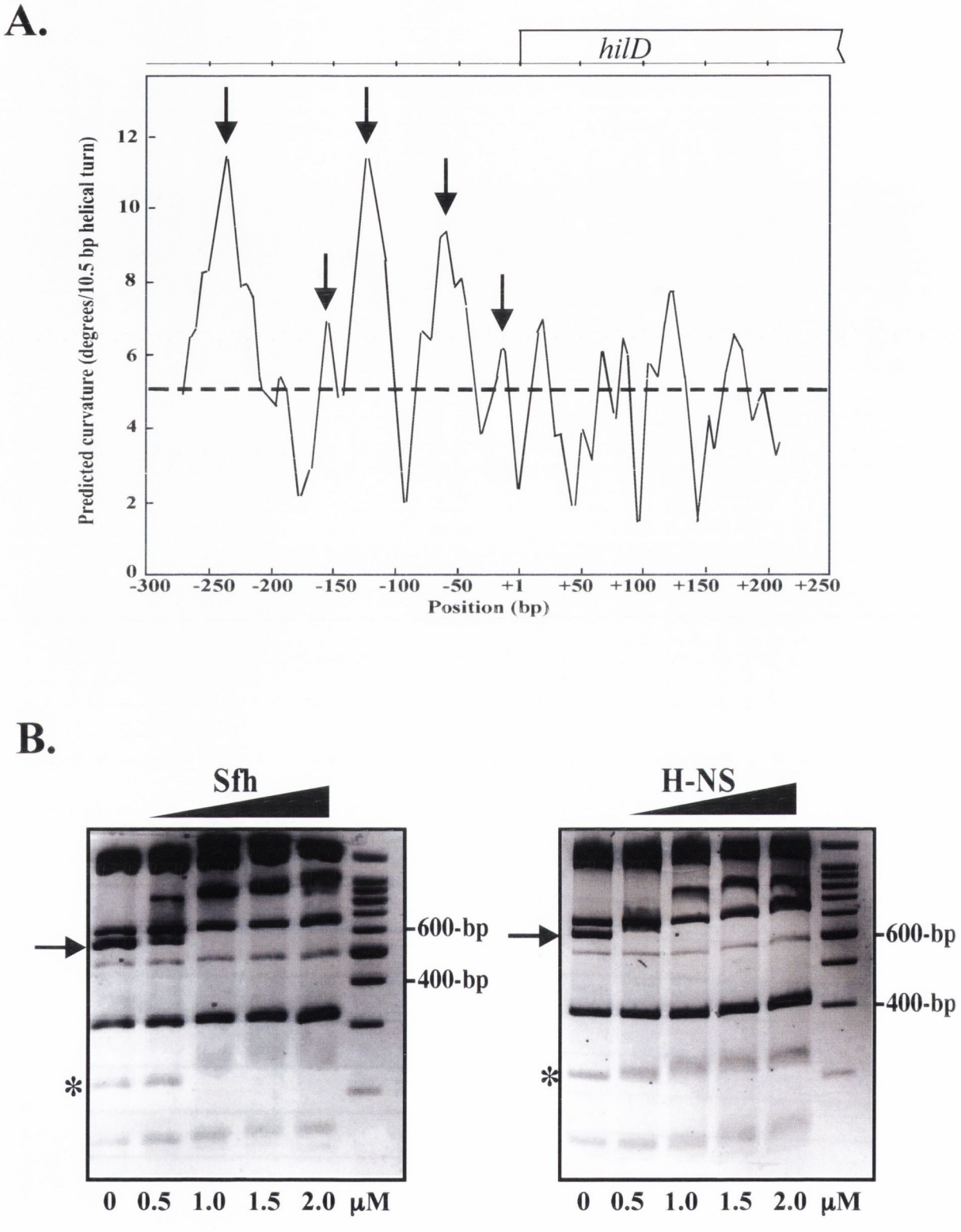
A.
hilD
Predicted curvature (degrees/10.5 bp helical turn)
0
2
4
6
8
10
12
-300
-250
-200
-150
-100
-50
+1
+50
+100
+150
+200
+250
Position (bp)
B.
Sfh
H-NS
600-bp
400-bp
600-bp
400-bp
*
*
0 0.5 1.0 1.5 2.0 μM
0 0.5 1.0 1.5 2.0 μM

Fig. 6.8. Direct interaction of Sfh and H-NS with the *sipB* promoter region.

(A) DNA curvature analysis of the *sipB* promoter region. Graph shows the predicted intrinsic curvature of the *sipB* regulatory region using the computer program BEND-IT. Curvature is expressed as degrees per helical turn and plotted against the position on the promoter sequence, with +1 corresponding to the *sipB* translation initiation codon. Curved and straight motifs have a value above or below 5 degrees per helical turn, respectively. Regions of intrinsic DNA curvature are arrowed. (B) Competitive gel retardation assays showing the specific binding of Sfh and H-NS to the *sipB* promoter region. A 468-bp DNA fragment encompassing the *sipB* regulatory region (nt –405 to +63 with respect to the translation initiation codon of the *sipB* gene) was amplified by PCR using the primer pair sipB-F and sipB-R (Table 2.3). The plasmid pBR322 was digested with restriction endonucleases *Taq*1 and *Ssp*I, and the resulting DNA fragments mixed with the 468-bp amplimer of the *sipB* promoter region. The DNA mixtures were incubated with increasing concentrations of Sfh or H-NS in the range 0 μM to 2 μM. An arrow and an asterisk indicate the position of the *sipB* and *bla* promoter fragments, respectively. The curved *bla* promoter is a positive control known to bind H-NS-like proteins. The positions of the 600-bp and 400-bp molecular size markers are also indicated.

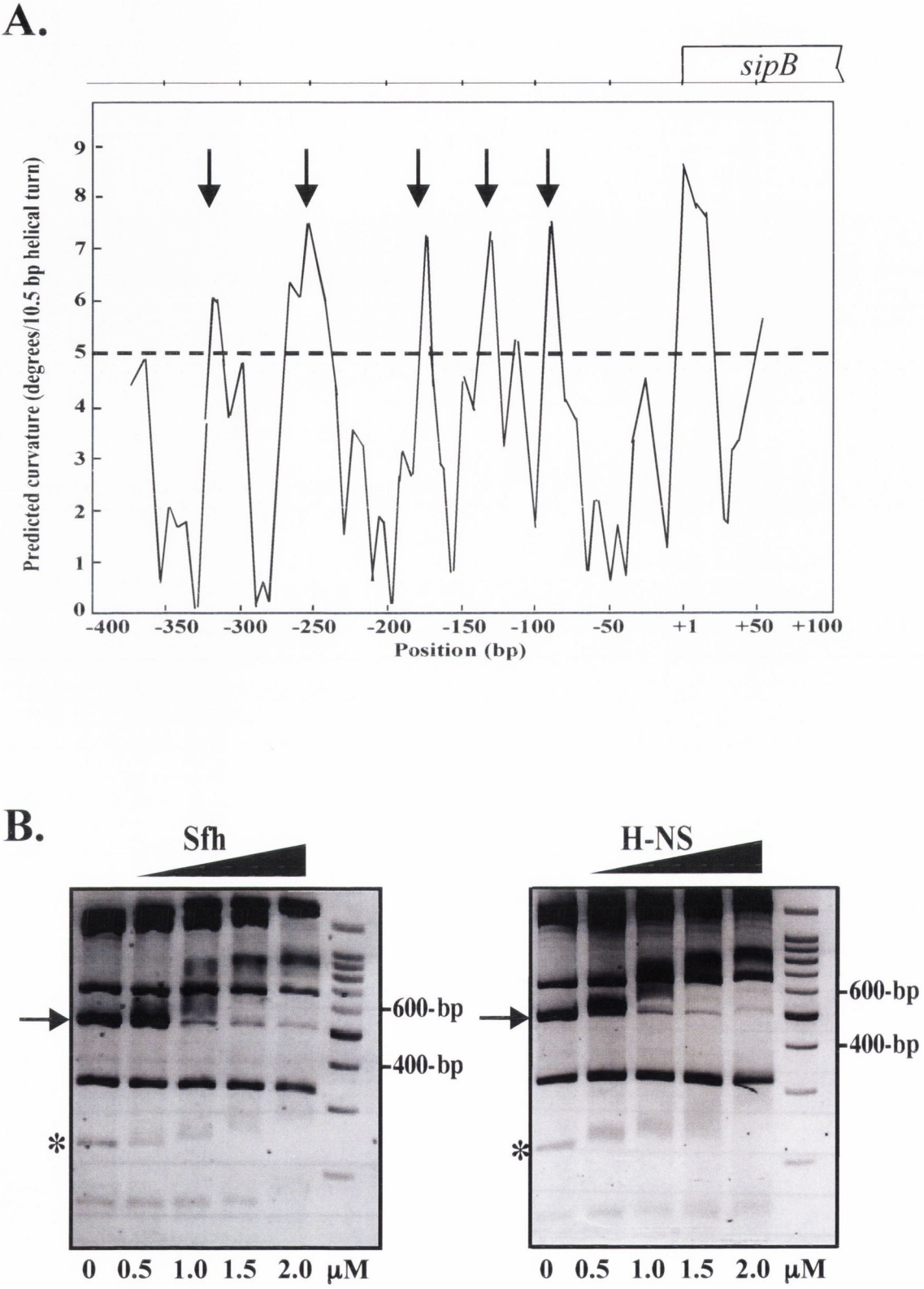
A.
sipB
Predicted curvature (degrees/10.5 bp helical turn)
0
1
2
3
4
5
6
7
8
9
-400
-350
-300
-250
-200
-150
-100
-50
+1
+50
+100
Position (bp)
B.
Sfh
H-NS
600-bp
400-bp
600-bp
400-bp
*
*
0 0.5 1.0 1.5 2.0 μM
0 0.5 1.0 1.5 2.0 μM

Fig. 6.9. Direct interaction of Sfh and H-NS with the *spvR* promoter region.

(A) DNA curvature analysis of the *spvR* promoter region. Graph shows the predicted intrinsic curvature of the *spvR* regulatory region using the computer program BEND-IT. Curvature is expressed as degrees per helical turn and plotted against the position on the promoter sequence, with +1 corresponding to the *spvR* translation initiation codon. Curved and straight motifs have a value above or below 5 degrees per helical turn, respectively. Regions of intrinsic DNA curvature are arrowed. (B) Competitive gel retardation assays showing the specific binding of Sfh and H-NS to the *spvR* promoter region. A 485-bp DNA fragment encompassing the *spvR* regulatory region (nt –374 to +111 with respect to the translation initiation codon of the *spvR* gene) was amplified by PCR using the primer pair spvR-FBS and spvR-RBS (Table 2.3). The plasmid pBR322 was digested with restriction endonucleases *Taq*1 and *Ssp*I, and the resulting DNA fragments mixed with the 485-bp amplimer of the *spvR* promoter region. The DNA mixtures were incubated with increasing concentrations of Sfh or H-NS in the range 0 μM to 2 μM. An arrow and an asterisk indicate the position of the *spvR* and *bla* promoter fragments, respectively. The curved *bla* promoter is a positive control known to bind H-NS-like proteins. The positions of the 600-bp and 400-bp molecular size markers are also indicated.

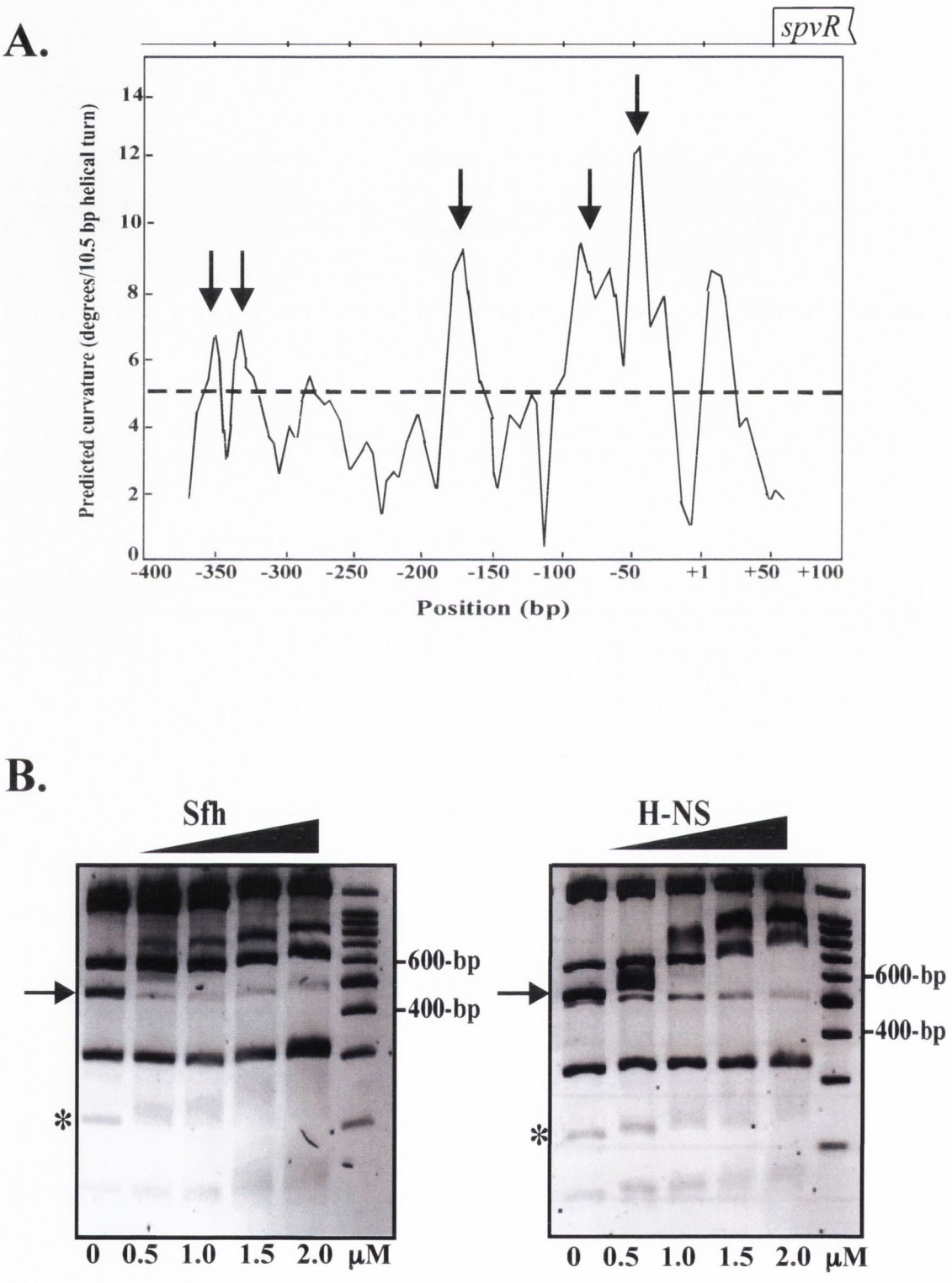
A.
spvR
Predicted curvature (degrees/10.5 bp helical turn)
0
2
4
6
8
10
12
14
-400
-350
-300
-250
-200
-150
-100
-50
+1
+50
+100
Position (bp)
B.
Sfh
H-NS
600-bp
400-bp
600-bp
400-bp
*
*
0 0.5 1.0 1.5 2.0 μM
0 0.5 1.0 1.5 2.0 μM

Fig. 6.10. Direct interaction of Sfh and H-NS with the *spvA* promoter region.

(A) DNA curvature analysis of the *spvA* promoter region. Graph shows the predicted intrinsic curvature of the *hilD* regulatory region using the computer program BEND-IT. Curvature is expressed as degrees per helical turn and plotted against the position on the promoter sequence, with +1 corresponding to the *spvA* translation initiation codon. Curved and straight motifs have a value above or below 5 degrees per helical turn, respectively. Regions of intrinsic DNA curvature are arrowed. (B) Compeitive gel retardation assays showing the specific binding of Sfh and H-NS to the *spvA* promoter region. A 480-bp DNA fragment encompassing the *spvA* regulatory region (nt –326 to +154 with respect to the translation initiation codon of the *spvA* gene) was amplified by PCR using the primer pair spvA-FBS and spvA-RBS (Table 2.3). The plasmidpBR322 was digested with restriction endonucleases *Taq*1 and *Ssp*I, and the resulting DNA fragments mixed with the 480-bp amplimer of the *spvA* promoter region. The DNA mixtures were incubated with increasing concentrations of Sfh or H-NS in the range 0 μM to 2 μM. An arrow and an asterisk indicate the position of the *spvA* and *bla* promoter fragments, respectively. The curved *bla* promoter is a positive control known to bind H-NS-like proteins. The positions of the 600-bp and 400-bp molecular size makers are also indicated.

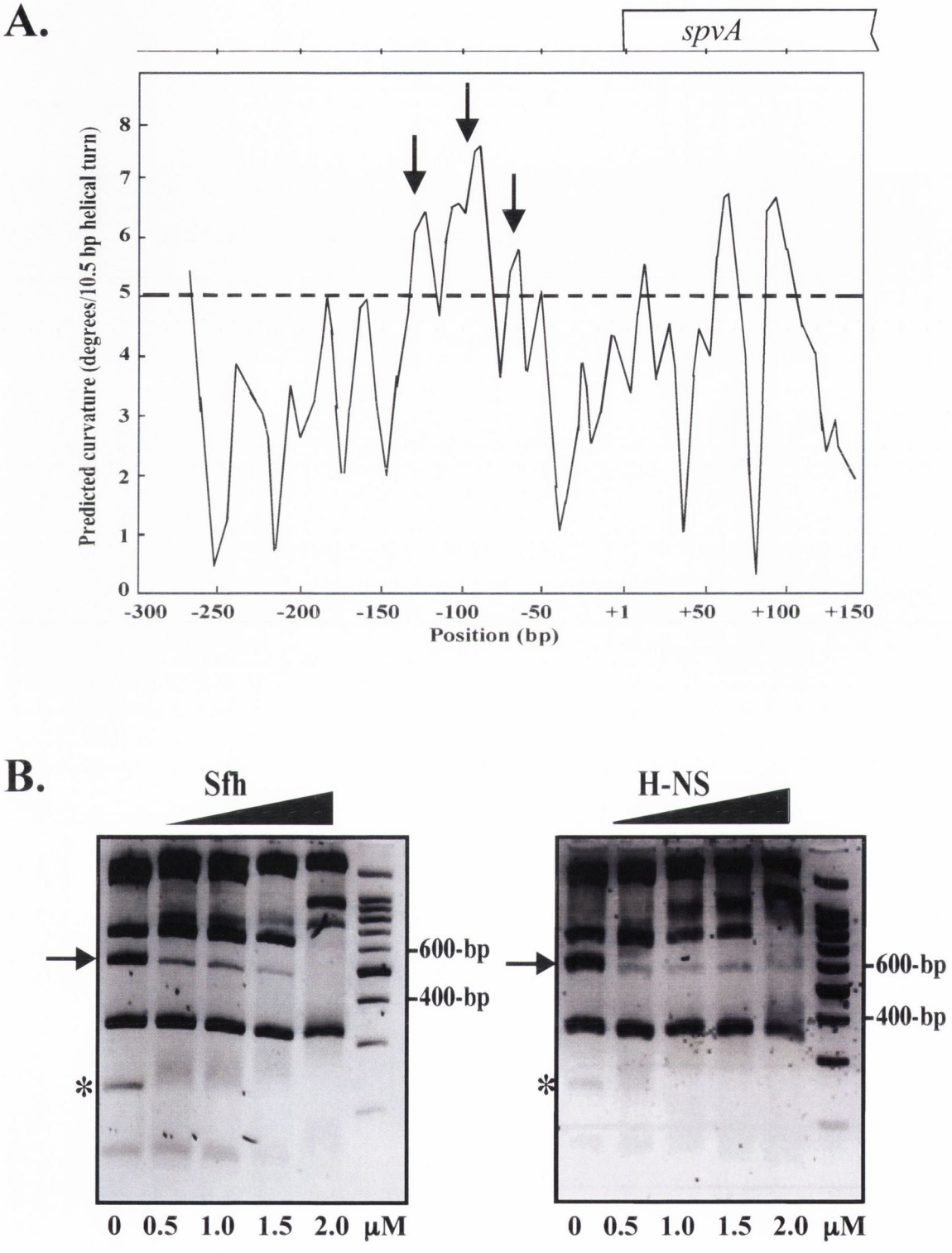
A.
spvA
Predicted curvature (degrees/10.5 bp helical turn)
0
1
2
3
4
5
6
7
8
-300
-250
-200
-150
-100
-50
+1
+50
+100
+150
Position (bp)
B.
Sfh
H-NS
600-bp
400-bp
600-bp
400-bp
*
*
0 0.5 1.0 1.5 2.0 µM
0 0.5 1.0 1.5 2.0 µM

Fig. 6.11. Direct interaction of Sfh and H-NS with the *ssrA* promoter region.

(A) DNA curvature analysis of the *ssrA* promoter region. Graph shows the predicted intrinsic curvature of the *ssrA* regulatory region using the computer program BEND-IT. Curvature is expressed as degrees per helical turn and plotted against the position on the promoter sequence, with +1 corresponding to the *ssrA* translation initiation codon. Curved and straight motifs have a value above or below 5 degrees per helical turn, respectively. Regions of intrinsic DNA curvature are arrowed. (B) Competitive gel retardation assays showing the specific binding of Sfh and H-NS to the *ssrA* promoter region. A 476-bp DNA fragment encompassing the *ssrA* regulatory region (nt –426 to +50 with respect to the translation initiation codon of the *ssrA* gee) was amplified by PCR using the primer pair ssrA-FBS and ssrA-RBS (Table 2.3). The plasmid pBR322 was digested with restriction endonucleases *Taq*1 and *Ssp*I, and the resulting DNA fragments mixed with the 539-bp amplimer of the *ssrA* promoter region. The DNA mixtures were incubated with increasing concentrations of Sfh or H-NS in the range 0 μM to 2 μM. An arrow and an asterisk indicate the position of the *ssrA* and *bla* promoter fragments, respectively. The curved *bla* promoter is a positive control known to bind H-NS-like proteins. The positions of the 600-bp and 400-bp molecular size markers are also indicated.

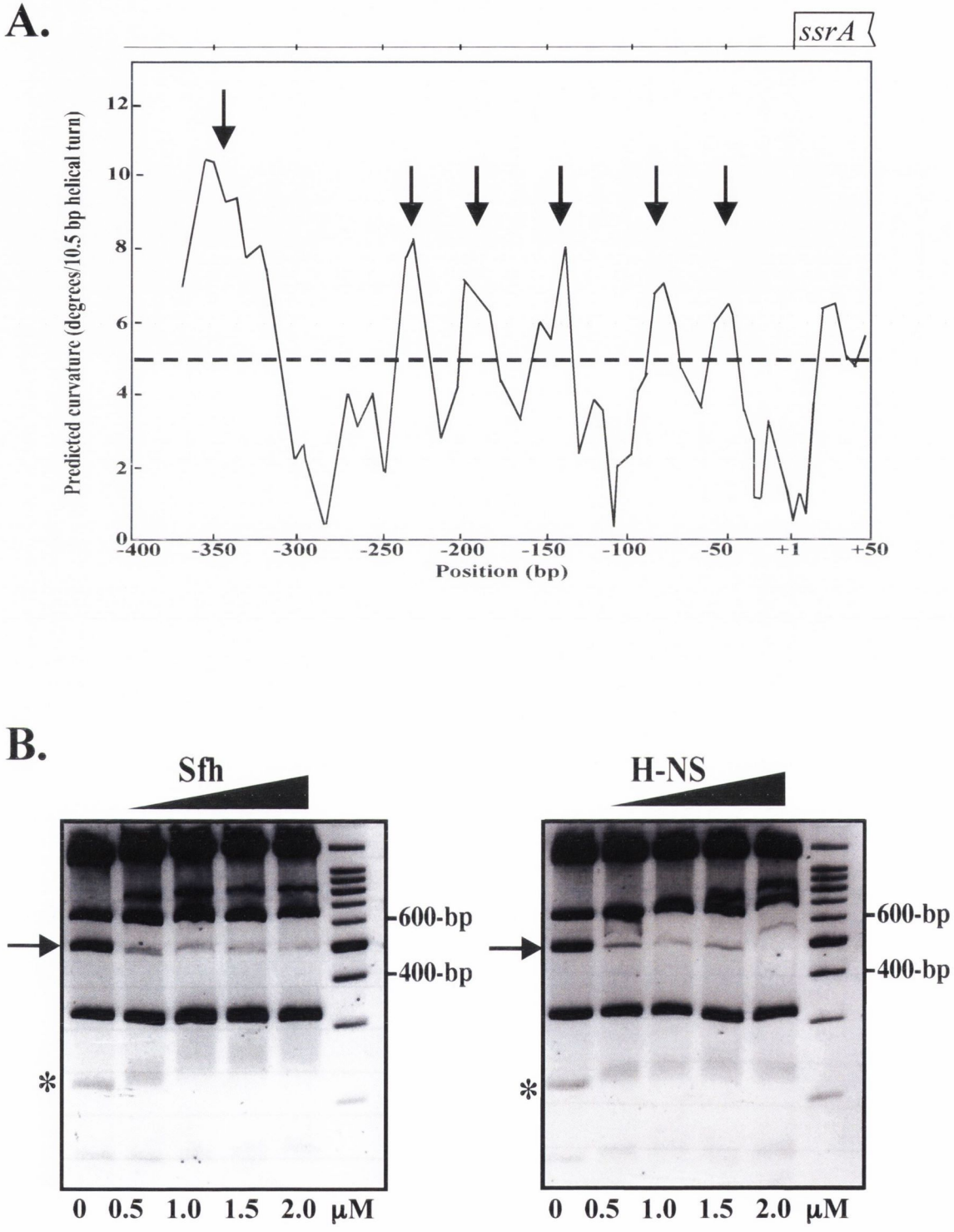
A.
ssrA
Predicted curvature (degrees/10.5 bp helical turn)
12
10
8
6
4
2
0
-400
-350
-300
-250
-200
-150
-100
-50
+1
+50
Position (bp)
B.
Sfh
H-NS
600-bp
400-bp
*
0 0.5 1.0 1.5 2.0 μM

Fig. 6.12. Direct interaction of Sfh and H-NS with the *sseA* promoter region.

(A) DNA curvature analysis of the *sseA* promoter region. Graph shows the pedicted intrinsic curvature of the *sseA* regulatory region using the computer program BEND-IT. Curvature is expressed as degrees per helical turn and plotted against the positio1 on the promoter sequence, with +1 corresponding to the *sseA* translation initiation codon. Curved and straight motifs have a value above or below 5 degrees per helical turn, respectively. Regions of intrinsic DNA curvature are arrowed. (B) Competitive gel retardation assays showing the specific binding of Sfh and H-NS to the *sseA* pomoter region. A 530-bp DNA fragment encompassing the *sseA* regulatory region (nt -493 to +37 with respect to the translation initiation codon of the *sseA* gene) was amplfied by PCR using the primer pair sseA-FBS and sseA-RBS (Table 2.3). The plasmid pBR322 was digested with restriction endonucleases *Taq*1 and *Ssp*I, and the resulting DNA fragments mixed with the 530-bp amplimer of the *sseA* promoter region. The DNA mixtures were incubated with increasing concentrations of Sfh or H-NS in the range 0 μM to 2 μM. An arrow and an asterisk indicate the position of the *sseA* and *bla* promoter fragments, respectively. The curved *bla* promoter is a positive control known to bind H-NS-like proteins. The positions of the 600-bp and 400-bp molecular size markers are also indicated.

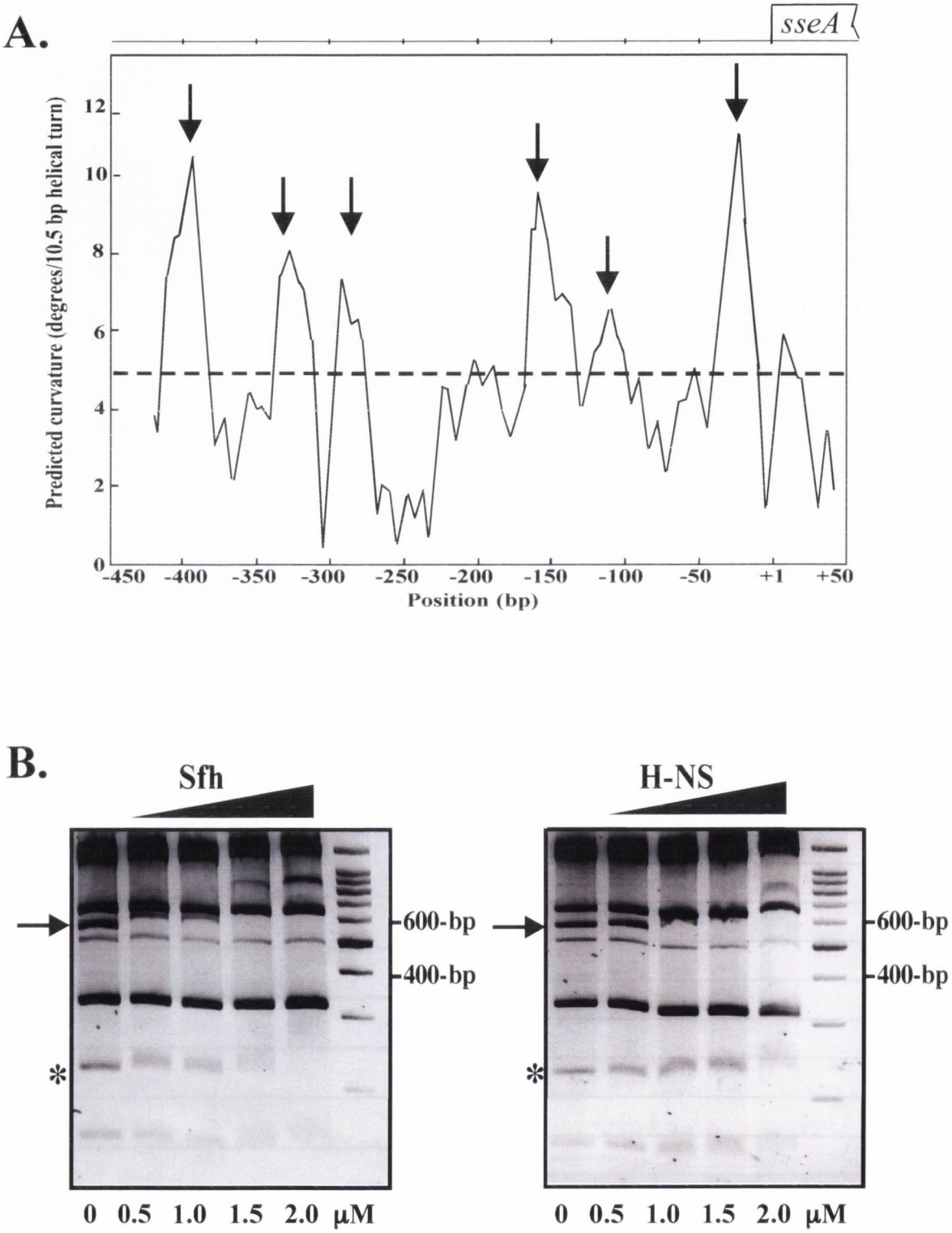
A.
sseA
Predicted curvature (degrees/10.5 bp helical turn)
0
2
4
6
8
10
12
-450
-400
-350
-300
-250
-200
-150
-100
-50
+1
+50
Position (bp)
B.
Sfh
H-NS
600-bp
400-bp
*
0 0.5 1.0 1.5 2.0 μM

confirmed by EMSA that H-NS binds to the promoter regions of *spvR* (Fig. 6.9) and *spvA* (Fig. 6.10) and further demonstrated a specific interaction between Sfh and the same DNA sequences (Fig. 6.9 and 6.10). Finally, the interaction of purified Sfh with the SPI-2 *ssrA* (Fig. 6.11) and *sseA* (Fig. 6.12) promoters revealed that they were also specifically shifted by Sfh in concentration-dependent manners. In addition, the H-NS protein also bound specifically to these regulatory regions (Fig. 6.11 and 6.12). In all the above electrophoretic mobility shift assays, the mobility of the DNA fragments harbouring the various virulence promoter regions were retarded more efficiently than the *bla* positive control band (Fig. 6.7 – 6.12). These data indicate that Sfh, like H-NS, has the potential to directly bind to and influence transcription of *Salmonella* virulence genes.

6.2.8 Impact of plasmids pSf-R27Gent^R and pSf-R27Δ*sfh*::Gent^R on intracellular survival

S. Typhimurium and other virulence plasmid-containing *Salmonella* serovars are facultative intracellular pathogens that survive and replicate within a variety of host cells, including epithelial cells and macrophage (Finlay and Falkow, 1989). Genes located within SPI-1 are required for the invasive phenotype (Mills *et al.*, 1995), while the second major pathogenicity island SPI-2 is associated with survival and proliferation of *Salmonella* inside macrophage (Hensel *et al.*, 1998; Ochman *et al.*, 1996). In addition, the *spv* gene cluster is also needed for intracellular pathogenesis (Gulig *et al.*, 1993). The discovery that Sfh can influence expression of the *spv* genes and also genes belonging to SPI-1 and SP1-2 strongly suggested Sfh might have an important role in *Salmonella* pathogenesis *in vivo.*

To ascertain whether plasmid pSf-R27Gent^R or plasmid pSf-R27Δ*sfh*::Gent^R could affect the invasive ability of strain SL1344, epithelial invasion assays were performed. Cultured CHO-K1 or CACO-II epithelial cells were infected with stationary phase L-broth cultures of strains SL1344, SL1344(pSf-R27Gent^R), or SL1344(pSf-R27Δ*sfh*::Gent^R) and 2 h post infection epithelial cells were lysed and the intracellular bacteria enumerated. Surprisingly, the results

revealed that the invasive capacity of strain SL1344 did not alter to any marked extent (≥1.5-fold) following the horizontal transfer of plasmids pSf-R27Gent^R and pSf-R27Δ*sfh*::Gent^R (Fig. 6.13). The plasmid-bearing strains abilities to invade CHO-K1 epithelial cells were observed to be slightly enhanced compared to that of the wild-type strain SL1344 (Fig. 6.13). In contrast, when the CACO-II epithelial cell line was used in the invasion assay, the presence of plasmid pSf-R27Gent^R correlated with a modest decrease in invasion, whereas plasmid pSf-R27Δ*sfh*::Gent^R slightly increased the invasive capacity of strain SL1344 (Fig. 6.13). These data imply that neither plasmid pSf-R27Gent^R nor Sfh have a significant role in the *Salmonella* invasive phenotype.

To determine whether plasmid pSf-R27Gent^R or plasmid pSf-R27Δ*sfh*::Gent^R could affect the uptake and intracellular survival of strain SL1344 in macrophage, amikacin protection assays were performed. The macrophage-like cell line J774-A.1 was infected with stationary phase L-broth cultures of strains SL1344, SL1344(pSf-R27Gent^R), or SL1344(pSf-R27Δ*sfh*::Gent^R) and at various time-points post infection macrophage were lysed and the intracellular bacteria enumerated. Comparison of the results obtained for the wild-type strain and for strain SL1344 harbouring plasmid pSf-R27Gent^R illustrates the considerable increase in intracellular survival following the acquisition of plasmid pSf-R27Gent^R (Fig. 6.14). The deletion of the *sfh* gene from plasmid pSf-R27 further enhanced bacterial survival (Fig. 6.14), consistent with the findings that Sfh negatively regulates *ssrA* (Section 6.2.5) and *spv* gene expression (Section 6.2.6). These data indicate a novel role for both plasmid pSf-R27Gent^R and Sfh in the proliferation and survival of *Salmonella* inside macrophage.

6.2.9 Environmental factors influencing SPI-2 expression and intracellular survival

SPI-2 genes are required for survival and replication inside macrophage, and are activated by certain macrophage-associated environmental signals such as low pH, and Mg^{2+}, Fe^{2+}, or phosphate concentration (Deiwick *et al.*, 1999; Garcia-del Portillo *et al.*, 1992; Lee *et al.*, 2000). Thus, the increased macrophage survival rates of strains harbouring plasmid pSf-

Fig. 6.13. The effect of plasmids pSf-R27Gent^R and pSf-R27Δ*sfh*::Gent^R on *Salmonella* invasion. (A) CACO-II and (B) CHO-KI cells were infected with strains SL1344, SL1344(pSf-R27Gent^R) and SL1344(pSf-R27Δ*sfh*::Gent^R) for 1 h. Cells were then washed and incubated for 1 h with amikacin-containing (400 μg ml^{-1}) culture medium. After incubation, cells were lysed with 0.5% Triton X-100, and lysates diluted and plated onto L-agar plates to determine the numbers of colony forming units. Data from representative experiments are shown. The values represent the means and standard deviations of strains tested in quadruplicate.

A.

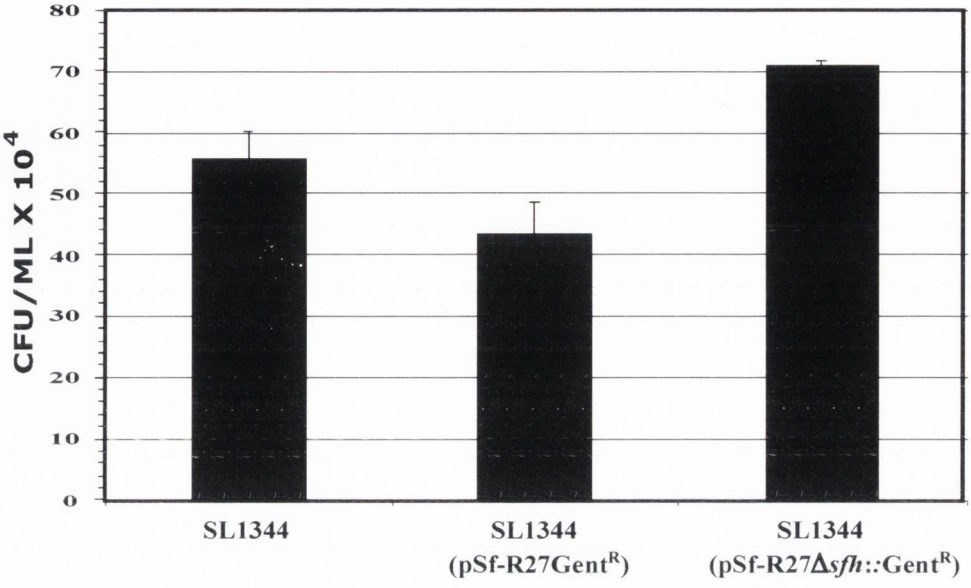
80
70
60
50
40
30
20
10
0
CFU/ML X 10^4
SL1344
SL1344 (pSf-R27Gent^R)
SL1344 (pSf-R27Δsfh::Gent^R)

B.

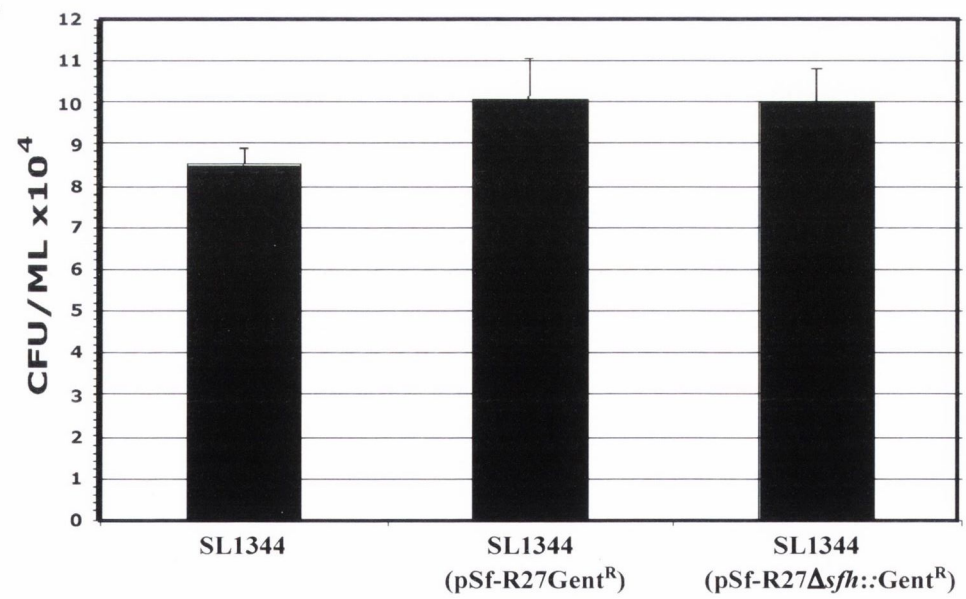
12
11
10
9
8
7
6
5
4
3
2
1
0
CFU/ML x10^4
SL1344
SL1344 (pSf-R27Gent^R)
SL1344 (pSf-R27Δsfh::Gent^R)

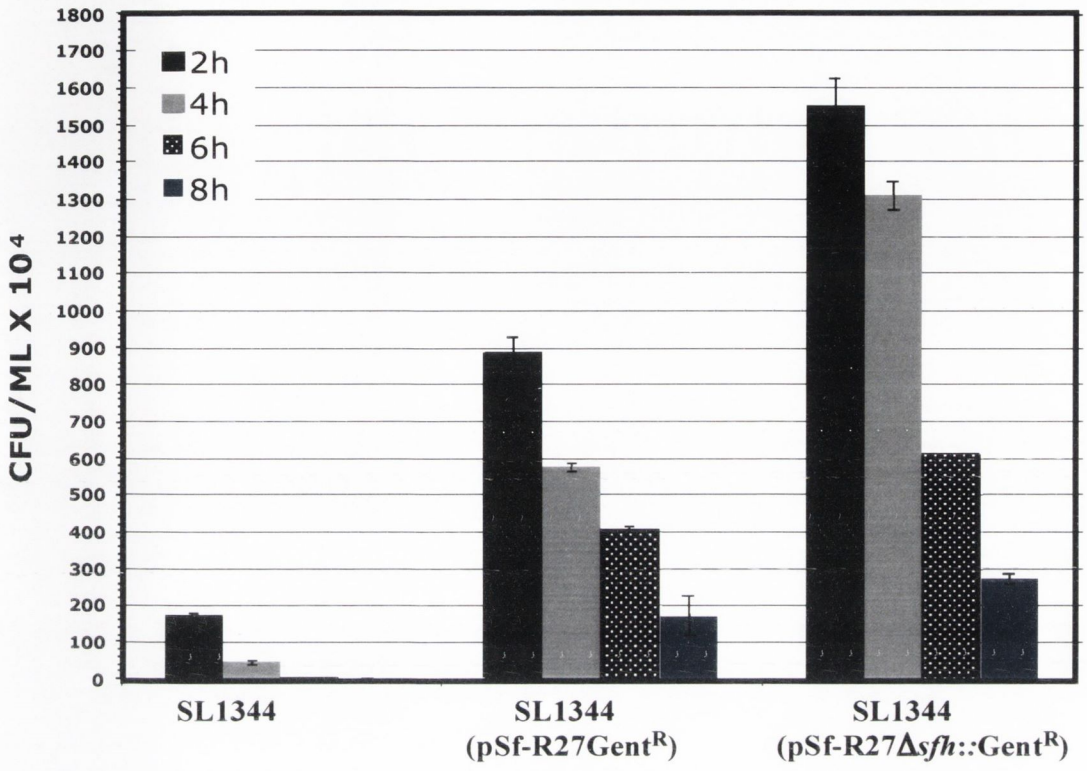

Fig. 6.14. The effect of plasmids pSf-R27Gent^R and pSf-R27Δ*sfh*::Gent^R on intracellular survival. JJ74-A.1 macrophage-like cells were infected with stationary phase L-broth cultures of strains SL1344, SL1344(pSf-R27Gent^R), and SL1344(pSf-R27Δ*sfh*::Gent^R) for 1 h. Cells were then washed and incubated for 1 h with amikacin-containing (400 μg ml^{-1}) culture medium. The monolayers were then either lysed with 0.5 % (v/v) Triton X-100 or incubated in fresh culture medium containing a minimum concentration of amikacin (80 μg ml^{-1}) and lysed 4, 6 or 8 h post-infection. Finally, cell lysates were diluted and plated onto L-agar plates to determine the numbers of colony forming units. The values represent the means and standard deviations of three independent experiments.

R27Gent^R or plasmid pSf-R27Δ*sfh*::Gent^R could be directly due to an upregulation of SPI-2 gene expression in these strains compared to that of the parental strain SL1344 in the intracellular milieu of the macrophage. To test this hypothesis, *ssrA* and *sseA* transcriptional activities were monitored in each of the strains following growth in the 'macrophage mimicking' minimal medium 5.8 (MM 5.8), containing 0.5-mM histidine as strain SL1344 is a histidine auxotroph. MM 5.8 is a low pH, minimal medium that has previously been used to stimulate the intracellular environment of the macrophage (Deiwick *et al.*, 1999; Kox *et al.*, 2000). Coombes *et al.* (2004) have shown that *sseA* gene expression is maximal in cells grown for 5 h in low phosphate, low magnesium-containing medium at pH 5.8. Consistent with these findings, expression of the SPI-2 genes *ssrA* and *sseA* was induced in strain SL1344 and its plasmid-bearing derivatives, SL1344(pSf-R27Gent^R), SL1344(pSf-R27Δ*sfh*::Gent^R) and SL1344(pSf-R27Δ*sfh*::Gent^R, pYC*sfh*$^+$) cultured for 5 h in MM 5.8 (Fig. 6.15). All the strains had a similar doubling time in MM 5.8 (data not shown) and there were only modest changes in *ssrA* and *sseA* gene expression between the wild-type strain SL1344 and its plasmid-bearing derivatives (Fig. 6.15). These results suggest that the increased macrophage survival rates of strains SL1344(pSf-R27Gent^R) and SL1344(pSf-R27Δ*sfh*::Gent^R) cannot be attributed to a significant increase in SPI-2 gene expression in these strains. Interestingly, over-expression of Sfh *in trans* from the plasmid pYCsfh did not repress *ssrA* transcription in MM 5.8 (Fig. 6.15), indicating that Sfh cannot exert its negative affect on *ssrA* gene expression under SPI-2 inducing conditions.

Macrophage cells express numerous antimicrobial factors such as reactive oxygen species, reactive nitrogen species, and antimicrobial peptides (Vazquez-Torres and Fang, 2001). Release of these antimicrobial factors into the phagosome results in killing of the invading microbe. Upon invasion of macrophages, *Salmonella* is exposed to large amounts of superoxide in its direct environment, generated by the antimicrobial defense mechanisms (oxidative burst) of the eukaryotic cell. To counteract this, *S.* Typhimurium possesses virulence genes including those for several superoxide dismutases –*sodA, sodB, sodCI, sodCII*– which function specifically to protect the cell from the phagocytic oxidative burst

(Fang *et al.*, 1999). Therefore, *Salmonella* displaying increased resistance to oxidative stress and DNA damage should survive better in the intracellular macrophage environment.

For this reason, hydrogen peroxide (H_2O_2) stress assays were performed on strains SL1344, SL1344(pSf-R27Gent^R) and SL1344(pSf-R27Δ*sfh*::Gent^R). Stationary phase cultures of all three strains were subjected to 20-mM H_2O_2 for 1 or 2 h and the survival rates of each strain compared. The results revealed a modest increase in the survival rate of cells harbouring plasmid pSf-R27Gent^R, whereas deletion of the *sfh* gene from plasmid pSf-R27 corresponded with a reduction in survival (Fig. 6.16). These findings are supported by microarray data, which show that the expression of several oxidative stress response genes such as *sodA*, *sodB*, and *dps* are downregulated in the *sfh* mutant (Supplementary data). However, the results of the H_2O_2 stress assays do not explain the enhanced survival rates of strain SL1344 harbouring plasmid pSf-R27 or plasmid pSf-R27Δ*sfh*::Gent^R. Clearly, further investigation will be required to decipher this issue.

Fig. 6.15. Expression of the *ssrA* and *sseA* genes during growth in MM 5.8. Histograms show the activity of (A) *ssrA–lacZ* and (B) *sseA–lacZ* transcriptional fusions in the wild-type strain SL1344 and its plasmid bearing derivatives SL1344(pSf-R27Gent^{R}), SL1344(pSf-R27Δ*sfh*::Gent^{R}), and SL1344(pSf-R27Δ*sfh*::Gent^{R}, pYCsfh^{+}). β–galactosidase assays were performed on strains cultured for 5 h in MM 5.8 containing 0.5-mM histidine at 37°C. The data represent an average of at least three independent experiments and error bars represent standard deviations.

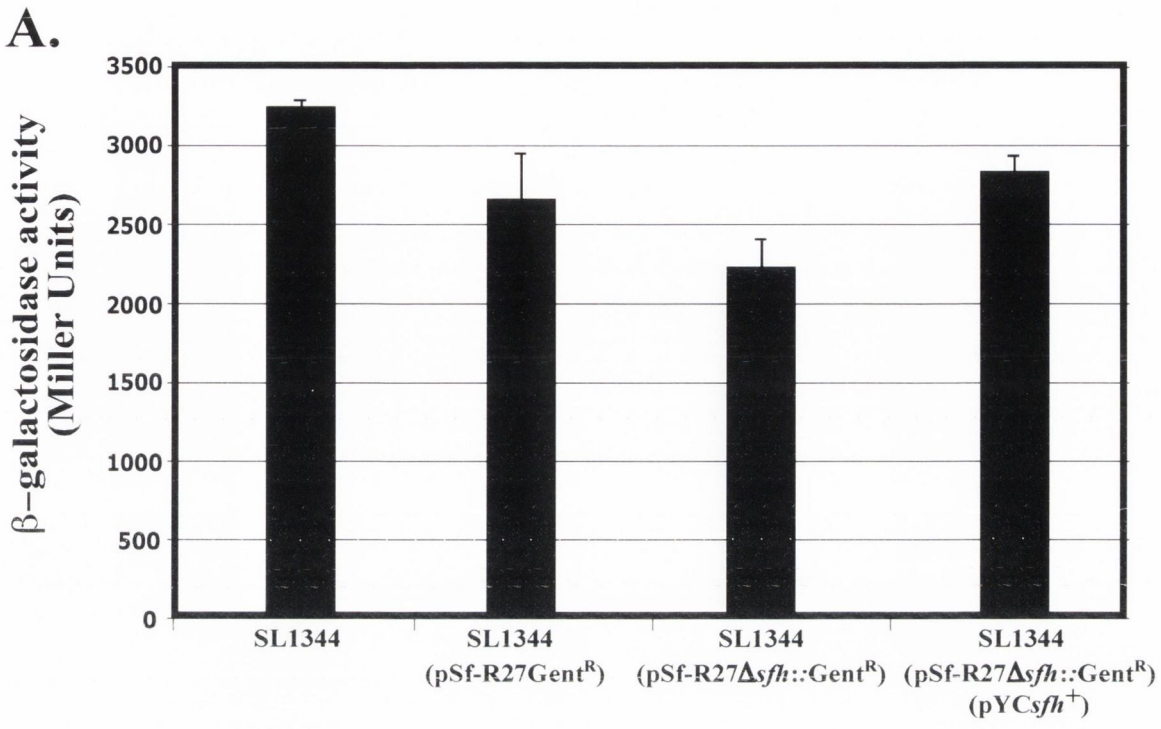
A.
β–galactosidase activity (Miller Units)
3500
3000
2500
2000
1500
1000
500
0
SL1344
SL1344 (pSf-R27Gent^R)
SL1344 (pSf-R27Δsfh::Gent^R)
SL1344 (pSf-R27Δsfh::Gent^R) (pYCsfh^+)

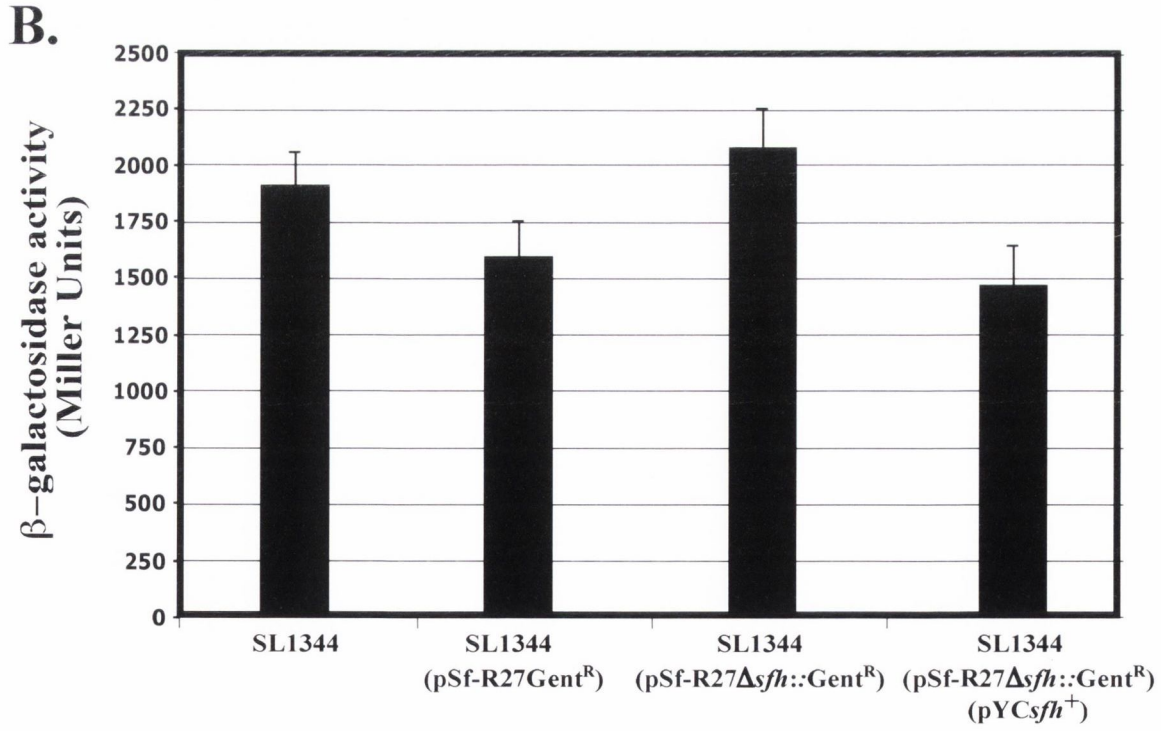
B.
β–galactosidase activity (Miller Units)
2500
2250
2000
1750
1500
1250
1000
750
500
250
0
SL1344
SL1344 (pSf-R27Gent^R)
SL1344 (pSf-R27Δsfh::Gent^R)
SL1344 (pSf-R27Δsfh::Gent^R) (pYCsfh^+)

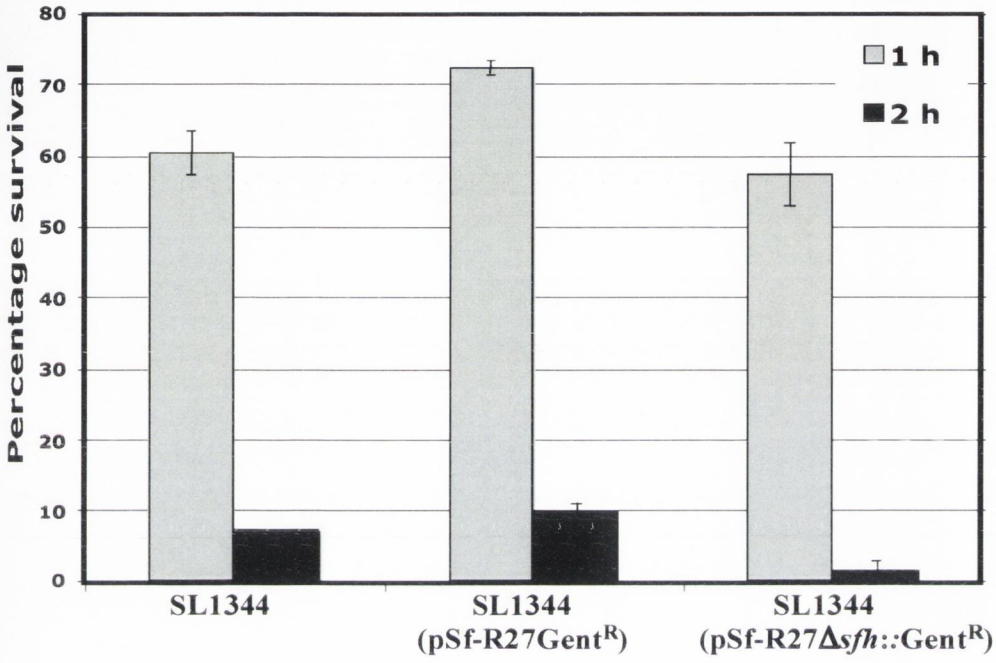

Fig. 6.16. Impact of plasmids pSf-R27Gent^R and pSf-R27Δ*sfh*::Gent^R on bacterial resistance to reactive oxygen species. Overnight L-broth cultures of strains SL1344, SL1344(pSf-R27Gent^R), and SL1344(pSf-R27Δ*sfh*::Gent^R) were treated with 20-mM hydrogen peroxide for either 1 or 2 h. The numbers of surviving bacteria were determined by plating the treated and untreated cultures onto L-agar plates and calculating the number of colony forming units. The percentage survival is an average of three independent experiments and error bars represent standard deviations.

6.3 Discussion

A role for nucleoid-associated proteins in virulence gene regulation has long been established for many different bacterial species (Dorman and Deighan, 2003). *S. flexneri* and *S.* Typhimurium are no exceptions. In both cases their virulence gene regulatory networks have been previously shown to involve several major nucleoid-associated proteins including H-NS, FIS, IHF and HU (Kelly *et al.*, 2004; Mangan *et al.*, 2006; Marshall *et al.*, 1999; O'Byrne and Dorman, 1994a; Schechter *et al.*, 2003). The exact composition and relative abundance of the major nucleoid-associated proteins in the cell varies dramatically depending on many factors including growth phase and environmental conditions (Azam *et al.*, 1999). In particular, nucleoid-associated proteins are sensitive to changes in temperature and osmolarity, two key signals experienced by pathogenic bacteria during infection (Dorman and Deighan, 2003). Thus, regulation of virulence genes by nucleoid-associated proteins is one mechanism used by bacteria to sense environmental shifts and to ensure that virulence gene expression is strictly restricted to permissive conditions. Preliminary data from DNA microarray analysis indicated a potential role for Sfh in *Salmonella* virulence gene expression. The aim of this study was to examine in more detail the role of Sfh in *S.* Typhimurium virulence gene regulation, and to investigate what role, if any, Sfh plays in the regulation of *Shigella* virulence.

Previous studies have shown that H-NS represses *Shigella* virulence gene expression under non-permissive conditions by binding to the promoter regions of the *virF* and *virB* genes, which encode the two essential regulatory proteins VirF and VirB, respectively (Beloin and Dorman, 2003; Maurelli and Sansonetti, 1988; Tobe *et al.*, 1993). Like H-NS, Sfh was shown to preferentially bind the promoter regions of the *virF* and *virB* genes, in competitive gel retardation assays (Fig. 6.2). These data strongly indicated Sfh could potentially regulate *Shigella* virulence gene expression. Subsequently, it was observed that virulence gene expression was derepressed in a *sfh hns* double mutant, but not in a *sfh* single mutant under non-permissive conditions (Fig. 6.1). When the *sfh* mutation was combined with the *hns* mutation, there was an enhancement of the transcriptional derepression of the virulence genes

normally associated with *hns* lesions. Taken in aggregate these data show that, in the absence of H-NS, Sfh can repress virulence gene expression and thus act as a 'molecular backup' for H-NS.

DNA microarray analysis revealed that virulence genes from all five *Salmonella* pathogenicity islands together with the *spv* genes encoded on the pSLT virulence plasmid show altered expression following the introduction of plasmid pSf-R27Δ*sfh*::Gent^R (but not plasmid pSf-R27Gent^R) into *S.* Typhimurium (Fig. 5.13 and Supplementary data). These findings strongly suggest that horizontal acquisition of Sfh on plasmid pSf-R27Gent^R can potentially contribute to *Salmonella* virulence signaling pathways. In this study, the negative effect of Sfh on *spv* gene expression (Fig. 6.6) and on the expression of the central SPI-2 regulator gene *ssrA* (Fig. 6.5) was confirmed. In addition, Sfh-mediated repression of the SPI-1 regulator HilD and the secreted effector SipB was also verified using transcriptional reporter fusions (Fig. 6.4).

The transcriptional control of *Salmonella* virulence gene expression is very complex. It is therefore important to distinguish between direct and indirect influences. For this reason, the Sfh protein was shown, using competitive gel retardation assays, to preferentially bind to selected promoters in all three genetic elements, namely, SPI-1, SPI-2, and pSLT (Fig. 6.7 – 6.12). Furthermore, *in silico* analysis of the same promoter sequences revealed that they possessed regions of curvature (Fig. 6.7 – 6.12), the structural features that are characteristic of high-affinity H-NS-like protein-binding sites. However, as discussed previously, the observed effect of Sfh on *Salmonella* gene expression is probably due to a titration effect exerted by the introduced plasmid pSf-R27Δ*sfh*::Gent^R (Chapter 5). The absence of Sfh in strain SL1344(pSf-R27Δ*sfh*::Gent^R) is thought to result in H-NS binding to the plasmid, consequently leading to an overall reduction in H-NS availability such that H-NS binding sites within the host genome, especially sites of lower affinity, might be occupied less often.

Consistent with this hypothesis, the H-NS protein was shown to preferentially bind to the same virulence regulatory regions as purified Sfh (Fig. 6.7 – 6.12). Consequently, it can be concluded that H-NS must repress the various virulence genes in wild-type *S.* Typhimurium strain SL1344. This model is strongly supported by previous studies, which demonstrated that H-NS directly represses the *spv* genes (O'Byrne and Dorman, 1994a) and also the SPI-1 gene *hilA* (Olekhnovich and Kadner, 2006). Therefore, the data from this study confirm that H-NS acts as a repressor of the *spv* genes. Importantly the data further suggest an extended role for H-NS in SPI-1 regulation (the *hilD* and *sipB* genes) and a novel role in SPI-2 expression (the *ssrA* and *sseA* genes). In addition, it cannot be discounted that under some circumstances Sfh modulates *Salmonella* gene expression.

Intriguingly, most *Salmonella* and *Shigella* virulence genes have been horizontally acquired and thus have a higher percentage A+T content compared to the chromosomal genes (Blanc-Potard *et al.*, 1999; Sansonetti, 1991a). Since H-NS-like proteins preferentially bind to AT-rich sequences it is unsurprising that H-NS binds to these virulence genetic elements and consequently represses transcription. One can envisage that maintaining the virulence genes in a constant state of repression is beneficial to the bacterium, as expression of a TTSS and other virulence genes represents a heavy metabolic burden, which would subsequently reduce bacterial fitness. However, it is crucial that during the infection process the virulence genes are expressed. Thus, the virulence genetic elements have evolved to overcome H-NS repression under permissive conditions.

This is exemplified by VirB, which acts as a H-NS antirepressor in the *Shigella* virulence cascade and is thought to have evolved from a redundant partitioning system of the LVP (Watanabe *et al.*, 1990). The SPI-I regulators HilC and HilD are also thought to function as H-NS anti-repressors at the *hilA* promoter (Schechter *et al.*, 2003). It is also noteworthy that *Shigella* and *Salmonella* virulence genetic elements encode a repertoire of AraC/XylS proteins, as members of this protein family are known to specifically counteract H-NS repression (Egan, 2002).

Importantly, the phenomenon of pathogenicity islands (PAI) encoding proteins that antagonize H-NS activity is not confined to *Salmonella* and *Shigella.* The virulence genes of enteropathogenic and enterohaemorrhagic *E. coli* located on a PAI known as the locus of enterocyte effacement (LEE) are induced by the LEE-encoded regulator (Ler), which acts specifically as a H-NS antirepressor (Bustamante *et al.*, 2001; Mellies *et al.*, 1999). Intriguingly, the Ler protein is itself a member of the H-NS protein family but has evolved to counteract H-NS-mediated repression (Mellies *et al.*, 1999). Recently Williamson *et al.* (2005) reported that a second PAI in enteropathogenic *E. coli* encoded a truncated H-NS protein, H-NST_{EPEC}, which has potent anti-H-NS activity (Williamson and Free, 2005).

It is easy to speculate that these H-NS-like proteins were originally repressors of the genetic elements that encode them, but following integration of the PAI into the chromosome they became redundant, as the chromosomally encoded H-NS replaced them. Perhaps, H-NS was a more effective repressor of the PAI and thus the proteins (Ler and H-NST_{EPEC}) evolved to overcome H-NS-mediated repression under permissive conditions. This hypothesis is supported by a previous study that revealed that integration of the *Shigella* LVP into the chromosome results in constant repression of virulence expression due to H-NS repressing *virB* transcription at both 30°C and 37°C (Colonna *et al.*, 1995). The hypothesis suggests that there might be a difference in H-NS repressive activity depending on whether the protein is expressed *in cis* or *in trans* and reinforces the model that H-NS-mediated repression of plasmid pSf-R27Δ*sfh*::$Gent^R$ gene expression requires copious amounts of H-NS.

Horizontal transfer of plasmid pSf-R27Δ*sfh*::$Gent^R$ into *S.* Typhimurium altered expression of virulence genes involved in most aspects of *Salmonella* pathogenesis. In light of this, the effect of plasmids pSf-R27$Gent^R$ and pSf-R27Δ*sfh*::$Gent^R$ on *Salmonella* invasion and intracellular survival was investigated. Surprisingly, the plasmids did not significantly affect the invasive ability of strain SL1344. In contrast, intracellular survival rates of strain SL1344 in macrophage increased dramatically following the acquisition of plasmid pSf-R27$Gent^R$ (Fig. 6.14) and were further augmented by the deletion of the *sfh* gene from plasmid pSf-R27

(Fig. 6.14). Transcriptional data obtained for the SPI-2 genes *ssrA* and *sseA* under inducing conditions indicated that the observed increase in intracellular survival of the plasmid-bearing strains is not mediated through an increase in SPI-2 expression (Fig. 6.15). Similarly, the enhanced macrophage survival rates of the plasmid-bearing strains cannot be attributed to increased resistance to oxidative damage (Fig. 6.16). Since the presence of both plasmids pSf-R27Gent^R and pSf-R27Δ*sfh*::Gent^R corresponded with an increase in bacterial survival, these findings suggest that these plasmids might encode novel virulence factors, which protect *Salmonella* in the macrophage intracellular environment and perhaps enhance the systemic spread of *Salmonella* in the host.

These data are of the utmost clinical importance as IncHI plasmids are now isolated from almost all cases of MDR *S.* Typhi worldwide (Hampton *et al.*, 1998). Significantly, *S.* Typhi strains harbouring MDR IncHI plasmids are associated with a more severe clinical outcome in children (Bhutta *et al.*, 2000) and blood bacterial counts are higher in infections caused by *S.* Typhi harbouring these plasmids (Wain *et al.*, 1998). Taken in aggregate, the results indicated that IncHI plasmids confer a selective advantage to *Salmonella* spp. in establishing a systemic infection (Wain and Kidgell, 2004). Interestingly, *S. flexneri* serotype 2a strain 2457T is the only *Shigella* strain known to harbour an IncHI plasmid, suggesting that IncHI plasmids might not confer a selective advantage to *Shigella* spp. This might be reflected in the opposing intracellular survival strategies used by *Salmonella* and *Shigella*. *Shigella* escapes the macrophage phagosomal vacuole, whereas *Salmonella* hijacks the eukaryotic cell by subverting the normal cellular trafficking processes, subsequently preventing lysosomal fusion and creating the unique *Salmonella*-containing vacuole. Perhaps, IncHI plasmids encode factors that facilitate the creation of, and survival in, the *Salmonella*-containing vacuole and therefore could explain the promiscuous nature of these plasmids in *Salmonella* spp. The data presented clearly show a novel role for the IncHI plasmid pSf-R27 in *Salmonella* intracellular survival, although further investigation is needed to elucidate the exact mechanism by which it leads to increased bacterial survival in macrophage.

Chapter 7

General Discussion

7.1 Discussion

During the past decade, advances in genomic technology have revolutionized molecular biology and led to a rapid increase in bacterial genome sequencing. Analysis of this new wealth of genome sequence information has revealed that H-NS-like proteins constitute a large family of proteins that are widespread in Gram-negative bacteria (Bertin *et al.*, 1999; Tendeng and Bertin, 2003). Sequencing studies have also highlighted the fact that that although some bacteria contain only one *hns* gene, many others contain multiple *hns*-related genes (Dorman, 2004; Tendeng and Bertin, 2003; Williamson and Free, 2005). Often these additional H-NS-like proteins are encoded on mobile genetic elements, such as large self-transmissible plasmids or within elements such as pathogenicity islands thought to have been acquired via horizontal transfer (Beloin *et al.*, 2003; Tendeng and Bertin, 2003; Williamson and Free, 2005). This is exemplified by the *S. flexneri* serotype 2a strain 2457T, which harbours three *hns*-like genes, namely the chromosomal genes *hns* and *stpA,* and also the novel *hns*-like gene *sfh* which is harboured on the large self-transmissible plasmid pSf-R27 (Beloin *et al.*, 2003). Although the family of known H-NS-like proteins has expanded rapidly in recent years, the physiological role of most of these newly identified H-NS-like proteins remains to be elucidated.

The Sfh protein has 59% and 61% amino acid identity to H-NS and StpA, respectively (Beloin *et al.*, 2003). Like all members of the H-NS protein family, Sfh has a bipartite structure consisting of an N-terminal oligomerization domain and a C-terminal nucleic acid binding domain, connected by a flexible linker (Beloin *et al.*, 2003; Bertin *et al.*, 1999; Dorman *et al.*, 1999). Consequently, Sfh is capable of forming homomeric complexes and also heteromeric complexes with both of its homologues H-NS and StpA (Deighan *et al.*, 2003). This has led to speculation that the properties of these homomeric and heteromeric complexes could vary depending on their protein subunit composition (Deighan *et al.*, 2003; Dorman *et al.*, 1999; Johansson and Uhlin, 1999). Like *stpA* mutants, no obvious phenotypes can be associated with mutations in the *sfh* gene. However, when overexpressed, Sfh can complement several unrelated *hns* mutant phenotypes (Beloin *et al.*, 2003). The aim of the

present studies was to elucidate the physiological role of Sfh and to discover if it had any functions that differed from those of its homologues, StpA and H-NS.

The first distinguishing feature of the *sfh* gene to be elucidated herein was its unique and complex growth phase-dependent expression pattern, which is regulated at the level of transcription and also post-transcriptionally, at the translational level (Fig. 3.22). The exact mechanism underlying the translational block of *sfh* mRNA during the exponential phase of growth was not deciphered in detail, but the data presented strongly suggest that *sfh* mRNA folds into a *cis*-inhibitory secondary structure that hinders efficient translation of the transcript. These data led to the hypothesis that expression of an unknown factor (perhaps a riboregulator or an RNA chaperone) is induced at the onset of stationary phase, which subsequently stimulates translation of the *sfh* transcript. As a result, Sfh expression *in vivo* is specifically induced only during the stationary phase of growth (Fig. 3.22). Significantly, the present study eliminated several prime candidate factors that might modulate *sfh* mRNA translation, including plasmid pSf-R27- or *Shigella*-specific factors. Importantly, H-NS and StpA were shown not to influence the translation of *sfh* transcript, but in agreement with previous reports (Deighan *et al.*, 2003) were observed to repress *sfh* transcription directly. Thus, Sfh cellular levels but not Sfh growth phase-dependent expression is directly modulated by the level of its homologous proteins *in vivo.* Moreover, all three proteins negatively cross-regulate each other's gene expression (Deighan *et al.*, 2003) highlighting the dynamic triangular relationship between H-NS, StpA, and Sfh (Fig. 7.1).

Intriguingly, the post-transcriptional regulation of *sfh* expression ensures that the two paralogues, Sfh and StpA, exhibit growth phase expression patterns that are the reciprocal of each other. Indeed, all three proteins –H-NS, StpA, and Sfh– have distinct growth-phase expression profiles in nutrient-rich broth (Deighan *et al.*, 2003). The differential expression of Sfh, StpA, and H-NS provides the cell with the capacity to vary the composition of its H-NS-like proteins as a function of growth phase. Consequently, the formation of homomeric and heteromeric protein complexes *in vivo* will alter as the different H-NS-like proteins

Fig. 7.1. Model summarizing the triangular relationship between Sfh, H-NS, and StpA. (A) Expression of H-NS, StpA, and Sfh is modulated by several environmental and cellular factors such as temperature and growth phase. Each protein negatively autoregulates transcription its own gene and can negatively cross-regulate each other's gene expression. Members of the H-NS protein family have the same overall domain structure with an N-terminal oligomerization domain connected by a flexible linker region to a C-terminal nucleic acid-binding domain. Consequently, Sfh, H-NS, and StpA are all capable of forming homodimers and each protein can form heterodimers with either of its homologues. (B) Venn diagram represents the different regulons of H-NS (blue set), Sfh (green set), and StpA (red set). The three proteins have both common and distinct regulatory properties and, therefore, are illustrated to have both overlapping and separate regulons. It is proposed that homomeric and heteromeric H-NS-like protein complexes have unique regulatory properties depending on their subunit composition. The speculated regulons of H-NS:Sfh, H-NS:StpA and Sfh:StpA heteromeric complexes are indicated by hashed sets in the Venn diagram.

A.

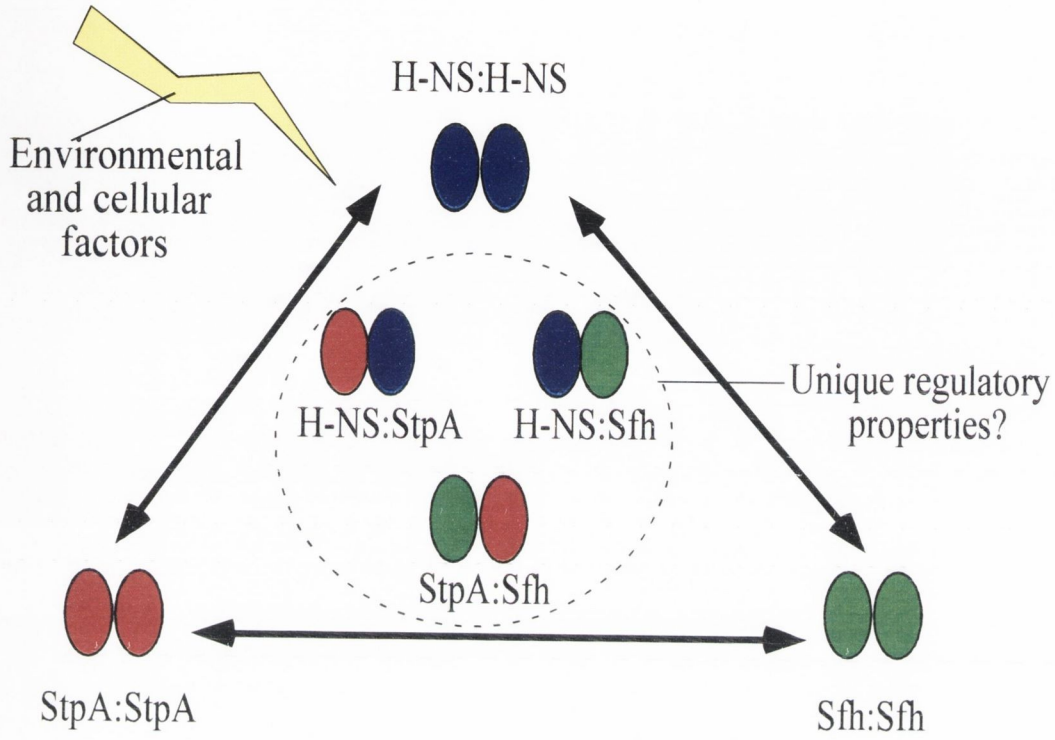
H-NS:H-NS
Environmental and cellular factors
H-NS:StpA
H-NS:Sfh
Unique regulatory properties?
StpA:Sfh
StpA:StpA
Sfh:Sfh

B.

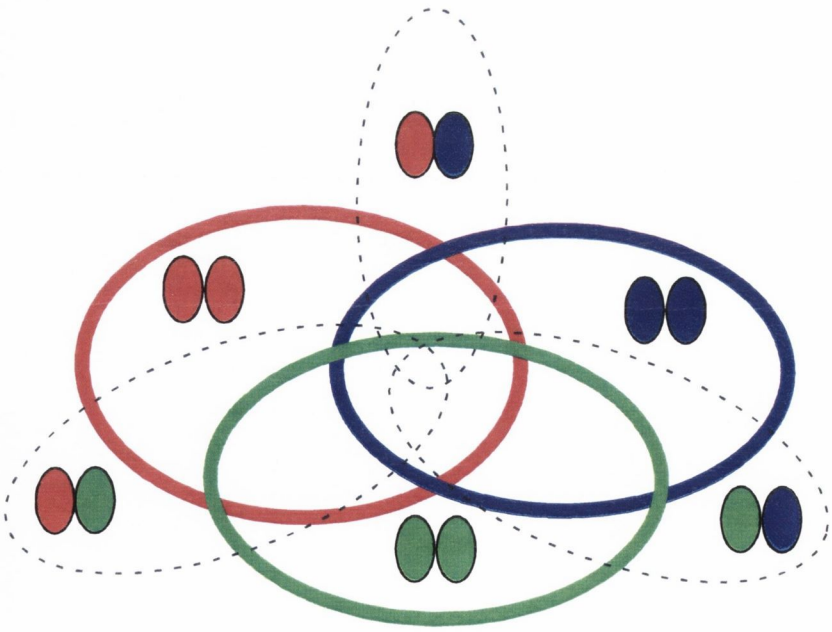

become the dominant species. It is speculated that the different protein complexes have distinct effects on cellular physiology depending on their subunit composition (Fig. 7.1). This hypothesis is strengthened by previous studies on the heterodimeric nucleoid-associated proteins HU and IHF. The different homomeric and heteromeric protein complexes formed by HU and IHF *in vivo* were demonstrated to have both common and distinct functions (Claret and Rouviere-Yaniv, 1997; Mangan *et al.*, 2006). Notably, the formation and ratio of different Sfh and StpA protein complexes *in vivo* is strictly controlled by regulated proteolysis (Fig. 3.20). Both Sfh and StpA (Johansson and Uhlin, 1999) are rapidly degraded in strains lacking H-NS. The protease mediating Sfh degradation in the absence of H-NS has not yet been identified, but several lines of evidence suggest that the Lon protease is responsible for the differential turnover of Sfh, as is the case for StpA (Johansson and Uhlin, 1999). Thus, the stoichiometry of the three proteins Sfh, H-NS and StpA is regulated not only by growth phase, but also proteolysis. These data strengthen the hypothesis of the physiological relevance of different H-NS-like protein complexes in the modulation of gene expression (Fig. 7.1).

In addition, this study revealed the significance of growth temperature on the expression Sfh, H-NS, and StpA. Consistent with previous findings, transcription of the *hns* and *stpA* genes was enhanced during cold shock and in response to increases in the temperature of the growth medium, respectively (Free and Dorman, 1997; La Teana *et al.*, 1991). In contrast, Sfh expression was more or less unaffected by either heat or cold shock. However, Sfh protein levels were observed to be significantly higher in a culture grown at 25°C than in a one grown at 37°C, whereas StpA and H-NS expression was downregulated at the lower growth temperature in accordance with previous findings (Free and Dorman, 1997; Lease *et al.*, 1998; Lease and Belfort, 2000; Sonden and Uhlin, 1996). The increase in Sfh expression at 25°C can be attributed to the low cellular levels of H-NS and StpA at this temperature, which consequently would result in derepression of *sfh* gene expression. These results highlight again the dynamic triangular relationship between H-NS, StpA, and Sfh *in vivo* and are consistent with the model in which different H-NS-like protein complexes have distinct

biological properties that potentially could modulate different subsets of genes in response to environmental change (Fig. 7.1).

Furthermore, H-NS regulates genes linked to the stress response and to changes in environmental conditions, albeit that expression of the *hns* gene itself does not alter significantly in response to heat shock, osmotic shock, carbon starvation, and growth in minimal medium (Dorman *et al.*, 1999; Hinton *et al.*, 1992). Therefore, how does H-NS regulate these genes? One very attractive possibility is that changes in *sfh* and *stpA* expression influence H-NS activity, either by repressing *hns* expression or as mentioned above by forming different homomeric and heteromeric complexes. Consistent with this model *stpA* expression is sensitive to several environmental conditions such as osmolarity, temperature and carbon starvation (Free and Dorman, 1997; Sonden and Uhlin, 1996).

The data presented in this study revealed a novel role for all three proteins, Sfh, H-NS and StpA, in the modulation of plasmid pSf-R27 conjugative transfer. Consistent with members of the H-NS protein family being transcriptional repressors, all three proteins were shown in general to negatively influence *tra* gene expression. Significantly, the results of conjugal transfer assays revealed that none of the *Shigella* H-NS-like proteins mediate the thermosensitive transfer of plasmid pSf-R27. In addition, the mating assays revealed that conjugative transfer of plasmid pSf-R27 from donor strains lacking one or more H-NS-like protein was dramatically reduced. This paradoxical observation suggests that plasmid pSf-R27 conjugative transfer is subject to complex regulation at both the transcriptional and post-transcriptional level. Therefore, derepression of *tra* gene expression would not necessarily correspond with a phenotypic increase in conjugative transfer.

All IncHI1 plasmids including plasmid pSf-R27 encode Dam, Hha and TlpA homologues (Parkhill *et al.*, 2001; Sherburne *et al.*, 2000; Wei *et al.*, 2003). Dam, Hha and TlpA are known transcriptional regulators of temperature-dependent expression systems (Dorman *et al.*, 2001; Rhen and Dorman, 2005) and previous reports have revealed that Dam and

members of the Hha protein family influence F-like plasmid conjugal transfer (Camacho and Casadesus, 2002; Camacho *et al.*, 2005a; Nieto *et al.*, 1998; Torreblanca and Casadesus, 1996). Importantly, the present study demonstrated by RT-PCR analyses that the *dam*-, *hha*- and *tlpA*-like genes encoded by plasmid pSf-R27 are all regulated by Sfh, H-NS, and StpA, in some instances in a temperature-dependent manner. These data indicate that the mechanism controlling the thermosensitive transfer of plasmid pSf-R27 could involve one or more of these proteins and therefore, indirectly Sfh, H-NS and StpA. However, further investigation is required to either confirm or discount this hypothesis.

The transcriptional data obtained herein also illustrate the complex regulatory network of plasmid pSf-R27. The results presented support a model in which Sfh, H-NS and StpA are the master regulators of plasmid pSf-R27 transcriptional regulatory cascades, although it was not determined if the Dam, Hha or TlpA homologues could influence *sfh, hns* and *stpA* expression. It is noteworthy that members of the Hha protein family are known to interact directly with H-NS-like proteins (Nieto *et al.*, 2002), consequently modulating their activity (Nieto *et al.*, 2000). This raises the possibility that the Hha homologue encoded by plasmid pSf-R27 could form heteromeric complexes with H-NS, Sfh, and StpA. Therefore, one must not only consider that the different homomeric and heteromeric H-NS-like protein complexes might regulate disparate subsets of plasmid pSf-R27 genes, but also the additional complexity that different Hha-H-NS-like protein complexes could also be required for the regulation of other distinct subsets of plasmid genes. Interestingly, transcription of several plasmid genes was repressed in an *sfh stpA* mutant background, but derepressed in *sfh* and *stpA* single mutant strains. This observation could be attributed to increased H-NS protein levels in a *sfh stpA* mutant due to the lack of negative cross-regulation by Sfh and StpA, but alternatively could also indicate that heteromeric H-NS-like complexes, especially StpA:Sfh complexes, are required for optimal control of plasmid pSf-R27 gene expression. The latter is consistent with the hypothesis that homomeric and heteromeric H-NS-like protein complexes have distinct regulatory properties depending on their subunit composition.

The results of this study highlight that pSf-R27 plasmid gene expression in *S. flexneri* serotype 2a strain 2457T is controlled by both plasmid- and chromosome-encoded regulators. Integration of horizontally acquired genetic elements into the host regulatory circuit is a widespread phenomenon and is thought to reduce the metabolic burden and thus 'fitness cost' associated with horizontally acquired genetic elements. The strain 2457T was isolated in Tokyo in 1954 (Formal *et al.*, 1958), but it is unclear whether at that time it contained plasmid pSf-R27 or whether it acquired the plasmid thereafter by horizontal transfer. Therefore, although it is obvious that there is cross-talk between the chromosomal and plasmid pSf-R27 regulatory circuits of strain 2457T, it is not known how quickly this phenomenon occurred following horizontal acquisition of plasmid pSf-R27. Perhaps it is possible that transmissible elements like plasmid pSf-R27, which encode paralogues of known global transcriptional regulators, could influence the transcriptome of transconjugants immediately or perhaps it is necessary for time to elapse for plasmid and chromosomal regulatory circuits to co-evolve. This fundamental issue was addressed in this study by determining the global gene response of *S.* Typhimurium strain SL1344 to the horizontal acquisition of plasmids pSf-R27Gent^R and pSf-R27Δ*sfh*::Gent^R.

Surprisingly, DNA microarray analysis revealed that introduction of plasmid pSf-R27Gent^R had only a minor influence on the transcriptome of strain SL1344, whereas in stark contrast horizontal transfer of plasmid pSf-R27 lacking a functional *sfh* gene (plasmid pSf-R27Δ*sfh*::Gent^R) resulted in widespread changes in the SL1344 transcriptome. Genes involved in motility, metabolism, virulence, and the response to DNA damage all showed significant changes in expression following the establishment of plasmid pSf-R27Δ*sfh*::Gent^R in strain SL1344. Consequently, acquisition of plasmid pSf-R27Δ*sfh*::Gent^R dramatically reduced the fitness of the recipient bacterium, whereas in comparison plasmid pSf-R27Gent^R had only a minor 'fitness cost'. Collectively these data revealed that plasmid pSf-R27 requires its H-NS-like gene *sfh* to minimize the impact of the plasmid on the host transcriptome and that, when expressed, the *sfh* gene appears to act like a 'stealth gene' allowing plasmid pSf-R27 to disseminate into a new host virtually without detection.

One puzzling observation was how the absence of Sfh could give rise to such widespread changes in the global expression profile of the transconjugant. Importantly, the phenotype of strain SL1344(pSf-R27Δ*sfh*::Gent^R) resembles that of an *hns* mutant and the plasmid pSf-R27 is very AT-rich (55%), which led to the hypothesis that H-NS is less active in strain SL1344(pSf-R27Δ*sfh*::Gent^R) due to a titration effect exerted by the introduced plasmid. Significantly, this study confirmed this hypothesis. Introduction of a specifically constructed AT-rich plasmid pUCA/T markedly reduced the fitness of a recipient cell by over 50%, whereas in comparison the backbone plasmid pUC18 had only a minor 'fitness cost'. Notably, the AT-rich DNA sequence cloned into pUC18 to generate plasmid pUCA/T did not code for any proteins and thus, the observed decrease in fitness associated with this plasmid could not be attributed to overexpression of a protein. Remarkably, expression of Sfh *in trans* completely negated the fitness cost of plasmid pUCA/T. Moreover, expression of Sfh *in cis* or *in trans* in cells harbouring different plasmids considerably decreased the 'fitness cost' associated with each of the plasmids. Importantly, H-NS could not reduce plasmid 'fitness costs' to the same degree. Therefore, the *sfh* gene can be truly regarded as a 'stealth gene' that can minimize the impact of plasmids on a host cell. This unique novel role for Sfh in plasmid biology could have potential applications in molecular biology research and the biotechnology industry. For example, cloning the *sfh* gene into expression vectors should reduce the fitness cost associated with the plasmid, which in turn might result in better product yields.

It is noteworthy that horizontally acquired genes in Gram-negative bacteria frequently have a high percentage A+T content compared to those of a host genome. Therefore, in light of the data presented herein, their acquisition will most likely correspond with a large reduction in bacterial fitness. Given the abundance of *hns*-related genes among mobile genetic elements, it is plausible that these genes represent a universal regulatory mechanism used by mobile genetic elements for promiscuous horizontal DNA transfer. Therefore, these genes could represent targets for new therapeutic agents, which could thwart the horizontal transfer of mobile genetic elements and thus the spread of virulence factors and antibiotic resistance

genes among pathogenic bacteria. Indeed, horizontal transfer of MDR IncHI1 plasmids has been implicated as the most significant factor in the persistence of typhoid fever worldwide (Lawley *et al.*, 2000; Parkhill *et al.*, 2001; Sherburne *et al.*, 2000; Wain *et al.*, 2003).

Notably, the results of the present study suggest that IncHI1 plasmids could also encode novel virulence factors, which confer a selective advantage upon *Salmonella* spp. in establishing a systemic infection. Strain SL1344 harbouring plasmids pSf-R27Gent^R and pSf-R27Δ*sfh*::Gent^R displayed a marked increase in intracellular macrophage survival rates in comparison to a wild-type strain. Moreover, *S.* Typhi strains harbouring different IncHI1 plasmids also display an increase in macrophage survival (J. Wain, Wellcome Trust Sanger Institute, Cambridge, U.K., personal communication). The exact mechanism by which IncHI1 plasmid carriage corresponds with an increase in *Salmonella* survival within the macrophage is currently unknown. Perhaps, IncHI plasmids encode factors that facilitate the creation of, and survival in, the *Salmonella*-containing vacuole and therefore this would explain the promiscuous nature of these plasmids in *Salmonella* spp.

Future work is required to identify these novel virulence factors and to determine if they are secreted into the host cell, and if so by what secretion system. One attractive possibility is that the factors could be secreted through the conjugation system encoded by IncHI1 plasmids. Although no conjugation occurs at 37°C, *tra* gene transcription can still be detected at this temperature and therefore, it is possible that at 37°C the T4SS secretes such putative virulence factors, while at lower temperatures it transfers plasmid DNA. This hypothesis is supported by previous studies on the *A. tumefaciens* conjugation system, which revealed that it transfers several proteins such as VirE2, SSB, and VirF into plant cells, in addition to oncogenic T-DNA (Vergunst *et al.*, 2000). Moreover, many important pathogens use T4SS's primarily for delivery of proteins rather than nucleic acids into host cells (Burns, 2003; Ding *et al.*, 2003; Nagai and Roy, 2003).

In conclusion, this work has identified novel common and disparate regulatory functions for Sfh and its homologous proteins, H-NS and StpA. All three proteins were shown to modulate plasmid pSf-R27 conjugative transfer, while Sfh was revealed to have a unique 'stealth-like' role in plasmid horizontal transmission. The complex regulation of *sfh* gene expression elucidated in this study highlights the elaborate regulation of *hns*-like genes and indicates the importance of these proteins in cell physiology. It is evident that there is a triangular relationship between Sfh, H-NS and StpA and that the cell dynamically links their expression to each another and to different environmental conditions. No doubt future research will reveal more distinct regulatory functions for these proteins and hopefully will provide concrete evidence that the different homomeric and heteromeric complexes formed by Sfh, H-NS, and StpA regulate both overlapping and distinct regulons.

Bibliography

Abeles, A.L., Friedman, S.A., and Austin, S.J. (1985) Partition of unit-copy miniplasmids to daughter cells. III. The DNA sequence and functional organization of the P1 partition region. *J Mol Biol* **185**: 261-272.

Adam, T., Arpin, M., Prévost, M.-C., Gounon, P., and Sansonetti, P.J. (1995) Cytoskeletal rearrangements and the functional role of T-plastin during entry of *Shigella flexneri* into HeLa cells. *J Cell Biol* **129**: 367-381.

Adler, B., Sasakawa, C., Tobe, T., Makino, S., Komatsu, K., and Yoshikawa, M. (1989) A dual transcriptional activation system for the 230 kb plasmid genes coding for virulence-associated antigens of *Shigella flexneri*. *Mol Microbiol* **3**: 627-635.

Adler, J., and Templeton, B. (1967) The effect of environmental conditions on the motility of *Escherichia coli*. *J Gen Microbiol* **46**: 175-184.

Akbar, S., Schechter, L.M., Lostroh, C.P., and Lee, C.A. (2003) AraC/XylS family members, HilD and HilC, directly activate virulence gene expression independently of HilA in *Salmonella typhimurium*. *Mol Microbiol* **47**: 715-728.

Aldridge, P., and Hughes, K.T. (2002) Regulation of flagellar assembly. *Curr Opin Microbiol* **5**: 160-165.

Alonso, A., Pucciarelli, M.G., Figueroa-Bossi, N., and García-del Portillo, F. (2005a) Increased excision of the *Salmonella* prophage ST64B caused by a deficiency in Dam methylase. *J Bacteriol* **187**: 7901-7911.

Alonso, G., Baptista, K., Ngo, T., and Taylor, D.E. (2005b) Transcriptional organization of the temperature-sensitive transfer system from the IncHI1 plasmid R27. *Microbiology* **151**: 3563-3573.

Alpuche-Aranda, C.M., Racoosin, E.L., Swanson, J.A., and Miller, S.I. (1994) *Salmonella* stimulate macrophage macropinocytosis and persist within spacious phagosomes. *J Exp Med* **179**: 601-608.

Althorpe, N.J., Chilley, P.M., Thomas, A.T., Brammar, W.J., and Wilkins, B.M. (1999) Transient transcriptional activation of the IncI1 plasmid anti-restriction gene (*ardA*) and SOS inhibition gene (*psiB*) early in conjugating recipient bacteria. *Mol Microbiol* **31**: 133-142.

Altschul, S.F., Gish, W., Miller, W., Myers, E.W., and Lipman, D.J. (1990) Basic local alignment search tool. *J Mol Biol* **215**: 403-410.

Altuvia, S., Weinstein-Fischer, D., Zhang, A., Postow, L., and Storz, G. (1997) A small, stable RNA induced by oxidative stress: role as a pleiotropic regulator and antimutator. *Cell* **90**: 43-53.

Amerik, A.Y., Antonov, V.K., Gorbalenya, A.E., Kotova, S.A., Rotanova, T.V., and Shimbarevich, E.V. (1991) Site-directed mutagenesis of La protease. A catalytically active serine residue. *FEBS Lett* **287**: 211-214.

Amit, R., Oppenheim, A.B., and Stavans, J. (2003) Increased bending rigidity of single DNA molecules by H-NS, a temperature and osmolarity sensor. *Biophys J* **84**: 2467-2473.

Anderson, E.S., and Smith, H.R. (1972) Chloramphenicol resistance in the typhoid bacillus. *Br Med J* **3**: 329-331.

Atlung, T., and Ingmer, H. (1997) H-NS: a modulator of environmentally regulated gene expression. *Mol Microbiol* **24**: 7-17.

Auner, H., Buckle, M., Deufel, A., Kutateladze, T., Lazarus, L., Mavathur, R., Muskhelishvili, G., Pemberton, I., Schneider, R., and Travers, A. (2003) Mechanism of transcriptional activation by FIS: role of core promoter structure and DNA topology. *J Mol Biol* **331**: 331-344.

Ausubel, F.M., Brent, R., Kingston, R.E., Moore, D.D., Seidman, J.G., Smith, J.A., and Struhl, K. (1990) *Current Protocols in Molecular Biology*. New York: John Wiley and Sons.

Aviv, M., Giladi, H., Schreiber, G., Oppenheim, A.B., and Glaser, G. (1994) Expression of the genes coding for the *Escherichia coli* integration host factor are controlled by growth phase, *rpoS*, ppGpp and by autoregulation. *Mol Microbiol* **14**: 1021-1031.

Azam, T.A., and Ishihama, A. (1999) Twelve species of the nucleoid-associated protein from *Escherichia coli*. Sequence recognition specificity and DNA binding affinity. *J Biol Chem* **274**: 33105-33113.

Azam, T.A., Iwata, A., Nishimura, A., Ueda, S., and Ishihama, A. (1999) Growth phase-dependent variation in protein composition of the *Escherichia coli* nucleoid. *J Bacteriol* **181**: 6361-6370.

Badaut, C., Williams, R., Arluison, V., Bouffartigues, E., Robert, B., Buc, H., and Rimsky, S. (2002) The degree of oligomerization of the H-NS nucleoid structuring protein is related to specific binding to DNA. *J Biol Chem* **277**: 41657-41666.

Bajaj, V., Hwang, C., and Lee, C.A. (1995) *hilA* is a novel *ompR/toxR* family member that activates the expression of *Salmonella typhimurium* invasion genes. *Mol Microbiol* **18**: 715-727.

Bajaj, V., Lucas, R.L., Hwang, C., and Lee, C.A. (1996) Co-ordinate regulation of *Salmonella typhimurium* invasion genes by environmental and regulatory factors is mediated by control of *hilA* expression. *Mol Microbiol* **22**: 703-714.

Bakshi, C.S., Singh, V.P., Wood, M.W., Jones, P.W., Wallis, T.S., and Galyov, E.E. (2000) Identification of SopE2, a *Salmonella* secreted protein which is highly homologous to SopE and involved in bacterial invasion of epithelial cells. *J Bacteriol* **182**: 2341-2344.

Balandina, A., Claret, L., Hengge-Aronis, R., and Rouviere-Yaniv, J. (2001) The *Escherichia coli* histone-like protein HU regulates *rpoS* translation. *Mol Microbiol* **39**: 1069-1079.

Ball, C.A., and Johnson, R.C. (1991a) Efficient excision of phage λ from the *Escherichia coli* chromosome requires the Fis protein. *J Bacteriol* **173**: 4027-4031.

Ball, C.A., and Johnson, R.C. (1991b) Multiple effects of Fis on integration and the control of lysogeny in phage λ. *J Bacteriol* **173**: 4032-4038.

Ball, C.A., Osuna, R., Ferguson, K.C., and Johnson, R.C. (1992) Dramatic changes in Fis levels upon nutrient upshift in *Escherichia coli*. *J Bacteriol* **174**: 8043-8056.

Bates, S., Roscoe, R.A., Althorpe, N.J., Brammar, W.J., and Wilkins, B.M. (1999) Expression of leading region genes on IncI1 plasmid ColIb-P9: genetic evidence for single-stranded DNA transcription. *Microbiology* **145**: 2655-2662.

Bäumler, A.J., Tsolis, R.M., and Heffron, F. (1996) Contribution of fimbrial operons to attachment to and invasion of epithelial cell lines by *Salmonella typhimurium*. *Infect Immun* **64**: 1862-1865.

Becker, G., Klauck, E., and Hengge-Aronis, R. (1999) Regulation of RpoS proteolysis in *Escherichia coli*: the response regulator RssB is a recognition factor that interacts with the turnover element in RpoS. *Proc Natl Acad Sci U S A* **96**: 6439-6444.

Beilharz, T.H., and Preiss, T. (2004) Translational profiling: the genome-wide measure of the nascent proteome. *Brief Funct Genomic Proteomic* **3**: 103-111.

Beloin, C., McKenna, S., and Dorman, C.J. (2002) Molecular dissection of VirB, a key regulator of the virulence cascade of *Shigella flexneri*. *J Biol Chem* **277**: 15333-15344.

Beloin, C., Deighan, P., Doyle, M., and Dorman, C.J. (2003) *Shigella flexneri* 2a strain 2457T expresses three members of the H-NS-like protein family: characterization of the Sfh protein. *Mol Genet Genomics* **270**: 66-77.

Beloin, C., and Dorman, C.J. (2003) An extended role for the nucleoid structuring protein H-NS in the virulence gene regulatory cascade of *Shigella flexneri*. *Mol Microbiol* **47**: 825-838.

Benson, N.R., Wong, R.M., and McClelland, M. (2000) Analysis of the SOS response in *Salmonella enterica* serovar *typhimurium* using RNA fingerprinting by arbitrarily primed PCR. *J Bacteriol* **182**: 3490-3497.

Bernardini, M.L., Mounier, J., d'Hauteville, H., Coquis-Rondon, M., and Sansonetti, P.J. (1989) Identification of *icsA*, a plasmid locus of *Shigella flexneri* that governs bacterial intra- and intercellular spread through interaction with F-actin. *Proc Natl Acad Sci U S A* **86**: 3867-3871.

Bertin, P., Terao, E., Lee, E.H., Lejeune, P., Colson, C., Danchin, A., and Collatz, E. (1994) The H-NS protein is involved in the biogenesis of flagella in *Escherichia coli*. *J Bacteriol* **176**: 5537-5540.

Bertin, P., Benhabiles, N., Krin, E., Laurent-Winter, C., Tendeng, C., Turlin, E., Thomas, A., Danchin, A., and Brasseur, R. (1999) The structural and functional organization of H-NS-like proteins is evolutionarily conserved in gram-negative bacteria. *Mol Microbiol* **31**: 319-329.

Bertin, P., Hommais, F., Krin, E., Soutourina, O., Tendeng, C., Derzelle, S., and Danchin, A. (2001) H-NS and H-NS-like proteins in Gram-negative bacteria andtheir multiple role in the regulation of bacterial metabolism. *Biochimie* **83**: 235-241.

Beuzon, C.R., Banks, G., Deiwick, J., Hensel, M., and Holden, D.W. (1999) pH-dependent secretion of SseB, a product of the SPI-2 type III secretion system of *Salmonella typhimurium*. *Mol Microbiol* **33**: 806-816.

Beuzon, C.R., Meresse, S., Unsworth, K.E., Ruiz-Albert, J., Garvis, S., Waterman, S.R., Ryder, T.A., Boucrot, E., and Holden, D.W. (2000) *Salmonella* maintains the integrity of its intracellular vacuole through the action of SifA. *EMBO J* **19**: 3235-3249.

Bhutta, Z.A., Khan, I.A., and Shadmani, M. (2000) Failure of short-course ceftriaxone chemotherapy for multidrug-resistant typhoid fever in children: a randomized controlled trial in Pakistan. *Antimicrob Agents Chemother* **44**: 450-452.

Bignell, C., and Thomas, C.M. (2001) The bacterial ParA-ParB partitioning proteins. *J Biotechnol* **91**: 1-34.

Bijlsma, J.J., and Groisman, E.A. (2005) The PhoP/PhoQ system controls the intramacrophage type three secretion system of *Salmonella enterica*. *Mol Microbiol* **57**: 85-96.

Bingle, L.E., and Thomas, C.M. (2001) Regulatory circuits for plasmid survival. *Curr Opin Microbiol* **4**: 194-200.

Blanc-Potard, A.B., and Groisman, E.A. (1997) The *Salmonella selC* locus contains a pathogenicity island mediating intramacrophage survival. *EMBO J* **16**: 5376-5385.

Blanc-Potard, A.B., Solomon, F., Kayser, J., and Groisman, E.A. (1999) The SPI-3 pathogenicity island of *Salmonella enterica*. *J Bacteriol* **181**: 998-1004.

Blattner, F.R., Weising, K., Banfer, G., Maschwitz, U., and Fiala, B. (2001) Molecular analysis of phylogenetic relationships among *Myrmecophytic macaranga* species (*Euphorbiaceae*). *Mol Phylogenet Evol* **19**: 331-344.

Bloch, V., Yang, Y., Margeat, E., Chavanieu, A., Auge, M.T., Robert, B., Arold, S., Rimsky, S., and Kochoyan, M. (2003) The H-NS dimerization domain defines a new fold contributing to DNA recognition. *Nat Struct Biol* **10**: 212-218.

Blocker, A., Gounon, P., Larquet, E., Niebuhr, K., Cabiaux, V., Parsot, C., and Sansonetti, P. (1999) The tripartite type III secreton of *Shigella flexneri* inserts IpaB and IpaC into host membranes. *J Cell Biol* **147**: 683-693.

Boddicker, J.D., Knosp, B.M., and Jones, B.D. (2003) Transcription of the *Salmonella* invasion gene activator, *hilA*, requires HilD activation in the absence of negative regulators. *J Bacteriol* **185**: 525-533.

Bonifield, H.R., and Hughes, K.T. (2003) Flagellar phase variation in *Salmonella enterica* is mediated by a posttranscriptional control mechanism. *J Bacteriol* **185**: 3567-3574.

Bonnefoy, E., Almeida, A., and Rouviere-Yaniv, J. (1989) Lon-dependent regulation of the DNA binding protein HU in *Escherichia coli*. *Proc Natl Acad Sci U S A* **86**: 7691-7695.

Boubrik, F., and Rouviere-Yaniv, J. (1995) Increased sensitvity to gamma radiation in bacteria lacking protein HU. *Proc Natl Acad Sci U S A* **92:** 3958-3962.

Bradford, M.M. (1976) A rapid and sensitive method for the quantitation of microgram quantities of protein utilizing the principle of protein-dye binding. *Anal Biochem* **72**: 248-254.

Bracco, L., Kotlarz, D., Kolb, A., Diekmann, S., and Buc, H. (1989) Synthetic curved DNA sequences can act as transcriptional activators in *Escherichia coli*. *EMBO J* **8**: 4289-4296.

Bradley, D.E., Hughes, V.M., Richards, H., and Datta, N. (1982) R plasmids of a new incompatibility group determine constitutive production of H pili. *Plasmid* **7**: 230-238.

Brau, B., Pilz, U., and Piepersberg, W. (1984) Genes for gentamicin-(3)-N-acetyltransferases III and IV: I. Nucleotide sequence of the AAC(3)-IV gene and possible involvement of an IS*140* element in its expression. *Mol Gen Genet* **193**: 179-187.

Brent, R., and Ptashne, M. (1981) Mechanism of action of the *lexA* gene product. *Proc Natl Acad Sci U S A* **78**: 4204-4208.

Brescia, C.C., Kaw, M.K., and Sledjeski, D.D. (2004) The DNA binding protein H-NS binds to and alters the stability of RNA *in vitro* and *in vivo*. *J Mol Biol* **339**: 505-514.

Broyles, S.S., and Pettijohn, D.E. (1986) Interaction of the *Escherichia coli* HU protein with DNA. Evidence for formation of nucleosome-like structures with altered DNA helical pitch. *J Mol Biol* **187**: 47-60.

Buchrieser, C., Glaser, P., Rusniok, C., Nedjari, H., d'Hauteville, H., Kunst, F., Sansonetti, P., and Parsot, C. (2000) The virulence plasmid pWR100 and the repertoire of proteins secreted by the type III secretion apparatus of *Shigella flexneri*. *Mol Microbiol* **38**: 760-771.

Bunny, K., Liu, J., and Roth, J. (2002) Phenotypes of *lexA* mutations in *Salmonella enterica*: evidence for a lethal *lexA* null phenotype due to the Fels-2 prophage. *J Bacteriol* **184**: 6235-6249.

Burns, D.L. (2003) Type IV transporters of pathogenic bacteria. *Curr Opin Microbiol* **6**: 29-34.

Burrus, V., and Waldor, M.K. (2003) Control of SXT integration and excision. *J Bacteriol* **185**: 5045-5054.

Bushman, W., Thompson, J.F., Vargas, L., and Landy, A. (1985) Control of directionality in lambda site specific recombination. *Science* **230**: 906-911.

Bustamante, V.H., Santana, F.J., Calva, E., and Puente, J.L. (2001) Transcriptional regulation of type III secretion genes in enteropathogenic *Escherichia coli*: Ler antagonizes H-NS-dependent repression. *Mol Microbiol* **39**: 664-678.

Camacho, E.M., and Casadesús, J. (2002) Conjugal transfer of the virulence plasmid of *Salmonella enterica* is regulated by the leucine-responsive regulatory protein and DNA adenine methylation. *Mol Microbiol* **44**: 1589-1598.

Camacho, E.M., and Casadesús, J. (2005) Regulation of *traJ* transcription in the *Salmonella* virulence plasmid by strand-specific DNA adenine hemimethylation. *Mol Microbiol* **57**: 1700-1718.

Camacho, E.M., Serna, A., and Casadesús, J. (2005a) Regulation of conjugal transfer by Lrp and Dam methylation in plasmid R100. *Int Microbiol* **8**: 279-285.

Camacho, E.M., Serna, A., Madrid, C., Marques, S., Fernandez, R., de la Cruz, F., Juárez, A., and Casadesuú, J. (2005b) Regulation of *finP* transcription by DNA adenine methylation in the virulence plasmid of *Salmonella enterica*. *J Bacteriol* **187**: 5691-5699.

Carpousis, A.J. (2002) The *Escherichia coli* RNA degradosome: structure, function and relationship in other ribonucleolytic multienzyme complexes. *Biochem Soc Trans* **30**: 150-155.

Carroll, R.K. (2003) Virulence gene regulation by nucleoid-associated proteins in *Salmonella typhimurium*: a role for Fis in *Salmonella* pathogenicity island 2 gene regulation. Ph.D. Thesis, Trinity College Dublin.

Casadaban, M.J. (1976) Transposition and fusion of the *lac* genes to selected promoters in *Escherichia coli* using bacteriophage lambda and Mu. *J Mol Biol* **104:** 541-555.

Cascales, E., and Christie, P.J. (2003) The versatile bacterial type IV secretion systems. *Nat Rev Microbiol* **1**: 137-149.

Case, R.B., Chang, Y.P., Smith, S.B., Gore, J., Cozzarelli, N.R., and Bustamante, C. (2004) The bacterial condensin MukBEF compacts DNA into a repetitive, stable structure. *Science* **305**: 222-227.

Catron, D.M., Sylvester, M.D., Lange, Y., Kadekoppala, M., Jones, B.D., Monack, D.M., Falkow, S., and Haldar, K. (2002) The *Salmonella*-containing vacuole is a major site of intracellular cholesterol accumulation and recruits the GPI-anchored protein CD55. *Cell Microbiol* **4**: 315-328.

Cerdan, R., Bloch, V., Yang, Y., Bertin, P., Dumas, C., Rimsky, S., Kochoyan, M., and Arold, S.T. (2003) Crystal structure of the N-terminal dimerisation domain of VicH, the H-NS-like protein of *Vibrio cholerae*. *J Mol Biol* **334**: 179-185.

Ceschini, S., Lupidi, G., Coletta, M., Pon, C.L., Fioretti, E., and Angeletti, M. (2000) Multimeric self-assembly equilibria involving the histone-like protein H-NS. A thermodynamic study. *J Biol Chem* **275**: 729-734.

Chakravortty, D., Hansen-Wester, I., and Hensel, M. (2002) *Salmonella* pathogenicity island 2 mediates protection of intracellular *Salmonella* from reactive nitrogen intermediates. *J Exp Med* **195**: 1155-1166.

Chakravortty, D., Rohde, M., Jager, L., Deiwick, J., and Hensel, M. (2005) Formation of a novel surface structure encoded by *Salmonella* Pathogenicity Island 2. *EMBO J* **24**: 2043-2052.

Chalfie, M., Tu, Y., Euskirchen, G., Ward, W.W., and Prasher, D.C. (1994) Green fluorescent protein as a marker for gene expression. *Science* **263**: 802-805.

Chaveroche, M.-K., Ghigo, J.-M., and d'Enfert, C. (2000) A rapid method for efficient gene replacement in the filamentous fungus *Aspergillus nidulans*. *Nucleic Acids Res* **28**: E97.

Chen, C.Y., Buchmeier, N.A., Libby, S., Fang, F.C., Krause, M., and Guiney, D.G. (1995) Central regulatory role for the RpoS sigma factor in expression of *Salmonella dublin* plasmid virulence genes. *J Bacteriol* **177**: 5303-5309.

Chilcott, G.S., and Hughes, K.T. (2000) Coupling of flagellar gene expression to flagellar assembly in *Salmonella enterica* serovar *typhimurium* and *Escherichia coli*. *Microbiol Mol Biol Rev* **64**: 694-708.

Chin, D.T., Goff, S.A., Webster, T., Smith, T., and Goldberg, A.L. (1988) Sequence of the *lon* gene in *Escherichia coli*. A heat-shock gene which encodes the ATP-dependent protease La. *J Biol Chem* **263**: 11718-11728.

Chomczynski, P. (1993) A reagent for the single-step simultaneous isolation of RNA, DNA and proteins from cell and tissue samples. *Biotechniques* **15**: 532-534, 536-537.

Christie, P.J., and Vogel, J.P. (2000) Bacterial type IV secretion: conjugation systems adapted to deliver effector molecules to host cells. *Trends Microbiol* **8**: 354-360.

Christie, P.J. (2004) Type IV secretion: the *Agrobacterium* VirB/D4 and related conjugation systems. *Biochim Biophys Acta* **1694**: 219-234.

Christie, P.J., Atmakuri, K., Krishnamoorthy, V., Jakubowski, S., and Cascales, E. (2005) Biogenesis, architecture, and function of bacterial type IV secretion systems. *Annu Rev Microbiol* **59**: 451-485.

Chu, C., Hong, S.-F., Tsai, C., Lin, W.-S., Liu, T.-P., and Ou, J.T. (1999) Comparative physical and genetic maps of the virulence plasmids of *Salmonella enterica* serovars *typhimurium*, *enteritidis*, *choleraesuis*, and *dublin*. *Infect Immun* **67**: 2611-2614.

Cirillo, D.M., Valdivia, R.H., Monack, D.M., and Falkow, S. (1998) Macrophage-dependent induction of the *Salmonella* pathogenicity island 2 type III secretion system and its role in intracellular survival. *Mol Microbiol* **30**: 175-188.

Claret, L., and Rouviere-Yaniv, J. (1996) Regulation of HUα and HUβ by CRP and FIS in *Escherichia coli*. *J Mol Biol* **263**: 126-139.

Claret, L., and Rouviere-Yaniv, J. (1997) Variation in HU composition during growth of *Escherichia coli*: the heterodimer is required for long term survival. *J Mol Biol* **273**: 93-104.

Clegg, S., Hancox, L.S., and Yeh, K.-S. (1996) *Salmonella typhimurium* fimbrial phase variation and FimA expression. *J Bacteriol* **178**: 542-545.

Coburn, G.A., and Mackie, G.A. (1999) Degradation of mRNA in *Escherichia coli*: an old problem with some new twists. *Prog Nucleic Acid Res Mol Biol* **62**: 55-108.

Collazo, C.M., and Galán, J.E. (1997) The invasion-associated type-III protein secretion system in *Salmonella*-a review. *Gene* **192**: 51-59.

Colonna, B., Casalino, M., Fradiani, P.A., Zagaglia, C., Naitza, S., Leoni, L., Prosseda, G., Coppo, A., Ghelardini, P., and Nicoletti, M. (1995) H-NS regulation of virulence gene expression in enteroinvasive *Escherichia coli* harboring the virulence plasmid integrated into the host chromosome. *J Bacteriol* **177**: 4703-4712.

Coombes, B.K., Brown, N.F., Valdez, Y., Brumell, J.H., and Finlay, B.B. (2004) Expression and Secretion of *Salmonella* Pathogenicity Island-2 Virulence genes in Response to Acidification Exhibit Differential Requirements of a Functional Type III Secretion Apparatus and SsaL. *J Biol Chem* **279:** 49804-49815.

Coombes, B.K., Wickham, M.E., Brown, N.F., Lemire, S., Bossi, L., Hsiao, W.W.L., Brinkman, F.S., and Finlay, B.B. (2005a) Genetic and molecular analysis of GogB, a phage-encoded type III-secreted substrate in *Salmonella enterica* serovar *typhimurium* with autonomous expression from its associated phage. *J Mol Biol* **348**: 817-830.

Coombes, B.K., Wickham, M.E., Lowden, M.J., Brown, N.F., and Finlay, B.B. (2005b) Negative regulation of *Salmonella* pathogenicity island 2 is required for contextual control of virulence during typhoid. *Proc Natl Acad Sci U S A* **102**: 17460-17465.

Coynault, C., Robbe-Saule, V., Popoff, M.Y., and Norel, F. (1992) Growth phase and SpvR regulation of transcription of *Salmonella typhimurium spvABC* virulence genes. *Microb Pathog* **13**: 133-143.

Craig, N.L., and Nash, H.A. (1984) *E. coli* integration host factor binds to specific sites in DNA. *Cell* **39**: 707-716.

Crellin, P., Sewitz, S., and Chalmers, R. (2004) DNA looping and catalysis; the IHF-folded arm of Tn*10* promotes conformational changes and hairpin resolution. *Mol Cell* **13**: 537-547.

Cunha, S., Odijk, T., Süleymanoglu, E., and Woldringh, C.L. (2001) Isolation of the *Escherichia coli* nucleoid. *Biochimie* **83**: 149-154.

Cusick, M.E., and Belfort, M. (1998) Domain Structure and RNA annealing activity of the *Escherichia coli* regulatory protein StpA. *Mol Microbiol* **28**: 847-857.

Dahlberg, C., and Chao, L. (2003) Amelioration of the cost of conjugative plasmid carriage in *Eschericha coli* K12. *Genetics* **165**: 1641-1649.

Dame, R.T., Wyman, C., and Goosen, N. (2000) H-NS mediated compaction of DNA visualised by atomic force microscopy. *Nucleic Acids Res* **28**: 3504-3510.

Dame, R.T., Wyman, C., Wurm, R., Wagner, R., and Goosen, N. (2002) Structural basis for H-NS-mediated trapping of RNA polymerase in the open initiation complex at the *rrnB* P1. *J Biol Chem* **277**: 2146-2150.

Dame, R.T. (2005) The role of nucleoid-associated proteins in the organization and compaction of bacterial chromatin. *Mol Microbiol* **56**: 858-870.

Darwin, K.H., and Miller, V.L. (1999a) InvF is required for expression of genes encoding proteins secreted by the SPI1 type III secretion apparatus *in Salmonella typhimurium*. *J Bacteriol* **181**: 4949-4954.

Darwin, K.H., and Miller, V.L. (1999b) Molecular basis of the interaction of *Salmonella* with the intestinal mucosa. *Clin Microbiol Rev* **12**: 405-428.

Darwin, K.H., and Miller, V.L. (2000) The putative invasion protein chaperone SicA acts together with InvF to activate the expression of *Salmonella typhimurium* virulence genes. *Mol Microbiol* **35**: 949-960.

Datsenko, K.A., and Wanner, B.L. (2000) One-step inactivation of chromosomal genes in *Escherichia coli* K-12 using PCR products. *Proc Natl Acad Sci U S A* **97**: 6640-6645.

Deighan, P., Free, A., and Dorman, C.J. (2000) A role for the *Escherichia coli* H-NS-like protein StpA in OmpF porin expression through modulation of *micF* RNA stability. *Mol Microbiol* **38**: 126-139.

Deighan, P., Beloin, C., and Dorman, C.J. (2003) Three-way interactions among the Sfh, StpA and H-NS nucleoid-structuring proteins of *Shigella flexneri* 2a strain 2457T. *Mol Microbiol* **48**: 1401-1416.

Deiwick, J., Nikolaus, T., Erdogan, S., and Hensel, M. (1999) Environmental regulation of *Salmonella* pathogenicity island 2 gene expression. *Mol Microbiol* **31**: 1759-1773.

Dempsey, W.B., and Fee, B.E. (1990) Integration host factor affects expression of two genes at the conjugal transfer origin of plasmid R100. *Mol Microbiol* **4**: 1019-1028.

Dersch, P., Schmidt, K., and Bremer, E. (1993) Synthesis of the *Escherichia coli* K-12 nucleoid-associated DNA-binding protein H-NS is subjected to growth-phase control and autoregulation. *Mol Microbiol* **8**: 875-889.

Dersch, P., Frisihi, H. and Bremer, E. (1994) Low-copy-number T7 vector for selective gene expression and efficient overproduction in *Escherichia coli*. *FEMS Microbiol Lett* **123:** 19-26.

Ding, Z., Atmakuri, K., and Christie, P.J. (2003) The outs and ins of bacterial type IV secretion substrates. *Trends Microbiol* **11**: 527-535.

Dockrell, D.H. (2001) Apoptotic cell death in the pathogenesis of infectious diseases. *J Infect* **42**: 227-234.

Doolittle, W.F., Boucher, Y., Nesbo, C.L., Douady, C.J., Andersson, J.O., and Roger, A.J. (2003) How big is the iceberg of which organellar genes in nuclear genomes are but the tip? *Philos Trans R Soc Lond B Biol Sci* **358**: 39-57.

Dorman, C.J., and Higgins, C.F. (1987) Fimbrial phase variation in *Escherichia coli*: dependence on integration host factor and homologies with other site-specific recombinases. *J Bacteriol* **169**: 3840-3843.

Dorman, C.J. (1995) 1995 Flemming Lecture. DNA topology and the global control of bacterial gene expression: implications for the regulation of virulence gene expression. *Microbiology* **141**: 1271-1280.

Dorman, C.J., and Porter, M.E. (1998) The *Shigella* virulence gene regulatory cascade: a paradigm of bacterial gene control mechanisms. *Mol Microbiol* **29**: 677-684.

Dorman, C.J., Hinton, J.C., and Free, A. (1999) Domain organization and oligomerization among H-NS-like nucleoid-associated proteins in bacteria. *Trends Microbiol* **7**: 124-128.

Dorman, C.J., McKenna, S., and Beloin, C. (2001) Regulation of virulence gene expression in *Shigella flexneri*, a facultative intracellular pathogen. *Int J Med Microbiol* **291**: 89-96.

Dorman, C.J., and Deighan, P. (2003) Regulation of gene expression by histone-like proteins in bacteria. *Curr Opin Genet Dev* **13**: 179-184.

Dorman, C.J. (2004) H-NS: a universal regulator for a dynamic genome. *Nat Rev Microbiol* **2**: 391-400.

Drlica, K., and Rouviere-Yaniv, J. (1987) Histone-like proteins of bacteria. *Microbiol Rev* **51**: 301-319.

DuPont, H.L., Levine, M.M., Hornick, R.B., and Formal, S.B. (1989) Inoculum size in shigellosis and implications for expected mode of transmission. *J Infect Dis* **159**: 1126-1128.

Ebel, W., Skinner, M.M., Dierksen, K.P., Scott, J.M., and Trempy, J.E. (1999) A conserved domain in *Escherichia coli* Lon protease is involved in substrate discriminator activity. *J Bacteriol* **181:** 2236-2243.

Egan, S.M. (2002) Growing repertoire of AraC/XylS activators. *J Bacteriol* **184**: 5529-5532.

Egile, C., d'Hauteville, H., Parsot, C., and Sansonetti, P.J. (1997) SopA, the outer membrane protease responsible for polar localization of IcsA in *Shigella flexneri*. *Mol Microbiol* **23**: 1063-1073.

Eguchi, Y., Ogawa, T., and Ogawa, H. (1988) Cleavage of bacteriophage ϕ80 CI repressor by RecA protein. *J Mol Biol* **202**: 565-573.

Ehrbar, K., and Hardt, W.D. (2005) Bacteriophage-encoded type III effectors in *Salmonella enterica* subspecies 1 serovar Typhimurium. *Infect Genet Evol* **5**: 1-9.

Eichelberg, K., and Galan, J.E. (1999) Differential regulation of *Salmonella typhimurium* type III secreted proteins by pathogenicity island 1 (SPI-1)-encoded transcriptional activators InvF and HilA. *Infect Immun* **67**: 4099-4105.

Eisenbrandt, R., Kalkum, M., Lurz, R., and Lanka, E. (2000) Maturation of IncP pilin precursors resembles the catalytic Dyad-like mechanism of leader peptidases. *J Bacteriol* **182**: 6751-6761.

El-Gedaily, A., Paesold, G., and Krause, M. (1997) Expression profile and subcellular location of the plasmid-encoded virulence (Spv) proteins in wild-type *Salmonella dublin*. *Infect Immun* **65**: 3406-3411.

Ellermeier, C.D., and Slauch, J.M. (2003) RtsA and RtsB coordinately regulate expression of the invasion and flagellar genes in *Salmonella enterica* serovar Typhimurium. *J Bacteriol* **185**: 5096-5108.

Eriksson, S., Lucchini, S., Thompson, A., Rhen, M., and Hinton, J.C. (2003) Unravelling the biology of macrophage infection by gene expression profiling of intracellular *Salmonella enterica*. *Mol Microbiol* **47**: 103-118.

Esposito, D., Thrower, J.S., and Scocca, J.J. (2001) Protein and DNA requirements of the bacteriophage HP1 recombination system: a model for intasome formation. *Nucleic Acids Res* **29**: 3955-3964.

Esposito, D., Petrovic, A., Harris, R., Ono, S., Eccleston, J.F., Mbabaali, A., Haq, I., Higgins, C.F., Hinton, J.C., Driscoll, P.C., and Ladbury, J.E. (2002) H-NS oligomerization domain structure reveals the mechanism for high order self-association of the intact protein. *J Mol Biol* **324**: 841-850.

Fahlen, T.F., Wilson, R.L., Boddicker, J.D., and Jones, B.D. (2001) Hha is a negative modulator of transcription of *hilA*, the *Salmonella enterica* serovar Typhimurium invasion gene transcriptional activator. *J Bacteriol* **183**: 6620-6629.

Falconi, M., Gualtieri, M.T., La Teana, A., Losso, M.A., and Pon, C.L. (1988) Proteins from the prokaryotic nucleoid: primary and quaternary structure of the 15-kDa *Escherichia coli* DNA binding protein H-NS. *Mol Microbiol* **2**: 323-329.

Falconi, M., Brandi, A., La Teana, A., Gualerzi, C.O., and Pon, C.L. (1996) Antagonistic involvement of FIS and H-NS proteins in the transcriptional control of *hns* expression. *Mol Microbiol* **19**: 965-975.

Falconi, M., Colonna, B., Prosseda, G., Micheli, G., and Gualerzi, C.O. (1998) Thermoregulation of *Shigella* and *Escherichia coli* EIEC pathogenicity. A temperature-dependent structural transition of DNA modulates accessibility of *virF* promoter to transcriptional repressor H-NS. *EMBO J* **17**: 7033-7043.

Falconi, M., Prosseda, G., Giangrossi, M., Beghetto, E., and Colonna, B. (2001) Involvement of FIS in the H-NS-mediated regulation of *virF* gene of *Shigella* and enteroinvasive *Escherichia coli*. *Mol Microbiol* **42**: 439-452.

Fang, F.C., DeGroote, M.A., Foster, J.W., Bäumler, A.J., Ochsner, U., Testerman, T., Bearson, S., Giárd, J.-C., Xu, Y., Campbell, G., and Laessig, T. (1999) Virulent *Salmonella typhimurium* has two periplasmic Cu, Zn-superoxide dismutases. *Proc Natl Acad Sci U S A* **96**: 7502-7507.

Farinha, M. A., and Kropinski, A. M. (1990) Construction of broad-host-range plasmid vectors for easy visible selection and analysis of promoters. *J. Bacteriol* **172**:3496-3499.

Farizo, K.M., Huang, T., and Burns, D.L. (2000) Importance of holotoxin assembly in Ptl-mediated secretion of pertussis toxin from *Bordetella pertussis*. *Infect Immun* **68**: 4049-4054.

Feng, X., Oropeza, R., and Kenney, L.J. (2003) Dual regulation by phospho-OmpR of *ssrA/B* gene expression in *Salmonella* pathogenicity island 2. *Mol Microbiol* **48**: 1131-1143.

Fernández de Henestrosa, A.R., Ogi, T., Aoyagi, S., Chafin, D., Hayes, J.J., Ohmori, H., and Woodgate, R. (2000) Identification of additional genes belonging to the LexA regulon in *Escherichia coli*. *Mol Microbiol* **35**: 1560-1572.

Fica, A., Fernandez-Beros, M.-E., Aron-Hott, L., Rivas, A., D'Ottone, K., Chumpitaz, J., Guevara, J.M., Rodríguez, M., and Cabello, F. (1997) Antibiotic-resistant *Salmonella typhi* from two outbreaks: few ribotypes and IS*200* types harbor Inc HI1 plasmids. *Microb Drug Resist* **3**: 339-343.

Figueroa-Bossi, N., and Bossi, L. (1999) Inducible prophages contribute to *Salmonella* virulence in mice. *Mol Microbiol* **33**: 167-176.

Figueroa-Bossi, N., Uzzau, S., Maloriol, D., and Bossi, L. (2001) Variable assortment of prophages provides a transferable repertoire of pathogenic determinants in *Salmonella*. *Mol Microbiol* **39**: 260-271.

Filutowicz, M., Ross, W., Wild, J., and Gourse, R.L. (1992) Involvement of Fis protein in replication of the *Escherichia coli* chromosome. *J Bacteriol* **174**: 398-407.

Finkel, S.E., and Johnson, R.C. (1992) The Fis protein: it's not just for DNA inversion anymore. *Mol Microbiol* **6**: 3257-3265.

Finlay, B.B., and Falkow, S. (1989) *Salmonella* as an intracellular parasite. *Mol Microbiol* **3**: 1833-1841.

Finlay, B.B., and Brumell, J.H. (2000) *Salmonella* interactions with host cells: *in vitro* to *in vivo*. *Philos Trans R Soc Lond B Biol Sci* **355**: 623-631.

Fleiszig, S.M., Arora, S.K., Van, R., and Ramphal, R. (2001) FlhA, a component of the flagellum assembly apparatus of *Pseudomonas aeruginosa*, plays a role in internalization by corneal epithelial cells. *Infect Immun* **69**: 4931-4937.

Flynn, J.M., Neher, S.B., Kim, Y.I., Sauer, R.T., and Baker, T.A. (2003) Proteomic discovery of cellular substrates of the ClpXP protease reveals five classes of ClpX-recognition signals. *Mol Cell* **11**: 671-683.

Folichon, M., Arluison, V., Pellegrini, O., Huntzinger, E., Regnier, P., and Hajnsdorf, E. (2003) The poly(A) binding protein Hfq protects RNA from RNase E and exoribonucleolytic degradation. *Nucleic Acids Res* **31**: 7302-7310.

Formal, S.B., Dammin, G.J., Labrec, E.H., and Schneider, H. (1958) Experimental *Shigella* infections: characteristics of a fatal infection produced in guinea pigs. *J Bacteriol* **75**: 604-610.

Forns, N., Baños, R.C., Balsalobre, C., Juárez, A., and Madrid, C. (2005) Temperature-dependent conjugative transfer of R27: role of chromosome- and plasmid-encoded Hha and H-NS proteins. *J Bacteriol* **187**: 3950-3959.

Francis, C.L., Starnbach, M.N., and Falkow, S. (1992) Morphological and cytoskeletal changes in epithelial cells occur immediately upon interaction with *Salmonella typhimurium* grown under low-oxygen conditions. *Mol Microbiol* **6**: 3077-3087.

Free, A. (1995) H-NS and the regulation of transcription in *Escherichia coli*. Ph.D. Thesis, Trinity College Dublin.

Free, A., and Dorman, C.J. (1995) Coupling of *Escherichia coli hns* mRNA levels to DNA synthesis by autoregulation: implications for growth phase control. *Mol Microbiol* **18**: 101-113.

Free, A., and Dorman, C.J. (1997) The *Escherichia coli stpA* gene is transiently expressed during growth in rich medium and is induced in minimal medium and by stress conditions. *J Bacteriol* **179**: 909-918.

Free, A., Porter, M.E., Deighan, P., and Dorman, C.J. (2001) Requirement for the molecular adapter function of StpA at the *Escherichia coli bgl* promoter depends upon the level of truncated H-NS protein. *Mol Microbiol* **42**: 903-917.

Freeman, J.A., Rappl, C., Kuhle, V., Hensel, M., and Miller, S.I. (2002) SpiC is required for translocation of *Salmonella* pathogenicity island 2 effectors and secretion of translocon proteins SseB and SseC. *J Bacteriol* **184**: 4971-4980.

Frost, A.J., Bland, A.P., and Wallis, T.S. (1997) The early dynamic response of the calf ileal epithelium to *Salmonella typhimurium*. *Vet Pathol* **34**: 369-386.

Frost, L.S., Leplae, R., Summers, A.O., and Toussaint, A. (2005) Mobile genetic elements: the agents of open source evolution. *Nat Rev Microbiol* **3**: 722-732.

Fry, R.C., Begley, T.J., and Samson, L.D. (2005) Genome-wide responses to DNA-damaging agents. *Annu Rev Microbiol* **59**: 357-377.

Fu, Y., and Galán, J.E. (1999) A *Salmonella* protein antagonizes Rac-1 and Cdc42 to mediate host-cell recovery after bacterial invasion. *Nature* **401**: 293-297.

Gabant, P., Newnham, P., Taylor, D., and Couturier, M. (1993) Isolation and location on the R27 map of two replicons and an incompatibility determinant specific for IncHI1 plasmids. *J Bacteriol* **175**: 7697-7701.

Gabant, P., Chahdi, A.O., and Couturier, M. (1994) Nucleotide sequence and replication characteristics of RepHI1B: a replicon specific to the IncHI1 plasmids. *Plasmid* **31**: 111-120.

Galán, J.E., and Curtiss, R., III (1989) Cloning and molecular characterization of genes whose products allow *Salmonella typhimurium* to penetrate tissue culture cells. *Proc Natl Acad Sci U S A* **86**: 6383-6387.

Galán, J.E. (1996) Molecular and cellular bases of *Salmonella* entry into host cells. *Curr Top Microbiol Immunol* **209**: 43-60.

Galyov, E.E., Wood, M.W., Rosqvist, R., Mullan, P.B., Watson, P.R., Hedges, S., and Wallis, T.S. (1997) A secreted effector protein of *Salmonella dublin* is translocated into eukaryotic cells and mediates inflammation and fluid secretion in infected ileal mucosa. *Mol Microbiol* **25**: 903-912.

García-del Portillo, F., Foster, J.W., Maguire, M.E., and Finlay, B.B. (1992) Characterization of the micro-environment of *Salmonella typhimurium*-containing vacuoles within MDCK epithelial cells. *Mol Microbiol* **6**: 3289-3297.

Geuskens, V., Mhammedi-Alaoui, A., Desmet, L., and Toussaint, A. (1992) Virulence in bacteriophage Mu: a case of *trans*-dominant proteolysis by the *Escherichia coli* Clp serine protease. *EMBO J* **11**: 5121-5127.

Giangrossi, M., Gualerzi, C.O., and Pon, C.L. (2001) Mutagenesis of the downstream region of the *Escherichia coli hns* promoter. *Biochimie* **83**: 251-259.

Gille, H., Egan, J.B., Roth, A., and Messer, W. (1991) The FIS protein binds and bends the origin of chromosomal DNA replication, *oriC*, of *Escherichia coli*. *Nucleic Acids Res* **19**: 4167-4172.

Gilmour, M.W., Lawley, T.D., Rooker, M.M., Newnham, P.J., and Taylor, D.E. (2001) Cellular location and temperature-dependent assembly of IncHI1 plasmid R27-encoded TrhC-associated conjugative transfer protein complexes. *Mol Microbiol* **42**: 705-715.

Gilmour, M.W., and Taylor, D.E. (2004) A subassembly of R27-encoded transfer proteins is dependent on TrhC nucleoside triphosphate-binding motifs for function but not formation. *J Bacteriol* **186**: 1606-1613.

Gilmour, M.W., Thomson, N.R., Sanders, M., Parkhill, J., and Taylor, D.E. (2004) The complete nucleotide sequence of the resistance plasmid R478: defining the backbone components of incompatibility group H conjugative plasmids through comparative genomics. *Plasmid* **52**: 182-202.

Gogarten, J.P., Doolittle, W.F., and Lawrence, J.G. (2002) Prokaryotic evolution in light of gene transfer. *Mol Biol Evol* **19**: 2226-2238.

Gogarten, J.P., and Townsend, J.P. (2005) Horizontal gene transfer, genome innovation and evolution. *Nat Rev Microbiol* **3**: 679-687.

Goldberg, A.L., and St John, A.C. (1976) Intracellular protein degradation in mammalian and bacterial cells. *Annu Rev Biochem* **45**: 747-803.

Goldberg, A.L., Moerschell, R.P., Chung, C.H., and Maurizi, M.R. (1994) ATP-dependent protease La (Lon) from *Escherichia coli*. *Methods Enzymol* **244**: 350-375.

Gomis-Rüth, F.X., Moncalián, G., Pérez-Luque, R., González, A., Cabezón, E., de la Cruz, F., and Coll, M. (2001) The bacterial conjugation protein TrwB resembles ring helicases and F1-ATPase. *Nature* **409**: 637-641.

González-Gil, G., Bringmann, P., and Kahmann, R. (1996) FIS is a regulator of metabolism in *Escherichia coli*. *Mol Microbiol* **22**: 21-29.

Goodier, R.I., and Ahmer, B.M. (2001) SirA orthologs affect both motility and virulence. *J Bacteriol* **183**: 2249-2258.

Goodsell, D.S., and Dickerson, R.E. (1994) Bending and curvature calculations in B-DNA. *Nucleic Acids Res* **22**: 5497-5503.

Gotoh, H., Okada, N., Kim, Y.G., Shiraishi, K., Hirami, N., Haneda, T., Kurita, A., Kikuchi, Y., and Danbara, H. (2003) Extracellular secretion of the virulence plasmid-encoded ADP-ribosyltransferase SpvB in *Salmonella*. *Microb Pathog* **34**: 227-238.

Gottesman, S., Trisler, P., and Torres-Cabassa, A. (1985) Regulation of capsular polysaccharide synthesis in *Escherichia coli* K-12: characterization of three regulatory genes. *J Bacteriol* **162:** 1111-1119.

Gottesman, S. (1989) Genetics of proteolysis in *Escherichia coli*. *Annu Rev Genet* **23**: 163-198.

Gottesman, S., Clark, W.P., and Maurizi, M.R. (1990) The ATP-dependent Clp protease of *Escherichia coli*. Sequence of *clpA* and identification of a Clp-specific substrate. *J Biol Chem* **265**: 7886-7893.

Gottesman, S., and Maurizi, M.R. (1992) Regulation by proteolysis: energy-dependent proteases and their targets. *Microbiol Rev* **56**: 592-621.

Gottesman, S. (1996) Proteases and their targets in *Escherichia coli*. *Annu Rev Genet* **30**: 465-506.

Gottesman, S., Wickner, S., and Maurizi, M.R. (1997) Protein quality control: triage by chaperones and proteases. *Genes Dev* **11**: 815-823.

Gottesman, S. (2003) Proteolysis in bacterial regulatory circuits. *Annu Rev Cell Dev Biol* **19**: 565-587.

Gottesman, S. (2004) The small RNA regulators of *Escherichia coli:* roles and mechanisms. *Annu Rev Microbiol* **58**: 303-328.

Gottesman, S. (2005) Micros for microbes: non-coding regulatory RNAs in bacteria. *Trends Genet* **21**: 399-404.

Goyard, S., and Bertin, P. (1997) Characterization of BpH3, an H-NS-like protein in *Bordetella pertussis*. *Mol Microbiol* **24**: 815-823.

Grob, P., and Guiney, D.G. (1996) *In vitro* binding of the *Salmonella dublin* virulence plasmid regulatory protein SpvR to the promoter regions of *spvA* and *spvR*. *J Bacteriol* **178**: 1813-1820.

Grohmann, E., Muth, G., and Espinosa, M. (2003) Conjugative plasmid transfer in gram-positive bacteria. *Microbiol Mol Biol Rev* **67**: 277-301.

Groisman, E.A., and Ochman, H. (1996) Pathogenicity islands: bacterial evolution in quantum leaps. *Cell* **87**: 791-794.

Grunberg-Manago, M. (1999) Messenger RNA stability and its role in control of gene expression in bacteria and phages. *Annu Rev Genet* **33**: 193-227.

Gulig, P.A. (1990) Virulence plasmids of *Salmonella typhimurium* and other *Salmonellae*. *Microb Pathog* **8**: 3-11.

Gulig, P.A., Caldwell, A.L., and Chiodo, V.A. (1992) Identification, genetic analysis and DNA sequence of a 7.8-kb virulence region of the *Salmonella typhimurium* virulence plasmid. *Mol Microbiol* **6**: 1395-1411.

Gulig, P.A., Danbara, H., Guiney, D.G., Lax, A.J., Norel, F., and Rhen, M. (1993) Molecular analysis of *spv* virulence genes of the *Salmonella* virulence plasmids. *Mol Microbiol* **7**: 825-830.

Gunton, J.E., Gilmour, M.W., Alonso, G., and Taylor, D.E. (2005) Subcellular localization and functional domains of the coupling protein, TraG, from IncHI1 plasmid R27. *Microbiology* **151**: 3549-3561.

Gupta, V., and Oliver, B. (2003) Drosophila microarray platforms. *Brief Funct Genomic Proteomic* **2**: 97-105.

Guy, R.L., Gonias, L.A., and Stein, M.A. (2000) Aggregation of host endosomes by *Salmonella* requires SPI2 translocation of SseFG and involves SpvR and the *fms-aroE* intragenic region. *Mol Microbiol* **37**: 1417-1435.

Haack, K.R., Robinson, C.L., Miller, K.J., Fowlkes, J.W., and Mellies, J.L. (2003) Interaction of Ler at the LEE5 (*tir*) operon of enteropathogenic *Escherichia coli*. *Infect Immun* **71**: 384-392.

Haffter, P., and Bickle, T.A. (1987) Purification and DNA-binding properties of FIS and Cin, two proteins required for the bacteriophage P1 site-specific recombination system, *cin*. *J Mol Biol* **198**: 579-587.

Hamilton, C.M., Lee, H., Li, P.-L., Cook, D.M., Piper, K.R., von Bodman, S.B., Lanka, E., Ream, W., and Farrand, S.K. (2000) TraG from RP4 and TraG and VirD4 from Ti plasmids confer relaxosome specificity to the conjugal transfer system of pTiC58. *J Bacteriol* **182**: 1541-1548.

Hampton, M.D., Ward, L.R., Rowe, B., and Threlfall, E.J. (1998) Molecular fingerprinting of multidrug-resistant *Salmonella enterica* serotype Typhi. *Emerg Infect Dis* **4**: 317-320.

Hanahan, D. (1983) Studies on transformation of *Escherichia coli* with plasmids. *J Mol Biol* **166:** 557-180.

Hansen-Wester, I., and Hensel, M. (2001) *Salmonella* pathogenicity islands encoding type III secretion systems. *Microbes Infect* **3**: 549-559.

Hardt, W.-D., Chen, L.-M., Schuebel, K.E., Bustelo, X.R., and Galán, J.E. (1998a) *S. typhimurium* encodes an activator of Rho GTPases that induces membrane ruffling and nuclear responses in host cells. *Cell* **93**: 815-826.

Hardt, W.-D., Urlaub, H., and Galán, J.E. (1998b) A substrate of the centisome 63 type III protein secretion system of *Salmonella typhimurium* is encoded by a cryptic bacteriophage. *Proc Natl Acad Sci U S A* **95**: 2574-2579.

Harnett, N., McLeod, S., AuYong, Y., Wan, J., Alexander, S., Khakhria, R., and Krishnan, C. (1998) Molecular characterization of multiresistant strains of *Salmonella typhi* from South Asia isolated in Ontario, Canada. *Can J Microbiol* **44**: 356-363.

Hautefort, I., Proenca, M.J., and Hinton, J.C.D. (1997) Single-Copy Green Fluorescent protein Gene Fusions Allow Accurate Measurement of *Salmonella* Gene Expression *In Vitro* and during Infection of Mammalian Cells. *Appl Environ Microbiol* **69**: 7480-7491.

Haykinson, M.J., Johnson, L.M., Soong, J., and Johnson, R.C. (1996) The Hin dimer interface is critical for Fis-mediated activation of the catalytic steps of site-specific DNA inversion. *Curr Biol* **6**: 163-177.

Hayward, R.D., and Koronakis, V. (1999) Direct nucleation and bundling of actin by the SipC protein of invasive *Salmonella*. *EMBO J* **18**: 4926-4934.

Hayward, R.D., Cain, R.J., McGhie, E.J., Phillips, N., Garner, M.J., and Koronakis, V. (2005) Cholesterol binding by the bacterial type III translocon is essential for virulence effector delivery into mammalian cells. *Mol Microbiol* **56**: 590-603.

Heithoff, D.M., Conner, C.P., Hanna, P.C., Julio, S.M., Hentschel, U., and Mahan, M.J. (1997) Bacterial infection as assessed by *in vivo* gene expression. *Proc Natl Acad Sci U S A* **94**: 934-939.

Hengen, P.N., Bartram, S.L., Stewart, L.E., and Schneider, T.D. (1997) Information analysis of Fis binding sites. *Nucleic Acids Res* **25**: 4994-5002.

Hengge, R., and Bukau, B. (2003) Proteolysis in prokaryotes: protein quality control and regulatory principles. *Mol Microbiol* **49**: 1451-1462.

Hengge-Aronis, R. (2002a) Recent insights into the general stress response regulatory network in *Escherichia coli*. *J Mol Microbiol Biotechnol* **4**: 341-346.

Hengge-Aronis, R. (2002b) Signal transduction and regulatory mechanisms involved in control of the σ^S (RpoS) subunit of RNA polymerase. *Microbiol Mol Biol Rev* **66**: 373-395.

Hensel, M., Shea, J.E., Gleeson, C., Jones, M.D., Dalton, E., and Holden, D.W. (1995) Simultaneous identification of bacterial virulence genes by negative selection. *Science* **269**: 400-403.

Hensel, M., Shea, J.E., Waterman, S.R., Mundy, R., Nikolaus, T., Banks, G., Vazquez-Torres, A., Gleeson, C., Fang, F.C., and Holden, D.W. (1998) Genes encoding putative effector proteins of the type III secretion system of *Salmonella* pathogenicity island 2 are required for bacterial virulence and proliferation in macrophages. *Mol Microbiol* **30**: 163-174.

Hensel, M. (2000) *Salmonella* pathogenicity island 2. *Mol Microbiol* **36**: 1015-1023.

Hensel, M. (2004) Evolution of pathogenicity islands of *Salmonella enterica*. *Int J Med Microbiol* **294**: 95-102.

Higgins, C.F., Dorman, C.J., Stirling, D.A., Waddell, L., Booth, I.R., May, G., and Bremer, E. (1988) A physiological role for DNA supercoiling in the osmotic regulation of gene expression in *S. typhimurium* and *E. coli*. *Cell* **52**: 569-584.

High, N., Mounier, J., Prévost, M.-C., and Sansonetti, P.J. (1992) IpaB of *Shigella flexneri* causes entry into epithelial cells and escape from the phagocytic vacuole. *EMBO J* **11**: 1991-1999.

Hinton, J.C., Santos, D.S., Seirafi, A., Hulton, C.S., Pavitt, G.D., and Higgins, C.F. (1992) Expression and mutational analysis of the nucleoid-associated protein H-NS of *Salmonella typhimurium*. *Mol Microbiol* **6**: 2327-2337.

Ho, T.D., Figueroa-Bossi, N., Wang, M., Uzzau, S., Bossi, L., and Slauch, J.M. (2002) Identification of GtgE, a novel virulence factor encoded on the Gifsy-2 bacteriophage of *Salmonella enterica* serovar Typhimurium. *J Bacteriol* **184**: 5234-5239.

Hochmann, H., Pust, S., von Figura, G., Aktories, K., and Barth, H. (2006) *Salmonella enterica* SpvB ADP-Ribosylates Actin at Position Arginine-177–Characterization of the Catalytic Domain within the SpvB Protein and a Comparison to Binary Clostridial Actin-ADP Ribosylating Toxins. *Biochemistry* **45:** 1271-1277.

Hoiseth, S.K., and Stocker, B.A. (1981) Aromatic-dependent *Salmonella typhimurium* are non-virulent and effective as live vaccines. *Nature* **291:** 238-239.

Hommais, F., Krin, E., Laurent-Winter, C., Soutourina, O., Malpertuy, A., Le Caer, J.P., Danchin, A., and Bertin, P. (2001) Large-scale monitoring of pleiotropic regulation of gene expression by the prokaryotic nucleoid-associated protein, H-NS. *Mol Microbiol* **40**: 20-36.

Hromockyj, A.E., Tucker, S.C., and Maurelli, A.T. (1992) Temperature regulation of *Shigella* virulence: identification of the repressor gene *virR*, an analogue of *hns*, and partial complementation by tyrosyl transfer RNA. *Mol Microbiol* **6**: 2113-2124.

Hübner, P., and Arber, W. (1989) Mutational analysis of a prokaryotic recombinational enhancer element with two functions. *EMBO J* **8**: 577-585.

Hurme, R., Berndt, K.D., Normark, S.J., and Rhen, M. (1997) A proteinaceous gene regulatory thermometer in *Salmonella*. *Cell* **90**: 55-64.

Hwang, B.J., Woo, K.M., Goldberg, A.L., and Chung, C.H. (1988) Protease Ti, a new ATP-dependent protease in *Escherichia coli*, contains protein-activated ATPase and proteolytic functions in distinct subunits. *J Biol Chem* **263**: 8727-8734.

Ish-Horowicz, D., and Burke, J.F. (1981) Rapid and efficient cosmid cloning. *Nucleic Acids Res* **9**: 2989-2998.

Ishihama, A. (1997) Adaptation of gene expression in stationary phase bacteria. *Curr Opin Genet Dev* **7**: 582-588.

Jackson, M.W., Silva-Herzog, E., and Plano, G.V. (2004) The ATP-dependent ClpXP and Lon proteases regulate expression of the *Yersinia pestis* type III secretion system via regulated proteolysis of YmoA, a small histone-like protein. *Mol Microbiol* **54**: 1364-1378.

Jacquet, M., Cukier-Kahn, R., Pla, J., and Gros, F. (1971) A thermostable protein factor acting on *in vitro* DNA transcription. *Biochem Biophys Res Commun* **45**: 1597-1607.

Janion, C. (2001) Some aspects of the SOS response system-a critical survey. *Acta Biochim Pol* **48**: 599-610.

Jáuregui, R., Abreu-Goodger, C., Moreno-Hagelsieb, G., Collado-Vides, J., and Merino, E. (2003) Conservation of DNA curvature signals in regulatory regions of prokaryotic genes. *Nucleic Acids Res* **31**: 6770-6777.

Jenal, U., and Hengge-Aronis, R. (2003) Regulation by proteolysis in bacterial cells. *Curr Opin Microbiol* **6**: 163-172.

Johansson, J., and Uhlin, B.E. (1999) Differential protease-mediated turnover of H-NS and StpA revealed by a mutation altering protein stability and stationary-phase survival of *Escherichia coli*. *Proc Natl Acad Sci U S A* **96**: 10776-10781.

Johansson, J., Eriksson, S., Sondén, B., Wai, S.N., and Uhlin, B.E. (2001) Heteromeric interactions among nucleoid-associated bacterial proteins: localization of StpA-stabilizing regions in H-NS of *Escherichia coli*. *J Bacteriol* **183**: 2343-2347.

Johnson, R.C., and Simon, M.I. (1985) Hin-mediated site-specific recombination requires two 26 bp recombination sites and a 60 bp recombinational enhancer. *Cell* **41**: 781-791.

Johnson, S.E., Dorman, C.M., and Bolanowski, S.A. (2002) Inhibition of myogenin expression by activated Raf is not responsible for the block to avian myogenesis. *J Biol Chem* **277**: 28742-28748.

Johnston, C., Pegues, D.A., Hueck, C.J., Lee, A., and Miller, S.I. (1996) Transcriptional activation of *Salmonella typhimurium* invasion genes by a member of the phosphorylated response-regulator superfamily. *Mol Microbiol* **22**: 715-727.

Jones, B.D., Ghori, N., and Falkow, S. (1994) *Salmonella typhimurium* initiates murine infection by penetrating and destroying the specialized epithelial M cells of the Peyer's patches. *J Exp Med* **180**: 15-23.

Jones, B.D., and Falkow, S. (1996) Salmonellosis: host immune responses and bacterial virulence determinants. *Annu Rev Immunol* **14**: 533-561.

Jones, B.D. (2005) *Salmonella* invasion gene regulation: a story of environmental awareness. *J Microbiol* **43**: 110-117.

Jordi, B.J., Dagberg, B., de Haan, L.A., Hamers, A.M., van der Zeijst, B.A., Gaastra, W., and Uhlin, B.E. (1992) The positive regulator CfaD overcomes the repression mediated by histone-like protein H-NS (H1) in the CFA/I fimbrial operon of *Escherichia coli*. *EMBO J* **11**: 2627-2632.

Kahmann, R., Rudt, F., Koch, C., and Mertens, G. (1985) G inversion in bacteriophage Mu DNA is stimulated by a site within the invertase gene and a host factor. *Cell* **41**: 771-780.

Kalkum, M., Eisenbrandt, R., and Lanka, E. (2004) Protein circlets as sex pilus subunits. *Curr Protein Pept Sci* **5**: 417-424.

Kaniga, K., Bossio, J.C., and Galán, J.E. (1994) The *Salmonella typhimurium* invasion genes *invF* and *invG* encode homologues of the AraC and PulD family of proteins. *Mol Microbiol* **13**: 555-568.

Kariuki, S., Gilks, C., Revathi, G., and Hart, C.A. (2000) Genotypic analysis of multidrug-resistant *Salmonella enterica* Serovar *typhi*, Kenya. *Emerg Infect Dis* **6**: 649-651.

Katayama, Y., Gottesman, S., Pumphrey, J., Rudikoff, S., Clark, W.P., and Maurizi, M.R. (1988) The two-component, ATP-dependent Clp protease of *Escherichia coli*. Purification, cloning, and mutational analysis of the ATP-binding component. *J Biol Chem* **263**: 15226-15236.

Kawula, T.H., and Orndorff, P.E. (1991) Rapid site-specific DNA inversion in *Escherichia coli* mutants lacking the histone-like protein H-NS. *J Bacteriol* **173**: 4116-4123.

Keane, O.M., and Dorman, C.J. (2003) The *gyr* genes of *Salmonella enterica* serovar Typhimurium are repressed by the factor for inversion stimulation, Fis. *Mol Genet Genomics* **270**: 56-65.

Kelly, A., Goldberg, M.D., Carroll, R.K., Danino, V., Hinton, J.C.D., and Dorman, C.J. (2004) A global role for Fis in the transcriptional control of metabolism and type III secretion in *Salmonella enterica* serovar Typhimurium. *Microbiology* **150**: 2037-2053.

Kelly, A. (2005) Gene Regulation and the Fis Nucleoid-associated Protein in *Salmonella enterica* serovar Typhimurium. Ph.D. Thesis, Trinity College Dublin.

Khil, P.P., and Camerini-Otero, R.D. (2002) Over 1000 genes are involved in the DNA damage response of *Escherichia coli*. *Mol Microbiol* **44**: 89-105.

Kim, C.C., and Falkow, S. (2004) Delineation of upstream signaling events in the *Salmonella* pathogenicity island 2 transcriptional activation pathway. *J Bacteriol* **186**: 4694-4704.

Kimbrough, T.G., and Miller, S.I. (2000) Contribution of *Salmonella typhimurium* type III secretion components to needle complex formation. *Proc Natl Acad Sci U S A* **97**: 11008-11013.

Kimbrough, T.G., and Miller, S.I. (2002) Assembly of the type III secretion needle complex of *Salmonella typhimurium*. *Microbes Infect* **4**: 75-82.

Kingsley, R.A., and Baumler, A.J. (2002) Pathogenicity islands and host adaptation of *Salmonella* serovars. *Curr Top Microbiol Immunol* **264**: 67-87.

Klein, J.R., and Jones, B.D. (2001) *Salmonella* pathogenicity island 2-encoded proteins SseC and SseD are essential for virulence and are substrates of the type III secretion system. *Infect Immun* **69**: 737-743.

Knodler, L.A., Celli, J., Hardt, W.D., Vallance, B.A., Yip, C., and Finlay, B.B. (2002) *Salmonella* effectors within a single pathogenicity island are differentially expressed and translocated by separate type III secretion systems. *Mol Microbiol* **43**: 1089-1103.

Ko, M., and Park, C. (2000) H-NS-Dependent regulation of flagellar synthesis is mediated by a LysR family protein. *J Bacteriol* **182**: 4670-4672.

Koch, C., Ninnemann, O., Fuss, H., and Kahmann, R. (1991) The N-terminal part of the *E. coli* DNA binding protein FIS is essential for stimulating site-specific DNA inversion but is not required for specific DNA binding. *Nucleic Acids Res* **19**: 5915-5922.

Koch, W.H., and Woodgate, R. (1998) The SOS response. In *DNA Damage and Repair:DNA Repair in Prokaryotes and Lower Eukaryotes*. Nickoloff, J.A. and Hoekstra, M.F. (eds). Towata, NJ: Humana Press, pp. 107-134.

Kostrewa, D., Granzin, J., Koch, C., Choe, H.W., Raghunathan, S., Wolf, W., Labahn, J., Kahmann, R., and Saenger, W. (1991) Three-dimensional structure of the *E. coli* DNA-binding protein FIS. *Nature* **349**: 178-180.

Kox, L.F., Wosten, M.M., and Groisman, E.A. (2000) A small protein that mediates the activation of a two-component system by another two-component system. *EMBO J* **19**: 1861-1872.

Kuhle, V., and Hensel, M. (2002) SseF and SseG are translocated effectors of the type III secretion system of *Salmonella* pathogenicity island 2 that modulate aggregation of endosomal compartments. *Cell Microbiol* **4**: 813-824.

La Teana, A., Brandi, A., Falconi, M., Spurio, R., Pon, C.L., and Gualerzi, C.O. (1991) Identification of a cold shock transcriptional enhancer of the *Escherichia coli* gene encoding nucleoid protein H-NS. *Proc Natl Acad Sci U S A* **88**: 10907-10911.

Lange, R., and Hengge-Aronis, R. (1994) The cellular concentration of the σ^S subunit of RNA polymerase in *Escherichia coli* is controlled at the levels of transcription, translation, and protein stability. *Genes Dev* **8**: 1600-1612.

Lawhon, S.D., Frye, J.G., Suyemoto, M., Porwollik, S., McClelland, M., and Altier, C. (2003) Global regulation by CsrA in *Salmonella typhimurium*. *Mol Microbiol* **48**: 1633-1645.

Lawley, T.D., Burland, V., and Taylor, D.E. (2000) Analysis of the complete nucleotide sequence of the tetracycline-resistance transposon Tn*10*. *Plasmid* **43**: 235-239.

Lawley, T.D., Gilmour, M.W., Gunton, J.E., Standeven, L.J., and Taylor, D.E. (2002) Functional and mutational analysis of conjugative transfer region 1 (Tra1) from the IncHI1 plasmid R27. *J Bacteriol* **184**: 2173-2180.

Lawley, T.D., Gilmour, M.W., Gunton, J.E., Tracz, D.M., and Taylor, D.E. (2003a) Functional and mutational analysis of conjugative transfer region 2 (Tra2) from the IncHI1 plasmid R27. *J Bacteriol* **185**: 581-591.

Lawley, T.D., Klimke, W.A., Gubbins, M.J., and Frost, L.S. (2003b) F factor conjugation is a true type IV secretion system. *FEMS Microbiol Lett* **224**: 1-15.

Lawley, T.D., and Taylor, D.E. (2003) Characterization of the double-partitioning modules of R27: correlating plasmid stability with plasmid localization. *J Bacteriol* **185**: 3060-3067.

Lease, R.A., Cusick, M.E., and Belfort, M. (1998) Riboregulation in *Escherichia coli*: DsrA RNA acts by RNA:RNA interactions at multiple loci. *Proc Natl Acad Sci U S A* **95**: 12456-12461.

Lease, R.A., and Belfort, M. (2000) A *trans*-acting RNA as a control switch in *Escherichia coli*: DsrA modulates function by forming alternative structures. *Proc Natl Acad Sci U S A* **97**: 9919-9924.

Lee, A.K., Detweiler, C.S., and Falkow, S. (2000) OmpR regulates the two-component system SsrA-SsrB in *Salmonella* pathogenicity island 2. *J Bacteriol* **182**: 771-781.

Lee, J., Nam, S., Hwang, S.B., Hong, M., Kwon, J.Y., Joeng, K.S., Im, S.H., Shim, J., and Park, M.C. (2004) Functional genomic approaches using the nematode *Caenorhabditis elegans* as a model system. *J Biochem Mol Biol* **37**: 107-113.

Lemoine, V.R., and Rowbury, R.J. (1975) Compatibility studies with the plasmid of *Salmonella typhimurium* LT2. *Rev Latinoam Microbiol* **17**: 79-85.

Lenski, R.E. (1991) Quantifying fitness and gene stability in microorganisms. *Biotechnology* **15**: 173-192.

Lesnick, M.L., Reiner, N.E., Fierer, J., and Guiney, D.G. (2001) The *Salmonella spvB* virulence gene encodes an enzyme that ADP-ribosylates actin and destabilizes the cytoskeleton of eukaryotic cells. *Mol Microbiol* **39**: 1464-1470.

Lewis, L.K., Harlow, G.R., Gregg-Jolly, L.A., and Mount, D.W. (1994) Identification of high affinity binding sites for LexA which define new DNA damage-inducible genes in *Escherichia coli*. *J Mol Biol* **241**: 507-523.

Li, C., Louise, C.J., Shi, W., and Adler, J. (1993) Adverse conditions which cause lack of flagella in *Escherichia coli*. *J Bacteriol* **175**: 2229-2235.

Lin-Chao, S., Wong, T.-T., McDowall, K.J., and Cohen, S.N. (1994) Effects of nucleotide sequence on the specificity of *rne*-dependent and RNase E-mediated cleavages of RNA I encoded by the pBR322 plasmid. *J Biol Chem* **269**: 10797-10803.

Linehan, S.A., Rytkonen, A., Yu, X.-J., Liu, M., and Holden, D.W. (2005) SlyA regulates function of *Salmonella* pathogenicity island 2 (SPI-2) and expression of SPI-2-associated genes. *Infect Immun* **73**: 4354-4362.

Little, J.W., Edmiston, S.H., Pacelli, L.Z., and Mount, D.W. (1980) Cleavage of the *Escherichia coli* LexA protein by the RecA protease. *Proc Natl Acad Sci U S A* **77**: 3225-3229.

Little, J.W., Mount, D.W., and Yanisch-Perron, C.R. (1981) Purified LexA protein is a repressor of the *recA* and *lexA* genes. *Proc Natl Acad Sci U S A* **78**: 4199-4203.

Little, J.W. (1993) LexA cleavage and other self-processing reactions. *J Bacteriol* **175**: 4943-4950.

Llosa, M., Gomis-Rüth, F.X., Coll, M., and de la Cruz, F. (2002) Bacterial conjugation: a two-step mechanism for DNA transport. *Mol Microbiol* **45**: 1-8.

Lucas, R.L., and Lee, C.A. (2000) Unravelling the mysteries of virulence gene regulation in *Salmonella typhimurium*. *Mol Microbiol* **36**: 1024-1033.

Lucas, R.L., Lostroh, C.P., DiRusso, C.C., Spector, M.P., Wanner, B.L., and Lee, C.A. (2000) Multiple factors independently regulate *hilA* and invasion gene expression in *Salmonella enterica* serovar *typhimurium*. *J Bacteriol* **182**: 1872-1882.

Lucht, J.M., Dersch, P., Kempf, B., and Bremer, E. (1994) Interactions of the nucleoid-associated DNA-binding protein H-NS with the regulatory region of the osmotically controlled *proU* operon of *Escherichia coli*. *J Biol Chem* **269**: 6578-6578.

Lusetti, S.L., Voloshin, O.N., Inman, R.B., Camerini-Otero, R.D., and Cox, M.M. (2004) The DinI protein stabilizes RecA protein filaments. *J Biol Chem* **279**: 30037-30046.

Lybarger, S.R., and Sandkvist, M. (2004) Microbiology. A hitchhiker's guide to type IV secretion. *Science* **304**: 1122-1123.

Macnab, R.M. (1986) Proton-driven bacterial flagellar motor. *Methods Enzymol* **125**: 563-581.

Macnab, R.M. (1996) Flagella and motility. In *Eschericha coli and Salmonella: Cellular and Molecular Biology*. Neidhardt, F.C., Curtiss R., III, Ingraham, J.L., Lin, E.C.C., Low, K.B., Magasanik, B., *et al.* (eds) Washington DC: ASM Press, pp. 123-145.

Madrid, C., Nieto, J.M., and Juárez, A. (2002a) Role of the Hha/YmoA family of proteins in the thermoregulation of the expression of virulence factors. *Int J Med Microbiol* **291**: 425-432.

Madrid, C., Nieto, J.M., Paytubi, S., Falconi, M., Gualerzi, C.O., and Juárez, A. (2002b) Temperature- and H-NS-dependent regulation of a plasmid-encoded virulence operon expressing *Escherichia coli* hemolysin. *J Bacteriol* **184**: 5058-5066.

Maher, D., Sherburne, R., and Taylor, D.E. (1993) H-pilus assembly kinetics determined by electron microscopy. *J Bacteriol* **175**: 2175-2183.

Majdalani, N., Chen, S., Murrow, J., St John, K., and Gottesman, S. (2001) Regulation of RpoS by a novel small RNA: the characterization of RprA. *Mol Microbiol* **39**: 1382-1394.

Majdalani, N., Hernandez, D., and Gottesman, S. (2002) Regulation and mode of action of the second small RNA activator of RpoS translation, RprA. *Mol Microbiol* **46**: 813-826.

Majtan, T., Bukovska, G., and Timko, J. (2004) DNA microarrays-techniques and applications in microbial systems. *Folia Microbiol (Praha)* **49**: 635-664.

Makris, J.C., Nordmann, P.L., and Reznikoff, W.S. (1990) Integration host factor plays a role in IS*50* and Tn*5* transposition. *J Bacteriol* **172**: 1368-1373.

Mandel, M., and Higa, A. (1970) Calcium-dependent bacteriophage DNA infection. *J Mol Biol* **53**: 159-162.

Mangan, M.W., Lucchini, S., Danino, V., O Croinin, T., Hinton, J.C.D., and Dorman, C.J. (2006) The integration host factor (IHF) integrates stationary-phase and virulence gene expression in *Salmonella enterica* serovar Typhimurium. *Mol Microbiol* **59**: 1831-1847.

Manna, D., and Gowrishankar, J. (1994) Evidence for involvement of proteins HU and RpoS in transcription of the osmoresponsive *proU* operon in *Escherichia coli*. *J Bacteriol* **176**: 5378-5384.

Marcus, S.L., Brumell, J.H., Pfeifer, C.G., and Finlay, B.B. (2000) *Salmonella* pathogenicity islands: big virulence in small packages. *Microbes Infect* **2**: 145-156.

Marlovits, T.C., Kubori, T., Sukhan, A., Thomas, D.R., Galán, J.E., and Unger, V.M. (2004) Structural insights into the assembly of the type III secretion needle complex. *Science* **306**: 1040-1042.

Marlovits, T.C., Kubori, T., Lara-Tejero, M., Thomas, D., Unger, V.M., and Galán, J.E. (2006) Assembly of the inner rod determines needle length in the type III secretion injectisome. *Nature* **441:** 637-640.

Marshall, D.G., Sheehan, B.J., and Dorman, C.J. (1999) A role for the leucine-responsive regulatory protein and integration host factor in the regulation of the *Salmonella* plasmid virulence (*spv*) locus in *Salmonella typhimurium*. *Mol Microbiol* **34**: 134-145.

Marshall, D.G., Bowe, F., Hale, C., Dougan, G., and Dorman, C.J. (2000) DNA topology and adaptation of *Salmonella typhimurium* to an intracellular environment. *Philos Trans R Soc Lond B Biol Sci* **355**: 565-574.

Masse, E., and Gottesman, S. (2002) A small RNA regulates the expression of genes involved in iron metabolism in *Escherichia coli*. *Proc Natl Acad Sci U S A* **99**: 4620-4625.

Masse, E., Escorcia, F.E., and Gottesman, S. (2003) Coupled degradation of a small regulatory RNA and its mRNA targets in *Escherichia coli*. *Genes Dev* **17**: 2374-2383.

Mathews, D.H., Sabina, J., Zuker, M., and Turner, D.H. (1999) Expanded sequence dependence of thermodynamic parameters improves prediction of RNA secondary structure. *J. Mol. Biol.* **288**: 911-940.

Matic, I., Taddei, F., and Radman, M. (2000) No genetic barriers between *Salmonella enterica* serovar *typhimurium* and *Escherichia coli* in SOS-induced mismatch repair-deficient cells. *J Bacteriol* **182**: 5922-5924.

Matsui, H., Bacot, C.M., Garlington, W.A., Doyle, T.J., Roberts, S., and Gulig, P.A. (2001) Virulence plasmid-borne *spvB* and *spvC* genes can replace the 90-kilobase plasmid in conferring virulence to *Salmonella enterica* serovar Typhimurium in subcutaneously inoculated mice. *J Bacteriol* **183**: 4652-4658.

Maurelli, A.T., Blackmon, B., and Curtiss, R., 3rd (1984) Temperature-dependent expression of virulence genes in *Shigella* species. *Infect Immun* **43**: 195-201.

Maurelli, A.T., Baudry, B., d'Hauteville, H., Hale, T.L., and Sansonetti, P.J. (1985) Cloning of plasmid DNA sequences involved in invasion of HeLa cells by *Shigella flexneri*. *Infect Immun* **49**: 164-171.

Maurelli, A.T., and Sansonetti, P.J. (1988) Identification of a chromosomal gene controlling temperature-regulated expression of *Shigella* virulence. *Proc Natl Acad Sci U S A* **85**: 2820-2824.

Maurizi, M.R. (1992) Proteases and protein degradation in *Escherichia coli*. *Experientia* **48**: 178-201.

McClelland, M., Sanderson, K.E., Spieth, J., Clifton, S.W., Latreille, P., Courtney, L., Porwollik, S., Ali, J., Dante, M., Du, F., Hou, S., Layman, D., Leonard, S., Nguyen, C., Scott, K., Holmes, A., Grewal, N., Mulvaney, E., Ryan, E., Sun, H., Florea, L., Miller, W., Stoneking, T., Nhan, M., Waterston, R., and Wilson, R.K. (2001) Complete genome sequence of *Salmonella enterica* serovar Typhimurium LT2. *Nature* **413**: 852-856.

McGovern, V., Higgins, N.P., Chiz, R.S., and Jaworski, A. (1994) H-NS over-expression induces an artificial stationary phase by silencing global transcription. *Biochimie* **76**: 1019-1029.

McKenna, S. (2002) Functional analysis of the VirB protein of *Shigella flexneri*. Ph.D. Thesis, Trinity College Dublin.

McKenna, S., Beloin, C., and Dorman, C.J. (2003) *In vitro* DNA-binding properties of VirB, the *Shigella flexneri* virulence regulatory protein. *FEBS Lett* **545:** 183-187.

McLeod, S.M., and Johnson, R.C. (2001) Control of transcription by nucleoid proteins. *Curr Opin Microbiol* **4**: 152-159.

Mellies, J.L., Elliott, S.J., Sperandio, V., Donnenberg, M.S., and Kaper, J.B. (1999) The Per regulon of enteropathogenic *Escherichia coli*: identification of a regulatory cascade and a novel transcriptional activator, the locus of enterocyte effacement (LEE)-encoded regulator (Ler). *Mol Microbiol* **33**: 296-306.

Ménard, R., Sansonetti, P.J., and Parsot, C. (1993) Nonpolar mutagenesis of the *ipa* genes defines IpaB, IpaC, and IpaD as effectors of *Shigella flexneri* entry into epithelial cells. *J Bacteriol* **175**: 5899-5906.

Ménard, R., Sansonetti, P., and Parsot, C. (1994) The secretion of the *Shigella flexneri* Ipa invasins is activated by epithelial cells and controlled by IpaB and IpaD. *EMBO J* **13**: 5293-5302.

Ménard, R., Prévost, M.-C., Gounon, P., Sansonetti, P., and Dehio, C. (1996) The secreted Ipa complex of *Shigella flexneri* promotes entry into mammalian cells. *Proc Natl Acad Sci U S A* **93**: 1254-1258.

Méresse, S., Unsworth, K.E., Habermann, A., Griffiths, G., Fang, F., Martínez-Lorenzo, M.J., Waterman, S.R., Gorvel, J.-P., and Holden, D.W. (2001) Remodelling of the actin cytoskeleton is essential for replication of intravacuolar *Salmonella*. *Cell Microbiol* **3**: 567-577.

Miao, E.A., Scherer, C.A., Tsolis, R.M., Kingsley, R.A., Adams, L.G., Bäumler, A.J., and Miller, S.I. (1999) *Salmonella typhimurium* leucine-rich repeat proteins are targeted to the SPI1 and SPI2 type III secretion systems. *Mol Microbiol* **34**: 850-864.

Miao, E.A., and Miller, S.I. (2000) A conserved amino acid sequence directing intracellular type III secretion by *Salmonella typhimurium*. *Proc Natl Acad Sci U S A* **97**: 7539-7544.

Miao, E.A., Freeman, J.A., and Miller, S.I. (2002) Transcription of the SsrAB regulon is repressed by alkaline pH and is independent of PhoPQ and magnesium concentration. *J Bacteriol* **184**: 1493-1497.

Miao, E.A., Alpuche-Aranda, C.M., Dors, M., Clark, A.E., Bader, M.W., Miller, S.I., and Aderem, A. (2006) Cytoplasmic flagellin activates caspase-1 and secretion of interleukin 1β via Ipaf. *Nature Immunology* **7:** 569-575.

Mika, F., and Hengge, R. (2005) A two-component phosphotransfer network involving ArcB, ArcA, and RssB coordinates synthesis and proteolysis of σ^S (RpoS) in *E. coli*. *Genes Dev* **19**: 2770-2781.

Miller, H.I., and Friedman, D.I. (1980) An *E. coli* gene product required for lambda site-specific recombination. *Cell* **20**: 711-719.

Miller, J.H. (1992) *A Short Course in Bacterial Genetics*. Cold Spring Harbor, NY: Cold Spring Harbor Laboratory Press.

Mills, D.M., Bajaj, V., and Lee, C.A. (1995) A 40 kb chromosomal fragment encoding *Salmonella typhimurium* invasion genes is absent from the corresponding region of the *Escherichia coli* K-12 chromosome. *Mol Microbiol* **15**: 749-759.

Mirza, S., Kariuki, S., Mamun, K.Z., Beeching, N.J., and Hart, C.A. (2000) Analysis of plasmid and chromosomal DNA of multidrug-resistant *Salmonella enterica* serovar *typhi* from Asia. *J Clin Microbiol* **38**: 1449-1452.

Moll, I., Afonyushkin, T., Vytvytska, O., Kaberdin, V.R., and Blasi, U. (2003) Coincident Hfq binding and RNase E cleavage sites on mRNA and small regulatory RNAs. *RNA* **9**: 1308-1314.

Møller, T., Franch, T., Udesen, C., Gerdes, K., and Valentin-Hansen, P. (2002) Spot 42 RNA mediates discoordinate expression of the *E. coli* galactose operon. *Genes Dev* **16**: 1696-1706.

Moncalián, G., Cabezón, E., Alkorta, I., Valle, M., Moro, F., Valpuesta, J.M., Goñi, F.M., and de la Cruz, F. (1999) Characterization of ATP and DNA binding activities of TrwB, the coupling protein essential in plasmid R388 conjugation. *J Biol Chem* **274**: 36117-36124.

More, M.I., Pohlman, R.F., and Winans, S.C. (1996) Genes encoding the pKM101 conjugal mating pore are negatively regulated by the plasmid-encoded KorA and KorB proteins. *J Bacteriol* **178**: 4392-4399.

Mukhopadhyay, S., Audia, J.P., Roy, R.N., and Schellhorn, H.E. (2000) Transcriptional induction of the conserved alternative sigma factor RpoS in *Escherichia coli* is dependent on BarA, a probable two-component regulator. *Mol Microbiol* **37**: 371-381.

Nagai, H., and Roy, C.R. (2003) Show me the substrates: modulation of host cell function by type IV secretion systems. *Cell Microbiol* **5**: 373-383.

Nakayama, S., and Watanabe, H. (1998) Identification of *cpxR* as a positive regulator essential for expression of the *Shigella sonnei virF* gene. *J Bacteriol* **180**: 3522-3528.

Newnham, P.J., and Taylor, D.E. (1994) Molecular analysis of RepHI1A, a minimal replicon of the IncHI1 plasmid R27. *Mol Microbiol* **11**: 757-768.

Nieto, J.M., Prenafeta, A., Miquelay, E., Torrades, S., and Juárez, A. (1998) Sequence, identification and effect on conjugation of the *rmoA* gene of plasmid R100-1. *FEMS Microbiol Lett* **169**: 59-66.

Nieto, J.M., Madrid, C., Prenafeta, A., Miquelay, E., Balsalobre, C., Carrascal, M., and Juárez, A. (2000) Expression of the hemolysin operon in *Escherichia coli* is modulated by a nucleoid-protein complex that includes the proteins Hha and H-NS. *Mol Gen Genet* **263**: 349-358.

Nieto, J.M., Madrid, C., Miquelay, E., Parra, J.L., Rodríguez, S., and Juárez, A. (2002) Evidence for direct protein-protein interaction between members of the enterobacterial Hha/YmoA and H-NS families of proteins. *J Bacteriol* **184**: 629-635.

Nikolaus, T., Deiwick, J., Rappl, C., Freeman, J.A., Schroder, W., Miller, S.I., and Hensel, M. (2001) SseBCD proteins are secreted by the type III secretion system of *Salmonella* pathogenicity island 2 and function as a translocon. *J Bacteriol* **183**: 6036-6045.

Niyogi, S.K. (2005) Shigellosis. *J Microbiol* **43**: 133-143.

Norris, F.A., Wilson, M.P., Wallis, T.S., Galyov, E.E., and Majerus, P.W. (1998) SopB, a protein required for virulence of *Salmonella dublin*, is an inositol phosphate phosphatase. *Proc Natl Acad Sci U S A* **95**: 14057-14059.

Nye, M.B., and Taylor, R.K. (2003) *Vibrio cholerae* H-NS domain structure and function with respect to transcriptional repression of ToxR regulon genes reveals differences among H-NS family members. *Mol Microbiol* **50**: 427-444.

O'Byrne, C.P., and Dorman, C.J. (1994a) Transcription of the *Salmonella typhimurium spv* virulence locus is regulated negatively by the nucleoid-associated protein H-NS. *FEMS Microbiol Lett* **121**: 99-105.

O'Byrne, C.P., and Dorman, C.J. (1994b) The *spv* virulence operon of *Salmonella typhimurium* LT2 is regulated negatively by the cyclic AMP (cAMP)-cAMP receptor protein system. *J Bacteriol* **176**: 905-912.

Oberto, J., and Rouviere-Yaniv, J. (1996) *Serratia marcescens* contains a heterodimeric HU protein like *Escherichia coli* and *Salmonella typhimurium*. *J Bacteriol* **178**: 293-297.

Ochman, H., Soncini, F.C., Solomon, F., and Groisman, E.A. (1996) Identification of a pathogenicity island required for *Salmonella* survival in host cells. *Proc Natl Acad Sci U S A* **93**: 7800-7804.

Ochman, H., Lawrence, J.G., and Groisman, E.A. (2000) Lateral gene transfer and the nature of bacterial innovation. *Nature* **405**: 299-304.

Odenbreit, S., Püls, J., Sedlmaier, B., Gerland, E., Fischer, W., and Haas, R. (2000) Translocation of *Helicobacter pylori* CagA into gastric epithelial cells by type IV secretion. *Science* **287**: 1497-1500.

Oh, T.J., and Kim, I.G. (1999) Identification of genetic factors altering the SOS induction of DNA damage-inducible *yebG* gene in *Escherichia coli*. *FEMS Microbiol Lett* **177**: 271-277.

Oh, T.J., Jung, I.L., and Kim, I.G. (2001) The *Escherichia coli* SOS gene *sbmC* is regulated by H-NS and RpoS during the SOS induction and stationary growth phase. *Biochem Biophys Res Commun* **288**: 1052-1058.

Ohl, M.E., and Miller, S.I. (2001) *Salmonella*: a model for bacterial pathogenesis. *Annu Rev Med* **52**: 259-274.

Ohya, K., Handa, Y., Ogawa, M., Suzuki, M., and Sasakawa, C. (2005) IpgB1 is a novel *Shigella* effector protein involved in bacterial invasion of host cells. Its activity to promote membrane ruffling via Rac1 and Cdc42 activation. *J Biol Chem* **280**: 24022-24034.

Olekhnovich, I.N., and Kadner, R.J. (2004) Contribution of the RpoA C-terminal domain to stimulation of the *Salmonella enterica hilA* promoter by HilC and HilD. *J Bacteriol* **186**: 3249-3253.

Olekhnovich, I.N., and Kadner, R.J. (2006) Crucial Roles of Both Flanking Sequences in Silencing of the *hilA* promoter in *Salmonella enterica*. *J Mol Biol*.

Ono, S., Goldberg, M.D., Olsson, T., Esposito, D., Hinton, J.C.D., and Ladbury, J.E. (2005) H-NS is a part of a thermally controlled mechanism for bacterial gene regulation. *Biochem J* **391**: 203-213.

Osiecki, J.C., Barker, J., Picking, W.L., Serfis, A.B., Berring, E., Shah, S., Harrington, A., and Picking, W.D. (2001) IpaC from *Shigella* and SipC from *Salmonella* possess similar biochemical properties but are functionally distinct. *Mol Microbiol* **42**: 469-481.

Osuna, R., Lienau, D., Hughes, K.T., and Johnson, R.C. (1995) Sequence, regulation, and functions of *fis* in *Salmonella typhimurium*. *J Bacteriol* **177**: 2021-2032.

Otto, H., Tezcan-Merdol, D., Girisch, R., Haag, F., Rhen, M., and Koch-Nolte, F. (2000) The *spvB* gene-product of the *Salmonella enterica* virulence plasmid is a mono(ADP-ribosyl)transferase. *Mol Microbiol* **37**: 1106-1115.

Owen-Hughes, T.A., Pavitt, G.D., Santos, D.S., Sidebotham, J.M., Hulton, C.S., Hinton, J.C.D., and Higgins, C.F. (1992) The chromatin-associated protein H-NS interacts with curved DNA to influence DNA topology and gene expression. *Cell* **71**: 255-265.

Page, A.L., Fromont-Racine, M., Sansonetti, P., Legrain, P., and Parsot, C. (2001) Characterization of the interaction partners of secreted proteins and chaperones of *Shigella flexneri*. *Mol Microbiol* **42**: 1133-1145.

Page, R.D. (1996) TreeView: an application to display phylogenetic trees on personal computers. *Comput Appl Biosci* **12**: 357-358.

Palchaudhuri, S., Tominna, B., and Leon, M.A. (1998) H-NS regulates DNA repair in *Shigella*. *J Bacteriol* **180**: 5260-5262.

Pang, T., Bhutta, Z.A., Finlay, B.B., and Altwegg, M. (1995) Typhoid fever and other salmonellosis: a continuing challenge. *Trends Microbiol* **3**: 253-255.

Pansegrau, W., and Lanka, E. (1996) Mechanisms of initiation and termination reactions in conjugative DNA processing. Independence of tight substrate binding and catalytic activity of relaxase (TraI) of IncPα plasmid RP4. *J Biol Chem* **271**: 13068-13076.

Parkhill, J., Dougan, G., James, K.D., Thomson, N.R., Pickard, D., Wain, J., Churcher, C., Mungall, K.L., Bentley, S.D., Holden, M.T., Sebaihia, M., Baker, S., Basham, D., Brooks, K., Chillingworth, T., Connerton, P., Cronin, A., Davis, P., Davies, R.M., Dowd, L., White, N., Farrar, J., Feltwell, T., Hamlin, N., Haque, A., Hien, T.T., Holroyd, S., Jagels, K., Krogh, A., Larsen, T.S., Leather, S., Moule, S., O'Gaora, P., Parry, C., Quail, M., Rutherford, K., Simmonds, M., Skelton, J., Stevens, K., Whitehead, S., and Barrell, B.G. (2001) Complete genome sequence of a multiple drug resistant *Salmonella enterica* serovar Typhi CT18. *Nature* **413**: 848-852.

Parsot, C. (2005) *Shigella* spp. and enteroinvasive *Escherichia coli* pathogenicity factors. *FEMS Microbiol Lett* **252**: 11-18.

Paytubi, S., Madrid, C., Forns, N., Nieto, J.M., Balsalobre, C., Uhlin, B.E., and Juárez, A. (2004) YdgT, the Hha paralogue in *Escherichia coli*, forms heteromeric complexes with H-NS and StpA. *Mol Microbiol* **54**: 251-263.

Perdomo, J.J., Gounon, P., and Sansonetti, P.J. (1994a) Polymorphonuclear leukocyte transmigration promotes invasion of colonic epithelial monolayer by *Shigella flexneri*. *J Clin Invest* **93**: 633-643.

Perdomo, O.J., Cavaillon, J.M., Huerre, M., Ohayon, H., Gounon, P., and Sansonetti, P.J. (1994b) Acute inflammation causes epithelial invasion and mucosal destruction in experimental shigellosis. *J Exp Med* **180**: 1307-1319.

Perwez, T., and Meyer, R.J. (1999) Stabilization of the relaxosome and stimulation of conjugal transfer are genetically distinct functions of the R1162 protein MobB. *J Bacteriol* **181**: 2124-2131.

Peterson, K.R., Wertman, K.F., Mount, D.W., and Marinus, M.G. (1985) Viability of *Escherichia coli* K-12 DNA adenine methylase (*dam*) mutants requires increased expression of specific genes in the SOS regulon. *Mol Gen Genet* **201**: 14-19.

Philpott, D.J., Yamaoka, S., Israël, A., and Sansonetti, P.J. (2000) Invasive *Shigella flexneri* activates NF-κB through a lipopolysaccharide-dependent innate intracellular response and leads to IL-8 expression in epithelial cells. *J Immunol* **165**: 903-914.

Porter, M.E., and Dorman, C.J. (1994) A role for H-NS in the thermo-osmotic regulation of virulence gene expression in *Shigella flexneri*. *J Bacteriol* **176**: 4187-4191.

Porter, M.E., and Dorman, C.J. (1997a) Positive regulation of *Shigella flexneri* virulence genes by integration host factor. *J Bacteriol* **179**: 6537-6550.

Porter, M.E., and Dorman, C.J. (1997b) Virulence gene deletion frequency is increased in *Shigella flexneri* following conjugation, transduction, and transformation. *FEMS Microbiol Lett* **147**: 163-172.

Porter, M.E. (1998) The Regulation of Virulence gene expression in *Shigella flexneri*. Ph.D. Thesis, Trinity College Dublin.

Porter, M.E., and Dorman, C.J. (2002) *In vivo* DNA-binding and oligomerization properties of the *Shigella flexneri* AraC-like transcriptional regulator VirF as identified by random and site-specific mutagenesis. *J Bacteriol* **184**: 531-539.

Postow, L., Hardy, C.D., Arsuaga, J., and Cozzarelli, N.R. (2004) Topological domain structure of the *Escherichia coli* chromosome. *Genes Dev* **18**: 1766-1779.

Prosseda, G., Fradiani, P.A., Di Lorenzo, M., Falconi, M., Micheli, G., Casalino, M., Nicoletti, M., and Colonna, B. (1998) A role for H-NS in the regulation of the *virF* gene of *Shigella* and enteroinvasive *Escherichia coli*. *Res Microbiol* **149**: 15-25.

Prosseda, G., Falconi, M., Giangrossi, M., Gualerzi, C.O., Micheli, G., and Colonna, B. (2004) The *virF* promoter in *Shigella*: more than just a curved DNA stretch. *Mol Microbiol* **51**: 523-537.

Pupo, G.M., Lan, R., and Reeves, P.R. (2000) Multiple independent origins of *Shigella* clones of *Escherichia coli* and convergent evolution of many of their characteristics. *Proc Natl Acad Sci U S A* **97**: 10567-10572.

Qian, X., Scheithauer, B.W., Kovacs, K., and Lloyd, R.V. (2005) DNA microarrays: recent developments and applications to the study of pituitary tissues. *Endocrine* **28**: 49-56.

Quinones, M., Kimsey, H.H., and Waldor, M.K. (2005) LexA cleavage is required for CTX prophage induction. *Mol Cell* **17**: 291-300.

Rasmussen, A.A., Eriksen, M., Gilany, K., Udesen, C., Franch, T., Petersen, C., and Valentin-Hansen, P. (2005) Regulation of *ompA* mRNA stability: the role of a small regulatory RNA in growth phase-dependent control. *Mol Microbiol* **58**: 1421-1429.

Rathman, M., Sjaastad, M.D., and Falkow, S. (1996) Acidification of phagosomes containing *Salmonella typhimurium* in murine macrophages. *Infect Immun* **64**: 2765-2773.

Redaschi, N., and Bickle, T.A. (1996) DNA Restriction and Modification Systems. In *Eschericha coli and Salmonella: Cellular and Molecular Biology.* Neidhardt, F.C., Curtiss R., III, Ingraham, J.L., Lin, E.C.C., Low, K.B., Magasanik, B., *et al.* (eds) Washington DC: ASM Press, pp. 773-781.

Repoila, F., and Gottesman, S. (2001) Signal transduction cascade for regulation of RpoS: temperature regulation of DsrA. *J Bacteriol* **183**: 4012-4023.

Repoila, F., Majdalani, N., and Gottesman, S. (2003) Small non-coding RNAs, co-ordinators of adaptation processes in *Escherichia coli*: the RpoS paradigm. *Mol Microbiol* **48**: 855-861.

Rhen, M., Riikonen, P., and Taira, S. (1993) Transcriptional regulation of *Salmonella enterica* virulence plasmid genes in cultured macrophages. *Mol Microbiol* **10**: 45-56.

Rhen, M., and Dorman, C.J. (2005) Hierarchical gene regulators adapt *Salmonella enterica* to its host milieus. *Int J Med Microbiol* **294**: 487-502.

Rice, P.A., Yang, S., Mizuuchi, K., and Nash, H.A. (1996) Crystal structure of an IHF-DNA complex: a protein-induced DNA U-turn. *Cell* **87**: 1295-1306.

Rice, P.A. (1997) Making DNA do a U-turn: IHF and related proteins. *Curr Opin Struct Biol* **7**: 86-93.

Rimsky, S., Zuber, F., Buckle, M., and Buc, H. (2001) A molecular mechanism for the repression of transcription by the H-NS protein. *Mol Microbiol* **42**: 1311-1323.

Rimsky, S. (2004) Structure of the histone-like protein H-NS and its role in regulation and genome superstructure. *Curr Opin Microbiol* **7**: 109-114.

Rolland, K., Lambert-Zechovsky, N., Picard, B., and Denamur, E. (1998) *Shigella* and enteroinvasive *Escherichia coli* strains are derived from distinct ancestral strains of *E. coli*. *Microbiology* **144**: 2667-2672.

Rooker, M.M., Sherburne, C., Lawley, T.D., and Taylor, D.E. (1999) Characterization of the Tra2 region of the IncHI1 plasmid R27. *Plasmid* **41**: 226-239.

Ross, W., Thompson, J.F., Newlands, J.T., and Gourse, R.L. (1990) *E. coli* Fis protein activates ribosomal RNA transcription *in vitro* and *in vivo*. *EMBO J* **9**: 3733-3742.

Roussel, A.F., and Chabbert, Y.A. (1978) Taxonomy and epidemiology of gram-negative bacterial plasmids studied by DNA-DNA filter hybridization in formamide. *J Gen Microbiol* **104**: 269-276.

Rouviere-Yaniv, J., Yaniv, M., and Germond, J.E. (1979) *E. coli* DNA binding protein HU forms nucleosome-like structure with circular double-stranded DNA. *Cell* **17**: 265-274.

Ruiz-Albert, J., Yu, X.J., Beuzon, C.R., Blakey, A.N., Galyov, E.E., and Holden, D.W. (2002) Complementary activities of SseJ and SifA regulate dynamics of the *Salmonella typhimurium* vacuolar membrane. *Mol Microbiol* **44**: 645-661.

Ruiz-Albert, J., Mundy, R., Yu, X.J., Beuzon, C.R., and Holden, D.W. (2003) SseA is a chaperone for the SseB and SseD translocon components of the *Salmonella* pathogenicity-island-2-encoded type III secretion system. *Microbiology* **149**: 1103-1111.

Ryan, V.T., Grimwade, J.E., Nievera, C.J., and Leonard, A.C. (2002) IHF and HU stimulate assembly of pre-replication complexes at *Escherichia coli oriC* by two different mechanisms. *Mol Microbiol* **46**: 113-124.

Sack, R.B., Rahman, M., Yunus, M., and Khan, E.H. (1997) Antimicrobial resistance in organisms causing diarrheal disease. *Clin Infect Dis* **24**: 102-105.

Safo, M.K., Yang, W.Z., Corselli, L., Cramton, S.E., Yuan, H.S., and Johnson, R.C. (1997) The transactivation region of the *fis* protein that controls site-specific DNA inversion contains extended mobile β-hairpin arms. *EMBO J* **16**: 6860-6873.

Saiki, R.K., Gelfand, D.H., Stoffel, S., Scharf, S.J., Higuchi, R., Horn, G.T., Mullis, K.B., and Erlich, H.A. (1988) Primer-directed enzymatic amplification of DNA with a thermostable DNA polymerase. *Science* **239**: 487-491.

Salazar-Gonzalez, R.M., and McSorley, S.J. (2005) *Salmonella* flagellin, a microbial target of the innate and adaptive immune system. *Immunol Lett* **101**: 117-122.\

Sambrook, J., and Russell, D.W. (2001) *Molecular Cloning: A Laboratory Manual.* Cold Spring Harbor, NY: Cold Spring Harbor Laboratory Press.

Sambrook, J., E.F. Fritsch, and T. Maniatis (1989) *Molecular cloning: A Laboratory Manual.* Cold Spring Harbor, NY: Cold Spring Harbor Laboratory Press.

Sansonetti, P.J., Hale, T.L., Dammin, G.J., Kapfer, C., Collins, H.H., Jr., and Formal, S.B. (1983) Alterations in the pathogenicity of *Escherichia coli* K-12 after transfer of plasmid and chromosomal genes from *Shigella flexneri. Infect Immun* **39**: 1392-1402.

Sansonetti, P.J. (1991a) Molecular and cellular bases of *Shigella flexneri* virulence. *Bull Acad Natl Med* **175**: 803-810.

Sansonetti, P.J. (1991b) Genetic and molecular basis of epithelial cell invasion by *Shigella* species. *Rev Infect Dis* **13**: 285-292.

Sansonetti, P.J., Arondel, J., Cantey, J.R., Prevost, M.C., and Huerre, M. (1996) Infection of rabbit Peyer's patches by *Shigella flexneri*: effect of adhesive or invasive bacterial phenotypes on follicle-associated epithelium. *Infect Immun* **64**: 2752-2764.

Sansonetti, P.J., Tran Van Nhieu, G., and Egile, C. (1999) Rupture of the intestinal epithelial barrier and mucosal invasion by *Shigella flexneri*. *Clin Infect Dis* **28**: 466-475.

Sansonetti, P.J. (2001) Rupture, invasion and inflammatory destruction of the intestinal barrier by *Shigella*, making sense of prokaryote-eukaryote cross-talks. *FEMS Microbiol Rev* **25**: 3-14.

Sasakawa, C., Kamata, K., Sakai, T., Makino, S., Yamada, M., Okada, N., and Yoshikawa, M. (1988) Virulence-associated genetic regions comprising 31 kilobases of the 230-kilobase plasmid in *Shigella flexneri* 2a. *J Bacteriol* **170**: **2480-2484.**

Saul, D., Lane, D., and Bergquist, P.L. (1988) A replication region of the IncHI plasmid, R27, is highly homologous with the RepFIA replicon of F. *Mol Microbiol* **2**: 219-225.

Schechter, L.M., Damrauer, S.M., and Lee, C.A. (1999) Two AraC/XylS family members can independently counteract the effect of repressing sequences upstream of the *hilA* promoter. *Mol Microbiol* **32**: 629-642.

Schechter, L.M., and Lee, C.A. (2001) AraC/XylS family members, HilC and HilD, directly bind and derepress the *Salmonella typhimurium hilA* promoter. *Mol Microbiol* **40**: 1289-1299.

Schechter, L.M., Jain, S., Akbar, S., and Lee, C.A. (2003) The small nucleoid-binding proteins H-NS, HU, and Fis affect *hilA* expression in *Salmonella enterica* serovar Typhimurium. *Infect Immun* **71**: 5432-5435.

Schneider, R., Travers, A., Kutateladze, T., and Muskhelishvili, G. (1999) A DNA architectural protein couples cellular physiology and DNA topology in *Escherichia coli*. *Mol Microbiol* **34**: 953-964.

Schroder, G., and Lanka, E. (2003) TraG-like proteins of type IV secretion systems: functional dissection of the multiple activities of TraG (RP4) and TrwB (R388). *J Bacteriol* **185**: 4371-4381.

Schroder, G., and Lanka, E. (2005) The mating pair formation system of conjugative plasmids-A versatile secretion machinery for transfer of proteins and DNA. *Plasmid* **54**: 1-25.

Schroder, O., and Wagner, R. (2002) The bacterial regulatory protein H-NS-a versatile modulator of nucleic acid structures. *Biol Chem* **383**: 945-960.

Schuch, R., Sandlin, R.C., and Maurelli, A.T. (1999) A system for identifying post-invasion functions of invasion genes: requirements for the Mxi-Spa type III secretion pathway of *Shigella flexneri* in intercellular dissemination. *Mol Microbiol* **34**: 675-689.

Schuch, R., and Maurelli, A.T. (2001) MxiM and MxiJ, base elements of the Mxi-Spa type III secretion system of *Shigella*, interact with and stabilize the MxiD secretin in the cell envelope. *J Bacteriol* **183**: 6991-6998.

Schweder, T., Lee, K.H., Lomovskaya, O., and Matin, A. (1996) Regulation of *Escherichia coli* starvation sigma factor (σ^s) by ClpXP protease. *J Bacteriol* **178**: 470-476.

Shanahan, P.M., Jesudason, M.V., Thomson, C.J., and Amyes, S.G. (1998) Molecular analysis of and identification of antibiotic resistance genes in clinical isolates of *Salmonella typhi* from India. *J Clin Microbiol* **36**: 1595-1600.

Shea, J.E., Hensel, M., Gleeson, C., and Holden, D.W. (1996) Identification of a virulence locus encoding a second type III secretion system in *Salmonella typhimurium. Proc Natl Acad Sci U S A* **93**: 2593-2597.

Shea, J.E., Beuzon, C.R., Gleeson, C., Mundy, R., and Holden, D.W. (1999) Influence of the *Salmonella typhimurium* pathogenicity island 2 type III secretion system on bacterial growth in the mouse. *Infect Immun* **67**: 213-219.

Sheehan, B.J., and Dorman, C.J. (1998) *In vivo* analysis of the interactions of the LysR-like regulator SpvR with the operator sequences of the *spvA* and *spvR* virulence genes of *Salmonella typhimurium. Mol Microbiol* **30**: 91-105.

Sherburne, C.K., Lawley, T.D., Gilmour, M.W., Blattner, F.R., Burland, V., Grotbeck, E., Rose, D.J., and Taylor, D.E. (2000) The complete DNA sequence and analysis of R27, a large IncHI plasmid from *Salmonella typhi* that is temperature sensitive for transfer. *Nucleic Acids Res* **28**: 2177-2186.

Shere, K.D., Sallustio, S., Manessis, A., D'Aversa, T.G., and Goldberg, M.B. (1997) Disruption of IcsP, the major *Shigella* protease that cleaves IcsA, accelerates actin-based motility. *Mol Microbiol* **25**: 451-462.

Shi, W., Zhou, Y., Wild, J., Adler, J., and Gross, C.A. (1992) DnaK, DnaJ, and GrpE are required for flagellum synthesis in *Escherichia coli. J Bacteriol* **174**: 6256-6263.

Shi, X., and Bennett, G.N. (1994) Plasmids bearing *hfq* and the *hns*-like gene *stpA* complement *hns* mutants in modulating arginine decarboxylase gene expression in *Escherichia coli. J Bacteriol* **176**: 6769-6775.

Shin, M., Song, M., Rhee, J.H., Hong, Y., Kim, Y.-J., Seok, Y.-J., Ha, K.-S., Jung, S.-H., and Choy, H.E. (2005) DNA looping-mediated repression by histone-like protein H-NS: specific requirement of $E\sigma^{70}$ as a cofactor for looping. *Genes Dev* **19**: 2388-2398.

Silhavy, T.J., Berman, M.l., and Enquist, L.W. (1984) *Experiments with gene fusions.* Cold Spring Harbor Laboratory, NY.: Cold Spring Harbor Laboratory Press.

Skoko, D., Wong, B., Johnson, R.C., and Marko, J.F. (2004) Micromechanical analysis of the binding of DNA-bending proteins HMGB1, NHP6A, and HU reveals their ability to form highly stable DNA-protein complexes. *Biochemistry* **43**: 13867-13874.

Sledjeski, D., and Gottesman, S. (1995) A small RNA acts as an antisilencer of the H-NS-silenced *rcsA* gene of *Escherichia coli*. *Proc Natl Acad Sci U S A* **92**: 2003-2007.

Sledjeski, D.D., Gupta, A., and Gottesman, S. (1996) The small RNA, DsrA, is essential for the low temperature expression of RpoS during exponential growth in *Escherichia coli*. *EMBO J* **15**: 3993-4000.

Smyth, C.P., Lundbäck, T., Renzoni, D., Siligardi, G., Beavil, R., Layton, M., Sidebotham, J.M., Hinton, J.C.D, Driscoll, P.C., Higgins, C.F., and Ladbury, J.E. (2000) Oligomerization of the chromatin-structuring protein H-NS. *Mol Microbiol* **36**: 962-972.

Sondén, B., and Uhlin, B.E. (1996) Coordinated and differential expression of histone-like proteins in *Escherichia coli*: regulation and function of the H-NS analog StpA. *EMBO J* **15**: 4970-4980.

Sonnenfield, J.M., Burns, C.M., Higgins, C.F., and Hinton, J.C.D. (2001) The nucleoid-associated protein StpA binds curved DNA, has a greater DNA-binding affinity than H-NS and is present in significant levels in *hns* mutants. *Biochimie* **83**: 243-249.

Southern, E.M. (1975) Detection of specific sequences among DNA fragments separated by gel electrophoresis. *J Mol Biol* **98**: 503-517.

Soutourina, O.A., and Bertin, P.N. (2003) Regulation cascade of flagellar expression in Gram-negative bacteria. *FEMS Microbiol Rev* **27**: 505-523.

Spassky, A., Rimsky, S., Garreau, H., and Buc, H. (1984) H1a, an *E. coli* DNA-binding protein which accumulates in stationary phase, strongly compacts DNA *in vitro*. *Nucleic Acids Res* **12**: 5321-5340.

Spurio, R., Durrenberger, M., Falconi, M., La Teana, A., Pon, C.L., and Gualerzi, C.O. (1992) Lethal overproduction of the *Escherichia coli* nucleoid protein H-NS: ultramicroscopic and molecular autopsy. *Mol Gen Genet* **231**: 201-211.

Spurio, R., Falconi, M., Brandi, A., Pon, C.L., and Gualerzi, C.O. (1997) The oligomeric structure of nucleoid protein H-NS is necessary for recognition of intrinsically curved DNA and for DNA bending. *EMBO J* **16**: 1795-1805.

Stanley, T.L., Ellermeier, C.D., and Slauch, J.M. (2000) Tissue-specific gene expression identifies a gene in the lysogenic phage Gifsy-1 that affects *Salmonella enterica* serovar *typhimurium* survival in Peyer's patches. *J Bacteriol* **182**: 4406-4413.

Starcic, M., Zgur-Bertok, D., Jordi, B.J.A.M., Wösten, M.M., Gaastra, W., and van Putten, J.P. (2003) The cyclic AMP-cyclic AMP receptor protein complex regulates activity of the *traJ* promoter of the *Escherichia coli* conjugative plasmid pRK100. *J Bacteriol* **185**: 1616-1623.

Starcic-Erjavec, M., van Putten, J.P., Gaastra, W., Jordi, B.J.A.M., Grabnar, M., and Zgur-Bertok, D. (2003) H-NS and Lrp serve as positive modulators of *traJ* expression from the *Escherichia coli* plasmid pRK100. *Mol Genet Genomics* **270**: 94-102.

Stella, S., Spurio, R., Falconi, M., Pon, C.L., and Gualerzi, C.O. (2005) Nature and mechanism of the *in vivo* oligomerization of nucleoid protein H-NS. *EMBO J* **24**: 2896-2905.

Stella, S., Falconi, M., Lammi, M., Gualerzi, C.O., and Pon, C.L. (2006) Environmental control of the *in vivo* oligomerization of nucleoid protein H-NS. *J Mol Biol* **355**: 169-174.

Stender, S., Friebel, A., Linder, S., Rohde, M., Mirold, S., and Hardt, W.-D. (2000) Identification of SopE2 from *Salmonella typhimurium*, a conserved guanine nucleotide exchange factor for Cdc42 of the host cell. *Mol Microbiol* **36**: 1206-1221.

Stephani, K., Weichart, D., and Hengge, R. (2003) Dynamic control of Dps protein levels by ClpXP and ClpAP proteases in *Escherichia coli*. *Mol Microbiol* **49**: 1605-1614.

Sternberg, N.L., and Maurer, R. (1991) Bacteriophage-mediated generalized transduction in *Escherichia coli* and *Salmonella typhimurium*. *Methods Enzymol* **204**: 18-43.

Suzuki, T., Ueguchi, C., and Mizuno, T. (1996) H-NS Regulates OmpF Expression through *micF* Antisense RNA in *Escherichia coli*. *J Bacteriol* **178**: 3650-3653.

Suzuki, T., and Sasakawa, C. (2001) Molecular basis of the intracellular spreading of *Shigella*. *Infect Immun* **69**: 5959-5966.

Takaya, A., Kubota, Y., Isogai, E., and Yamamoto, T. (2005) Degradation of the HilC and HilD regulator proteins by ATP-dependent Lon protease leads to downregulation of *Salmonella* pathogenicity island 1 gene expression. *Mol Microbiol* **55**: 839-852.

Takayanagi, Y., Tanaka, K., and Takahashi, H. (1994) Structure of the 5' upstream region and the regulation of the *rpoS* gene of *Escherichia coli*. *Mol Gen Genet* **243**: 525-531.

Taludker, A.A., Iwata, A., Nishimura, A., Ueda, S., and Ishihama, A. (1999) Growth phase-dependent variation in protein composition of the *Escherichia coli* nucleoid. *J Bacteriol* **181**: 6361-6370.

Talukder, A.A., and Ishihama, A. (1999) Twelve species of the nucleoid-associated protein from *Escherichia coli*. Sequence recognition specificity and DNA binding affinity. *J Biol Chem* **274**: 33105-33113.

Taylor, D.E., and Levine, J.G. (1980) Studies of temperature-sensitive transfer and maintenance of H incompatibility group plasmids. *J Gen Microbiol* **116**: 475-484.

Taylor, D.E., and Brose, E.C. (1985) Characterization of incompatibility group HI1 plasmids from *Salmonella typhi* by restriction endonuclease digestion and hybridization of DNA probes for Tn*3*, Tn*9*, and Tn*10*. *Can J Microbiol* **31**: 721-729.

Taylor, D.E., Hedges, R.W., and Bergquist, P.L. (1985) Molecular homology and incompatibility relationships between F and IncH1 plasmids. *J Gen Microbiol* **131**: 1523-1530.

Taylor, D.E., and Brose, E.C. (1988) Modified Birnboim-Doly method for rapid detection of plasmid copy number. *Nucleic Acids Res* **16**: 9056.

Tendeng, C., and Bertin, P.N. (2003) H-NS in Gram-negative bacteria: a family of multifaceted proteins. *Trends Microbiol* **11**: 511-518.

Tendeng, C., Soutourina, O.A., Danchin, A., and Bertin, P.N. (2003) MvaT proteins in *Pseudomonas* spp.: a novel class of H-NS-like proteins. *Microbiology* **149**: 3047-3050.

Tezcan-Merdol, D., Nyman, T., Lindberg, U., Haag, F., Koch-Nolte, F., and Rhen, M. (2001) Actin is ADP-ribosylated by the *Salmonella enterica* virulence-associated protein SpvB. *Mol Microbiol* **39**: 606-619.

Thompson, J.D., Higgins, D.G., and Gibson, T.J. (1994) CLUSTAL W: improving the sensitivity of progressive multiple sequence alignment through sequence weighting, position-specific gap penalties and weight matrix choice. *Nucleic Acids Res* **22**: 4673-4680.

Thompson, J.F., Moitoso de Vargas, L., Koch, C., Kahmann, R., and Landy, A. (1987) Cellular factors couple recombination with growth phase: characterization of a new component in the lambda site-specific recombination pathway. *Cell* **50**: 901-908.

Thomson, N., Baker, S., Pickard, D., Fookes, M., Anjum, M., Hamlin, N., Wain, J., House, D., Bhutta, Z., Chan, K., Falkow, S., Parkhill, J., Woodward, M., Ivens, A., and Dougan, G. (2004) The role of prophage-like elements in the diversity of *Salmonella enterica* serovars. *J Mol Biol* **339**: 279-300.

Tietze, E., and Tschäpe, H. (1994) Temperature-dependent expression of conjugation pili by IncM plasmid-harbouring bacteria: identification of plasmid-encoded regulatory functions. *J Basic Microbiol* **34**: 105-116.

Tippner, D., Afflerbach, H., Bradaczek, C., and Wagner, R. (1994) Evidence for a regulatory function of the histone-like *Escherichia coli* protein H-NS in ribosomal RNA synthesis. *Mol Microbiol* **11**: 589-604.

Tippner, D., and Wagner, R. (1995) Fluorescence analysis of the *Escherichia coli* transcription regulator H-NS reveals two distinguishable complexes dependent on binding to specific or nonspecific DNA sites. *J Biol Chem* **270**: 22243-22247.

Tobe, T., Nagai, S., Okada, N., Adler, B., Yoshikawa, M., and Sasakawa, C. (1991) Temperature-regulated expression of invasion genes in *Shigella flexneri* is controlled through the transcriptional activation of the *virB* gene on the large plasmid. *Mol Microbiol* **5**: 887-893.

Tobe, T., Yoshikawa, M., Mizuno, T., and Sasakawa, C. (1993) Transcriptional control of the invasion regulatory gene *virB* of *Shigella flexneri*: activation by *virF* and repression by H-NS. *J Bacteriol* **175**: 6142-6149.

Tolstorukov, M.Y., Virnik, K.M., Adhya, S., and Zhurkin, V.B. (2005) A-tract clusters may facilitate DNA packaging in bacterial nucleoid. *Nucleic Acids Res* **33**: 3907-3918.

Tomoyasu, T., Ohkishi, T., Ukyo, Y., Tokumitsu, A., Takaya, A., Suzuki, M., Sekiya, K., Matsui, H., Kutsukake, K., and Yamamoto, T. (2002) The ClpXP ATP-dependent protease regulates flagellum synthesis in *Salmonella enterica* serovar *typhimurium*. *J Bacteriol* **184**: 645-653.

Tomoyasu, T., Takaya, A., Isogai, E., and Yamamoto, T. (2003) Turnover of FlhD and FlhC, master regulator proteins for *Salmonella* flagellum biogenesis, by the ATP-dependent ClpXP protease. *Mol Microbiol* **48**: 443-452.

Torreblanca, J., and Casadesus, J. (1996) DNA adenine methylase mutants of *Salmonella typhimurium* and a novel *dam*-regulated locus. *Genetics* **144**: 15-26.

Tran Van Nhieu, G., Caron, E., Hall, A., and Sansonetti, P.J. (1999) IpaC induces actin polymerization and filopodia formation during *Shigella* entry into epithelial cells. *EMBO J* **18**: 3249-3262.

Tran Van Nhieu, G., Bourdet-Sicard, R., Dumenil, G., Blocker, A., and Sansonetti, P.J. (2000) Bacterial signals and cell responses during *Shigella* entry into epithelial cells. *Cell Microbiol* **2**: 187-193.

Travers, A., and Muskhelishvili, G. (2005) Bacterial chromatin. *Curr Opin Genet Dev* **15**: 507-514.

Ubeda, C., Maiques, E., Knecht, E., Lasa, I., Novick, R.P., and Penades, J.R. (2005) Antibiotic-induced SOS response promotes horizontal dissemination of pathogenicity island-encoded virulence factors in staphylococci. *Mol Microbiol* **56**: 836-844.

Uchiya, K., Barbieri, M.A., Funato, K., Shah, A.H., Stahl, P.D., and Groisman, E.A. (1999) A *Salmonella* virulence protein that inhibits cellular trafficking. *EMBO J* **18**: 3924-3933.

Ueguchi, C., Suzuki, T., Yoshida, T., Tanaka, K., and Mizuno, T. (1996) Systematic mutational analysis revealing the functional domain organization of *Escherichia coli* nucleoid protein H-NS. *J Mol Biol* **263**: 149-162.

Ueguchi, C., Seto, C., Suzuki, T., and Mizuno, T. (1997) Clarification of the dimerization domain and its functional significance for the *Escherichia coli* nucleoid protein H-NS. *J Mol Biol* **274**: 145-151.

Valdivia, R.H., and Falkow, S. (1997) Fluorescence-based isolation of bacterial genes expressed within host cells. *Science* **277**: 2007-2011.

Valentin-Hansen, P., Eriksen, M., and Udesen, C. (2004) The bacterial Sm-like protein Hfq: a key player in RNA transactions. *Mol Microbiol* **51**: 1525-1533.

Van Bogelen, R.A., Olsen, E.R., Wanner, B.L., and Neidhardt, F.C. (1996) Global analysis of proteins synthesised during phosphorus restriction in *Escherichia coli*. *J Bacteriol* **178**: 4344-4366.

van der Velden, A.W., Lindgren, S.W., Worley, M.J., and Heffron, F. (2000) *Salmonella* pathogenicity island 1-independent induction of apoptosis in infected macrophages by *Salmonella enterica* serotype *typhimurium*. *Infect Immun* **68**: 5702-5709.

van der Woude, M., Braaten, B., and Low, D. (1996) Epigenetic phase variation of the *pap* operon in *Escherichia coli*. *Trends Microbiol* **4**: 5-9.

van Noort, J., Verbrugge, S., Goosen, N., Dekker, C., and Dame, R.T. (2004) Dual architectural roles of HU: formation of flexible hinges and rigid filaments. *Proc Natl Acad Sci U S A* **101**: 6969-6974.

Varshavsky, A.J., Nedospasov, S.A., Bakayev, V.V., Bakayeva, T.G., and Georgiev, G.P. (1977) Histone-like proteins in the purified *Escherichia coli* deoxyribonucleoprotein. *Nucleic Acids Res* **4**: 2725-2745.

Vazquez-Torres, A., Jones-Carson, J., Bäumler, A.J., Falkow, S., Valdivia, R., Brown, W., Le, M., Berggren, R., Parks, W.T., and Fang, F.C. (1999) Extraintestinal dissemination of *Salmonella* by CD18-expressing phagocytes. *Nature* **401**: 804-808.

Vazquez-Torres, A., and Fang, F.C. (2001) *Salmonella* evasion of the NADPH phagocyte oxidase. *Microbes Infect* **3**: 1313-1320.

Vergunst, A.C., Schrammeijer, B., den Dulk-Ras, A., de Vlaam, C.M., Regensburg-Tuïnk, T.J., and Hooykaas, P.J. (2000) VirB/D4-dependent protein translocation from *Agrobacterium* into plant cells. *Science* **290**: 979-982.

Wagner, R. (2000) *Transcription Regulation in Prokaryotes*. Oxford: Oxford University Press.

Wain, J., Diep, T.S., Ho, V.A., Walsh, A.M., Hoa, N.T.T., Parry, C.M., and White, N.J. (1998) Quantitation of bacteria in blood of typhoid fever patients and relationship between counts and clinical features, transmissibility, and antibiotic resistance. *J Clin Microbiol* **36**: 1683-1687.

Wain, J., Nga, L.T.D., Kidgell, C., James, K., Fortune, S., Song Diep, T., Ali, T., O Gaora, P., Parry, C., Parkhill, J., Farrar, J., White, N.J., and Dougan, G. (2003) Molecular analysis of IncHI1 antimicrobial resistance plasmids from *Salmonella* serovar Typhi strains associated with typhoid fever. *Antimicrob Agents Chemother* **47**: 2732-2739.

Wain, J., and Kidgell, C. (2004) The emergence of multidrug resistance to antimicrobial agents for the treatment of typhoid fever. *Trans R Soc Trop Med Hyg* **98**: 423-430.

Waldor, M.K., and Friedman, D.I. (2005) Phage regulatory circuits and virulence gene expression. *Curr Opin Microbiol* **8**: 459-465.

Walker, G.C. (1996) The SOS response of *Escherichia coli*. In *Eschericha coli and Salmonella: Cellular and Molecular Biology*. Neidhardt, F.C., Curtiss R., III, Ingraham, J.L., Lin, E.C.C., Low, K.B., Magasanik, B., *et al.* (eds) Washington DC: ASM Press, pp. 1400-1416.

Wallis, T.S., and Galyov, E.E. (2000) Molecular basis of *Salmonella*-induced enteritis. *Mol Microbiol* **36**: 997-1005.

Wassef, J.S., Keren, D.F., and Mailloux, J.L. (1989) Role of M cells in initial antigen uptake and in ulcer formation in the rabbit intestinal loop model of shigellosis. *Infect Immun* **57**: 858-863.

Watanabe, H., Arakawa, E., Ito, K., Kato, J., and Nakamura, A. (1990) Genetic analysis of an invasion region by use of a Tn*3*-lac transposon and identification of a second positive regulator gene, *invE*, for cell invasion of *Shigella sonnei*: significant homology of *invE* with ParB of plasmid P1. *J Bacteriol* **172**: 619-629.

Waterman, S.R., and Holden, D.W. (2003) Functions and effectors of the *Salmonella* pathogenicity island 2 type III secretion system. *Cell Microbiol* **5**: 501-511.

Watson, P.R., Paulin, S.M., Bland, A.P., Jones, P.W., and Wallis, T.S. (1995) Characterization of intestinal invasion by *Salmonella typhimurium* and *Salmonella dublin* and effect of a mutation in the *invH* gene. *Infect Immun* **63**: 2743-2754.

Wei, B.L., Brun-Zinkernagel, A.-M., Simecka, J.W., Prüß, B.M., Babitzke, P., and Romeo, T. (2001) Positive regulation of motility and *flhDC* expression by the RNA-binding protein CsrA of *Escherichia coli*. *Mol Microbiol* **40**: 245-256.

Wei, J., Goldberg, M.B., Burland, V., Venkatesan, M.M., Deng, W., Fournier, G., Mayhew, G.F., Plunkett, G., 3rd, Rose, D.J., Darling, A., Mau, B., Perna, N.T., Payne, S.M., Runyen-Janecky, L.J., Zhou, S., Schwartz, D.C., and Blattner, F.R. (2003) Complete genome sequence and comparative genomics of *Shigella flexneri* serotype 2a strain 2457T. *Infect Immun* **71**: 2775-2786.

Weinstein-Fischer, D., Elgrably-Weiss, M., and Altuvia, S. (2000) *Escherichia coli* response to hydrogen peroxide: a role for DNA supercoiling, topoisomerase I and Fis. *Mol Microbiol* **35**: 1413-1420.

Welch, T.J., Farewell, A., Neidhardt, F.C., and Bartlett, D.H. (1993) Stress response of *Escherichia coli* to elevated hydrostatic pressure. *J Bacteriol* **175**: 7170-7177.

Werner, M.H., Clore, G.M., Gronenborn, A.M., and Nash, H.A. (1994) Symmetry and asymmetry in the function of *Escherichia coli* integration host factor: implications for target identification by DNA-binding proteins. *Curr Biol* **4**: 477-487.

West, R.B., and van de Rijn, M. (2006) The role of microarray technologies in the study of soft tissue tumours. *Histopathology* **48**: 22-31.

Whelan, K.F., Maher, D., Colleran, E., and Taylor, D.E. (1994) Genetic and nucleotide sequence analysis of the gene *htdA*, which regulates conjugal transfer of IncHI plasmids. *J Bacteriol* **176**: 2242-2251.

Whiteley, M., and Taylor, D.E. (1983) Identification of DNA homologies among H incompatibility group plasmids by restriction enzyme digestion and Southern transfer hybridization. *Antimicrob Agents Chemother* **24**: 194-200.

Wickner, S., Maurizi, M.R., and Gottesman, S. (1999) Posttranslational quality control: folding, refolding, and degrading proteins. *Science* **286**: 1888-1893.

Will, W.R., Lu, J., and Frost, L.S. (2004) The role of H-NS in silencing F transfer gene expression during entry into stationary phase. *Mol Microbiol* **54**: 769-782.

Williams, R.M., Rimsky, S., and Buc, H. (1996) Probing the structure, function, and interactions of the *Escherichia coli* H-NS and StpA proteins by using dominant negative derivatives. *J Bacteriol* **178**: 4335-4343.

Williams, R.M., and Rimsky, S. (1997) Molecular aspects of the *E. coli* nucleoid protein, H-NS: a central controller of gene regulatory networks. *FEMS Microbiol Lett* **156**: 175-185.

Williamson, H.S., and Free, A. (2005) A truncated H-NS-like protein from enteropathogenic *Escherichia coli* acts as an H-NS antagonist. *Mol Microbiol* **55**: 808-827.

Wilson, R.L., Libby, S.J., Freet, A.M., Boddicker, J.D., Fahlen, T.F., and Jones, B.D. (2001) Fis, a DNA nucleoid-associated protein, is involved in *Salmonella typhimurium* SPI-1 invasion gene expression. *Mol Microbiol* **39**: 79-88.

Wojtkowiak, D., Georgopoulos, C., and Zylicz, M. (1993) Isolation and characterization of ClpX, a new ATP-dependent specificity component of the Clp protease of *Escherichia coli*. *J Biol Chem* **268**: 22609-22617.

Wolf, S.G., Frenkiel, D., Arad, T., Finkel, S.E., Kolter, R., and Minsky, A. (1999) DNA protection by stress-induced biocrystallization. *Nature* **400**: 83-85.

Woo, K.M., Chung, W.J., Ha, D.B., Goldberg, A.L., and Chung, C.H. (1989) Protease Ti from *Escherichia coli* requires ATP hydrolysis for protein breakdown but not for hydrolysis of small peptides. *J Biol Chem* **264**: 2088-2091.

Wood, M.W., Jones, M.A., Watson, P.R., Hedges, S., Wallis, T.S., and Galyov, E.E. (1998) Identification of a pathogenicity island required for *Salmonella* enteropathogenicity. *Mol Microbiol* **29**: 883-891.

Worley, M.J., Ching, K.H.L., and Heffron, F. (2000) *Salmonella* SsrB activates a global regulon of horizontally acquired genes. *Mol Microbiol* **36**: 749-761.

Yamada, H., Muramatsu, S., and Mizuno, T. (1990) An *Escherichia coli* protein that preferentially binds to sharply curved DNA. *J Biochem* **108**: 420-425.

Yanisch-Perron, C., Vieira, J., and Messing, J. (1985) Improved M13 phage cloning vectors and host strains: nucleotide sequences of the M13mp18 and pUC19 vectors. *Gene* **33:**103-119.

Yasuda, T., Morimatsu, K., Horii, T., Nagata, T., and Ohmori, H. (1998) Inhibition of *Escherichia coli* RecA coprotease activities by DinI. *EMBO J* **17**: 3207-3216.

Yona-Nadler, C., Umanski, T., Aizawa, S., Friedberg, D., and Rosenshine, I. (2003) Integration host factor (IHF) mediates repression of flagella in enteropathogenic and enterohaemorrhagic *Escherichia coli*. *Microbiology* **149**: 877-884.

Yu, R.R., and DiRita, V.J. (2002) Regulation of gene expression in *Vibrio cholerae* by ToxT involves both antirepression and RNA polymerase stimulation. *Mol Microbiol* **43**: 119-134.

Yu, X.-J., Ruiz-Albert, J., Unsworth, K.E., Garvis, S., Liu, M., and Holden, D.W. (2002) SpiC is required for secretion of *Salmonella* Pathogenicity Island 2 type III secretion system proteins. *Cell Microbiol* **4**: 531-540.

Yuan, H.S., Finkel, S.E., Feng, J.A., Kaczor-Grzeskowiak, M., Johnson, R.C., and Dickerson, R.E. (1991) The molecular structure of wild-type and a mutant Fis protein: relationship between mutational changes and recombinational enhancer function or DNA binding. *Proc Natl Acad Sci U S A* **88**: 9558-9562.

Zablewska, B., and Kur, J. (1995) Mutations in HU and IHF affect bacteriophage T4 growth: HimD subunits of IHF appear to function as homodimers. *Gene* **160**: 131-132.

Zeng, H., Carlson, A.Q., Guo, Y., Yu, Y., Collier-Hyams, L.S., Madara, J.L., Gewirtz, A.T., and Neish, A.S. (2003) Flagellin is the major proinflammatory determinant of enteropathogenic *Salmonella*. *J Immunol* **171**: 3668-3674.

Zhang, A., and Belfort, M. (1992) Nucleotide sequence of a newly-identified *Escherichia coli* gene, *stpA*, encoding an H-NS-like protein. *Nucleic Acids Res* **20**: 6735.

Zhang, A., Derbyshire, V., Salvo, J.L., and Belfort, M. (1995) *Escherichia coli* protein StpA stimulates self-splicing by promoting RNA assembly *in vitro*. *RNA* **1**: 783-793.

Zhang, A., Rimsky, S., Reaban, M.E., Buc, H., and Belfort, M. (1996) *Escherichia coli* protein analogs StpA and H-NS: regulatory loops, similar and disparate effects on nucleic acid dynamics. *EMBO J* **15**: 1340-1349.

Zhang, A., Wassarman, K.M., Rosenow, C., Tjaden, B.C., Storz, G., and Gottesman, S. (2003) Global analysis of small RNA and mRNA targets of Hfq. *Mol Microbiol* **50**: 1111-1124.

Zhou, D., Mooseker, M.S., and Galán, J.E. (1999) Role of the *S. typhimurium* actin-binding protein SipA in bacterial internalization. *Science* **283**: 2092-2095.

Zhou, Y., Gottesman, S., Hoskins, J.R., Maurizi, M.R., and Wickner, S. (2001) The RssB response regulator directly targets σ^S for degradation by ClpXP. *Genes Dev* **15**: 627-637.

Zuber, F., Kotlarz, D., Rimsky, S., and Buc, H. (1994) Modulated expression of promoters containing upstream curved DNA sequences by the *Escherichia coli* nucleoid protein H-NS. *Mol Microbiol* **12**: 231-240.

Zuker, M. (2003) Mfold web server for nucleic acid folding and hybridization prediction. *Nucleic Acids Res*. **31**: 3406-3415.

Zulianello, L., de la Gorgue de Rosny, E., van Ulsen, P., van de Putte, P., and Goosen, N. (1994) The HimA and HimD subunits of integration host factor can specifically bind to DNA as homodimers. *EMBO J* **13**: 1534-1540.

Zychlinsky, A., Prévost, M.-C., and Sansonetti, P.J. (1992) *Shigella flexneri* induces apoptosis in infected macrophages. *Nature* **358**: 167-169.

Supplementary Data